Contributions to the Micropaleontology and Paleoceanography of the Northern North Atlantic

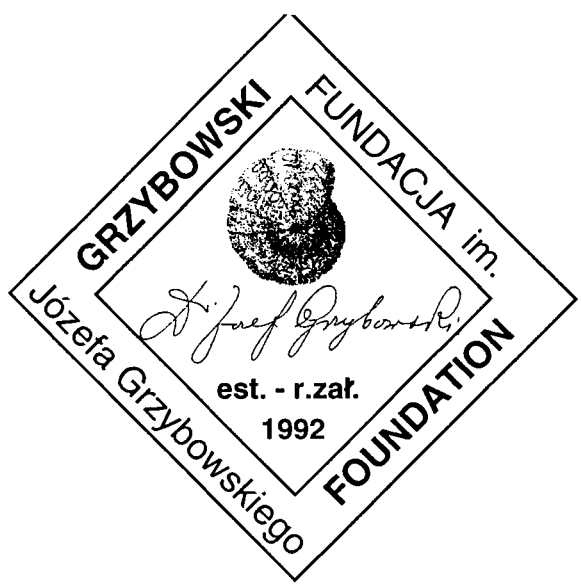


Edited by
H. Christian Hass &
Michael A. Kaminski

Contributions to the Micropaleontology and Paleoceanography of the Northern North Atlantic

edited by

H. Christian Hass & Michael A. Kaminski



Grzybowski Foundation, 1997

Contributions to the Micropaleontology and Paleoceanography of the Northern North Atlantic

(Collected Results from the GEOMAR Bungalow Working Group)

Edited by

H. Christian Hass
GEOMAR
Wischhofstraße 1-3,
D-24148 Kiel, Germany
Present address:
Sonderforschungsbereich 313,
Christian-Albrechts-Universität zu Kiel,
Heinrich-Hecht-Platz 10,
D-24118 Kiel, Germany

&

Michael A. Kaminski
Research School of Geological
and Geophysical Sciences,
Birkbeck College & University College London
Gower Street, London, WC1E 6BT, U.K.

Published by

The Grzybowski Foundation

Grzybowski Foundation Special Publication No. 5

First published in 1997 by the

Grzybowski Foundation

a charitable scientific foundation which associates itself with the Geological Society of Poland, founded in 1992.
The Grzybowski Foundation promotes and supports education and research in the field of Micropalaeontology through its Library (located at the Geological Museum of the Jagiellonian University), Special Publications, Student Grant-in-Aid Programme, and by organising symposia at scientific conferences. More information can be obtained from our website:
http://www.ucl.ac.uk/geolsci/Grzybowski/gf.html

The Grzybowski Foundation

Board of Trustees (1996-2000):
M.A. Gasinski (PL) M.A. Kaminski (GB) W. Kuhnt (D) E. Platon (for RO) P. Sikora (TX)
R. Coccioni (I) J. Van Couvering (NY) P. Geroch (CA) M.Bubik (Cz.R.)

Secretary: U. Mazurkiewicz (PL)

Webmaster: S. Filipescu

Special Publication Editor: M.A. Kaminski

Distributors:

Poland: The Grzybowski Foundation, c/o Geological Museum, Jagiellonian University, ul. Oleandry 2a,

30-063 Kraków, Poland.

North America: Micropaleontology Press, American Museum of Natural History, New York, N.Y. 10024

U.K.: The British Micropalaeontological Society Foraminiferal Group.

The Special Publications Editor (Email: ucfbmak@ucl.ac.uk), or any of the Trustees of the Grzybowski Foundation

This book can be cited as:
Hass, H.C. & Kaminski, M.A. 1997. Contributions to the Micropaleontology and Paleoceanography of the Northern North Atlantic. Grzybowski Foundation Special Publication No. 5, 275 + vi pp.

© **1997,** Hass, H.C. & M.A. Kaminski

British Library Cataloguing in Publication Data
Contributions to the Micropaleontology and Paleoceanography of the Northern North Atlantic
1. Micropalaeontology
I. Hass, H.C.(Hanns-Christian), 1962-
II. Kaminski, M.A. (Michael Anthony), 1957 -

ISBN: 83 - 901164 - 5 - 6

Printed in Poland by:
Drukarnia Narodowa, Kraków.

Cover Design by H.C. Hass & M.A. Kaminski, based on an original design by Nick Lloyd. The front-cover photo shows an island off northern Norway.

COPYRIGHT NOTICE
All rights reserved. No part of this publication may be reproduced, stored in any retrieval system, or transmitted, in any form or by any means, electronic, mechanical, photocopying, recording, or otherwise, without the permission of the Grzybowski Foundation, c/o Geological Museum U.J., ul. Oleandry 2a, 30-063 Kraków, Poland.

Preface

The Bungalow Book: What is it all about, anyway?
It was a hot day in August, 1990 ... Well, that's not exactly how a book on Paleoceanology is supposed to start, I guess. It was a hot day in August 1990, anyway, that the man in charge of the GEOMAR staff, guided me (HCH) from the GEOMAR main building to the Bungalow.

Recently graduated, I was lucky enough to get the opportunity to carry out my PhD thesis in the Department of Paleoceanology of the famous GEOMAR Research Center. Thus, I was a bit confused to leave the main building that housed so many well known researchers, and walk past the fish wholesalers and canneries, Gerd Rost's Auto Garage, a run-down green warehouse, and a few shipping containers, only to reach the "Bungalow".

Flat-roofed, painted in a dirty white color it sat in the corner of a parking place. Wild herbs crept over the three steps to the entrance door, and a young willow tree was busy breaking through the concrete of the upper steps. Altogether, it looked like a cheap 1970ies spectacle frame that somebody had forgotten to throw away.

To be honest, I didn't exactly love it from the first glance but that soon changed. I was welcomed with a good cup of coffee, while at least 3 radios (all tuned to different stations) provided the typical sound of micropaleontologists at work at their microscopes. Four of the five offices were occupied at that time; all of the office doors stood ajar to allow communication between those who formed the genuine "Bungalow Crew". There was Michaela Kubisch who was finishing her PhD thesis on dropstones in Arctic sediments; Henning Bauch, Stefan Nees, and Uli Struck working on their PhD theses on foraminifers of the Nordic Seas, and Mike Kaminski, halfway through his post doc at GEOMAR, working on agglutinated foraminifera from the Norwegian Sea. Happy with the frank atmosphere, I took the empty office that I would be occupying during the next 4 1/2 years whilst working on sediments of the Skagerrak for my PhD thesis, and later on Laptev Sea data during a post-doc.

The early years of 1990-91 were genuinely exciting times - we witnessed the fall of the Berlin wall and the re-unification of Germany; we listened attentively to the BBC world service on Mike's shortwave radio for the latest news when Saddam Hussain's forces invaded Kuwait; and we played host for the first visits to GEOMAR by Russian researchers and research ships as the spirit of scientific cooperation extended further to the East. When the situation arose the Bungalow Crew always banded together in mutual support, whether to lend a hand to unpack a shipping container, or in joyful times to celebrate the birth of a child.

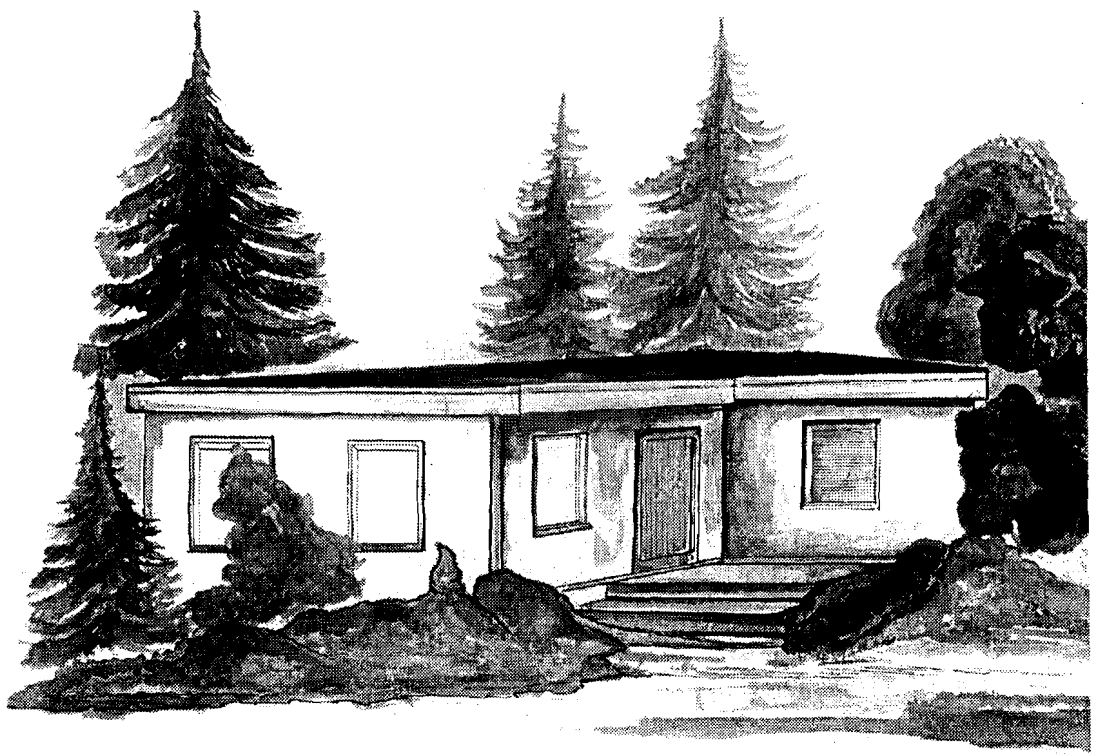
During the year I (MAK) spent at the Bungalow, surprisingly enough, the language of choice spoken at most times was English. Jörn Thiede had originally suggested that I take up residence in the Bungalow because he thought that having an English-speaking post doc among the PhD students housed there would be a good influence. Whether the influence was good or not is a matter of opinion, but our secluded location at the corner of a shipping container storage lot did mean that we developed a special sort of comradery that is rare in other places. The Bungalow was surrounded by shipping containers that served as portable laboratories - and as we had the only comfort/kitchen facilities in the immediate area - our ranks always grew in number during the morning coffee break. Stefan Lammers, Ingo Wollenburg, and others who worked in the laboratory containers would join us regularly for coffee. Because the Bungalow had turned into a little English-speaking corner of GEOMAR, Rainer Zahn (recently returned from Canada), Robin and Angela Keir (just arrived from Scripps), and Ron Boyd (spending his sabbatical at GEOMAR) became frequent guests who visited us from the other buildings. Every now and then Jörn Thiede (who also was the supervisor of all the students' theses projects) popped in for coffee, which gave us the feeling that we hadn't been quite forgotten by the rest of the world. Taking into account the Bungalow computer and telephone equipment as well as the frequent burglar raids (and last but not least the wasps' nests during summer...) we were very much convinced that the Bungalow was situated in the outer perimeter of Jurassic Park.

Our humble Bungalow actually served as a hospitality centre for some important visitors as well. Jenö Nagy came down from Oslo to spend a couple of weeks working with Mike on the agglutinated foraminifera from the Barents Sea, and Stan Geroch travelled from Krakow to spend a week at the Bunglow working on the taxonomy of agglutinated foraminifera from the Indian Ocean and North Atlantic. Jörg Mutterlose paid a brief visit to collaborate with Mike on the ODP Leg 123 biostratigraphical synthesis chapter. These meetings provided a convenient excuse for some welcome social activity, and on one memorable occasion the whole Bungalow crew went out for a nice Chinese meal with one of the distinguished visitors. Against this background of a warm and friendly working environment scientific cooperation flourished, and some of the scientific results of this joint research are presented in this book.

Fluctuations in the Bungalow Crew were, however, immense. Michaela passed her PhD the following winter and Mike left the Bungalow in April 1991 to become a lecturer at University College London. Soon after Stefan, Uli, and Henning also left in order to occupy an office in the new "SFB 313" (Special Research Project 313: Environmental Change: The Northern North Atlantic) building at Kiel University. In the following months a number of people moved into the bungalow only to leave it again after a couple of weeks. Meanwhile, Henning and Uli passed their PhDs, and Britta Jünger moved in to carry out her PhD thesis on deep-water

renewal in the Greenland Sea. Horst Bohrmann was in the Bungalow for one year in which he participated in ODP Leg 135, while Helge Meggers and Harry Andruleit completed their diploma theses in the Bungalow before they started off PhDs at Kiel and Bremen Universities. Although not based in Kiel, Martin Antonow had his place in the Bungalow, where he carried out the major part of his PhD thesis on sedimentation around the Vesteris Seamount in the Greenland Sea. Jan Rumohr joined the crew in 1992 to fulfill his duties as the man in charge of the Steno-Lab for the disabled at GEOMAR, and to work on sedimentologic aspects of the Barents and Norwegian shelves. Jens Matthießen became a honorary guest of the Bungalow. Abandoning his office in the main building (and sometimes also sacrificing precious time for his research on dinoflagellates of the Baltic Sea and the North Atlantic) he shared more than one night shift in the Bungalow writing research proposals.

The same day at the end of 1993, Stefan, who was still based at the SFB 313, and myself (HCH) passed our PhDs. Harry Hommers joined the Bungalow crew to start off his PhD on planktic foraminifers from the Arctic and Antarctic, and among one or two other students Susanne Geiselhart and Niels Andresen finished their diploma theses under the roof of the Bungalow. Peter Goldschmidt moved into the Bungalow after having finished his PhD thesis on sedimentological aspects of the Greenland Sea. Stefan Nees returned to the Bungalow in 1995 after a one-year post doc at the ANU in Canberra, Australia. I (HCH) left the Bungalow in 1995 after a 1 year post-doc working on Laptev Sea oceanography to commence a post-doc with Mike at University College London. Michaela Kubisch, Jan Rumohr, Stefan Nees, Harry Hommers, and the diploma students Claudia Didié, Jan Malte Wolfsdorf, Carmen Jung, and Jan Helmke formed the last of the Bungalow Crew.



The GEOMAR Bungalow, drawn by Jaroslaw Migacz (after a photograph taken by Claudia Didié)

While it was always an event of fun and joy to visit the Bungalow, its future existence is jeopardized if not already over. A new research centre has been built at GEOMAR and the Bungalow Crew had to vacate the building as leaks in the roof of the Bungalow began to adversely affect the safety of the whole structure. It is planned to either modernize the Bungalow and/or turn it into a guest house in the future. However, rumours that the Bungalow will be pulled down because of its rotten structure and the potential of asbestos contamination are resurfacing with even greater intensity.

Already several years ago we were planning to collect scientific papers from the Bungalow Crwe to turn them into a book. On one of those hot August afternoons one of us (MAK) had just returned home to the bunglow after a long and tiring visit in Tübingen (to assist with the editing of the Proceedings of the Third International Workshop on Agglutinated Foramininfera). As the Bungalow Crew was sitting on the front steps enjoying lunch, we began talking about compiling our joint results into a coherent thematic volume. After all, the one thing we all had in common was our shared interest in the paleoceanography of the northern North

Atlantic. We all agreed it was a worthwhile undertaking. However, everybody knows about the gap between talking about something and actually doing it... All the students at the time unanimously agreed that the first step was to write their thesis - then they could prepare a chapter for a book. Our plans had to wait on a back burner for a few years - and the book really began as a project coordinated in London by "Bungalow Graduates". Therefore, we take pride in presenting the project that carried the working title "The Bungabook" during the past 18 months. We are also grateful to the Grzybowski Foundation which gives the book a scientific home. Unfortunately, not everyone from the Bungalow was able to spare the time in order to write an original paper - we also regret that we could only accept papers that dealt with scientific aspects of the *North Atlantic*.

The papers

The book we present here contains original refereed articles on various topics relating to the micropaleontology and paleoceanography of the northern North Atlantic. It is chronologically organized starting with a paper that deals with Paleogene sediments from the Barents Sea and ending with a study of the seasonal development of coccolithophore communities in the Norwegian-Greenland Sea in the years 1990, 1991, and 1995. Two additional papers introduce a new benthic foraminifer species and a new planktic foraminifer morphotype, respectively. Last not least, one paper highlights an important link between micropaleontology and sedimentology.

In particular, the following papers are included: Nagy *et al.* present a study that focuses on the Paleocene-Eocene transition as recorded in clastic sediments of the Torsk Formation located in the Tromsø Basin. Paleo-environment reconstructions from 3.2-0.8 Ma in the Rockall Plateau area based on coccolith and planktic foraminifer data are presented by Meggers & Baumann. Struck focuses on the late Quaternary productivity-climate relation of benthic foraminifers from the Norwegian-Greenland Sea, whereas Bauch's paper places particular emphasis on the planktic foraminifer and stable isotope records of the northern North Atlantic. Antonow *et al.* elucidate the late Pleistocene paleoceanographic setting around the Vesteris seamount in the Greenland Sea. Analyzing ice-rafted material from the Norwegian-Greenland Sea, Goldschmidt presents an IRD classification scheme that suggests sources and timing of ice surges during the past ca. 170,000 years. Costello & Bauch present benthic foraminifer productivity records related to climate change from the Iceland Plateau. Matthiessen & Baumann's paper shows significantly changing surface water conditions off eastern Greenland through the late Weichselian and the Holocene as inferred from dinoflagellate cyst records. Nees focuses on the relation between benthic foraminiferal records from the Rockall Plateau up to the Fram Strait and atmospheric temperature reconstructions at the termination of the last glacial. Hass shows if and how benthic foraminifers from the North Sea react to late Holocene climate fluctuations as well as recent and subrecent agglutinated foraminifer assemblages from the Skagerrak. Baumann *et al.* highlight the reaction of calcareous phytoplankton during low production phases throughout the Norwegian-Greenland Sea. Kaminski *et al.* present new insights into seasonally changing microhabitats of live benthic foraminifers from the New Jersey continental margin. Kaminski & Geroch's paper introduces a new agglutinated foraminifer species that turns out to be a stratigraphic index species for the Eocene to Miocene interval. Hommers introduces a new morphotype of the planktic foraminifer species *Neogloboquadrina pachyderma* (sin) that is distributed in the high latitudes of both hemispheres. Finally, Michels & Meggers' investigations cast new light on the ultrastructure of planktic foraminifer tests in order to provide a means for differentiation of effects of dissolution and those produced through bed-load transport.

Acknowledgements
This book would have never come to fruition without the efforts of a number of people who carried out the scientific reviews, the language reviews, and final proof readings of the papers as well as those who helped in many ways during the production of the book.

The editors especially acknowledge scientific reviews by (alphabetical order): E. Alve (Oslo, Norway), W. Austin (Durham, UK), K.-H. Baumann (Bremen, Germany), H. Bergsten (Göteborg, Sweden), A. Holbourn (London, UK; Kiel, Germany), K.L. Knudsen (Aarhus, Denmark), W. Kuhnt (Kiel, Germany), M. Maslin (London, UK), J. Matthießen (Bremerhaven, Germany), J. Murray (Southhampton, UK), J. Nagy (Oslo, Norway), K. Nordberg (Göteborg, Sweden), H. Schulz (Hannover, Germany), M.-S. Seidenkrantz (Aarhus, Denmark), R. Spielhagen (Kiel, Germany), M. Spindler (Kiel, Germany), R. Stein (Bremerhaven, Germany), J. Young (London, UK), as well as two anonymous referees.

Language reviews and technical aid provided by A. Holbourn (London, UK; Kiel, Germany), Claudia Didié (Kiel, Germany), S. Kinsey (Kiel, Germany), P. Goldschmidt (Kiel, Germany), T. Paramor (London, UK), and R. Preece (London, UK) are greatly acknowledged. B. Fürst (Freiberg, Germany) considerably accelerated the computerized type setting process.

We thank the Grzybowski Foundation for including this book into their Special Publication Series. Last but not least, the editors would like to thank all the authors who contributed original papers to this special publication of the Grzybowski Foundation, and who showed patience and discipline during review, revision and typesetting processes.

This book is dedicated to all the people of the Bungalow and those of kindred spirit in the past, present and future. The GEOMAR Bungalow may not survive another season, but the spirit of collaboration and companionship will long outlive the physical structure that once contained it.

Christian Hass and Mike Kaminski
Kiel/London, May 1997

TABLE OF CONTENTS

Preface by the editors i

Table of contents v

Foreword by Jörn Thiede and Priska Schäfer vii

Evolution of the North Atlantic Ocean: An overview
H. CHRISTIAN HASS 1

Foraminiferal, palynomorph, and diatom biostratigraphy and paleoenvironments of the Torsk Formation: A reference section for the Paleocene-Eocene transition in the western Barents Sea
JENÖ NAGY, MICHAEL A. KAMINSKI, KARL JOHNSEN and ALEXANDER G. MITLEHNER 15

Late Pliocene/Pleistocene North Atlantic calcareous plankton and paleoceanography of the North Atlantic
HELGE MEGGERS and KARL-HEINZ BAUMANN 39

Paleoecology of benthic foraminifera in the Norwegian-Greenland Sea during the past 500 ka
ULRICH STRUCK 51

Paleoceanography of the North Atlantic Ocean during the past 450 ky deduced from planktic foraminiferal assemblages and stable isotopes
HENNING A. BAUCH 83

The climate-sensitive Vesterisbanken area (central Greenland Sea): depositional environment and paleoceanography during the past 250,000 years
MARTIN ANTONOW, PETER M. GOLDSCHMIDT and HELMUT ERLENKEUSER 101

The ice-rafting history of coarse-grained sediments in the Norwegian-Greenland Sea for the last two glacial/interglacial cycles
PETER M. GOLDSCHMIDT 119

Late Pleistocene-Holocene productivity record of benthic foraminifera from the Iceland Plateau
ORAN COSTELLO and HENNING A. BAUCH 141

Dinoflagellate cyst records from the East Greenland continental margin during the last 15,000 years: Implications for paleoceanographic reconstructions
JENS MATTHIESSEN and ASTRID BAUMANN 149

High resolution benthic foraminiferal records of the last glacial termination in the northern North Atlantic
STEFAN NEES 167

The benthic foraminiferal response to late Holocene climate change over northern Europe
H. CHRISTIAN HASS 199

Recent and subrecent agglutinated foraminifers in four box cores from the Skagerrak (NE North Sea)
H. CHRISTIAN HASS 217

Spatial and temporal dynamics of coccolithophore communities during low production phases in the Norwegian-Greenland Sea.
KARL-HEINZ BAUMANN, HARALD ANDRULEIT, ANDREA SCHRÖDER-RITZRAU and CHRISTIAN SAMTLEBEN 227

Seasonality in microhabitats of rose bengal stained deep-sea benthic foraminifera from the New Jersey continental margin
MICHAEL A. KAMINSKI, AMAL M. AL HASSAWI and WOLFGANG KUHNT 245

***Psamminopelta gradsteini* n.sp., a new species of Paleogene deep-water agglutinated foraminifera from the northern North Atlantic and Polish Outer Carpathians**
MICHAEL A. KAMINSKI and STANISŁAW GEROCH 249

Wurstkammer specimens of *Neogloboquadrina pachyderma* (sinistral): A new morphotype from the Arctic Ocean and the Weddell Sea
HARALD HOMMERS 253

Effects of bed-load transport on planktic foraminifer tests
KLAUS H. MICHELS and HELGE MEGGERS 263

MICROPALEONTOLOGY AND PALEOCEANOGRAPHY OF THE NORTHERN NORTH ATLANTIC OCEAN

A foreword by

JÖRN THIEDE[1,2] and PRISKA SCHÄFER[2,3]

[1]GEOMAR Research Center for marine Geosciences of Kiel University, Wischhofstraße 1-3, D-24148 Kiel, Germany

[2]Sonderforschungsbereich 313 ("Veränderungen der Umwelt: Der nördliche Nordatlantik") of Kiel University, Heinrich-Hecht-Platz 10, D-24118 Kiel, Germany

[3]Geologisch-Paläontologisches Institut und Museum der Christian-Albrechts-Universität zu Kiel, Olshausenstraße 40, D-24118 Kiel, Germany

This collection of papers about a variety of themes on the micropaleontology and paleoceanography of the northern North Atlantic Ocean which is being published by the Grzybowski Foundation tells the story of some exceptional coincidences, namely of an exciting scientific subject, of young scientific entrepreneurs, of a small building housing this young group of researchers in the sometimes depressing surrounding of an old factory complex, and of a new Europe.

The scientific subject is of immediate concern to northwestern Europe, if not to the entire northern Hemisphere. There is no question that many aspects of climatic zonation, in particular its regional perturbation over NW Europe has much to do with the fact the the geologically young northernmost North Atlantic Ocean allows the exchange of surface as well as deep water masses between the Arctic Ocean and the temperate to tropical Atlantic. In modern times, during the present interglacial, the North Atlantic Drift and its northward continuation, the Norwegian Current, are advecting much heat to high northern latitudes that entire NW Europe including its extreme northern parts enjoy a climate which is favorable for the highly developed modern European societies living in these territories. Based on the long oceanographic tradition and the original definition of the Norwegian Current by the Norwegian oceanographer Mohn in the 19th century, it is pertinent that Hans Holtedahl (1959) from the same university was the first one to take a series of sediment cores across the Norwegian current and to detect that the Norwegian-Greenland Sea not all that long ago was ice covered and interglacial conditions only developed in the course of the last deglaciation. Today we know that interglacials are indeed exceptional and that they represent short spells of interruptions of a long history of glacial paleoenvironments. Since the interglacial inflow of temperate to the Norwegian-Greenland Sea is balanced by the outflow of cold and sometimes ice-covered waters of the East Greenland current as well by the overflow across the Greenland-Scotland Ridge of deep, cold and oxygen-rich waters feeding the North Atlantic Deep Water, this small subbasin of the world Ocean is today influencing the environment of our entire globe.

Studies which allow to tap the history of paleoclimate in this region which is highly sensitive to change are therefore in the limelight of many nations which are directly or indirectly concerned about the possibility of change in the near future. The SFB 313 ("Sonderforschungsbereich 313: Veränderungen der Umwelt: Der nördliche Nordatlantik", Kiel University 1985-1998) from which many of the studies published in this book originated is only but one in the concert of international efforts which conducted by European and North American nations with the aim to unravel the recent, historic and potentially future impact of processes in the Norwegian-Greenland Sea on the global climate. Based on substantial funding relatively large paleoceanographic communities have developed on both sides of the Atlantic to collaborate and sometimes to friendly compete in attempts to solve the causal relationships generating the fast and dramatic climate changes of the late Cenozoic. This book will therefore only be one in considerable series of publications all closing in onto attempts to describe this history as detailed as possible and draw information from these studies for an evaluation of future properties of marine and terrestrial habitats in and around the North Atlantic. Major scientific investigations with this aim are today conducted by the international Ocean Drilling Program ("North Atlantic-Arctic Ocean Gateway-program), by the PONAM (Polar North Atlantic Margins)-program of the European Science Foundation, by the "Climate and Ozone-Program" of Norwegian research institutions and some major research establishments in Russia, USA, UK and France, to name a few.

Beside the research subject, however, this book tells also the story of a young, enthusiastic and internationally oriented group of researchers who converged for some limited time in the so-called "Bungalow" on the premises of the former "Seefischmarkt" (=fish market) which had been established in difficult times after the second world war on the eastern shores of Kiel Bay. Somebody had forgotten to demolish the "Bungalow"

and in times when space for research is scarce it did not take long time before even this building was occupied. The "Bungalow" was neither elegant nor suited for science as described vividly in the "preface" of the editors of this book. However, it obviously offered something which is often lacking in new buildings, namely "atmosphere" where graduate students were able to work towards their masters- and PhD-theses, loosely supervised by some postdocs and the academic staff of the SFB 313 and of GEOMAR. Other parts of the SFB and of GEOMAR were housed in much more comfortable offices, and in close neighbourhood the "Bungalow"-crew could see the new building of GEOMAR rising. Times are changing and today this group has partly spread to other countries, other institutions, though some remain in Kiel. But obviously all carry some fond memories of their time in the "Bungalow" because otherwise they would not have been willing to sacrifice their time and efforts to contribute to this book.

The book reflects also some of the changes which have affected Europe over the past decade. The book is being published by the Grzybowski Foundation which is an international foundation associated with the Geological Society of Poland and which promotes as well as supports research and education in the field of micropaleontology. The foundation is housed at the Geological Museum of the Jagellonian University in Kraków, Poland. Since the SFB 313 is project funded through support from the German Research Foundation (DFG=Deutsche Forschungsgemeinschaft) and through Kiel University by the State goverment of Schleswig-Holstein, most of the authors are German. Most have not remained at Kiel University after completing their degree, but have moved on to virtually all major marine geoscientific research institutions in Germany, some of which have only been founded after the reunification of the former East and West Germany. The list of authors shows also characteristics which are typically for these changing times. Some of the papers have been authored by a colleague originally from the US, and another author is from one of the "Neue Bundesländer". Another paper originated mainly from Oslo documenting the close relationship which have developed between the geoscientific institutions of Oslo and Kiel Universities. The book is a good document for the new times in Europe, for the growth of paleoceanography and for the internationalization of the marine geosciences.

Oslo/Kiel, Jan. 1997

The North Atlantic Ocean: An Overview

H. CHRISTIAN HASS

Department of Geological Sciences, University College London, Gower Street, London WC1E 6BT, U.K.

Present address: SFB 313, Kiel University, Heinrich-Hecht-Platz 10, D-24118 Kiel, Germany

INTRODUCTION

The North Atlantic is one of the most important oceans for virtually any subject of scientific interest. Geophysicists investigating rifting and plate tectonics, as well as marine geologists and marine micropaleontologists, appreciate that even the birth of the North Atlantic is still recorded in the form of sediments in the eastern- and westernmost parts of the equatorial North Atlantic. Like all other oceans, much of the geological history of the North Atlantic has been reconstructed due to the success of the Ocean Drilling Program (ODP) and its predecessor the Deep Sea Drilling Project (DSDP). Since the launch of the drilling programs, many cores have recovered sediments, including subsediment crustal structures, that led to the understanding of the evolution of (not only!) the North Atlantic Ocean, its paleoceanography and the Earth's climatic development through the past 155 million years.

From its earliest stages, when it formed the westernmost part of the Tethys Ocean as early as the Early Cretaceous (DSDP Leg 44, ODP Leg 101), the Atlantic started to play a critical role in the climatic and oceanographic history of the Earth. Later on, the Atlantic Ocean became the only entirely open waterway that until today connects both polar regions, providing a „deep sea highway" for Arctic-Antarctic water masses as well as interhemispherical heat exchange. Today, the northern North Atlantic is characterized by two major surface current systems and water masses that couldn't be more different (see also Baumann *et al., this volume*). In the western part, the East Greenland Current conveys cold, mainly Arctic water masses south. These are less saline and significantly colder than their counterparts on the eastern side which emerge from the Carribean, transporting temperate water masses far north via the North Atlantic and Norwegian Currents. Altogether, these currents together with the associated deep currents play a crucial role in global climate dynamics.

A further important North Atlantic aspect is the epicontinental seas that are adjacent to and part of the North Atlantic. All bear their own important evolutional histories:

The Gulf of Mexico and the Carribean Sea, presently forming the Atlantic's warm water pool, carry some of the oldest sediments found in the entire Atlantic, some of them oil-bearing (e.g. Jenkyns, 1994).

The Mediterranean turns out to be an excellent example for the impact that even a small sea, blocked by huge continents, may have on the Earth's climate: during the latest Miocene - the Earth was already in a glacial mode, and decreasing sea levels cut-off the connection between the Mediterranean and the World Ocean. Water evaporated and eventually reached the World Ocean again but the salt remained on site. Thus, the World Ocean became more prone to freezing over because of slightly decreased salinity which in turn slightly increased the Earth's Albedo and finally caused a global cooling during what is called the „Mediterranean salinity crisis" (e.g. Hodell *et al.*, 1986; Weijermars, 1988; Kastens, 1992).

Further north, the Baltic Sea forms the largest reservoir of brackish water in the world. Its oscillations between marine and freshwater stages due to iso- and eustasy at least during the past 13,000 years had a tremendous effect not only on the biology of the Baltic Sea but perhaps also on the climate of the northern North Atlantic (Bergsten & Nordberg, 1992). Its gateway to the North Sea, and thus its only connection with the World Ocean, the Skagerrak-Kattegat, bears extreme high-resolution Holocene sedimentary records (e.g. Stabell & Thiede, 1985; Hass, 1996). The North Sea basin itself, bearing the North Atlantic's most important hydrocarbon province, has a colorful tectonic history. Rifting commenced in the earliest Triassic and terminated during the Paleocene, thus leaving major structures like the Central and Viking Grabens (Ziegler & Van Hoorn, 1989).

The Norwegian Sea is situated at one of the most crucial gateways of the World Ocean circulation. It was not before the middle Miocene that the

In: Hass, H.C. & Kaminski, M.A. (eds.) 1997. Contributions to the Micropaleontology and Paleoceanography of the Northern North Atlantic. *Grzybowski Foundation Special Publication*, no. 5, pp. 1-14

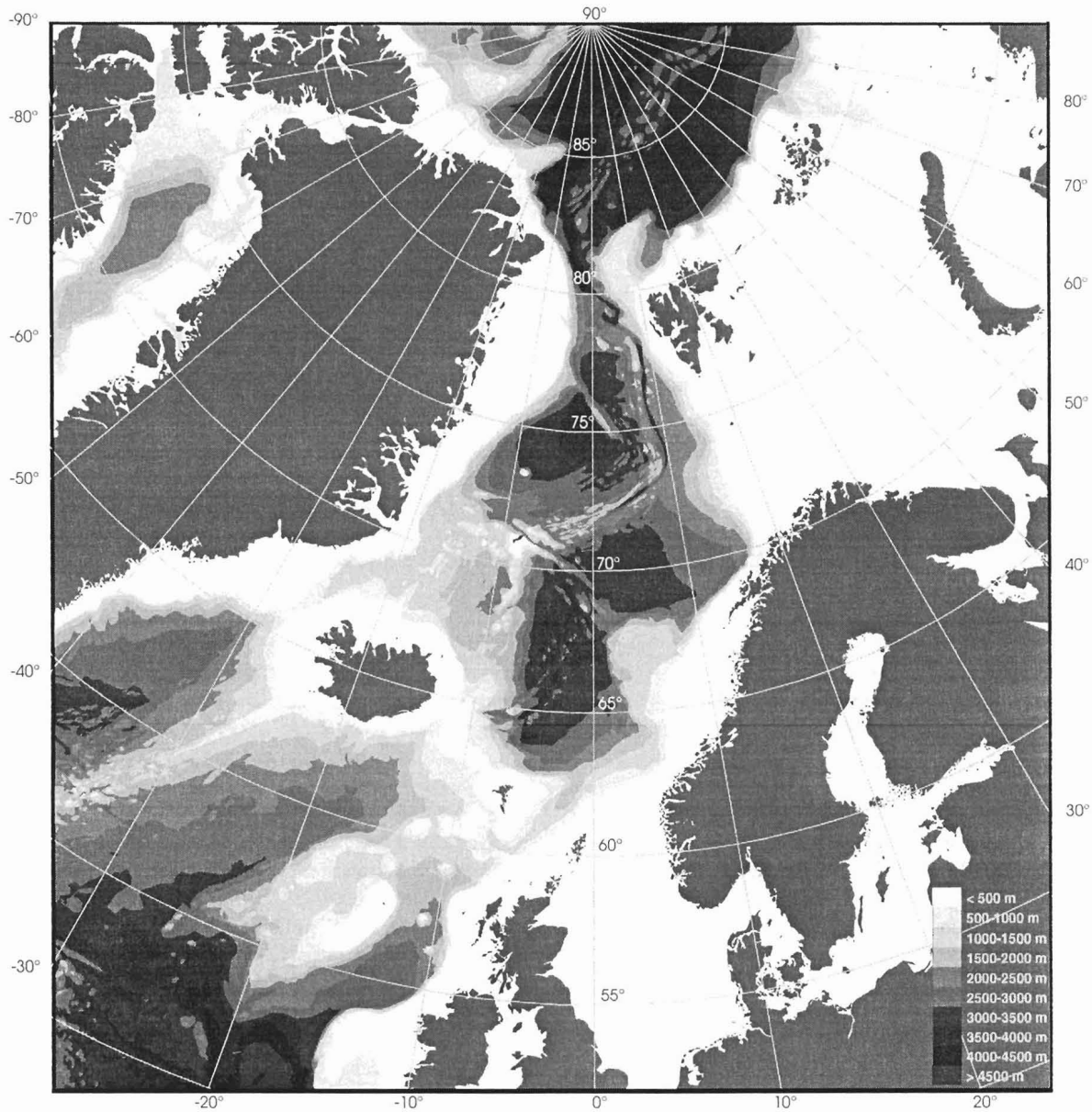


Figure 1. The northern North Atlantic (bathymetric data from GEBCO).

Greenland-Scotland Ridge submerged below sea level, thus terminating the isolation of the northern North Atlantic and providing a connection between the central Atlantic and the Arctic Ocean heat sink (Eldholm *et al.*, 1987; Berggren & Schnitker, 1983). Eventually, a proto-modern Atlantic circulation commenced as cold and dense deep water masses headed south and were replaced by warmer and less dense surface water masses from the south (Kennett, 1982); the highly climate effective Norwegian Current that passes along the Norwegian shelf and through the Norwegian Sea was born.

Regarding the present global ocean circulation and climate, the initial pacemaker of the Ocean Conveyor (Broecker, 1991) is considered to be in the North Atlantic. Cold Arctic winds cause evaporation and cooling of surface water masses and thus contribute to the sinking of huge cells of denser cooled surface water (Broecker & Denton, 1990). This produces a gigantic flow of cold and salty deep and intermediate water which then travels from the North Atlantic south around Africa and through the Indian Ocean (see also Sy *et al.*, 1997). The stability of the deep water flow is controlled by the freshwater balance of the North Atlantic basin (Rahmstorf, 1996). The major part of this cold water mass upwells in the northern Paci-

fic due to intense wind forcing, releasing salt and incorporating freshwater and heat. According to the model, this water mass returns to the North Atlantic as a warm and less saline surficial return flow, increases its salinity and temperature in the Carribean and eventually conveys heat up to the higher latitudes in the form of the North Atlantic Current. If this process is disturbed, the deep circulation may become shallower and weaker and the areas of deep water renewal may migrate further south (Rahmstorf, 1994). As a result, less heat is conveyed north and the northern North Atlantic regions rapidly cool down (the „glacial" mode of deep circulation).

Presently, a legion of researchers is working on paleoclimatic reconstructions on Milankovitch and sub-Milankovitch time scales from Quaternary sediments in order to exactly reconstruct rapid climate change with regard to the paleoceanographic setting of the North Atlantic. While deep-sea drilling is very expensive and takes a long time for planning and organization, dozens of large and small research vessels collected sediment cores and water samples, and carried out measurements at hundreds of sites in the North Atlantic Ocean during the last 20-30 years in order to understand the present oceanographic and climatic conditions as well as those of the past few hundred thousends of years. This small armada of research ships includes vessels as small as a rubber dinghy (to take water and plankton samples from coastal areas) up to huge icebreakers such as the German „Polarstern" that are able to enter pack ice covered basins in the northernmost areas of the North Atlantic and elsewhere.

TECTONIC EVOLUTION OF THE NORTH ATLANTIC

Today, the Atlantic forms the second largest basin of the World Ocean. Through time it undertook a variety of forms, from a narrow, tropical part of the Tethyan Ocean at the time the reptiles began to rule the surrounding supercontinents to the present elongated, more than 11,000-km long basin that connects both polar regions. While the South Atlantic is slightly younger, the evolution of the North Atlantic can be traced back as far as the Triassic.

The following sections deal exclusively with the North Atlantic in general and the northern North Atlantic in particular. This chapter is based on a great number of references as listed in the reference section. Basically, where not specified, the tectonics chapter is based on papers in Ziegler (1975), Kennett (1982), Sheridan (1986), Eldholm *et al.* (1987), Srivastava & shipboard scientific party (1987), Ziegler & van Hoorn (1989), Myhre & Thiede (1995), and Scrutton *et al.* (1995).

The birth of an ocean

Long before the splitting of the African and North American continents in the middle Jurassic, early tectonic activity affected the northern North Atlantic area when late Hercynian suturing marked the future breakup of Gondwana and Laurasia.

While rifting in the Norwegian-Greenland Sea started as early as in the Namurian, the southward propagation of rifting processes was presumably inhibited by oppositely directed stress fields emerging from the peak Variscan orogenic activities.

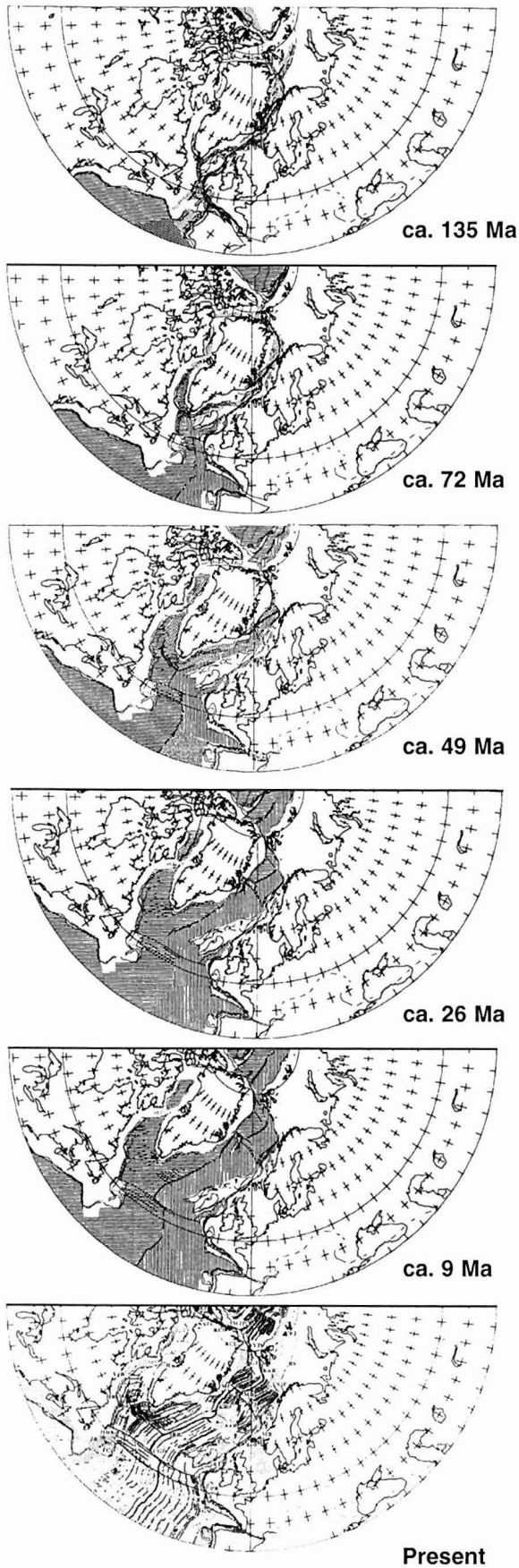
As the stress fields changed, rifting may have expanded to the south during the early Permian. During the Permo-Triassic, the northern North Atlantic area was covered with red beds that were trapped in rapidly forming graben structures. Rifting further increased and eventually formed a complicated pattern from the Norwegian Sea to the western Tethys, where rifting processes from the early Permian heralded a major reorganization of the plates. Although there were no late Paleozoic marine ingressions into the North Atlantic area, the structures that eventually led to the formation of the early North Atlantic Ocean established themselves during the Late Carboniferous at the latest.

The Mesozoic development of the North Atlantic

It was not until the early Triassic that Permo-Carboniferous fracture zones of the Mediterranean were reactivated through strong rifting processes related to the tectonic activity in the Tethys. These structures eventually enabled marine advances further west. By the end of the Triassic and at the dawn of the Jurassic, marine conditions had established themselves through rapidly subsiding basins as far as the Rockall Trough and the NW African, New England and Canadian shelves. East of the Rockall Trough, a number of basins formed; these now carry up to 6 km of clastic Triassic sediments (Ebdon *et al.*, 1995). Further advances finally led to a connection with the cyclically advancing Arctic Ocean through the Rockall Trough and the grabens of the Irish Sea during the Raethian and Hettangian. Early Lias then saw the development of open marine conditions between the Tethys, which had meanwhile advanced to the Carribean, and the Arctic Ocean.

Although this connection was suspended during a short period of extensive doming in the North Sea (Ziegler & van Hoorn, 1989), the breakup of Pangaea, and thus the development of a major ocean, did not stop.

Intensive volcanism accompanied the prograding rift system that advanced from the south through the Labrador Sea, while the main sea floor



spreading axis of the central Atlantic could not overcome the Azores fracture zone until the Early Cretaceous. Later, rifting reached Baffin Bay and the central Atlantic spreading axis advanced into the northern North Atlantic, where strong tectonic activity resulted in rapid doming and subsidence.

During the Cretaceous, crustal separation between Europe and Greenland advanced as seafloor spreading continued in the Norwegian-Greenland Sea. The North Atlantic spreading axis reached the North American continent and succeeded in separating Greenland. Until the Early Tertiary (mostly within Anomalies 24-25), major changes took place: crustal separation isolated Greenland from Norway and Rockall, crustal separation also took place in the Baffin Bay, major ridges formed in the North Atlantic and Arctic Oceans and the Eurasian Basin opened (e.g. Srivastava, 1978; Eldholm *et al.*, 1987).

Cenozoic development

Spreading continued in the Norwegian-Greenland and Labrador Seas; this eventually caused enormous compressional stress on Greenland's shelf until the early Oligocene when the Labrador-Baffin Bay spreading axis became extinct. The Greenland-Scotland Ridge, one of the most important structures for global ocean circulation (see e.g. Bott *et al.*, 1983), appears to be the track of a mantle plume that was situated underneath eastern Greenland. During the divergence of Norway and Greenland, this hot spot left a trace of up to 30 km thick igneous rocks that formed the ridge (White, 1988). Activity of this hot spot caused uplift of up to 1,500 m in the Shetland-Faeroe area (Joppen & White, 1990). Due to this process, large submarine fans formed in the North Sea and eventually became excellent hydrocarbon reservoirs (Anderton, 1993; Ebdon *et al.*, 1995).

Due to continued spreading in the Norwegian-Greenland Sea, Greenland was eventually pushed back to the North American Plate.

Until the mid-Miocene, tectonic and volcanic activitiy remained high: Jan Mayen as well as the northeastern part of the Barents Shelf separated from Greenland. Meanwhile, a connection between the North Atlantic and the Arctic spreading centers was established by the Knipovitch Ridge.

Until today, major sea floor spreading is slow to moderate (Norwegian-Greenland Sea at 0.95 cm/yr; Eldholm *et al.*, 1987).

Figure 2. Paleophysiographic evolution of the northern North Atlantic area from Early Cretaceous (Valanginian, ca. 135 Ma) to the Present according to several sources (after Rowley & Lottes, 1988). Ridge axes, different crust types, and magnetic anomalies (Present) are displayed (see Rowley & Lottes, 1988).

PALEOCEANOGRAPHIC AND PALEOCLIMATIC HISTORY OF THE NORTH ATLANTIC

The section above could only provide a glimpse of the long history of rifting prior to the eventual formation of the present day North Atlantic. In the following section a short overview of the paleoceanographic evolution of the North Atlantic and its role in global climate change will be given. Of course it can not be complete. The main emphasis will be placed on the northern North Atlantic.

Mesozoic paleoenvironments

The lack of Mesozoic glacial deposits suggests that there were no glaciated areas anywhere in the world (Frakes, 1986). Among many theories to explain the vast global warming that followed the glaciation of Gondwana, an increased greenhouse effect through volcanogenic CO_2 is only one (see Graedel & Crutzen, 1993). Towards the middle Jurassic, substantial parts of the continental margins worldwide became drowned, mostly due to eustatic sea level rise. What is Europe today consisted of widespread epicontinental seas and intercalated land areas (Ziegler, 1975). There is a reasonably good correlation of sea-level highstands and periods of fast seafloor spreading during the Jurassic and Cretaceous (Sheridan, 1986; see also Pittman, 1978).

Unlike the crucial role the North Atlantic played in the paleoclimatic evolution of the Cenozoic, Mesozoic sediments suggest that the young North Atlantic Ocean was built up of mostly restricted basins (Kennett, 1982). At least temporally, these basins must have been cut off from the World Ocean, as evidenced by evaporites of probably early or middle Jurassic age (Thiede, 1979). These oldest sediments in the North Atlantic were deposited near the spreading axis of this ca. 500 km wide, tropical ocean (Robertson & Ogg, 1986).

Favored by the warm climate and high atmospheric CO_2 concentrations, calcareous nannoplankton began to shift the major part of carbonate production from the shallow shelves to the deep sea during the late Jurassic (Roth, 1986). Towards the middle Cretaceous, when the central North Atlantic approached probably half of its present size, water mass circulation was controlled by a large cyclonic gyre. There was a gateway that opened to the Tethys Ocean and probably a narrow strait that allowed surficial water mass exchange with the Pacific through the Carribean, whereas the south was blocked by land masses and there was no connection to the northern North Atlantic until the Eocene (Myhre & Thiede, 1995; Roth & Krumbach, 1986). Deep water was thus generated in marginal evaporitic basins, which resulted in warm and saline deep and bottom waters. A very stable water column with low-saline and very warm surface waters and high saline but only slightly cooler bottom waters resulted (Roth, 1986; Saltzman & Barron, 1982); low oxygen values kept marine life low (Bralower & Thierstein, 1986). These conditions became even more pronounced during the Cenomanian transgression, when warm, saline South Atlantic water masses fueled the North Atlantic and widespread epicontinental seas contributed increasing amounts of low oxygen, high saline water to the bottom water (Roth, 1986). DSDP Leg 76 (Site 534, Blake-Bahama Basin) sediments revealed 2 major cycles of carbon-poor to carbon-rich sediments starting in the middle Jurassic; these extend as far as in the eastern Tethys (Baumgartner, 1983). These sediments may be the result of a cyclic occurrence of anoxic conditions and eustatic sea-level changes that, in turn, led to CCD fluctuations (Sheridan, 1986). Hallam (1986) discusses possible Milankovich forcing that may be the reason for obvious sedimentary cycles of 10,000 to 100,000 years superimposed on the large cycles of Cretaceous ocean ventilation.

From the Turonian, Tethyan planktic foraminifers that were found in cores from the South Atlantic (e.g. DSDP Leg 39) suggest the establishment of strong currents connecting the North and the South Atlantic oceans (Premoli Silva & Boersma, 1977).

Cenozoic paleoenvironments

The basins that formed in the Norwegian-Greenland Sea were framed by a complex tectonic pattern of ridges and fracture zones (see Myhre *et al.*, 1982; Nunns & Peacock, 1982; Eldholm *et al.*, 1987). These still prevented major water mass exchange with the World Ocean. The Greenland-Scotland Ridge remained subaerial at least until the late early Eocene, when the most easterly parts began to subside (Myhre & Thiede, 1995). Complex sedimentary patterns (sediment drifts) suggest that a large portion of the bottom waters made their way through the Faeroe channels that formed the deepest passage of the Greenland-Scotland Ridge (Andersen & Boldreel, 1995). Faunal exchange (deep water agglutinated foraminifers) between the North Atlantic and Norwegian Sea is already evident in the middle Eocene (Kaminski *et al.*, 1990). Subsidence of the ridge apparently followed the trace of the mantle plume to the west. By the middle Miocene the ocean basins had almost their modern shapes (Schnitker, 1980). The Denmark Strait section of the ridge became submerged in the late Miocene, as evidenced by changes in the benthic foraminiferal faunas in the Norwegian-Greenland Sea (Berggren & Schnitker, 1983). Cold bottom waters that had formed since the Miocene

in the Nordic Seas were now able to flow across the ridge. The Earth's climate system had already entered a glacial mode during this time and a worldwide ca. 40 m sea level drop took place (Kennett, 1982). Partly due to this sea level drop, the Mediterranean became isolated from the World Ocean (see also Weijermars, 1988). As a result, evaporation transformed the Mediterranean into a series of salty inland lakes until the beginning of the Pliocene, leaving behind a huge series of evaporites. Eventually, this salt was withdrawn from the World Ocean; thus, its salinity decreased by 2 PSU. Since less saline waters freeze earlier, which in turn increases the Earth's Albedo, the isolation of the Mediterranean was the cause of a remarkable world-wide cooling during a period that is called the „Mediterranean salinity crisis" (Kennett, 1982).

Continuing deterioration of the climate led to a permanently frozen Arctic Ocean, probably from the late Miocene (Clark, 1982; however, see Wolf & Thiede, 1991; Repenning *et al.*, 1987). During the late Pliocene, sedimentation of ice-rafted debris in the North Atlantic began (Shackleton *et al.*, 1984), although first indications of an unstable ice cover or icebergs in the Labrador and Norwegian-Greenland Seas could be dated back as far as the middle/late Miocene (Wolf & Thiede, 1991; Fronval & Jansen, 1996; Thiede & Myhre, 1996; Wolf-Welling *et al.*, 1996). In the continuation of the Cenozoic, the growths and decays of the major ice sheets around the northern North Atlantic, which had another amplification around 1 MyBP, led to the deposition of huge masses of glacial sediments that were transported as far as the deep-sea basins through ice rafting or in the form of mass movements through channel systems on the slope. Shelves prograded considerably into the North Atlantic as huge submarine fans formed, such as on the West Hebrides and West Shetland shelves (Stoker, 1995) and all around the northern North Atlantic from Newfoundland to Norway (e.g. Piper *et al.*, 1990; Vorren *et al.*, 1991; Aksu & Hiscott, 1992; Elverhøi, 1992;).

The climate deteriorated stepwise during the past 55 Ma. From at least 3 MyBP, strong orbital forcing is suggested from SST records and ice volume (Myhre & Thiede, 1995; see also DSDP Leg 94 results). Maslin *et al.* (1995a) consider a sharp increase in insolation through increased obliquity and precession amplitudes the main trigger for the intensification of the Northern Hemisphere galciation between 2.75 and 2.55 MyBP. The final closure of the Panama Isthmus around 1.8 MyBP (Keller *et al.*, 1989) is thought to have either delayed the formation of ice sheets through increased heat transport to the north (Maslin *et al.*, 1995a) or stimulated ice sheet formation as a result of increased transport of moisture to the north (Mikolajewicz *et al.*, 1993). Burton *et al.* (1997) present geochemical evidence for increased North Atlantic Deep Water (NADW) flow since the closure of the central American Isthmus suggesting the onset of modern North Atlantic water mass circulation at that time.

Of the Plio-Pleistocene, which is characterized by an increasingly significant climate deterioration, the last ca. 900 ka (Mid Pleistocene Revolution 900-920 kyBP, Berger & Jansen, 1994) - i.e. oxygen isotope Stages 22-1 - and especially the last 650 ka attracted major interest as the Earth's climate system then switched from 41,000 and 23,000 into a powerful 100,000 year cycle (e.g. Pisias *et al.*, 1984; Martinson *et al.*, 1987). During this period, the advancing and retreating Laurentide and Eurasian ice sheets had their major maxima (e.g. Last Glacial Maximum, LGM, ~18 kyBP) and minima (e.g. Eemian, ~125 kyBP). Since mathematically, the glacial/interglacial cycles should have been more continuous than they obviously were, a couple of theories were established in order to explain rapid climate change (see e.g. Ruddiman & McIntyre, 1981; Boyle & Keigwin, 1987; Berger & Jansen, 1994). Most likely, variations in the formation of NADW such as the southward movement of the source area of NADW, switching to a weaker production mode or a complete shutdown of the flow of the global ocean circulation system (the Ocean Conveyor) led to changes in global heat transport which subsequently caused rapid climate change (Broecker, 1987, 1991; Broecker & Denton, 1990; see also Rahmstorf, 1994, 1996; Sarnthein *et al.*, 1994; Weinelt *et al.*, 1996). Thus, aside from orbital parameters, the northern North Atlantic in general and the NADW production cells in particular are considered to be the principal pace maker of global climate. Recently, new hypotheses (mainly based on geochemical evidence and atmospheric general circulation models) challenged this view by proposing a significant drop in *tropical* sea surface temperatures that may have led to a series of feedback mechanisms affecting atmospheric water vapour and thus the greenhouse effect finally resulting in global cooling (Webb *et al.*, 1997; Beck *et al.*, 1997; Bard *et al.*, 1997; Curry & Oppo, 1997; see also Zahn, 1994).

The production rate of NADW appears to be in close conformity with the climate variability as recorded in Greenland's ice cores (e.g. Keigwin *et al.*, 1994). Recently, North Atlantic deep-sea sediment analyses (op. cit.) suggested stable climate conditions during the Eemian interglacial as no change in NADW production could be detected, thus challenging earlier interpretations from ice cores (GRIP Members, 1993). However, Maslin

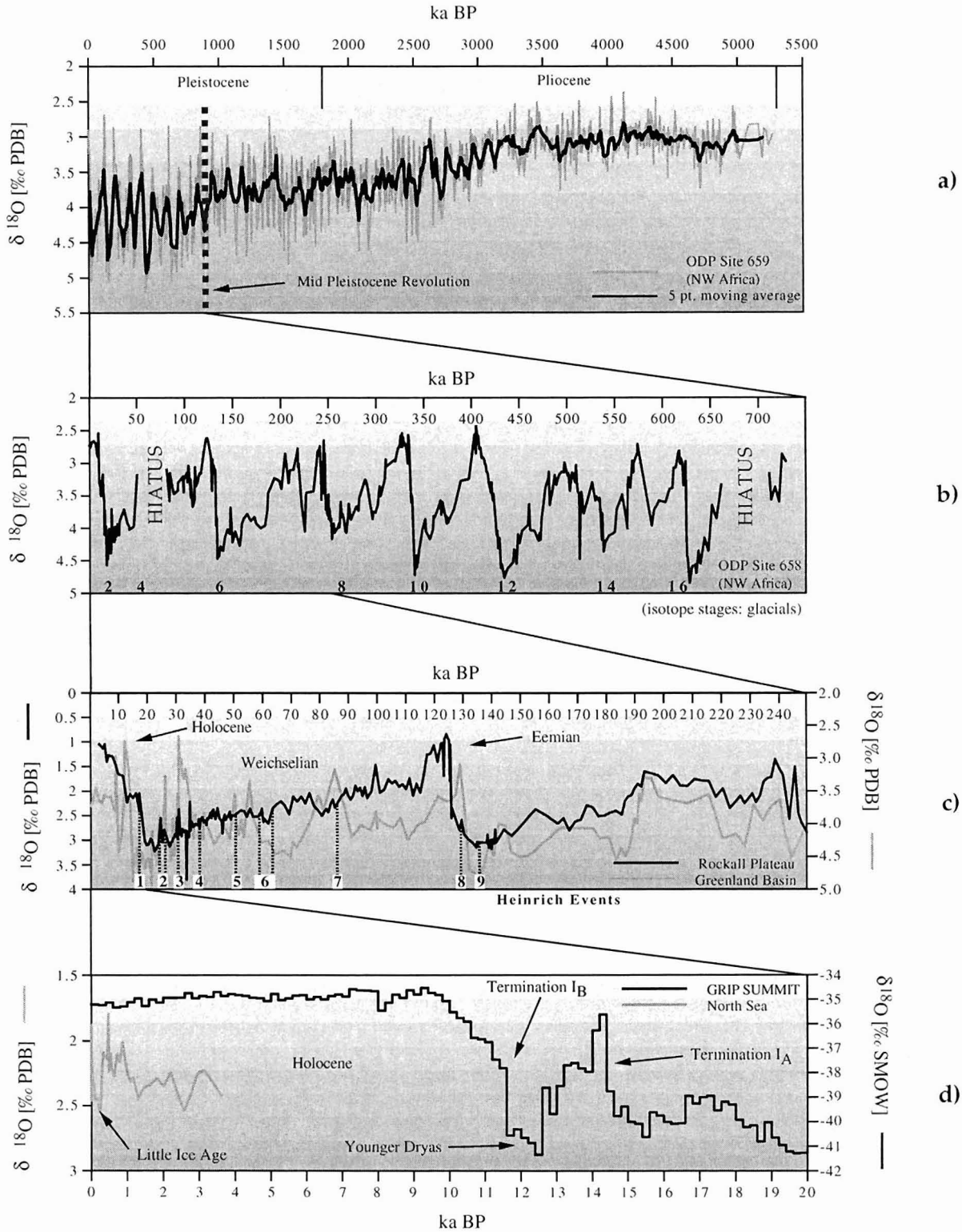


Figure 3. a) Oxygen isotope profile of Site 659 (ODP Leg 108, off NW Africa) (after Tiedemann *et al.*, 1994); b) oxygen isotope profile of Site 658 (ODP Leg 108, off NW Africa) (after Sarnthein & Tiedemann, 1989) including glacial isotope stages; c) solid line: oxygen isotope profile of Core 23414 from the Rockall Plateau including Heinrich Events (age scale: calender years) (after Jung, 1996); grey line: oxygen isotope profile of several cores from the Greenland Basin combined to a „standard" profile (after Antonow, 1995; Antonow *et al.*, *this volume*); d) black line: oxygen isotope profile of Greenland ice core GRIP SUMMIT (after Dansgaard *et al.*, 1993; data from Dansgaard, W., Johnsen, S. J., Clauson, H. B., Dahl-Jensen, D., Gundestrup, N. S., Hammer, C. U., Hvidberg, C. S., Steffensen, J. P., Sveinbjornsdottir, A. E., and J. Jouzel); grey line: oxygen isotope profile of Core III KAL, Skagerrak (after Hass, 1996; *this volume*).

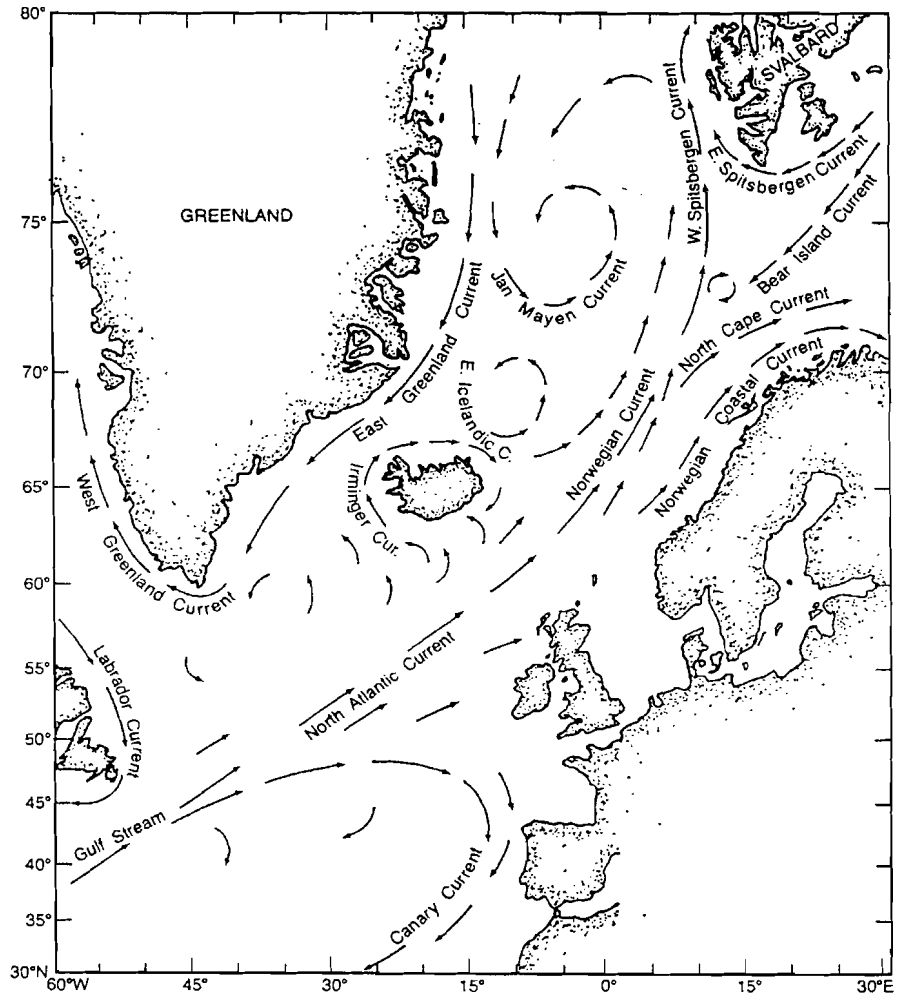


Figure 4. Present-day surface water mass circulation of the northern North Atlantic (adapted from Eldholm *et al.*, 1987, after data from Kellogg, 1975, 1976).

(1996) was able to present stable isotope evidence (ODP Site 658, eastern Atlantic) for a short term (<400 yrs) intra-Eemian shutdown of deep water formation and a synchronous cold spell. Keigwin *et al.* (1991) and Lehman *et al.* (1991) showed that during the last deglaciation (15-10 ka), multiple meltwater events were followed by decreased NADW production and cold spells. The sudden shutdown of NADW production was found to cause SST shifts of ≥ 5° C in fewer than 40 years (Lehman & Keigwin, 1992).

Apparently, the pattern of glacial/interglacial changes during the Brunhes Epoch basically repeated itself through time. As an example, the conditions from the LGM to the beginning of the Holocene in the northern North Atlantic are now shortly described.

There is much debate about the surface and deep water circulation of the northern North Atlantic during the LGM. Earlier interpretations of SSTs suggest a sluggishly cyclonically rotating, though permanently frozen, Norwegian-Greenland Sea (CLIMAP Project Members, 1976, 1981, 1984) whereas Henrich (1990, 1992) and Henrich *et al.* (1995) inferred at least seasonally open cyclonically rotating waters in the Norwegian-Greenland Sea from IRD facies, carbonate contents and carbonate preservation studies. From stable isotope measurements of planktic foraminifers, Sarnthein & Altenbach (1995) and others (e.g. Ruddiman & McIntyre, 1976; Robinson *et al.*, 1995; Weinelt *et al.*, 1996; Bauch, *this volume*) postulate a seasonally ice-free, weakly cyclonic rotating Norwegian-Greenland Sea. According to this theory, the Norwegian Sea was entirely isolated from the North Atlantic by ice sheets of Iceland, the Shetlands, and Norway. Furthermore, a persistent anticyclonic rotating meltwater lens west of Ireland not only blocked the connection to the northeast but also supported the Irminger Current that conveyed temperate water masses north across the Denmark Strait (Sarnthein & Altenbach, 1995).

Aside from unequivocally astronomically steered climate change, there is still strong and rapid climate change on a much shorter -millenial- timescale: A strange pattern of ice-rafted debris (IRD) that was deposited approximately every 12 ky during the past ca. 60 ka was discovered in the North Atlantic, stretching from Labrador to the British Islands (e.g. Bond *et al.*, 1992; Broecker *et al.*, 1992) including associated events further north (e.g. Stein *et al.*, 1994, 1996). Termed Heinrich Layers after H. Heinrich, who was the first to describe them (Heinrich, 1988), most of these layers result

from massive iceberg discharge out of Baffin Bay; the icebergs were transported northeast by the cyclonic polar gyre (Grousset *et al.*, 1993). These events of massive iceberg release into the North Atlantic Ocean during the last glaciation appear to be parallel to recurring episodes of unusually cold North Atlantic surface water (Bond cycles; Bond *et al.*, 1992) and cold air temperatures over Greenland (Dansgaard-Oeschger events; Dansgaard *et al.*, 1993). Interpreting sea surface properties (SST, SSS, $\delta^{18}O$ of planktic foraminifers), Maslin *et al.* (1995b) could not substantiate a sea surface cooling prior to Heinrich events, thus adding support to the largely climate-independent free-oscillating system theory of MacAyeal and Wang (1992) as a cause for the Heinrich Events. After each Heinrich event (except H1, which occurred during the Milankovitch forced insolation rise) an episode of increased SST and air temperature over Greenland lasting up to 2,000 years is suggested before the climate trend continued further into the glacial maximum (GRIP Members, 1993; Grootes *et al.*, 1993; Maslin *et al.*, 1995b). As NADW production was possibly halted by Heinrich events H3 and H4, and there was basically no or only very weak deep water production between 30 and 13 kyBP, it was inferred that Heinrich events were at least partly responsible for amplifying glacial conditions (Broecker, 1994; Maslin *et al.*, 1995b; Sarnthein & Altenbach, 1995). Seidov & Haupt (1997) showed that NADW production was low although the glacial conveyor was rather intensive; deep-water convection was restricted to the center of the subpolar gyre. However, Oppo & Lehman (1995) postulate that NADW production was already weak prior to Heinrich events H2, 3, and 4 and that there was no additional weakening in response to the massive iceberg discharge. Although still part of scientific debate, it turns out that the Heinrich events are not only in phase with the air temperature above Greenland (Bond *et al.*, 1993) but that corresponding events left worldwide traces (e.g. Broecker, 1996, 1994; Porter & An-Zhisheng, 1995; see also Stein *et al.*, 1994; Goldschmidt, *this volume*).

Based on AMS ^{14}C and planktic $\delta^{18}O$ results, Sarnthein *et al.* (1992) dated the beginning of the last deglaciation at 14.7 kyBP peaking at 13.5 kyBP. A giant meltwater lens formed off northern Norway and cold water masses were conveyed south, whereas the influx of temperate waters into the Norwegian-Greenland Sea across the Denmark Strait persisted since the LGM (Sarnthein & Altenbach, 1995). During the recovery from the LGM, this unusual current regime in the Norwegian-Greenland Sea caused a decrease or even shutdown of the NADW production (e.g. Jansen & Veum, 1990; Keigwin & Lehman, 1994; Seidov *et al.*, 1996; Seidov & Haupt, 1997). As a result, the Oldest Dryas (equivalent to H1) cold spell forced the climate system back towards late glacial conditions at around 14.5 kyBP; $\delta^{13}C$ values of planktic foraminifers indicate the lowest NADW production rate of the past 20 ky (Keigwin & Lehman, 1994). However, insolation increased rapidly; thus, the Oldest Dryas soon saw another reorganization of water mass circulation in the North Atlantic that eventually brought the Bølling warm period at glacial Termination I_A. The maximum melting of the Fennoscandian icesheet has been dated at around 12.5 kyBP, the peak warm phase during the Bølling (Andersen *et al.*, 1995). Koç Karpuz and Jansen (1992), working on diatom SST transfer functions of high resolution cores from the southwestern Norwegian shelf, were able to distinguish a series of short-term climate episodes within the period of the meltwater peak that characterizes Termination I_A.

Still within the Allerød warm interval, around 11.2 kyBP, calculated SSTs suggest that Polar and Arctic fronts in the northern North Atlantic rapidly readvanced to near-glacial conditions. Sea surface temperatures may have dropped as rapidly by more than 6° C as the air temperatures over Greenland did (Dansgaard *et al.*, 1989; Koç Karpuz & Jansen, 1992; Lehman & Keigwin, 1992; see also Costello & Bauch, *this volume*). Sea ice drifted as far south as to the latitudes of northern Spain (Keigwin & Lehman, 1994) during the most recent extreme cooling episode of the Younger Dryas (11.2-10.2 kyBP after Koç Karpuz & Jansen, 1992). Despite the enormous impact, the role of the North Atlantic during the Younger Dryas cold spell remains enigmatic: stable isotope data suggest a regular Holocene-style meridional circulation regime, however, with SST's indicating strong seasonality of the sea ice cover (Sarnthein *et al.*, 1995) that ceased in the course of the Holocene. Around 8.5 kyBP the end of iceberg drifting in the Norwegian Sea that is suggested by disappearing IRD deposits (Bauch & Weinelt, *in press*) heralds the begin of the Holocene climate optimum (Hypsithermal) (see also Nesje & Dahl, 1993) after a few centuries of slightly dropped sea surface temperatures (Younger Dryas II, Koç-Karpuz & Jansen, 1992; Koç *et al.*, 1996). Around this time, the English Channel was already open and a powerful current system that includes the Jutland and Norwegian Coastal Currents established itself in the North Sea (e.g. Stabell & Thiede, 1985). The interplay between eustasy and isostasy in the course of the Holocene lead to marine and freshwater stages of the Baltic Sea, which may have had impact on the oceanography of the northeastern North Atlantic (Bauch & Weinelt, *in press*; see also Bergsten & Nordberg, 1992). The Skager-

rak, which forms the gateway between the Baltic Sea and the North Atlantic, proved to be a high resolution archive of Holocene climate fluctuations (e.g. Stabell & Thiede, 1985; Conradsen & Heier-Nielsen, 1995; Hass, 1996, *this volume*). Periods such as the Little Ice Age (ca. 1350-1900 AD) are characterized by wind forced-fluctuations in current strengths (Hass & Kaminski, 1994).

Regarding the large scale oceanographic patterns, no exceptional longer term paleoceanographic changes occurred during the past 10,000 years in the northern North Atlantic. Moderate climate fluctuations are recorded mainly in shelf sediments (e.g. Stabell & Thiede, 1985) because limited temporal resolution mostly prevents the accurate dating of short-term oceanographic and climatic events in sediment cores from the deep sea. During the Holocene - like today - water mass circulation in the North Atlantic is characterized by the Gulf Stream that forms the northern part of the Subtropical Gyre. Towards the northeast, it forms the southern part of the Subpolar Gyre as the North Atlantic Current. It passes Scotland and eventually meets the Norwegian Coastal Current, which adds North Sea water masses, reducing its salinity from 35.1-35.3 PSU to <34.7 PSU (Johannessen, 1986). Providing heat and moisture to Europe, this current continues further northward as the Norwegian Current. Through cooling and evaporation, these northbound water masses gain density; eventually portions sink and form NADW in the Greenland and Iceland Seas, thus fuelling the Ocean Conveyor that links the oceans of the world (e.g. Veum *et al.*, 1992). Meridionally separated from Atlantic water masses by the Arctic Front, the East Greenland Current conveys cold Arctic water masses south along Greenland's coastline.

ACKNOWLEDGEMENTS

This paper was meant to be a short introduction to the topics that are addressed by the authors contributing to this book. It took me a while to figure out that it is kind of impossible to even produce a snap-shot of the state-of-the-art of a scientific field that is so lively discussed as is the paleoceanography of the North Atlantic. Thus, snowed under papers, journals, and books I decided to finally give up although knowing quite well that there are still important papers left to add. I tried to take any care not to misrepresent conclusions drawn in the various papers referred to in this introduction. If I did anyway in the heat of finishing this book I apologize herewith.

I would like to thank Ralf Tiedemann, Simon Jung and Martin Antonow for providing data for Figure 3, and Mara Weinelt, Bernd Haupt, Henning Bauch, Jens Matthiessen, Peter Goldschmidt, Mike Kaminski and a number of colleagues for fruitfull discussion and help.

This is contribution no. 320 of the Sonderforschungsbereich 313 (Special Research Project 313) of the University of Kiel.

REFERENCES

Aksu, A.E. & Hiscott, R.N. 1992. Shingled Quaternary debris flow lenses on the north-east Newfoundland Slope. *Sedimentology*, **39**, 193-206.

Andersen, E.S., Ostmo, S.R., Forsberg, C.F. & Lehman, S.J. 1995. Late- and post-glacial depositional environments in the Norwegian Trench, northern North Sea. *Boreas*, **24**, 47-64.

Andersen, M.S. & Boldreel, L.O. 1995. Effect of Eocene-Miocene compression structures on bottom-water currents in the Faeroe-Rockall area. *In*: Scrutton, R.A., Stoker, M.S., Shimmield, G.B. & Tudhope, A.W. (eds.), *The tectonics sedimentation and Palaeoceanography of the North Atlantic region*, **Vol. 90**, 141-143, Geological Society London.

Anderton, R. 1993. Sedimentation and basin evolution in the Paleogene of the northern North Sea and Faeroe-Shetland Basins. *In*: Parker, J.R. (ed.), *Petroleum Geology of northwest Europe: Proceedings of the 4th conference*, 31, Geological Society London.

Antonow, M., Goldschmidt, P. & Erlenkeuser, H. *this volume*. The climate-sensitive Vesterisbanken area (central Greenland Sea): depositional environment and paleoceanography during the past 250,000 years.

Antonow, M. 1995. Sedimentationsmuster um den Vesteris Seamount (zentrale Grönlandsee) in den letzten 250.000 Jahren. *Geomar Report*, **44**, 1-121.

Bard, E., Rostek, F. & Sonzogni, C. 1997. Interhemispheric synchrony of the last deglaciation inferred from alkenone palaeothermometry. *Nature*, **385**, 707-710.

Bauch, H.A. *this volume*. Paleoceanography of the North Atlantic Ocean (68-76°N) during the past 450 ky deduced from planktic foraminiferal assemblages and stable isotopes.

Bauch, H.A. & Weinelt, M.S. 1997. Surface water changes in the Norwegian Sea during last deglacial and Holocene times. *Quaternary Science Reviews, in press.*

Baumann, K.-H., Andruleit, H., Schröder-Ritzrau, A. & Samtleben, C. *this volume*. Spatial and temporal dynamics of coccolithophore communities during low production phases in the Norwegian-Greenland Sea.

Baumgartner, P.O. 1983. Summary of middle Jurassic-early Cretaceous radiolarian biostratigraphy of Site 534 (Blake-Bahama Basin) and correlations to the Tethyan sections. *Initial Reports of the Deep Sea Drilling Project*, **76**, 569-571.

Beck, J.W., Récy, J., Taylor, F., Edwards, R.L. & Cabloch, G. 1997. Abrupt changes in early Holocene tropical sea surface temperature derived from coral records. *Nature*, **385**, 705-707.

Berger, W.H. & Jansen, E. 1994. Mid-Pleistocene climate shift - the Nansen connection. *Geophysical Monograph*, **84**, 295-311.

Berggren, W.A. & Schnitker, D. 1983. Cenozoic marine environments in the North Atlantic and Norwegian-Greenland Sea. *In*: Bott, M.H.P., Saxov, S., Talwani, M. & Thiede, J. (eds.) *Structure and development of the Greenland-Scotland Ridge; new methods and concepts. IV. Marine Sciences*, **Vol. 8**, 495-548, Univ. Durham, Durham, United-Kingdom. NATO Conference Series.

Bergsten, H. & Nordberg, K. 1992. Late Weichselian marine stratigraphy of the southern Kattegat, Scandi-

navia: evidence for drainage of the Baltic Ice Lake between 12,700 and 10,300 years B.P. *Boreas*, **21**, 223-252.

Bond, G., Broecker, W.S., McManus, J., Labeyrie, L., Jouzel, J. & Bonani, G. 1993. Correlations between climate records from North Atlantic sediments and Greenland ice. *Nature*, **365**, 143-147.

Bond, G., Heinrich, H., Huon, S., Broecker, W.S., Labeyrie, L., Andrews, J., McManus, J., Clasen, S., Tedesco, K., Jantschik, R., Simet, C. & Klas, M. 1992. Evidence for massive discharge of icebergs into the glacial North Atlantic. *Nature*, **360**, 245-249.

Bott, M.H.P., Saxov, S., Talwani, M. & Thiede, J. (eds.) 1983. *Structure and development of the Greenland-Scotland Ridge; new concepts and methods*. NATO Conference Series IV, 685 pp., Plenum Press, New York.

Boyle, E.A. & Keigwin, L. 1987. North Atlantic thermohaline circulation during the past 20,000 years linked to high-latitude surface temperature. *Nature*, **330**, 35-40.

Bralower, T.J. & Thierstein, H.R. 1986. Organic carbon and metal accumulation in Holocene and mid-Cretaceous marine sediments: paleoceanographic significance. *In*: Brooks, J. & Fleet, A. (eds.), *Marine petroleum source rocks*, **Vol. 26**, 345-369, Blackwell Scientific Publishers, Geological Society Special Publication.

Broecker, W.S., Bond, G., Klas, M., Clark, E. & McManus, J. 1992. Origin of the northern Atlantic's Heinrich events. *Climate Dynamics*, **6**, 91-109.

Broecker, W.S. 1987. The biggest chill. *Natural History*, **10**, 74-82.

Broecker, W.S. 1991. The great ocean conveyor. *Oceanography*, **4**, 79-89.

Broecker, W.S. 1994. Massive ice berg discharge as triggers for global climate change. *Nature*, **372**, 421-424.

Broecker, W.S. 1996. Glacial cooling: is water vapour the villain? *EOS*, **77 (19)**, 283.

Broecker, W.S. & Denton, G.H. 1990. The role of ocean-atmosphere reorganizations in glacial cycles. *Quaternary Science Reviews*, **9**, 305-341.

Clark, D.L. 1982. Origin, nature and world climate effect of Arctic Ocean ice-cover. *Nature*, **300**, 321-325.

CLIMAP Project Members 1976. The surface of the ice-age earth. *Science*, **191**, 1131-1137.

CLIMAP Project Members 1981. Seasonal reconstructions of the earth's surface at the last glacial maximum. *Geological Society America*, GSA Map Chart Series MC-36, Boulder, Colorado.

CLIMAP Project Members 1984. The last interglacial ocean. *Quaternary Research*, **21**, 123-224.

Conradsen, K. & Heier-Nielsen, S. 1995. Holocene paleoceanography and paleoenvironments of the Skagerrak-Kattegat, Scandinavia. *Paleoceanography*, **10**, 801-813.

Costello, O.P. & Bauch, H.A. *this volume*. Late Pleistocene-Holocene productivity record of benthic foraminifera from the Iceland Plateau (Core PS1246-2).

Curry, W. B. & Oppo, D.W. 1997. Synchronous high-frequency oscillations in tropical sea surface temperatures and North Atlantic Deep Water production during the last glacial cycle. *Paleoceanography*, **12**, 1-14.

Dansgaard, W., Johnson, S.J., Clausen, H., Dahl-Jensen, D., Gundestrup, N.S., Hammer, C.U., Hvidberg, C.S., Steffensen, J.P., Sveinbjörnsdotir, A.E., Jouzel, J. & Bond, G. 1993. Evidence for general instability of past climate from a 250-kyr ice-core record. *Nature*, **364**, 218-220.

Dansgaard, W.J., White, W.C. & Johnson, S.J. 1989. The abrupt termination of the Younger Dryas climate event. *Nature*, **339**, 532-533.

Ebdon, C.C., Granger, P.J., Johnson, H.D. & Evans, A.M. 1995. Early Tertiary evolution and sequence stratigraphy of the Faeroe-Shetland Basin: implications for hydrocarbon prospectivity. *In*: Scrutton, R.A., Stoker, M.S., Shimmield, G.B. & Tudhope, A.W. (eds.), *The tectonics, sedimentation and palaeoceanography of the North Atlantic region*, **Vol. 90**, 51-69, Geological Society London.

Eldholm, O., Thiede, J. & Taylor, E. 1987. Evolution of the Norwegian continental margin: background and objectives. *Proceedings of the Ocean Drilling Program Part A- Initial Reports*, **104**, 5-25.

Elverhøi, A. 1992. A presentation of the ESF PONAM Programme: a study of the last 5 million years of the Norwegian-Greenland Sea and its margins. *Oceanology International 92, abstract volume*, Brighton, UK.

Frakes, L.A. 1986. Mesozoic-Cenozoic climatic history and causes of the glaciation. *In*: Hsü, K.J. (ed.), *Mesozoic and Cenozoic oceans*, **Vol. 15**, 33-48, AGU, GSA.

Fronval, T. & Jansen, E. 1996. Late Neogene paleoclimates and paleoceanography in the Iceland-Norwegian Sea: Evidence from the Iceland and Vøring Plateaus. *Proceedings of the Ocean Drilling Program, Scientific Results*, **151**, 455-468.

Goldschmidt, P.M. *this volume*. The ice-rafting history of coarse-grained sediments in the Norwegian-Greenland Sea for the last two glacial/interglacial cycles.

Graedel, T.E. & Crutzen, P.J. 1993. *Atmospheric Change*, 446 pp., W.H. Freeman and Company, New York.

GRIP Members 1993. Climate instability during the last interglacial period recorded in the Grip ice core. *Nature*, **364**, 203-207.

Grootes, P.M., Stuiver, M., White, J.W.C., Johnsen, S. & Jouzel, J. 1993. Comparison of oxygen isotope records from the GISP2 and GRIP Greenland ice cores. *Nature*, **366**, 552-554.

Grousset, F.E., Labeyrie, L., Sinko, J.A., Cremer, M., Bond, G., Duprat, J., Cortijo, E. & Huon, S. 1993. Patterns of ice-rafted detritus in the North Atlantic (40-55° N). *Paleoceanography*, **8**, 175-92.

Hallam, A. 1986. Role of climate affecting late Jurassic and early Cretaceous sedimentation in the North Atlantic. *In*: Summerhayes, C.P. & Shackleton, N.J. (eds.), *North Atlantic Paleoceanography*, **Vol. 21**, 277-282, Blackwell Scientific Publishers.

Hass, H.C. 1996. Northern Europe climate variations during late Holocene: evidence from marine Skagerrak. *Palaeogeography, Palaeoclimatology, Palaeoecology*, **123**, 121-145.

Hass, H.C. *this volume*. The benthic foraminiferal response to late Holocene climate change over northern Europe.

Hass, H.C. & Kaminski, M.A. 1994. Change in atmospheric and ocean circulation reflected in North Sea sediments during late Holocene. *Zentralblatt für Geologie und Paläontologie Teil I*, **1/2**, 51-65.

Heinrich, H. 1988. Origin and consequences of cyclic icerafting in the northeast Atlantic Ocean during the past 130,000 years. *Quaternary Research*, **29**, 143-152.

Henrich, R. 1990. Cycles, rhythms and events in Arctic and Antarctic glaciomarine deposits. *In*: Bleil, U. & Thiede, J. (eds.), *Geological history of the polar oceans. Arctic versus Antarctic*, NATO ASI Series, **C 308**, 213-244, Kluwer.

Henrich, R. (1992) Beckenanalyse des Europäischen Nordmeeres: Pelagische und glaziomarine Sedimentflüsse im Zeitraum 2,6 Ma bis rezent. Unpubl. habil. thesis, Math.-Nat. Fak. Universität Kiel.

Henrich, R., Wagner, T., Goldschmidt, P. & Michels, K.

1995. Depositional regimes in the Norwegian-Greenland Sea: the last two glacial to interglacial transitions. *Geologische Rundschau*, **84**, 28-48.

Hodell, D.A., Elmstrom, K.M. & Kennett, J.P. 1986. Latest Miocene benthic delta (super 18) O changes, global ice volume, sea level and the „Messinian salinity crisis". *Nature*, **320**, 411-414.

Jansen, E. & Veum, T. 1990. Evidence for two-step deglaciation and its impact on North Atlantic deep water circulation. *Nature*, **343**, 612-616.

Jenkyns, H.C. 1994. Early history of the oceans. *Oceanus*, **36**, 49-52.

Joppen, M. & White, R.S. 1990. The structure and subsidence of Rockall trough from two-ship experiments. *Journal of Geophysical Research*, **95**, 19,821-19,837.

Johannessen, O.M. 1986. Brief overview of the physical oceanography. *In:* Hurdle, B.G. (ed.), *The Nordic Seas*, 103-127, Springer-Verlag.

Jung, S. 1996. Wassermassenaustausch zwischen NE-Atlantik und Nordmeer während der letzten 300.000/80.000 Jahre im Abbild stabiler O- und C-Isotope. *Berichte aus dem Sonderforschungsbereich 313*, **61**, 1-104.

Kaminski, M.A., Gradstein, F.M., Goll, R.M., & Grieg, D. 1990. Biostratigraphy and paleoecology of deep-water agglutinated foraminifera at ODP Ste 643, Norwegian-Greenland Sea. *In:* Hemleben, C., Kaminski, M.A., Kuhnt, W., and Scott, D.B. (eds.), *Paleoecology, Biostratigraphy, Paleoceanography and Taxonomy of Agglutinated Foraminifera*, NATO ASI Series, Kluwer Acad. Publ. 345-386.

Kastens, K.A. 1992. Did glacio-eustatic sea level drop trigger the Messinian salinity crisis? New evidence from Ocean Drilling Program Site 654 in the Tyrrhenian Sea. *Paleoceanography*, **7**, 333-356.

Keigwin, L.D., Jones, G.A., Lehman, S.J. & Boyle, E.A. 1991. Deglacial meltwater discharge, North Atlantic deep circulation, and abrupt climate change. *Journal of Geophysical Research*, **96**, 16,811-16,826.

Keigwin, L.D., Curry, W.B., Lehmann, S.J. & Johnsen, S. 1994. The role of the deep ocean in North Atlantic climate change between 70 and 130 kyr ago. *Nature*, **371**, 323-326.

Keigwin, L.D. & Lehmann, S.J. 1994. Deep circulation change linked to HEINRICH event 1 and Younger Dryas in a middepth North Atlantic core. *Paleoceanography*, **9**, 185-194.

Keller, C., Zenker, C.E. & Stone, S.M. 1989. Late Neogene history of the Pacific-Caribbean gateway. *Journal of South American Earth Sciences*, **2**, 73-108.

Kennett, J. 1982. *Marine Geology*, 813 pp., Prentice-Hall Inc.

Koç-Karpuz, N. & Jansen, E. 1992. A high resolution diatom record of the last deglaciation from the SE Norwegian Sea: Documentation of rapid climatic changes. *Paleoceanography*, **7**, 499-520.

Koç, N., Jansen, E., Hald, M. & Labeyrie, L.D. 1996. Late glacial-Holocene sea surface temperatures and gradients between the North Atlantic and the Norwegian Sea: implications for the Nordic heat pump. *In:* Andrews, J.T., Austin, W.E.N., Bergsten, H. & Jennings, A.E. (eds.), *Late Quaternary Palaeoceanography of the Atlantic Margins*, 177-185, Geological Society Special Publication, **Vol. 111**.

Lehman, S.J., Jones, G.A., Keigwin, L.D., Andersen, E.S., Butenko, G. & Østmo, S.-R. 1991. Initiation of Fennoscandian ice-sheet retreat during the last deglaciation. *Nature*, **349**, 513-516.

Lehman, S.J. & Keigwin, L.D. 1992. Sudden changes in North Atlantic circulation during the last deglaciation. *Nature*, **356**, 757-762.

MacAyeal, D.R. & Wang, H.-L. 1992. A glaciological throttle on freshwater input to the North Atlantic Ocean during glacial climates. *EOS* (supplement to Fall Meeting), **73**, 158.

Maslin, M.A., Haug, G.H., Sarnthein, M., Tiedemann, R., Erlenkeuser, H. & Stax, R. 1995. Northwest Pacific Site 882: The initiation of northern hemisphere glaciation. *Proceedings of the Ocean Drilling Program, Scientific Results*, **145**, 315-327.

Maslin, M.A. 1996. Sultry last interglacial gets sudden chill. *EOS*, **77**, 353-354.

Maslin, M.A., Shackleton, N.J. & Pflaumann, U. 1995b. Surface water temperature, salinity, and density changes in the northeast Atlantic during the last 45,000 years: Heinrich events, deep water formation, and climatic rebounds. *Paleoceanography*, **10**, 527-544.

Martinson, D.G., Pisias, N.G., Hays, J.D., Imbrie, J., Moore, T. C. & Shackleton, N.J. 1987. Age dating and the orbital theory of the ice ages: development of a high-resolution 0 to 300,000-year chronostratigraphy. *Quaternary Research*, **27**, 1-29.

Mikolajewicz, U., Maier-Reimer, E., Crowley, T. J. & Kim, K.-Y. 1993. Effect of Drake and Panamanian gateways on the circulation of an ocean model. *Paleoceanography*, **8**, 409-426.

Myhre, A.M., Eldholm, O. & Sundvor, E. 1982. The margin between Senja and Spitsbergen Fracture Zones: implications from plate tectonics. *Tectonophysics*, **89**, 33-50.

Myhre, A.M. & Thiede, J. 1995. North Atlantic-Arctic gateways. *Proceedings of the Ocean Drilling Program Part A- Initial Reports*, **151**, 5-26.

Nesje, A. & Dahl, S. 1993. Lateglacial and Holocene glacier fluctuations and climate variations in western Norway: A review. *Quaternary Science Reviews*, **12**, 255-261.

Nunns, A.G. & Peacock, J.H. 1982. Correlation, indentification and inversion of magnetic anomalies in the Norway Basin. *In:* Warnke, D.A. & Vogel, A. (eds.), *The structure, evolution and present geodynamics of the Norwegian-Greenland Sea*, 130-138, Earth Evolution Sciences, **Vol. 2**.

Oppo, D.W. & Lehmann, S.J. 1995. Suborbital timescale variability of North Atlantic deep water during the past 200 000 years. *Paleoceanography*, **10**, 901-910.

Piper, D.J.W., Mudie, P.J., Josenhans, H.W., MacLean, B. & Vilks, G. 1990. Quaternary geology. *In:* Keen, M.J. & Williams, G.L. (eds.), *Geology of the continental margin of eastern Canada*, **Vol. 2**, 475-607, Geological Survey of Canada.

Pittman, W.C.I. 1978. Relationship between eustatic and stratigraphic sequences of passive margins. *Bulletin of the American Geological Society*, **89**, 1389-1403.

Porter, S.C. & An-Zhisheng 1995. Correlation between climate events in the North Atlantic and China during the last glaciation. *Nature*, **375**, 305-308.

Premoli Silva, I. & Boersma, A. 1977. Cretaceous planktic foraminifers - DSDP Leg 39 (South Atlantic). *Initial Reports of the Deep Sea Drilling Project*, **39**, 615-641.

Pisias, N.G., Martinson, N.G., Moore, T.C., Shackleton, N.J., Prell, W., Hays, J. & Boden, G. 1984. High resolution stratigraphic correlation of benthic oxygen isotopic records spanning the last 300,000 years. *Marine Geology*, **56**, 119-136.

Rahmstorf, S. 1994. Rapid climate transitions in a coupled ocean-atmosphere model. *Nature*, **372**, 82.

Rahmstorf, S. 1996. What drives the Atlantic conveyor belt? *EOS (suppl.)*, **77**, 19.

Repenning, C.A., Brouwers, E.M., Carter, L.D., Marincovitch, L. & Ager, T.A. 1987. The Beringian ancestry of *Phenacomys* (Rodentia: Cricetidae) and the beginning of the modern Arctic Ocean borderland biota. *U.S. Geological Survey Bulletin*, **1687**, 1-28.

Robertson, A.H.F. & Ogg, J.G. 1986. Palaeoceanographic setting of the Callovian North Atlantic. *In*: Summerhayes, C.P. & Shackleton, N.J. (eds.), *North Atlantic Paleoceanography*, **Vol. 21**, 283-293, Blackwell Scientific Publishers.

Robinson, S.G., Maslin, M.A. & McCave, I.N. 1995. Magnetic susceptibility variations in Upper Pleistocene deep-sea sediments of the NE Atlantic: implications for ice rafting and palaeocirculation at the last glacial maximum. *Paleoceanography*, **10**, 221-250.

Roth, H.R. 1986. Mesozoic palaeoceanography of the North Atlantic and Tethys Oceans. *In*: Summerhayes, C.P. & Shackleton, N.J. (eds.), *North Atlantic Paleoceanography*, **Vol. 21**, 299-320, Blackwell Scientific Publishers.

Roth, P.H. & Krumbach, K.R. 1986. Middle Cretaceous calcareous nannofossil biogeography and preservation in the Atlantic and Indian Oceans. *Marine Micropaleontology* **10**, 235-266.

Ruddiman, W.F. & McIntyre, A. 1976. Northeast Atlantic paleoclimatic changes over the last 600,000 years. *Geological Society of America Memoir*, **145**, 111-146.

Ruddiman, W.F. & McIntyre, A. 1981. The North Atlantic Ocean during the Last Deglaciation. *Palaeogeography, Palaeoclimatology, Palaeoecology*, **35**, 145-214.

Saltzman, E.S. & Barron, E.J. 1982. Deep circulation in the late Cretaceous: oxygen isotope paleotemperatures from Inoceramus remains in DSDP cores. *Palaeogeography, Palaeoclimatology, Palaeoecology*, **40**, 167-181.

Sarnthein, M. & Altenbach, A.V. 1995. Late Quaternary changes in surface water masses of the Nordic Seas and north-eastern North Atlantic. *Geologische Rundschau*, **84**, 89-107.

Sarnthein, M. & Tiedemann, R. 1989. Toward a high resolution stable isotope stratigraphy of the last 3.4 million years: sites 658 and 659 off northwest Africa. *Proceedings of the Ocean Drilling Program, Scientific Results*, **108**, 167-158.

Sarnthein, M., Jansen, E., Arnold, M., Duplessy, J.-C., Erlenkeuser, H., Flatøy, A., Veum, T., Vogelsang, E. & Weinelt, M.S. 1992. $\delta^{18}O$ Time-slice reconstruction of meltwater anomalies at Termination I in the North Atlantic between 50° and 80° N. *In*: Bard, E. & Broekker, W. S. (eds.), *NATO ASI Series*, **Vol. 12**, 183-200, Springer Verlag.

Sarnthein, M., Jansen, E., Weinelt, M., Arnold, M., Duplessy, J.C., Erlenkeuser, H., Flatøy, A., Johannessen, G., Johannessen, T., Jung, S., Koç, N., Labeyrie, L., Maslin, M., Pflaumann, U. & Schulz, H. 1995. Variations in Atlantic surface ocean paleoceanography, 50-80°N: A time slice record of the last 30,000 years. *Paleoceanography*, **10**, 1063-1094.

Sarnthein, M., Winn, K., Jung, S.J.A., Duplessy, J.-C., Labeyrie, L., Erlenkeuser, H. & Ganssen, G. 1994. Change in east Atlantic deepwater circulation over the last 30,000 years: Eight time slice reconstructions. *Paleoceanography*, **9**, 209-267.

Schnitker, D. 1980. Quaternary deep-sea benthic foraminifers and bottom water masses. *Annual Review of Earth and Planetary Sciences*, **8**, 343-370.

Scrutton, R.A., Stoker, M.S., Shimmield, G.B. & Tudhope, A.W. 1995. *The tectonics, sedimentation and palaeoceanography of the North Atlantic region*, **Vol. 90**, Geological Society London.

Seidov, D. & Haupt, B.J. 1997. Simulated ocean circulation and sediment transport in the North Atlantic during the last glacial maximum and today. *Paleoceanography*, **12**, 281-305.

Seidov, D., Sarnthein, M., Stattegger, K., Prien, R. & Weinelt, M. 1996. North Atlantic Ocean circulation during the last glacial maximum and subsequent meltwater event: A numerical model. *Journal of Geophysical Research*, **101**, 16,305-16,332.

Shackleton, N.J., Backman, J., Zimmermann, H., Kent, D.V., Hall, M.A., Roberts, D.G., Schnitker, D., Baldauf, J.G., Desprairies, A., Homrighausen, R., Huddlestun, P., Keene, J.B., Kaltenback, A.J., Krumsiek, K.A.O., Morton, A.C., Murray, J.W. & Westberg-Smith, J. 1984. Oxygen isotope calibration of the onset of ice-rafting and history of glaciation in the North Atlantic region. *Nature*, **307**, 620-623.

Sheridan, R.E. 1986. Pulsation tectonics as the control of North Atlantic paleoceanography. *In*: Summerhayes, C.P. & Shackleton, N.J. (eds.), *North Atlantic Paleoceanography*, **Vol. 21**, 255-275, Blackwell Scientific Publishers.

Srivastava, S.P. 1978. Evolution of the Labrador Sea and its bearing on the early evolution of the North Atlantic. *Geophysical Journal of the Royal Astronomical Society*, **52**, 313-357.

Srivastava, S.P. & Shipboard Scientific Party 1987. Introduction. *Proceedings of the Ocean Drilling Program Part A - Initial Reports*, **105**, 5-20.

Stabell, B. & Thiede, J. (1985) Upper Quaternary marine Skagerrak (NE North Sea) deposits; stratigraphy and depositional environment. *Norsk Geologisk Tidsskrift*, **65**, 1-149.

Stoker, M.S. 1995. The influence of glacigenic sedimentation on slope-apron development on the continental margin off Northwest Britain. *In*: Scrutton, R.A., Stoker, M.S., Shimmield, G.B. & Tudhope, A.W. (eds.), *The tectonics sedimentation and Palaeoceanography of the North Atlantic region*, 159-177, Geological Society Special Publication, **Vol. 90**.

Stein, R., Nam, S.-I., Grobe, H. & Hubberten, H. 1996. Late Quaternary glacial history and short-term ice-rafted debris fluctuations along the East Greenland continental margin. *In:* Andrews, J.T., Austin, W.E.N., Bergsten, H. & Jennings, A.E. (eds.), *Late Quaternary Palaeoceanography of the Atlantic Margins*, 135-152, Geological Society Special Publication, **Vol. 111**.

Stein, R., Nam, S.-I., Schubert, C., Vogt, C., Fütterer, D. & Heinemeier, J. 1994. The last deglaciation event in the eastern Central Arctic Ocean. *Science*, **264**, 692-696.

Sy, A., Rhein, M., Lazler, J.R.N., Koltermann, K.P., Meincke, J., Putzka, A. & Bersch, M. 1997. Surprisingly rapid spreading of newly formed intermediate waters across the North Atlantic Ocean. *Nature*, **386**, 375-379.

Tiedemann, R., Sarnthein, M. & Shackleton, N.J. 1994. Astronomic timescale for the Pliocene Atlantic $\delta^{18}O$ and dust flux records of Ocean Drilling Program site 659. *Paleoceanography*, **9**, 619-638.

Thiede, J. 1979. Paleogeography and paleobathymetry of the Mesozoic and Cenozoic North Atlantic. *Geojournal*, **3**, 263-272.

Thiede, J. & Myhre, A.M. 1996. The paleoceanographic history of the North Atlantic-Arctic gateways: Synthesis of the Leg 151 Drilling Results. *Proceedings of the Ocean Drilling Program, Scientific Results*, **151**, 645-658.

Veum, T., Jansen, E., Arnoldt, M., Beyer, I. & Duplessy, J.-

C. 1992. Water mass exchange between the North Atlantic and the Norwegian Sea during the past 28.000 years. *Nature*, **356**, 783-785.

Vorren, T.O., Richardsen, G., Knutsen, S.M. & Henriksen, E. 1991. Cenozoic erosion and sedimentation in the western Barents Sea. *Marine Petroleum Geology*, **8**, 317-340.

Webb, R.S., Rind, D.H., Lehman, S.J., Healy, R.J. & Sigman, D. 1997. Influence of ocean heat transport on the climate of the Last Glacial Maximum. *Nature*, **385**, 695-699.

Weijermars, R. 1988. Neogene tectonics in the western Mediterranean may have caused the Messinian salinity crisis and an associated glacial event. *Tectonophysics*, **148**, 211-219.

Weinelt, M., Sarnthein, M., Pflaumann, U., Schulz, H., Jung, S. & Erlenkeuser, H. 1996. Ice-free Nordic Seas during the last Glacial Maximum? Potential sites of deepwater formation. *Palaeoclimates*, **1**, 283-309.

White, R.S. 1988. A hot-spot model for early Tertiary volcanism in the N. Atlantic. *In*: Morton, A.C. & Parson, L.M. (eds.), *Early Tertiary volcanism and the opening of the North Atlantic*, 3-13, Geological Society Special Publication, **Vol. 39**.

Wolf, T.C.W. & Thiede, J. 1991. History of terrigenous sedimentation during the past 10 m.y. in the North Atlantic (ODP Legs 104, 105 and DSDP 81). *Marine Geology*, **101**, 83-102.

Wolf-Welling, T.C.W., Cremer, M., O'Connel, S., Winkler, A. & Thiede, J. 1996. Cenozoic Arctic gateway paleoclimate variability: Indications from changes in coarse-fraction composition. *Proceedings of the Ocean Drilling Program, Scientific Results*, **151**, 515-525.

Wright, J.D. & Miller, K.G. 1996. Control of North Atlantic deep water circulation by the Greenland-Scotland Ridge. *Paleoceanography*, **11**, 157-170.

Zahn, R. 1994. Fast flickers in the tropics. *Nature*, **372**, 621-622.

Ziegler, P.A. 1975. Geologic evolution of the North Sea and its tectonic frame work. *AAPG Memoir*, **59**, 1073-1097.

Ziegler, P.A. 1979. Geology and hydrocarbon provinces of the North Sea. *Geojournal*, **1**, 7-31.

Ziegler, P.A. & van Hoorn, B. 1989. Evolution of the North Sea rift system. *In*: Tankard, A.J. & Balkwill, H.R. (eds.), *Extensional tectonics and stratigraphy of the North Atlantic margins*, AAPG Memoir, **Vol. 46**, 111-130, American Assossiation of Petroleum Geologists/Canadian Geological Foundation.

Foraminiferal, palynomorph, and diatom biostratigraphy and paleoenvironments of the Torsk Formation: A reference section for the Paleocene–Eocene transition in the western Barents Sea

JENÖ NAGY[1], MICHAEL A. KAMINSKI[2], KARI JOHNSEN[3] and ALEXANDER G. MITLEHNER[4]

1. Department of Geology, University of Oslo, P.O. Box 1047 Blindern, N-0316 Oslo, Norway
2. Research School of Geological and Geophysical Sciences, Birkbeck College and University College London, Gower Street, London, WCIE 6BT, U.K.
3. Saga Petroleum a.s., Kjörboveien 16, P.O. Box 496, N-1301, Norway
4. Department of Geography, Edinburgh University, Drummond Street, Edinburgh, EH8 9XP, U.K.

ABSTRACT

A microfossil-based biostratigraphic reference section is selected for the Paleogene Torsk Formation in the 7119/9-1 well, located in the Tromsø Basin of the southwestern Barents Sea. Benthic foraminifera, dinoflagellate cysts, and diatom infillings indicate an early late Paleocene to early Eocene age for the Torsk Formation on the eastern flank of the basin. A comparison of benthic foraminiferal last occurrences in the reference section with that established in neighbouring wells illustrates the potential use of these events for high-resolution stratigraphic correlation. Though differing in detail, the record of microfossil last occurrences in the western Barents Sea compares well with the biostratigraphy of the Central North Sea area. A morphogroup analysis of the Paleogene foraminiferal succession of the Tromsø Basin reveals a bathymetric deepening of the depositional area culminating near the Paleocene-Eocene transition, followed by a shallowing.

INTRODUCTION

The Barents Sea covers a continental shelf area that is of a comparable size to the entire North Sea, but the subsurface geology of the area is constrained by fewer than 53 wells, mostly concentrated in the Hammerfest and Tromsø basins (Fig. 1). This area has been subjected to intense Mesozoic and Cenozoic tectonic movements that have affected the configuration of seaways linking the North Atlantic with the Arctic Ocean. Therefore, studies of the sedimentary and biotic record preserved in the Barents Sea basins are important for reconstructing the history of faunal connections between the North Atlantic and Arctic oceans, and constraining paleobiogeographic patterns in the Boreal Realm.

Reconstructing the development and history of marine connections through the Norwegian-Greenland Sea is the prime objective of the „Arctic Gateways" legs of the Ocean Drilling Program. As the oldest oceanic crust in the Norwegian Sea region is of early Eocene age, the early Paleogene biotic record can only be obtained from continental margin wells. Fortunately, Paleocene to Eocene sediments have been recovered from a number of exploratory wells drilled in the Tromsø and Hammerfest basins, off the northern coast of Norway. These basins are situated just east of the oceanic areas of the Norwegian-Greenland Sea, and constitute the northernmost offshore basins of the North Sea / Norwegian Sea rift system explored by conventional drilling. The main objective of this study is to assess the stratigraphic and paleoenvironmental significance of early Paleogene benthic foraminifera, dinoflagellate cysts, and diatoms from a key section in the western Barents Sea. This study is intended to complement the assessment of microfossil assemblages from younger Cenozoic material carried out under the auspices of the ODP „Arctic Gateways" initiative.

Among 12 wells that we have examined from

In: Hass, H.C. & Kaminski, M.A. (eds.) 1997. Contributions to the Micropaleontology and Paleoceanography of the Northern North Atlantic. *Grzybowski Foundation Special Publication*, no. 5, pp. 15-38

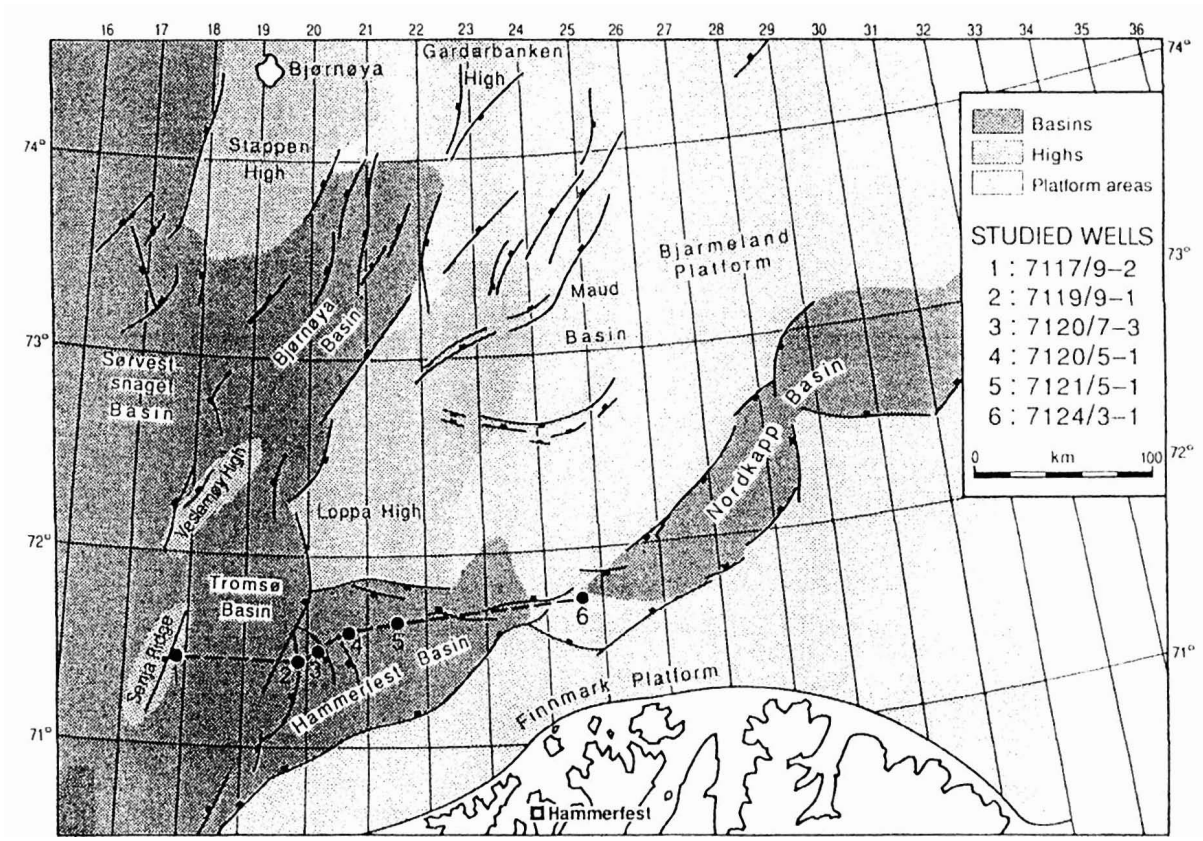


Figure 1. Location map of the western Barents Sea, with main structural features and locations of 6 of the studied wells.

the western Barents Sea area, well 7119/9-1 was chosen as a reference section because of the presence of a thick Paleogene succession (1030 m according to electric logs), rich microfossil assemblages, and the availability of continuous sampling. In addition, Knutsen *et al.* (1992) published a seismic line that crosses the well site and defined seismic units in this well, so it is now possible to more accurately assess the age and significance of regional seismic reflectors. Altogether, 129 ditch cutting samples were analysed from this well, with few exceptions spaced at 10 m intervals. The biostratigraphy from well 7119/9-1 is compared with data from nearby wells in the Hammerfest and Tromsø basins.

STUDY AREA

Geological Setting

The Barents Sea overlies an intracratonic area of structural basins, platforms, and highs. In the west, the area borders the oceanic Norwegian-Greenland Sea with a passive shear margin marked by the Senja Fracture Zone in the south and the Hornsund Fault Zone in the north. The Barents Sea margin started to develop in the early Paleogene in connection with the opening of the Norwegian-Greenland Sea, but the structural basins on the Barents Sea platform were formed as a result of earlier (Cretaceous to Paleocene) rifting phases.

The geology and structural development of the Barents Sea has been the subject of numerous studies published mainly after drilling in the area commenced in the early 1980's. The subsurface geology of the area based on seismic evidence has been discussed by Rønnevik (1981), Rønnevik & Jacobsen (1984), Roufosse (1987), and Faleide *et al.* (1993a,b). Recently, Riis (1992), Cloetingh *et al.* (1992), Walderhaug (1992), and Richardsen *et al.* (1993) have provided estimates of the amount of Cenozoic uplift and erosion in the western Barents Sea based on geophysical and petrophysical evidence. The early Cenozoic sedimentary history of the area has been discussed by Knutsen & Vorren (1991).

The area of this study is located in the southwestern part of the Barents Sea close to the continental margin. The region is divided into four main basins: Bjørnøya, Tromsø, Hammerfest, and Nordkapp, with intervening structural highs such as the Senja Ridge, Loppa High, and Veslemøy High (Fig. 1). The Tromsø Basin is connected with the Hammerfest Basin over the Ringvassoy-Loppa Fault

Complex. In an easterly direction, the Hammerfest basin is linked to the Nordkapp Basin over a shallow threshold on the southernmost extension of the Bjarmeland Platform. The reference well chosen was drilled on the eastern flank of the Tromsø Basin.

Stratigraphical Framework

The Mesozoic and Cenozoic lithostratigraphy of the western Barents Sea was formally outlined by Worsley *et al.* (1988). The Paleogene Torsk Formation has a rather monotonous lithology consisting of light grey to greenish grey, essentially non-calcareous claystones. Thin beds of siltstone or limestone occur rarely throughout the formation, and tuffaceous horizons are commonly reported in the lower part. The thickness of the formation varies from 200-300 m in wells drilled in marginal areas of the Hammerfest Basin, to over 1 km in the central parts of the basin. The formation thickens to over 2 km in the undrilled deepest parts of the Tromsø Basin.

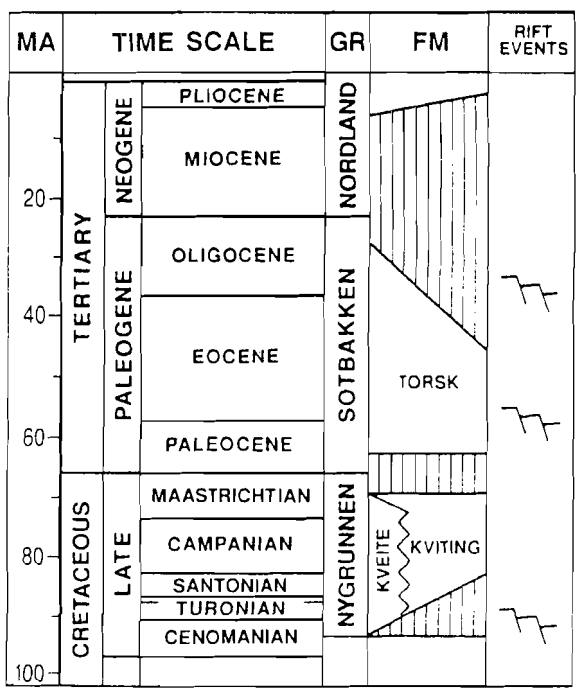


Figure 2 Lithostratigraphic scheme of Upper Cretaceous and Cenozoic deposits of the southwestern Barents Sea (modified after Worsley *et al.* (1988) and Faleide *et al.* (1993)).

The basal contact of the Torsk Formation is unconformable, and represents an important depositional hiatus encompassing the latest Cretaceous and early Paleocene (Fig. 2). This hiatus can be traced on seismic lines throughout the southwestern Barents Sea (Rønnevik, 1981; Faleide *et al.*, 1993a,b). The top of the Torsk Formation is cut by an erosional unconformity, and it is overlain by Plio-Pleistocene glacial and glacial-marine sediments.

Large areas of the Barents Shelf east of the Senja Ridge were uplifted and subjected to multiple phases of erosion, lasting to the early Pliocene. As a result, the upper parts of the Torsk Formation (as much as 1500 m) have been removed, particularly in marginal parts of the basins where the formation thickness is strongly reduced.

MATERIAL & METHODS

Well 7119/9-1 was a wildcat well drilled in the summer of 1984 at 71°24'53.19"N, and 19°49'43.26"E in 201 m of water, with Elf Aquitaine Norge a.s. acting as the operator. Samples for this micropaleontological study were provided by the Norwegian Petroleum Directorate in Stavanger. The material analysed consists wholly of washed ditch cutting samples ranging in dry weight from 25 to 45 grams. The micropaleontological samples were disintegrated by boiling in sodium carbonate, and washed over a 63µm sieve. Foraminifera and diatoms were picked from the >125µm fraction and mounted on cardboard slides. Palynological samples were analysed in accordance with standard techniques. All depths reported in this paper are quoted below rotary kelly bushing (therefore, a value of 226 m must be subtracted from the reported depth to convert to depth below sea floor).

RESULTS

The succession of palynomorphs, diatoms, and benthic foraminifera in the 7119/9-1 well can each be subdivided into distinct assemblages based on the distribution of dominant taxa, the occurrences of stratigraphically important species, and fluctuations in diversity and abundance (Fig. 3). The chronostratigraphy of the well is based primarily on palynomorph assemblages, which can be correlated with the zonations of the northern North Sea published by Schröder (1992) and Mudge & Bujak (1994, 1996).

a. Palynomorph assemblages

Altogether, 70 samples have been analysed for palynomorphs with a spacing of 10 m except in the upper 400 m of the well, where the sample spacing is mostly 30 m. The studied interval contains 99 palynomorph taxa, and their stratigraphical distribution is presented in Table 1. The palynomoph succession is subdivided into six stratigraphically significant assemblages (Fig. 3).

From the uppermost part of the formation (at 330 m), a single sample was analysed which contains a poor palynomorph assemblage. No age-dia-

gnostic species were recorded, and most of the palynomophs present are reworked from Cretaceous deposits, a feature that is typical of the Pliocene – Pleistocene deposits of the area. The palynomorph succession from the 7119/9-1 well is discussed below in order from youngest to oldest.

1. *Alisocysta* sp. 2 assemblage

Interval: 405-720 m.

Age: early Eocene

Samples from this interval contain rich and diverse palynomorph assemblages. The persistent occurrence of *Alisocysta* sp. 2 (Heilmann-Clausen, 1985) and *Deflandrea oebisfeldensis* below 405 m suggest an age no younger than early Eocene. This age assignment is supported by the presence of *Charlesdowniea edwardsii* at 435 m and *Charlesdowniea crassiramosa* at 570 m. The persistent occurrence of *Alisocysta* sp. 2 and *D. oebisfeldensis* and the high content of terrestrial material (pollen, spores, plant tissue fragments) indicates that the interval belongs to the lower part of the lower Eocene, and corresponds to the top of the lower Eocene Subzone E2A of Mudge & Bujak (1994) in the northern North Sea.

Dracodinium varielongitudum was recorded at 405 m and below. This species is characteristic of the early Eocene. However, *D. varielongitudum* is thought not to coexist with *Alisocysta* sp. 2, but in slightly younger sediments (Heilmann-Clausen, 1985). Younger early Eocene sediments are therefore thought to be present between 405 and 330 m.

A certain number of species occurring in the assemblage are probably caved. The presence of *Rhombodinium draco* at 435 and 470 m suggests that sediments younger than the middle part of the Middle Eocene (Costa & Manum, in Vinken, 1988) are present above 405 m. *Svalbardella cooksoniae* was recorded at 405 m. This species has a known strati-

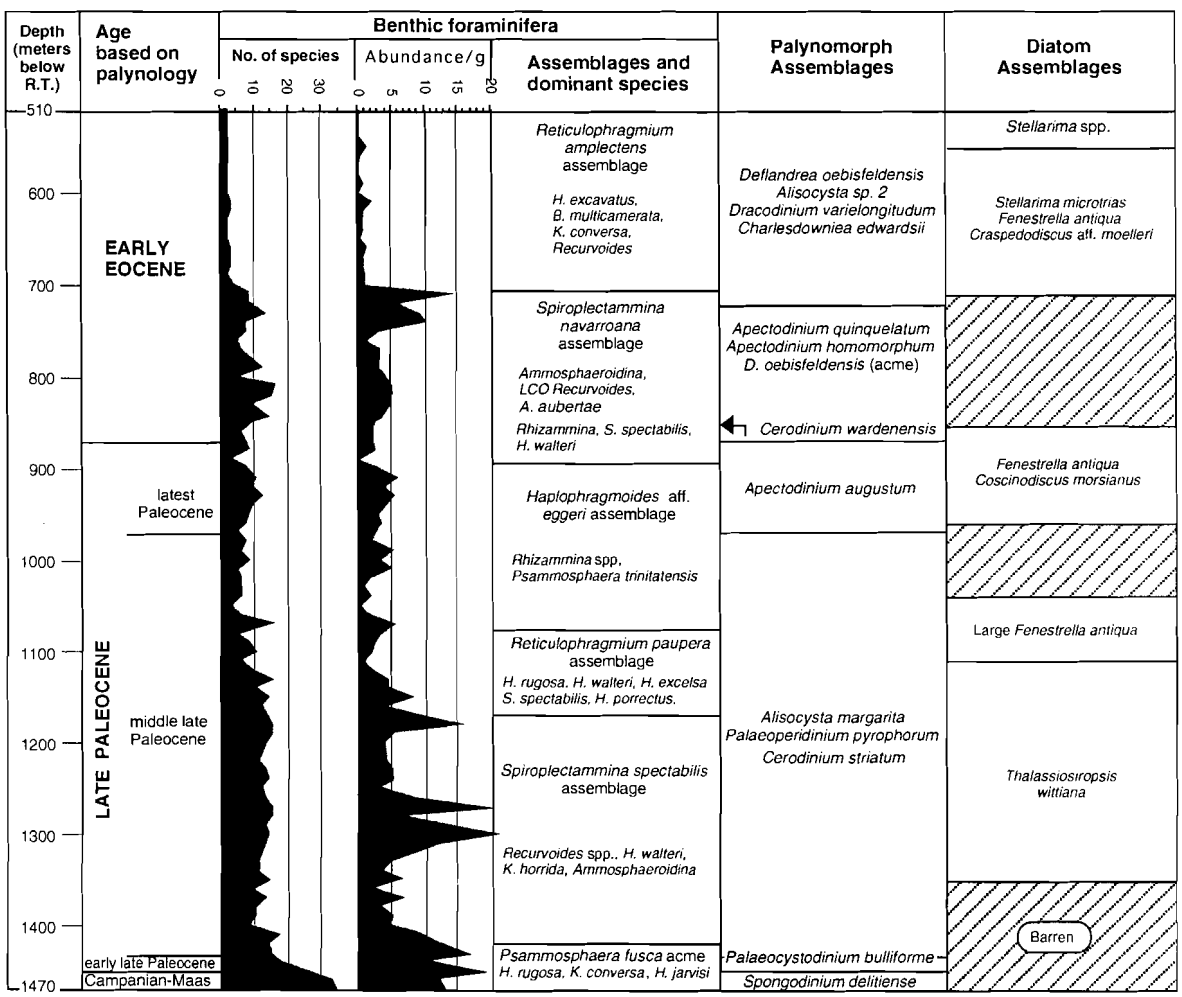


Figure 3. Chronostratigraphy, foraminiferal distribution, palynomorph assemblages, and diatom assemblages in well 7119/9-1.

graphic range spanning from late Eocene to early Oligocene (Costa & Manum, in Vinken, 1988). In this assemblage there is also evidence of reworking from the Cretaceous.

2. *Deflandrea oebisfeldensis* assemblage

Interval: 720-890 m.

Age: earliest Eocene

The consistent occurrence of *Apectodinium quinquelatum* below 720 m and the presence of the *Apectodinium homomorphum/parvum* complex at 720 m suggests an early Eocene age. The relatively common occurrence of *Deflandrea oebisfeldensis* at 720 m supports this age assignment. The top of the *D. oebisfeldensis* acme defines the top of the lowermost Eocene Subzone E1c of Mudge & Bujak (1994), and correlates with the top of the Balder Formation in the northern North Sea.

The LO of *Cerodinium wardenense* is observed at 845 m and it occurs consistently below 850 m. The LO of *C. wardenense* defines the top of the lowermost Eocene E1b Subzone of Mudge & Bujak (1994).

3. *Apectodinium augustum* assemblage

Interval: 890-970 m.

Age: latest Paleocene

The LO of *Apectodinium augustum* at 890 m indicates the latest Paleocene „P6" palynomorph zone of Mudge & Bujak (1996). The individuals reveal considerable morphological variability. Some specimens have less well-developed horns, and especially the apical horn displays variation in size. The characteristic acme of *Apectodinium* spp. was not recorded in this well.

4. *Alisocysta margarita* assemblage

Interval: 970-1420 m.

Age: middle late Paleocene

The LO of *Alisocysta margarita* at 970 m together with the occurrence of *Palaeoperidinium pyrophorum* at 1020 m suggests a middle late Paleocene age, corresponding to the „P5" palynomorph zone of Mudge & Bujak (1996). Schröder (1992) noted that the range of *A. margarita* is limited to the lowermost part of the Lista Formation in the southern Viking Graben. In the studied well, the species *Areoligera* cf. *senonensis* displays an acme at 1000 m. This species usually occurs in high numbers in the middle part of the upper Paleocene, and this event probably corresponds to dinoflagellate cyst zone 4 of Heilmann-Clausen (1985). The common occurrence of *Palaeoperidinium pyrophorum* at 1370 m probably corresponds to the upper part of dinoflagellate cyst zone 3 of Heilmann-Clausen (1985), which is equivalent to the middle part of the „P4" palynomorph zone of Mudge & Bujak (1996).

5. *Palaeocystodinium bulliforme* assemblage

Interval: 1420-1450 m.

Age: early late Paleocene

The LO of the species *Palaeocystodinium bulliforme* (=*P. australinum* of Mudge & Bujak, 1996) at 1420 m indicates an early late Paleocene age. The common occurrence of *P. bulliforme*, *P. pyrophorum* and *Isabelidinium* cf. *viborgense* below 1440 m supports this age assignment. This interval corresponds to dinoflagellate cyst zone 3 and the upper zone 2 of Heilmann-Clausen (1985).

The presence of *Spongodinium delitiense* at 1450 m may be due to reworking. This species is known to have its last occurrence in the earliest early Paleocene (Hansen, 1977). According to Schröder (1992) it ranges only to the top of the Ekofisk Formation in the southern Viking Graben.

6. *Spongodinium delitiense* – *Odontochitina* cf. *costata* – *Cleistosphaeridium* sp. 1 assemblage

Interval: 1460-1570 m.

Age: late Campanian

An abrupt change in the organic content of the samples takes place at 1460 m, with an increase in the amount of coal particles and the occurrence of abundant *Cleistosphaeridium* sp. 1 and common *Chatangiella* spp.

Spongodinium delitiense is relatively common at 1460 m. This species is known to occur in the upper Campanian (Lucas-Clark, 1987), but is more characteristic of sediments of Maastrichtian and early Paleocene age (Hansen, 1977). The LO of *Odontochitina* cf. *costata* at 1460 m suggests an age not younger than the late Campanian or early Maastrichtian (Tocher, 1987).

b. Benthic Foraminiferal Assemblages

Samples examined from the uppermost part of the Torsk Formation (410-500 m) were barren of foraminifera. Ninety-three samples were analysed in the interval from 510 to 1470 m, mostly at a sample

spacing of 10 m. A total of 84 species and open nomenclature taxa were recognised, all of which are agglutinated (Table 2). The succession of foraminiferal events can be compared with the integrated microfossil zonation of the northern North Sea and Haltenbanken areas recently established by Gradstein *et al.* (1994) and by Gradstein & Bäckström (1996). The benthic foraminiferal succession in the well can be subdivided into six main assemblages:

1. *Reticulophragmium amplectens* assemblage

Interval: 510-710 m.

Age: early Eocene

At the top of the Torsk Formation from 510 m to 700 m, both abundance and diversity are low. The assemblage consists mainly of *Haplophragmoides excavatus* and *Budashevaella multicamerata*. At 710 m there is a sharp increase in foraminiferal abundance, and a peak in the frequency of *Reticulophragmium amplectens* (= the early Eocene morphotype called *Reticulophragmium intermedium* (Mjatliuk)) is observed. This assemblage also contains common *Rhizammina* spp., *Recurvoides* spp., *Karrerulina* spp., *Haplophragmoides excavatus*, and *Budashevaella multicamerata*. The species *R. intermedium* is the nominate taxon of the late early Eocene to early middle Eocene Zone NSR5A of Gradstein & Bäckström (1996).

2. *Spiroplectammina navarroana* assemblage

Interval: 710-890 m.

Age: latest Paleocene to earliest Eocene

The LOs of many taxa are observed near 710 m, including that of *Spiroplectammina navarroana*, *Ammosphaeroidina pseudopauciloculata*, *Haplophragmoides kirki*, and *Ammodiscus macilentus*. In the Central North Sea, the LO of *S. navarroana* is an important event within the lower Eocene *Subbotina patagonica* Zone of Gradstein *et al.* (1994). In the Haltenbanken area of offshore Norway, the LO of *S. navarroana* is observed within the middle part of Zone NSR5A of Gradstein & Bäckström (1996). Mudge & Bujak (1996) correlate the LO of *S. navarroana* with the top of the Ypresian.

The interval from 790 to 890 m is characterised by the occurrence of a diminuative form of *Ammomarginulina aubertae*, a species first described from the North Sea and Labrador Shelf by Gradstein & Kaminski (1989). This species is apparently diachronous in offshore Norway, as it characterises the late middle Eocene Zone NSR6 of Gradstein & Bäckström (1996) in Haltenbanken and in the northern North Sea. It is rare in our samples. The assemblage is numerically dominated by *Rhizammina* spp., with *Recurvoides* spp., *Karrerulina* spp., and *Spiroplectammina spectabilis* present in low numbers. The whole interval is characterised by a taxonomic turnover, and a plateau in the species range chart occurs near 810 m, coincident with a peak in the abundance of tubular forms. At this level the LOs of several typically Paleocene to lower Eocene species are observed, including *Saccammina placenta*, *Sphaerammina* sp., *Kalamopsis grzybowskii*, and *Glomospira* spp. Both diversity and abundance decrease to minimum values near the base of this assemblage.

We did not observe any planktonic foraminifera or calcareous benthic foraminifera in the lower Eocene interval of the well, nor did we find any calcareous specimens in adjacent wells in the western Barents Sea. Calcareous assemblages belonging to the *Subbotina patagonica* Zone of Gradstein *et al.* (1994) have been observed as far north as Haltenbanken (Gradstein & Bäckström, 1996) and the outer Vøring Plateau (Hulsbos *et al.*, 1989). Either the northern boundary of the early Eocene planktonic foraminifera must have existed south of the Barents Sea area, or the deep waters of the basin were too corrosive to allow the preservation of calcareous microfossils.

3. *Haplophragmoides* aff. *eggeri* assemblage

Interval: 890-1070 m.

Age: late Paleocene

From 890 m to ca. 1070 m the diversity of benthic foraminifera is low, and the assemblage is dominated by tubular forms and a species of *Haplophragmoides* tentatively designated *H.* aff. *eggeri*. The LO of this species was observed at 910 m, but foraminiferal abundance near the top of this interval is especially low. We therefore arbitrarily placed the top of this assemblage at the abundance minimum at 890 m. The foraminifera in this interval are not age-diagnostic.

4. *Reticulophragmium paupera* assemblage

Interval: 1080-1160 m.

Age: middle late Paleocene

Between 1080 and 1160 m, both the abundance and diversity of the benthic foraminifera steadily

increase downhole. This interval is characterised by the consistent common occurrence of *Reticulophragmium paupera*, an index taxon for the upper Paleocene in the North Sea and Haltenbanken. It is the nominate taxon of the late late Paleocene Zone NSR2B of Gradstein & Bäckström (1996). Other important species include *Haplophragmoides walteri* and tubular forms belonging mainly to *Rhizammina*. *Spiroplectammina spectabilis* is occasionally present in this interval in low numbers. The LO of *Hyperammina rugosa* is observed together with that of *R. paupera* at 1080 m.

5. *Spiroplectammina spectabilis* assemblage

Interval: 1180-1400 m.

Age: middle late Paleocene

A distinct maximum in the abundance of *Spiroplectammina spectabilis* is observed in the interval from 1180 to 1400 m. The last common occurrence (LCO) of *S. spectabilis* occurs within the upper Paleocene in the North Sea, and is placed near the base of Zone NSR2B of Gradstein & Bäckström (1996). In the studied well, this event occurs between the LO of *Alisocysta margarita* and the LCO of *Palaeoperidinium pyrophorum* (at 1370 m), which agrees with its relative position in the RASC zonal model of Gradstein & Bäckström. One unusual feature of this assemblage is the large proportion of of juvenile forms of *S. spectabilis*. Other common taxa include *Rhizammina* spp., *Ammosphaeroidina pseudopauciloculata*, *Haplophragmoides walteri*, and *Reticulophragmium paupera*. In the lower part of the interval, single occurrences of the species *Rzehakina minima* and *Reticulophragmoides jarvisi* were observed.

In the studied western Barents Sea wells, the species *Ammoanita ruthvenmurrayi* (the nominate taxon of the mid Paleocene Zone NSR 2A of Gradstein & Bäckström) is rare or absent. We therefore selected an event that occurs regionally in the western Barents Sea to characterise this assemblage. Our *S. spectabilis* assemblage is roughly equivalent to the *T. ruthvenmurrayi* Zone in the North Sea and Haltenbanken.

6. *Psammosphaera fusca* assemblage

Interval: 1410-1450 m.

Age: early middle Paleocene

The benthic foraminiferal assemblage at the base of the Torsk Formation (1430-1480 m) displays strongly increased abundance and the highest diversity in the well. There is an abrupt downhole expansion in abundance at 1410 m. The assemblage is distinguished from overlying assemblages because it is dominated by species that agglutinate coarse material for the construction of their test, such as *Hyperammina rugosa*, *Psammosphaera fusca*, and an unnamed species of *Recurvoides*. *Psammosphaera fusca* increases in relative abundance at 1430 m, near the base of the Torsk Formation. Other common forms in this interval include *Recurvoides* spp., *Rhabdammina* spp., *Karrerulina* sp., and *Ammosphaeroidina pseudopauciloculata*. Three distinctive species are restricted to this assemblage: *Praecystammina* sp., *Caudammina ovulum*, and *Rzehakina epigona*.

Samples from the underlying Cretaceous Kviting Formation display further increased abundance and diversity compared with the Torsk Formation. The species *Ammodiscus glabratus*, *Spirosigmoilinella* sp. 1, *Hormosina velascoensis*, and *Trochammina* cf. *subvesicularis* display LOs at 1460 m, coincident with the top of the Kviting Formation. However, these are taxa that are known to range into younger stratigraphic levels in other areas of the North Atlantic. The Upper Cretaceous index form *Caudammina gigantea* was observed at 1470 m, confirming a Campanian to Maastrichtian age for this level.

c. Diatom assemblages

A total of 35 diatom taxa were identified from 70 samples. Although poorly preserved (being infilled and/or replaced by pyrite) and in relatively small numbers (due to the effects of differential preservation bias towards more robust forms), enough stratigraphically important taxa were present to enable the Paleogene succession to be subdivided into five stratigraphically significant assemblages (Fig. 3). Diatoms occur sporadically in the samples studied, with a major abundance peak developed between 850 and 870 m, at around the Paleocene/Eocene boundary. This correlates with a similar abundance peak in the North Sea Basin. Diatoms are also relatively abundant between 1110 and 1310 m. The diatom succession is discussed below in order from youngest to oldest.

1. *Stellarima* spp. assemblage

Interval: 510-550 m.

Various morphologies belonging to the genus *Stellarima* occur in the uppermost diatomaceous samples studied. Although some of these are difficult to identify to species level due to poor preservation, their biconvex shape, small size (<100 μm) and centrally-positioned labiate processes, are

characteristic of *Stellarima*. Usually these are normal (i.e. vegetative) cells of the species *S. microtrias*, but sometimes resting spores are encountered, distinguished by having a depression at the centre of the valve face. The latter are a morphological adaptation found in many diatom species, and are formed in response to seasonal depletions of nutrients (see Round *et al.* 1990, pp. 37-40 for a fuller discussion). Smaller morphologies bearing a strong resemblance to *S. microtrias* also occur in some samples in the lower Eocene interval.

2. *Stellarima microtrias, Fenestrella antiqua, Craspedodiscus* aff. *moelleri* assemblage

Interval: 560-710 m.

This assemblage is characterised by the continued presence of *Stellarima microtrias*, though in low abundance; in addition to the first occurrence of the large, biconvex species *Fenestrella antiqua*, also in small numbers. Sporadic appearances of the „doughnut-shaped" genus *Craspedodiscus* (which bear a resemblance to the species *C. moelleri*.) are also present in this assemblage. Poor preservation precludes species determination. In the interval 720 to 810 m, diatoms are completely absent.

3. *Fenestrella antiqua, Coscinodiscus morsianus* assemblage

Interval: 850-960 m.

Diatoms reappear at 820 m, slightly above the Paleocene/Eocene boundary as delimited by palynomorphs. From 850 m, a rich diatom assemblage is present, dominated by *Fenestrella antiqua*. Other species include *Stellarima microtrias*, the biconcave species *Coscinodiscus morsianus*, the triangular taxon *Triuacria regina*, and sporadic occurrences of *Thalassiosiropsis wittiana*. The latter is similar in shape to *Stellarima microtrias* but much larger, with an extremely smooth surface and with a pronounced dimple at the centre of the valve. Other species include the benthic taxa *Actinoptychus senarius* and *Aulacodiscus hirtus*, indicative of shallowing conditions. Diatoms appear only sparsely between 970 and 1030 m.

4. *Fenestrella antiqua* assemblage

Interval: 1040-1110 m.

Huge (<250 µm) specimens of *F. antiqua* dominate this assemblage, often characterised by the presence of a veneer of original silica on the surface. Both vegetative cells and resting spores are found; the latter distinguished by their lenticular shape, smooth surface and lack of a girdle. Auxospores of *F. antiqua* also occur, which are barrel-shaped with a very wide girdle. Other species present in the assemblage include *Stellarima* sp. and *Coscinodiscus morsianus*.

5. *Thalassiosiropsis wittiana* assemblage

Interval: 1120-1350 m.

The late Paleocene interval is dominated by relatively great numbers of the large, discoidal species *Thalassiosiropsis wittiana*. This taxon is found in other areas during this interval, including the Russian Platform and the North Sea, and indicates fairly unrestricted connections between these areas. The interval from 1350 to 1470 m is barren of diatoms.

DISCUSSION

a. Stratigraphic Correlation

For the purposes of assessing the utility of the assemblages observed in the 7119/9-1 well for regional stratigraphic correlation, we compiled a graphic overview of foraminiferal stratigraphic events that were observed in six wells comprising an east-west transect from the Senja Ridge to the transition between the Hammerfest and Nordkapp basin (Fig. 1). For these purposes, only the last occurrences (LO) and last common occurrences (LCO) of selected common, cosmopolitan, deep-water benthic foraminifera were included (Fig. 4).

Parts of the well sections analysed display low abundance and diversity of benthic foraminifera. In spite of this, the strata reveal several important biostratigraphical events, such as the LOs of *Reticulophragmium amplectens, Spiroplectammina navarroana*, and of the dinoflagellate cyst *Apectodinium angustum*. In the Paleocene part of the transect the LOs of *Reticulophragmium paupera, Hyperammina rugosa*, and the LCO of *Spiroplectammina spectabilis* are observed in all wells, whereas the LOs of *Hormosina excelsa, Rzehakina minima, Praecystammina* sp., and *Caudammina gigantea* are restricted to fewer wells. The events included in the transect have also been recorded from in the Viking Graben of the Central North Sea (i.e. Gradstein *et al.*, 1994), and may serve as the basis for a wider foraminiferal zonation of the lower Paleogene of offshore Norway.

In the three westernmost wells, the LO of *R. amplectens* is observed near the eroded upper contact of the Torsk Formation, therefore its last stratigraphic occurrence in this area is probably not correlative to its true extinction. The occurrence of *S. navarroana* near the top of the studied interval in

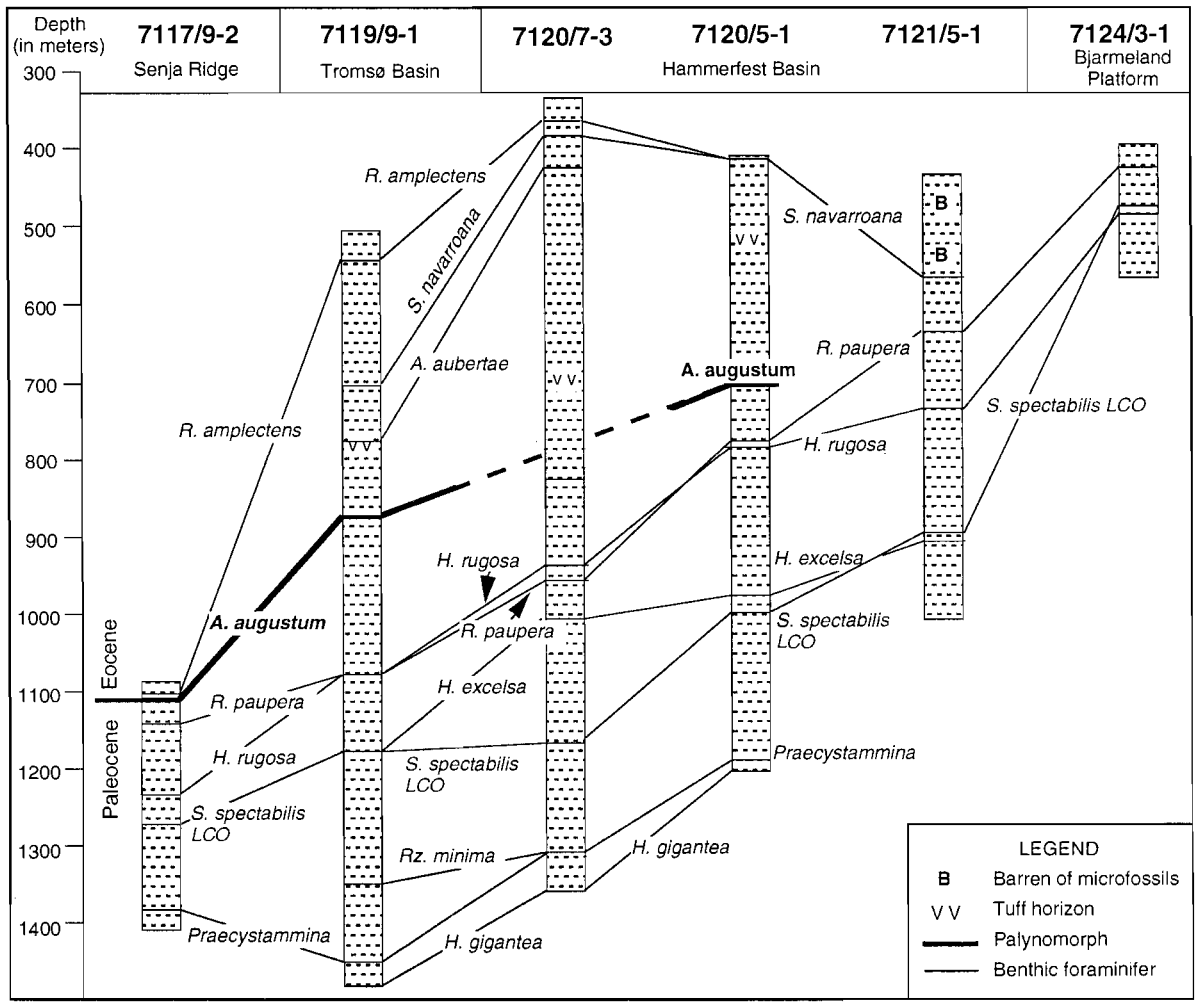


Figure 4. Foraminiferal last occurrences in an W-E transect of wells from the Tromsø and Hammerfest basins, plotted at a common depth scale (meters below rig floor) to give an impression of the subsurface geometry of the Torsk Formation. The position of a distinctive tuff horizon and the LO of a dinocyst approximating the Paleocene/Eocene boundary is also indicated.

the three western wells suggests correlation with the lower Eocene *Subbotina patagonica* Zone of Gradstein *et al.* (1988; 1994), although we did not observe any specimens of the nominate species of this zone, or any other calcareous benthic foraminifera that are known to occur in the lower Eocene of the North Sea.

East of Block 7120, the Eocene sediments have been removed by erosion, and the Torsk Formation penetrated by the two eastern wells is dated as wholly within the late Paleocene according to palynomorphs. The top of the *R. paupera* assemblage in the studied wells is easily recognised by an abrupt change to more a diversified foraminiferal assemblage downhole. The LO of a distinct, very coarsely agglutinated tubular species, here identified as *H. rugosa*, is closely associated with that of *R. paupera*. These events, together with the last common occurrence of *S. spectabilis* are remarkably continuous over the whole study area despite obvious variations in sedimentation and paleobathymetry. However, the earliest late Paleocene *Psammosphaera* assemblage (indicated in Fig. 4 by the LO of *Praecystammina* sp.) is not present in the two easternmost wells, suggesting that the pre-Cenozoic topography of the basin did influence the composition of the benthic foraminiferal assemblages. In the North Sea region, *Praecystammina* sp. is regarded to

be a deep-water species (middle bathyal) in the Paleocene, therefore, its absence from the eastern wells may be a result of ecological exclusion.

A total of 74 stratigraphic last occurrences of foraminifera were recorded in the nearby 7120/7-3 well in the western Hammerfest Basin, with 50 events in common with those in the 7119/9-1 well. These two wells give the best correlation of last occurrence data observed between any two records investigated so far from the Torsk Formation. When the depths of all shared LOs are plotted in a standard graphic correlation plot, a regression equation can be calculated (Fig. 5). The regression coefficient can be interpreted as a measure of the „reliability" of the last occurrence events. The correlation between the LOs in the two holes can best be described by a linear regression. Polynomial and exponential solutions of the regression equation did not yield markedly higher regression coefficients, suggesting that there were no observable significant hiatuses or changes in sedimentation rate between the two sites. In this solution, the regression coefficient calculated using all the observed LOs gave a value of R^2=0.71. Outliers from the regression line in all cases consist of rare species. In a later stage of biostratigraphic analysis, these outliers are normally deleted from the data set. The „scatter" in the data points is greater among Eocene last occurrences than among events recorded from the Paleocene. However, in this case the outliers can be partially explained by sampling bias. This is attributed to the small size of the studied samples resulting in low specimen numbers in many Eocene samples.

A second regression curve was calculated from a subset of data points, indicated as shaded squares in Fig. 5. These points represent species found in the Tromsø Basin, which are listed as stratigraphically important in the Paleocene to middle Eocene probabilistic stratigraphy of the Central North Sea by Gradstein *et al.* (1994). The regression line constructed from the important North Sea species alone does not differ greatly from the previous curve, but the regression coefficient is much higher (R^2=0.91). This suggests that the North Sea benthic foraminiferal zonation of Gradstein *et al.* (1994) can give excellent stratigraphic results in the western Barents Sea. However, other points also fall close the correlation line as well, indicating that additional index forms are also present in the Tromsø-Hammerfest Basin area. A complete discussion of the stratigraphic utility of faunal events is beyond the scope of this study, and must be based on detailed analysis of a greater number of well sections.

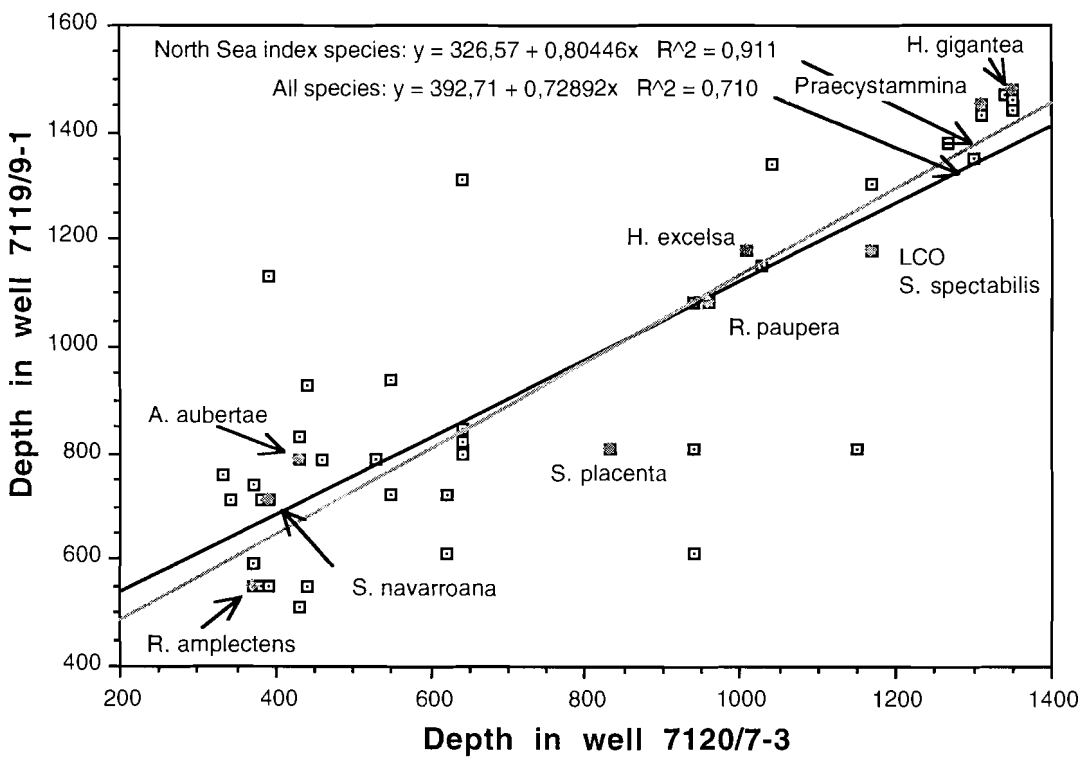


Figure 5. Graphic correlation of foraminiferal LOs and LCOs in Wells 7119/9-1 and 7120/7-3 in the Tromsø and Hammerfest basins. Axes values are the depths in meters BKB of events observed in both wells.

b. Unconformities

The benthic foraminiferal and dinoflagellate cyst biostratigraphy investigated here provides significant new constraints for the age and nature of unconformities, which are expressed as important seismic horizons in the western Barents Sea. Two seismic horizons were examined here in detail:

The Basal Tertiary: This is the „Sequence boundary B" horizon of Rønnevik (1981), which marks the top of the rotated fault blocks east of the contact between oceanic and continental crust. Rønnevik correlated this reflector with the oldest Tertiary sediments in Spitsbergen, and correctly regarded it as representing the base of the upper Paleocene. He added that older Paleocene sediments may be present in the eastern part of the Barents Sea area. Faleide *et al.* (1993b) recognised the regional nature of the „Base Tertiary" reflector, and noted that it constitutes a hiatus spanning the Cretaceous-Tertiary transition. On the southwestern Loppa High this reflector defines an angular unconformity truncating Cretaceous strata (Knutsen & Vorren, 1991).

Our observations suggest that the „Base Tertiary" reflector in the basin areas indeed represents a submarine hiatus. Earlier studies of the southwestern Barents Sea (e.g. Worsley *et al.*, 1988) have suggested an early Campanian age for the underlying Kviting Formation, but based on the occurrence of *Caudammina gigantea* and *Spongodinium deltiense* in our samples, the formation may include strata as young as late Campanian to Maastrichtian in places. In the wells where we sampled both the lowermost Torsk Formation and the uppermost Kviting Formation, we observed little change in the paleobathymetric significance of the benthic foraminiferal assemblage on either side of the disconformity. Assemblages from both formations in the Tromsø Basin and central part of the Hammerfest basin contain deep-water benthic foraminiferal taxa such as *Praecystammina, Caudammina, Pseudobolivina, Rzehakina,* and abundant tubular forms such as *Rhizammina* and *Rhabdammina,* which indicate a middle bathyal (or deeper) depositional environment.

In the Tromsø Basin and western part of the Hammerfest Basin, the basal assemblage of the Torsk Formation contains numerous tubular forms and several other taxa that utilize coarse agglutinated material in the construction of their test. At some localities, a maximum in *Psammosphaera fusca* is observed. The distinctive composition of the basal assemblage in the Torsk Formation invites comparison with areas affected by deep-sea bottom currents. In the modern North Atlantic, high abundances of coarsely agglutinated forms, suspension-feeding tubular forms, and the opportunistic species *P. fusca* are found beneath the Western Boundary Undercurrent (Kaminski, 1985). The late Paleocene deep water conditions in the southwestern Barents Sea appear to have developed during a longer time period, because during the Late Cretaceous the Tromsø and Sørvestsnaget basins continued to subside (Faleide *et al.*, 1993a). It is likely that fine-grained sediments bypassed the area, and that the coarse agglutinated assemblage is testimony to the presence of periodic bottom currents that affected the sea floor.

Top Torsk Formation: The Torsk Formation is unconformably overlain by Plio-Pleistocene glacial marine and glacial sediments of the Nordland Group. Seismic lines interpreted by Faleide *et al.* (1993a,b) show truncation of seismic reflectors within the Torsk Formation in an easterly direction, indicating that the top of the Paleogene succession has been clearly eroded, while thicker and younger Paleogene sediments are present in the west. Our results confirm this interpretation. In the easternmost locality the top of the Torsk formation is within the middle late Paleocene *R. paupera* Zone (*sensu* Gradstein *et al.*, 1988), whereas in the west, sediments belonging to the late early Eocene *R. amplectens* Zone underlie the Cenozoic unconformity.

The timing and causes of the Cenozoic erosion is a matter of discussion. In the western part of the Barents Sea, in the region of the Sørvestsnaget Basin and the Senja Ridge, uplift of rift flanks is associated with Paleogene continental breakup. The main phase of deformation took place during initial breakup in the early Eocene, but some faults were active into early Oligocene times. Faleide *et al.* (1993b) estimated that as much as 1 km of Paleogene sediments were removed by erosion in this area. This erosion is related to uplift along the Senja Fracture Zone during Eocene time (Vignes, 1995). This event created a western source area for some sediments in the Tromsø Basin. Erosion in the Hammerfest Basin was of greater magnitude, according to estimates from vitrinite reflectance and fission track analysis in the range of 1200-1500 m. A study of the porosity, cementation, and oxygen isotopes in the Jurassic Stø Formation in the 7120/9-1 well (present depth = 1500 m) indicated that the at least 1500 m of overburden has been removed at this locality (Walderhaug, 1992). Regional uplift in the southwestern Barents Sea may have been associated with or caused by Oligocene volcanism (Faleide *et al.*, 1991), a Miocene sea-level fall (Reemst & Cloetingh, 1994), increased levels of intraplate compression in the Neogene (Cloetingh *et al.*, 1990, 1992), and neotectonic activity resulting from Pleistocene deglaciations (Karpuz *et al.*, 1991).

c. Benthic foraminiferal paleoecology and paleobathymetry

A striking feature of the foraminiferal assemblages in the studied wells is the absence of calcareous taxa (both benthic and planktonic). The assemblages include significant proportions of deep-water agglutinated foraminifera belonging to the single-chambered (tubular and globular forms) and multichambered groups. The low availability of carbonate in the southwestern Barents sea during the early Paleogene has probably produced unfavorable conditions for the development of calcareous faunas, as well as for the preservation of any calcareous microfossil tests originally present. The wholly agglutinated nature of the assemblages and the presence of taxa that are known from basinal facies in the Central North Sea points to deep-water (middle bathyal) conditions in the Tromsø Basin. However, it is a well known fact that deep-sea organisms can be found living in shallower environments at high latitudes (Murray, 1895), so this estimate must be regarded as a lower limit.

The accumulation rate of benthic foraminifera at a given locality can change in response to fluctuations in water depth, the flux of marine organic matter to the sea floor, as well as the sedimentation rate (Herguera & Berger, 1991). The foraminiferal abundance has been measured quantitatively in well 7119/9-1 (Fig. 3). The record displays fluctuations of two orders of magnitude within the Torsk Formation. Fluctuations of this magnitude cannot be explained by changes in surface productivity and water depth alone, and more likely reflect variations in the flux of terrigenous sediments. In sequence stratigraphic terms, intervals with high benthic foraminiferal abundance and diversity reflect condensed horizons. The nature of the benthic foraminiferal abundance pattern in the 7119/9-1 well suggests cycles of higher sediment input, although changes in sediment texture are not apparent from gamma ray logs.

Knutsen & Vorren (1991) and Knutsen *et al.* (1992) noted that the Loppa High served as a sediment source area during the late Paleocene, and that in the northwestern part of the Tromsø Basin prograding clinoforms are visible in seismic reflection profiles. The decrease in foraminiferal abundance and diversity in this part of the section (above the *Spiroplectammina spectabilis* assemblage) may reflect high terrigenous influx related to increased sediment supply from the north, which caused conditions unfavorable for the fauna.

The functional morphology of benthic foraminifera can provide important insights into the ecology of the benthic environment. Foraminiferal test shape is thought to reflect differences in life position and feeding strategy (Jones & Charnock, 1985). Changes in the relative proportions of the various morphogroups through time can reflect changes in environmental parameters such as water depth, current strength, and organic flux to the sea floor.

For this study, we have devised a morphogroup scheme for classifying the benthic foraminifera according to test morphology, and by analogy with modern faunas, for interpreting their paleoecology. Paleogene assemblages from the Barents Sea can be subdivided into four groups and nine subgroups (Fig. 6). Forms in Group 1 (tubular taxa) are normally found in higher abundance in bathyal to abyssal habitats, reaching an acme in the lower bathyal zone in the modern North Atlantic (Schroeder, 1986). Because they are epifaunal suspension feeders, they are adapted to life in areas of low organic flux. In the modern Norwegian-Greenland Sea, an abrupt shift from infaunal to predominantly epifaunal morphogroups is observed at a water depth of 1,500 m (Corliss & Chen, 1988). The infaunal Group 3, by contrast, is better adapted to life in areas of increased organic flux and hig-

Morphogroup		Test morphology & Habitat	Examples
1	1 a	Rigid tubular Epifaunal, elevated, suspension feeding	*Bathysiphon, Rhabdammina*
	1 b	Flexible and flattened Epifaunal surficial, detritivores	*Rhizammina, Nothia*
2	2 a	Globular, surficial or shallow infaunal, feeding at the sediment surface	*Saccammina, Psammosphaera*
	2 b	Rounded planoconvex, trocho- spiral, and streptospiral, surficial	*Recurvoides* &some *Trochammina*
	2 c	Keeled planispiral and elongated, surficial	*R. amplectens* *S. spectabilis*
3	3 a	Rounded planispiral, intermediate infaunal to surficial	*Haplo. eggeri*
	3 b	Elongated subcylindrical, tapered, deeper infaunal	*Karrerulina, Verneuilinoides*
4	4 a	Flattened planispiral and flattened irregular, epifaunal or climbing	*Ammodiscus* some *Glomospira*
	4 b	Flattened trochospiral Epifaunal or attached on elevated substrate	*some Trochammina*

Figure 6. Morphogroup scheme and inferred paleoecology of Paleogene agglutinated foraminifera from the western Barents Sea.

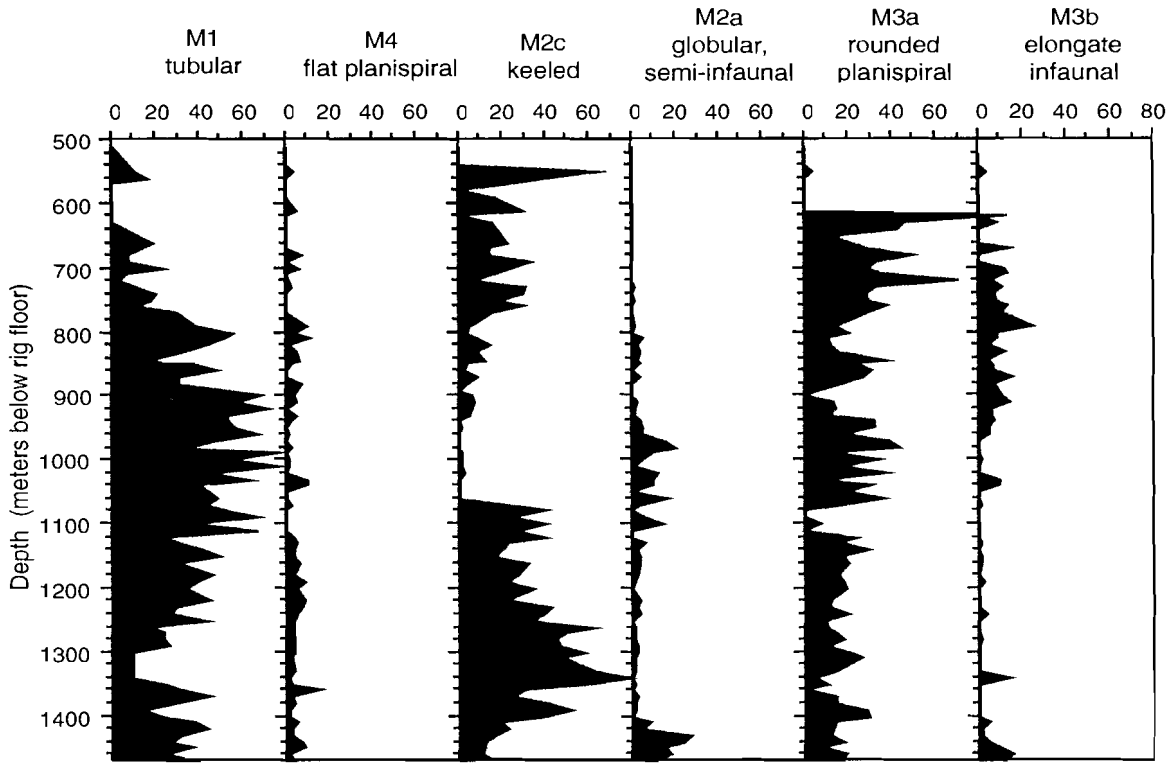


Figure 7. Relative proportions (in percent) of agglutinated foraminiferal morphogroups in the Paleogene of well 7119/9-1.

her nutrient supply. This group is often observed in large proportions near the shelf/slope break in the Gulf of Mexico, or in areas where the surface layer of the sea floor is affected by bottom currents (Kaminski, 1985).

We have undertaken a morphogroup analysis of the assemblages from the 7119/9-1 well, and results are shown in Figure 7. Taxa belonging to the tubular morphogroup 1a are common to dominant throughout the studied interval, except in the upper 170 m where they are rare or absent. High abundances of this group recalls the so-called flysch-type agglutinated assemblages of the Paleocene of the North Sea and Alpine-Carpathian regions. The frequency variations of the tubular morphogroup are interpreted as reflecting changes in the paleobathymetry of the site. In the lower part of the section, the relative proportion of tubes increases upsection, suggesting a gradual subsidence of the basin. Maximum water depth is represented by the interval between 900 and 1100 m, where the proportion of this morphogroup reaches 70%. It is natural to assume that the water depth during the latest Paleocene was middle bathyal or deeper. In the seismic section published by Knutsen *et al.* (1992, Fig. 11) a double high-intensity reflector is present between 900 and 1000 m which correlates precisely to our double peak in the proportions of the tubular morphogroup. We believe that the maximum proportions of the tubular morphogroup at this level reflect the maximum extent of the Paleocene transgression in the Barents Sea area, and therefore represent a maximum flooding surface in sequence stratigraphic terms.

Above this interval, a shallowing of the site is indicated by the decreasing frequency of the tubular morphogroup 1 and its partial disappearance in the later part of the early Eocene. The keeled morphogroup 2c displays a maximum in the lower and upper parts of the interval, expressing the first phases of the transgression and the subsequent regression, respectively. It is of interest to note that the infaunal rounded planispiral morphogroup 3a attains maximum frequency in the upper part of the interval, corresponding to the early Eocene portion of the Torsk Formation. As a general rule, infaunal organisms can only exist in large numbers in areas where organic matter is buried in sufficient amounts. This observation agrees with the general trend of increasing surface-water paleoproductivity in the North Atlantic region during the latter part of the early Eocene, reflected by the onset of biosiliceous sedimentation (Berggren & Olsson, 1985).

The „deep infaunal" morphogroup 3b displays variable but low abundance throughout the

studied interval. Since this group normally reaches maximum proportions in eutrophic areas or in dysaerobic environments such as those found beneath the oxygen minimum zone (Kaminski *et al.* 1995), we conclude that the bottom water in the Tromsø Basin was not oxygen-deficient during the deposition of the Torsk Formation. However, increased numbers of the genus *Karrerulina* are observed in the *Psammosphaera* assemblage at the base of the Torsk Formation. This is consistent with the finding of elevated proportions of deep infauna in areas disturbed by bottom currents (Kaminski, 1985). The above patterns are complex, and analysis of additional sections is needed to provide a more complete picture of the subsidence history of the western Barents Sea.

d. Diatom paleoecology

The most commonly occurring diatom taxon in the samples studied is *Stellarima microtrias*, a species found intermittently through the entire Paleogene. It occurs in all of the samples from 510 to 710 m, and between 845 and 1240 m. This species also has an intermittent stratigraphic distribution in the Paleogene of the North Sea (Mudge & Bujak 1994; Mitlehner, 1994). Some of the diatom taxa recognised in well 7119/9-1 are more stratigraphically restricted. *Thalassioriopsis wittiana* occurs more or less continuously through the upper Paleocene section, but is absent thereafter; whilst appearing sporadically between 560 and 1100 m is the large (up to 300 µm diameter) species *Fenestrella antiqua* (= *Coscinodiscus* sp. 1 of Bettenstaedt *et al.*, 1962), a taxon which marks the base of the Eocene in the North Sea but which has a longer range in the Barents Sea, extending from the upper Paleocene through the lower Eocene. It has a similar range in the Paleogene of the Urals and Volga Basin (Glezer *et al.* 1974), suggesting a connection of the Barents Sea with the Turgai Sea which extended across the Russian Platform during the Paleogene. Other species co-occurring with *F. antiqua* include *Coscinodiscus morsianus* and *Trinacria regina*. This assemblage as a whole is very similar to coeval diatom assemblages from the North Sea area (Hughes, 1981; Malm *et al.*, 1984; Homann, 1991; Mitlehner, 1994) as well as the Arctic Ocean (Dell'Agnese & Clark, 1994), although there are fewer similarities to the Paleogene assemblages sporadically recovered by DSDP Leg 38 from the less restricted Norwegian Basin (Schrader & Fenner 1976; Dzinoridze *et al.*, 1978). This assemblage similarity documents the beginning of the early Eocene transgressive phase, related to a worldwide warming event which occurred in all areas (Rea *et al.*, 1990; Robert & Chamley, 1991). Other pyritised diatom assemblages, recovered from the Labrador Sea (Thomas & Gradstein, 1981), and the MacKenzie Basin of offshore northern Canada (McNeil, 1990) have certain similarities with those from the Barents Sea, in particular the occurrence of *Stellarima* species.

The sporadic occurrence of diatoms in the samples studied is related to periods of restricted water circulation as a result of lowered sea-level, in conjunction with increased nutrient influxes leading to diatom blooms (Calvert, 1966; Thunell *et al.*, 1994) in a relatively small and insolated basin. These periods often coincide with a decline in both species numbers and diversity of benthic foraminifera, a pattern also found in the North Sea (Mitlehner, 1994; 1996). This phenomenon can be attributed to periods of high surface water productivity, with increased nutrient levels leading to diatom blooms and eutrophication in the upper water column, and oxygen depletion of the lower water column (Codispoti, 1989). Conversely, increased numbers of benthic foraminifera coincide with a general absence of diatoms, a situation which signifies improved water circulation and increased oxygenation in the lower water column.

A particularly significant period of increased diatom productivity occurred at the Paleocene-Eocene transition, and is represented in well 7119/9-1 by an abundant and diverse diatom assemblage. The presence of benthic species (*Actinoptychus senarius*, *Aulacodiscus* sp.) indicates that there were shallow neritic conditions in the vicinity. A similar diatom abundance peak is recorded in the North Sea at the same interval, and it is likely that similar mechanisms, involving a lowered sea-level with increased influxes of waterborne and windblown terrigenously and volcanically derived nutrients to a restricted basin led to the proliferation of diatoms at that time.

CONCLUSIONS

Among the six wells located along a transect from the Senja Ridge through the Tromsø Basin to the Hammerfest Basin, well 7119/9-1 is chosen as a stratigraphic reference section. Analysis of foraminiferal, palynomorph, and diatom assemblages in this well in the Tromsø Basin enable a reliable determination of the chronostratigraphy of the Torsk Formation. A total of 86 palynomorph, 84 foraminiferal, and 35 diatom taxa have been found. The succession of late Paleocene to early Eocene assemblages compares well with the North Sea zonations of Mudge & Bujak (1994, 1996), Gradstein *et al.* (1994), Gradstein & Bäckström (1996), and Mitlehner (1994). The stratigraphic occurrences of several foraminiferal and dinocyst last occurrence events are consistent in wells across the Senja Ridge - Hammerfest Basin transect, suggesting that the biostratigraphical record of the 7119/9-1 well

may serve as a standard for stratigraphic correlation in the southwestern Barents Sea. Micropaleontological and palynological evidence suggest that the top of the Kviting Formation may be as young as late Campanian to Maastrichtian.

The foraminiferal assemblages of the studied wells consist exclusively of agglutinated taxa, suggesting reduced availability of dissolved calcium carbonate in the depositional basins. The composition of the benthic foraminiferal assemblages at the base of the Torsk Formation and in the uppermost part of the underlying Kviting Formation reflects a deep-water (middle or upper bathyal) depositional environment. There is no paleontological evidence of a shallowing of the environment in connection with the „basal Tertiary unconformity" in the Tromsø Basin. Analysis of the benthic foraminiferal morphogroups in the reference section indicates a deepening of the basin until the latest Paleocene, followed by a shallowing of the basin in the early Eocene. As with the benthic foraminifera, the Paleogene diatom assemblages recovered show marked similarities to those present in the North Sea, although there are a number of differences in the stratigraphic ranges of some taxa.

ACKNOWLEDGEMENTS

We thank the Norwegian Petroleum Directorate and STATOIL for kindly providing samples. We are grateful to the STATOIL-VISTA Programme for funding the project. Mufak Naoroz kindly assisted with the sample processing. The manuscript benefited from comments by Geoff Eaton, Jan-Inge Faleide, Felix Gradstein, and Ann Holbourn. This is contribution no. 49 of the Deep-water Agglutinated Foraminifera Project.

REFERENCES

Barron, J.A. 1993. Diatoms. *In*: Lipps, J.H. (ed.) *Fossil Prokaryotes and Protists*, 155-167, Blackwell, Boston.

Berggren, W.A., & Olsson, R.K. 1985. North Atlantic Mesozoic and Cenozoic paleoceanography. *In:* Vogt, P.R. & Tucholke, B.E. (eds.). *The Geology of North America, volume M, The North Atlantic Region,* 565-587, Geological Society of America.

Bettenstaedt, F., Fahrion, H., Hiltermann, H., & Wick, W. 1962. Tertiär Norddeutschlands. *In*: Simon, W. & Bartenstein, H. (eds.) *Arbeitskreis deutscher Mikropaläontologen: Leitfossilien der Mikropaläontologie*, 432 pp. & pls., 2 vols. Gebrüder Bornträger, Berlin.

Calvert, S.E. 1966. Accumulation of diatomaceous silica in sediments of the Gulf of California. *Bulletin of the Geological Society of America*, **77**, 569-596.

Cloetingh, S., Gradstein, F.M., Kooi, H., Grant, A.C., & Kaminski, M.A. 1990. Did plate reorganisation cause rapid late Neogene subsidence around the Atlantic? *Journal of the Geological Society of London*, **144**, 43-58.

Cloetingh, S., Reemst, P., Kooi, H., & Fanavoll, S. 1992. Intraplate stresses and the Post-Cretaceous uplift and subsidence in northern Atlantic basins. *Norsk Geologisk Tidskrift*, **72**, 229-235.

Codispoti, L.A. 1989. Phosphorus vs. nitrogen limitation of new and export production. *In:* Berger, W.H., Smetacek, V.S. & Wefer, G. (eds.), *Productivity of the Ocean: Present and Past*, 377-394, Wiley & Sons, Chichester.

Corliss, B.H., & Chen, C. 1988. Morphotype patterns of Norwegian Sea deep-sea benthic foraminifera and ecological implications. *Geology*, **16**, 716-719.

Dell'Agnese, D.J. & Clark, D.L. 1994. Siliceous microfossils from the warm late Cretaceous and early Cenozoic Arctic Ocean. *Journal of Paleontology*, **68**, 31-47.

Dzinoridze, R.N., Jousé, A.P., Koroleva-Golikova, G.S., Koslova, G.E., Nagaeva, G.S., Petrushevskaya, M.G. & Strelnikova, N.I. 1978. Diatom and radiolarian Cenozoic stratigraphy, Norwegian Basin. DSDP Leg 38 *Initial Reports, Deep Sea Drilling Project, Supplement*, **38-41**, 289-427.

Faleide, J.I., Gudlaugsson, S.T., Eldholm, O., Myhre, A.M., & Jackson, H.R. 1991. Deep seismic transects across the sheared western Barents Sea-Svalbard continental margin. *Tectonophysics*, **189**, 73-89.

Faleide, J.I., Vågnes, E., & Gudlaugsson, S.T. 1993a. Late Mesozoic - Cenozoic evolution of the southwestern Barents Sea. *In:* Parker, J.R. (ed.) *Petroleum Geology of northwest Europe: Proceedings of the 4th Conference*, 933-950, Geological Society, London.

Faleide, J.I., Vågnes, E., & Gudlaugsson, S.T. 1993b. Late Mesozoic - Cenozoic evolution of the southwestern Barents Sea in a regional rift-shear tectonic setting. *Marine and Petroleum Geology*, **10**, 186-214.

Glezer, Z.I., Jousé, A.P., Makarova, I.P., Proshkina-Lavrenko, A.I. & Sheshukova-Poretskaya, V.S. 1974. *The Diatoms of the USSR Fossil and Recent. Vol. 1.* Akademii Nauk SSSR, Botanical Institute, Leningrad, 403 pp., 16 figs., 20 tbs., 93 pls. (In Russian).

Gradstein, F.M., & Bäckström, S. 1996. Cainozoic biostratigraphy and palaeobathymetry, northern North Sea and Haltenbanken. *Norsk Geologisk Tidskrift*, **76**, 3-32.

Gradstein, F.M., & Kaminski, M.A. 1989. Taxonomy and biostratigraphy of new and emended species of Cenozoic deep-water agglutinated foraminifera from the Labrador and North Seas. *Micropaleontology*, **35**, 72-92.

Gradstein, F.M., Kaminski, M.A., & Berggren, W.A. 1988. Cenozoic foraminiferal biostratigraphy of the central North Sea. *Abhandlungen der Geologischen Bundesanstalt*, **41**, 97-108.

Gradstein, F.M., Kaminski, M.A., Berggren, W.A., Kristiansen, I.L., & D'Ioro, M.A. 1994. Cenozoic biostratigraphy of the North Sea and Labrador Shelf. *Micropaleontology*, **40** (Supplement), 1-152.

Hansen, J.M. 1977. Dinoflagellate stratigraphy and echinoid distribution in upper Maastrichtian and Danian deposits from Denmark. *Bulletin of the Geological Society of Denmark*, **26**, 1-26.

Heilmann-Clausen, C. 1985. Dinoflagellate stratigraphy of the upper Danian to Ypresian in the Viborg 1 Borehole, central Jylland. *Denmarks Geologiske Undersøkelse, Series* **A7**, 1-69.

Herguera, J.C., & Berger, W.H. 1991. Paleoproductivity from benthic foraminifera abundance - glacial to postglacial change in the West-Equatorial Pacific. *Geology*, **19**, 1173-1176.

Homann, M. 1991. Die Diatomeen der Fur-Formation (Alt-tertiär) aus dem Limfjord-Gebiet, Nordjutland/Dänemark. *Geologisches Jahrbuch*, Hannover, Reihe A, **123**, 285 pp., 57 pl.

Hughes, M.J. 1981. Contribution on Oligocene and Eocene microfossils from the southern North Sea. *In:* Neale, J.W. & Brasier, M.D. (eds.) *Microfossils from Fos-*

sil and Recent Shelf Seas, 186-294, Ellis Horwood, Chichester.

Jacqué, M. & Thouvenin, J. 1975. Lower Tertiary tuffs and volcanic activity in the North Sea. *In*: Woodland, A.W. (ed.) *Petroleum and the Continental Shelf of Northwest Europe, Vol. 1: Geology*, 455-465, Elsevier, Barking.

Jones, R.W., & Charnock, M.A. 1985. „Morphogroups" of agglutinating foraminifera, their life positions and feeding habits and potential applicability in (paleo)ecological studies. *Revue de Paléobiologie*, **4**, 311-320.

Kaminski, M.A. 1985. Evidence for control of abyssal agglutinated foraminiferal community structure by substrate disturbance - results from the HEBBLE area. *Marine Geology*, **66**, 113-131.

Kaminski, M.A., Boersma, A., Tyszka, J., & Holbourn, A.E.L. 1995. Response of deep-water agglutinated foraminifera to dysoxic conditions in the California Borderland basins. *Grzybowski Foundation Special Publication*, **3**, 131-140.

Kaminski, M.A., Gradstein, F.M., & Berggren, W.A. 1989. Paleogene benthic foraminifer biostratigraphy and paleoecology at Site 647, southern Labrador Sea. *Proceedings of the Ocean Drilling Program, Scientific Results*, **105**, 705-730.

Karpuz, M.R., Gabrielsen, R.H., Engell-Sorensen, L., & Anundsen, K. 1991. Seismotectonic significance of the January 29, 1989 Etne Earthquake, southwest Norway. *Terra Nova*, 3, 540-549.

King, C. 1983. *Cainozoic Micropalaeontological Biostratigraphy of the North Sea*. Institute of Geological Sciences Report 82/7, H.M.S.O., London, 40 pp., 6 pls.

King, C. 1989. Cenozoic of the North Sea. *In*: Jenkins, D.G. & Murray, J.W. (eds.), *A Stratigraphical Atlas of Fossil Foraminifera*, 418-489, 2nd Edition. Ellis Horwood, Chichester.

Knutsen, S.-M., & Vorren, T.O. 1991. Early Cenozoic sedimentation in the Hammerfest Basin. *Marine Geology*, **101**, 31-48.

Knutsen, S.-M., Skjold, L.-J., & Skott, P.H. 1992. Palaeocene and Eocene development of the Tromsø Basin - sedimentary response to rifting and early sea-floor spreading in the Barents Sea area. *Norsk Geologisk Tidskrift*, **72**, 191-207.

Lucas-Clark, J. 1987. *Wigginsiella* n.gen., *Spongodinium*, and *Apteodinium* as members of the Aptiana-Ventriosum complex (fossil Dinophyceae). *Palynology*, **11**, 155-184.

Malm, O.A., Christensen, O.B., Furnes, H., Løvlie, R., Ruselåtten, H. & Østby, K.L. 1984. The Lower Tertiary Balder Formation: an organogenic and tuffaceous deposit in the North Sea region, 149-170. *In*: Spencer, A.M. *et al.* (eds.) *Petroleum Geology of the North European Margin*, Graham & Trotman, London.

McNeil, D.H. 1990. Stratigraphy and paleoecology of the Eocene *Stellarima* assemblage zone (pyrite diatom steinkerns) in the Beaufort-Mackenzie Basin, Arctic Canada. *Bulletin of Canadian Petroleum Geology*, **38**, 17-27.

Mitlehner, A.G. 1994. The occurrence and preservation of diatoms in the Palaeogene of the North Sea Basin. Unpublished Ph.D. thesis, University of London, 292 pp.

Mitlehner, A.G. 1996. Palaeoenvironments in the North Sea Basin around the Palaeocene/Eocene boundary: evidence from diatoms and other siliceous microfossils. *In*: Knox, R.W.O'B., Corfield, R.M., & Dunay, R.E. (eds.) *Correlation of the Early Paleogene in Northwest Europe*. Geological Society Special Publication, **101**, 255-273.

Mudge, D.C., & Bujak, J.P., 1994. Eocene stratigraphy of the North Sea Basin. *Marine and Petroleum Geology*, **11**, 166-181.

Mudge, D.C., & Bujak, J.P., 1996. An integrated stratigraphy for the Paleocene and Eocene of the North Sea. *In*: Knox, R.W.O'B., Corfield, R.M., & Dunay, R.E. (eds.) *Correlation of the Early Paleogene in Northwest Europe*. Geological Society Special Publication, **101**, 91-113.

Murray, J., 1895. A summary of scientific results. *Reports of the Scientific Results of the HMS Challenger*, 1608 pp. Eyre & Spottiswoode, London.

Rea, D.K., Zachos, J.C., Owen, R.M. & Gingerlich, P.D. 1990. Global change at the Paleocene - Eocene boundary: climatic and evolutionary consequences of tectonic events. *Palaeogeography, Palaeoclimatology, Palaeoecology*, **79**, 117-128.

Reemst, P., & Cloetingh, S. 1994. Tectonostratigraphic modelling of Cenozoic uplift and erosion in the southwestern Barents Sea. *Marine and Petroleum Geology*, **11**, 478-490.

Richardsen, G., Vorren, T.O., & Tørudbakken, B.O. 1993. Post-Early Cretaceous uplift and erosion in the southern Barents Sea: a discussion based on analysis of seismic interval velocities. *Norsk Geologisk Tidskrift*, **73**, 3-20.

Riis, F. 1992. Dating and measuring of erosion, uplift, and subsidence in Norway and the Norwegian shelf in glacial periods. *Norsk Geologisk Tidskrift*, **72**, 325-331.

Robert, C. & Chamley, H. 1991. Development of early Eocene warm climates, as inferred from clay mineral variations in oceanic sediments. *Palaeogeography, Palaeoclimatology, Palaeoecology (Global and Planetary Change Section)*, **89**, 315-331.

Rønnevik, H.C. 1981. Geology of the Barents Sea. *In*: *Petroleum Geology of the Continental Shelf of North-West Europe*. 395-406.

Rønnevik, H.C., & Jacobsen, H.P. 1984. Structures and basins in the western Barents Sea. *In:* Spencer, A.M. (ed.) *Petroleum Geology of the North European Margin*. 19-32, Graham & Trotman, London.

Roufosse, M.C. 1987. The formation and evolution of sedimentary basins in the western Barents Sea. *In:* Brooks, J. & Glennie, K. (eds.) *Petroleum Geology of Northwest Europe*, 1149-1161, Graham & Trotman, London.

Round, F.E., Crawford, R.M., & Mann, D.G. 1990. *The Diatoms. Biology and Morphology of the Genera*, 741 pp., Cambridge University Press.

Schröder, T. 1992. A palynological zonation for the Paleocene of the North Sea Basin. *Journal of Micropalaeontology* **11**, 113-126.

Schroeder, C.J. 1986. Deep-water arenaceous foraminifera in the Northwest Atlantic Ocean. *Canadian Technical Report of Hydrography and Ocean Sciences*, **71**, 1-191.

Thomas, F.C. & Gradstein, F.M. 1981. Tertiary subsurface correlations using pyritised diatoms, offshore eastern Canada. *In: Current Research, Part B, Geological Survey of Canada*, **81-1B**, 17-23.

Thunell, R.C., Pride, C.J., Tappa, E. & Muller-Karger, F.E. 1994. Biogenic silica fluxes and accumulation rates in the Gulf of California. *Geology*, **22**, 303-306.

Tocher, B.A. 1987. Campanian to Maestrichtian dinoflagellate cysts from the United States Atlantic Margin, Deep Sea Drilling Site 612. *Initial Reports of the Deep Sea Drilling Project*, **95**, 419-428.

Vinken, R. (ed.) 1988. The Northwest European Tertiary Basin: Results of the International Geological Correlation Programme Project 124. *Geologisches Jahrbuch, Reihe A*, **100**, 1-508.

Walderhaug, O., 1992. Magnitude of uplift of the Stø and

Nordmela Formations in the Hammerfest Basin - a diagenetic approach. *Norsk Geologisk Tidskrift*, **72**, 321-323.

Worsley, D., Johansen, R., & Kristensen, S.E. 1988. The Mesozoic and Cenozoic succession of Tromsøflaket. *In:* Dalland, A., Worsley, D., & Ofstad, K. (eds.) A lithostratigraphic scheme for the Mesozoic and Cenozoic succession offshore mid- and northern Norway. *NPD Bulletin*, **4**, 42-61.

Table 1. Palynomorph distribution in samples from Well 7119/9-1. Depth in metres.

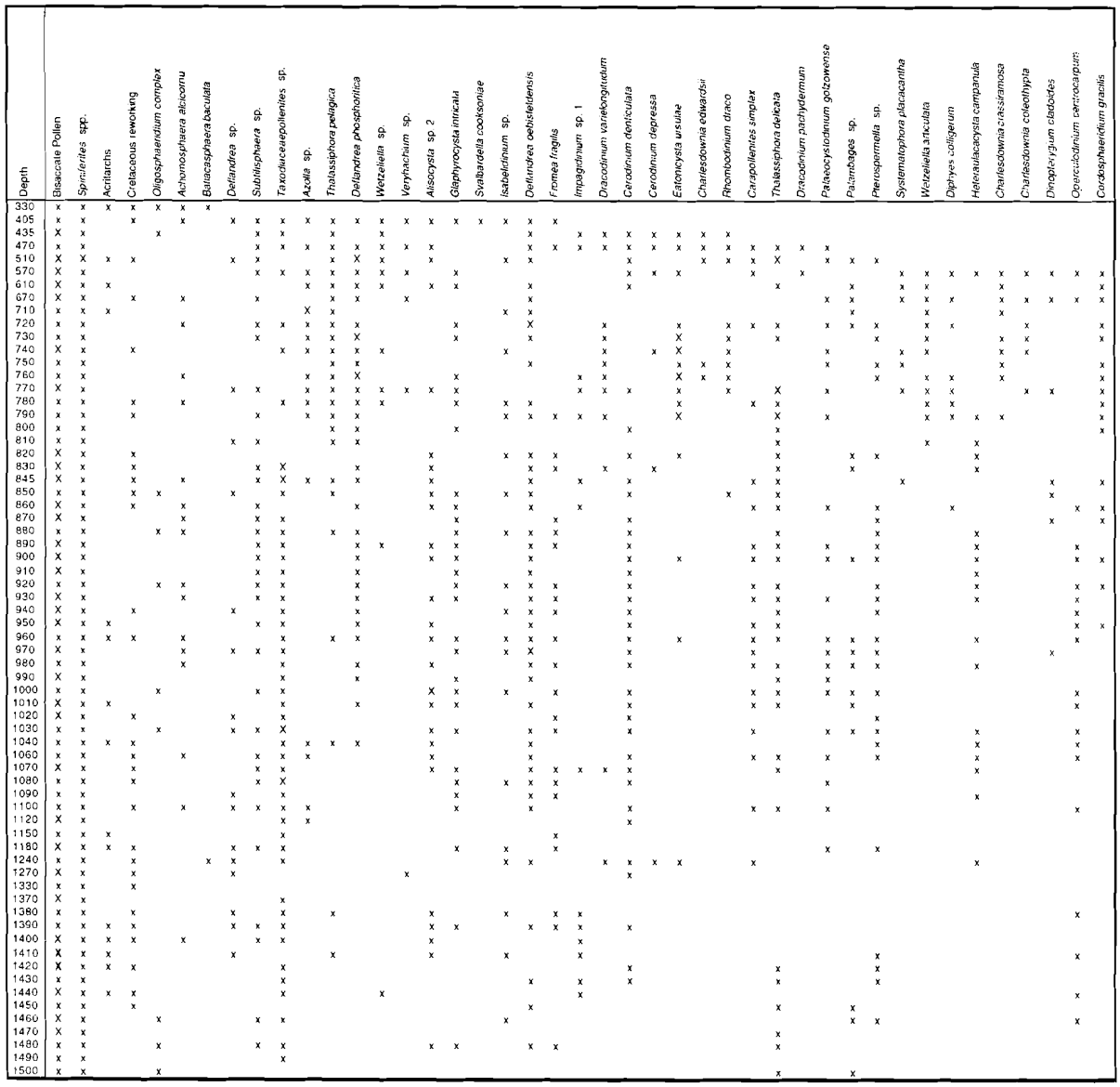


Table 1 (cont.). Palynomorph distribution in samples from Well 7119/9-1. Depth in metres.

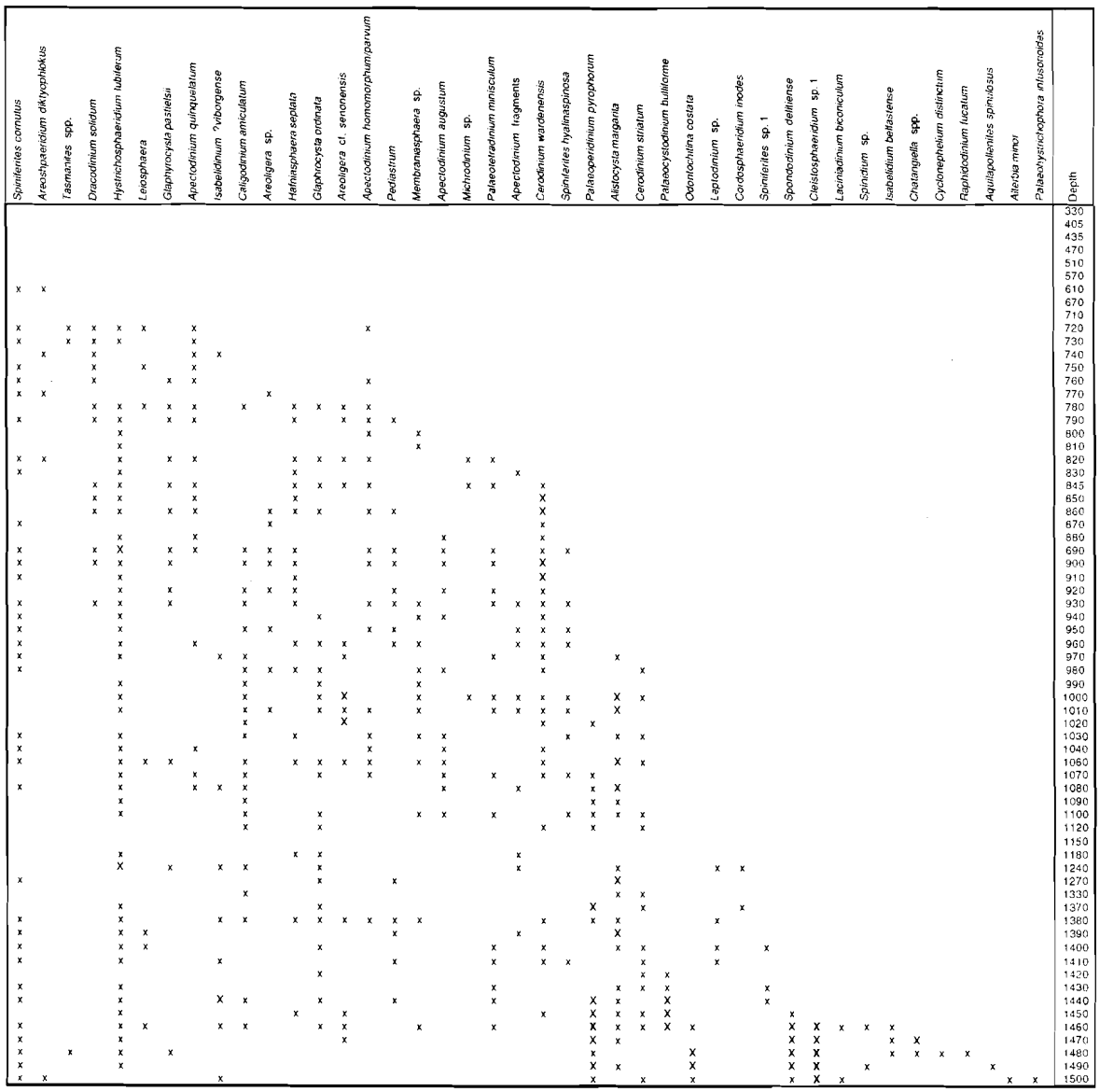


Table 2. Benthic foraminiferal distribution in samples from Well 7119/9-1. Depth in metres.

Depth in well 7119/9-1	*Labrospira sctula*	*Karrerulina horrida*	*Rhizammina indivisa*	*Haplophragmoides excavatus*	*Ammodiscus planus*	*Reticulophragmium amplectens*	*Haplophragmoides porrectus*	*Karrerella conversa*	*Lagenammina*	*Recurvoides* spp.	*Haplophragmoides* spp.	*Haplophragmoides subroticularis*	*Budashevella multicamerata*	*Haplophragmoides eggeri*	*Recurvoidella lamella*	*Cyclammina placenta*	*Hyperammina* spp.	*Trochammina* spp.	*Ammodiscus* spp.	*Eggerella* sp.	*Haplophragmoides* sp. A	*Ammodiscus macilentus*	*Haplophragmoides horridus*	*Haplophragmoides kirki*	*Spiroplectammina navarroana*	*Ammosphaeroidina pseudopauciloculata*	*Rhabdammina* spp.	*Verneuilinoides* spp.	*Trochammina challengeri*	*Rhizammina* sp.	*Psammosphaera bilitalentata*	*Bathysiphon* spp.	*Haplophragmoides* sp. B	*Karrerulina tenuis*	*Trochammina* sp. 6	*Spiroplectammina spectabilis*	*Textularia* sp.	*Nothia robusta*	*Ammodiscus peruvianus*	*Glomospirella hedbergi*	*Ammomarginulina aubertae*	*Glomospira charoides*	*Ammobaculites* sp.
510	2	3																																							
520			1																																							
530			1																																							
540	1		2																																							
550	4		3	6	1	11	1	1																																	
560	3		1	1		1																																			
570				1					1																																
580	1									1																																
590				1							1	2	2																													
600																																									
610				5	1	2								15	1																											
620							2						7	1		5																											
630						2	3	1		1			2	4																													
640				3		1							3																														
650			1	6									1																													
660			4	6			2						4	10			1																									
670			2	1				1		1			1					1																								
680			1	2							2		7	1					1																						
690	3		1	4									4																													
700			4	4			3	2					2									1	1																			
710	29		11	18		14		22		51			9				1	7					8	2	1	5															
720	10		3	8				5		74			4								1	1				1	2	2	1												
730	8		6	20		37	2	12		47			6								4	4			2	2			6	15	2	2	2	6	1						
740		4	5	11		26	6	5		27	17		3					1												19		1			1	1					
750		5	5			12				19	10																		5	5	1	2		1							
760		3				7				6		1	2													1			2								2					
770	6	2	3			6	1			9															2		1			7			1								
790	4	14	7				1			7										1		2					4		1	13	1				2		2	2	1		
800		4	16		2					8	5																			11									2	1	
810		8	4	1	2		2			6	6											6				3	3			40	1	5				3		2		
820	19	4	7					1		9																	2		5	23		12			6	1		1	3	1	
830	10	7			2		5			4								2												16	1	3			5			1			
845	13	2	1				14			13								2				4	2		1	1				10		1			2				1		
850		2	15				4			7	12											1								3	2			1		1			1		
860	5	1	10				8			4															1					9					1						
870	2	4	4				4			3								1												4					2	1					
880	9	2	1							5												2					1			6		1			1	1					
890		1																												1											
900	7	5	4					1														2					1			33					1						
910		7	8			1		2										1				3								32									1		
920		2	15				3	1																						41	1	1			3						
930	14	5			1		1			10								3				4					2			60	2				3	2			3		
940		1	5		1					3								1							1				1	23	2										
950		3	15							7																	3			16	2				1						
960		4	14		1																									37	4					1				1	
970			3				1			5																				13	5										
980			2							5												1					2			10	6										
990				1																							4			47	6										
1000			12		1				1	7																1		1		12	3	10									
1010			2		1				1	2																				46	1										
1020			4				1		1	3								1												12	4										
1030					1																							1		7	1										
1040		2			1					3																	2			8	2								1		
1050										1	2																			2											
1060			1				1																							11	3										
1070			12		1					7			3									1				6	14	1		19	4	2			15						
1080			7								3																			10											
1090			11														1										1			4	2										
1100										1																				13	5										
1110									1		1																			9											
1120							4			2				1													1	3		1		2			4			1			
1130										15				7								1					5	9	3	12	5	6			5			3			
1140			7										25														4	7		10	2	11			2			3			
1150		1					2			12			3						3								4	4	4	43					4						
1160		1	6		2		5			11				3													1	7	1	12	3				15			2			
1180							14		1	12			2														6	46		34	3	3			29						
1190			4				4			9			6									2					7	24	1	5	1	8			21						
1200							4			5																	1	5	2	4		2			11		1				
1220			8		3					8	3		2									4					4	13		16	2				13						
1230			8		4					10			2									3					5			22		1			28						
1240		1	4				3			4		1	2						3						1		2	1	1	11	2				19				2		
1250			3		2		3			2			1					2									2	5		16					7						1
1260			10		2		4			11			3														4	4		11	3	7			72		1				
1270			26		1					29			5					4									13	11		10	1				66		2				
1280			3		2					20			4					1						1			6	17		5	1				33		2				
1290		1	22		3		5			25			1														20	28		23	7				83		8				1
1300			5		2		5			46			3									2					18	6		12	4				92		1				
1310			6		1					68				4													28	13		5					79						
1330			1		1					9	1							2				1					1				1				34	1					
1340			3				1			2												1					2			2					45						
1350			4				3			8								2				3					4	9			1				68						
1360																								2			4	1													
1370			7				2			10																	6	11		3	1				8						
1380			4							9				1													7	8		7	1				17		2				
1390			1				14			5												1					2	1		7	1				22						
1400			9		1					13															16		8					4			22						
1410			22		5		3	1		22	1															7	21			4	7	25			18		3			1	
1420			19		1		2	2		16																	18	1		15	2				14		3				
1430			1		5		1			35								5				4					18	40		3					12					2	
1440								4		34												5				5	14	1		17	6				5		7			2	
1450		5	12		9		2	11		14			1				1	4								3	17	15		10	7	4		1	10		10			1	
1460		14			2		1	14		39		2						3								1	16	9		10		15			14		1			6	
1470		11	7				3	4		20												2				1	11	33		7		5			12		2			2	

Table 2 (continued). Benthic foraminiferal distribution in samples from Well 7119/9-1. Depth in metres.

Kalamopsis grzybowskii	*Psammosphaera irregularis*	*Saccammina placenta*	*Haplophragmoides stomatus*	*Sphaeammina gerochi*	*Glomospira gordialis*	*Haplophragmoides walteri*	*Saccammina grzybowskii*	*Textularia* sp. 3	*Reophax* spp.	*Haplophragmoides* sp. aff. *eggeri*	*Bigenerina* spp.	*Evolutinella rotulata*	*Ammodiscus cretaceus*	*Hyperammina rugosa*	*Reticulophragmium paupera*	*Reticulophragmium* sp. (robust)	*Dorothia* spp.	*Aschemocella grandis*	*Bathysiphon microrhaphidus*	*Hormosina excelsa*	*Eratidus foliaceus*	*Psammosphaera fusca*	*Haplophragmoides* sp. 5	*Parathurammina* spp. ind.	*Reticulophragmoides jarvisi*	*Rzehakina minima*	*Haplophragmoides walteri/jarvisi*	*Rzehakina epigona*	*Jaculella obtusa*	*Glomospira irregularis*	*Spiroplectammina dentata*	*Hormosina ovulum*	*Hormosina velascoensis*	*Ammodiscus glabratus*	*Praecystammina* sp.	*Glomospira glomerata*	*Spirosigmoilinella* sp. 1 (Ch & J)	*Pseudobolivina lagenaria*	*Trochammina subvesicularis*	*Hormosina ganntea*	S	SUM	Depth in well 7119/9-1
																																									2	5	510
																																									1	1	520
																																									1	1	530
																																									2	3	540
																																									7	27	550
																																									4	6	560
																																									2	2	570
																																									2	2	580
																																									4	6	590
																																									0	0	600
																																									5	24	610
																																									4	15	620
																																									6	13	630
																																									3	7	640
																																									3	8	650
																																									6	27	660
																																									6	7	670
																																									6	14	680
																																									4	12	690
																																									7	17	700
																																									13	178	710
																																									12	112	720
																																									19	184	730
																																									14	127	740
																																									10	65	750
																																									8	24	760
																																									10	38	770
																																									15	62	790
																																									8	49	800
2	1	1	1	2																																					21	104	810
		1		1	1	6																																		18	103	820
							1																																		12	57	830
				1		6	1																																		17	75	845
								1																																	12	50	850
									1																																9	40	860
							1																																		10	26	870
																																									10	29	880
																																									2	2	890
						2																																			9	56	900
						3	2			8	1																														12	69	910
						2				8	2																														11	79	920
											2	2																													15	114	930
									1	14																															11	53	940
	1									12																															9	60	950
										14																															8	76	960
										7																															6	34	970
										13																															7	41	980
										9																															5	67	990
										14																															10	62	1000
										9																															7	62	1010
										9																															8	35	1020
										1																															5	11	1030
										3																															7	20	1040
																																									3	5	1050
	1									8																															6	25	1060
1						12		2		8			1																													17	109	1070
														4	16																										5	40	1080
						8								6																											7	33	1090
						14	1			1				3	3	1																										9	42	1100
						2								1	1																											6	15	1110
						6																																			10	25	1120
						14									1		1	1																							15	88	1130
															15																										10	86	1140
	3					6								1	6		1		1																						15	98	1150
						4							1		6																											16	80	1160
1						20	1	2					6				1				1																					17	182	1180
													7		4		2	2	2																						17	103	1190
						5							1						5	1																					13	47	1200
	1					3									3																											14	83	1220
	2			1		11									4		4					2																			15	107	1230
						4								1			2																									18	64	1240
						13									1		1		3																							15	62	1250
						36							4		2		4																									16	178	1260
					2	48							4	8				1					1																		17	232	1270
						27								7			3	1		2																					17	135	1280
	1					49									2		4																									17	283	1290
						51							3		1								1	1																		17	253	1300
	1	1				39							4		6								1		1																15	257	1310
1						5								4																												13	62	1330
						10		1	1					2												2																12	72	1340
1			3			7								20										4			1														15	138	1350
						3								7																												7	26	1360
		1				12							1	16						3							1														14	82	1370
						9																						1													11	66	1380
						10																						2													11	66	1390
						17								10																												9	100	1400
				3		13	1							19								1	3																		21	182	1410
		1				15								26								1	4																		17	141	1420
						38			4					53									83	1	2																17	307	1430
		3				15								35									36	3	1							1									18	194	1440
		1	1			12	2							36					1	4			24	3																28	221	1450
1	1	1				6	2		4					24								1	35	4	4						1		1	1	3	3	4	2	1	2	2	1		27	233	1460
3	2	2	1			5	2		1				1							2	2	2	1	2						1		3	2	1	1		1	1		1	2	8	28	147	1470

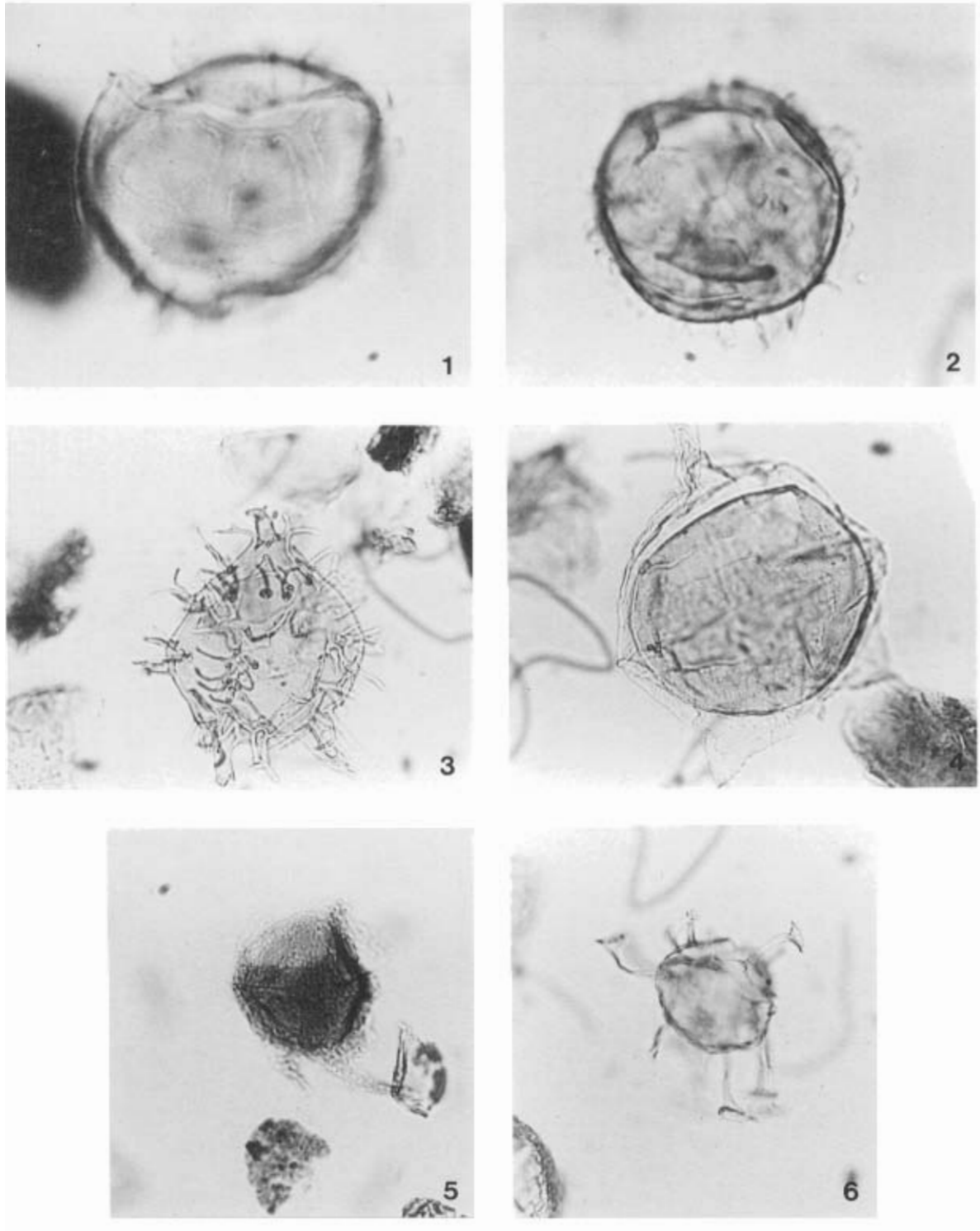


Plate 1. Stratigraphically important palynomorphs from the western Barents Sea. **1,2.** *Alisocysta* sp. 2 Heilmann-Clausen, 1985, x1000. **3.** *Apectodinium quinquelatum* (Williams & Downie) Costa & Downie, 1979, x500. **4.** *Deflandrea oebisfeldensis* Alberti, 1959b, x500. **5.** *Deflandrea denticulata* Alberti, 1959b, x500. **6.** *Hystrichosphaeridium tubiferum* (Ehrenberg) Deflandre emend. Davey & Williams, 1966b, x500.

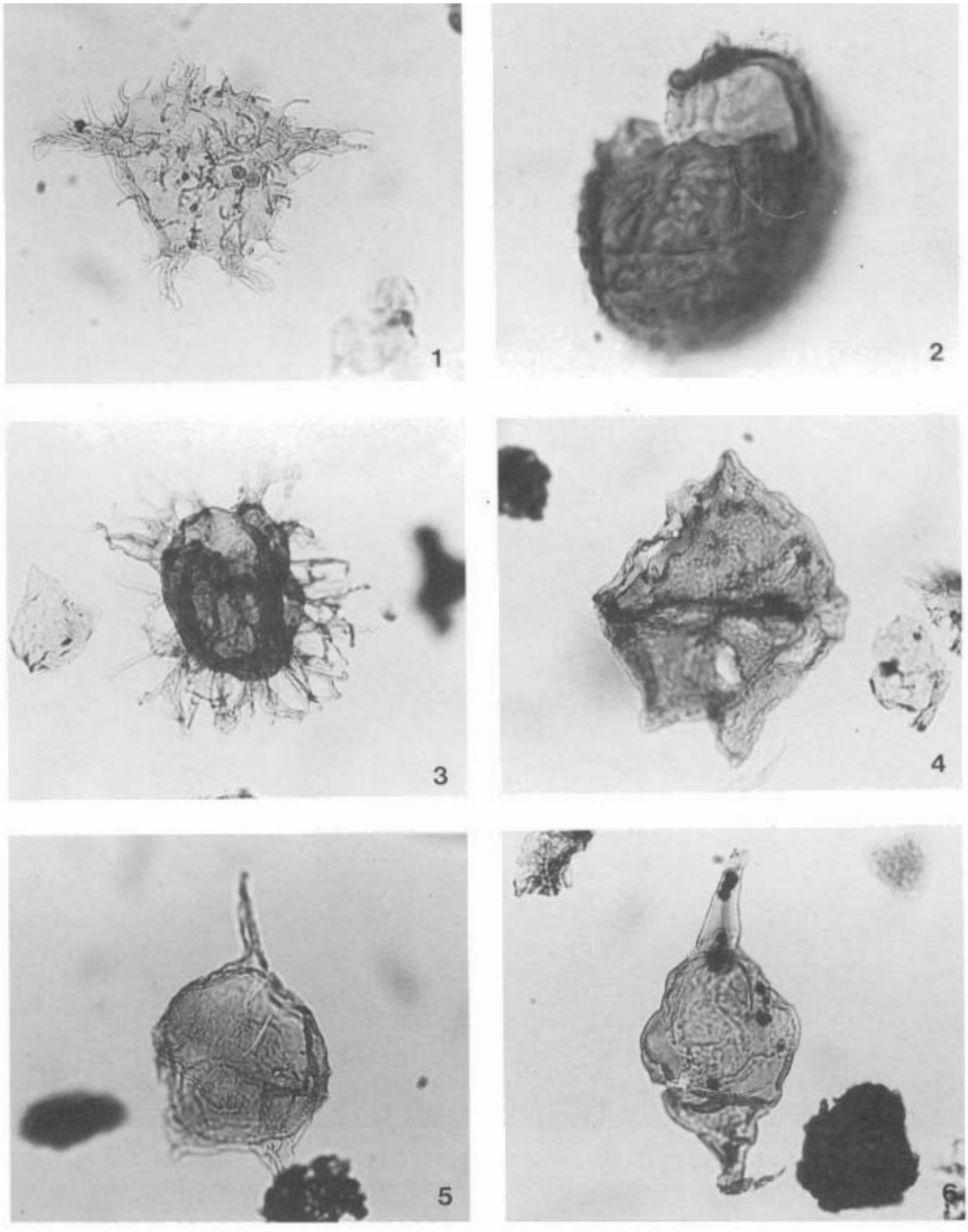


Plate 2. Stratigraphically important palynomorphs from the western Barents Sea. **1.** *Apectodinium augustum* (Harland) Lentin & Williams, 1981, x300. **2.** *Alisocysta margarita* (Harland) Harland, 1979a, x1000. **3.** *Areoligera* cf. *senonensis* Lejeune-Carpenter, 1938, x500. **4.** *Palaeoperidinium pyrophorum* (Ehrenberg) Sarjeant, 1967b, x500. **5.** *Cerodinium striatum* (Drugg) Lentin & Williams, 1987, x500. **6.** *Palaeocystodinium bulliforme* Ioannides, 1986, x250.

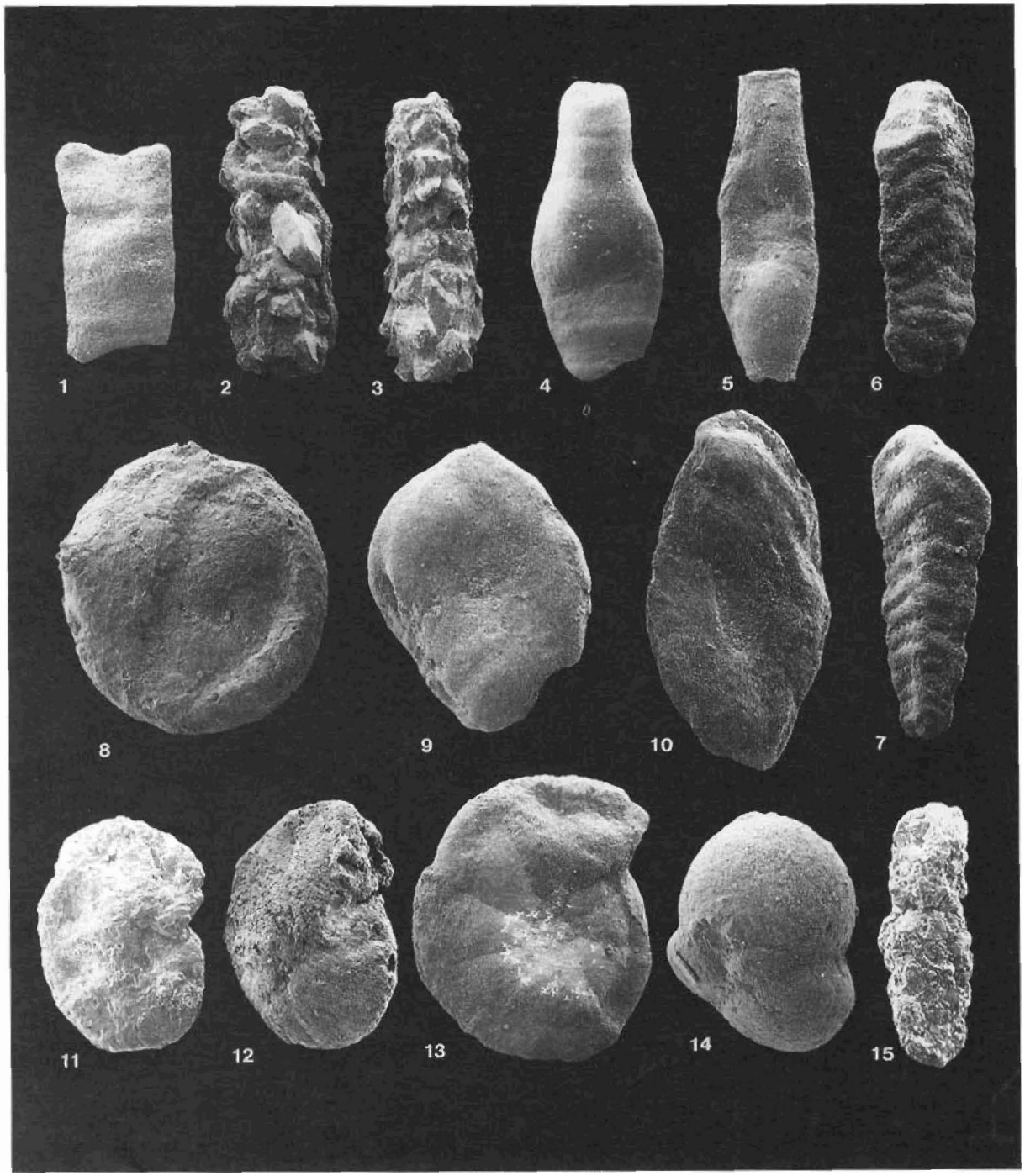


Plate 3. Stratigraphically important benthic foraminifera from Well 7119/1. **1.** *Nothia robusta* (Grzybowski), x37. **2.** *Hyperammina rugosa* Verdenius & Van Hinte, 1320m, x28. **3.** *Hyperammina rugosa*, x45. **4.** *Caudammina excelsa* (Dylazanka), 1350m, x33. **5.** *Kalamopsis grzybowskii* (Dylazanka), 1349, x140. **6.** *Spiroplectammina spectabilis* (Grzybowski) megalosphaeric, 1370m, x80. **7.** *Spiroplectammina spectabilis* microspaeric, 1370m, x80. **8.** *Saccamina placenta* (Grzybowski), 1320m, x78. **9.** *Rzehakina epigona* (Rzehak), 1380m, x70. **10.** *Rzehakina minima* Cushman & Renz, 1330m, x145. **11.** *Haplophragmoides excavatus* Cushman, x93. **12.** *Reticulophragmium amplectens* (Grzybowski), x90. **13.** *Reticulophragmium pauperu* (Chapman), 1380m, x45. **14.** *Praecystammina* sp., 1380m, x160. **15.** *Karrerulina* sp., x115.

Late Pliocene/Pleistocene calcareous plankton and paleoceanography of the North Atlantic

HELGE MEGGERS and KARL-HEINZ BAUMANN

Fachbereich Geowissenschaften, Bremen University, D-28334 Bremen, Postfach 330 440, Germany

ABSTRACT

The calcium carbonate record, abundances and numbers of planktonic foraminifera and coccolithophorids, and the biometry of the foraminifera species *Neogloboquadrina pachyderma* sin. and *Neogloboquadrina atlantica* sin. from DSDP Site 552 have been analyzed for the time interval 3.2 Ma to 0.8 Ma. The different records are used to examine environmental changes in the North Atlantic, especially on the Rockall Plateau, and for comparison in the northern Labrador Sea (ODP Site 646).

The planktonic assemblages in the late Pliocene consisted mainly of subpolar to temperate species; warm-water adapted species were relatively rare. The increase in the influence of polar surface waters at 2.5-2.4 Ma is indicated by an increase in the abundance of cold-water adapted coccolithophore *Coccolithus pelagicus*. However, this corresponds to an increase in subpolar *N. pachyderma* dex., indicating that conditions during this „cold" phase would be analogous to intermittent interglacials of the late Pleistocene. Today's cold water-adapted *N. pachyderma* sin. first occurred at 1.8 Ma. Relatively high abundances during the interval 1.8-1.35 Ma seem to indicate relatively cold surface temperatures, whereas the absence of *N. pachyderma* sin. during the short interval 1.35-1.2 Ma probably indicates somewhat warmer surface water temperatures. However, using factor analysis, it is shown here that *N. pachyderma* sin. first showed a polar biogeographical distribution at 1.1 Ma, while it is a subpolar indicator between 1.8 Ma and 1.1 Ma.

The biometric data of *Neogloboquadrina* tests at both sites indicate an evolutionary trend from large-sized *N. atlantica* sin. before 2.4 Ma via morphological integrade-forms („*N. atlantica-pachyderma* integrade") to small-sized *N. pachyderma* sin. between 1.8 Ma and 1.1 Ma.

INTRODUCTION

The circulation system in the North Atlantic has a strong impact on both the climate of the adjacent continents and the storage of carbon in the ocean. Therefore, details about the paleoceanographic development of the surface circulation system are invaluable for understanding the environmental changes of the northern hemisphere climate. The major northern hemisphere climatic cooling in the open North Atlantic is generally observed close to 2.7-2.5 Ma when extreme ice rafting occurred for the first time (Shackleton *et al.*, 1984; Ruddiman *et al.*, 1986a; Raymo *et al.*, 1989). However, Shackleton *et al.* (1984) demonstrated that considerable climatic variability existed during the million year prior to the initial glacial event. A pattern of regular climate oscillations which become progressively „colder", more positive in $\delta^{18}O$, was observed between 3.2 Ma and 2.6 Ma (e.g., Shackleton *et al.*, 1984; Raymo, 1992). This is also shown by sea surface temperature (SST) estimates from planktonic foraminifera using transfer functions (Dowsett & Poore, 1990). The problem in doing this is that the ecologic preferences of extinct species like *Neogloboquadrina atlantica* and *Globorotalia puncticulata* cannot be exactly characterized. To solve this problem a similar but less rigorous transfer function has been used to quantify the ecological niche of extinct species by comparing with stable isotope data (Hooper & Funnell, 1986). Extinct species are

In: Hass, H.C. & Kaminski, M.A. (eds.) 1997. Contributions to the Micropaleontology and Paleoceanography of the Northern North Atlantic. *Grzybowski Foundation Special Publication*, no. 5, pp. 39-50

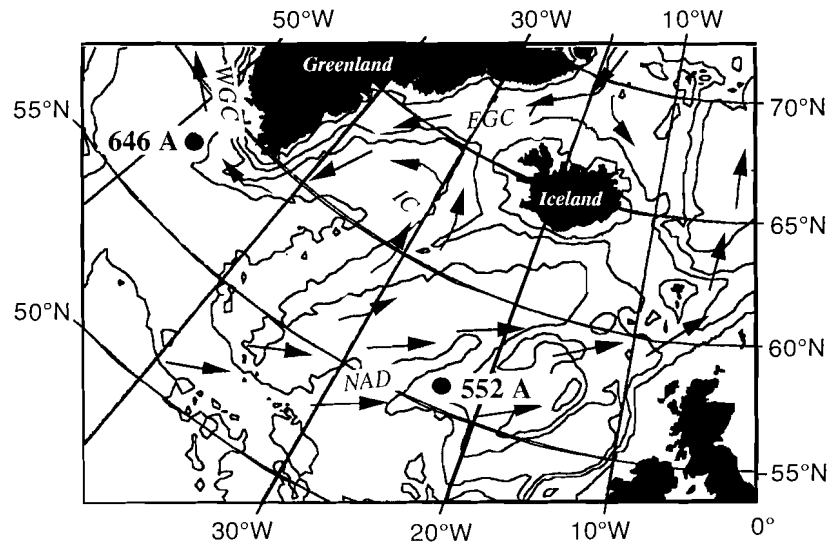


Figure 1. Locations of DSDP Site 552 and ODP Site 646, as well as present-day major surface water circulation (EGC - East Greenland Current,WGC - West Greenland Current, IC - Irminger Current, NAD - North Atlantic Drift).

then substituted by modern analogues, to enable paleotemperatures to be calculated for the Pliocene.

The general evolution of North Atlantic surface water conditions over the last three million years has been described in detail in several key papers (e.g., Shackleton *et al.*, 1984; Zimmerman *et al.*, 1984; Ruddiman *et al.*, 1986a, 1989; Raymo, 1992). Prior to about 1.2 Ma climate variations are characterized by a strong 41 kyr obliquity frequency (Raymo *et al.*, 1989; Ruddiman *et al.*, 1989). For most of the interval from 2.6-1.2 Ma, cold extremes are most analogous to interglaciations (Substage 5d), whereas many warm extremes had more ice and/or probably colder ocean temperatures than are observed today (Raymo, 1992). Thus, except for some low-carbonate spikes during extreme glacial episodes, most of the sediment is of high carbonate content and, therefore, contains planktonic foraminifers (Zimmerman *et al.*, 1984). This is in drastic contrast to both the Norwegian Sea to the north and the Labrador Sea to the west. Here, most of the interval before 1.1 Ma is characterized by glacial conditions, very low productivity of the surface waters, and thus, very low carbonate contents (Henrich & Baumann, 1994; Meggers, 1996; Baumann *et al.*, in press). The most prominent increase in carbonate as well as the change in the number and composition of the calcareous plankton assemblages occurred at approximately 1.1 Ma to 0.9 Ma (Jansen *et al.*, 1989; Henrich & Baumann, 1994; Meggers, 1996; Baumann & Meggers, 1996). It is now well documented that during this interval the climate cyclicity changed, involving a substantial change in mean state and in amplitude of climatic variations (Ruddiman *et al.*, 1986b, 1989; Ruddiman & Raymo, 1988; Raymo, 1992; Berger & Jansen, 1994).

In this study we present records of calcareous plankton assemblages as well as biometrical data of distinct species from Site 552. On the basis of these data we present an overview of the paleoceanographic evolution of the North Atlantic during the late Pliocene - early Pleistocene. These data are combined with existing data from the northeastern Labrador Sea (Site 646) to examine latitudinal variations of the surface current system. In addition, biometric data of *Neogloboquadrina* tests of both sites provide the foundation for a proposed evolutionary trend within this genus.

DATA AND METHODS

DSDP Site 552 was drilled in 2301m water depth on the southwest flank of the Rockall Plateau (Fig. 1). The site is located beneath the diffuse eastern extension of the North Atlantic Current. All cores from Hole 552A were extremely well preserved with the exception of Core 552A-6 (24-29 mbsf). However, despite severe disturbance during core recovery, samples of Core 552A-6 were incorporated in this investigation to compare the test size range of *N. pachyderma* sin. within the lower and upper sediment sections. Interpretations of these samples have to be considered very carefully. Site 646 was drilled on the northern flank of the Eirik Ridge in the northern Labrador Sea and is located beneath the present-day subpolar West Greenland Current in a water depth of 3451m (Fig. 1).

The chronology of the investigated sites is based on oxygen isotope stratigraphies and paleomagnetic data, which have previously been published (e.g., Krumsiek & Roberts, 1984; Shackleton & Hall, 1984; Shackleton *et al.*, 1984). The stratigraphies were updated and/or summarized by Raymo *et al.* (1989) for Site 552, and by Aksu *et al.* (1992) and Baumann & Meggers (1996) for Site 646. All ages were converted to the new time scale of Shackleton *et al.* (1995), proposed for the last 14.8 m.y. (Chron C1 through Chron C5AD). All ages (including previously published ages) used in the following have been converted to this new time scale.

Sediment samples were freeze-dried, weighed and washed on a 63µm-mesh sieve, and then further split into subfractions. The total abundance of planktonic foraminifera was determined, and specimens counted for the 125-500µm fraction. Samples were split into aliquots of at least 500 specimens. Total foraminifer abundances were converted to „specimens per gram dry weight sediment" (spec./g).

The identification of individual specimens, especially of *N. pachyderma* sin. and *N. atlantica* sin. was sometimes difficult, and was further complicated by test sizes which were in the size range of both species from 2.75 Ma (in the Labrador Sea) and 2.4 Ma (on the Rockall Plateau) to 1.8 Ma. Therefore, forms which integrate morphologically between *N. atlantica* sin. and *N. pachyderma* sin. in this study were called the „*N. atlantica-pachyderma* integrate" and were placed together with *N. pachyderma* sin. within the polar planktonic foraminifera group. All other planktonic foraminifera were interpreted as subpolar. Rare numbers of Pliocene species such as *G. puncticulata* or *Globorotalia crassula* were put into „diverse species".

Coccolith species of 37 samples from Site 552 were counted under the scanning electron microscope (SEM). For quantitative analysis, the <2µm fraction was separated, and micrographs of an arbitrarily selected part of the scanned sample were taken (Baumann, 1990). All particles (usually >1000 particles), including up to about 500 coccoliths, were counted in each sample using x2000 magnification. The quantitative data were recorded as particle percent (grain percent of <63µm fraction) for coccolith species.

Estimates of factor analysis on the planktonic foraminifer assemblage of Site 646 were calculated with the program SYSTAT. For factor analysis we used *N. atlantica* sin. and dex., *N. pachyderma* sin. and dex., *Globigerina bulloides*, and *Turborotalia quinqueloba*. *Globigerinita glutinata* and *Globigerinita uvula*, as well as *Globorotalia inflata*, *Globorotalia truncatulinoides*, and *Globorotalia scitula* are calculated as genus (*Globigerinita* and *Globorotalia*).

For biometric analysis of sinistral *Neogloboquadrina*, the maximum diameter of individual *N. atlantica* sin. and *N. pachyderma* sin. tests (in umbilical view) were measured under SEM at a magnification of x150. All maximum diameters were converted into a median diameter per sample. From 61 samples which are counted to determine the planktonic foraminifer assemblage 37 samples were analysed biometrically (with more than 800 individual measurements).

RESULTS

Planktonic foraminifer assemblages from Site 552 are generally characterized by relatively low diversities (Fig. 2). The total numbers range from 200 to 100,000 spec./g sediment. Warmer water indicators such as *G. bulloides*, *T. quinqueloba*, and *Globigerinita* spp. are present in relatively high steady abundances throughout the investigated interval (Fig. 2). However, there are typical faunal changes which can be summarized as follows:

The interval 3.2-2.4 Ma is generally characterized by relatively high numbers of *N. atlantica* sin. (up to 18,000 spec./g) and *N. pachyderma* dex. (up to 10,000 spec./g). Polar planktonic foraminifer species were not found during this interval. The mean sizes of *N. atlantica* sin. are in the range 275-300µm (compare also with Fig. 5). However, the extreme range in its maximum diameter (200-450µm) possibly indicate that species of „*N. atlantica-pachyderma* integrate" were already present within this interval. A drastic decrease in maximum test size to generally <250µm at around 2.4 Ma corresponds well with counting results. *N. atlantica* sin. is nearly absent from the planktonic foraminifer assemblage, while *N. pachyderma* dex. is the most dominant species (numbers >75,000 spec./g) and forms around 50% of the fauna. In addition, the amount of *Globorotalia* spp. increased.

A significant change within the planktonic foraminifer assemblage at 1.8 Ma is indicated by the first occurrence of the modern polar species *N. pachyderma* sin. (Fig. 2). Until 1.4 Ma *N. pachyderma* sin. dominated the assemblage, while the number of *N. pachyderma* dex. decreased to <10,000 spec./g, and *N. atlantica* sin. as well as „*N. atlantica-pachyderma* integrate" disappeared from the assemblage. *N. pachyderma* sin. can only be differentiated from the „*N. atlantica-pachyderma* integrate" by its smaller size and not by its ultrastructure. The maximum test sizes are in the range from 150µm to 250µm. These small sizes lead to the impression that this species is more encrusted than the older *Neogloboquadrina* species or than the modern type of *N. pachyderma* sin.

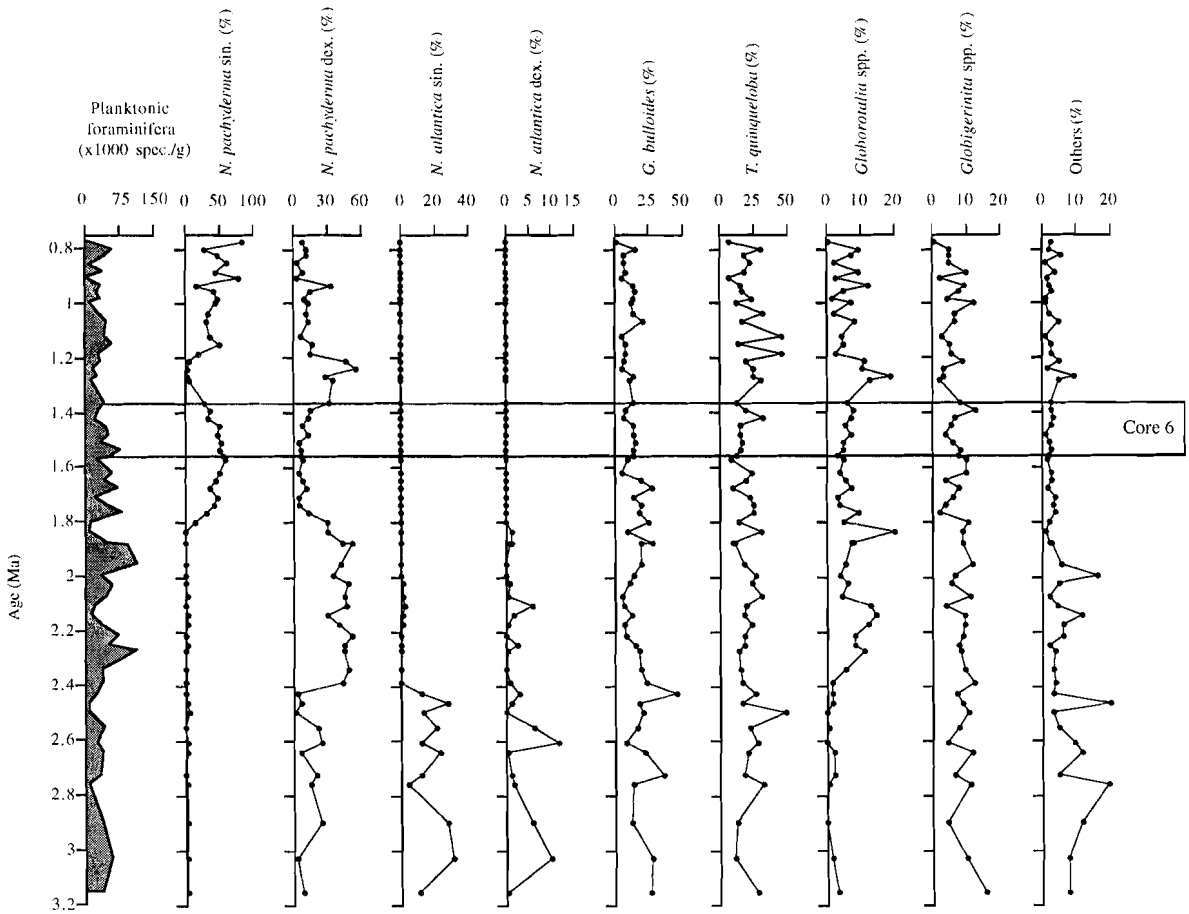


Figure 2. Number of planktonic foraminifera (specimens per gram sediment) and percent-abundance of the main species and species groups of DSDP Site 552 in the interval 3.2 Ma to 0.8 Ma.

Another shift within the planktonic foraminifer assemblage occurred between 1.4 Ma and 1.2 Ma (Fig. 2). *N. pachyderma* sin. nearly disappeared from the assemblage (<10%), whereas *N. pachyderma* dex. increased and formed >30% of the fauna (up to 13,000 spec./g). The sparse tests of *N. pachyderma* sin. only show maximum sizes in the range from 200 µm to about 250 µm, indicating that *N. pachyderma* sin. is the only sinistral *Neogloboquadrina* species which is present during this interval. After 1.2 Ma, the mean size obviously increased and is up to about 350 µm in maximum (compare also with Fig. 5). The foraminifer assemblage again is dominated by *N. pachyderma* sin., but subpolar species such as *G. bulloides*, *T. quinqueloba* (up to 50%) and *N. pachyderma* dex. are also present.

The total abundance of calcareous nannofossils at Site 552 varied strongly and was between 5 and about 60 grain-% in the investigated interval (Fig. 3). The assemblage was generally dominated by few species, usually of *Gephyrocapsa* spp. or *Reticulofenestra* spp.. However, individuals of warmer water-adapted species such as *Helicosphaera carteri*, *Pontosphaera* spp., *Calcidiscus leptoporus*, *Umbilicosphaera sibogae*, *Oolithotus fragilis*, and *Discoaster* spp. were present in low numbers in most of the samples. The development of the assemblage can be summarized as follows:

The total amount of nannofossils was about >40 grain-% prior to 2.5 Ma, and reticulofenestrids (*R. minuta*, *R. minutula*, *R. productella*) dominate the assemblage (Fig. 3). In addition, warmer water-adapted species were also present in moderate abundances. Species of *Gephyrocapsa* as well as *Coccolithus pelagicus*, which is related to cold surface-water temperatures, only occurred in very low numbers.

The total number of nannofossils decreased between 2.5 Ma to 2.4 Ma, and the following interval until 1.1 Ma was characterized by moderate abundances of nannofossils (10-40 grain-%). Gephyrocapsids dominated the assemblage except for the interval 2.5-2.3 Ma and between 2.0-1.7 Ma. Here, cold-water adapted *C. pelagicus* formed up to

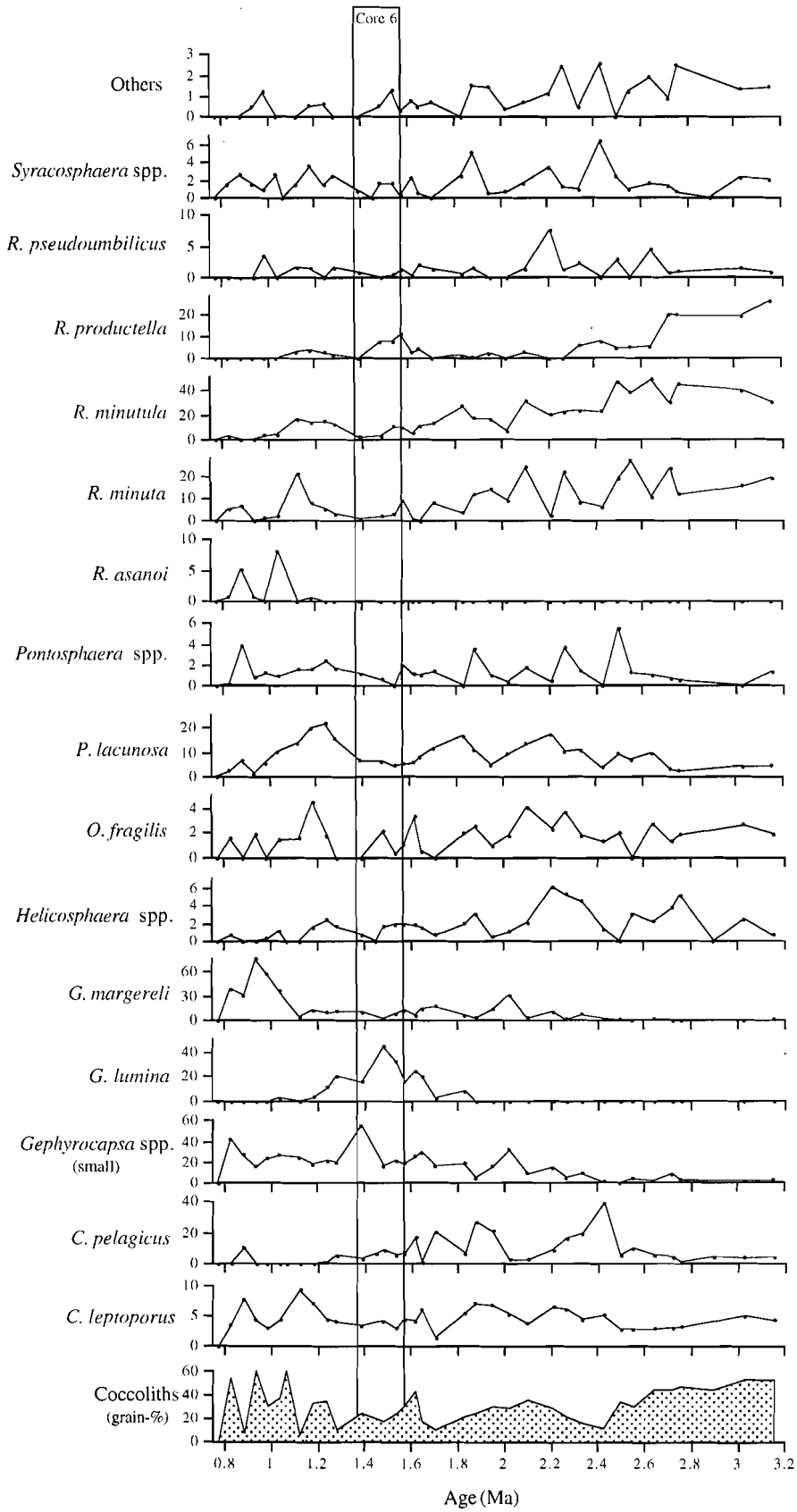


Figure 3. Number of coccolithophores (grain-%), and composition of the coccolithophore assemblage (%) at DSDP Site 552 in the interval 3.2 Ma to 0.8 Ma.

40% of the floral assemblage.

The interval after about 1.1 Ma was characterized by large fluctuations in the abundance of calcareous nannofossils (Fig. 3). They were abundant especially in interglacial stages, whereas during glacials the number drastically decreased. Generally, abundance peaks are higher (up to >60 grain-%) during this interval than observed before. *Gephyrocapsa* species dominated the assemblage while other species reached less than 10%.

PREVIOUSLY PUBLISHED RESULTS

Results of ODP Site 646 in the Labrador Sea have previously been published by Aksu *et al.* (1989, 1992), Aksu & Kaminski (1989), and Baumann & Meggers (1996). In general, the calcareous plankton assemblages are less diverse than the assemblage of the Rockall Plateau. This is most probably due to the influence of cold surface waters as well as the closer proximity of Site 646 to the Greenland ice-shield. In addition, carbonate in the Labrador Sea is far less well preserved than observed on the Rockall Plateau (Meggers, 1996; Baumann & Meggers, 1996). The development of calcareous plankton and the surface water paleoceanography at Site 646 can be summarized as follows:

Relatively low numbers of calcareous nannofossils and planktonic foraminifera, dominated by subpolar species, indicate that the northern Labrador Sea was weakly influenced by warm Atlantic surface waters during parts of the interval 3.1 Ma to 2.8 Ma. The calcareous plankton assemblages indicated an increase in the influence of polar surface waters 2.8 Ma ago. The assemblages were characterized by very low numbers of strongly corroded, cold-water adapted species (*C. pelagicus*, *N. pachyderma* sin.) until 2.3 Ma. Subpolar foraminifera species *T. quinqueloba* and *N. atlantica* sin. temporarily occurred between 2.3 Ma and 1.8 Ma, indicating an episodic inflow of relatively warm surface waters into the northern Labrador Sea. The interval 1.8 Ma to 1.5 Ma was marked by a series of strong environmental shifts in the surface water regime. Relatively high amplitudes in the biogenic calcareous records and abundant warm-adapted species indicate the presence of relatively warm surface waters during climatic optima, although cold-adapted species dominated throughout this interval. A significant decrease in the numbers of calcareous nannofossils and planktonic foraminifers at 1.5 Ma was related to another cooling that lasted until about 1.1 Ma. During the last 1.1 m.y., abundant warm-adapted species indicate the presence of relatively warm surface waters during interglacials, while scarce polar assemblages are related to variable conditions dominated by at least seasonal sea-ice cover during glacials.

In addition, a morphological transformation from large *N. atlantica* via median-sized „*N. pachyderma* integrate" to modern *N. pachyderma* sin. was evident at Site 646 between 2.4 Ma and 1.8 Ma.

Based on the high-resolution faunal data of Site 646 a factor analysis has been carried out. Factor analysis indicate two different paleoecological interpretations of the *Neogloboquadrina* taxon. Two factors (polar and subpolar) are statistically relevant for Site 646 within the limits of confidence by the Kaiser-criterion (compare with Backhaus *et al.*, 1994). Over 80% of the variance can be explained by the two varimax rotated factors.

While *N. pachyderma* sin. scores highly on the polar factor after the mid-Pleistocne transition, it shows high factor loadings on the subpolar factor before 1.1 Ma (Table 1). Within the time-period between 3.2 Ma and 1.1 Ma *N. atlantica* sin., the „*N. atlantica-pachyderma* integrate" and the small individuals of *N. pachyderma* sin. (between 1.8 Ma and 1.1 Ma) were combined with species like *G. bulloides*, *T. quinqueloba*, *G. inflata*, *G. glutinata* in the subpolar group.

Table 1. Factor matrix for the samples of ODP Site 646.

Factor matrix Site 646	3.2 Ma -1.1 Ma	1.1 Ma - 0 Ma
	"subpolar"	"polar"
N. pachyderma sin.	0.871	-0.522
N. pachyderma dex.	0.866	0.469
N. atlantica	-0.034	
G. bulloides	0.643	0.444
T. quinqueloba	0.793	0.654
Globorotalia	0.635	0.608
Globigerinita	0.776	0.575
Variance	50.820	30.274

DISCUSSION

Surface-water paleoceanography: Comparison of Sites 552 and 646 calcareous plankton data

The fluctuations in Pliocene/Pleistocene calcareous faunal and floral data at Site 552 suggest periodic changes in surface water conditions, although the sampling resolution was not high enough to demonstrate cyclicity. However, as previously shown, variations in high-resolution records of $\delta^{18}O$ and $CaCO_3$ at Site 552 were dominated by the 41 kyr component of the orbital obliquity during most of the late Pliocene/early Pleistocene (Shackleton & Hall, 1984; Raymo *et al.*, 1989). A development of the calcareous plankton and surface water paleoceanography as observed at Site 646 could not be determined. It seems reasonable to suggest that over the time-scale con-

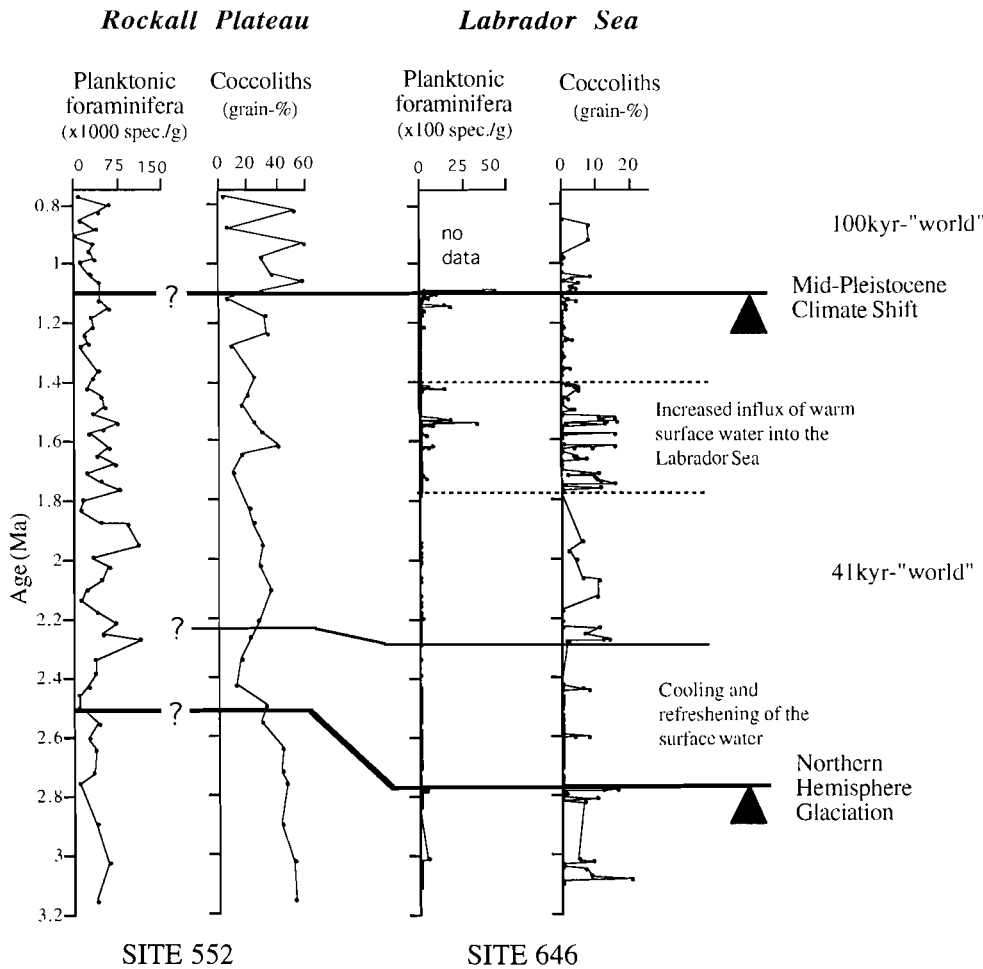


Figure 4. Comparison of the absolute abundances of both coccolithophores and planktonic foraminifera at Sites 646 and 552. Main palaeoceanographic events are indicated by horizontal lines.

sidered here the ecological conditions during interglacials did not change appreciably on the Rockall Plateau. Only spikes of low coarse fraction carbonate associated with glacial stages suggest particularily intense cold periods during which surface productivity was reduced (Zimmerman *et al.*, 1984).

Thus, between 3.2 Ma and 0.8 Ma strong gradients in the number of calcareous planktic organisms were present between the Rockall Plateau and the northern Labrador Sea (Fig. 4). The number of planktonic foraminifers is several times higher in the northeastern North Atlantic compared to the area south of Greenland. In addition, the latter area is characterized by long-lasting intervals nearly barren in foraminifers and calcareous nannofossils, whereas on the Rockall Plateau the calcareous fauna and flora is present throughout the investigated interval. These differences are not only due to strong carbonate dissolution in the Labrador Sea (Baumann & Meggers, 1996), but are probably caused by drastic differences in the productivity of calcareous plankton. Although there is no clear evidence for a strong cooling trend in the latest Pliocene to Pleistocene calcareous plankton record at Site 552, it is notable that *N. atlantica* and the reticulofenestrids nearly disappeared in the latest Pliocene-earliest Pleistocene. The last appearance as well as the drastic decrease in abundance of these taxa must also be interpreted as a response to changed environmental conditions. Similar regional extinctions, which were also described for other planktonic organisms in the study area (e.g. dinoflagellates, de Vernal & Mudie, 1992), probably suggest the onset of harsh environmental conditions and may be attributed to surface water cooling. At Site 552, this is also shown by the increase in abundance of cold-water adapted coccolithophore species *C. pelagicus* during the interval 2.4-2.2 Ma. Nevertheless, a disappearance of most of

the taxa in response to the development of an extensive sea ice cover and to cooling and/or refreshening of the surface water as observed in the Labrador Sea are not inferred for the northeastern North Atlantic.

These data indicate that the thermal gradient between the two areas was strong throughout most of the late Pliocene to early Pleistocene interval. Site 552 is located beneath the diffuse eastern extension of the North Atlantic Current, whereas Site 646 is influenced by the subpolar West Greenland Current which is fed by both the polar East Greenland Current and the subpolar Irminger Current, a branch of the North Atlantic Drift. Hence, the Labrador Sea was heavily influenced by polar, ice-ladden surface water after the northern hemisphere cooling started. The calcareous fauna and flora indicate that surface paleoceanographic conditions off southern Greenland were mostly very different compared to that in the Rockall Plateau area. The assemblages are characterized by very low numbers of cold-water adapted species during most of the interval until about 1.1 Ma. Almost monospecific assemblages of *N. pachyderma* sin. at Site 552 are first observed in the upper Pleistocene (Hooper & Funnell, 1986). Thus, repeated migrations of the polar front across this site did not occur before 1.1 Ma when amplitudes of glacial /interglacial cycles drastically increased (Jansen *et al.*, 1989; Ruddiman *et al.*, 1986a). These changes indicate the initiation of warmer interglacials with warmer surface water influx not only into the Labrador Sea (Aksu *et al.*, 1989; Baumann & Meggers, 1996) but also into the Norwegian-Greenland Sea (Henrich *et al.*, 1989; Jansen *et al.*, 1989; Baumann *et al.*, in press).

Despite all these gradients, there are similarities in the biometrical evolution of *Neogloboquadrina* species indicating a convergent biometrical evolution of this genus in both the northeasten North Atlantic and the northwestern North Atlantic.

Surface water temperature in the Pliocene - early Pleistocene North Atlantic: The possibility of a reconstruction

All paleoecological work on plankton is based on the fundamental assumption that the pelagic ecosystem being sampled today has remained unchanged during the examined time period. The most common technique used with planktonic foraminifers is the transfer-function pioneered by Imbrie & Kipp (1971). The downcore use of different transfer functions to calculate SST back in the early Pleistocene and in the Pliocene has been carried out by various working groups (Thunell, 1979; Hooper & Funnell, 1986; Dowsett & Poore, 1990; Dowsett, 1991). Thunell (1979) used the Imbrie & Kipp (1971) model to calculate paleotemperatures for the last 5.0 m.y. in the Mediterranean area, making the basic assumption that evolving lineages of planktonic foraminifera retain nearly the same ecological requirements throughout their history. Dowsett & Poore (1990) and Dowsett (1991) used such a technique to calculate Pliocene to Pleistocene SST in the North Atlantic. Mostly extinct Pliocene species were assumed to be ecologically equivalent to closely related modern forms. For example the extinct planktonic foraminifer *G. puncticulata* is compared with the modern related species *G. inflata* (Dowsett & Poore, 1990). In the Pliocene *N. atlantica* was substituted for sinistral *N. pachyderma* to enable paleotemperatures for this time period by Hooper & Funnell (1986). From the results of Hooper & Funnell (1986), we consider *N. atlantica* sin. to be a polar species, since it shows highest abundances during glacial intervals. In contrast to this, *N. atlantica* sin. was regarded as a subpolar species by Poore & Berggren (1975) and by Kennett & Srinivasan (1980) by morphological comparison between *N. atlantica* sin. and *Neogloboquadrina dutertrei.*

In the present study we have concentrated on both the planktonic foraminifer assemblage and the morphological characteristics of key-species. Although there are strong thermal gradients in surface water between the Labrador Sea and the Rockall Plateau (see above) the comparison of the biometrical record with assemblage and isotope data (compare Ruddiman *et al.*, 1986b) indicate that the calculation of Pliocene - early Pleistocene SST by using transfer functions is very difficult and should be performed with caution.

A similarity between both sites is the time-transgressive disappearance of *N. atlantica* sin. after the intensification of the northern hemisphere cooling at 2.4 Ma (Fig. 5). The number of sinistral *Neogloboquadrina* decreased between 2.4 Ma and 1.8 Ma within the sediments of both the northern Labrador Sea and the Rockall Plateau. In the North Atlantic the last appearance of *N. atlantica* sin. provides a useful biostratigraphic datum. Several analyses indicate a last occurrence of this species between 2.4 Ma and the Pliocene/Pleistocene boundary. Hooper & Weaver (1987) give an extinction point of 2.3 Ma at ODP Sites 609, 610 and 611. This axgrees well with the extinction points in this study and in the investigations of Spiegler & Jansen (1989) for the Vøring-Plateau, Pujol & Duprat (1985) for the Goban Spur, and Zachariasse *et al.* (1990) for the Mediterranean. Further investigations on test sizes of *N. atlantica* sin. and *N. pachyderma* sin. may help to distinguish these species in the upper Pliocene to lower Pleistocene sediment

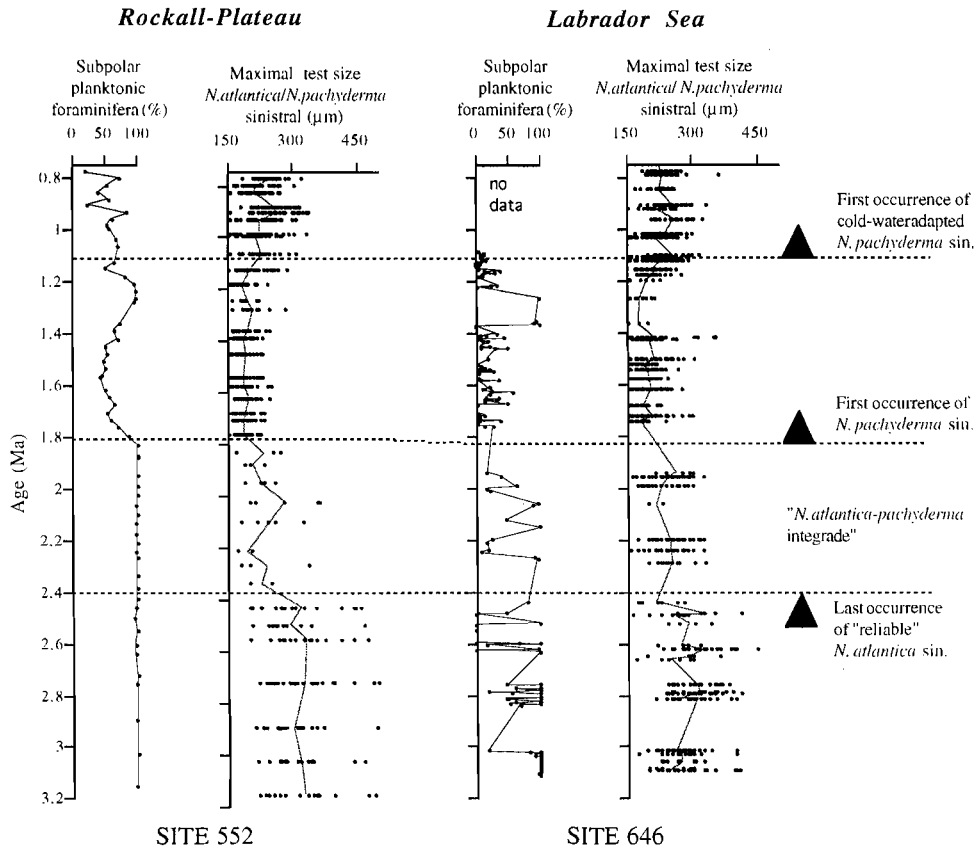


Figure 5. Biometrical measurements of *N. pachyderma* sin./*N. atlantica* sin. (maximum diameter) as well as the amount of subpolar planktonic foraminifera during the time interval 3.2-0.8 Ma for DSDP Site 552 and ODP Site 646. Median test size of each sample is indicated by the traced line. Note that *N. pachyderma* sin. in the abundance-plots is used as a polar species although this interpretation is not supported by the results presented in this paper.

sections of the North Atlantic

The second synchronous event is the appearance of the small *N. pachyderma* sin. at 1.8 Ma. The small size of *N. pachyderma* sin. in this interval gives the impression that this species are more heavily encrusted (compare Hooper & Weaver, 1987) than *N. atlantica* sin. or the „*N. atlantica-pachyderma* integrate". Also synchronous is the redisappearance of *N. pachyderma* sin. from the planktonic foraminifer assemblage between 1.35 Ma and 1.2 Ma. This may indicate that there are morphological changes in the taxon *Neogloboquadrina* due to the drastic climatic and ecological changes of the Northern Hemisphere in this time. Also the last synchronous pattern, the trend to larger sized *N. pachyderma* sin. in the whole North Atlantic, suggests an evolutionary trend in cold-water adapted *Neogloboquadrina* (Fig. 5). This evolution influenced the temperature preferences of the species *N. atlantica* sin. and *N. pachyderma* sin. Due to the strong similarities in the biometrical evolution of *Neogloboquadrina*, it could be stated that the cooling of the Northern Hemisphere influenced the planktonic foraminifer assemblages, as it is shown for the lineage *Neogloboquadrina acostaensis - Neogloboquadrina humerosa - N. dutertrei* by Biolzi (1991), for the lineage *G. puncticulata - G. inflata* by Wei (1994) and for the lineage *Globorotalia crassaformis - Globorotalia tosaensis - G. truncatulinoides* by Lazarus *et al.* (1995). In all these lineages changes in the oceanographic conditions triggered the disappearence of ancient species followed by a first appearance of new species. The coincidence between paleoceanographic events and biometrical/morphometrical changes suggest that paleoenvironmental changes cause developmental perturbations. Oceanic conditions influence the size, the shape and the developmental timing of planktonic foraminifera (Wei, 1994). The different planktonic foraminifer lineages responded to the Northern Hemisphere cooling events by morphological variations and by diversification.

In Site 552 a no-analogue assemblage (compared with the isotope record of benthic foraminifers) precludes making credible SST estimates in the interval 1.3-1.2 Ma (Ruddiman *et al.*, 1986b). Only the record above 1.1 Ma is suitable for SST estimates and related time-series analysis. Low numbers of *Globigerinoides ruber* and other low-latitude species indicate that warm subtropical conditions did not develop during this interval. The fauna in this time-period consisted of *N. pachyderma* dex. (see also Ruddiman *et al.*, 1986b). Within this interval, there are three brief pulses of heavier benthic foraminiferal oxygen isotopic values, suggesting a greater ice-volume on the surrounding continents (Shackleton & Hall, 1984; Shackleton *et al.*, 1984). Also the $CaCO_3$-record shows synchronous minima (Zimmerman *et al.*, 1984), implying dissolution of carbonate particles on the sea-floor, increased dilution by IRD, or suppression of productivity in surface waters. Analyses concerning the carbonate dissolution on the Rockall Plateau indicate a relatively good carbonate preservation over the whole time period from 3.2 Ma to 0.8 Ma (Diester-Haass & Schnitker, 1989; Meggers, 1996). Investigations of the benthic foraminifer assemblage also indicate that the main body of benthic species are characteristic of North Atlantic Deep Water (NADW) (Murray, 1984). It may therefore be assumed that either non-corrosive NADW has occupied the Rockall Plateau area throughout most of the Neogene. While the northern Labrador Sea is a very sensitive area for NADW-production, depending on the establishment of meridional circulation, the Rockall Plateau was influenced by relatively warm Atlantic surface water for the whole time. Therefore, the out-of-phase link between SST and oxygen isotope record at Site 552 could not be explained with the preservation of carbonate.

Dilution by IRD is much more important in the interpretation of carbonate minima on the Rockall Plateau. For example, after 1.3 Ma, inputs of IRD to the Norwegian Sea generally increased, which is supposed to be due to an intensified glaciation (Jansen *et al.*, 1988). In addition, Spiegler (1989) showed that redeposition of microfossils from the shelf areas increased during glacials after 1.2 Ma. This suggests that continental ice-sheets expanded much further onto the continental shelves after 1.2 Ma than during the interval between 2.5 Ma and 1.35 Ma. Therefore, the explanation for the non-analogue link between SST and oxygen isotope data could be more easily seen in several significant coolings of the North Atlantic ocean that occurred between 1.3 Ma and 1.2 Ma. These coolings are registered in an anomalous way in the genus *Neogloboquadrina* because of a fundamental change in environmental responses of *N. pachyderma* sin., which is the polar end-member in the planktonic foraminifer assemblage. The same pattern of a low-frequency oscillation toward warm SST values near the interval 1.35-1.2 Ma was also seen at Site 607 (Ruddiman *et al.*, 1989). In both cases there are out-of-phase links between SST and benthic oxygen isotope records which are probably artifacts caused only by the absence of the species *N. pachyderma* sin. The speculations of Ruddiman *et al.* (1986b, 1989) are confirmed by the biometrical/paleoceanographical results of this study. In addition, factor analysis of Site 646 planktonic foraminifer data shows that from 1.1 Ma *N. pachyderma* sin. first exhibits a polar adaptation. Raymo *et al.* (1986) have shown that *N. pachyderma* sin. did not take on a distinct „cold-indicator" role in the North Atlantic until 1.7 Ma. This role was abandoned by *N. pachyderma* sin. from 1.3 Ma to 1.2 Ma and finally reacquired at 1.2 Ma to 1.1 Ma with the mid-Pleistocene transition (Ruddiman *et al.*, 1986b). Late Pliocene to Holocene biometrical analyses in the Labrador Sea clearly indicate an increase in maximum diameter of *N. pachyderma* sin. after 1.1 Ma, most probably related to a better adaptation of this species to the extreme glacial conditions (Baumann & Meggers, 1996).

Next to changing surface water conditions between 1.3 Ma and 1.1 Ma changes in deep water chemistry can be detected from carbon isotope studies (Raymo *et al.*, 1990). Raymo *et al.* (1990) concluded that a significant decrease in NADW-production occurred between 1.2 Ma and 1.1 Ma. During the same interval poor carbonate preservation could be seen in the Labrador Sea (Baumann & Meggers, 1996) and in the Norwegian-Greenland Sea (Henrich & Baumann, 1994; Meggers, 1996). It is generally believed that the thermohaline circulation is largely driven through the production of NADW (Johnson, 1982; Raymo *et al.*, 1990). Therefore, the breakdown of this thermohaline circulation cannot only be seen within carbonate preservation patterns and $\delta^{13}C$-values, but also in its influence on the planktonic foraminifer assemblage (Meggers, 1996; Baumann & Meggers, 1996) and on the ecological niches of benthic foraminifers (Schönfeld, 1996), which showed several extinctions in the middle Pleistocene.

CONCLUSIONS

The planktonic assemblages in the upper Pliocene at Site 552 consist mainly of subpolar to temperate species. The increase in the influence of polar surface waters at about 2.5 Ma is indicated mainly by an increase in the abundance of the cold-water adapted coccolithophore species *C. pelagicus*. However, this corresponds to an increase in subpolar *N. pachyderma* dex., indicating that conditions

during this „cold" phase would be analogous to intermittent interglacials of the late Pleistocene. The drastic decrease in abundance of „Pliocene" taxa is interpreted as a response to the onset of harsh environmental conditions and may be attributed to surface water cooling. In general, the calcareous faunal and floral data indicate that the thermal gradient between Sites 552 and 646 was strong throughout most of the late Pliocene to early Pleistocene interval.

The biometric data of *Neogloboquadrina* tests at both sites indicate an evolutionary trend from large-sized *N. atlantica* sin. before 2.4 Ma via morphological integrate-forms („*N. atlantica-pachyderma* integrate") to small-sized *N. pachyderma* sin. between 1.8 Ma and 1.1 Ma. Therefore, the use of transfer functions on cold-water adapted *Neogloboquadrina* in sediment sections of the northern North Atlantic older than about 1.1 Ma should be treated with caution. From factor analyses it can be shown that *N. pachyderma* sin. first becomes a cold-water adapted species at 1.1 Ma, while it is a subpolar indicator between 1.8 Ma and 1.1 Ma.

ACKNOWLEDGEMENTS

The authors want to thank Nicolas Dittert and Robert Huber for a constructive review on an earlier version of the manuscript. We also thank Bill Austin for his helpful review which greatly improved this paper. Thanks are to Claudia Venhern who provided technical assistance in preparation of the data sets. This work was financially supported by the Deutsche Forschungsgemeinschaft (Grant He 1671/4).

REFERENCES

Aksu, A.E., de Vernal, A., & Mudie, P.J. 1989. High-resolution foraminifer, palynologic, and stable isotopic records of Upper Pleistocene sediments from the Labrador Sea: Palaeoclimatic and palaeoceanographic trends. *In:* Srivastava, S.P., Arthur, M., Clement, B. *et al.* (eds), *Proc. ODP, Sci. Results*, **105**, 617-642, College Station, TX.

Aksu, A.E. & Kaminski, M.A. 1989. Neogene planktonic foraminiferal biostratigraphy and biochronology in Baffin Bay and the Labrador Sea. *In:* Srivastava, S.P., Arthur, M., Clement, B. *et al.* (eds), *Proc. ODP, Sci. Results*, **105**, 287-304, College Station, TX.

Aksu, A.E., Mudie, P.J., de Vernal, A. & Gillespie, H. 1992. Ocean-atmosphere responses to climatic change in the Labrador Sea: Pleistocene plankton and pollen records. *Palaeogeography, Palaeoclimatology, Palaeoecology*, **92**, 121-137.

Backhaus, K., Erichson, B., Plinke, W. & Weiber, R. 1994. *Multivariate Analysenmethoden - eine anwenderorientierte Einführung*, 594 pp, Springer.

Baumann, K.-H. 1990. Veränderlichkeit der Coccolithophoridenflora des Europäischen Nordmeeres im Jungquartär. *Berichte aus dem Sonderforschungsbereich 313*, **22**, 1-146.

Baumann, K.H. & Meggers, H. 1996. Palaeoceanographic changes in the Labrador Sea during the past 3.0 My: Evidence from calcareous plankton records. *In:* Moguilevsky, A. & Whatley, R. (eds.), *Microfossils and oceanic environments*, 131-153, The University of Wales, Aberystwyth Press,

Baumann, K.H., Meggers, H. & Henrich, R. in press. Variations in surface water mass conditions in the Norwegian-Greenland Sea: Evidence from Plio-/Pleistocene calcareous plankton records (ODP Sites 644, 907, 909). *In:* Myhre, A., Thiede, J. , Firth, J. *et al.* (eds.), *Proc. ODP, Sci. Results*, **151**, College Station, TX (Ocean Drilling Program).

Berger, W.H. & Jansen, E. 1994. Mid-Pleistocene climate shift - The Nansen Connection.- *In:* Johannessen, O.M., Muench, R.D. & Overland, J.E. (eds.), *The polar oceans and their role in shaping the global environment*, Geophysical Monograph Series, **85**, 295-311.

Biolzi, M. 1991. Morphometric analyses of the Late Neogene planktonic foraminiferal lineage *Neogloboquadrina dutertrei*. *Marine Micropaleontology*, **18**, 129-142.

de Vernal, A. & Mudie, P.J. 1992. Pliocene and Quaternary dinoflagellate cyst stratigraphy in the Labrador Sea: Paleoenvironmental implications. *In:* Head, M.J. & Wrenn, J.H. (eds.), *Neogene and Quaternary dinoflagellate cysts and acritarchs*, 329-346. AASP Foundation, Dallas.

Diester-Haass, L. & Schnitker, D. 1989. Plio-Pleistocene sedimentation regimes leading to chalk-marl-cycles in the North Atlantic (DSDP Site 552 - Hole 552A). *Geologische Rundschau*, **78**, 959-985.

Dowsett, H.J. 1991. The development of a long-range foraminifer transfer function and application to Late Pleistocene North Atlantic climatic extremes. *Paleoceanography*, **6**, 259-273.

Dowsett, H.J. & Poore, R.Z. 1990. A new planktic foraminifer transfer function for estimating Pliocene-Holocene paleoceanographic conditions in the North Atlantic. *Marine Micropaleontology*, **16**, 1-23.

Henrich, R. & Baumann, K.-H. 1994. Evolution of the Norwegian Current and the Scandinavian ice sheets during the past 2.6 m.y.: evidence from ODP Leg 104 biogenic carbonate and terrigenous records. *Palaeogeography, Palaeoclimatology, Palaeoecology*, **108**, 75-94.

Henrich, R., Wolf, T.C.W., Bohrmann, G. & Thiede, J. 1989. Cenozoic paleoclimatic and paleoceanographic changes in the northern hemisphere revealed by variability of coarse-fraction composition in sediments from the Vøring-Plateau-ODP Leg 104 drill sites. *In:* Eldholm, O., Thiede, J., Taylor, E., *et al.* eds.), *Proc. ODP, Sci. Results*, **104**, 75-188, College Station, TX (Ocean Drilling Program).

Hooper, P.W.P. & Funnell, B.M. 1986. Late Pliocene to recent planktonic foraminifera from the North Atlantic (DSDP Site 552A): quantitative palaeotemperatures analysis. *In:* Summerhayes, C.P. & Shackleton, N.J. (eds.), *North Atlantic Palaeoceanography*, Geological Society Special Publication **21**, 181-190.

Hooper, P.W.P. & Weaver, P.P.E. 1987. Late Neogene species of the genus *Neogloboquadrina* Bandy, Frerichs, and Vincent in the North Atlantic: a biostratigrephic, palaeoceanographic, and phylogenetic review. *In:* Hart, M.B. (ed.): *Micropalaeontology of carbonate environments*, 21-43, British Micropalaeontological Society Series.

Imbrie, J. & Kipp, N.G. 1971. A new micropaleontological method for quantitative paleoclimatology: applications to a late Pleistocene Caribbean core. *In:* Turekian, K.K. (ed.), *Late Cenozoic Glacial Ages*, 71-181, Yale University Press, Hartford.

Jansen, E., Bleil U., Henrich, R., Kringstad L. & Slettemark, B. 1988. Paleoenvironmental changes in the Norwegian Sea and the northeast Atlantic during the last 2.8 My: Deep Sea Drilling Project/Ocean Drilling

Program Sites 610, 642, 643 and 644. *Paleoceanography*, **3**, 563-581.

Jansen, E., Slettermark, B., Bleil, U., Henrich, R., Kringstad, L. & Rolfsen, S. 1989. Oxygen and carbon isotope stratigraphy and magnetostratigraphy of the last 2.8 Ma: Paleoclimatic comparisons between the Norwegian Sea and the North Atlantic. *In:* Eldholm, O., Thiede, J., Taylor, E., *et al.* (eds.), *Proc. ODP, Sci. Results*, **104**, 255-269, College Station, TX (Ocean Drilling Program).

Johnson, D.A. 1982. Abyssal teleconnections; interactive dynamics of the deep ocean circulation. *Palaeogeography, Palaeoclimatology, Palaeoecology*, **38**, 93-128.

Kennett, J.P. & Srinivasan, M.S. 1980. Surface ultrastructural variation in *Neogloboquadrina pachyderma* (Ehrenberg): Phenotypic variation and phylogeny in the late Cenozoic. *Cushman Found. Special Publication*, **19**, 134-162.

Krumsiek, K. & Roberts, D.G. 1984. Paleomagnetics of Tertiary sediments from the southwest Rockall-Plateau, Deep Sea Drilling Project Leg 81. *In:* Roberts, D.G., Schnitker, D., *et al., Initial Reports. DSDP*, **81**, 837-851, Washington (U.S. Govt. Printing Office).

Lazarus, D., Hilbrecht, H., Spencer-Cervato, C. & Thierstein, H. 1995. Sympatric speciation and phyletic change in *Globorotalia truncatulinoides*. *Paleobiology*, **21**, 28-51.

Meggers, H. 1996. Pliozän-quartäre Karbonatsedimentation und Paläozeanographie des Nordatlantiks und des Europäischen Nordmeeres - Hinweise aus planktischen Foraminiferengemeinschaften, *Berichte FB Geowissenschaften, Universität Bremen*, **71**, 1-143.

Murray, J.W. 1984. Paleogene and Neogene benthic foraminifers from Rockall Plateau. *In:* Roberts, D.G., Schnitker, D., *et al.* (eds.), *Initial Reports. DSDP*, **81**, 503-534, Washington (U.S. Govt. Printing Office).

Poore, R.Z. & Berggren; W.A. 1975. The morphology and classification of *Neogloboquadrina atlantica* (Berggren). *Journal of Foraminiferal Research*, **5**, 76-84.

Pujol, C. & Duprat, J. 1985. Quaternary and Pliocene planktonic foraminifers of the Northeastern Atlantic (Goban Spur), Deep Sea Drilling Project Leg 80. *In:* de Graciansky, P.C., Poag, C.W., *et al.* (eds.), *Initial Reports. DSDP*, **80**, 683-723, Washington (U.S. Govt. Printing Office).

Raymo, M.E., Ruddiman, W.F., Backman, J., Clement, B.M. & Martinson, D.G. 1989. Late Pliocene variation in northern hemisphere ice sheets and North Atlantic deep water circulation. *Paleoceanography*, **4**, 413-446.

Raymo, M.E., Ruddiman, W.F. & Clement, B.M. 1986. Pliocene-Pleistocene paleoceanography of the North Atlantic at Deep Sea Drilling Project Site 609. *In:* Ruddiman, W.F., Kidd, R.B., Thomas, E., *et al.* (eds.), *Initial Reports. DSDP*, **94**, 895-901, Washington (US Govt. Printing Office).

Raymo, M.E., Ruddiman, W.F., Shackleton, N.J. & Oppo, D.W. 1990. Evolution of Atlantic-Pacific $\delta^{13}C$ gradients over the last 2.5 m.y. *Earth and Planetary Science Letters*, **97**, 353-368.

Raymo, M.E., 1992. Global climate change: A three million year perspective. *In:* Kukla, G.J. & Went, E. (eds.), *Start of a glacial*, NATO ASI Series, **3**, 207-223, Springer.

Ruddiman, W.F., McIntyre, A. & Raymo, M.E. 1986a. Paleoenvironmental results from North Atlantic Sites 607 and 609. *In:* Ruddiman, W.F., Kidd, R.B., Thomas, E., *et al.* (eds.), *Initial Reports. DSDP*, **94**, 855-878, Washington (U.S. Govt. Printing Office).

Ruddiman, W.F. & Raymo, M.E. 1988. Northern hemisphere climate regimes during the past 3 Ma: possible tectonic connections. *Philosophical Transactions of the Royal Society London*, **B 318**, 411-430.

Ruddiman, W.F., Raymo, M.E., Martinson, D.G., Clement, B.M. & Backman, J., 1989. Pleistocene evolution: Northern hemisphere ice sheets and North Atlantic Ocean. *Paleoceanography*, **4**, 353-412.

Ruddiman, W.F., Shackleton, N.J. & McIntyre, A. 1986b. North Atlantic sea-surface temperatures for the last 1.1 million years. *In:* Summerhayes, C.P. & Shackleton, N.J. (eds.), *North Atlantic Palaeoceanography*. Geological Society Special Publication **21**, 155-173.

Schönfeld, J. 1996. The *Stilostomella* Extinction. Structure and dynamics of the last turnover in deep-sea benthic foraminiferal assemblages. *In:* Moguilevsky, A. & Whatley, R. (eds.), *Microfossils and Oceanic Environments*, 27-37, The University of Wales, Aberystwyth Press.

Shackleton, N.J., Backman, J., Zimmerman, H., Kent, D.V., Hall, M.A., Roberts, D.G., Schnitker, D., Baldauf, J.G., Desprairies, A., Homrighausen, R., Huddlestun, P., Keene, J.B., Kaltenback, A.J., Krumsiek, K.A.O., Morton, A.C., Murray, J.W. & Westberg-Smith, J. 1984. Oxygen isotope calibration of the onset of ice-rafting and history of glaciation in the North Atlantic region. *Nature*, **307**, 620-623.

Shackleton, N.J., Crowhorst, S., Hagelberg, T., Pisias, N. & Schneider, D.A. 1995. A new late Neogene timescale: Application to ODP Leg 138 sites. *In:* Pisias, N., Mayer, L.A., Janecek, T.R., Palmer-Julson, A. & van Andel, T.H. (eds.), *Proc. ODP, Sci. Results*, **138**, 73-101, College Station, TX (Ocean Drilling Program).

Shackleton, N.J. & Hall, M.A. 1984. Oxygen and carbon isotope stratigraphy of Deep Sea Drilling Project Hole 552A: Plio- Pleistocene glacial history. *In:* Roberts, D.G., Schnitker, D., *et al.* (eds.), *Initial Reports. DSDP*, **81**, 599-609, Washington (U.S. Govt. Printing Office).

Spiegler, D., 1989. Ice-rafted Cretaceous and Tertiary fossils in Pleistocene-Pliocene sediments, ODP Leg 104, Norwegian Sea. *In:* Eldholm, O., Thiede, J., Taylor, E., *et al., Proc. ODP, Sci. Results*, **104**, College Station, TX (Ocean Drilling Program), 739-744.

Spiegler, D. & Jansen, E. 1989. Planktonic foraminifer biostratigraphy of Norwegian Sea sediments: ODP Leg 104. *In:* Eldholm, O., Thiede, J., Taylor, E., *et al., Proc. ODP, Sci. Results*, **104**, College Station, TX (Ocean Drilling Program), 681-696.

Thunell, R.C. 1979. Climatic evolution of the Mediterranean Sea during the last 5.0 million years. *Sedimentary Geology*, **23**, 67-79.

Wei, K.Y. 1994. Allometric heterochrony in the Pliocene-Pleistocene planktic foraminiferal clade *Globoconella*. *Paleobiology*, **20**, 66-84.

Zachariasse, W.J., Gudjonsson, L., Hilgen, F.J., Langereis, C.G., Lourens, L.J., Verhallen, P.J.J.M. & Zijderveld, J.D.A. 1990. Late Gauss to early Matuyama invasions of *Neogloboquadrina atlantica* in the Mediterranean and associated record of climatic change. *Paleoceanography*, **5**, 239-252.

Zimmerman, H.B., Shackleton, N.J., Backman, J., Kent, D.V., Baldauf, J.G., Kaltenback, A.J. & Morton, A.C. 1984. History of Plio- Pleistocene climate in the Northeastern Atlantic, Deep Sea Drilling Project Hole 552A. *In:* Roberts, D.G., Schnitker, D., *et al.* (eds.), *Initial Reports. DSDP*, **81**, 861-875, Washington (U.S. Govt. Printing Office).

Paleoecology of benthic foraminifera in the Norwegian-Greenland Sea during the past 500 ka

ULRICH STRUCK

Institut für Ostseeforschung Warnemünde, Seestraße 15, D-18119 Rostock, Germany

ABSTRACT

Eleven long sediment cores from the Norwegian-Greenland Sea have been investigated for their benthic foraminiferal content. Fourty-two benthic foraminiferal species were found and five taxonomic groups were described. The most abundant species during the past 500,000 years are *Oridorsalis umbonatus* (Reuss), *Cibicidoides wuellerstorfi* (Schwager), *Cassidulina teretis* Tappan, *Triloculina tricarinata* d'Orbigny, and *Pyrgo rotalaria* Loeblich & Tappan.

Stratigraphically useful layers are indicated by abundance peaks of *Siphotextularia rolshauseni* (Phleger & Parker) in Stage 2, *Pullenia bulloides* (d'Orbigny) in Substage 5.1 and *Globocassidulina subglobosa* (Brady) in Substage 11.3. Interglacial conditions are well documented by high amounts of *C. wuellerstorfi*.

The calculation of test accumulation rates reveals three to four times higher foraminiferal productivity during interglacials, with four remarkably high-productivity events in Substages 11.3, 9.3, 7.1, and 5.5. The regional pattern of test accumulation rates shows highest amounts in the southeastern part of the Norwegian-Greenland Sea with decreasing westward and northward trends.

The ecological interpretation of fossil foraminiferal habitats show dominant suspension-feeding foraminiferal faunas (i.e. *C. wuellerstorfi*) during interglacials, contrasting glacial periods with dominant deposit feeding foraminifers.

Both the dominance of suspension feeding foraminifera and higher benthic foraminiferal accumulation rates during interglacials indicate an increased food supply at the sea floor and consequently enhanced productivity of the northernmost Atlantic Ocean during interglacials. A link is observed between the benthic foraminiferal assemblages and the climatic mode of the surface ocean (glacial/interglacial) attributed to changes in the surface productivity.

INTRODUCTION

The habitat at the sea floor in the high latitude deep sea is marked by the strong seasonality of food supply and long starvation periods (Linke, 1989; Gooday & Lambshead, 1989). Here, living benthic foraminifera have to react to such conditions with distinct survival strategies. Therefore, a comparatively small number of specialized foraminifera species occupy this realm (Thies, 1991).

A major factor controlling the benthic species composition in the deep ocean is the amount of food supply and its availability at the sea floor, which in turn is primarily a function of the surface productivity and the degree of remineralization. The first large scale study that attributed the composition of the benthic foraminiferal assemblages to the amount of organic carbon in sediments examined the upwelling influenced regime at the continental margin off northwest Africa (Lutze & Coulburn, 1984). Afterwards several other studies on modern benthic foraminifera have suggested that these organisms are well adapted to specific habitats and respond to changes in near bottom lateral advection of food and to the seasonality of organic carbon flux from the sea surface (e.g. Corliss, 1985; Linke & Lutze, 1992).

The climate in the northern hemisphere over the past 500 ka is dominated by „Milankovitch"-

In: Hass, H.C. & Kaminski, M.A. (eds.) 1997. Contributions to the Micropaleontology and Paleoceanography of the Northern North Atlantic. *Grzybowski Foundation Special Publication*, no. 5, pp. 51-82

forced insolation variability which induced strong fluctuations of ice-sheets in high latitudes (Thiedemann *et al.*,1994). Times of advance or retreat of ice sheets, had a major impact on the modern type circulation pattern in the Norwegian-Greenland Sea. The productivity in the surface ocean of northern high latitudes (i.e. the Norwegian-Greenland Sea) also responds to climate change (Altenbach, 1992). Consequently the fossil benthic foraminiferal assemblages ought to serve a recorder of these processes, in terms of their species composition and abundances. In this study, I trace the benthic foraminiferal response to environmental changes in eleven sediment cores of pelagic sediments from the Norwegian-Greenland Sea covering the past 500 ka.

Modern and paleoceanography of the Norwegian-Greenland Sea

The oceanographic conditions of the study area are determined by the northward flowing warm, saline surface waters of the Norwegian Current, which is a northern continuation of the Atlantic Drift, and by the southward flowing cold, less saline surface waters of the East Greenland Current (Fig. 1). Cooling of the Atlantic Water upon heat release to the atmosphere generates deep water convection and thermohaline circulation, variations of which affect European climate today as they did in the past (Broecker & Denton, 1989).

The surface water masses define two major fronts (Fig. 1): The Polar Front is the boundary between low saline Polar waters and cold higher saline Arctic waters, and the Arctic Front is the boundary between cold Arctic waters and warm Atlantic waters (Helland-Hansen & Nansen, 1909; Swift & Aagard, 1981). The maximum winter sea ice limit lies slightly west of the Arctic Front, while the summer sea ice limit lies west of the Polar Front. The area of seasonal ice cover basically comprises Arctic Water masses, i. e. the water masses where winter convection occurs.

In contrast to today, the Atlantic of the Last Glacial Maximum (LGM) had a strongly reduced deep water circulation, which is probably the result of reduced deep water convection in the Norwegian Greenland-Sea (Duplessy *et al.*, 1988). Therefore, the Norwegian-Greenland Sea is an important oceanic basin that exerted a major control on the deep water circulation of the worlds ocean.

MATERIAL AND METHODS

For this study, eleven long sediment cores were selected from undisturbed pelagic to hemipelagic sediments collected in the southern part of the Norwegian-Greenland Sea. The study area covers all modern water-mass domains (Fig. 1, Table 1). The cores were retrieved during cruises of the German research vessels „Polarstern" and „Meteor". The cores were sampled at 5 to 10 cm intervals. A 10 - 20 gram sample was weighed and freeze-dried, and washed through a 63 micron sieve. The subsample (>63µm) was sieved into four size-fractions (63-125µm; 125-250µm; 250-500µm; >500µm). At least 300 specimens per sample were counted in the quantitatively split sample.

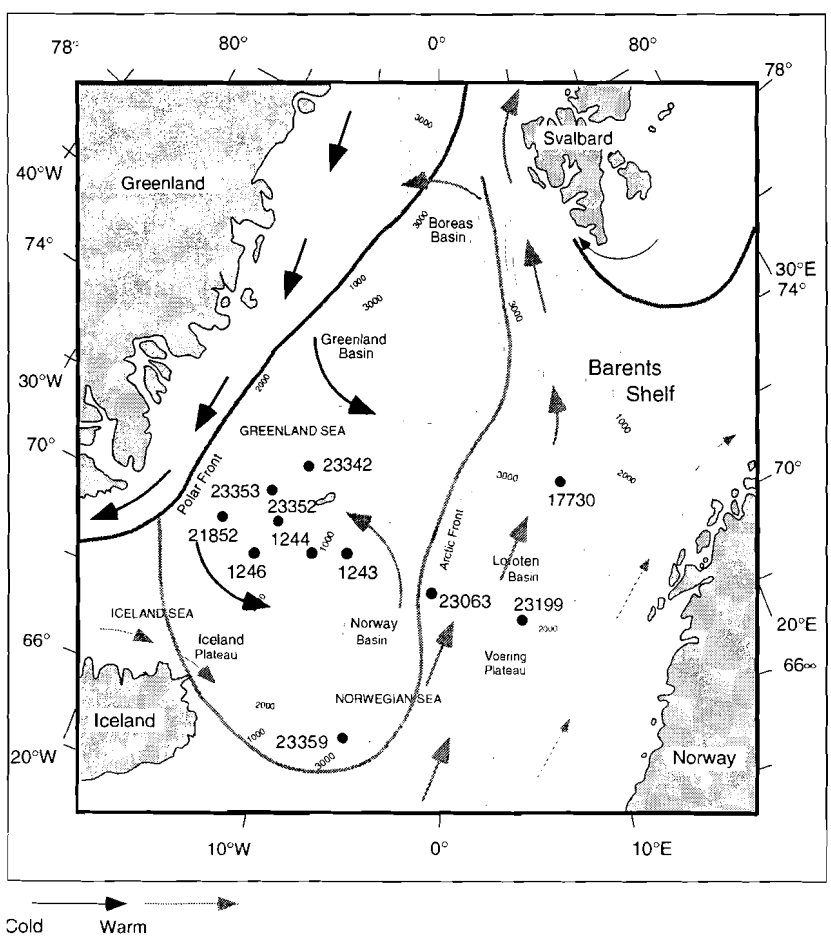


Figure 1. Location map of investigated cores including modern surface circulation regime.

Table 1. List of investigated cores

Core #	Longitude	Latitude	Waterdepth	Length	source of $\delta^{18}O$-data
23359	04°09.6 E	65°31.7 N	2820m	599cm	Gehring, 1989
23063	00°00.0 E	68°45.0 N	2299m	918cm	Vogelsang, 1990
23352	12°25.8 E	70°00.4 N	1819m	826cm	Henrich, 1992
1243	06°32.1 W	69°22.3 N	2710m	767cm	Birgisdottir,1992
23199	05°13.5 E	68°22.5 N	1968m	555cm	Haake & Pflaumann, 1989
1244	08°40.0 W	69°22.0 N	2162m	665cm	*correlated*
1246	12°55.0 W	69°23.0 N	1902m	706cm	Birgisdottir, 1992
23353	12°43.3 W	70°34.2 N	1394m	1068cm	Jünger, 1990
23342	08°38.2 W	71°38.2 N	1974m	599cm	Henrich, 1992
17730	07°23.3 E	72°06.7 N	2749m	550cm	Weinelt, 1993
21852	15°49.5 W	70°15.7 N	1117m	573cm	Lackschewitz, 1991

The data shown in this work are converted to a size fraction larger 125µm. The chronostratigraphy of the investigated cores is taken from Struck (1992). The oxygen isotopic values from *Neogloboquadrina pachyderma* (sin. versus PDB) are from several authors shown on Table 1. The high resolution Core 17730 is dated by AMS-^{14}C mass spectrometry (Weinelt, 1993).

With the information of age-/depth relation linear sedimentation rates (LSR) were calculated. Dry bulk densities (DBD) for every sample have been published by several authors (Holler & Kassens, 1989; Kassens, 1990; Kassens *in prep.*; Birgisdottir, 1992). Bulk accumulation rates (ARBULK) are calculated after:

$$ARBULK\ (g*cm^{-2}*ky^{-1}) = LSR\ (cm*ky^{-1})*DBD(g*cm^{-3})$$

Test accumulation of benthic foraminifera (BFAR) is calculated as the product of:

$$Specimens\ (gram^{-1}) * ARBULK\ (g*cm^{-2}*ky^{-1}) = BFAR\ (Spec.*cm^{-2}*ky^{-1})$$

All data for calculating the BFAR-values (sedimentation rates, dry bulk densities, and age-depth relation) as well as species abundances (tests per gram) are provided in Struck, 1992).

TAXONOMY AND ECOLOGY

The species distribution in this study follows in general the taxonomic interpretations of previous studies on modern benthic foraminifera in the area. The species list consists of 42 recognized foraminiferal species and 4 taxonomical groups (Annex 1).

Owing to our limited knowledge about the ecological habitats of benthic foraminifera, the following discussion of the investigated core profiles focuses on 10 foraminiferal species/groups that are of great importance for the paleoecological interpretation.

Ecology and modern habitat of some important benthic foraminiferal species

A comparitively small number of benthic foraminifera species dominate the modern habitat in the deep basins of the Norwegian-Greenland Sea. In a study of Recent living (Rose Bengal stained) foraminifera below 1000 m waterdepth, Lutze & Thiel (1987) found assemblages dominated by only three species (>250µm in high abundances (up to 100 foraminifera per 10 cm^2). Dominant species in the area are *C. subglobosus*, *C. wuellerstorfi* and *P. murrhina* (*P. rotalaria* in this study). According to Linke & Lutze (1992) the modern habitat of *C. subglobosus* in the Norwegian Sea characterizes an environment of low sedimentation. Linke & Lutze also speculated that scavenging foraminifera such as *C. subglobosus* are able to react rapidly to organic flux events and utilize large amounts of organic matter originating from plankton blooms.

Lutze & Thiel (1987) found *C. wuellerstorfi* living in an elevated position, feeding on laterally advected organic material. Therefore, *C. wuellerstorfi* is well adapted to suspension-feeding and probably requires permanent lateral advective currents at the sea floor. Altenbach (1992) associated *C. wuellerstorfi* to a faunal assemblage of foraminifera related to a flux of organic carbon in the range of 1.5-2.5g $m^{-2}yr^{-1}$. *Pyrgo rotalaria* is reported to be an ubiquitous foraminifer that lives endo- to epifaunally possibly with endosymboints (Heeger, 1990; Linke & Lutze, 1992). It characteristically lives in a deep sea environment with a low flux of organic carbon (<1.5g $m^{-2}yr^{-1}$, Altenbach, 1992).

The work of Lutze & Salomon (1987) only considered the size-fraction >250µm. This leads to an under-estimate of small foraminifera which are typical in the modern deep sea environment (Schröder *et al.*, 1987). One of the most important of these species is *O. umbonatus*, commonly reported as an important inhabitant of the deep sea fauna and is adapted to low flux of organic carbon (Altenbach, 1992). Another abundant small foraminifer is *Triloculina tricarinata*, which is supposed to be a deposit feeding endo- to epifaunal species well adapted to a low flux of organic carbon (Murray, 1991; Altenbach pers. comm.; Thies, 1991).

Some species not present today in the deep basin (below 1200m) of the Norwegian-Greenland Sea, but known from fossil assemblages and/or shallower parts are *Pullenia bulloides*, *Siphotextularia rolshauseni*, and *Globocassidulina subglobosa*. Unfortunately little ecological information is available on *S. rolshauseni*. Hermelin & Scott (1985) reported occurrences of this species in low percentages in Holocene sediments of the central North Atlantic Ocean. The biserial tapered shape of the foraminiferal test implies an endo- to semi endobenthic life style (Corliss, 1985). The tube shaped aperture may be helpful for stabilizing the pseudopodii to trap particles of organic material delivered through

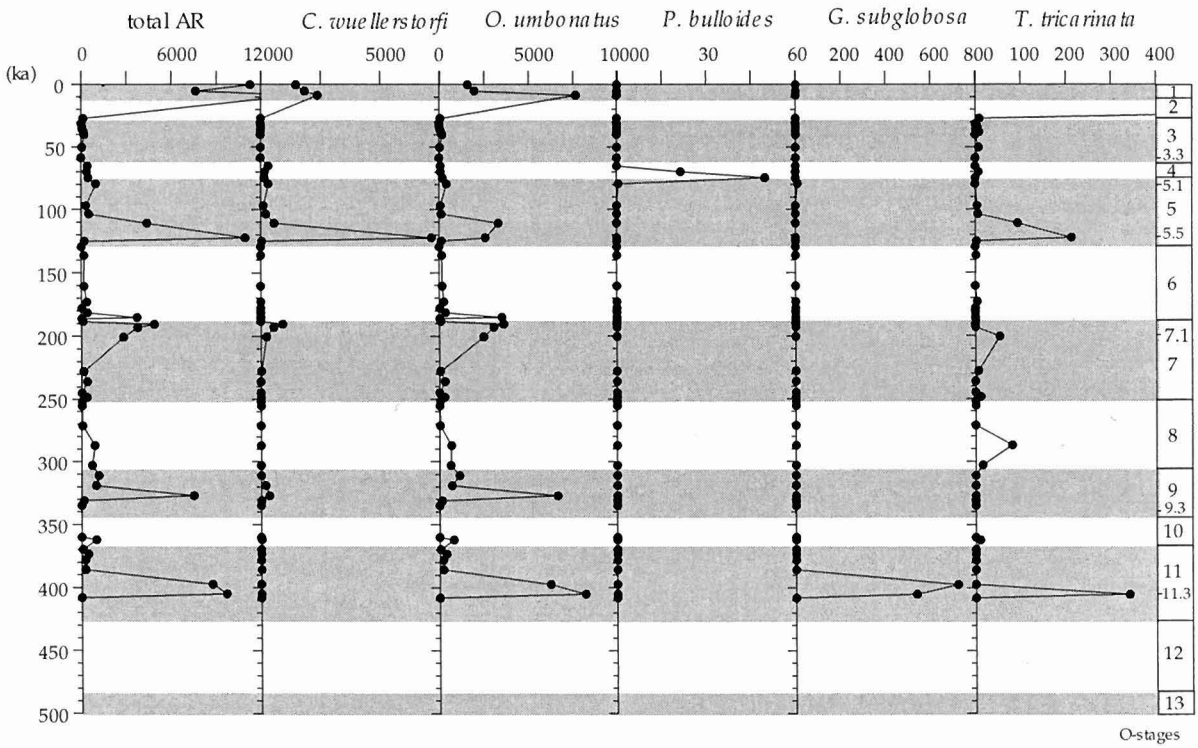


Figure 2. BFAR (Spec.*cm^{-2}*ky^{-1}) of total benthic foraminiferal assemblage and five important species of Core 23359. Oxygen isotope stages are indicated.

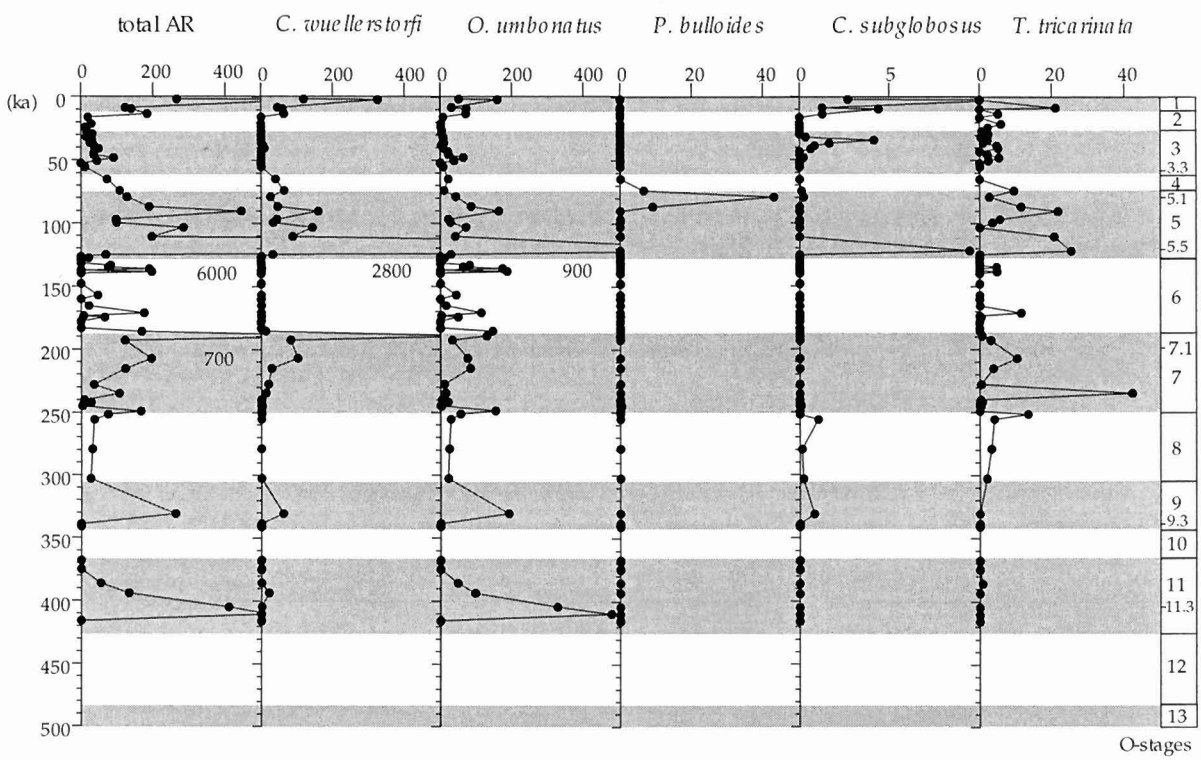


Figure 3. BFAR (Spec.*cm^{-2}*ky^{-1}) of total benthic foraminiferal assemblage and five important species of Core 23063. Oxygen isotope stages are indicated.

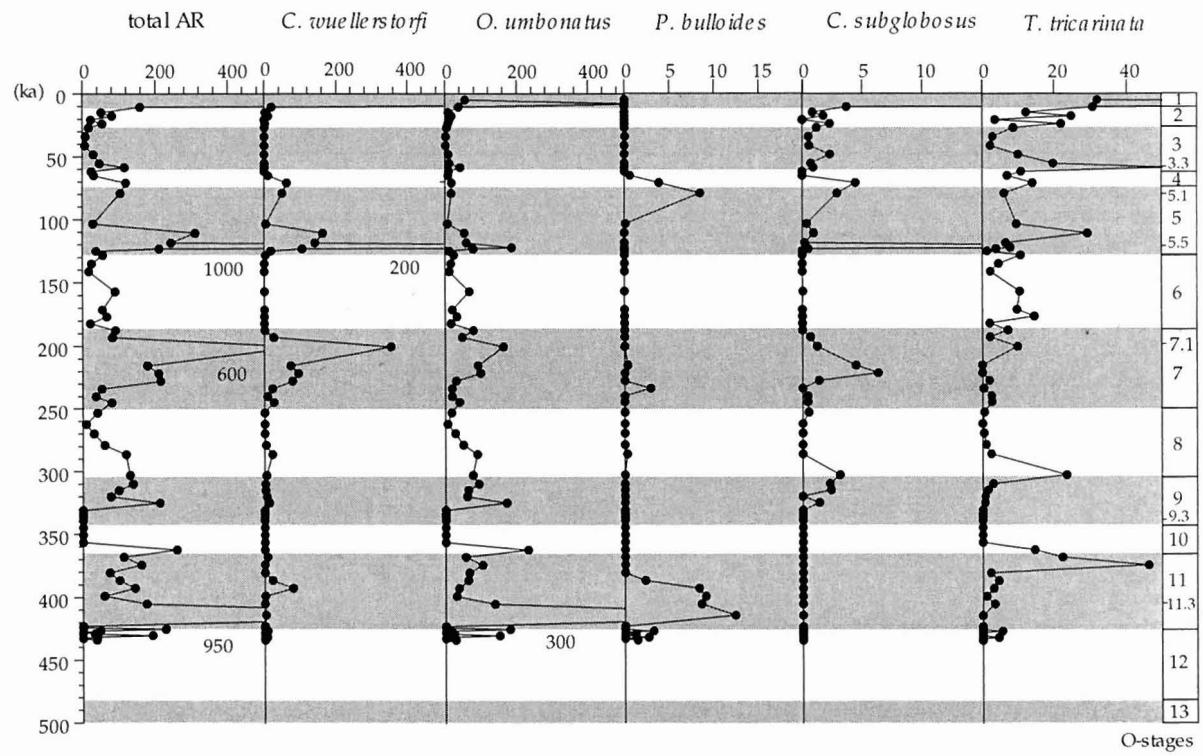


Figure 4. BFAR (Spec.*cm^{-2}*ky^{-1}) of total benthic foraminiferal assemblage and five important species of Core 23352. Oxygen isotope stages are indicated.

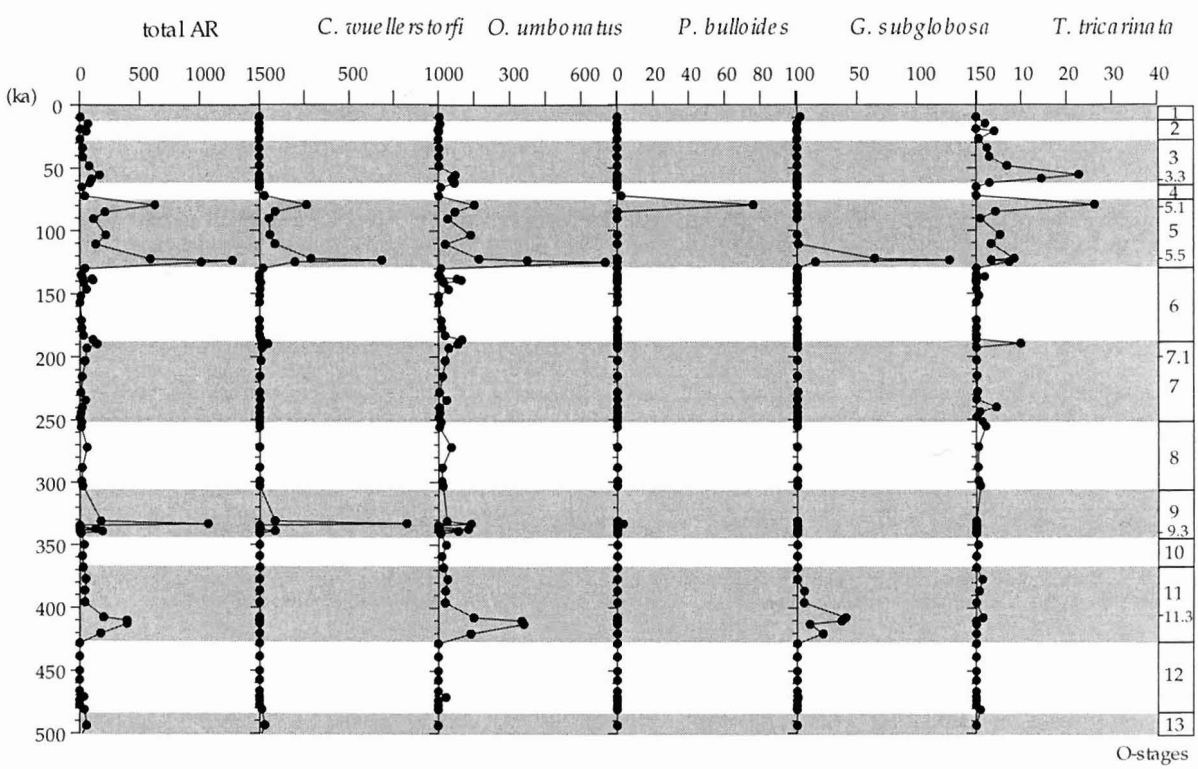


Figure 5. BFAR (Spec.*cm^{-2}*ky^{-1}) of total benthic foraminiferal assemblage and five important species of Core 1243. Oxygen isotope stages are indicated.

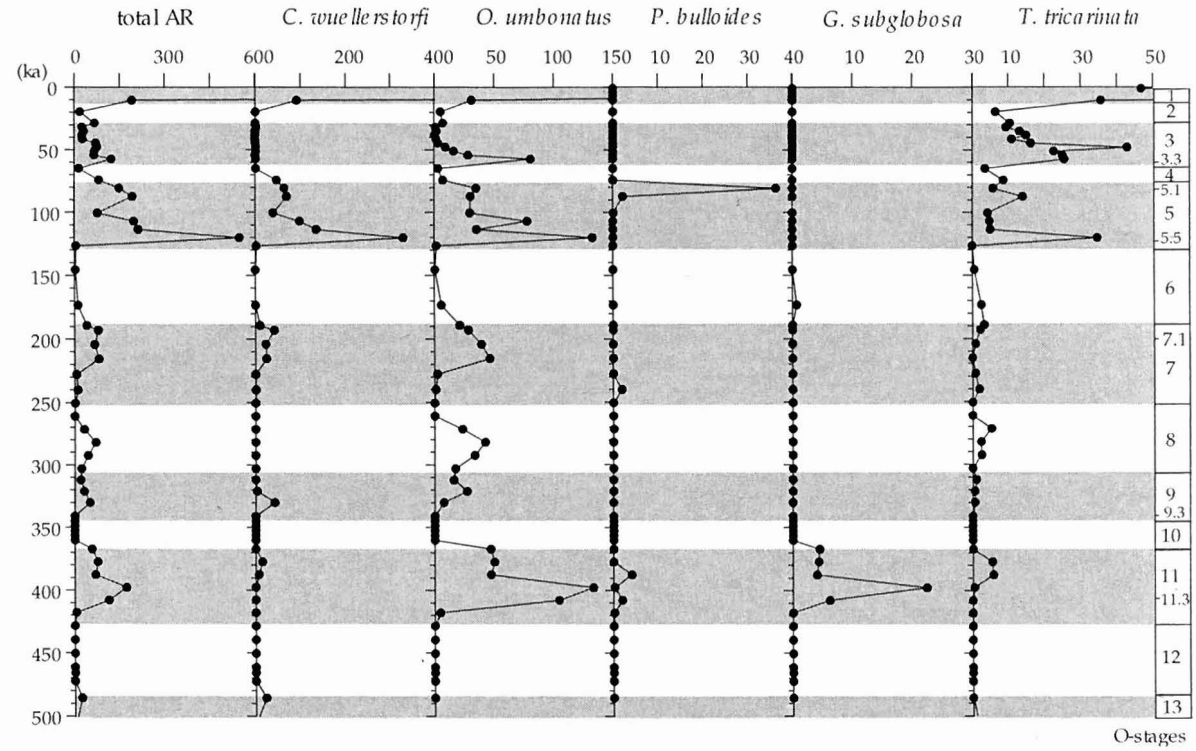


Figure 6. BFAR (Spec.*cm^{-2}*ky^{-1}) of total benthic foraminiferal assemblage and five important species of Core 1244. Oxygen isotope stages are indicated.

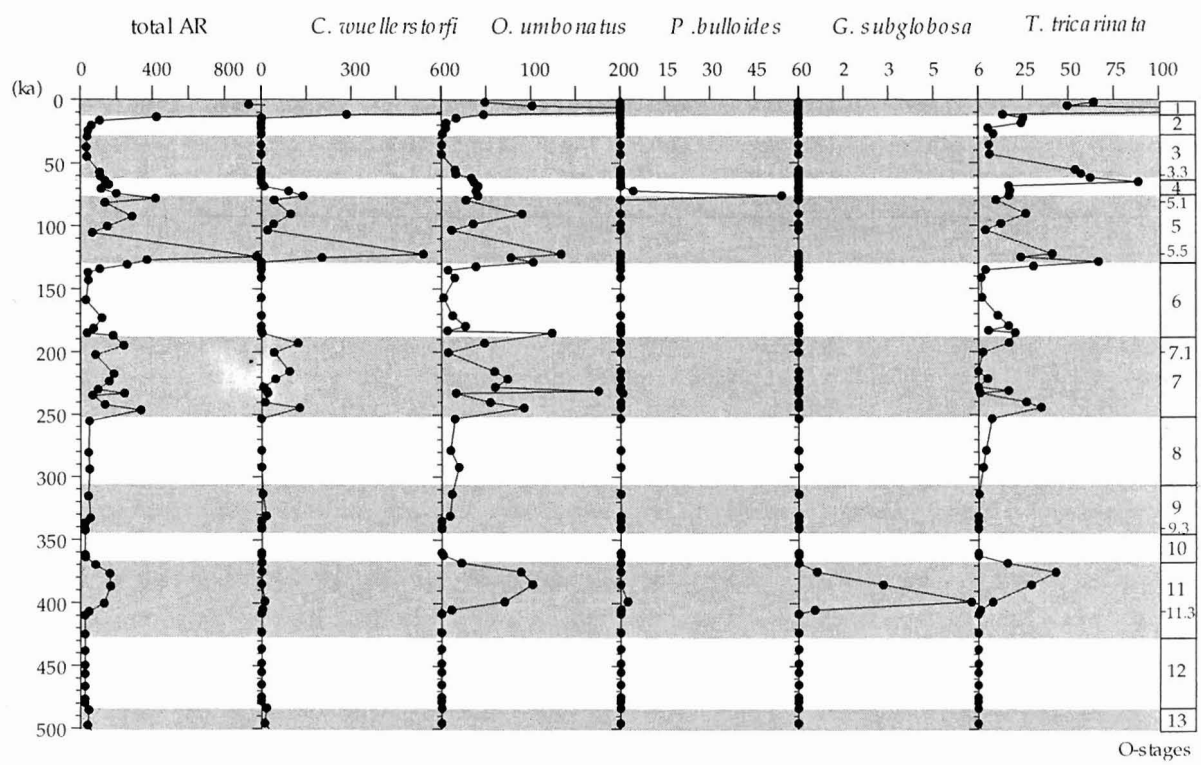


Figure 7. BFAR (Spec.*cm^{-2}*ky^{-1}) of total benthic foraminiferal assemblage and five important species of Core 1246. Oxygen isotope stages are indicated.

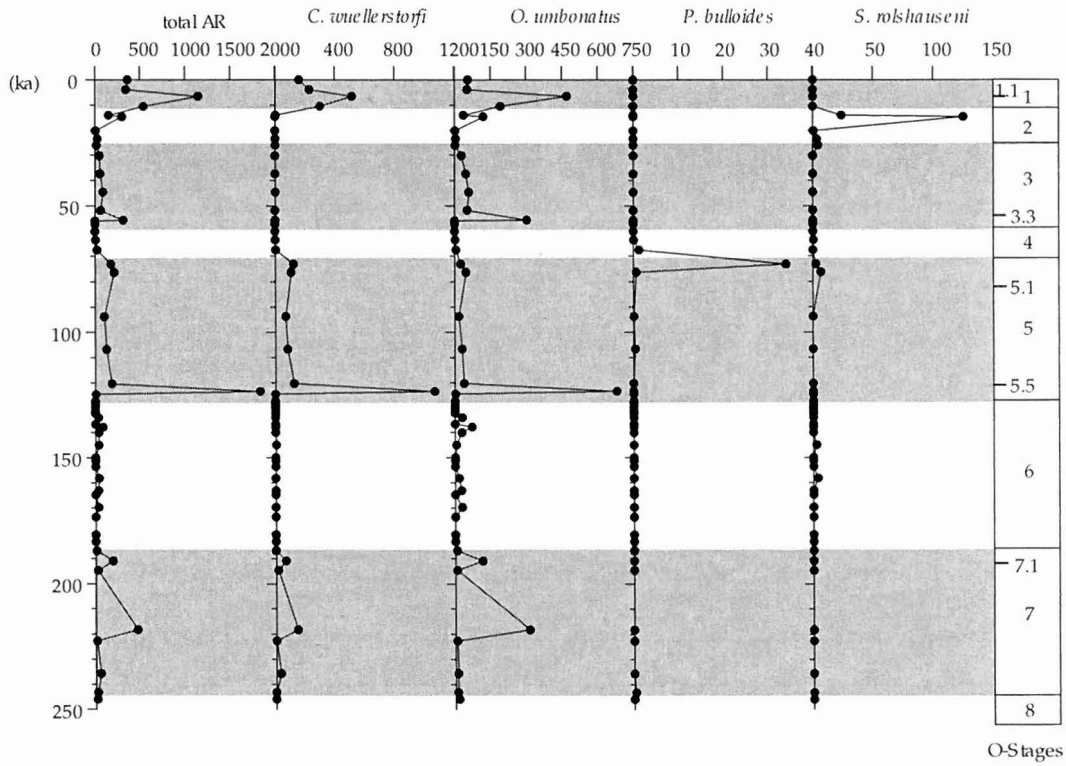


Figure 8. BFAR (Spec.*cm^{-2}*ky^{-1}) of total benthic foraminiferal assemblage and four important species of Core 23199. Oxygen isotope stages are indicated.

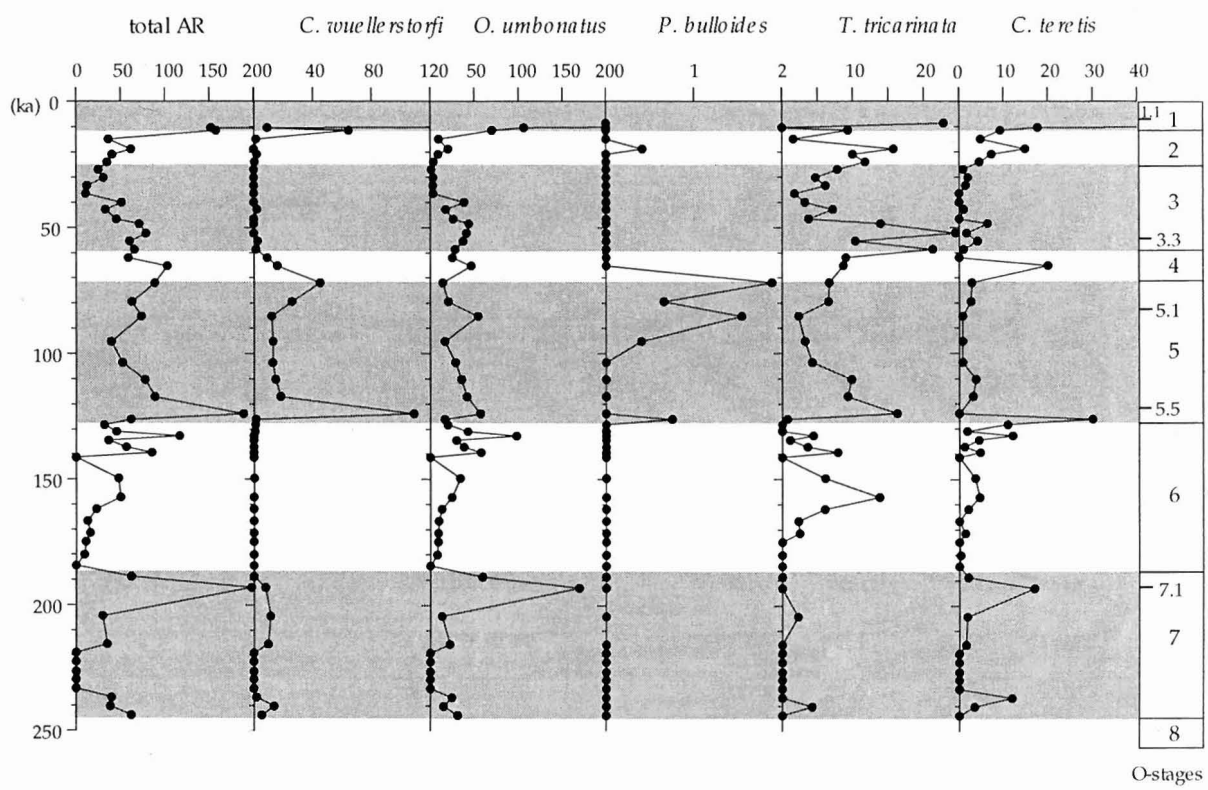


Figure 9. BFAR (Spec.*cm^{-2}*ky^{-1}) of total benthic foraminiferal assemblage and five important species of Core 23342. Oxygen isotope stages are indicated.

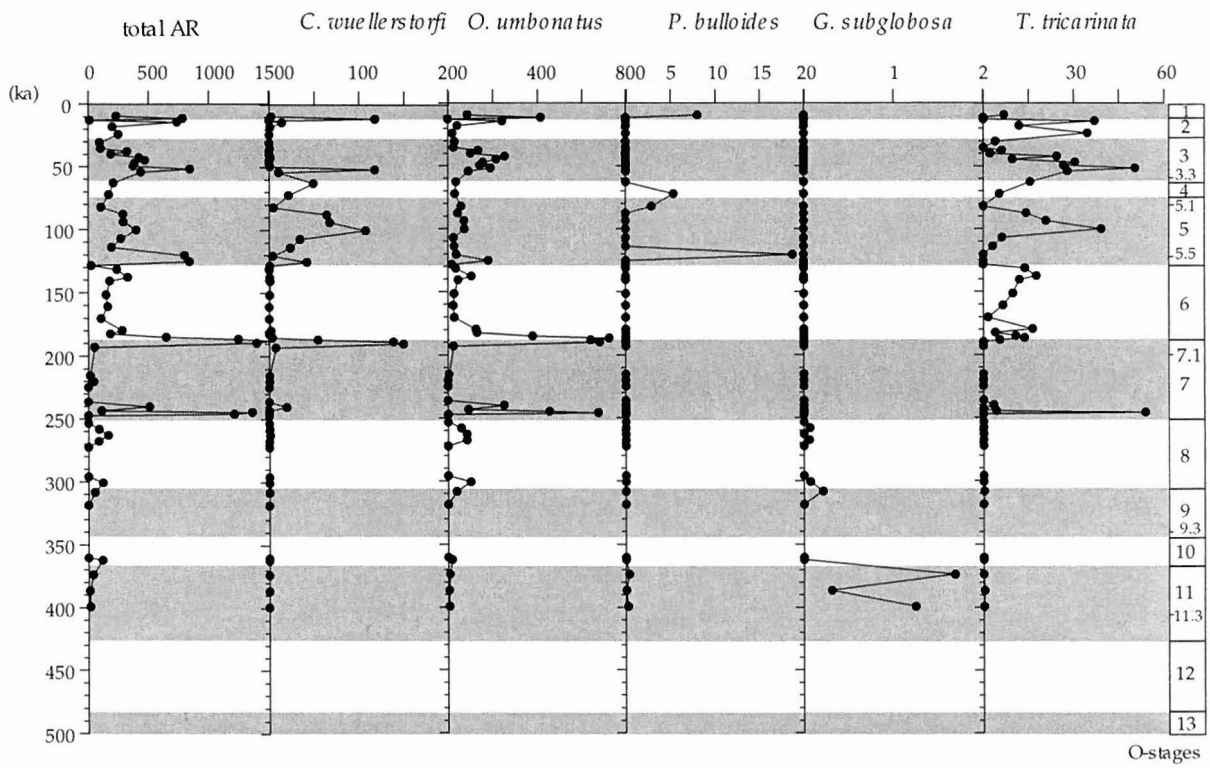


Figure 10. BFAR (Spec.*cm^{-2}*ky^{-1}) of total benthic foraminiferal assemblage and five important species of Core 23353. Oxygen isotope stages are indicated.

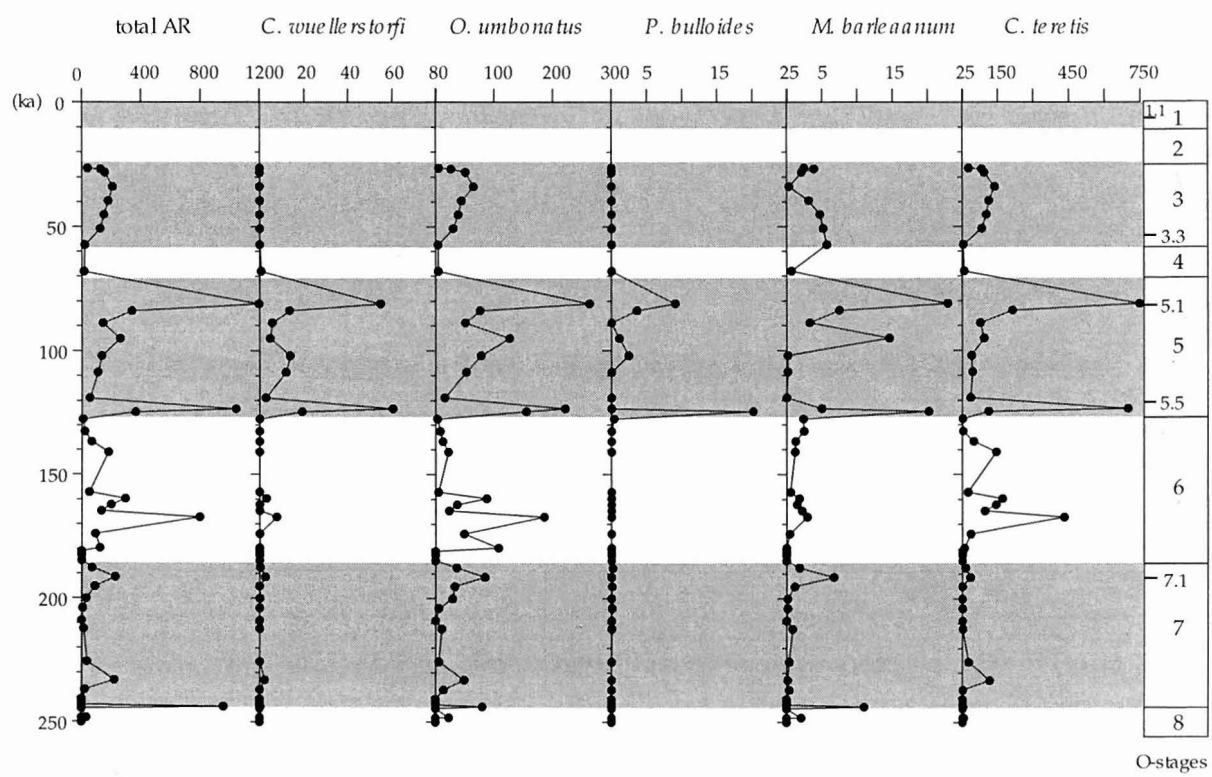


Figure11. BFAR (Spec.*cm^{-2}*ky^{-1}) of total benthic foraminiferal assemblage and five important species of Core 21852. Oxygen isotope stages are indicated.

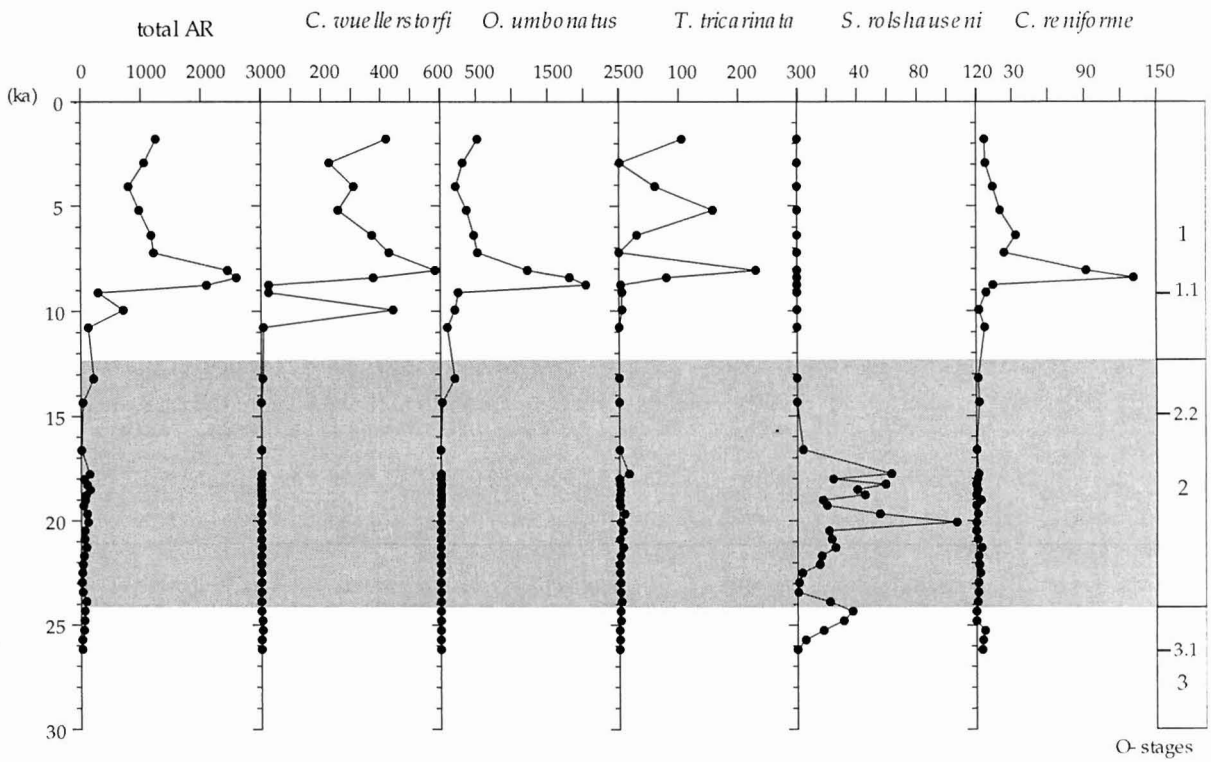


Figure 12. BFAR (Spec.*cm^{-2}*ky^{-1}) of total benthic foraminiferal assemblage and five important species of Core 17730. Oxygen isotope stages are indicated.

the water column (Nees & Struck, 1994). *Pullenia bulloides* is thought to live infaunally (*sensu* Corliss, 1985; Murray, 1991). Mackensen *et al.*, (1994) found *P. bulloides* characteristic in a „Southern High Productivity" assemblage at the Polar Front in the South Atlantic associated with a high flux of organic carbon. *Globocassidulina subglobosa* is not known from modern benthic foraminiferal fauna in the deep parts of the Norwegian-Greenland Sea (Mackensen, 1987; Thies, 1991). It is thought to be infaunal *sensu* Corliss (1985).

RESULTS AND DISCUSSION

Faunal variability

The total accumulation rates (BFAR) as well as accumulation rates of individual species (species-AR) of five important foraminiferal species in the investigated cores are documented in figures 2-12. The time interval recovered in the cores spans the last 500,000 years. The oldest sediments are found in Cores 1244, 1246 and 1243 from the central Iceland-Sea. Core 17730 (Fig. 12) provides a high resolution time series over the last 30,000 years with an average time resolution between samples of about 1,000 years.

Core 23359 from the Aegir Ridge (Fig. 2) shows the highest BFAR of all cores. Highest BFAR are correlated to peak interglacial periods located at Stage 5.5, 7.1, 9.3, and 11.3 (at 123 ka, 193 ka, 331 ka, and 405 ka). As many as 10,000 tests cm^{-2} ka^{-1} are observed in Stage 5.5 (Fig. 2). Normal interglacial BFAR values are closer to 1,000 tests cm^{-2} ka^{-1}. Lower BFAR values are related to cold phases during interglacials such as Stage 5.2, 5.4, and 11.2. Glacial periods in the investigated sequence are marked by reduced BFAR. An interval without benthic foraminifera was found in the samples of cold Stage 10.

The main constituents of the fossil assemblage in Core 23359 are *C. wuellerstorfi*, *O. umbonatus*, and *T. tricarinata*. *Cibicidoides wuellerstorfi* has occurrences only in interglacial and interstadial sediments, and has highest abundances in peak interglacials 5.5 and 7.1. *Oridorsalis umbonatus* is present in most of the samples and follows the distribution of the total fauna with BFAR-values in interglacials and reduced ones in glacials. The *T. tricarinata*-AR reveals varying fluctuations of this species in the faunal succession with BFAR-peaks in Stages 11.3, 9.1, 7.1 and 5.5. *Pullenia bulloides* and *G. subglobosa* are species that occur during distinct stratigraphical horizons in the studied time interval (Stages 5.1 and 11.3, Fig. 2).

The faunal distribution in Core 23359 is also typical for several other cores. In Core 23063, 23352, 1243, 1244, 1246 about the same time interval is recovered and the faunal distribution is also very similar with the exception of differences in the

amount of foraminifera (see Fig. 3, 4, 5, 6, 7). Core 23199 (Fig. 8) from the Voering Plateau recovered only the past 250 ky and is presented in comparison with the results of Haake & Pflaumann (1989; data are kindly provided by the authors). The data of Core 23199 fit very well into the general pattern of the previously described sediment cores (Figs. 2-8).

In comparison, the faunal distribution in Cores 1342, 23353, and 21852 shows some distinct differences. In general contrast between the BFAR in glacial and interglacial assemblages is less pronounced (Figs. 9-11). Highest BFAR occur in Substage 7.1 (Core 23342, 23353) and 5.1 (Core 21852) respectively. Another difference is the distinct stratigraphic occurence of *P. bulloides* in Substage 5.5 (at 123 ka). As in the other cores, the presence of *C. wuellerstorfi* is restricted to interglacial sediments.

Stage 1 (Holocene) comprises only a few samples in most of the cores (or is not recovered) which leads to uncertainties in the calculation of accumulation rates. Therefore, absolute abundances and species-AR show possibly overestimated results. To obtain a realistic view of the quantitative and qualitative succession of the benthic foraminiferal assemblage over the last glacial to interglacial transition, the high resolution Core 17730 was investigated (Fig. 12). The analyzed sequence of Core 17730 spans the time interval of the last 30 ka. During Stage 2, low numbers of foraminifera accumulated. The glacial assemblage consists of *O. umbonatus, T. tricarinata, C. reniforme,* and *S. rolshauseni* whereas *S. rolshauseni* has a stratigraphic occurence mainly restricted to Stage 2 (see also Nees & Struck, 1994; Struck, 1995). The maximum abundance of foraminiferal tests was found at about 9 ka (Fig. 12). Like in other cores, *C. wuellerstorfi* is restricted to interglacial sediments younger than 10.6 ka.

Discussion of the faunal succession during the past 500,000 years

In the sediments of **Stage 12** and **10** no benthic foraminifera are preserved. In comparison with the distribution of benthic foraminifera in the modern ocean where no oxygenated environment is known without any living foraminifera, it is obvious that the assemblage is totally dissolved. Other investigations on microfossils from this time interval indicate strongly or totally reduced calcareous (Bleil & Gard, 1989; Baumann, 1990; Bauch, 1996) as well as biosiliceous (Bohrmann, 1988; Wolf, 1990) fossil assemblages.

Foraminiferal data from **Stage 11** sediments is available from seven cores. The highest abundances of foraminifera were found in early Stage 11 sediments corresponding to Substage 11.3 at 405 ka from southeasternmost Core 23359. There is a decreasing trend in BFAR directed towards the north and west (Figs. 2-11) during early Stage 11. The species distribution in this interval reveals an assemblage that is presently unknown from the deep Norwegian-Greenland Sea (Belanger & Streeter, 1980; Mackensen, 1985; Mackensen, 1987; Thies, 1991) characterized by foraminifera such as *G. subglobosa, P. bulloides,* and *O. umbonatus* (Figs. 2-11). Mackensen *et al.* (1994) found *P. bulloides* to be characteristic of a „Southern High Productivity"-assemblage at the Polar Front in the South Atlantic, and related to a high flux of organic carbon. *Globocassidulina subglobosa* and *O. umbonatus* are thought to be infaunal as well as *P. bulloides* (*sensu* Corliss, 1985). This implies a relatively high vertical flux of organic carbon to the sea floor. Suspension-feeding foraminifera such as *C. wuellerstorfi* are present in low concentrations in upper Stage 11 sediments, which could be interpreted as reflecting the onset of a lateral advection of food. The steep gradient in total abundances of foraminifera between southeastern Core 23359 and northern and western cores implies strongly reduced surface productivity over a small area. An oceanic front with an enhanced advection of nutrients could be an explanation for this strong gradient. Selective corrosion of foraminiferal tests owing to a change in the carbonate lysocline may be neglected as Core 23359 with highest BFAR is the deepest of the investigated cores.

However, the „warm" period of Stage 11 as well as other interglacials are documented in the benthic foraminiferal record as phases of enhanced test accumulation. However, in the deep ocean differences in water temperatures between glacial and interglacial times are obviously not the primary reason for significant changes in ecological conditions at the sea floor. It seems to be clear that only a change in trophic conditions (i.e. flux of organic material to the sea floor) could explain the enhanced test accumulation.

The „warm" Oxygen-Isotope **Stages 9, 7,** and **5** are *C. wuellerstorfi* dominated periods (Figs. 2-11). The quantity of the suspension-feeding foraminifer *C. wuellerstorfi* in the sediments may reflect the importance of bottom currents which supply particulate organic matter to the foraminifera in the Norwegian-Greenland Sea. The steep gradient of test abundance from south to north and from east to west, discussed in Stage 11.3 (see above) is also present in peak interglacial situations 9.3, 7.1, and 5.5. It is concluded that maxima in benthic productivity parallel peak „warm" phases in late Pleistocene sediments, as indicated by the temperature-dependent oxygen isotope record of

planktic foraminifera in this area (Vogelsang, 1990; Weinelt, 1993). Higher secondary production at the sea floor is related to an increased flux of usable organic matter to the sea floor. The accumulation rates of calcium carbonate ($CaCO_3$), consisting mainly of coccoliths and planktic foraminifera (Kellogg, 1977; Henrich & Baumann, 1994; Birgisdottir, 1992; Bauch, 1996) may be used as a relative measure of the surface productivity. Peaks of $CaCO_3$-AR and abundance maxima of planktic foraminifera also parallel the abundance peaks of benthic foraminifera, and therefore demonstrate the direct coupling between benthic and pelagic realm (Struck & Bauch, 1994). Benthic foraminifera that are indicative of high productivity such as *G. subglobosa* and *P. bulloides* (Mackensen *et al.*, 1994) are restricted to very short intervals in the sedimentary history (*P. bulloides* in Substage 5.1, 5.5, and 7.5 as well as *G. subglobosa* in Substage 5.5). These species are not found in every core (Figs. 2-11) possibly owing to differences in the paleo surface productivity and/or differences in the water depth of the investigated cores.

The benthic foraminiferal assemblage of **Stage 6** and **4** sediments is strongly dominated by *O. umbonatus*. Test production (BFAR) is strongly reduced in comparison with interglacial periods. It is therefore concluded that the lowered glacial surface productivity in the Norwegian-Greenland Sea leads to lower secondary production on he seafloor. Altenbach (1992) regarded *O. umbonatus* dominated foraminifera assemblages as indicative of a low flux of organic carbon to the sea floor. Streeter *et al.*, (1981) and Haake & Pflaumann (1989) found the same *O. umbonatus* dominated glacial assemblage in cores from the Norwegian Sea. Taking into account the AR of *O. umbonatus* during interglacials and the absence of high productivity indicating foraminifera such as *P. bulloides* and *G. subglobosa*, the high dominance of *O. umbonatus* in glacial sediments could be interpreted as a faunal reduction during glacials owing to the limited flux of organic carbon. However, glacial benthic foraminiferal assemblages without suspension-feeding foraminifera such as *C. wuellerstorfi* do not necessarily constitute evidence for the absence of near bottom-currents.

In relation to the insolation forcing Oxygen-Isotope **Stage 3** is comparable to more or less interstadial conditions (Imbrie *et al.*, 1993). The lowered BFAR during this period gives evidence that the coupling between lower pelagic production leads to reduced production conditions at the seafloor. A brief occurrence of *C. wuellerstorfi* in Core 23063 in Substage 3.3 (Fig. 3) can be interpreted as indicating a short period with enhanced flux of organic carbon in combination with bottom near currents in that area. Specimens of *T. tricarinata* are common in Stage 3 sediments, and its morphology suggests an infaunal habitat (e. g. Corliss, 1985). Today, this species is abundant in the deepest parts of the Norwegian-Greenland Sea with lowest flux of organic carbon (Thies, 1991). It is therefore apparent that *T. tricarinata* as well as *O. umbonatus* is well adapted to a low flux of organic material.

For a closer look at glacial and interglacial (**Stage 2** and **1**) conditions at the sea floor in the Norwegian-Greenland Sea, Core 17730 provides a high-resolution record of benthic foraminifera over the last glacial/interglacial cycle (Fig. 12). Data from this core were presented by Struck (1995), who discussed the stepwise migration of benthic foraminiferal species into the postglacial Norwegian Sea. The last glacial interval in Core 17730 is dominated by *O. umbonatus* and *S. rolshauseni* in low AR. As in the other glacials, low AR and the predominance of *O. umbonatus* represents conditions of low food supply at the seafloor. In modern sediments of the Norwegian-Greenland Seas, *S. rolshauseni* is unknown except for two specimens reported by Belanger & Streeter (1980) from unstained deep sea surface samples. Investigation of shelf - to deep-sea sediments from this area (Mackensen, 1985; Hald & Vorren, 1984; Thies, 1991) did not report any occurrences of this species.

The distribution of BFAR during the last deglaciation shows low values until 10.5 ka. An initial brief AR-peak occurs at 10 ka, immediately followed by a reduction to „glacial" BFAR-values, which presumedly reflects the faunal response to the „Younger Dryas" climatic event (Mangerud *et al.*, 1974). The following BFAR-maximum at 8.5 to 7.5 ka reveals the highest test production rates of benthic foraminifera in Holocene sediments. These values are comparable to BFAR-values of Stage 5.5 from the area (Cores 23199 and 23063). The subsequent Holocene sequence has half as large BFAR-values. The faunal distribution through the deglaciation and the Holocene appears to be comparable to the Stage 6/5-transition. Another paper in this volume (Nees, *this volume*) focuses on the last deglaciation on a south/north transect of cores in high sampling resolution from the North Atlantic to the Fram Strait between Spitsbergen and Greenland.

Can major changes in the regional oceanography be seen in benthic foraminiferal assemblages?

In general, a direct deduction of information about surface circulation from fossil benthic foraminiferal assemblages is impared by the usual decoupling of surface water masses from the deep ocean. In particular the oceanography of the Norwegian-Green-

land Sea is today strongly dominated by the generation of deep water, which is formed from previously warm, saline surface waters by heat release to the atmosphere. This thermohaline circulation leads to the formation of bottom currents in the deep sea of the study area. The modern deep-sea environment of the Norwegian-Greenland Sea is dominated by *C. wuellerstorfi* (Belanger & Streeter, 1982; Mackensen, 1987; Thies, 1990). Lutze & Thiel (1987) found *C. wuellerstorfi* living in an elevated position, feeding on laterally advected organic material. Therefore, *C. wuellerstorfi* is well adapted to suspension feeding and in need of permanent lateral advective currents at the sea floor. The predominance of *C. wuellerstorfi* in fossil benthic foraminiferal faunas may therefore be an indicator for the presence of such bottom currents.

Figure 13 shows the percentage distribution of *C. wuellerstorfi* in Core 23352. High percentage values of this species are typical of sediments from interglacial periods in each of the investigated cores (see also in Struck, 1992, 1995), which seem to indicate active bottom currents during those periods. However, benthic foraminiferal assemblages without suspension feeding foraminifera such as *C. wuellerstorfi* do not necessarily suggest evidence for the absence of near bottom-currents. Nevertheless, it is reasonable to postulate a similar surface circulation system with deep water convection as in the modern environment during phases of dominant *C. wuellerstorfi* (i. e. Stage 1, 5, 7 and partly in Stage 9 and 11; see Fig. 13).

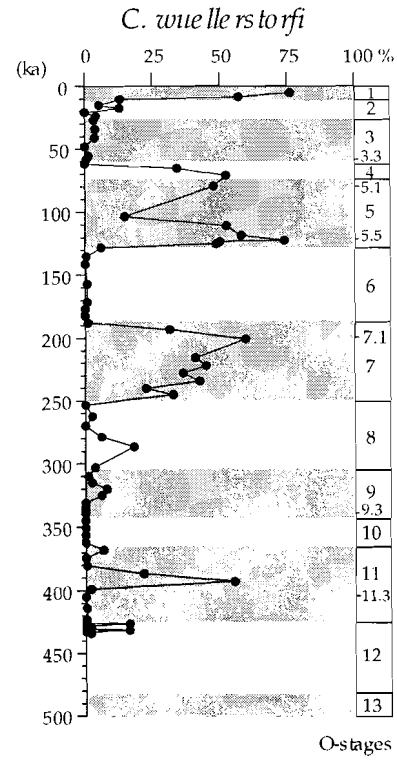


Figure 13. Percentage distribution of suspension feeding foraminifer *C. wuellerstorfi* in the sediments of Core 23352, which indicates the presence of bottom currents possibly related to phases of active deep water production in that area during times of high dominance of that species.

SUMMARY AND CONCLUSIONS

Fossil benthic foraminiferal assemblages (>0.125µm) were analyzed in sediment samples from 11 cores from the Norwegian-Greenland Sea covering the past 500.000 years. Fourty-two species and four taxonomic groups were found.

Only a few species were dominant for longer periods: *C. wuellerstorfi*, *O. umbonatus*, *T. tricarinata*, *S. rolshauseni* (see also in Nees & Struck, 1994), *P. bulloides* (also in Haake *et al.*, 1992) and *G. subglobosa*. Only *O. umbonatus* is present in every sample with a recorded foraminiferal fauna. Assemblages with dominant *C. wuellerstorfi* indicate interglacial conditions in Stages 9.3, 7, 5 and 1. The interglacial Stage 11.3 has a different benthic foraminiferal assemblage characterized by the occurence of the infaunal species *G. subglobosa* and/or *P. bulloides*. Interstadial Stage 3 has no dominant occurences of *C. wuellerstorfi*.

In the sediments of glacial Stages 12 and 10 no benthic foraminifera were found owing to calcite dissolution. The remaining glacial Stages 2, 4, 6, and 8 consist of an assemblage dominated by *O. umbonatus*, *S. rolshauseni*, and *T. tricarinata*.

The interpretation of quantitative fluctuations provides insights into surface productivity as a result of pelagic/benthic coupling. During the past 500,000 years, five brief high productivity periods (Stages 11.3, 9.3, 7.1, 5.5, and 1.1) with five- to ten-fold changes in BFAR are observed. „Normal" interglacial conditions had 2-3 times higher test production than glacials.

The interpretation of ecological habitats of benthic foraminifera revealed that suspension feeding foraminifera, which dominate interglacials, indicate the presence of bottom currents during Interglacials 7, 5 and 1 possibly originated from deep water formation in that area. Opportunistic foraminifera such as *O. umbonatus* can survive during glacial periods with low food supply, but had highest test production during interglacials.

The quantitative and qualitative investigation of foraminiferal assemblages from upper Pleistocene to Holocene sediments of the Norwegian-Greenland Sea reveals a link between climatic change, the changes in surface water productivity, surface circulation, and the response of the benthic community.

ACKNOWLEDGEMENTS

Research on this study was conducted during my tenure in the GEOMAR Bungalow. I thank Julia Soetje and the editors of this book for careful corrections. The review of Helene Bergsten has improved this manuscript particularly. The results of this investigations are part (contribution no. 321) of joint research project „SFB 313" funded by the Deutsche Forschungsgemeinschaft.

REFERENCES

Altenbach, A.V. 1992. Verbreitungsmuster benthischer Foraminiferen im Arktischen Ozean und in glazialen und interglazialen Sedimenten des Europäischen Nordmeeres. Habil. an der Math. Nat. Fak. der Christian-Albrechts-Universität zu Kiel, 111pp.

Barker, R.W. 1960. Taxonomic Notes on the Species figured by H.B. Brady in his Report on the Foraminifera dredged by H.M.S. Challenger during the years 1873-1876. *Society of Economical Paleontologists and Mineralogists, Special Publication*, **9**, 1-238.

Bauch, H. *this volume*. Paleoceanography of the N. Atlantic (68°-76°N) during the past 450 ky deduced from planktic foraminiferal assemblages and stable isotopes.

Baumann, K.-H. 1990. Veränderlichkeit der Coccolithophoridenflora des Europäischen Nordmeeres im Jungquartär. *Berichte aus dem Sonderforschungsbereich 313*, **22**, 1-146.

Belanger, P.E. & Streeter, S. S. 1980. Distribution and ecology of benthic foraminifera in the Norwegian-Greenland Sea. *Marine Micropaleontology*, **5**, 401-428.

Birgisdottir, L. 1992. Die paläo-ozeanographische Entwicklung der Islandsee in den letzten 550,000 Jahren. *Berichte aus dem Sonderforschungsbereich 313*, **34**, 1-186.

Bleil, U. & Gard, G. 1989. Chronology and correlation of Quaternary magnetostratigraphy and nannofossil biostratigraphy in Norwegian-Greenland Sea sediments. *Geologische Rundschau*, **78**: 1173-1187.

Bohrmann, G. 1988. Zur Sedimentationsgeschichte biogenen Opals im nördlichen Nordatlantik und im Europäischen Nordmeer. *Berichte aus dem Sonderforschungsbereich 313*, **9**, 1-221.

Broecker, W.S. & Denton, G. H. 1989. The role of ocean-atmosphere reorganizations in glacial cycles. *Geochimica Cosmochimica Acta*, **53**, 2465-2501.

Cushman, J.A. 1930. The foraminifera of the Atlantic Ocean. Part VII: Nonoinidae, Camerinidae, Peneroplidae and Alveolinidae. *Smithonian Institution of the U.S. National Museum, Bulletin*, **104**, 1-79.

Corliss, B. H. 1985, Microhabitats of benthic Foraminifera within deep -sea sediments. *Nature*, **314**, 435-438.

Duplessy, J.-C., Labeyrie, L., & Blanc, P.L. 1988. Norwegian Sea deep water variations over the last climatic cycle: paleo-oceanographic implications. *In*: Wanner, H. & Siegenthaler, U. *et al.*, (eds.), *Long and Short Term Variability of Climate, Lecture Notes in Earth Sciences*, **16**, 83-116.

Gehring, H. 1989. Beitrag zur paläo-ozeanographischen Entwicklung der südwestlichen Norwegischen See während der letzten 405,000 Jahre. *unpubl. master-thesis*, Kiel Univ., 1-65.

Gooday, A.J. & Lambshead, P.J.D. 1989. Influence of seasonally deposited phytodetritus on the benthic foraminiferal populations in the bathyal northeast Atlantic: the species response. *Marine Ecology Progress Series*, **58**, 53-67.

Haake, F.W. & Pflaumann, U. 1989. Late Pleistocene foraminiferal stratigraphy on the Vöring Plateau, Norwegian Sea. *Boreas*, **18**, 343-356.

Haake, F.W., Erlenkeuser, H. & Pflaumann, U. 1992. *Pullenia bulloides* (Orbigny) in sediments of the Norwegian Greenland Sea and the northeastern Atlantic Ocean: Paleo-Oceanographic evidence. *In*. Takayanagi, Y. & Saito, T. (eds.), *Studies in Benthic Foraminifera, BENTHOS '90*, Sendai 1990, TOKAI, Univ. Press., 235-244.

Hald, M. & Vorren, T.O., 1984, Modern and Holocene foraminifera and sediments on the continental shelf off Troms, North Norway. *Boreas*, **13**: 133-154.

Heeger, T. 1990. Elektronenmikroskopische Untersuchungen zur Ernährungsbiologie benthischer Foraminiferen. *Berichte aus dem Sonderforschungsbereich 313*, **21**, 1-139.

Helland-Hansen, B. & Nansen, F. 1909. The Norwegian Sea. Its physical oceanography based upon Norwegian researches 1900-1904. *Reports on Norwegian Fishery and Marine Investigations*, **2**, 1-359.

Henrich, R. 1992. Beckenanalyse des Europäischen Nordmeeres: Pelagische und glaziomarine Sedimenteinflüsse im Zeitraum 2.6 Ma bis rezent. *Habilitationsschrift, Kiel Univ.*, 1-342.

Henrich, R. & Baumann, K.-H. 1994. Evolution of the Norwegian current and the Scandinavian ice-sheets during the past 2.6 m.y.: evidence from ODP Leg 104 biogenic carbonate and terrigenous records. *Palaeogeography, Palaeoclimatology, Palaeoecology*, **108**, 75-94.

Hermelin, J.O.R. & Scott, D.B. 1985, Recent benthic foraminifera from the central North Atlantic Ocean. *Micropaleontology*, **31/3**: 199-220.

Holler, P. & Kassens, H. 1989. Sedimentphysikalische Eigenschaften aus dem Europäischen Nordmeer. *Berichte aus dem Sonderforschungsbereich 313*, **15**, 1-69.

Imbrie, J., Berger, A., Boyle, E.A., Clemens, S.C., Duffy, A., Howard, W.R., Kukla, G., Kutzbach, J., Martinson, D.G., McIntyre, A., Mix, A.C., Molfino, B., Morlino, J. J., Peterson, L.C., Pisias, N.G., Prell, W.L., Raymo, M. E., Shackleton, N.J. and Toggweiler, J.R. 1993, On the structure and origin of major glaciation cycles: 2. The 100,000 year-cycle. *Paleoceanography*, **8**, 699-735.

Jünger, B. 1990. Zur paläo-ozeanographischen Entwicklung der Islandsee während der letzten 360,000 Jahre. unpubl. master thesis, Kiel Univ., 1-69.

Kassens, H. 1990. Verfestigte Sedimentlagen und seismische Reflektoren: Frühdiagenese und Paläo-Ozeanographie. *Berichte aus dem Sonderforschungsbereich 313* **24**, 1-117.

Kassens, H. in prep.. The environmental history of the Nordic Seas: Implications from physical properties. (*in prep.*).

Kellogg, T.B. 1977. Paleoclimatology and paleoceanography of the Norwegian and Greenland Seas: The last 450,000 years. *Marine Micropaleontology*, **2**: 235-249.

Knudsen, K.L. 1971. Late Quaternary foraminifera from Vendsyssel, Denmark and Sandnes, Norway. *Bulletin of the Geological Society of Denmark*, **21**, 185-291.

Lackschewitz, K. 1991. Sedimentation am aktiven mittelozeanographischen Kolbeinsey Rücken (N' Island) - vulkanisch und klimatisch gesteuerte Ablagerungsprozesse im Spätquartär. unpubl. PhD Thesis, Kiel Univ.: 1-135.

Linke, P. 1989. Lebendbeobachtungen und Untersuchungen des Energiestoffwechsels benthischer Foraminiferen aus dem Europäischen Nordmeer. *Berichte aus dem Sonderforschungsbereich 313*, **18**, 1-108.

Linke, P. & Lutze, G.F. 1992. Microhabitats preference of benthic foraminifera - a static concept or a dynamic

adaptation to optimize food acquisition? *Marine Micropaleontology*, **20**, 215-234.

Lutze, G.F. & Coulburn, W.T. 1984. Recent benthic Foraminifera from the continental margin off Northwest Africa: Community structure and distribution. *Marine Micropaleontology*, **8**, 361-401.

Loeblich, A.R. & Tappan, H. 1953. Arctic foraminifera. *Smith. Miscellan. Coll.*, **121**, 1-150.

Loeblich, A.R. & Tappan, H. 1964. Sarcodina, chiefly thecamoebians and foraminiferids. *In*: H. R. Moore (ed.), *Treatise on invertebrate paleontology. Part C, Protista 2*, 900pp, Kansas Univ. Press.

Loeblich, A.R. & Tappan, H. 1988. *Foraminiferal genera and their classification*. Van Norstrand Reinholdy, 970pp, New York, 2 volumes.

Lutze, G.F. 1979. Benthic foraminifers at Site 397: faunal fluctuations and ranges in the Quaternary. *Initial Reports of the DSDP*, **471**, 419-431.

Lutze, G.F. & Altenbach, A.V. 1988. *Rupertina stabilis* WALLICH, a highly adapted suspension feeding foraminifer. *Meyniana*, **40**, 55-69.

Lutze, G.F. & Thiel, H. 1989. Epibenthic foraminifera from elevated microhabitats: *Cibicidoides wuellerstorfi* and *Planulina ariminensis*. *Journal of Foraminiferal Research*, **19**, 153-158.

Lutze, G.F. & Salomon. B. 1987. Foraminiferen-Verbreitung zwischen Norwegen und Grönland: ein Ost-West Profil. *Berichte aus dem Sonderforschungsbereich 313*, **6**, 69-78.

Mackensen, A. 1985. Verbreitung und Umwelt benthischer Foraminiferen in der Norwegischen See. Unpubl. PhD thesis, Kiel Univ., 1-126.

Mackensen, A. 1987. Benthische Foraminiferen auf dem Island-Schottland Rücken: Umweltanzeiger an der Grenze zweier ozeanischer Räume. *Paläontologische Zeitschrift*, **613/4**, 149-179.

Mackensen, A. & Hald, M. 1988. *Cassidulina teretis* (Tappan) and *Cassidulina laevigata* (D'Orbigny): their modern and late Quaternary distribution in northern seas. *Journal of Foraminiferal Research*, **18**, 16-24.

Mackensen, A., Grobe, H., Hubberten, H.-W. & Kuhn, G. 1994. Benthic foraminiferal assemblages and the $\delta^{13}C$-signal in the Atlantic sector of the southern ocean: glacial to interglacial contrasts. *In:* Zahn *et al.* (eds.): *Carbon cycling in the glacial ocean: constraints on the ocean's role in global change*. NATO ASI series I, **17**, 105-145.

Mangerud, J., Andersen, S.T., Berglund, B.E. & Donner, J. J. 1974. Quaternary stratigraphy of Norden, a proposal for terminology and classification. *Boreas*, **3**, 109-128.

Murray, J.W. 1991. Ecology and Palaeoecology of Benthic Foraminifera. Essex, Longman Scientific & Technical, London, 397pp.

Nees, S. *this volume*. **A** high resolution benthic foraminiferal record of the last glacial termination in the northern North Atlantic.

Nees, S. & Struck, U. 1994. The biostratigraphical and paleoceanographic significance of *Siphotextularia rolshauseni* (Phleger & Parker) in Norwegian-Greenland Sea sediments. *Journal of Foraminiferal Research*, **24**, 233-240.

Oki, K. 1989. Ecological Analysis of Benthonic Foraminifera in Kagoshima Bay, South Kyushu, Japan. *South Pacific Study*, **101**, 1-191.

Parr, W. J. 1950. Foraminifera in some sediment samples-from the Greenland Arctic. *Journal of Foraminiferal Research*, **3**, 80-89.

Phleger, F.B. & Parker, F.L. 1951. Ecology of foraminifera, Northwest Gulf of Mexico, Part II, Foraminifera species. *Geological Society of America, Memoir*, **46**, 1-64.

Phleger, F. B., Parker F. L. & Peirson, J. F. 1953. *North Atlantic foraminifera of the Swedish Deep Sea Expedition*. **7**, 1-22.

Reuss, A.E. 1851. Ueber die fossilen Foraminiferen und Entromostraceen der Septarienthone der Umgegend von Berlin. *Zeitschrift der deutschen geologischen Gesellschaft*, **1**, 49-92.

Schröder, C.J., Scott, D.B. & Medioli, F.S. 1987. Can smaller benthic foraminifera be ignored in paleo-environmental analysis? *Journal of Foraminiferal Research*, **17**, 101-105.

Scott, D.B. & Vilks, G. 1991. Benthic foraminifera in the surface sediments of the deep-sea Arctic Ocean. *Journal of Foraminiferal Research*, **201**, 20-39.

Sejrup, H.P., Fjæran, T., Hald, M., Beck, L., Hagen, J., Miljeteig, I., Morvik, I. & Norvik, O. 1981. Benthonic foraminifera in surface samples from the Norwegian continental margin between 62° N and 65° N. *Journal of Foraminiferal Research*, **11**, 277-295.

Sejrup, H.P. &. Guilbault, J.P 1980. *Cassidulina reniforme* and *C. obtusa* Foraminifera, distribution and ecology. *Sarsia*, **65**, 79-85.

Streeter, S.S., Belanger, P.E., Kellogg, T.B. & Duplessy, J. C. 1982. Late Pleistocene paleo-oceanography of the Norwegian Greenland Sea: Benthic foraminiferal evidence. *Quaternary Research*, **18**, 72-90.

Struck, U. 1992. Zur Paläo-Ökologie benthischer Foraminiferen im Europäischen Nordmeer während der letzten 600,000 Jahre. *Berichte aus dem Sonderforschungsbereich 313*, **38**, 1-129.

Struck, U. 1995. Stepwise migration of benthic foraminifera into the abyssal northeastern Norwegian Sea. *Marine Micropaleontology*, **26**, 207-213.

Struck, U. & Bauch, H. 1994. Plankton versus benthos: Glacial/interglacial paleoproductivity in the Norwegian-Greenland Seas. *Paleo Bios*, **16**, 61.

Swift, J.H. & Aargard, B. 1981. Seasonal transitions and water mass formation in the Iceland and Greenland seas. *Deep-Sea Research*, **28A**, 1107-1129.

Thies, A. 1991. Benthosforaminiferen im Europäischen Nordmeer. *Berichte aus dem Souderforschungsbereich 313*, **31**, 1-97.

Tiedemann, R., Sarnthein, M. & Shackleton, N.J. 1994. Astronomic timescale for the Pliocene Atlantic $\delta^{18}O$- and dust flux records of Ocean Drilling Program Site 659. *Paleoceanography*, **9**, 619-638.

Todd, R. & Low, D. 1967. Recent foraminifera of Alaska and southeastern Alaska. *Contributions on Paleontology, Geological Survey Professional Papers*, **573A**, 1-46.

Vogelsang, E. 1990. Paläoozeanographie des Europäischen Nordmeeres an Hand stabiler Kohlenstoff- und Sauerstoffisotope. *Berichte aus dem Sonderforschungsbereich 313*, **23**, 1-127.

Weinelt, M. 1993. Schmelzwasserereignisse und klimatische Verstärkerimpulse im Europäischen Nordmeer während der letzten 60.000 Jahre - Hinweise aus hochauflösenden Isotopenkurven. *Berichte aus dem Sonderforschungsbereich 313*, **41**, 1-104.

Wolf, T.C.W. 1991. Paläo-ozeanographische-klimatische Entwicklung des nördlichen Nordatlantiks seit dem späten Neogen (ODP Legs 104 und 105, DSDP Leg 81). *GEOMAR Report*, **5**, 1-92.

APPENDIX 1. Faunal list

For each species at least one recent reference is listed which provides an illustration:

Pyrgo rotalaria LOEBLICH & TAPPAN
1953 *Pyrgo rotalaria* - LOEBLICH & TAPPAN, p. 47, pl. 6/5-6

Cribrostomoides subglobosum (SARS)
1964 *Cribrostomoides subglobosum* (SARS) - LOEBLICH & TAPPAN, p. 225, pl. 136/1,2.

Pyrgo murrhina (SCHWAGER)
1953 *Pyrgo murrhina* (SCHWAGER) - PHLEGER *et al.*, p. 28, pl. 5/7-8.

Triloculina tricarinata d'ORBIGNY
1960 *Triloculina tricarinata* d'ORBIGNY - BARKER, p. 6, pl. 3/17a-b.

Marginulina glabra d'ORBIGNY
1967 *Marginulina glabra* d'ORBIGNY - TODD & LOW, p. 22, pl. 3/8-9.

Parafissurina groenlandica (STSCHEDRINA)
1980 *Parafissurina groenlandica* (STSCHEDRINA) - TODD & LOW, p. 24, pl. 2/6a-b.

Cibicidoides wuellerstorfi (SCHWAGER)
1953 *Planulina wuellerstorfi* (SCHWAGER) - PHLEGER *et al.*, p. 53, pl. 11/1-2.

Cibicides lobatulus (WALKER & JACOB)
1953 *Cibicides lobatulus* (WALKER & JACOB) - PHLEGER *et al.*, p. 49, pl. 11/9, 14.

Planispirinoides bucculentus (BRADY)
1980 *Planispirinoides bucculentus* (BRADY) - TODD & LOW, p. 24, pl. 2/17a-b.

Nonion labradoricum (DAWSON)
1981 *Nonion labradoricum* (DAWSON) - SEJRUP *et al.*, p. 293, pl. 2/5-6

Melonis barleeanum (WILLIAMSON)
1979 *Melonis zaandami* (VOORTHUYSEN) - LUTZE, p. 426, pl. 1/7.

Oridorsalis umbonatus REUSS
1981 *Eponides umbonatus* (REUSS) - SEJRUP *et al.*, p. 293, pl. 2/2-3.

Elphidium excavatum (TERQUEM)
1981 *Elphidium excavatum* (TERQUEM) - SEJRUP *et al.*, p. 293, pl. 1/10.

Reophax nodulosum BRADY
1960 *Reophax nodulosum* BRADY - BARKER, p. 64, pl. 31/1-9.

Quinqueloculina seminula (LINNÉ)
1960 *Quinqueloculina seminula* (LINNÉ) - BARKER, p. 10, pl. 5/6.

Pyrgo oblonga (d'ORBIGNY)
1953 *Pyrgo oblonga* (d' ORBIGNY) - PHLEGER *et al.*, p. 29, pl. 5/25-26.

Dentalina pauperata d'ORBIGNY
1953 *Dentalina pauperata* d' ORBIGNY - LOEBLICH & TAPPAN, p. 57, pl. 8/7-9.

Lenticulina gibba (d'ORBIGNY)
1960 *Lenticulina gibba* (d' ORBIGNY) - BARKER, p. 144, pl. 69/8-9.

Cassidulina laevigata d'ORBIGNY
1981 *Cassidulina laevigata* d' ORBIGNY - SEJRUP *et al.*, p. 290, pl. 1/5.

Cassidulina teretis TAPPAN
1988 *Cassidulina teretis* TAPPAN - MACKENSEN & HALD, p. 17, pl. 1/8-15.

Islandiella norcrossi (CUSHMAN)
1988 *Islandiella norcrossi* (CUSHMAN) - LOEBLICH & TAPPAN, p. 506, pl. 559/3-7.

Epistominella exigua (BRADY)
1960 *Epistominella exigua* (BRADY) - BARKER, pl. 103/14.

Pullenia bulloides (d'ORBIGNY)
1981 *Pullenia bulloides* (d' ORBIGNY) - SEJRUP *et al.*, p. 293, pl. 2/8.

Elphidium arcticum (PARKER & JONES)
1930 *Elphidium arcticum* (PARKER & JONES) - CUSHMAN, p. 27, pl. 11/1-6.

Eponides tumidulus (BRADY)
1960 *Eponides tumidulus* (BRADY) - BARKER, pl. 95/8.

Oolina hexagona (WILLIAMSON 1848)
953 *Oolina hexagona* (WILLIAMSON) - PHLEGER & PARKER, p. 69, pl. 14/1-2.

Oolina sp.
1851 *Lagena acuticosta* n - REUSS, p. 305, pl. 1/4.
1971 cf. *Oolina acuticosta* (REUSS) - KNUDSEN, pl. 6/1 u. pl. 17/1.
1953 *Lagena apiopleura* n - LOEBLICH & TAPPAN, p. 59, pl. 10/10+15.

Pattelina corrugata WILLIAMSON
1953 *Pattelina corrugata* WILLIAMSON - PHLEGER *et al.*, pl. 9/14.

Cassidulina reniforme NÖRVANG
1980 *Cassidulina reniforme* NÖRVANG - SEJRUP & GUILBAULT, p. 79-85, Abb. 2.

Globocassidulina subglobosa (BRADY)
1960 *Cassidulina subglobosa* BRADY - BARKER, pl. 54/17.

Sigmoilopsis schlumbergeri (SILVESTRI)
1960 *Sigmoilopsis schlumbergeri* (SILVESTRI) - BARKER, p. 16, pl. 8/1-4.

Ammobaculites agglutinans (d' ORBIGNY)
1960 *Ammobaculites agglutinans* (d' ORBIGNY) - BARKER, p. 66, pl. 32/19-21+24-26.

Trifarina angulosa (WILLIAMSON)
1981 *Trifarina angulosa* (WILLIAMSON) - SEJRUP *et al.* T2/10.

Stetsonia arctica (GREEN)
1991 *Stetsonia arctica* (GREEN) - SCOTT & VILKS, pl. 1/-6.

Siphotextularia rolshauseni PHLEGER & PARKER
1951 *Siphotextularia rolshauseni* PHLEGER & PARKER - PHLEGER & PARKER, p. 4, pl. 1/23-24.

Rupertina stabilis WALLICH
1988 *Rupertina stabilis* WALLICH - LUTZE & ALTENBACH, p. 31-46, Fig. 3-5.

Bulimina marginata d' ORBIGNY
1960 *Bulimina marginata* d' ORBIGNY - BARKER, pl. 51/3-5.

Pullenia quinqueloba (REUSS)
1989 *Pullenia quinqueloba* (REUSS) - OKI, pl. 20/7a-c.

Parafissurina ovata (WIESNER)
1950 *Parafissurina ovata* (WIESNER) - PARR, p. 316, p. 316, pl.

10/4.

Textularia sagittula DEFRANCE
1960 *Textularia sagittula* DERFANCE - BARKER, pl. 42/17-18.

Cyclogyra planorbis (SCHULTZE)
1964 *Cyclogyra planorbis* (SCHULTZE) - LOEBLICH & TAPPAN, pl. 329/2a-2b.

Cibicides fletcheri GALLOWAY & WISSLER
visus 1991 *Cibicides fletcheri* GALLOWAY & WISSLER, LUTZE-collection.

Footnote to Annex 1:
Taxonomic Groups

a. Morphological Group „*Lagena* spp."
This group includes calcitic elongated monothalamous foraminiferal tests, hyaline to opaque, 63-250µm in length. Relative abundance of this group is typically less than 1‰.

b. *Cassidulina teretis* and *Cassidulina laevigata* -group
In samples from subrecent sedimentary samples it is difficult to distinguish between specimens of *C. teretis* and *C. laevigata*. (Mackensen & Hald 1988). In the modern Norwegian Sea (Mackensen 1985) *C. laevigata* is restricted to water depth above 800m. It is therefore concluded that most of the specimens in the samples are *C. teretis*. In the following discussion the taxon „*C. teretis*" documents data of both species.
c. „arenaceous tubes"-group. Due to the poor preservation of tube shaped agglutinated foraminifera in the fossil assemblages, used this morphological group. The group is mainly composed of the genera *Sacchoriza* and *Hyperamina*.
d. Group *Elphidium* spp.
In the distribution of live benthic foraminifera in the deep basins of the Norwegian-Greenland Sea the genus *Elphidium* is not present (Thies 1991; Lutze & Salomon, 1987). The occurrence of tests of the typically „shelf" genus in the investigated core sediments indicates the input of shelf material reworked by ice rafting. The most important species in the samples are *E. excavatum* and *E. arcticum*. *Elphidium* spp.. They occur in relative abundances mainly below 5‰.

Appendix 1. Data for Core 23359 (Spec/g)

Depth [cm]	Age [ka]	DBD [g/ccm]	Dry Weight [g]	Isotope-Event	LSR [cm/ka]	*Pyrgo rotalaria*	*Cibicidoides wuellerstorfi*	*Epistominella exigua*	*Oinqueloculina seminula*	*Elphidium* spp.	*Triloculina tricarinata*	*Cribrostomoides subglobosus*	agglutinated Tubes	*Ammobaculites agglutinans*	*Pullenia bulloides*	*Cassidulina teretis*
0.5	0.27	0.80	38.49		1.88	42.87	981.48	2048.59	6.65	6.65	771.55	24.53	29.93	79.82	0.00	0.00
10.0	5.33	0.53	45.22		2.98	72.62	1149.91	679.33	0.00	5.66	498.18	64.13	0.00	271.73	0.00	5.66
20.0	8.68	1.02	40.34		1.58	114.19	1466.74	0.00	0.00	0.00	1573.98	58.38	0.00	660.06	0.00	6.35
31.0	11.00	1.00	38.80		1.50	19.18	97.32	0.00	0.00	4.33	265.17	5.46	0.62	0.00	0.00	0.00
49.0	27.00	1.68	39.89	3.1	1.14	2.73	4.84	0.00	2.46	0.03	4.81	3.33	0.00	0.00	0.00	0.00
54.0	31.40	0.47	49.04		4.62	0.75	0.00	0.00	1.49	0.84	0.33	0.04	0.00	0.00	0.00	0.16
66.0	34.00	1.20	33.35		1.66	7.89	9.45	0.00	0.60	0.06	2.40	0.84	0.18	0.00	0.00	0.72
69.0	35.81	0.77	29.99		2.27	2.13	2.80	0.00	1.73	1.60	0.83	0.93	0.17	0.00	0.00	0.00
74.0	38.01	0.61	43.08		2.27	2.02	3.34	0.00	11.14	0.19	6.31	0.26	0.56	0.00	0.00	0.00
79.0	40.21	1.05	50.15		0.98	1.06	0.00	0.00	10.21	0.00	0.00	0.04	0.00	0.00	0.00	0.00
89.0	50.37	0.78	45.72		1.20	0.09	1.57	0.00	1.22	2.80	8.40	0.00	0.00	0.00	0.00	0.00
94.0	55.45			3.3												
99.0	58.71	1.26	47.10		1.54	0.06	0.25	0.00	0.00	0.00	0.00	0.00	0.02	0.00	0.00	0.00
109.0	65.22	0.96	48.14	4.2.2	1.05	0.98	318.87	0.00	0.33	15.95	0.00	0.00	3.66	0.00	0.00	0.33
114.0	69.97	0.85	39.66		1.05	1.99	196.76	0.00	30.41	10.49	8.09	0.03	2.87	0.00	23.80	0.00
119.0	74.71	0.75	24.16		1.05	4.30	201.79	0.00	28.56	2.65	0.33	0.00	2.36	0.00	62.92	0.00
124.0	79.46	1.12	35.81	5.1	0.57	7.71	506.30	0.00	123.66	0.00	0.00	0.00	42.50	0.00	0.89	0.00
134.0	97.04	1.06	46.40		0.77	9.94	146.24	0.00	51.56	2.76	5.52	0.00	43.32	0.00	0.00	0.00
139.0	103.55	0.72	32.15	5.3	1.38	4.45	220.99	3.98	78.88	0.00	5.97	0.00	10.36	0.00	0.00	0.00
149.0	110.79	0.87	40.55	5.4	0.86	23.18	760.98	0.00	211.74	0.00	126.26	0.00	15.96	0.00	0.00	0.00
159.0	122.38	0.66	33.38	5.5.1	3.81	140.73	2832.64	0.00	0.18	0.00	84.37	0.00	0.00	0.00	0.00	0.00
169.0	125.00	1.03	57.12	5.5.3	2.20	1.21	21.90	0.00	0.00	2.80	1.26	0.00	0.07	0.00	0.00	0.63
179.0	129.54	1.18	55.40		2.20	0.51	0.58	0.00	0.00	1.16	0.00	0.00	0.00	0.00	0.00	0.00
194.0	136.34	3.49	54.50		0.82	0.17	0.59	0.59	0.00	4.11	0.59	0.00	0.00	0.00	0.00	0.00
196.0	141.33			6.3												
199.0	157.10			6.4												
214.0	160.67	1.59	44.95		1.70	0.27	0.09	0.00	0.00	0.09	0.00	0.53	2.49	0.00	0.00	0.00
219.0	171.37			6.5												
235.0	173.04	1.25	50.23		2.79	1.00	1.27	0.00	0.00	7.64	1.27	0.00	0.00	0.00	0.00	1.27
249.0	178.06	0.96	42.71		2.89	0.28	0.00	0.00	0.00	2.34	0.00	0.00	0.56	0.00	0.00	0.00
259.0	181.52	1.23	46.15		2.18	1.24	0.00	0.00	0.00	0.69	0.00	0.00	6.93	0.00	0.00	0.69
267.0	185.19	0.96	44.36		4.06	3.16	0.00	0.00	0.00	30.96	0.00	0.00	9.03	0.00	0.00	1.29
270.0	186.00			7.0												
271.0	186.18	1.29	49.64		4.06	0.00	0.00	0.00	0.00	0.39	0.00	0.00	0.00	0.00	0.00	0.00
280.0	188.39	0.96	41.18		4.06	0.63	0.37	0.00	0.00	0.47	0.21	0.00	3.19	0.00	0.00	0.00
289.0	190.61	0.95	37.94		4.06	11.71	238.50	0.00	0.00	25.85	0.00	0.00	40.21	0.00	0.00	0.00
299.0	193.07	0.94	44.57	7.1	1.33	17.61	435.98	0.00	0.00	0.00	0.00	0.00	35.41	0.00	0.00	0.00
309.0	200.57	1.22	41.57	7.2	0.55	15.62	355.19	0.00	0.00	0.00	81.04	0.00	25.33	0.00	0.00	0.00
324.0	228.00	0.96	37.91	7.3	1.23	4.57	17.30	0.00	0.00	9.37	5.77	0.00	20.90	0.00	0.00	5.77
334.0	236.13	1.04	44.40		1.13	15.77	0.00	0.00	0.00	0.00	0.00	0.00	7.55	0.00	0.00	0.00
344.0	245.00	1.10	33.92	8.0	2.88	1.49	0.00	0.00	0.00	1.71	0.00	0.00	0.50	0.00	0.00	0.00
354.0	248.48	1.16	39.71		2.88	1.88	2.39	0.02	0.00	1.19	3.58	0.00	8.95	0.00	0.02	0.00
364.0	251.95	0.82	53.64		2.88	1.10	0.00	0.00	0.00	0.00	0.16	0.16	2.77	0.00	0.00	0.00
374.0	255.43	1.00	24.55	8.3	0.63	0.93	13.52	0.67	0.00	2.59	0.77	0.00	0.19	0.00	0.00	0.58
384.0	271.29	0.98	41.73		0.63	0.81	0.27	0.00	0.00	5.75	0.00	6.35	15.11	0.00	0.00	0.00
394.0	287.14	1.05	33.36		0.63	2.25	0.00	0.00	3.05	12.00	123.05	15.03	63.01	0.00	0.00	0.00
404.0	303.00	0.91	42.66	9.0	1.25	6.60	0.00	0.00	0.00	0.00	13.68	14.61	12.82	0.00	0.00	0.00
414.0	311.00	0.80	37.44		1.25	3.03	2.40	0.00	0.00	0.00	0.00	6.48	3.20	0.00	0.00	0.00
424.0	319.00	0.68	40.00		1.25	36.66	231.07	1.92	1.92	0.00	0.00	9.76	7.69	0.00	0.00	0.00
434.0	327.00	0.58	33.31		1.25	40.14	486.03	0.00	0.00	0.00	0.00	13.00	0.00	0.00	0.00	0.00
439.0	331.00	0.90	29.85	9.3	1.25	4.56	17.42	0.00	0.02	0.00	0.00	2.15	0.69	0.00	0.00	0.00
444.0	335.00	0.58	46.49		2.60	0.00	0.00	0.00	0.00	0.00	0.00	0.00	0.00	0.00	0.00	0.00
509.0	360.00	0.77	42.72		2.50	0.00	0.00	0.00	0.00	0.00	0.00	0.00	0.00	0.00	0.00	0.00
514.0	362.00	1.15	47.83	10.0	2.61	2.45	8.70	2.68	0.00	10.70	3.35	0.00	28.79	0.00	0.00	0.67
534.0	369.67	1.00	36.10		3.00	0.00	0.00	0.00	0.00	0.00	0.00	6.43	0.00	0.00	0.00	0.00
545.0	373.33	1.97	29.22		1.90	0.44	2.29	0.00	0.00	0.00	0.00	6.67	0.00	0.00	0.00	0.00
554.0	378.08	2.53	47.12		1.30	1.68	0.00	2.72	0.00	0.00	0.00	0.51	0.00	0.00	0.00	0.00
564.0	385.77	0.89	26.22		1.30	3.81	10.72	0.00	0.00	0.00	0.00	0.31	0.31	0.00	0.00	0.00
579.0	397.31	0.74	33.64		1.30	93.58	0.00	0.00	0.00	0.00	0.00	0.00	0.00	0.00	0.00	0.00
589.0	405.00	0.74	34.57	11.3	1.30	126.63	11.11	0.00	0.00	0.00	355.50	0.00	0.00	0.00	0.00	0.00
593.0	408.08	0.80	29.40		1.45	0.00	0.00	0.00	0.00	0.00	0.00	0.00	0.00	0.00	0.00	0.00

Appendix 1. continued

Depth [cm]	*Oridorsalis umbonatus*	*Globocassidulina subglobosa*	*Margin ulina glabra*	*Dentalina pauperata*	*Siphotextularia rolshauseni*	*Cassidulina reniforme*	*Miliolinella sp.*	*Oolina hexagona*	*Cyclamina sp.*	*Pneafissurina ovata*	*Lenticulina gibba*	*Lagenides tunidulus*	*Lingena spp.*	Total [Spec/g]
0.5	1064.20	0.00	0.00	0.00	0.00	26.61	0.00	0.00	0.00	53.21	0.00	216.17	53.21	7513.89
10.0	1234.12	0.00	0.00	5.84	0.00	45.29	0.00	0.00	0.00	5.66	0.00	45.29	0.00	4785.39
20.0	4728.28	0.00	0.00	0.00	0.00	50.77	0.00	0.00	0.00	12.69	0.00	50.77	57.12	8849.19
31.0	848.29	0.00	0.00	0.00	0.00	69.28	0.00	0.00	0.00	0.00	0.00	3.30	0.00	1319.76
49.0	31.29	0.00	0.00	0.00	0.00	4.81	11.23	0.00	0.00	0.00	1.60	0.00	3.21	70.34
54.0	1.79	0.00	0.00	0.00	0.00	0.65	2.28	0.00	0.00	0.00	0.00	0.16	0.33	8.85
66.0	10.08	0.00	0.00	0.00	0.24	0.72	2.16	0.00	0.00	0.00	1.08	0.00	0.06	39.22
69.0	27.75	0.00	0.00	0.13	0.00	3.74	0.93	0.00	0.00	0.00	0.00	1.60	1.07	45.42
74.0	80.23	0.00	0.00	0.00	0.00	2.97	15.04	0.00	0.00	0.00	1.86	0.00	0.00	125.77
79.0	165.27	1.28	0.00	0.00	0.00	2.55	14.36	0.00	0.00	0.00	0.00	1.28	2.73	198.77
89.0	48.12	0.00	0.00	0.00	0.00	0.00	1.40	0.00	0.00	0.00	0.00	0.00	1.40	65.00
94.0														
99.0	2.89	0.34	0.00	0.00	0.00	0.00	0.00	0.00	0.00	0.00	0.00	0.00	0.00	3.57
109.0	80.44	0.00	0.00	5.32	1.00	0.00	0.33	0.00	0.00	0.33	0.00	0.00	0.00	427.88
114.0	97.22	0.00	0.00	0.00	3.63	0.00	22.62	0.00	0.00	2.82	1.61	12.91	0.00	418.07
119.0	240.74	0.00	0.08	0.00	12.25	0.33	13.25	0.00	0.00	7.95	0.00	6.62	1.32	593.41
124.0	650.56	14.30	0.03	0.00	0.00	0.00	76.88	0.00	0.00	58.09	0.00	0.00	0.00	1538.99
134.0	89.66	0.00	0.00	0.00	0.00	2.76	20.69	0.00	0.00	2.76	0.00	2.76	5.52	386.23
139.0	119.44	0.00	0.00	0.00	0.00	11.94	15.93	0.00	0.00	15.93	0.00	0.00	1.00	509.76
149.0	4434.97	0.00	0.00	3.16	0.00	28.41	157.83	0.00	0.00	0.00	25.25	50.51	31.57	5879.28
159.0	1023.98	0.00	0.00	0.03	0.00	149.57	0.00	0.00	0.00	0.00	0.00	30.68	15.34	4323.55
169.0	59.38	0.00	0.00	0.00	0.00	3.99	0.00	0.00	0.00	1.12	0.00	1.68	1.12	96.44
179.0	3.47	0.00	0.00	0.07	0.00	0.58	0.00	0.00	0.00	0.00	0.00	0.00	0.00	6.35
194.0	51.08	0.00	0.00	0.02	0.00	1.17	0.00	0.00	0.00	0.00	0.00	7.05	0.59	65.95
196.0														
199.0														
214.0	61.13	0.00	0.00	0.00	0.00	0.71	0.00	0.00	0.00	0.00	0.00	0.71	0.00	66.03
219.0														
235.0	74.37	0.00	0.00	0.00	3.82	2.55	0.00	0.00	0.00	0.00	0.00	1.27	1.27	106.10
249.0	12.07	0.00	0.00	0.00	0.00	0.00	0.00	0.00	0.00	0.00	0.00	0.00	0.02	15.37
259.0	127.58	0.00	0.00	2.77	0.00	0.00	0.00	0.00	0.00	0.00	0.00	5.55	2.77	151.00
267.0	899.93	0.00	0.00	0.00	0.00	10.31	0.00	0.00	0.00	0.00	0.00	0.00	1.29	955.97
270.0														
271.0	4.27	0.00	0.00	0.00	0.00	0.78	0.00	0.00	0.00	0.00	0.00	0.00	0.00	5.44
280.0	22.43	0.00	0.00	0.00	0.00	1.05	0.00	0.00	0.00	0.00	0.42	0.00	0.45	29.46
289.0	941.98	0.00	0.09	2.87	0.00	0.00	0.00	0.00	0.00	0.00	0.00	0.00	2.87	1266.95
299.0	2439.93	0.00	0.00	0.00	0.00	0.00	0.00	0.00	0.00	0.00	0.00	4.62	0.00	3009.00
309.0	3709.30	0.00	0.00	0.00	0.00	0.00	0.00	27.01	0.00	0.00	0.00	0.00	0.00	1213.48
324.0	46.85	0.00	0.02	0.72	0.05	5.77	0.00	0.00	0.00	0.00	0.00	0.00	0.00	123.84
334.0	271.70	0.00	0.00	0.00	0.00	0.00	0.00	0.00	0.00	0.00	0.00	45.28	0.00	340.57
344.0	1.61	0.00	0.00	0.10	0.03	0.81	0.00	0.81	0.00	0.00	0.00	0.00	0.00	8.74
354.0	89.48	0.00	0.00	0.00	0.00	2.98	0.00	0.00	0.00	1.19	0.00	0.00	0.00	112.87
364.0	15.86	0.00	0.00	0.00	0.00	0.00	0.00	0.00	0.00	0.00	0.00	0.00	0.00	20.00
374.0	22.24	0.00	0.00	0.10	0.48	1.44	0.00	0.00	0.00	0.10	0.00	1.92	1.73	48.07
384.0	58.51	0.00	0.00	0.00	0.00	0.96	0.00	0.00	0.00	0.12	0.00	2.88	0.00	98.79
394.0	996.18	0.00	0.00	0.02	0.00	24.00	0.00	0.00	0.00	0.00	0.00	0.00	0.00	1334.60
404.0	547.93	0.00	0.00	0.00	0.00	0.00	0.00	0.00	0.00	0.00	0.00	0.00	0.00	610.17
414.0	1113.73	0.00	0.00	0.03	0.00	0.00	0.00	12.80	0.00	0.00	0.00	0.00	0.00	1142.48
424.0	814.75	0.00	0.06	0.00	0.00	15.37	0.00	0.00	0.00	0.00	0.00	30.75	0.00	1149.95
434.0	9143.41	0.00	4.52	0.00	0.00	446.02	0.00	34.31	34.31	0.00	0.00	34.31	68.62	10317.53
439.0	123.93	0.00	0.02	0.00	0.00	0.00	0.00	0.00	0.00	0.00	0.00	0.00	0.00	148.79
444.0	0.00	0.00	0.00	0.00	0.00	0.00	0.00	0.00	0.00	0.00	0.00	0.00	0.00	0.00
509.0	0.00	0.00	0.00	0.00	0.00	0.00	0.00	0.00	0.00	0.00	0.00	0.00	0.00	0.00
514.0	262.92	0.00	0.00	0.00	0.00	2.68	0.00	0.00	0.00	0.00	0.00	0.00	0.00	326.31
534.0	17.73	0.00	0.00	0.00	0.00	0.00	0.00	0.00	0.00	0.00	0.00	1.77	0.00	25.93
545.0	105.13	0.00	0.03	0.00	0.00	0.00	0.00	0.00	0.00	0.00	0.00	4.38	0.00	118.96
554.0	62.64	0.00	0.02	0.00	0.00	2.72	0.00	0.00	0.00	0.00	0.00	2.72	0.00	78.09
564.0	185.50	0.00	0.04	0.00	0.00	9.76	0.00	0.00	0.00	1.83	0.00	0.00	0.00	214.71
579.0	6456.83	749.55	0.24	0.00	0.00	24.02	0.00	0.00	0.00	171.22	0.00	0.00	0.00	9019.98
589.0	8532.00	562.88	0.00	3.70	0.00	14.35	0.00	0.00	0.00	7.41	0.00	0.00	0.00	10073.22
593.0	0.00	0.00	0.00	0.00	0.00	0.00	0.00	0.00	0.00	0.00	0.00	0.00	0.00	0.00

Appendix 2. Data for Core 23063 (Spec/g)

Depth [cm]	Age [ka]	DBD [g/ccm]	Dry Weight [g]	Isotope Event	LSR [cm/ka]	*Pyrgo rotalaria*	*Cibicidoides wuellerstorfi*	*Epistominella exigua*	*Quinqueloculina seminula*	*Elphidium* spp.	*Triloculina tricarinata*	*Cribrostomoides subglobosus*	agglutinated Tubes	*Ammobaculites agglutinans*	*Pullenia bulloides*	*Cassidulina teretis*
1.0	2.00	0.60	6.71		1.63	12.33	121.24	57.64	0.00	0.00	0.00	1.66	0.00	0.00	0.00	0.00
4.0	3.98	0.60	4.00		1.63	4.42	333.57	59.59	0.00	7.45	0.00	7.45	0.00	0.00	0.00	0.00
11.0	8.60	0.76	4.07	1.1	2.50	6.89	23.99	0.00	0.00	0.00	8.42	0.51	4.59	0.00	0.00	0.00
14.0	9.75	0.75	6.47		2.50	0.16	31.67	0.00	0.00	0.00	0.00	1.77	0.00	0.00	0.00	0.00
15.5	10.1			Vo												
24.0	13.60	0.93	8.38	Vo	5.77	2.12	11.80	0.00	0.00	0.89	0.89	0.22	0.89	0.00	0.00	0.22
31.0	14.9			2.2												
34.0	16.40	0.95	8.79		1.88	0.60	0.24	0.00	0.00	0.12	0.00	0.00	0.12	0.00	0.00	0.00
44.0	21.40	0.95	9.61		3.57	0.21	0.00	0.00	0.00	0.83	1.67	0.00	0.00	0.00	0.00	0.00
54.0	24.20	0.95	9.36		3.57	0.00	0.00	0.00	0.11	1.07	0.64	0.00	0.00	0.00	0.00	0.21
64.0	27.00	0.96	14.16	3.1	4.15	0.21	0.07	0.00	0.42	0.78	0.14	0.00	0.00	0.00	0.00	0.07
74.0	29.41	0.96	13.66		4.15	1.24	0.15	0.00	1.98	0.44	0.59	0.00	0.07	0.00	0.00	0.59
84.0	31.82	0.96	12.30		4.15	0.73	0.08	0.00	0.33	0.16	0.08	0.08	0.00	0.00	0.00	0.00
94.0	34.23	0.96	14.95		4.15	1.14	0.00	0.00	0.67	0.00	0.54	1.00	0.00	0.00	0.00	0.00
104.0	36.64	0.96	12.49		4.15	0.00	0.00	0.08	0.00	0.40	0.24	0.40	0.00	0.00	0.00	0.00
112.0	38.57	0.96	14.83		4.15	0.81	1.48	0.00	0.00	0.94	1.15	0.20	0.00	0.00	0.00	0.00
122.0	40.98	0.96	19.93		4.15	0.80	2.41	0.00	0.00	1.35	1.25	0.15	0.00	0.00	0.00	0.00
132.0	43.39	0.96	13.82		4.15	1.45	0.00	0.00	0.00	0.43	0.00	0.00	0.00	0.00	0.00	0.00
142.0	45.81	0.96	15.39		4.15	1.49	0.00	0.00	0.00	0.00	0.52	0.00	0.00	0.00	0.00	0.00
152.0	48.22	0.96	18.31		4.15	2.73	0.00	0.00	0.00	0.00	1.31	0.05	0.00	0.00	0.00	0.05
162.0	50.63	0.96	15.31		4.15	0.13	0.00	0.00	0.00	0.13	0.59	0.00	0.00	0.00	0.00	0.00
170.0	52.56	0.96	17.43		4.15	0.00	0.00	0.00	0.00	0.00	0.00	0.00	0.00	0.00	0.00	0.00
182.0	55.45	0.96	10.21	3.3	1.02	0.49	0.88	0.00	0.00	0.49	0.10	0.00	0.00	0.00	0.00	0.00
192.0	65.22	0.96	11.79	4.2.2	1.11	2.79	37.63	0.00	0.00	0.00	0.00	0.00	0.10	0.00	0.10	0.00
202.0	72.92	0.99	12.04		1.11	2.54	58.32	0.00	0.00	1.56	8.58	0.10	0.10	0.00	6.05	0.00
207.5	77.15	0.99	11.63		1.11	1.01	23.73	0.00	1.31	0.00	2.42	0.20	0.00	0.00	39.49	0.00
210.5	79.455			5.1												
216.0	83.27	0.99	11.11		1.54	1.29	42.22	0.00	14.70	2.12	10.35	0.00	0.47	0.00	8.35	0.94
220.0	86.03	0.99	9.85		1.54	1.53	104.68	0.00	25.98	0.00	14.14	0.00	4.97	0.00	0.00	0.00
226.5	90.525			5.2												
230.0	93.91	0.99	11.80		1.54	1.09	28.61	0.00	12.93	0.00	3.66	0.00	0.06	0.00	0.00	0.00
234.0	97.76	0.99	9.36		1.54	0.65	21.93	0.00	18.47	0.00	2.31	0.00	0.00	0.00	0.00	0.00
240.0	103.55	0.99	9.20	5.3	1.38	5.11	104.82	0.00	23.49	0.00	0.00	0.00	7.18	0.00	0.00	0.00
250.0	110.79	0.95	10.70	5.4	0.86	3.83	106.20	5.98	9.72	0.00	23.93	0.00	3.74	0.00	0.00	0.00
260.0	122.38	0.90	9.63	5.5.1	3.55	14.15	858.06	43.66	11.58	0.00	7.13	2.67	22.28	0.00	0.00	7.13
270.0	125.00	1.00	14.10	5.5.3	6.05	0.00	5.38	0.00	0.00	0.53	0.00	0.00	0.00	0.00	0.00	0.00
280.0	126.76	1.00	10.11		6.05	0.00	0.00	0.00	0.00	0.00	0.00	0.00	0.00	0.00	0.00	0.00
287.0	128.00	1.00	9.50	6.0	7.13	0.00	0.00	0.00	0.00	0.21	0.00	0.00	0.95	0.00	0.00	0.00
291.0	128.42	1.30	13.32		7.13	0.00	0.00	0.00	0.00	0.00	0.00	0.00	0.00	0.00	0.00	0.00
316.0	132.07	1.30	19.36		7.13	0.00	0.00	0.00	0.00	0.00	0.00	0.00	0.00	0.00	0.00	0.00
327.0	133.61	1.30	10.72		7.13	0.00	0.00	0.00	0.00	0.00	0.00	0.00	0.00	0.00	0.00	0.00
337.0	135.02	1.30	12.29		7.13	0.00	0.00	0.00	0.00	0.33	0.65	0.00	0.00	0.00	0.00	0.00
347.0	136.42	1.30	12.71		7.13	0.16	0.16	0.00	0.00	0.24	0.00	0.00	0.00	0.00	0.00	0.00
355.0	137.54	1.30	11.45		7.13	0.00	0.00	0.00	0.00	0.00	0.00	0.00	0.00	0.00	0.00	0.00
363.0	138.66	1.30	13.37		7.13	0.07	0.00	0.00	0.00	0.00	0.67	0.00	0.00	0.00	0.00	0.00
372.0	139.93	1.15	14.79		7.13	0.00	0.00	0.00	0.00	0.00	0.00	0.00	0.00	0.00	0.00	0.00
382.0	141.33			6.3												
392.0	148.08	1.15	17.29		1.48	0.00	0.00	0.00	0.00	0.00	0.00	0.00	0.00	0.00	0.00	0.00
405.5	157.19	1.20	15.43		1.48	0.39	0.06	0.00	0.00	0.65	0.00	0.00	0.00	0.00	0.00	0.13
410.5	160.57	1.20	14.61		1.48	0.00	0.00	0.00	0.00	0.00	0.00	0.00	0.00	0.00	0.00	0.00
418.5	165.97	1.10	15.63		1.48	0.26	0.13	0.00	0.00	1.15	0.06	0.00	0.00	0.00	0.00	0.19
426.5	171.37	1.10	13.09	6.5	3.73	10.02	0.00	0.00	0.00	0.62	3.08	0.00	0.62	0.00	0.00	0.00
435.5	173.76	1.10	16.98		3.73	0.48	0.00	0.00	0.00	0.24	0.00	0.00	0.12	0.00	0.00	0.00
439.5	174.83	1.17	20.04		3.73	2.77	0.00	0.00	0.00	0.40	0.10	0.00	0.00	0.00	0.00	0.00
451.0	177.89	1.17	19.74		3.73	0.00	0.00	0.00	0.00	0.00	0.00	0.00	0.00	0.00	0.00	0.00
471.0	183.21	1.17	21.84		3.73	0.00	0.00	0.00	0.00	0.00	0.00	0.00	0.00	0.00	0.00	0.00
481.5	186.00	1.03	15.58	6.0	2.40	3.74	4.98	0.00	0.12	0.00	0.00	0.00	0.00	0.00	0.00	0.00
490.5	189.86	1.03	14.29		2.40	4.62	237.43	0.00	0.00	0.00	0.27	0.00	0.00	0.00	0.00	0.00
498.0	193.07	1.03	19.51	7.1	0.62	3.84	126.68	0.00	0.00	0.00	4.92	0.00	0.00	0.00	0.00	0.00
507.0	207.52	1.03	13.53		0.62	8.28	157.91	0.00	0.00	0.00	16.56	0.00	0.00	0.00	0.00	0.00
512.0	215.54	1.10	10.67	7.3	0.80	4.59	32.72	0.00	0.09	0.00	4.69	0.00	0.00	0.00	0.00	0.00
522.0	228.00	1.05	11.91	7.4	1.15	2.86	15.62	0.00	0.00	0.00	0.34	0.00	0.00	0.00	0.00	0.00
530.0	234.97	1.05	13.94		1.15	16.50	10.90	0.00	0.00	2.30	36.73	0.00	0.00	0.00	0.00	0.00
536.0	240.19	1.05	13.79	7.5	3.74	0.00	0.07	0.00	0.00	0.15	0.07	0.00	0.00	0.00	0.00	0.00
543.0	242.01	1.05	11.30		3.74	0.73	0.00	0.00	0.00	0.18	0.18	0.00	0.00	0.00	0.00	0.18
546.5	242.92	1.18	15.40		3.74	0.00	0.00	0.00	0.00	0.13	0.00	0.00	0.00	0.00	0.00	0.13
554.5	245.00	1.30	18.13	8.0	2.39	1.03	0.00	0.00	0.00	0.00	0.00	0.00	0.00	0.00	0.00	0.00
564.5	249.27	1.10	8.26		2.39	1.31	0.12	0.00	0.00	0.24	0.00	0.00	0.47	0.00	0.00	0.47
570.0	251.63	1.10	12.42		2.39	0.00	0.32	0.00	0.00	0.32	5.60	0.00	0.00	0.00	0.00	0.16
580.0	255.90	1.10	13.62	8.4	0.42	1.32	0.15	0.00	0.00	0.00	9.47	2.42	0.00	0.00	0.00	0.00
590.0	279.45	1.10	13.84		0.42	1.01	0.00	0.00	0.00	0.00	7.51	0.29	0.72	0.00	0.00	0.00
600.0	303.00	1.14	17.67	9.1	0.36	2.60	0.40	0.00	0.00	0.00	5.43	0.57	0.23	0.00	0.00	0.00
610.0	331.00	1.14	10.89	9.3	1.25	1.56	42.62	0.00	0.00	0.09	0.00	0.64	0.18	0.00	0.00	0.00
620.0	339.00	1.14	17.79	10.0	22.00	0.00	0.00	0.00	0.00	0.00	0.00	0.00	0.00	0.00	0.00	0.00
664.0	341.00	1.26	18.32	10.2	0.85	0.00	0.00	0.00	0.00	0.00	0.00	0.00	0.00	0.00	0.00	0.00
687.0	368.00	1.16	18.53	11.1	1.29	0.00	0.00	0.00	0.00	0.00	0.00	0.00	0.00	0.00	0.00	0.00
696.0	375.00	1.16	18.09	11.2	0.90	0.00	0.00	0.00	0.00	0.00	0.00	0.00	0.00	6.00	0.00	0.00
706.0	386.11	1.16	19.05		0.90	3.52	0.21	0.00	0.00	0.00	0.84	0.00	0.00	0.00	0.00	0.00
713.0	393.89	1.16	13.12		0.90	3.66	20.20	0.00	0.00	0.00	0.00	0.00	0.00	0.00	0.00	0.00
723.0	405.00	1.16	13.87	11.3	1.39	10.88	0.86	0.00	0.00	0.00	0.00	0.00	0.00	0.00	0.00	0.00
731.0	410.76	1.16	14.34		1.39	0.00	0.07	0.00	0.00	0.00	0.00	0.00	0.00	0.00	0.00	0.00
738.0	415.80	1.16	18.25		1.39	0.00	0.00	0.00	0.00	0.00	0.00	0.00	0.00	0.00	0.00	0.00

Appendix 2. continued

Depth [cm]	*Oridorsalis umbonatus*	*Globocassidulina subglobosa*	*Marginulina glabra*	*Dentalina pauperata*	*Siphotextularia rolshauseni*	*Cassidulina reniforme*	*Miliolinella* sp.	*Oolina hexagona*	*Cyclammina* sp.	*Parafissurina ovata*	*Lenticulina gibba*	*Eponides tumidulus*	*Lagena* spp.	Total [Spec/g]
1.0	53.21	0.00	0.00	0.00	0.00	4.43	0.00	0.00	0.00	4.43	0.00	8.87	0.00	272.69
4.0	163.88	0.00	0.00	0.00	0.00	74.49	0.00	0.00	0.00	0.00	0.00	7.45	0.00	673.20
11.0	16.59	0.00	0.00	0.00	0.00	2.04	0.00	0.00	0.00	0.00	0.00	0.00	0.00	65.34
14.0	38.74	0.00	0.00	0.00	0.00	1.29	0.00	0.00	0.00	0.00	0.00	1.29	0.00	74.91
15.5														
24.0	13.36	0.00	0.00	0.00	0.00	0.89	0.00	0.00	0.00	0.00	0.00	0.00	0.00	34.40
31.0														
34.0	4.47	0.00	0.00	0.00	4.83	0.00	0.00	0.00	0.00	0.00	0.00	0.00	0.48	10.87
44.0	0.62	0.00	0.00	0.00	4.16	0.21	0.00	0.00	0.00	0.00	0.00	0.21	0.21	8.53
54.0	0.43	0.00	0.00	0.00	0.00	0.21	0.11	0.00	0.00	0.21	0.00	0.00	0.00	3.52
64.0	1.20	0.00	0.00	0.00	0.64	0.07	0.00	0.00	0.00	0.07	0.07	0.00	0.07	4.02
74.0	0.88	0.00	0.00	0.00	0.00	1.17	0.00	0.00	0.00	0.44	0.00	0.00	0.00	7.98
84.0	1.95	0.00	0.00	0.24	0.00	0.00	0.00	0.00	0.00	0.00	0.08	0.00	0.00	3.74
94.0	2.14	0.00	0.00	0.07	0.00	0.54	0.00	0.00	0.00	0.00	0.00	1.07	0.00	7.70
104.0	2.64	0.00	0.00	0.00	0.00	0.40	0.00	0.00	0.00	0.40	0.00	1.68	0.00	6.40
112.0	0.61	0.00	0.00	0.00	0.00	1.89	0.00	0.27	0.00	0.74	0.07	1.08	0.00	9.24
122.0	2.06	0.00	0.00	0.05	0.00	1.61	0.00	0.40	0.00	0.15	0.00	2.01	0.00	12.24
132.0	5.36	0.00	0.00	0.00	0.00	0.72	0.00	0.00	0.00	0.00	0.00	1.45	0.00	9.41
142.0	5.72	0.00	0.00	0.00	0.00	0.00	0.00	0.00	0.00	0.19	0.00	0.78	0.00	8.97
152.0	16.16	0.00	0.00	0.00	0.00	0.87	0.00	0.44	0.00	0.11	0.00	0.93	0.00	22.72
162.0	9.67	0.00	0.00	0.00	0.00	0.39	0.00	0.00	0.00	0.00	0.00	0.20	0.00	11.17
170.0	0.00	0.00	0.00	0.00	0.00	0.00	0.00	0.00	0.00	0.00	0.00	0.00	0.00	0.00
182.0	7.93	0.00	0.00	0.00	0.00	0.49	0.00	0.00	0.00	0.00	0.00	0.69	0.00	11.16
192.0	20.71	0.00	0.00	0.00	0.00	4.78	0.00	0.00	0.00	0.10	0.00	1.59	0.00	67.79
202.0	9.36	0.00	0.00	0.00	0.00	9.36	0.00	0.00	0.00	1.17	0.00	1.56	0.00	98.70
207.5	39.09	0.00	0.00	0.00	0.00	1.62	0.00	0.00	0.00	2.02	0.00	6.46	0.00	117.36
210.5														
216.0	78.67	0.00	0.00	0.00	0.94	5.64	0.00	0.94	0.00	4.12	0.00	1.88	0.00	173.57
220.0	107.73	0.00	0.00	0.00	0.00	21.39	0.00	0.00	0.00	3.82	0.00	4.58	0.00	293.78
226.5														
230.0	14.70	0.00	0.00	0.00	0.00	0.00	0.00	0.00	0.00	0.11	0.00	2.75	0.00	63.97
234.0	18.47	0.00	0.00	0.00	0.00	0.00	0.00	0.00	0.00	0.00	0.00	2.31	0.00	65.29
240.0	52.41	0.00	0.00	0.00	0.00	0.00	0.00	0.00	0.00	1.74	0.22	10.44	0.00	208.88
250.0	50.11	13.46	0.00	0.00	0.00	0.00	0.00	0.00	0.00	2.99	0.00	0.00	0.00	239.41
260.0	278.00	226.32	0.00	0.00	0.00	42.77	0.00	0.00	0.00	48.12	0.00	21.38	0.00	1,869.26
270.0	4.85	0.00	0.00	0.00	0.00	0.53	0.00	0.00	0.00	0.00	0.00	0.00	0.00	11.36
280.0	0.00	0.00	0.00	0.00	0.00	0.00	0.00	0.00	0.00	0.00	0.00	0.00	0.00	0.00
287.0	1.68	0.00	0.00	0.00	0.00	0.00	0.00	0.00	0.00	0.00	0.00	0.00	0.00	2.95
291.0	0.00	0.00	0.00	0.00	0.00	0.00	0.00	0.00	0.00	0.00	0.00	0.00	0.00	0.00
316.0	0.00	0.00	0.00	0.00	0.00	0.00	0.00	0.00	0.00	0.00	0.00	0.00	0.00	0.00
327.0	8.77	0.00	0.00	0.00	0.00	0.00	0.00	0.00	0.00	0.00	0.00	0.00	0.00	8.86
337.0	6.83	0.00	0.00	0.00	0.00	0.00	0.00	0.00	0.00	0.00	0.00	0.33	0.00	8.14
347.0	18.72	0.00	0.00	0.00	0.00	0.00	0.00	0.00	0.00	0.31	0.16	0.63	0.00	20.46
355.0	0.00	0.00	0.00	0.00	0.00	0.00	0.00	0.00	0.00	0.00	0.00	0.00	0.00	0.00
363.0	20.12	0.00	0.00	0.00	0.00	0.00	0.00	0.00	0.00	0.00	0.00	0.30	0.00	21.17
372.0	0.00	0.00	0.00	0.00	0.00	0.00	0.00	0.00	0.00	0.00	0.00	0.00	0.00	0.00
382.0														
392.0	0.00	0.00	0.00	0.00	0.00	0.00	0.00	0.00	0.00	0.00	0.00	0.00	0.00	0.00
405.5	24.56	0.00	0.00	0.00	0.00	0.13	0.00	0.00	0.00	0.00	0.00	0.00	0.00	26.11
410.5	0.00	0.00	0.00	0.00	0.00	0.00	0.00	0.00	0.00	0.00	0.00	0.00	0.00	0.00
418.5	9.59	0.00	0.00	0.00	0.00	0.13	0.00	0.00	0.00	0.00	0.13	0.77	0.00	13.24
426.5	27.76	0.00	0.00	0.00	0.00	0.00	0.00	0.00	0.00	0.62	0.00	0.00	0.00	42.72
435.5	0.71	0.00	0.00	0.00	0.00	0.12	0.00	0.00	0.00	0.00	0.00	0.00	0.00	1.66
439.5	11.28	0.00	0.00	0.00	0.00	0.40	0.00	0.00	0.00	0.00	0.00	0.00	0.00	14.95
451.0	0.00	0.00	0.00	0.00	0.00	0.00	0.00	0.00	0.00	0.00	0.00	0.00	0.00	0.00
471.0	0.00	0.00	0.00	0.00	0.00	0.00	0.00	0.00	0.00	0.00	0.00	0.00	0.00	0.00
481.5	58.81	0.00	0.06	0.00	0.00	0.00	0.00	0.00	0.00	0.00	0.06	0.00	0.00	67.90
490.5	52.16	0.00	0.07	0.54	0.00	0.00	0.00	0.00	0.00	4.35	0.00	0.00	0.00	299.71
498.0	50.84	0.00	0.00	0.00	0.00	0.00	0.00	0.00	0.00	0.00	0.00	0.00	0.00	189.97
507.0	118.28	0.00	0.00	0.00	0.00	2.37	0.00	0.00	0.00	0.00	0.00	0.00	0.00	303.98
512.0	94.59	0.00	0.00	0.00	0.00	0.00	0.00	1.50	0.00	0.00	0.00	0.00	0.00	139.68
522.0	8.40	0.00	0.00	0.00	0.00	0.00	0.00	0.00	0.00	0.00	0.00	0.00	0.00	27.72
530.0	12.05	0.00	0.00	0.00	0.00	9.18	0.00	0.00	0.00	0.00	0.00	0.00	0.00	88.24
536.0	1.19	0.00	0.00	0.00	0.00	0.00	0.00	0.00	0.00	0.00	0.00	0.00	0.00	2.31
543.0	5.37	0.00	0.00	0.00	0.00	0.00	0.00	0.00	0.00	0.00	0.00	0.00	0.00	6.91
546.5	0.93	0.00	0.00	0.00	0.00	0.40	0.00	0.00	0.00	0.00	0.00	0.00	0.00	1.60
554.5	0.00	0.00	0.00	0.00	0.00	0.00	0.00	0.00	0.00	0.00	0.00	0.00	0.00	1.03
564.5	58.42	0.00	0.00	0.00	0.00	0.47	0.00	0.00	0.00	0.00	0.00	0.00	0.47	63.05
570.0	21.23	0.00	0.00	0.08	0.16	0.16	0.00	0.00	0.00	0.08	0.00	0.16	0.00	28.34
580.0	61.10	0.00	0.00	0.00	0.00	0.00	0.00	0.00	0.00	2.35	0.00	0.00	0.00	77.70
590.0	51.45	0.00	0.00	0.00	0.00	0.58	0.00	0.00	0.00	0.58	0.00	0.00	0.00	65.75
600.0	52.51	0.00	0.00	0.06	0.00	0.00	0.00	0.00	0.00	0.00	0.00	0.00	0.00	63.77
610.0	133.73	0.00	0.00	0.00	0.00	0.00	0.00	0.00	0.00	0.00	0.00	1.47	0.00	183.52
620.0	0.00	0.00	0.00	0.00	0.00	0.00	0.00	0.00	0.00	0.00	0.00	0.00	0.00	0.00
664.0	0.00	0.00	0.00	0.00	0.00	0.00	0.00	0.00	0.00	0.00	0.00	0.00	0.00	0.00
687.0	0.00	0.00	0.00	0.00	0.00	0.00	0.00	0.00	0.00	0.00	0.00	0.00	0.00	0.00
696.0	0.00	0.00	0.00	0.00	0.00	0.00	0.00	0.00	0.00	0.00	0.00	0.00	0.00	0.00
706.0	46.19	0.00	0.00	0.00	0.00	0.84	0.00	0.00	0.00	0.00	0.00	0.00	0.00	51.59
713.0	92.68	1.30	0.00	0.00	0.00	4.88	0.00	0.00	0.00	1.37	0.00	0.00	0.00	127.12
723.0	203.27	19.17	0.00	0.00	0.00	9.23	0.00	4.61	0.00	0.14	0.00	0.00	0.00	253.80
731.0	297.14	9.62	0.00	0.00	0.00	13.39	0.00	0.00	0.00	2.30	0.00	0.00	0.00	322.53
738.0	0.00	0.00	0.00	0.00	0.00	0.00	0.00	0.00	0.00	0.00	0.00	0.00	0.00	0.00

Appendix 3. Data for Core 23352 (Spec/g)

Depth [cm]	Age [ka]	DBD [g/ccm]	Dry Weight [g]	Isotope Event	LSR [cm/ka]	*Pyrgo rotalaria*	*Cibicidoides wuellerstorfi*	*Epistominella exigua*	*Quinqueloculina seminula*	*Elphidium spp.*	*Triloculina tricarinata*	*Cribrostomoides subglobosus*	agglutinated Tubes	*Ammobaculites agglutinans*	*Pullenia bulloides*	*Cassidulina teretis*
10.0	5.00	0.70	24.04		4.29	3.66	445.68	13.31	0.00	5.33	10.65	56.25	8.99	0.00	0.00	13.31
24.0	8.27	0.67	23.02		4.29	6.69	442.04	0.00	0.00	0.00	47.96	45.00	13.90	0.00	0.00	0.00
29.0	8.60			1.1												
34.0	10.60	0.98	38.48		2.79	0.23	7.56	0.00	0.00	0.00	11.23	1.35	4.94	0.00	0.00	14.97
46.0	14.90	0.90	34.07	2.2	3.22	0.35	0.97	0.00	0.00	0.23	4.23	0.29	1.47	0.00	0.00	2.82
55.0	17.69	0.78	34.15		3.22	0.23	4.22	0.00	0.00	0.94	9.84	0.70	3.75	0.00	0.00	0.47
65.0	20.79	0.83	41.00		3.22	0.12	0.00	0.00	0.07	0.39	1.37	0.00	1.17	0.00	0.00	0.20
75.0	23.90	0.93	41.61		3.22	0.02	0.77	0.38	0.02	0.00	7.31	0.77	2.69	0.00	0.00	1.54
85.0	27.00	0.96	39.59	3.1	1.41	0.03	0.43	0.00	0.03	0.00	6.47	0.88	0.20	0.00	0.00	0.81
95.0	34.11	0.88	38.36		1.41	0.08	0.26	0.05	0.00	0.21	2.40	0.42	0.21	0.05	0.05	0.21
105.0	41.23	0.90	40.06		1.41	0.92	0.20	0.00	0.00	0.00	1.80	0.45	0.00	0.00	0.00	0.40
115.0	48.34	0.91	36.48		1.41	0.93	0.00	0.00	0.00	0.00	7.89	1.81	0.00	0.00	0.00	0.88
125.0	55.45	0.89	34.80	3.3	3.07	1.03	0.23	0.11	0.00	0.00	7.24	0.26	0.72	0.00	0.00	0.57
135.0	58.71	0.87	38.13		3.07	0.50	0.21	0.00	0.00	0.63	19.09	0.34	2.10	0.00	0.00	1.05
145.0	61.96	0.83	41.31		3.07	0.17	0.00	0.00	0.00	0.19	4.26	0.00	0.10	0.00	0.00	0.00
155.0	65.22	0.93	41.93	4.2.2	1.73	0.12	6.68	0.57	0.00	0.00	4.39	0.00	0.57	0.00	0.38	0.19
165.0	71.00	1.00	40.10	5.0	1.21	0.07	51.47	0.80	0.00	0.40	11.57	3.67	4.56	0.00	3.19	4.39
175.0	79.46	0.87	40.55	5.1	0.62	0.07	92.78	1.58	0.00	1.18	11.47	5.43	22.76	0.39	15.78	2.76
190.0	103.55	0.75	33.32	5.3	1.38	0.00	4.20	0.00	0.00	0.12	9.24	0.36	2.64	0.00	0.12	0.60
200.0	110.79	0.84	39.30	5.4	2.59	0.05	74.94	0.41	0.00	0.41	13.44	0.43	10.20	0.00	0.00	0.00
220.0	118.51	0.79	29.65		2.59	1.15	69.14	1.08	0.00	1.08	3.24	0.10	6.37	0.00	0.00	2.16
230.0	122.38	0.60	27.78	5.5.1	2.59	13.10	413.88	0.00	0.00	0.00	2.30	11.41	51.12	0.00	0.00	3.46
235.0	123.25	0.70	36.73	5.5.2	5.71	0.94	101.65	0.47	0.00	0.00	3.76	0.47	3.76	0.00	0.00	6.59
245.0	125.00	0.88	33.37	5.5.3	1.49	0.82	14.00	0.00	0.00	0.59	1.06	0.00	0.35	0.00	0.00	0.12
250.0	128.37	0.87	45.07		1.49	2.70	2.18	0.00	0.00	0.00	6.97	0.00	0.87	0.00	0.00	2.61
260.0	135.10	0.77	36.29	6.2	1.77	0.60	0.24	0.48	0.00	0.00	10.55	0.00	0.00	0.00	0.00	2.64
271.0	141.33	1.02	33.11	6.3	0.57	1.07	0.00	0.36	0.00	0.00	3.20	0.00	0.71	0.00	0.00	1.42
280.0	157.10	0.84	35.45	6.4	0.70	0.08	0.39	1.32	0.00	0.47	6.78	0.03	0.08	0.00	0.00	0.99
290.0	171.37	0.91	43.44	6.5	1.84	0.12	0.24	1.21	0.00	2.42	5.80	0.00	6.40	0.00	0.00	2.66
300.0	176.80	0.83	37.88		1.84	0.51	0.00	0.00	0.00	0.45	9.48	0.00	4.99	0.00	0.00	5.87
310.0	182.22	0.96	40.63		1.84	0.28	0.00	0.00	0.00	0.64	1.20	0.00	0.00	0.00	0.00	0.46
320.0	187.65	0.85	43.32		1.84	0.00	0.84	0.00	0.00	0.84	6.34	0.00	0.42	0.00	0.00	1.27
330.0	193.07	0.85	40.19	7.1	1.33	0.00	45.28	0.39	0.00	0.39	3.94	1.18	0.79	0.00	0.00	7.48
340.0	200.57	1.00	42.26	7.2	0.67	0.00	217.86	0.00	0.00	0.00	6.05	0.76	4.54	0.00	0.00	31.76
350.0	215.54	1.06	23.40	7.3	1.62	0.00	42.40	0.20	0.00	0.60	0.00	2.59	1.79	0.00	0.20	1.59
360.0	221.70	1.03	44.48		1.62	0.00	56.22	0.00	0.00	0.76	0.00	3.79	4.54	0.00	0.00	0.57
370.0	227.87	0.90	43.71		1.62	0.00	53.34	0.00	0.00	0.00	1.37	0.94	67.41	0.00	0.00	2.74
380.0	234.03	0.97	37.54		1.62	0.00	10.97	0.00	0.00	0.36	0.18	0.00	1.44	0.00	1.44	0.54
390.0	240.19	0.97	30.98	7.5	2.08	0.02	6.98	0.00	0.00	0.37	2.20	0.37	3.29	0.00	0.00	0.73
400.0	245.00	0.87	37.87	8.0	1.21	0.00	24.72	0.00	0.00	0.43	2.56	0.43	0.43	0.00	0.00	5.54
410.0	253.29	0.81	42.90		1.21	0.00	0.00	0.00	0.00	0.78	0.52	0.52	1.81	0.00	0.00	13.44
421.0	262.40	0.87	35.22		1.21	0.00	0.21	0.00	0.00	0.21	0.00	0.00	0.21	0.00	0.00	0.42
430.0	269.86	0.90	28.15		1.21	0.00	0.00	0.00	0.00	1.12	0.37	0.00	0.00	0.00	0.00	0.37
441.0	278.97	0.80	41.15		1.21	0.00	3.18	0.00	0.00	0.45	0.91	0.00	0.00	0.00	0.00	2.27
450.0	286.43	0.67	41.28		1.43	0.00	22.27	0.00	0.00	0.00	2.56	0.00	0.28	0.00	0.28	1.99
470.0	303.00	1.00	39.03	9.1	1.43	0.00	2.33	0.00	0.00	0.00	11.66	1.56	0.39	0.00	0.00	5.05
480.0	310.00	0.97	36.39		2.00	0.00	0.78	0.00	0.00	1.16	1.55	1.16	0.39	0.00	0.00	4.26
490.0	315.00	0.96	32.87		2.00	0.00	1.23	0.00	0.00	0.00	0.82	1.23	0.41	0.00	0.00	0.41
500.0	320.00	0.87	27.43		2.00	0.00	3.52	0.00	0.00	0.00	0.44	0.00	0.00	0.00	0.00	1.76
510.0	325.00	0.82	45.06		2.00	0.00	4.38	0.00	0.00	0.73	0.24	0.49	0.00	0.00	0.00	0.24
522.0	331.00	0.65	48.81	9.3	3.50	0.00	0.00	0.00	0.00	0.00	0.00	0.00	0.00	0.00	0.00	0.00
532.0	333.86	0.98	41.80		3.50	0.00	0.00	0.00	0.00	0.00	0.00	0.00	0.00	0.00	0.00	0.00
541.0	336.43	1.08	45.53		1.72	0.00	0.00	0.00	0.00	0.00	0.00	0.00	0.00	0.00	0.00	0.00
550.0	339.00	1.20	41.83		1.72	0.00	0.00	0.00	0.00	0.00	0.00	0.00	0.00	0.00	0.00	0.00
560.0	344.80	1.15	49.82		1.72	0.00	0.00	0.00	0.00	0.00	0.00	0.00	0.00	0.00	0.00	0.00
570.0	350.60	1.22	37.92		1.72	0.00	0.00	0.00	0.00	0.00	0.00	0.00	0.00	0.00	0.00	0.00
580.0	356.40	1.39	46.67		1.72	0.00	0.00	0.00	0.00	0.00	0.00	0.00	0.00	0.00	0.00	0.00
590.0	362.20	0.92	42.31		1.72	0.00	0.00	0.42	0.00	0.00	9.70	0.00	0.00	0.00	0.00	7.17
600.0	368.00	1.01	40.95	11.1	1.62	0.17	4.50	8.57	0.17	0.36	13.54	0.00	0.00	0.00	0.00	3.26
610.0	374.17	0.96	42.07		1.62	0.12	0.00	0.00	0.00	0.00	29.50	0.00	0.00	0.00	0.00	1.89
620.0	380.33	0.90	31.94		1.62	0.20	0.20	0.00	0.00	0.00	1.56	0.00	0.00	0.00	0.00	0.98
630.0	386.50	0.92	20.12		1.62	0.38	14.45	0.00	0.00	0.00	3.04	0.00	0.00	0.00	1.52	1.14
640.0	392.67	0.85	25.34		1.62	0.25	57.11	0.00	0.00	0.00	2.25	0.00	0.00	0.00	6.01	5.26
650.0	398.83	0.64	28.00		1.62	0.00	1.59	0.80	0.00	0.00	1.59	0.00	0.00	0.00	12.72	17.49
660.0	405.00	0.61	59.94	11.3	1.11	0.00	0.00	0.00	0.00	0.00	5.05	0.00	0.00	0.00	12.63	27.78
670.0	414.00	0.66	39.78		1.11	0.00	0.57	0.00	0.00	0.00	0.00	0.00	0.00	0.00	2.29	0.57
680.0	423.00	1.00	43.93	12.0	8.18	0.00	0.00	0.00	0.00	0.00	0.00	0.00	0.00	0.00	0.00	0.00
690.0	424.22	1.18	43.16		8.18	0.00	0.00	0.00	0.00	0.00	0.00	0.00	0.00	0.00	0.00	0.00
700.0	425.44	1.17	53.95		8.18	0.00	0.00	0.00	0.00	0.18	0.00	0.00	0.00	0.00	0.00	0.82
710.0	426.67	1.20	48.61		8.18	0.00	0.79	0.00	0.00	0.05	0.56	0.00	0.00	0.00	0.32	0.23
720.0	427.89	1.05	43.93		8.18	0.00	0.00	0.00	0.00	0.00	0.00	0.00	0.00	0.00	0.00	0.00
730.0	429.11	0.88	43.16		8.18	0.00	0.08	0.00	0.00	0.25	0.00	0.00	0.00	0.00	0.16	0.00
740.0	430.33	0.98	53.95		8.18	0.00	0.00	0.00	0.00	0.18	0.00	0.00	0.00	0.00	0.00	0.82
751.0	431.68	0.99	48.81		8.18	0.00	0.79	0.00	0.00	0.05	0.56	0.00	0.00	0.00	0.32	0.23
760.0	432.78	1.17	46.56		8.18	0.00	0.00	0.00	0.00	0.00	0.00	0.00	0.00	0.00	0.00	0.00
770.0	434.00	1.03	55.40		8.18	0.00	0.08	0.00	0.00	0.25	0.00	0.00	0.00	0.00	0.16	0.00

Appendix 3. continued

Depth [cm]	*Oridorsalis umbonatus*	*Globocassidulina subglobosa*	*Margimulina glabra*	*Dentalina pauperata*	*Siphotextularia rolshauseni*	*Cassidulina reniforme*	*Miliolinella* sp.	*Oolina hexagona*	*Cyclamina* sp.	*Parafissurina ovata*	*Lenticulina gibba*	*Eponides tumidulus*	*Lagena* spp.	Total [Spec./g]
18.0	18.64	0.00	0.33	0.00	0.00	2.66	0.00	0.00	0.00	0.00	0.00	0.00	0.00	584.14
24.0	189.05	8.34	0.00	0.00	0.00	5.56	0.00	0.00	0.00	0.00	0.00	2.78	0.00	772.45
29.0														
34.0	13.72	0.42	0.00	0.00	0.42	1.25	0.00	0.00	0.00	0.42	0.00	0.42	0.00	57.74
46.0	3.05	0.00	0.00	0.00	3.52	0.00	0.00	0.00	0.00	0.00	0.23	0.00	0.47	17.87
55.0	7.03	0.00	0.00	0.00	1.87	0.00	0.00	0.00	0.00	0.00	0.00	0.00	0.94	32.33
65.0	4.49	0.00	0.00	0.20	0.00	0.39	0.00	0.00	0.00	0.00	0.00	0.00	0.00	8.59
75.0	2.69	0.00	0.00	0.00	0.00	0.00	0.00	0.38	0.00	0.00	0.07	0.00	0.00	18.19
85.0	3.44	0.00	0.00	0.00	0.00	0.20	0.00	0.00	0.00	0.00	0.00	0.20	0.00	12.88
95.0	1.72	0.00	0.00	0.00	0.00	0.21	0.00	0.00	0.00	0.21	0.00	0.57	0.05	6.70
105.0	0.90	0.00	0.00	0.00	0.00	0.20	0.00	0.00	0.00	0.20	0.00	0.30	0.00	5.47
115.0	7.46	0.00	0.00	0.00	0.00	1.10	0.00	0.00	0.00	0.88	0.00	2.19	0.00	23.79
125.0	4.48	0.00	0.00	0.00	0.00	0.69	0.00	0.00	0.00	0.23	0.00	0.80	0.00	17.19
135.0	15.74	0.00	0.03	0.00	0.21	1.68	0.00	0.00	0.00	0.21	0.00	1.26	0.21	43.25
145.0	3.87	0.00	0.00	0.00	0.00	0.00	0.00	0.00	0.00	0.10	0.00	0.58	0.10	9.56
155.0	5.15	0.00	0.00	0.00	0.00	0.19	0.00	0.00	0.00	0.19	0.00	0.57	0.00	19.39
165.0	14.76	0.00	0.02	0.00	0.80	0.40	0.00	0.00	0.00	0.80	0.00	0.80	0.00	98.09
175.0	31.96	0.02	0.07	0.00	0.39	0.39	0.00	0.00	0.00	4.34	0.00	1.58	0.00	193.38
190.0	6.48	0.00	0.00	0.00	0.00	0.24	0.00	0.00	0.00	0.48	0.00	0.60	0.00	28.21
200.0	24.84	0.00	0.00	0.00	0.00	0.41	0.41	1.22	0.00	1.63	0.00	2.85	0.41	142.63
220.0	29.14	0.00	0.17	0.00	0.00	1.08	0.00	0.00	0.00	0.00	0.03	1.08	0.00	119.05
230.0	54.14	0.00	0.18	0.00	0.00	0.00	0.00	0.00	0.04	0.00	0.32	1.15	0.00	558.03
235.0	75.76	1.88	0.00	0.47	0.00	0.00	0.00	0.00	0.94	4.71	0.00	0.47	0.47	202.35
245.0	8.24	0.00	0.00	0.00	0.00	0.00	0.00	0.00	0.00	0.59	0.24	0.59	0.12	28.59
250.0	15.68	0.00	0.00	0.00	0.00	0.00	0.00	0.00	0.44	0.44	0.00	3.92	0.00	36.24
260.0	35.96	0.00	0.00	0.00	0.00	0.00	0.24	0.00	0.00	0.72	0.24	4.55	0.00	56.45
271.0	15.98	0.00	0.00	0.00	0.00	0.00	0.00	0.00	0.00	0.36	0.00	0.71	0.00	24.14
280.0	43.51	0.00	0.00	0.00	1.38	0.00	0.00	0.00	0.00	0.44	0.00	1.76	0.00	57.81
290.0	11.60	0.00	0.00	0.00	0.00	0.00	0.00	0.24	0.00	0.72	0.00	0.24	0.48	32.37
300.0	21.21	0.00	0.00	0.03	0.00	0.45	0.00	0.00	0.00	0.00	0.00	0.00	0.00	43.44
310.0	8.93	0.00	0.00	0.00	0.00	0.09	0.00	0.09	0.00	0.09	0.00	0.00	0.09	11.97
320.0	69.06	0.21	0.00	0.21	0.00	0.00	0.00	0.00	0.00	0.21	0.00	0.00	0.00	79.62
330.0	82.69	0.00	0.00	0.00	0.00	0.00	0.00	0.00	0.00	0.39	0.00	0.00	0.79	143.73
340.0	99.82	0.76	0.00	0.00	0.00	0.00	0.00	0.76	0.00	0.76	0.00	0.00	0.00	365.32
350.0	52.95	0.20	0.00	0.00	0.00	0.40	0.00	0.00	0.00	0.00	0.00	0.00	0.00	103.31
360.0	58.87	0.00	0.00	0.00	0.00	0.19	0.00	0.00	0.00	0.00	0.00	0.00	0.00	124.93
370.0	20.52	0.00	0.00	0.00	0.00	0.00	0.00	0.00	0.00	0.00	0.00	0.00	0.00	146.31
380.0	9.17	0.00	0.00	0.00	0.00	0.18	0.00	0.00	0.97	0.00	0.00	0.00	0.00	23.79
390.0	16.11	0.00	0.00	0.00	0.00	0.73	0.00	0.00	0.00	0.00	0.00	0.00	0.00	30.80
400.0	37.50	0.43	0.00	0.43	0.00	0.43	0.00	0.00	0.00	0.00	0.00	0.00	0.00	75.44
410.0	17.31	0.26	0.00	0.00	0.00	1.29	0.00	0.00	0.78	0.00	0.00	0.00	0.00	40.82
421.0	5.49	0.00	0.00	0.00	0.00	0.00	0.00	0.21	0.00	0.00	0.00	0.00	0.00	8.45
430.0	24.99	0.00	0.00	0.00	0.00	0.00	0.00	0.00	0.00	0.00	0.00	0.00	0.00	27.98
441.0	43.61	0.00	0.11	0.00	0.00	0.91	0.00	0.00	0.00	0.00	0.00	0.00	0.45	52.36
450.0	92.64	0.00	0.21	0.00	0.00	0.00	0.00	0.00	0.00	0.00	0.00	0.00	0.85	123.37
470.0	38.10	0.00	0.00	0.00	0.00	0.78	0.00	0.00	0.00	0.00	0.39	0.00	0.00	64.54
480.0	48.06	0.00	0.53	0.00	0.00	0.00	0.00	0.00	0.00	0.00	0.00	0.00	0.00	70.69
490.0	33.20	0.00	0.03	0.00	0.00	0.41	0.00	0.00	0.00	0.00	0.00	0.00	0.00	51.26
500.0	34.74	0.00	0.00	0.00	0.00	0.00	0.00	0.44	0.00	0.00	0.00	0.00	0.00	43.97
510.0	59.62	0.00	0.00	0.00	0.00	0.24	0.00	0.00	0.00	0.00	0.00	0.00	0.49	73.49
522.0	0.00	0.00	0.00	0.00	0.00	0.00	0.00	0.00	0.00	0.00	0.00	0.00	0.00	0.00
532.0	0.00	0.00	0.00	0.00	0.00	0.00	0.00	0.00	0.00	0.00	0.00	0.00	0.00	0.00
541.0	0.00	0.00	0.00	0.00	0.00	0.00	0.00	0.00	0.00	0.00	0.00	0.00	0.00	0.00
550.0	0.00	0.00	0.00	0.00	0.00	0.00	0.00	0.00	0.00	0.00	0.00	0.00	0.00	0.00
560.0	0.00	0.00	0.00	0.00	0.00	0.00	0.00	0.00	0.00	0.00	0.00	0.00	0.00	0.00
570.0	0.00	0.00	0.00	0.00	0.00	0.00	0.00	0.00	0.00	0.00	0.00	0.00	0.00	0.00
580.0	0.00	0.00	0.00	0.00	0.00	0.00	0.00	0.00	0.00	0.00	0.00	0.00	0.00	0.00
590.0	154.41	0.42	0.00	0.00	0.00	0.00	0.00	0.00	0.00	0.00	0.00	0.00	0.00	172.97
600.0	34.11	0.00	0.00	0.00	0.34	0.17	0.00	0.00	0.00	0.00	0.00	0.69	0.17	67.81
610.0	66.18	0.00	0.00	0.00	0.00	1.89	0.00	0.00	0.00	1.13	0.00	1.89	0.00	102.60
620.0	45.13	0.00	0.20	0.00	0.00	1.37	0.00	0.00	0.00	0.00	0.00	0.59	0.00	50.21
630.0	42.21	0.00	0.00	0.00	0.00	2.66	0.00	0.00	0.00	0.38	0.00	0.38	0.00	66.93
640.0	26.80	0.00	0.00	0.00	0.00	2.25	0.25	0.00	0.00	0.50	0.00	0.00	0.50	103.20
650.0	42.14	0.00	0.00	0.00	0.00	0.00	0.00	0.00	0.00	0.00	0.80	0.00	0.00	81.89
660.0	202.06	0.00	0.00	0.00	0.00	7.58	0.00	0.00	0.00	2.53	0.00	0.00	0.00	257.62
670.0	208.01	0.00	0.00	0.00	0.00	3.43	0.00	0.00	0.00	0.00	0.00	0.00	0.57	215.44
680.0	0.00	0.00	0.00	0.00	0.00	0.00	0.00	0.00	0.00	0.00	0.00	0.00	0.00	0.00
690.0	0.00	0.00	0.00	0.00	0.00	0.00	0.00	0.00	0.00	0.00	0.00	0.00	0.00	0.00
700.0	18.76	0.27	0.00	0.00	0.00	2.82	0.00	0.00	0.00	0.00	0.00	0.00	0.00	23.77
710.0	1.48	0.00	0.00	0.00	0.00	1.20	0.00	0.00	0.00	0.05	0.00	0.05	0.05	4.82
720.0	0.00	0.00	0.00	0.00	0.00	0.00	0.00	0.00	0.00	0.00	0.00	0.00	0.00	0.00
730.0	3.29	0.00	0.00	0.00	0.00	0.58	0.00	0.00	0.00	0.00	0.00	0.00	0.00	4.44
740.0	18.76	0.27	0.00	0.00	0.00	2.82	0.00	0.00	0.00	0.00	0.00	0.00	0.00	23.77
751.0	1.48	0.00	0.00	0.00	0.00	1.20	0.00	0.00	0.00	0.05	0.00	0.05	0.05	4.82
760.0	0.00	0.00	0.00	0.00	0.00	0.00	0.00	0.00	0.00	0.00	0.00	0.00	0.00	0.00
770.0	3.29	0.00	0.00	0.00	0.00	0.58	0.00	0.00	0.00	0.00	0.00	0.00	0.00	4.44

Appendix 4. Data for Core 1243 (Spec/g)

Corrected Depth [cm]	Age [ky]	DBD [g/cm]	Dry Weight [g]	LSR [cm/ka]	Isotope Event	1243GKG Depth [cm]	*Pyrgo rotalaria*	*Cibicidoides wuellerstorfi*	*Epistominella exigua*	*Quinqueloculina seminula*	*Elphidium* spp.	*Trilocul. feicarinata*	*Crithionina subglobosa*	agglutinated Tubes	*Ammobaculites agglutinans*	*Pullenia bulloides*
1.5	1.29					1.5	17.04	362.01	217.29	0.00	0.00	137.55	14.09	0.74	62.07	0.00
2.5	1.58			AMS C14-Dates		2.5	8.67	198.11	153.14	0.00	0.00	134.10	8.62	0.20	25.52	0.00
4.5	2.14			unpublished		4.5	0.00	157.94	171.11	0.00	0.00	148.07	3.29	0.00	59.23	0.00
6.5	2.71			BAUCH		6.5	11.42	149.05	148.84	0.00	0.00	81.61	8.77	0.00	20.30	0.00
8.5	3.28					8.5	18.91	149.19	221.94	0.00	0.00	67.42	16.98	0.81	61.94	0.00
10.5	3.85					10.5	20.51	168.79	188.32	0.00	0.36	125.90	11.23	0.13	39.95	0.00
12.5	4.42					12.5	26.60	202.12	72.32	0.00	0.38	189.60	14.74	0.09	114.50	0.00
14.5	4.99					14.5	33.21	191.99	6.14	0.00	0.00	69.10	18.04	0.00	55.28	0.00
16.5	5.38					16.5	72.78	255.02	0.00	0.00	0.00	129.04	16.71	0.00	30.72	0.00
18.5	5.77					18.5	49.27	157.14	0.00	0.00	0.00	149.81	11.99	0.00	58.59	0.00
20.5	6.06					20.5	6.18	197.68	0.00	0.00	0.00	186.87	3.09	0.00	49.42	0.00
22.5	6.55					22.5	29.79	98.25	5.46	0.68	0.00	107.90	6.83	0.00	34.14	0.00
24.5	6.94					24.5	56.26	121.82	0.00	0.00	0.00	190.27	25.12	0.00	30.14	0.00
26.5	7.33					26.5	59.80	163.85	0.00	0.00	0.00	168.92	16.22	0.00	5.41	0.00
28.5	7.72					28.5	81.45	276.23	0.00	0.00	0.00	192.33	27.97	0.00	0.00	0.00
30.5	8.00					30.5	56.81	167.53	0.00	0.00	0.00	382.09	14.47	0.00	0.00	0.00
32.5	8.28					32.5	27.13	33.30	0.00	0.00	0.00	6.29	7.05	0.00	0.00	0.00
34.5	8.56					34.5	4.06	26.84	0.00	0.00	0.00	100.29	4.26	0.00	0.00	0.00
36.5	8.84					36.5	10.82	45.20	0.00	0.00	0.00	115.47	4.35	0.00	0.00	0.00
38.5	9.11					38.5	4.91	33.95	0.00	0.00	0.00	33.15	3.11	0.00	0.00	0.00
40.5	9.39					40.5	6.11	43.70	0.00	0.28	0.00	74.53	2.95	0.00	0.00	0.00
42.5	9.67															
44.5	9.95					1243SL										
46.5	10.23															
44.5	10.51					36.0	2.99	0.77	0.00	0.00	0.00	0.31	3.07	0.84	0.00	0.00
45.5	10.78					37.0	2.17	0.23	0.00	0.00	0.47	0.00	0.78	0.00	0.00	0.00
46.5	11.06					38.0	3.23	0.27	0.13	0.00	0.40	0.13	1.78	0.13	0.00	0.00
47.5	11.34					39.0	1.39	0.32	0.26	0.00	0.03	0.39	1.13	0.13	0.00	0.00
48.5	11.61					40.0	1.09	0.07	0.13	0.00	0.13	0.40	1.06	0.03	0.00	0.00
49.5	11.89					41.0	0.76	2.24	0.00	0.00	0.00	3.79	0.81	0.39	0.00	0.00
50.5	12.16					42.0	1.02	5.77	0.03	0.00	0.00	12.68	1.73	0.46	0.00	0.00
51.5	12.44					43.0	0.08	0.15	0.00	0.00	0.15	0.81	0.84	1.23	0.00	0.00
52.5	13.00					44.0	0.29	0.75	0.00	0.00	0.18	0.58	0.38	1.29	0.00	0.00
53.5	13.57					45.0	0.12	0.24	0.12	0.00	0.36	0.60	1.46	4.08	0.12	0.00
54.5	14.13					46.0	0.08	0.76	0.00	0.00	0.21	1.88	2.90	3.21	0.00	0.00
55.5	14.70					47.0	0.36	2.18	0.00	0.00	0.00	2.70	3.97	1.19	0.00	0.00
56.5	15.26					48.0	0.67	5.73	0.03	0.00	0.85	6.81	3.01	3.71	0.00	0.00
57.5	15.83					49.0	0.28	2.63	0.00	0.00	1.50	8.63	0.31	3.03	0.00	0.00
58.5	16.39					50.0	0.20	1.16	0.00	0.00	1.93	2.27	0.31	7.56	0.00	0.00
59.5	16.82					51.0	0.15	0.24	0.00	0.00	1.71	2.12	0.15	3.47	0.00	0.00
60.5	17.25					52.0	0.14	0.66	0.00	0.00	0.66	1.09	0.03	2.48	0.00	0.00
61.5	18.10					53.0	0.05	0.00	0.00	0.05	2.34	1.03	0.05	3.01	0.00	0.00
62.5	18.53					54.0	0.03	0.06	0.00	0.00	0.78	0.24	0.03	0.69	0.00	0.00
63.5	18.96					55.0	0.35	1.27	0.23	0.00	2.08	1.16	0.00	8.50	0.23	0.00
64.5	19.39					56.0	0.08	0.22	0.22	0.00	0.95	0.90	0.06	10.05	0.00	0.00
65.5	19.79					57.0	0.06	0.18	0.00	0.00	0.18	0.03	0.00	0.00	0.00	0.00
66.5	20.19					58.0	0.50	0.39	0.11	0.00	0.19	0.94	0.08	0.44	0.00	0.00
67.5	20.59					59.0	0.44	0.44	0.00	0.00	0.98	0.91	0.84	2.22	0.00	0.00
68.5	20.99					60.0	0.68	0.11	0.00	0.00	0.93	0.90	0.28	0.20	0.00	0.00
69.5	22.59					61.0	0.23	0.29	0.00	0.03	2.28	1.60	0.17	6.91	0.00	0.00
70.5	22.99					62.0	0.23	0.00	0.00	0.06	1.87	1.05	0.09	2.13	0.00	0.00
71.5	23.49					63.0	0.17	0.00	0.00	0.14	0.45	0.22	0.00	0.95	0.00	0.00
72.5	23.99					64.0	0.21	0.12	0.12	0.30	0.80	0.97	0.06	0.65	0.00	0.00
73.5	24.49					65.0	0.31	0.00	0.00	0.84	0.31	1.76	0.31	0.84	0.00	0.00
74.5	25.00					66.0	0.04	0.00	0.00	0.63	1.48	0.07	0.07	0.81	0.00	0.00
75.5	25.50					67.0	0.54	0.08	0.19	1.11	1.11	2.34	1.53	1.69	0.00	0.00
78.5	27.00	0.990	20.470	1.41	3.10	70.0	0.06	0.00	0.06	0.50	1.69	0.56	0.00	0.44	0.00	0.00
88.5	34.41	1.070	22.770	1.41		80.0	0.06	0.00	0.00	6.24	2.20	2.45	0.55	9.11	0.00	0.00
98.5	41.23	1.090	24.880	1.41		90.0	4.23	0.00	0.00	6.95	0.48	2.96	1.21	1.87	0.00	0.00
108.5	48.34	1.050	23.120	1.41		100.0	5.70	0.53	0.00	20.68	1.06	6.89	0.80	32.41	0.00	0.00
118.5	55.45	0.870	31.640	3.07	3.30	110.0	8.15	0.00	0.00	47.58	0.00	22.82	6.01	10.70	0.00	0.00
128.5	58.71	0.800	17.650	3.07		120.0	2.42	0.00	1.21	12.11	2.42	14.53	0.91	2.72	0.00	0.00
138.5	61.96	0.930	19.710	3.07		130.0	0.12	0.37	0.00	5.36	1.00	2.99	0.12	0.12	0.00	0.00
148.5	65.22	0.910	17.220	1.40	4.20	140.0	0.98	0.60	0.00	2.65	2.42	0.00	0.00	0.68	0.00	0.00
158.5	72.34	0.810	18.640	1.40		150.0	0.07	28.36	0.00	4.24	1.09	0.00	0.00	0.14	0.00	2.26
168.5	79.46	0.870	19.670	1.81	5.10	160.0	3.73	262.36	0.00	40.85	0.00	26.24	0.07	19.08	0.00	76.10
178.5	84.99	0.980	23.120	1.81		170.0	3.95	88.27	0.00	23.09	1.09	4.36	0.00	6.20	0.00	0.00
183.0	87.48	0.850	18.000	1.81		174.5	0.00	104.96	0.00	33.11	3.15	7.88	0.00	3.15	0.00	0.00
188.5	90.53	0.860	12.610	0.77	5.20	180.0	0.98	52.91	0.00	15.64	0.00	0.88	0.00	2.23	0.00	0.00
198.5	103.55	0.750	21.260	1.38	5.30	190.0	5.70	58.63	0.00	0.11	1.79	5.36	0.00	1.79	0.00	0.00
208.5	110.79	0.650	21.520	0.86	5.40	200.0	4.18	85.68	0.00	0.00	0.12	3.37	0.00	0.00	0.00	0.00
218.5	122.38	0.620	15.380	3.14	5.51	210.0	26.97	286.82	0.00	0.00	0.00	8.50	0.00	4.25	0.00	0.00
228.5	123.69	0.640	18.260	3.14		220.0	24.87	684.15	0.00	0.85	0.00	3.42	0.00	3.42	0.00	0.00
238.5	125.00	1.040	17.340	3.14		230.0	39.10	197.58	0.00	0.00	0.00	7.43	0.00	10.44	0.00	0.00
248.5	130.05	0.990	22.830	3.14		240.0	2.00	20.05	0.00	0.00	1.15	0.00	0.00	0.14	0.00	0.00
250.5	135.10	0.880	24.750	4.82	6.20	242.0	0.39	0.19	0.00	0.00	7.71	0.00	0.00	0.77	0.00	0.00
266.5	136.76	1.210	35.740	4.82		258.0	0.00	0.00	0.00	0.00	0.00	1.90	0.00	0.00	0.00	0.00
268.5		0.880	30.000	4.82		260.0	0.00	0.00	0.00	0.00	0.00	0.00	0.00	0.00	0.00	0.00
273.5	138.22	0.920	24.970	4.82		265.0	0.00	0.17	0.00	0.00	1.36	0.00	0.00	12.57	0.00	0.00
278.5	139.25	1.140	31.060	4.82		270.0	0.00	0.00	0.00	0.00	3.43	0.00	0.00	3.71	0.00	0.00
288.5	141.33	1.030	29.040	1.90	6.30	280.0	0.00	6.71	0.00	0.00	2.39	0.00	0.00	0.15	0.00	0.00
298.5	146.59	1.150	26.480	1.90		290.0	0.00	3.10	0.00	0.00	1.77	0.00	0.00	0.96	0.00	0.00
308.5	151.84	0.870	30.710	1.90		300.0	0.00	1.00	0.00	0.00	2.85	0.57	0.00	0.14	0.00	0.00
318.5	157.10	1.040	22.600	0.70	6.40	310.0	0.08	0.03	0.00	0.00	0.22	0.00	0.00	0.00	0.00	0.00
328.5	171.37	1.110	26.960	1.68	6.50	320.0	0.00	0.06	0.00	0.00	1.55	0.00	0.00	0.00	0.00	0.00
338.5	177.34	0.920	24.210	1.68		330.0	0.00	0.00	0.00	0.00	1.85	0.00	0.00	0.00	0.00	0.00
348.5	183.30	0.860	23.740	3.07	6.60	340.0	0.00	0.00	0.00	0.00	0.00	0.00	0.00	0.24	0.00	0.00
358.5	186.56	1.000	26.700	3.07		350.0	0.98	8.41	0.00	0.00	0.00	0.00	0.00	0.40	0.00	0.00
368.5	189.81	1.130	22.630	3.07		360.0	0.95	45.72	0.00	0.00	1.36	9.90	0.00	4.75	0.00	0.00
378.5	193.07	0.840	26.980	0.89	7.10	370.0	0.04	13.49	0.00	0.00	0.04	0.00	0.00	0.30	0.00	0.00
387.5	203.18	0.670	24.830	0.89		379.0	0.63	7.47	0.00	0.00	0.00	0.03	0.00	7.77	0.00	0.00
393.5		0.820	22.000	0.89		385.0	0.19	1.25	0.00	0.00	0.00	0.00	0.00	1.71	0.00	0.00
398.5	215.54	0.990	20.440	0.80	7.30	390.0	0.19	1.09	0.00	0.00	0.00	0.13	0.10	1.61	0.00	0.00
408.5	228.00	1.090	26.600	1.64	7.40	400.0	0.24	0.92	0.00	0.00	1.22	0.24	0.00	0.55	0.00	0.00
418.5	234.10	0.980	25.680	1.64		410.0	4.52	2.85	0.00	0.00	1.18	0.07	0.00	0.84	0.00	0.00
428.5	240.19	1.000	35.940	2.55	7.50	420.0	1.88	0.00	0.00	0.00	1.67	4.52	0.00	0.49	0.00	0.00
438.5	244.12	1.310	26.380	2.55		430.0	0.00	0.00	0.00	0.00	0.77	0.77	0.00	0.00	0.00	0.00
448.5	248.05	0.770	33.510	2.55		440.0	0.00	0.00	0.00	0.00	0.00	0.00	0.00	0.10	0.00	0.00
458.5	251.97	0.860	22.620	2.55		450.0	1.91	0.09	0.00	0.00	0.78	1.39	0.00	0.69	0.00	0.00
468.5	255.90	1.080	27.700	0.67	8.30	460.0	0.00	0.10	0.00	0.00	0.74	2.15	0.02	1.36	0.00	0.00
478.5	272.04	0.900	25.090	0.67		470.0	1.18	0.00	0.00	0.00	0.00	0.46	1.20	1.95	0.00	0.00
488.5	288.17	0.850	24.740	0.67		480.0	1.38	0.00	0.00	0.00	0.00	0.39	0.24	0.39	0.00	0.00
498.5	299.00	1.270	20.790	0.67		490.0	0.44	0.08	0.00	0.00	0.44	0.46	0.38	0.11	0.00	0.00
508.5	303.00	0.890	21.210	0.67		500.0	2.35	0.08	0.00	0.00	0.00	0.96	0.40	0.28	0.00	0.00
518.5	331.00	1.390	21.710	6.00	9.30	510.0	10.58	84.86	0.00	0.00	7.38	0.00	18.20	15.50	0.00	0.00
531.5	333.08	1.350	30.220	6.00		523.0	0.00	822.41	4.42	0.00	3.31	0.00	2.21	1.10	0.00	3.31
540.5	334.52	1.280	32.300	6.00		532.0	0.00	0.00	0.00	0.00	0.00	0.00	0.00	0.00	0.00	0.00
548.5	335.80	0.920	24.070	6.00		540.0	0.00	0.00	0.00	0.00	0.00	0.00	0.00	0.00	0.00	0.00
558.5	337.40	0.880	23.880	6.00		550.0	0.00	4.16	0.00	0.00	2.08	0.00	0.00	0.46	0.00	0.00
562.5	338.04	1.110	37.400	6.00		554.0	0.00	0.00	0.00	0.00	0.00	0.00	0.00	0.00	0.00	0.00
568.5	339.00	0.960	23.440	6.00		560.0	0.00	86.38	6.82	0.00	4.55	0.00	0.00	0.00	0.00	0.00
578.5	341.00	1.010	23.420	1.11	10.20	570.0	0.00	0.09	0.00	0.00	0.23	0.00	0.23	0.00	0.00	0.00
588.5	350.00	0.970	22.920	1.11		580.0	0.00	0.00	0.00	0.00	0.44	0.39	0.15	0.00	0.00	0.00
598.5	359.00	0.940	23.770	1.11		590.0	0.09	0.18	0.00	0.00	0.00	0.00	0.05	0.00	0.00	0.00
608.5	368.00	0.830	24.950	0.54	11.10	600.0	1.71	1.95	0.00	0.00	0.02	0.00	0.00	0.00	0.00	0.00
613.5	377.25	0.740	20.610	0.54		605.0	0.00	0.00	0.00	0.00	0.00	1.39	0.00	0.00	0.00	0.00
618.5	386.50	0.690	20.080	0.54		610.0	3.29	0.00	0.00	0.00	0.00	0.64	0.00	0.00	0.00	0.00
623.5	395.75	0.730	20.450	0.54		615.0	5.49	0.00	0.00	0.00	0.00	0.00	0.02	0.00	0.00	0.00
633.5	407.57	0.700	18.920	1.23	11.30	625.0	5.02	0.00	0.00	0.00	0.00	1.52	0.00	0.00	0.00	0.00
638.5	410.11	0.700	20.130	1.23		630.0	0.00	0.00	0.00	0.00	0.00	0.00	0.00	0.00	0.00	0.00
643.5	412.71	0.650	21.230	1.23		635.0	0.00	0.00	0.00	0.00	0.00	0.00	0.00	0.00	0.00	0.00
648.5		1.130	18.000	1.23		640.0	0.00	0.00	0.00	0.00	0.00	0.00	0.00	0.00	0.00	0.00
658.5	420.43	0.960	16.960	1.23		650.0	5.97	0.00	0.00	0.00	0.00	0.00	0.00	0.00	0.00	0.00
668.5	428.22	1.210	28.510	1.23		660.0	0.00	0.00	0.00	0.00	0.00	0.00	0.00	0.00	0.00	0.00
678.5	438.65	1.000	27.650	1.23		670.0	0.00	0.00	0.00	0.00	0.00	0.00	0.00	0.00	0.00	0.00
688.5	450.13	1.220	23.430	1.23		681.0	0.00	0.00	0.00	0.00	0.00	0.00	0.00	0.00	0.00	0.00
696.5	457.44	0.990	33.610	1.23		688.0	0.00	0.00	0.00	0.00	0.00	0.00	0.00	0.00	0.00	0.00
705.5	466.30	1.010	32.270	1.23		697.0	0.00	0.00	0.00	0.00	0.00	0.00	0.00	0.00	0.00	0.00
709.5	471.00	1.270	26.820	2.60	12.40	701.0	0.00	0.00	0.00	0.00	0.78	0.00	0.00	0.00	0.00	0.00
716.5	473.69	1.160	32.760	2.60		708.0	0.00	0.00	0.00	0.00	0.00	0.00	0.00	0.00	0.00	0.00
726.5	477.54	1.220	27.110	2.60		718.0	0.00	0.00	0.00	0.00	0.00	0.00	0.00	0.00	0.00	0.00
735.5	481.00	0.950	28.100	2.80	13.11	727.0	8.02	13.13	0.00	0.00	5.84	0.97	0.00	0.00	0.00	0.00
746.5	493.57	1.050	31.040	2.80		738.0	15.68	30.59	0.00	0.00	1.54	0.00	0.00	0.00	0.00	0.00
755.5	503.86	1.000	25.720	2.80		747.0	0.00	4.12	0.00	0.00	0.00	0.00	0.00	0.00	0.00	0.00
763.0		1.090	25.870	2.80	13.12											

Appendix 4. continued

Corrected Depth [cm]	Cassidulina teretis	Oridorsalis umbonatus	Globocassidulina subglobosa	Marginulina glabra	Dentalina pauperata	Siphotextularia rolshauseni	Cassidulina reniforme	Miliolinella sp.	Oolina hexagona	Cyclandra sp.	Parafissurina ovata	Lenticulina gibba	Eponides tumidulus	Lagena spp.	Total [Spec./g]
1.5	0.00	689.01	0.00	0.00	0.00	0.00	6.21	0.00	0.00	0.00	19.12	0.00	31.04	0.00	1569.09
2.5	0.00	382.85	0.00	0.00	0.00	0.00	19.14	0.00	0.00	0.00	0.00	0.00	95.71	19.14	1044.92
4.5	0.00	302.72	0.00	0.00	0.00	0.00	23.03	0.00	0.00	0.00	3.29	0.00	6.58	3.29	957.53
6.5	0.00	196.19	0.00	0.00	0.00	0.00	20.30	0.00	0.00	0.00	7.19	0.00	6.77	13.53	664.38
8.5	0.00	196.13	0.00	0.00	0.32	0.00	15.48	0.00	0.00	0.00	5.81	0.00	10.32	3.16	771.37
10.5	0.00	188.68	0.00	0.00	0.00	0.00	22.83	0.00	0.00	0.00	18.19	0.00	22.83	0.00	859.13
12.5	0.00	385.69	0.00	0.00	0.00	0.00	30.13	0.00	0.00	0.00	6.78	0.00	12.05	0.00	975.38
14.5	0.00	178.12	0.00	0.00	0.00	0.00	18.43	0.00	0.00	0.00	7.68	0.00	12.28	0.00	592.13
16.5	0.00	141.33	0.00	0.00	0.00	0.00	24.58	0.00	0.00	0.00	6.91	0.00	6.14	6.14	690.16
18.5	0.00	218.39	0.00	0.00	0.00	0.00	31.96	0.00	0.00	0.00	7.32	0.67	5.33	10.65	701.12
20.5	0.00	159.07	0.00	0.00	0.00	0.00	15.44	0.00	0.00	0.00	4.63	0.00	6.18	0.00	636.29
22.5	0.00	110.63	0.00	0.00	0.00	0.00	9.56	0.00	0.00	0.00	1.37	0.00	1.37	1.37	408.02
24.5	0.00	171.43	0.00	0.00	0.00	0.00	10.05	0.00	0.00	0.00	1.88	0.00	2.51	0.63	609.73
26.5	0.00	235.81	0.00	0.00	0.00	0.00	10.81	0.00	0.00	0.00	6.08	0.00	2.70	2.70	678.38
28.5	0.00	307.15	0.00	0.00	0.00	0.00	19.63	0.00	0.00	0.00	10.79	0.00	3.93	1.96	911.57
30.5	0.00	223.61	0.00	0.00	0.00	0.00	55.00	0.00	0.00	0.00	7.24	0.00	2.89	0.72	921.94
32.5	0.00	0.00	0.00	0.00	0.10	0.00	0.00	0.00	0.00	0.00	0.10	0.00	0.00	0.00	67.97
34.5	0.00	180.69	0.00	0.00	0.00	0.00	4.70	0.00	0.00	0.00	0.20	0.00	1.57	0.00	242.80
36.5	0.00	150.66	0.00	0.00	0.00	0.00	14.56	0.00	0.00	0.00	2.43	0.00	3.24	0.00	348.74
38.5	0.00	44.73	0.00	0.00	0.17	0.00	6.04	0.00	0.00	0.00	0.17	0.00	4.70	0.00	124.30
40.5	0.00	82.33	0.00	0.00	0.00	0.00	6.74	0.00	0.00	0.00	0.42	0.00	3.37	0.00	220.86
42.5															
44.5															
46.5															
44.5	0.00	1.53	0.00	0.00	0.00	0.00	0.00	0.00	0.00	0.00	0.00	0.00	0.61	0.00	10.28
45.5	0.00	1.40	0.00	0.00	0.00	0.00	0.31	0.00	0.00	0.00	0.00	0.00	1.48	0.16	7.30
46.5	0.00	1.41	0.00	0.00	0.24	0.00	0.94	0.00	0.00	0.00	0.00	0.00	1.34	0.13	10.15
47.5	0.00	4.42	0.00	0.00	0.00	0.00	0.00	0.00	0.00	0.00	0.00	0.00	0.90	0.03	9.64
48.5	0.00	15.02	0.00	0.00	0.03	0.00	0.27	0.00	0.00	0.00	0.03	0.00	1.46	0.00	19.90
49.5	0.00	23.79	0.00	0.00	0.00	0.00	2.36	0.00	0.00	0.00	0.00	0.00	0.79	0.00	35.57
50.5	0.00	33.25	0.00	0.00	0.00	0.00	3.41	0.00	0.00	0.00	0.09	0.00	0.46	0.03	59.10
51.5	0.15	13.21	0.00	0.00	0.00	0.00	1.07	0.00	0.00	0.00	0.00	0.00	0.00	0.15	18.09
52.5	0.00	13.66	0.00	0.00	0.00	0.18	0.35	0.00	0.00	0.00	0.00	0.00	0.00	0.00	18.03
53.5	0.00	14.50	0.00	0.00	0.00	0.00	0.24	0.00	0.00	0.00	0.12	0.00	0.00	0.00	22.10
54.5	0.42	24.05	0.00	0.00	0.03	0.21	0.21	0.00	0.00	0.00	0.21	0.00	0.63	0.03	34.80
55.5	0.16	35.86	0.00	0.00	0.00	0.00	0.00	0.00	0.00	0.00	0.00	0.00	0.79	0.87	48.29
56.5	0.26	43.11	0.00	0.00	0.00	1.40	0.50	0.00	0.00	0.03	0.99	0.00	0.91	2.46	70.84
57.5	0.00	7.86	0.00	0.00	0.00	3.60	0.24	0.00	0.00	0.00	0.24	0.00	2.51	1.25	31.55
58.5	0.11	3.29	0.00	0.00	0.00	7.48	0.23	0.00	0.00	0.00	1.25	0.00	3.17	0.00	29.07
59.5	0.18	4.82	0.00	0.00	0.00	14.88	0.24	0.00	0.00	0.00	0.00	0.00	6.59	0.00	35.34
60.5	0.44	1.97	0.00	0.00	0.00	15.28	0.22	0.00	0.00	0.00	0.33	0.00	3.71	0.22	27.05
61.5	0.21	1.65	0.00	0.03	0.00	21.12	0.41	0.00	0.00	0.00	0.21	0.00	5.77	0.00	35.99
62.5	0.00	1.23	0.00	0.00	0.00	5.93	0.48	0.00	0.00	0.00	0.09	0.00	0.48	0.00	10.05
63.5	0.00	1.85	0.00	0.00	0.00	21.06	0.00	0.00	0.00	0.00	0.12	0.00	0.23	0.23	38.47
64.5	0.06	1.85	0.00	0.00	0.08	13.61	0.00	0.00	0.00	0.00	0.34	0.00	0.28	0.00	28.98
65.5	0.00	0.35	0.00	0.00	0.00	1.32	0.00	0.00	0.00	0.00	0.15	0.00	0.00	0.00	2.28
66.5	0.00	0.72	0.00	0.00	0.00	6.01	0.00	0.00	0.00	0.00	0.33	0.00	0.53	0.17	10.57
67.5	0.15	1.05	0.00	0.00	0.07	10.95	0.00	0.00	0.00	0.00	0.11	0.00	0.29	0.47	15.92
68.5	0.23	0.70	0.00	0.00	0.03	1.66	0.79	0.00	0.00	0.00	0.03	0.00	0.11	0.25	7.07
69.5	0.97	0.46	0.00	0.00	0.06	4.97	0.00	0.00	0.00	0.00	0.00	0.00	0.00	0.74	18.98
70.5	0.06	1.23	0.00	0.00	0.03	7.13	0.23	0.00	0.00	0.00	0.26	0.00	0.00	0.29	14.73
71.5	0.00	0.33	0.00	0.00	0.08	0.92	0.00	0.00	0.00	0.00	0.11	0.00	0.11	0.42	3.93
72.5	0.00	0.83	0.00	0.00	0.00	1.54	0.00	0.00	0.00	0.00	0.00	0.00	0.00	0.95	6.56
73.5	0.00	0.44	0.00	0.00	0.00	4.09	0.26	0.00	0.00	0.00	0.04	0.00	0.00	0.22	9.51
74.5	0.00	0.00	0.00	0.00	0.00	3.32	0.15	0.00	0.00	0.00	0.00	0.00	0.00	0.15	7.27
75.5	0.34	0.31	0.00	0.00	0.00	3.49	0.15	0.00	0.00	0.00	0.00	0.03	0.00	0.15	13.03
78.5	0.38	0.56	0.00	0.00	0.00	0.69	0.50	0.00	0.00	0.00	0.19	0.03	0.00	0.00	6.00
88.5	0.00	4.65	0.00	0.00	0.00	0.00	0.98	0.00	0.00	0.00	0.24	0.00	0.00	0.00	26.65
98.5	0.00	2.42	0.00	0.00	0.00	0.00	0.97	0.00	0.06	0.00	1.15	0.00	3.93	0.00	26.91
108.5	1.06	3.18	0.00	0.00	0.00	0.00	2.12	0.00	0.00	0.00	0.53	0.00	5.30	0.53	80.80
118.5	0.00	71.72	0.00	0.00	0.00	0.00	0.00	0.00	0.00	0.00	0.31	0.00	0.00	0.00	167.39
128.5	0.00	57.05	0.00	0.00	0.00	0.00	2.42	0.00	0.00	0.00	0.00	0.00	4.81	0.00	100.63
138.5	0.00	68.16	0.00	0.00	0.00	0.00	1.00	0.00	0.00	0.00	1.00	0.00	4.98	0.12	85.36
148.5	0.00	10.28	0.00	0.00	0.00	0.00	0.00	0.00	0.00	0.00	0.60	0.00	1.21	0.00	20.11
158.5	0.00	2.19	0.00	0.00	0.00	1.09	0.00	0.00	0.00	0.00	0.14	0.00	3.28	0.00	42.85
168.5	0.00	151.16	0.00	0.00	0.00	16.70	7.16	0.00	0.00	0.00	2.98	0.00	14.31	4.77	625.50
178.5	0.00	69.74	0.00	0.00	0.00	0.00	0.00	0.00	0.00	0.00	3.27	0.00	7.63	3.09	210.87
183.0	0.00	67.80	0.00	0.00	0.00	1.58	0.00	0.00	1.58	0.00	12.61	0.00	11.04	1.58	249.12
188.5	0.00	39.35	0.00	0.00	0.00	0.00	0.00	0.05	0.00	0.00	1.19	0.00	2.39	0.00	115.71
198.5	0.00	136.23	0.00	0.00	0.00	0.00	0.00	0.00	0.00	0.00	2.68	0.00	3.57	1.79	218.09
208.5	0.00	29.84	0.96	0.00	0.00	0.00	0.00	0.00	0.00	0.00	3.49	0.48	3.37	2.41	131.86
218.5	0.00	170.05	64.83	0.00	0.00	0.00	0.00	0.00	0.00	0.00	19.66	0.00	4.25	0.00	586.39
228.5	0.00	373.13	127.22	0.00	0.00	0.00	6.83	0.00	3.42	0.00	11.95	0.85	27.32	3.42	1274.26
238.5	0.00	702.15	15.31	0.00	0.00	0.00	11.14	0.00	0.00	0.00	6.96	0.23	18.56	4.18	1013.08
248.5	0.00	10.60	0.00	0.00	0.00	0.00	0.00	0.00	0.00	0.00	0.00	0.00	8.02	2.43	44.96
250.5	0.00	1.74	0.00	0.00	0.00	0.00	0.00	0.00	0.00	0.00	0.19	0.00	0.00	0.00	12.53
266.5	0.47	9.14	0.00	0.00	0.00	0.00	0.00	0.00	0.00	0.00	0.47	0.00	5.22	4.39	21.72
268.5	0.00	13.22	0.00	0.00	0.00	0.00	0.00	0.00	0.00	0.00	0.00	0.00	0.78	0.00	14.77
273.5	0.17	77.97	0.00	0.00	0.00	0.00	0.00	0.00	0.00	0.00	1.36	0.00	8.15	1.36	103.28
278.5	0.00	96.08	0.00	0.00	0.00	0.00	1.14	0.00	0.00	0.00	0.00	0.00	4.57	1.14	110.22
288.5	0.67	23.27	0.00	0.00	0.00	0.00	0.60	0.00	0.00	0.00	0.00	0.00	0.00	0.00	33.91
298.5	0.00	42.72	0.00	0.00	0.00	7.09	0.00	0.00	0.00	0.00	0.00	0.00	0.00	0.00	56.09
308.5	0.71	0.57	0.00	0.00	0.00	1.14	0.57	0.00	0.00	0.00	0.07	0.00	0.57	0.00	9.46
318.5	0.00	0.86	0.00	0.00	0.00	0.00	0.43	0.00	0.00	0.00	0.00	0.00	0.00	0.03	1.67
328.5	0.00	11.90	0.00	0.00	0.00	0.00	0.00	0.00	0.00	0.00	0.00	0.00	0.00	0.00	13.58
338.5	0.00	14.25	0.00	0.00	0.00	0.00	0.00	0.00	0.00	0.00	0.00	0.00	0.00	0.00	16.41
348.5	0.00	27.72	0.00	0.00	0.24	0.00	1.43	0.00	0.00	0.00	0.00	0.00	0.00	0.48	30.69
358.5	0.00	98.29	0.00	0.10	0.00	0.00	0.00	0.00	0.00	0.00	0.00	0.00	0.00	0.00	109.27
368.5	0.00	81.40	0.00	0.00	0.00	0.00	0.00	0.00	0.00	0.00	0.00	0.00	0.00	0.14	114.21
378.5	0.00	42.68	0.00	0.00	0.07	0.00	0.00	0.00	0.00	0.00	0.00	0.00	0.00	0.00	58.74
387.5	0.00	28.49	0.00	0.00	0.00	0.00	0.00	0.00	0.00	0.00	0.00	0.00	0.00	0.24	44.62
393.5	0.00	6.10	0.00	0.00	0.00	0.00	0.00	0.00	0.00	0.00	0.00	0.00	0.00	0.00	9.24
398.5	0.00	16.87	0.00	0.00	0.00	0.00	0.13	0.00	0.00	0.00	0.00	0.00	0.00	0.13	20.25
408.5	0.00	4.15	0.49	0.00	0.00	0.00	1.46	0.00	0.00	0.00	0.00	0.00	0.00	0.31	9.58
418.5	0.00	34.53	0.00	0.00	0.00	0.00	0.00	0.00	0.00	0.00	1.18	0.00	0.00	1.25	48.03
428.5	0.28	4.52	0.00	0.00	0.00	0.00	1.95	0.00	0.00	0.00	0.07	0.00	0.00	0.35	18.63
438.5	0.58	6.96	0.00	0.00	0.00	0.00	0.39	0.00	0.00	0.00	0.00	0.00	0.00	0.39	10.44
448.5	0.00	1.59	0.00	0.00	0.00	0.00	0.00	0.00	0.00	0.00	0.00	0.00	0.00	0.00	1.69
458.5	0.00	11.11	0.00	0.00	0.00	0.00	0.00	0.00	0.00	0.00	0.00	0.00	0.00	0.69	16.67
468.5	0.37	4.44	0.00	0.00	0.00	0.66	0.52	0.00	0.00	0.00	0.00	0.17	0.33	0.17	11.13
478.5	0.46	54.11	0.00	0.00	0.00	0.00	0.46	0.00	0.00	0.00	0.00	0.00	0.00	0.00	59.87
488.5	0.02	16.28	0.00	0.00	0.00	0.00	0.00	0.00	0.00	0.00	1.55	0.00	0.00	0.00	20.25
498.5	0.00	13.94	0.00	0.00	0.03	0.00	0.00	0.00	0.00	0.00	0.03	0.00	0.00	0.00	15.92
508.5	0.36	19.45	0.00	0.00	0.00	0.00	0.32	0.00	0.00	0.00	0.00	0.00	0.00	0.00	24.20
518.5	0.00	35.42	0.00	0.00	0.00	0.00	0.00	0.00	0.00	0.00	0.00	0.00	0.00	0.00	175.87
531.5	67.34	136.88	0.00	0.00	0.00	0.00	0.00	0.00	0.00	0.00	1.10	2.21	0.00	0.00	1069.68
540.5	0.00	0.00	0.00	0.00	0.00	0.00	0.00	0.00	0.00	0.00	0.00	0.00	0.00	0.00	0.00
548.5	0.00	1.60	0.00	0.00	0.00	0.00	0.00	0.00	0.00	0.00	0.00	0.00	0.00	0.00	1.60
558.5	0.92	125.75	0.00	0.00	0.00	0.00	0.00	0.00	0.00	0.00	0.00	0.00	0.00	0.00	133.38
562.5	0.00	0.00	0.00	0.00	0.00	0.00	0.00	0.00	0.00	0.00	0.00	0.00	0.00	0.00	0.00
568.5	0.57	84.10	0.00	0.00	0.00	2.27	2.27	0.00	0.00	0.00	0.00	0.00	0.00	0.00	186.96
578.5	0.05	8.74	0.00	0.00	0.00	0.00	0.18	0.00	0.00	0.00	0.14	0.00	0.18	0.00	9.88
588.5	0.00	32.51	0.00	0.00	0.00	0.00	1.96	0.00	0.00	0.00	0.39	0.00	1.57	0.00	37.50
598.5	0.00	13.87	0.00	0.00	0.00	0.00	5.80	0.00	0.00	0.00	0.54	0.00	0.36	0.00	21.67
608.5	0.00	20.85	0.16	0.00	0.00	0.00	2.61	0.00	0.00	0.00	0.41	0.00	0.00	0.00	28.17
613.5	0.00	38.31	0.00	0.00	0.00	0.00	9.75	0.00	0.00	0.00	0.00	0.00	0.00	0.00	52.21
618.5	0.00	29.32	5.90	0.00	0.00	0.00	0.96	0.00	0.00	0.00	0.92	0.00	0.00	0.32	43.64
623.5	0.00	28.01	5.62	0.00	0.00	0.00	1.17	0.00	0.00	0.00	0.64	0.00	0.00	0.00	42.71
633.5	0.00	148.55	40.58	0.00	0.00	0.00	1.52	0.00	0.00	0.00	0.00	0.05	0.00	0.00	197.23
638.5	0.00	349.79	37.30	0.00	0.00	0.00	5.46	0.00	0.00	0.00	0.04	0.00	0.00	0.00	392.60
643.5	0.00	357.97	10.56	0.00	0.00	0.00	23.31	0.00	0.00	0.00	0.00	0.00	0.00	0.00	391.81
648.5	0.00	120.55	0.00	0.00	0.00	0.00	1.42	0.00	0.00	0.00	0.00	0.00	0.00	0.00	121.97
658.5	0.00	136.15	21.51	0.00	0.00	0.00	7.85	0.00	0.00	0.00	3.19	0.00	0.00	0.00	174.66
668.5	0.00	0.00	0.12	0.00	0.00	0.00	0.00	0.00	0.00	0.00	0.00	0.00	0.00	0.00	0.12
678.5	0.00	0.00	0.00	0.00	0.00	0.00	0.00	0.00	0.00	0.00	0.00	0.00	0.00	0.00	0.00
689.5	0.00	0.00	0.00	0.00	0.00	0.00	0.00	0.00	0.00	0.00	0.00	0.00	0.00	0.00	0.00
696.5	0.00	0.00	0.00	0.00	0.00	0.00	0.00	0.00	0.00	0.00	0.00	0.00	0.00	0.00	0.00
705.5	0.00	0.00	0.00	0.00	0.00	0.00	0.00	0.00	0.00	0.00	0.00	0.00	0.00	0.00	0.00
709.5	0.00	32.12	0.78	0.00	0.00	0.00	1.57	0.00	0.00	0.00	0.00	0.00	0.00	0.00	35.25
716.5	0.00	0.00	0.00	0.00	0.00	0.00	0.40	0.00	0.00	0.00	0.00	0.00	0.00	0.00	0.40
726.5	0.00	0.00	0.00	0.00	0.00	0.00	0.00	0.00	0.00	0.00	0.00	0.00	0.00	0.00	0.00
735.5	0.00	0.00	0.00	0.00	0.00	0.00	4.86	0.00	0.97	0.00	1.95	0.00	0.00	0.00	39.63
746.5	0.00	0.00	0.00	0.00	0.00	0.00	5.48	0.00	0.00	0.00	0.00	0.00	0.00	0.09	58.19
755.5	0.00	0.00	0.00	0.00	0.00	0.00	0.46	0.00	0.46	0.00	0.00	0.00	0.00	0.00	5.19
763.0															

Appendix 5. Data for Core 1244 (Spec/g)

Depth [cm]	Age [ka]	DBD [g/ccm]	Dry Weight [g]	AMS14C dates [ky]	LSR [cm/ka]	*Pyrgo ratularia*	*Cibicidoides wuellerstorfi*	*Epistominella exigua*	*Oinqueloculina seminula*	*Elphidium* spp.	*Triloculina tricarinata*	*Cribrostomoides subglobosus*	agglutinated Tubes	*Ammobaculites agglutinans*	*Pullenia bulloides*	*Cassidulina teretis*
0.0	1.00	0.73	19.85		3.18	4.89	863.69	51.58	0.00	0.00	20.15	25.38	6.70	0.00	0.00	0.00
10.0	4.14	0.76	17.91		3.18	36.90	1014.57	14.29	0.00	0.00	121.46	80.77	0.00	0.00	0.00	7.14
20.0	7.29	0.73	16.40		3.18	38.78	650.66	0.00	0.00	0.00	87.80	28.53	23.41	7.80	0.00	15.61
30.0	10.43	0.89	26.06		3.18	1.15	32.58	0.00	0.00	0.61	12.59	2.49	3.45	0.00	0.00	1.23
40.0	19.50	1.00	27.00		0.67	0.96	1.22	0.00	0.00	0.59	9.78	0.56	1.85	0.00	0.00	0.59
50.0	28.60	0.88	20.99		3.13	0.81	0.19	0.00	0.00	2.29	3.81	0.43	0.86	0.00	0.00	0.76
60.0	31.80	0.90	21.72		3.13	0.09	0.78	0.00	0.00	0.64	3.36	0.46	0.05	0.00	0.00	0.00
70.0	35.00	0.95	23.36		3.13	0.04	0.00	0.00	0.04	0.69	4.45	0.51	4.07	0.00	0.00	0.00
80.0	38.20	0.93	20.13		3.13	0.15	0.00	0.00	0.00	0.00	5.17	0.40	3.13	0.00	0.00	0.00
90.0	41.40	0.93	20.08		3.13	0.55	0.00	0.00	0.00	0.55	3.79	0.60	2.54	0.00	0.00	0.05
100.0	44.60	0.96	22.28		3.13	0.94	0.18	0.00	0.36	0.09	5.43	2.06	10.28	0.00	0.00	0.36
110.0	47.80	1.04	22.56		3.13	1.11	0.44	0.00	0.00	0.09	13.21	1.60	1.64	0.00	0.00	0.00
120.0	51.00	0.95	18.83		3.13	0.85	0.48	0.00	0.00	0.00	7.65	0.21	3.40	0.00	0.00	0.00
130.0	54.20	0.98	15.65		3.13	1.66	0.00	0.00	0.00	0.00	8.18	0.13	0.06	0.00	0.00	0.00
140.0	57.40	0.91	16.47		3.13	0.61	0.49	0.00	0.00	0.06	8.99	0.12	0.91	0.00	0.00	0.00
150.0	65.00	0.98	25.09		0.83	0.60	1.67	0.00	0.00	1.43	4.46	0.00	4.54	0.00	0.00	0.08
160.0	74.28	0.96	16.15		1.53	0.06	32.44	1.98	0.12	0.00	5.94	0.25	2.79	0.00	0.00	2.97
170.0	80.83	0.78	16.34		1.53	0.00	54.03	0.00	0.55	0.06	4.96	0.49	1.10	0.00	30.65	0.00
180.0	87.38	1.03	23.24		1.53	0.86	44.41	0.00	2.07	0.00	8.95	0.00	24.79	0.00	1.38	1.38
200.0	100.48	0.67	15.31		1.53	1.76	38.74	0.00	0.00	0.07	4.25	0.07	0.65	0.00	0.07	0.00
210.0	107.03	0.84	16.83		1.53	3.57	76.66	0.00	0.00	0.00	3.80	0.00	1.49	0.00	0.00	0.00
220.0	113.59	0.67	12.88		1.53	6.21	132.63	0.00	0.23	0.00	4.97	1.01	6.13	0.00	0.00	0.00
230.0	120.14	0.60	10.15		1.53	8.38	360.33	0.00	0.00	0.00	37.85	7.79	0.79	0.00	0.00	0.00
240.0	126.69	1.10	15.91		1.53	0.00	1.51	0.00	0.00	0.00	0.00	0.00	0.00	0.00	0.00	0.00
249.0	145.65	1.04	22.43		0.40	0.00	0.00	0.00	0.00	0.71	1.43	0.00	0.00	0.00	0.00	0.00
260.0	173.39	0.94	26.12		0.40	0.34	0.31	0.00	0.00	0.00	6.74	0.11	4.06	0.00	0.00	0.61
270.0	189.28	1.07	23.52		1.53	0.43	6.38	0.00	0.00	0.04	2.04	0.04	2.13	0.00	0.00	0.04
280.0	193.07	1.10	27.76		0.89	0.07	42.66	0.00	0.00	0.14	2.31	1.48	4.68	0.00	0.00	0.00
290.0	204.31	0.96	16.00		0.89	1.25	26.88	0.00	0.00	0.00	1.00	0.25	0.75	0.00	0.00	1.00
300.0	215.54	0.96	19.11		0.81	0.00	31.60	0.00	0.00	0.00	0.00	0.00	0.00	0.00	0.00	10.94
310.0	227.87	1.12	17.77		0.81	0.06	0.06	0.00	0.00	2.25	0.90	0.00	0.06	0.00	0.00	0.00
320.0	240.19	1.11	17.68		0.96	0.00	0.90	0.00	0.00	0.00	1.81	0.00	1.81	0.00	1.81	0.00
330.0	250.66	0.87	15.95		0.96	0.19	0.00	0.00	0.00	0.31	0.00	0.00	0.13	0.00	0.00	0.75
340.0	261.13	0.77	13.33		0.96	0.00	0.00	0.00	0.00	0.00	0.00	0.00	0.00	0.00	0.00	0.00
350.0	271.60	0.96	16.08		0.96	0.00	0.00	0.00	0.00	0.06	5.75	0.00	0.00	0.00	0.11	0.44
360.0	282.06	1.13	21.64		0.96	0.00	0.00	0.00	0.00	0.74	2.22	2.86	1.48	0.00	0.00	18.11
370.0	292.53	1.03	18.79		0.96	0.00	0.00	0.00	0.00	0.00	2.56	0.32	0.00	0.00	0.00	7.67
380.0	303.00	0.98	16.05		1.11	0.06	0.00	0.00	0.00	0.00	0.00	0.31	0.00	0.00	0.00	3.99
390.0	312.00	1.00	17.36		1.11	0.52	0.12	0.00	0.00	0.58	0.92	0.00	0.92	0.00	0.00	0.46
400.0	321.00	0.85	13.34		1.11	0.22	3.22	0.00	0.00	0.00	0.60	0.07	0.00	0.00	0.00	0.00
410.0	330.00	0.74	10.34		0.56	0.00	102.93	0.00	0.00	0.00	1.55	0.00	0.00	0.00	0.00	0.00
420.0	340.92	0.86	10.53		2.61	0.00	0.00	0.00	0.00	0.00	0.00	0.00	0.00	0.00	0.00	0.00
430.0	344.75	1.25	16.86		2.61	0.00	0.00	0.00	0.00	0.00	0.00	0.00	0.00	0.00	0.00	0.00
440.0	348.58	1.27	17.68		2.61	0.00	0.00	0.00	0.00	0.00	0.00	0.00	0.00	0.00	0.00	0.00
450.0	352.42	1.26	14.05		2.61	0.00	0.00	0.00	0.00	0.00	0.00	0.00	0.00	0.00	0.00	0.00
460.0	356.25	1.07	10.58		2.61	0.00	0.00	0.00	0.00	0.00	0.00	0.00	0.00	0.00	0.00	0.00
470.0	360.08	1.27	18.75		2.61	0.00	0.00	0.00	0.00	0.00	0.00	0.00	0.00	0.00	0.00	0.00
480.0	367.08	1.09	15.42		0.98	0.39	0.06	0.00	0.00	0.00	0.06	0.06	0.00	0.00	0.00	0.00
490.0	377.25	1.00	14.58		0.98	1.23	15.02	0.00	0.00	0.07	5.55	0.00	0.00	0.00	0.00	0.00
500.0	387.42	0.81	13.54		0.98	0.66	8.49	0.00	0.00	0.00	7.24	0.00	0.00	0.00	5.10	0.00
510.0	397.58	0.72	12.28		0.98	9.85	0.00	0.00	0.00	0.00	0.65	0.00	0.00	0.00	0.33	10.42
520.0	407.75	0.67	11.13		0.98	0.90	0.00	0.00	0.00	0.00	0.00	0.00	0.00	0.00	2.96	0.00
530.0	417.92	0.70	13.02		0.98	0.00	0.08	0.00	0.00	0.00	0.00	0.00	0.00	0.00	0.23	0.00
540.0	428.50	1.15	18.54		0.91	0.00	0.00	0.00	0.00	0.00	0.00	0.00	0.00	0.00	0.00	0.00
550.0	439.50	1.30	22.43		0.91	0.00	0.00	0.00	0.00	0.00	0.00	0.00	0.00	0.00	0.00	0.00
560.0	450.50	1.33	23.84		0.91	0.00	0.00	0.00	0.00	0.00	0.00	0.00	0.00	0.00	0.00	0.00
570.0	461.50	1.09	18.70		0.91	0.00	0.00	0.00	0.00	0.00	0.00	0.00	0.00	0.00	0.00	0.00
574.0	465.90	1.08	17.01		0.91	0.00	0.00	0.00	0.00	0.71	0.00	0.00	0.00	0.00	0.00	0.00
580.0	472.50	1.31	15.97		0.91	0.00	0.00	0.00	0.00	0.00	0.00	0.00	0.00	0.00	0.00	0.00
590.0	485.67	1.07	16.73		0.65	0.18	33.18	0.00	0.00	0.00	0.00	0.00	0.00	0.00	0.00	0.00
600.0	501.00	1.05	16.93		0.65	0.00	8.56	0.00	0.00	1.89	1.89	0.00	0.00	0.00	0.00	0.00
610.0	516.33	0.89	18.94		0.65	0.00	16.90	0.00	0.00	0.00	0.00	0.00	0.00	0.00	0.00	0.00
620.0	528.56	1.15	17.38		1.10	0.00	0.00	0.00	0.00	0.00	0.00	0.00	0.00	0.00	0.00	0.00
630.0	537.67	1.16	14.92		1.10	0.00	0.00	0.00	0.00	0.00	0.00	0.00	0.00	0.00	0.00	0.00
640.0	546.78	1.33	17.99		1.10	0.00	0.00	0.00	0.00	0.00	0.00	0.00	0.00	0.00	0.00	0.00
650.0	555.89	1.52	17.20		1.10	0.00	0.00	0.00	0.00	0.00	0.00	0.00	0.00	0.00	0.00	0.00
660.0	565.00	1.55	17.06		1.10	0.00	0.00	0.00	0.00	0.00	0.00	0.00	0.00	0.00	0.00	0.00
665.0	568.00	1.01	13.10		1.67	0.61	0.98	15.87	0.00	0.61	1.22	0.00	1.37	0.00	0.61	14.04

Appendix 5. continued

Depth [cm]	*Oridorsalis umbonatus*	*Globocassidulina subglobosa*	*Marginulina glabra*	*Dentalina pauperata*	*Siphotextularia rolshauseni*	*Cassidulina reniforme*	*Melonella* sp.	*Oolina hexagona*	*Cyclammina* sp.	*Parafissurina ovata*	*Lenticulina gibba*	*Ejamides tumidulus*	*Liggena* spp.	Total [Spec./g]
0.0	141.83	0.00	0.00	1.61	0.00	6.45	0.00	0.00	0.00	0.00	0.00	0.00	6.45	1128.72
10.0	164.33	0.00	0.00	0.00	0.00	28.58	0.00	0.00	0.00	0.00	0.00	7.14	3.57	1478.77
20.0	124.86	0.00	0.00	0.00	7.80	15.61	0.00	0.00	0.00	0.00	0.00	7.80	0.00	1008.67
30.0	11.05	0.00	0.00	0.00	0.00	1.23	0.00	0.00	0.00	0.00	0.00	0.61	0.61	67.61
40.0	8.00	0.00	0.00	0.00	2.37	0.00	0.00	0.00	0.00	0.00	0.00	1.78	0.59	28.30
50.0	2.67	0.00	0.00	0.19	10.29	0.76	0.00	0.00	0.00	0.00	0.00	1.52	0.00	24.58
60.0	0.37	0.00	0.00	0.05	2.21	0.74	0.37	0.00	0.00	0.00	0.00	0.00	0.00	9.12
70.0	0.69	0.00	0.00	0.17	0.00	0.00	0.00	0.00	0.00	0.00	0.00	0.00	0.00	10.66
80.0	0.10	0.00	0.00	0.00	0.00	0.00	0.00	0.00	0.00	0.00	0.00	0.00	0.00	8.94
90.0	0.60	0.00	0.00	0.00	0.00	0.40	0.00	0.00	0.00	0.00	0.00	0.40	0.00	9.46
100.0	1.08	0.00	0.00	0.00	0.00	0.36	0.00	0.00	0.00	0.00	0.00	2.87	0.00	24.02
110.0	2.93	0.00	0.00	0.00	0.00	0.71	0.00	0.00	0.00	0.18	0.00	1.06	0.35	23.31
120.0	5.52	0.00	0.00	0.00	0.00	3.40	0.00	0.00	0.00	0.00	0.00	1.27	0.00	22.78
130.0	9.26	0.00	0.00	0.00	0.00	1.02	0.00	0.00	0.00	0.13	0.00	1.02	0.00	21.47
140.0	28.42	0.00	0.00	0.00	0.00	1.46	0.00	0.00	0.00	0.00	0.00	1.94	0.00	42.99
150.0	3.91	0.00	0.00	0.00	0.00	0.00	0.00	0.00	0.00	0.00	0.00	1.91	0.00	18.62
160.0	4.95	0.00	0.00	0.00	0.00	0.99	0.00	0.00	0.00	0.12	0.00	2.97	0.00	55.60
170.0	29.49	0.00	0.06	0.00	0.12	0.98	0.00	0.00	0.00	1.35	0.00	0.98	0.00	124.81
180.0	19.28	0.00	0.00	0.00	0.00	4.13	0.00	0.00	0.00	5.51	0.00	5.51	1.38	122.38
200.0	29.27	0.00	0.00	0.00	0.00	0.00	0.00	0.00	0.00	0.13	0.00	0.00	0.00	74.99
210.0	60.85	0.00	0.00	0.00	0.00	1.90	0.00	0.00	0.00	0.00	0.00	5.70	0.00	153.97
220.0	34.79	0.00	0.00	0.00	0.00	5.59	0.00	0.00	0.00	5.59	0.00	9.94	0.00	207.10
230.0	145.08	0.00	0.00	0.00	0.00	26.02	0.00	0.00	0.00	0.00	0.00	6.31	6.31	398.84
240.0	1.01	0.00	0.00	0.00	0.00	0.50	0.00	0.00	0.00	0.00	0.00	0.00	0.00	3.02
249.0	1.43	0.00	0.00	0.00	0.00	1.43	0.00	0.00	0.00	0.00	0.00	2.14	0.00	7.13
260.0	15.62	1.84	0.00	0.00	0.00	0.00	0.00	0.00	0.00	0.00	0.00	0.61	0.61	30.86
270.0	13.01	0.00	0.00	0.00	0.00	0.00	0.68	0.00	0.00	0.00	0.00	0.68	0.00	24.87
280.0	28.97	0.00	0.00	0.00	0.00	0.00	0.00	0.00	0.00	0.00	0.00	0.00	0.00	80.31
290.0	46.00	0.00	0.00	0.00	0.00	0.00	0.00	0.00	0.00	0.00	0.00	0.00	1.00	78.13
300.0	59.44	0.00	0.00	0.00	0.00	1.67	0.00	0.00	0.00	0.00	0.00	0.00	0.00	105.65
310.0	2.70	0.00	0.00	0.06	0.00	0.90	0.00	0.00	0.00	0.00	0.00	0.00	0.00	6.98
320.0	0.90	0.00	0.00	0.00	0.00	2.71	0.00	0.00	0.00	0.00	0.00	0.00	0.00	9.95
330.0	0.00	0.00	0.00	0.00	0.06	0.00	0.00	0.00	0.00	0.00	0.00	0.00	0.00	1.44
340.0	0.00	0.00	0.00	0.00	0.00	0.00	0.00	0.00	0.00	0.00	0.00	0.00	0.00	0.00
350.0	25.38	0.00	0.00	0.00	0.00	0.44	0.00	0.00	0.00	0.11	0.06	1.77	0.00	34.12
360.0	39.18	0.00	0.00	0.00	0.00	0.00	0.00	0.00	0.00	0.00	0.00	0.00	0.00	64.59
370.0	34.07	0.00	0.00	0.00	0.00	0.00	0.00	0.00	0.00	0.00	0.00	0.00	0.00	44.61
380.0	15.95	0.00	0.00	0.00	0.00	0.00	0.00	0.00	0.00	0.00	0.06	0.00	0.00	20.37
390.0	14.28	0.00	0.00	0.00	0.00	0.00	0.00	0.00	0.00	0.00	0.00	0.00	0.00	17.80
400.0	28.78	0.00	0.00	0.00	0.00	0.00	0.00	0.00	0.00	0.00	0.00	0.00	0.00	32.93
410.0	18.57	0.00	0.00	0.00	0.00	0.00	0.00	0.00	0.00	0.00	0.00	0.00	0.00	125.06
420.0	0.00	0.00	0.00	0.00	0.00	0.00	0.00	0.00	0.00	0.00	0.00	0.00	0.00	0.00
430.0	0.00	0.00	0.00	0.00	0.00	0.00	0.00	0.00	0.00	0.00	0.00	0.00	0.00	0.00
440.0	0.00	0.00	0.00	0.00	0.00	0.00	0.00	0.00	0.00	0.00	0.00	0.00	0.00	0.00
450.0	0.00	0.00	0.00	0.00	0.00	0.00	0.00	0.00	0.00	0.00	0.00	0.00	0.00	0.00
460.0	0.00	0.00	0.00	0.00	0.00	0.00	0.00	0.00	0.00	0.00	0.00	0.00	0.00	0.00
470.0	0.00	0.00	0.00	0.00	0.00	0.00	0.00	0.00	0.00	0.00	0.00	0.00	0.00	0.00
480.0	43.71	4.15	0.00	0.00	0.00	4.15	0.00	0.00	0.00	0.00	0.00	4.15	0.00	52.59
490.0	50.81	4.39	0.00	0.00	0.00	4.39	0.00	0.00	0.00	0.27	0.07	0.00	0.00	77.41
500.0	59.09	5.02	0.00	0.00	0.00	5.02	0.00	0.00	0.00	0.07	0.15	0.00	0.00	85.83
510.0	187.91	31.59	0.16	0.00	0.00	31.59	0.00	0.00	0.00	0.33	0.33	0.00	0.00	241.56
520.0	158.07	9.34	0.00	0.00	0.00	9.34	0.00	0.00	0.00	0.00	0.18	0.00	0.00	171.46
530.0	6.84	0.00	0.00	0.00	0.00	0.00	0.00	0.00	0.00	0.00	0.00	0.00	0.00	7.14
540.0	0.00	0.00	0.00	0.00	0.00	0.00	0.00	0.00	0.00	0.00	0.00	0.00	0.00	0.00
550.0	0.00	0.00	0.00	0.00	0.00	0.00	0.00	0.00	0.00	0.00	0.00	0.00	0.00	0.00
560.0	0.00	0.00	0.00	0.00	0.00	0.00	0.00	0.00	0.00	0.00	0.00	0.00	0.00	0.00
570.0	0.00	0.00	0.00	0.00	0.00	0.00	0.00	0.00	0.00	0.00	0.00	0.00	0.00	0.00
574.0	0.00	0.00	0.00	0.00	0.00	0.12	0.00	0.00	0.00	0.00	0.00	0.00	0.00	0.82
580.0	0.00	0.00	0.00	0.00	0.00	0.00	0.00	0.00	0.00	0.00	0.00	0.00	0.00	0.00
590.0	0.00	0.00	0.00	0.06	0.00	0.00	0.00	0.00	0.00	0.00	0.00	0.00	0.00	33.42
600.0	0.00	0.00	0.00	0.06	0.00	0.00	0.00	0.00	0.00	0.00	0.00	0.00	0.94	13.55
610.0	0.00	0.00	0.00	0.00	0.00	0.00	0.00	0.00	0.00	0.00	0.00	0.00	0.00	16.90
620.0	0.00	0.00	0.00	0.00	0.00	0.00	0.00	0.00	0.00	0.00	0.00	0.00	0.00	0.00
630.0	0.00	0.00	0.00	0.00	0.00	0.00	0.00	0.00	0.00	0.00	0.00	0.00	0.00	0.00
640.0	0.00	0.00	0.00	0.00	0.00	0.00	0.00	0.00	0.00	0.00	0.00	0.00	0.00	0.00
650.0	0.00	0.00	0.00	0.00	0.00	0.00	0.00	0.00	0.00	0.00	0.00	0.00	0.00	0.00
660.0	0.00	0.00	0.00	0.00	0.00	0.00	0.00	0.00	0.00	0.00	0.00	0.00	0.00	0.00
665.0	0.00	0.00	0.00	0.00	0.61	1.83	6.87	0.00	0.00	0.00	0.61	0.61	0.00	44.95

Appendix 6. Data for Core 1246 (Spec/g)

[cm]	[ka]	[g/ccm]	[g]	Event	[cm/ka]	*rotularia*	*wuellerstorfi*	*exigua*	*caribula*	*spp.*	*tricarinata*	*subglobosus*	Tubes	*agglutinans*	*bulloides*	*teretis*
5.5	2.00	0.70	19.21	Vo	1.67	16.50	529.56	0.00	0.10	13.85	54.97	54.55	0.00	0.00	0.00	61.84
10.5	5.00	0.70	16.61		2.22	6.74	845.14	0.00	0.00	17.88	31.85	16.92	0.00	0.00	0.00	39.73
18.5	8.60	0.68	16.81	1.1	5.33	8.33	744.94	0.00	0.12	0.95	54.27	11.07	0.95	0.00	0.00	15.23
20.5	10.1			Vo												
30.5	11.85	1.01	20.42		2.86	0.93	98.81	0.00	0.78	0.10	4.80	4.80	2.74	0.00	0.00	7.05
35.5	13.6			Vo												
40.5	14.68	0.99	21.83		4.62	0.87	0.37	0.00	0.00	0.37	5.50	0.23	0.73	0.00	0.00	0.00
45.5	14.9			2.2												
50.5	18.53	0.89	22.24		2.48	0.09	0.13	0.00	0.04	0.40	10.88	0.00	1.48	0.00	0.00	0.36
60.5	22.56	0.91	19.83		2.48	0.25	0.00	0.00	0.00	0.40	2.47	0.05	2.17	0.00	0.00	0.00
71.5	27.00	0.97	19.18	3.1	1.06	0.42	0.47	0.00	0.42	0.00	8.24	0.16	0.52	0.00	0.00	1.04
80.5	35.52	0.94	23.52		1.06	0.13	0.00	0.00	0.00	0.34	6.12	0.13	0.43	0.00	0.00	0.34
88.5	43.09	1.00	21.72		1.06	0.14	0.00	0.00	0.05	0.37	5.98	0.87	1.24	0.00	0.00	0.41
100.5	55.45	1.00	23.96	3.3	3.07	1.09	0.00	0.00	0.17	0.17	17.53	0.71	0.42	0.00	0.00	0.88
110.5	58.71	0.90	20.37		3.07	1.08	0.00	0.00	0.20	0.20	20.62	0.83	0.49	0.00	0.00	1.03
120.5	61.96	0.90	22.40		3.07	1.61	0.04	0.00	0.09	0.00	22.50	0.27	1.70	0.00	0.00	0.00
130.5	65.22	0.94	22.29	4.2.2	2.88	0.40	0.22	0.00	0.22	0.18	32.75	0.00	0.40	0.00	0.00	1.08
139.5	68.35	0.95	20.79		2.88	0.96	3.37	0.00	0.05	3.94	6.21	0.05	0.67	0.00	0.05	1.97
150.5	72.17	0.94	20.31		2.88	0.69	33.67	0.00	0.25	0.39	6.55	1.33	2.46	0.00	1.58	2.36
161.5	75.99	0.84	20.36		2.88	1.77	57.56	0.00	10.17	0.00	7.07	6.97	30.70	0.00	22.40	0.79
171.5	79.46	0.90	21.55	5.1	0.77	1.76	61.68	0.00	16.52	0.74	14.29	1.30	21.25	0.00	0.00	0.00
180.5	90.53	0.86	24.46	5.2	1.38	2.98	82.71	0.00	9.81	2.62	22.24	0.04	7.60	0.00	0.00	3.92
191.5	98.49	0.76	14.77		1.38	3.38	39.26	0.00	6.23	0.00	12.05	0.07	5.41	0.00	0.00	3.38
198.5	103.55	0.84	21.13	5.3	0.58	4.26	42.79	0.00	0.00	0.80	8.33	0.00	2.79	0.00	0.00	0.95
209.5	122.38	0.66	14.41	5.5.1	4.57	9.99	179.85	0.00	0.07	0.00	13.60	11.80	44.96	0.00	0.00	2.22
221.5	125.00	0.91	24.74	5.5.3	2.87	2.55	77.48	0.00	0.00	0.00	9.05	0.69	3.68	0.00	0.00	2.59
232.5	128.83	0.83	23.19		2.87	4.79	0.43	0.00	0.00	0.00	27.94	0.00	14.01	0.00	0.00	2.07
242.5	132.31	1.02	25.37		2.87	0.32	0.00	0.32	0.00	0.00	10.48	0.00	0.79	0.00	0.00	1.02
250.5	135.10	1.08	26.76	6.2	1.28	0.00	0.22	0.00	0.00	0.60	2.99	0.00	0.45	0.00	0.00	0.60
258.5	141.33	0.95	22.06	6.3	0.70	0.14	0.09	0.00	0.00	0.77	2.54	0.09	0.82	0.00	0.00	0.36
269.5	157.10	0.98	25.64	6.4	0.77	0.16	0.00	0.00	0.00	0.70	2.81	0.04	0.16	0.00	0.00	0.00
280.5	171.37	0.93	22.85	6.5	1.07	0.70	0.00	0.00	0.00	0.00	10.94	0.00	65.26	0.00	0.00	3.50
289.5	179.73	1.03	23.90		1.94	0.42	0.00	0.00	0.00	0.42	8.45	0.00	0.04	0.00	0.00	0.00
296.5	183.33	1.27	30.20	6.6	3.31	0.00	0.00	0.00	0.00	0.00	1.36	0.00	0.00	0.00	0.00	0.00
302.5	185.19	0.98	24.49		2.41	0.37	1.18	0.00	0.16	0.90	8.70	0.00	0.24	0.00	0.00	0.49
321.5	193.07	1.00	32.71	7.1	1.07	0.15	114.88	0.00	0.00	0.00	16.02	4.92	2.14	0.00	0.00	15.90
329.5	200.57	1.03	30.19	7.2	0.60	0.07	69.19	0.00	0.00	0.17	4.24	3.94	0.36	0.00	0.00	4.24
338.5	215.54	1.06	28.69	7.3	2.01	0.00	44.13	0.00	0.00	0.56	0.00	1.99	0.38	0.00	0.00	0.00
350.5	221.52	0.82	19.98		2.01	0.00	28.53	0.00	0.00	0.00	3.20	1.35	3.20	0.00	0.00	0.00
354.5	228.00	0.80	20.31	7.4	1.64	0.00	4.92	0.00	0.00	0.00	0.00	0.30	3.35	0.00	0.00	0.00
359.5	231.05	0.95	23.62		1.64	0.00	11.86	0.00	0.00	1.36	10.84	0.17	2.50	0.00	0.00	0.04
362.5	232.88	0.95	24.60		1.64	0.00	13.62	0.00	0.00	0.00	0.65	0.89	0.04	0.00	0.49	0.00
370.5	240.19	0.99	26.38	7.5	2.11	0.00	5.91	0.00	0.00	0.61	12.77	0.04	0.04	0.00	0.00	3.07
379.5	244.45	0.91	22.01		2.11	3.41	66.14	0.00	0.00	0.00	18.17	2.36	10.90	0.00	0.00	5.81
398.5	253.43	1.07	24.31	8.2	0.52	0.00	0.08	0.00	0.00	0.00	13.90	0.45	0.00	0.00	0.00	0.08
411.5	278.64	1.02	27.80		0.52	0.00	0.00	0.00	0.00	0.00	8.20	0.72	0.00	0.00	0.00	1.73
418.5	292.22	0.98	23.39		0.52	0.09	0.34	0.00	0.00	0.00	5.47	0.47	1.37	0.00	0.00	0.85
429.5	313.55	0.90	17.23		0.52	0.00	8.82	0.00	0.00	0.06	0.93	0.00	0.00	0.00	0.00	0.00
438.5	331.00	0.92	22.80	9.3	0.81	0.00	21.06	0.00	0.00	1.40	0.00	0.22	2.15	0.00	0.00	0.70
450.5	335.00	1.35	37.33		0.81	0.00	0.00	0.00	0.00	0.00	0.00	0.00	0.00	0.00	0.00	0.00
459.5	340.00	1.29	32.24		0.81	0.00	0.00	0.00	0.00	0.00	0.00	0.00	0.00	0.00	0.00	0.00
469.5	340.20	1.28	28.80		0.81	0.00	0.00	0.00	0.00	0.00	0.00	0.00	0.00	0.00	0.00	0.00
480.5	340.50	1.30	39.14		0.81	0.00	0.00	0.00	0.00	0.00	0.00	0.00	0.00	0.00	0.00	0.00
487.5	340.75	1.34	34.18	10.0	24.25	0.00	0.00	0.00	0.00	0.00	0.00	0.00	0.00	0.00	0.00	0.00
489	340.80	1.38	12.25		24.25	0.00	0.00	0.00	0.00	0.00	0.00	0.00	0.00	0.00	0.00	0.00
490.5	360.00	1.38	30.56		24.25	0.00	0.00	0.00	0.00	0.00	0.00	0.00	0.00	0.00	0.00	0.00
493.5	362.00	1.20	17.81	11.0	0.11	0.00	0.00	0.00	0.00	0.06	0.00	0.00	0.00	0.00	0.00	0.00
496.5	368.00	1.20	24.44	11.1	1.57	0.08	0.82	0.00	0.00	1.31	8.59	0.00	0.00	0.00	0.00	6.71
507.5	375.00	1.00	26.01		1.00	0.65	0.73	0.00	0.00	0.62	42.95	0.00	0.00	0.00	0.00	1.31
517.5	385.00	1.10	24.96		1.00	0.40	0.24	0.00	0.00	0.00	26.72	0.00	0.00	0.00	0.00	3.89
531	398.50	0.98	27.19		1.00	1.65	10.99	0.00	0.00	1.18	8.27	0.00	0.00	0.00	2.43	2.35
537.5	405.00	0.91	22.57	11.3	0.42	0.80	9.04	0.00	0.00	8.15	2.92	0.00	0.00	0.00	0.27	8.55
540	408.00	0.91	25.00		0.42	0.00	0.00	0.00	0.00	0.00	0.00	0.00	0.00	0.00	0.00	0.00
552.5	423.00	1.21	31.24	12.0	1.05	0.03	0.00	0.00	0.00	0.10	0.00	0.00	0.00	0.00	0.00	0.00
559	436.28	1.00	24.08		1.05	0.00	0.00	0.00	0.00	0.00	0.00	0.00	0.00	0.00	0.00	0.00
571	447.66	1.11	25.34		1.05	0.00	0.00	0.00	0.00	0.00	0.00	0.00	0.00	0.00	0.00	0.00
578.5	454.77	1.04	27.89		1.05	0.00	0.00	0.00	0.00	0.00	0.00	0.00	0.00	0.00	0.00	0.00
589	464.72	1.01	26.26		1.05	0.00	0.00	0.00	0.00	0.00	0.00	0.00	0.00	0.00	0.00	0.00
595	474.68	1.22	32.25		1.05	0.00	0.00	0.00	0.00	0.00	0.00	0.00	0.00	0.00	0.00	0.00
599.5	478.00	1.06	23.59	13.0	0.91	0.00	0.00	0.00	0.00	0.00	0.00	0.00	0.00	0.00	0.00	0.00
608	483.48	1.03	25.50		0.91	0.04	18.43	0.00	0.00	0.08	0.00	0.00	0.00	0.00	0.00	3.77
619	495.52	1.12	25.25		0.91	0.00	10.77	0.00	0.00	0.83	0.00	0.08	0.00	0.00	0.00	2.69
628.5	505.93	1.10	27.97		0.91	0.00	40.87	0.00	0.00	0.00	3.43	0.00	0.00	0.00	0.00	10.30
640.5	519.07	1.21	27.68		0.91	0.00	14.09	0.00	0.00	0.00	0.00	0.00	0.00	0.00	0.00	0.00
651	530.15	0.89	28.05	14.0	0.98	0.00	27.88	0.00	0.00	0.00	0.00	0.00	0.00	0.00	0.00	0.07
657.5	540.00	1.05	28.52		0.98	0.00	0.00	0.00	0.00	0.00	0.00	0.00	0.00	0.00	0.00	0.00
662.5	545.00	0.92	23.56		0.98	0.00	0.00	0.00	0.00	0.00	0.00	0.00	0.00	0.00	0.00	0.00
667	550.00	1.22	24.70		0.98	0.00	0.00	0.00	0.00	0.00	0.00	0.00	0.00	0.00	0.00	0.00
672.5	555.00	1.37	35.42		0.98	0.00	0.00	0.00	0.00	0.00	0.00	0.00	0.00	0.00	0.00	0.00
677.5	560.00	1.33	39.92		0.98	0.00	0.00	0.00	0.00	0.00	0.00	0.00	0.00	0.00	0.00	0.00
679.5	565.00	1.41	36.34		0.98	0.00	0.00	0.00	0.00	0.00	0.00	0.00	0.00	0.00	0.00	0.00
688.5	568.26	0.82	21.96	15.0	1.08	0.00	0.00	0.00	0.00	0.00	0.00	0.00	0.00	0.00	0.00	0.00
694.5	573.84	0.76	20.14		1.08	0.05	64.76	0.00	0.00	0.00	0.00	0.00	0.00	0.00	0.00	16.29
699.5	578.49	0.62	17.75		1.08	0.00	0.00	0.00	0.00	0.00	0.00	0.00	0.00	0.00	0.00	0.00
706.5	585.00	0.83	17.64		1.08	0.00	14.40	0.00	0.00	3.74	0.23	0.00	0.00	0.00	0.11	18.71

Appendix 6. continued

Depth [cm]	*Oridorsalis umbonatus*	*Globocassidulina subglobosa*	*Marginulina glabra*	*Dentalina pauperata*	*Siphotextularia rolshauseni*	*Cassidulina reniforme*	*Miliolinella sp.*	*Oolina hexagona*	*Cyclamina sp.*	*Parafissurina ovata*	*Lenticulina gibba*	*Eponides tumidulus*	*Lagena spp.*	Total [Spec./g]
5.5	42.06	0.00	0.10	0.00	0.00	0.00	0.00	0.00	0.00	0.00	0.00	0.00	6.87	780.39
10.5	65.50	0.00	0.06	0.00	0.00	0.00	0.00	0.00	0.00	0.00	0.00	0.00	15.89	1055.73
18.5	102.82	0.00	0.00	0.00	0.00	0.00	0.00	0.00	0.00	0.00	0.00	0.00	3.81	946.36
20.5														
30.5	16.45	0.00	0.05	0.00	0.00	0.00	0.00	0.00	0.00	0.00	0.00	0.00	1.57	138.38
35.5														
40.5	3.66	0.00	0.00	0.00	5.13	0.00	0.00	0.00	0.00	0.00	0.00	0.00	0.00	18.14
45.5														
50.5	2.52	0.00	0.00	0.00	0.04	0.00	0.00	0.00	0.00	0.00	0.00	0.00	0.76	17.22
60.5	2.22	0.00	0.00	0.10	0.00	0.00	0.00	0.20	0.00	0.00	0.00	0.00	0.00	8.37
71.5	1.25	0.00	0.00	0.10	0.00	0.21	0.00	0.21	0.00	0.00	0.00	0.00	0.00	13.03
80.5	0.68	0.00	0.00	0.00	0.04	0.00	0.00	0.00	0.00	0.00	0.00	0.00	0.00	8.55
88.5	0.41	0.00	0.00	0.05	0.74	0.00	0.00	0.00	0.00	0.00	0.00	0.00	0.00	11.42
100.5	5.01	0.00	0.00	0.00	0.00	0.00	0.00	0.00	0.00	0.33	0.00	0.00	0.00	26.67
110.5	5.89	0.00	0.00	0.00	0.00	0.00	0.00	0.00	0.00	0.00	0.00	0.00	0.00	31.18
120.5	12.14	0.00	0.00	0.00	0.00	1.07	0.00	0.00	0.00	0.71	0.00	0.00	0.00	40.63
130.5	13.46	0.00	0.00	0.00	0.00	0.00	0.00	0.00	0.00	0.00	0.00	0.36	0.18	49.30
139.5	15.01	0.00	0.00	0.00	0.00	0.00	0.00	0.00	0.00	0.00	0.00	0.00	0.00	33.00
150.5	14.28	0.00	0.00	0.00	0.00	0.00	0.00	0.00	0.00	0.00	0.00	0.39	0.00	64.20
161.5	16.90	0.00	0.00	0.00	0.79	0.00	0.00	0.00	0.00	0.00	0.00	0.00	0.00	162.37
171.5	39.54	0.00	0.00	0.00	0.79	0.74	0.00	0.00	0.00	0.00	0.00	0.00	0.00	161.50
180.5	75.88	0.00	0.00	0.33	0.00	3.92	0.00	0.00	0.00	0.65	0.00	0.00	1.31	220.53
191.5	33.98	0.00	0.00	0.00	0.00	2.17	0.00	0.00	0.00	1.22	0.14	2.17	0.00	119.05
198.5	23.48	0.00	0.00	0.00	0.00	0.00	0.00	0.00	0.00	0.95	0.00	0.76	0.00	86.85
209.5	44.41	0.00	0.28	0.00	0.00	0.00	0.00	0.00	0.00	0.83	0.00	0.00	0.00	315.22
221.5	29.75	0.00	0.00	0.00	0.00	1.29	0.00	0.00	0.00	1.94	0.00	0.00	0.00	131.75
232.5	43.11	0.00	0.00	0.69	0.00	0.00	0.00	0.00	0.00	2.07	0.00	2.76	0.00	98.69
242.5	13.16	0.00	0.00	0.16	0.00	0.00	0.00	0.00	0.00	0.79	0.00	0.63	0.00	28.30
250.5	5.42	0.00	0.00	0.07	0.90	0.30	0.00	0.00	0.00	0.00	0.00	0.30	0.00	12.33
258.5	22.49	0.00	0.00	0.00	1.00	0.00	0.00	0.00	0.00	0.95	0.00	0.00	0.00	30.06
269.5	3.35	0.00	0.08	0.00	0.00	0.62	0.00	0.00	0.00	0.23	0.00	0.31	0.00	8.46
280.5	12.60	0.00	0.00	0.00	0.00	0.00	0.00	0.00	0.00	0.35	0.00	0.00	0.70	94.75
289.5	13.39	0.00	0.00	0.00	0.00	0.67	0.00	0.00	0.00	0.00	0.00	0.00	0.00	24.14
296.5	1.62	0.00	0.00	0.00	0.00	0.00	0.00	0.00	0.00	0.00	0.00	0.00	0.00	2.98
302.5	52.31	0.00	0.00	0.04	0.00	0.49	0.00	0.00	0.00	0.08	0.00	0.00	0.82	66.15
321.5	45.12	0.00	0.00	0.00	0.00	0.00	0.00	0.00	0.00	0.00	0.00	0.00	0.00	201.09
329.5	12.19	0.00	0.00	0.13	0.00	0.00	0.00	0.00	0.00	0.53	0.00	0.00	0.00	95.09
338.5	27.89	0.00	0.00	0.00	0.00	0.00	0.00	0.00	0.00	0.00	0.00	0.00	0.00	74.94
350.5	44.89	0.00	0.00	0.00	0.00	0.00	0.00	0.00	0.00	0.00	0.00	0.00	0.00	81.18
354.5	45.69	0.00	0.00	0.00	0.00	0.00	0.00	0.00	0.00	0.00	0.00	0.00	0.00	55.04
359.5	112.68	0.00	0.00	0.00	0.00	0.00	0.00	0.00	0.25	0.00	0.00	0.00	0.00	139.69
362.5	10.41	0.00	0.00	0.00	0.00	0.65	0.00	0.00	0.12	0.00	0.00	0.00	0.00	26.87
370.5	26.08	0.00	0.00	0.64	0.00	0.00	0.00	0.00	0.00	0.00	0.00	0.00	0.00	52.84
379.5	47.97	0.00	0.00	0.00	0.00	0.00	0.00	0.00	0.00	0.00	0.00	0.00	0.00	160.58
398.5	26.98	0.00	0.04	0.04	0.00	0.00	0.00	0.00	0.00	0.00	0.08	0.00	0.00	43.72
411.5	18.99	0.00	0.00	0.00	0.00	0.58	0.00	0.00	0.00	0.00	0.00	0.00	0.00	35.68
418.5	38.30	0.00	0.00	0.00	0.00	0.00	0.00	0.00	0.00	0.00	0.00	0.00	0.00	48.60
429.5	25.08	0.00	0.12	0.46	0.00	0.00	0.00	0.00	0.00	0.00	0.00	0.00	0.06	39.59
438.5	12.63	0.00	0.00	0.00	0.00	0.00	0.00	0.00	0.09	0.00	0.00	0.00	0.70	39.57
450.5	0.00	0.00	0.00	0.00	0.00	0.00	0.00	0.00	0.00	0.00	0.00	0.00	0.00	0.00
459.5	0.00	0.00	0.00	0.00	0.00	0.00	0.00	0.00	0.00	0.00	0.00	0.00	0.00	0.00
469.5	0.00	0.00	0.00	0.00	0.00	0.00	0.00	0.00	0.00	0.00	0.00	0.00	0.00	0.00
480.5	0.00	0.00	0.00	0.00	0.00	0.00	0.00	0.00	0.00	0.00	0.00	0.00	0.00	0.00
487.5	0.00	0.00	0.00	0.00	0.00	0.00	0.00	0.00	0.00	0.00	0.00	0.00	0.00	0.00
489	0.00	0.00	0.00	0.00	0.00	0.00	0.00	0.00	0.00	0.00	0.00	0.00	0.00	0.00
490.5	0.00	0.00	0.00	0.00	0.00	0.00	0.00	0.00	0.00	0.00	0.00	0.00	0.00	0.00
493.5	14.37	0.00	0.00	0.00	0.00	0.00	0.00	0.00	0.00	0.00	0.00	0.00	0.00	14.43
496.5	11.78	0.00	0.00	0.00	0.65	0.00	0.00	0.00	0.00	0.00	0.00	0.00	0.00	30.60
507.5	88.62	0.00	0.04	0.00	0.00	0.62	0.00	0.00	0.00	0.62	0.00	0.62	0.00	136.84
517.5	92.43	0.00	0.00	0.04	0.00	2.56	0.00	0.00	0.00	0.64	0.00	0.64	0.00	127.24
531	71.78	0.00	0.04	0.00	0.00	5.88	0.00	0.00	0.00	1.18	0.00	0.00	1.18	106.93
537.5	29.82	0.00	0.00	0.00	0.00	1.42	0.00	0.00	0.00	0.04	0.00	0.00	0.00	58.22
540	0.00	0.00	0.00	0.00	0.00	0.00	0.00	0.00	0.00	0.00	0.00	0.00	0.00	0.00
552.5	0.00	0.00	0.00	0.00	0.00	0.00	0.00	0.00	0.00	0.00	0.00	0.00	0.00	0.13
559	0.00	0.00	0.00	0.00	0.00	0.00	0.00	0.00	0.00	0.00	0.00	0.00	0.00	0.00
571	0.00	0.00	0.00	0.00	0.00	0.00	0.00	0.00	0.00	0.00	0.00	0.00	0.00	0.00
578.5	0.00	0.00	0.00	0.00	0.00	0.00	0.00	0.00	0.00	0.00	0.00	0.00	0.00	0.00
589	0.00	0.00	0.00	0.00	0.00	0.00	0.00	0.00	0.00	0.00	0.00	0.00	0.00	0.00
595	0.00	0.00	0.00	0.00	0.00	0.00	0.00	0.00	0.00	0.00	0.00	0.00	0.00	0.00
599.5	0.00	0.00	0.00	0.00	0.00	0.00	0.00	0.00	0.00	0.00	0.00	0.00	0.00	0.00
608	0.63	0.00	0.00	0.00	0.00	0.00	0.00	0.00	0.00	0.00	0.00	0.00	0.00	22.94
619	0.16	0.00	0.00	0.00	0.00	0.08	0.00	0.00	0.00	0.00	0.00	0.00	0.00	14.77
628.5	0.00	0.00	0.00	0.00	0.00	0.00	0.00	0.00	0.00	0.14	0.00	0.00	0.00	56.89
640.5	0.00	0.00	0.00	0.00	0.00	0.00	0.00	0.00	0.00	0.00	0.00	0.00	0.00	14.09
651	0.00	0.00	0.00	0.00	0.00	0.00	0.00	0.00	0.00	0.00	0.00	0.00	0.00	28.52
657.5	0.00	0.00	0.00	0.00	0.00	0.00	0.00	0.00	0.00	0.00	0.00	0.00	0.00	0.00
662.5	0.00	0.00	0.00	0.00	0.00	0.00	0.00	0.00	0.00	0.00	0.00	0.00	0.00	0.00
667	0.00	0.00	0.00	0.00	0.00	0.00	0.00	0.00	0.00	0.00	0.00	0.00	0.00	0.00
672.5	0.00	0.00	0.00	0.00	0.00	0.00	0.00	0.00	0.00	0.00	0.00	0.00	0.00	0.00
677.5	0.00	0.00	0.00	0.00	0.00	0.00	0.00	0.00	0.00	0.00	0.00	0.00	0.00	0.00
679.5	0.00	0.00	0.00	0.00	0.00	0.00	0.00	0.00	0.00	0.00	0.00	0.00	0.00	0.00
688.5	0.00	0.00	0.00	0.00	0.00	0.00	0.00	0.00	0.00	0.00	0.00	0.00	0.00	0.00
694.5	0.00	0.00	0.00	0.00	0.00	3.18	0.00	0.00	0.00	0.00	0.00	0.00	0.00	87.45
699.5	0.00	0.00	0.00	0.00	0.00	0.00	0.00	0.00	0.00	0.00	0.00	0.00	0.00	0.00
706.5	0.00	0.00	0.00	0.00	0.00	0.00	0.00	0.00	0.00	0.00	0.00	0.00	0.00	37.18

Appendix 7. Data for Core 23342 (Spec/g)

Depth [cm]	Age [ka]	DBD [g/ccm]	Dry Weight [g]	Isotope Event	LSR [cm/ka]	*Turgo rotalinra*	*Cibicidoides wuellerstorfi*	*Epistominella exigua*	*Oinqueloculina seminula*	*Elphidium* spp.	*Triloculina tricarinata*	*Cribrostomoides subglobosus*	agglutinated Tubes	*Ammobaculites agglutinans*	*Paliculn bulloides*	*Cassidulina teretis*
14.0	8.65	0.90	23.34		0.00	1.59	186.99	6.86	0.00	1.37	2.74	17.95	0.17	0.00	0.00	26.05
30.0	10.38	1.01	33.69		0.00	0.00	0.98	0.47	0.00	0.47	0.00	0.59	0.47	0.00	0.00	1.90
40.0	11.46	0.89	28.15		0.00	0.00	7.81	0.00	0.00	0.00	1.14	0.00	0.00	0.00	0.00	1.14
50.0	14.90	0.91	29.91	2.2	0.00	0.37	0.53	0.00	0.00	0.53	0.53	0.00	0.00	0.00	0.00	1.60
63.0	18.83	1.10	35.07		0.00	0.00	0.00	0.11	0.00	0.11	4.33	0.00	1.57	0.00	0.11	4.11
70.0	20.95	0.99	26.21		0.00	0.00	0.65	0.00	0.00	0.71	3.05	0.00	0.88	0.00	0.00	2.25
80.0	23.98	1.02	25.22		0.00	0.04	0.16	0.08	0.00	0.79	3.49	0.59	1.15	0.00	0.00	1.35
90.0	27.00	1.14	29.03	3.1	0.00	0.00	0.00	0.00	0.00	2.48	2.17	0.00	0.00	0.00	0.00	0.24
100.0	30.16	1.07	27.75		0.00	0.04	0.00	0.00	0.00	0.15	1.39	0.37	4.87	0.00	0.00	0.59
110.0	33.32	1.05	27.08		0.00	0.04	0.00	0.00	0.00	0.07	1.85	0.07	0.00	0.00	0.00	0.44
120.0	36.48	0.99	28.65		0.00	0.10	0.00	0.00	0.00	1.12	0.56	0.00	0.56	0.00	0.00	0.00
131.0	39.96	1.03	32.52		0.00	0.37	0.00	0.00	0.00	0.98	0.98	0.00	1.23	0.00	0.00	0.00
140.0	42.81	1.00	24.80		0.00	0.65	0.65	0.00	0.00	0.40	2.26	0.00	0.00	0.00	0.00	0.32
152.0	46.60	1.03	27.77		0.00	2.34	0.00	0.00	0.00	0.00	1.15	0.58	0.61	0.00	0.00	0.00
158.0	48.50	1.03	24.72		0.00	0.74	0.00	0.00	0.00	0.33	4.28	0.00	0.33	0.00	0.00	1.97
170.0	52.29	1.00	22.74		0.00	0.35	0.00	0.00	0.00	0.00	7.74	0.18	0.35	0.00	0.00	0.53
180.0	55.45	0.97	23.02	3.3	0.00	0.00	0.87	0.00	0.00	0.17	3.47	0.17	0.69	0.00	0.00	1.39
190.0	58.71	1.00	24.81		0.00	0.04	0.48	0.32	0.00	0.16	6.93	0.00	0.16	0.00	0.00	0.72
200.0	61.96	1.02	27.87		0.00	0.04	2.87	0.29	0.00	1.44	2.87	0.00	0.29	0.00	0.00	0.00
210.0	65.22	1.08	23.55	4.2	0.00	0.17	9.98	0.34	0.00	0.00	5.43	1.66	3.44	0.00	0.00	12.57
220.0	72.00	1.03	25.80		0.00	0.70	29.58	0.00	0.00	0.00	4.38	3.18	3.76	0.00	1.24	1.86
231.0	79.46	0.99	29.04	5.1	0.00	0.00	21.73	0.00	0.00	0.00	5.51	0.03	2.72	0.00	0.55	2.20
238.0	85.27	1.14	28.50		0.00	0.00	8.74	0.00	0.00	0.28	1.68	0.00	0.04	0.00	1.12	0.56
250.0	95.24	1.00	23.90		0.00	0.04	10.75	0.00	0.00	0.00	2.68	0.00	2.01	0.00	0.33	0.67
260.0	103.55	1.07	26.59	5.2	0.00	0.34	9.93	0.00	0.00	0.00	3.31	0.00	1.28	0.00	0.00	0.60
270.0	110.31	0.94	29.50		0.00	0.88	10.61	0.00	0.00	0.00	7.05	0.27	1.66	0.00	0.00	2.71
280.0	117.06	0.95	29.15		0.00	0.69	12.93	0.00	0.00	0.00	6.59	0.55	2.74	0.00	0.00	2.20
290.0	123.82	0.96	22.37	5.5	0.00	0.00	76.62	0.00	0.00	0.00	11.44	0.00	0.00	0.00	0.00	0.00
300.0	126.01	0.70	33.66		0.00	0.00	0.48	0.00	0.00	0.00	0.24	0.24	1.66	0.00	0.24	9.51
310.0	128.25	1.02	33.51		0.00	0.00	0.24	0.00	0.00	0.00	0.00	0.00	0.00	0.00	0.00	2.39
322.0	130.91	1.31	26.61		0.00	0.00	0.15	0.00	0.00	0.00	0.00	0.00	0.00	0.00	0.00	0.30
330.0	132.69	0.99	32.52		0.00	0.00	0.00	0.00	0.00	0.25	0.98	0.00	0.00	0.00	0.00	2.71
338.0	134.46	1.16	37.98		0.00	0.00	0.00	0.00	0.00	0.00	0.21	0.00	0.00	0.00	0.00	0.84
350.0	137.12	0.95	28.70		0.00	0.00	0.00	0.14	0.00	0.28	0.84	0.14	0.84	0.00	0.00	0.28
360.0	139.34	0.90	34.06		0.00	0.00	0.00	0.12	0.00	0.12	1.76	0.82	1.64	0.00	0.00	1.06
369.0	141.33	1.48	46.44	6.3	0.00	0.00	0.00	0.00	0.00	0.00	0.00	0.00	0.00	0.00	0.00	0.00
380.0	149.59	0.88	33.91		0.00	0.74	0.24	0.00	0.00	0.47	5.19	0.00	0.47	0.00	0.00	3.07
390.0	157.10	0.91	30.03	6.4	0.00	0.00	0.00	0.00	0.00	0.27	7.19	0.00	0.27	0.00	0.00	2.40
400.0	161.86	0.92	30.81		0.00	0.65	0.00	0.00	0.00	0.00	3.12	0.00	0.26	0.00	0.00	1.04
410.0	166.61	0.93	34.20		0.00	0.00	0.00	0.00	0.00	0.47	1.17	0.00	0.00	0.00	0.00	0.00
420.0	171.37	1.02	34.35	6.5	0.00	0.00	0.00	0.00	0.00	0.23	1.05	0.00	0.23	0.00	0.00	0.58
428.0	174.84	1.10	38.68		0.00	0.00	0.00	0.00	0.00	0.41	0.00	0.00	0.00	0.00	0.00	0.00
440.0	180.05	1.00	31.24		0.00	0.00	0.00	0.00	0.00	0.32	0.00	0.00	0.03	0.00	0.00	0.13
450.0	184.39	1.02	32.01		0.00	0.00	0.00	0.00	0.00	0.00	0.00	0.00	0.00	0.00	0.00	0.00
460.0	188.73	0.94	34.14		0.00	0.00	0.00	0.00	0.00	0.12	0.00	0.00	0.12	0.00	0.00	0.94
470.0	193.07	1.04	33.92	7.1	0.00	0.00	3.30	0.00	0.00	0.71	0.00	0.00	0.24	0.00	0.00	7.07
480.0	204.31	1.00	21.75		0.00	0.00	12.66	0.00	0.00	0.25	2.52	0.00	0.50	0.00	0.00	2.02
490.0	215.54	1.12	36.58	7.3	0.00	0.00	9.73	0.00	0.00	0.66	0.00	0.00	0.55	0.00	0.00	1.53
500.0	219.06	1.06	38.66		0.00	0.00	0.00	0.00	0.00	0.00	0.00	0.00	0.00	0.00	0.00	0.00
510.0	222.58	1.06	26.40		0.00	0.00	0.00	0.00	0.00	0.00	0.00	0.00	0.00	0.00	0.00	0.00
521.0	226.46	0.84	17.92		0.00	0.00	0.00	0.00	0.00	0.00	0.00	0.00	0.00	0.00	0.00	0.00
530.0	229.63	0.94	29.12		0.00	0.00	0.00	0.00	0.00	0.00	0.00	0.00	0.00	0.00	0.00	0.00
540.0	233.15	1.00	36.28		0.00	0.00	0.00	0.00	0.00	0.00	0.00	0.00	0.00	0.00	0.00	0.00
550.0	236.67	0.99	31.65		0.00	0.00	0.63	0.00	0.00	0.13	0.00	0.00	0.00	0.00	0.00	4.25
560.0	240.19	0.99	29.47	7.4	0.00	0.00	4.89	0.00	0.00	0.14	1.49	0.00	0.27	0.00	0.00	1.22
570.0	243.71	0.92	22.94		0.00	0.00	2.09	0.00	0.00	1.05	0.00	0.00	5.93	0.00	0.00	0.00

Appendix 7. continued

Depth [cm]	*Oridorsalis umbonatus*	*Globocassidulina subglobosa*	*Marginulina glabra*	*Dentalina pauperata*	*Siphotextularia colshanseni*	*Cassidulina reniforme*	*Miliolinella* sp.	*Cotton hexagona*	*Cyclammina* sp.	*Parafissurina ovata*	*Lenticulina gibba*	*Eponiides tumidulus*	*Lagena* spp.	Total [Spec/g]
14.0	103.52	0.00	0.00	1.37	0.00	4.11	0.00	0.00	0.00	0.00	0.00	0.00	1.37	362.28
30.0	11.40	0.00	0.00	0.00	0.00	0.00	0.00	0.00	0.00	0.00	0.00	0.00	0.00	16.30
40.0	8.52	0.00	0.00	0.28	0.00	0.00	0.00	0.00	0.14	0.00	0.14	0.00	0.00	19.18
50.0	3.21	0.00	0.00	0.00	3.21	0.00	0.00	0.00	0.00	0.00	0.00	1.60	0.00	12.14
63.0	5.59	0.00	0.00	0.00	0.57	0.00	0.00	0.00	0.00	0.11	0.00	0.00	0.00	17.00
70.0	2.79	0.00	0.00	0.04	0.00	0.15	0.00	0.00	0.00	0.00	0.00	0.00	0.15	12.40
80.0	1.11	0.00	0.00	0.00	0.40	0.71	0.00	0.08	0.00	0.00	0.00	0.00	0.08	10.35
90.0	0.34	0.00	0.00	0.03	0.00	0.96	0.00	0.00	0.00	0.00	0.00	0.00	0.07	6.96
100.0	1.02	0.00	0.00	0.00	0.00	0.44	0.00	0.00	0.00	0.00	0.00	0.00	0.15	9.15
110.0	0.96	0.00	0.00	0.00	0.00	0.00	0.07	0.00	0.00	0.00	0.00	0.00	0.00	3.66
120.0	1.12	0.00	0.00	0.00	0.00	0.00	0.00	0.00	0.00	0.00	0.00	0.00	0.00	3.36
131.0	11.81	0.00	0.00	0.00	0.00	0.00	0.00	0.00	0.00	0.00	0.00	0.00	0.25	15.62
140.0	5.48	0.00	0.00	0.00	0.00	0.65	0.00	0.00	0.00	0.00	0.00	0.00	0.00	10.40
152.0	8.07	0.00	0.00	0.00	0.00	0.00	0.00	0.00	0.00	0.00	0.00	0.00	0.00	13.90
158.0	13.49	0.00	0.00	0.00	0.00	0.00	0.00	0.00	0.00	0.00	0.00	0.00	0.66	0.00	21.80
170.0	13.02	0.00	0.00	0.00	0.00	1.41	0.00	0.00	0.00	0.00	0.00	0.00	0.88	0.18	24.80
180.0	12.51	0.00	0.00	0.00	0.00	0.87	0.00	0.00	0.00	0.00	0.00	0.00	0.00	0.00	20.15
190.0	9.19	0.00	0.00	0.00	0.00	2.90	0.00	0.00	0.00	0.00	0.00	0.00	0.16	0.16	21.32
200.0	8.04	0.29	0.00	0.00	0.00	0.29	0.00	0.00	0.00	0.00	0.00	0.00	0.57	0.00	18.69
210.0	29.21	0.00	0.00	0.00	0.00	1.70	0.00	0.00	0.00	0.00	0.00	0.00	0.00	0.00	64.49
220.0	9.30	0.00	0.00	0.00	0.00	1.86	0.00	0.00	0.00	1.24	0.00	0.62	0.62	58.34
231.0	17.08	0.00	0.00	0.00	0.00	0.55	0.00	0.00	0.00	0.55	0.55	1.10	0.00	52.58
238.0	39.59	0.00	0.00	0.00	0.00	0.28	0.00	0.00	0.00	0.00	0.00	0.28	0.28	53.41
250.0	13.72	0.00	0.00	0.00	0.00	0.00	0.00	0.00	0.00	0.00	0.00	2.01	0.00	32.93
260.0	22.26	0.00	0.00	0.00	0.00	0.90	0.00	0.00	0.00	0.30	0.00	0.90	0.30	40.12
270.0	25.49	0.00	0.00	0.00	0.00	0.81	0.00	0.27	0.00	0.00	0.00	4.61	0.00	55.74
280.0	29.64	0.00	0.00	0.00	0.00	0.55	0.00	0.55	0.00	1.10	0.00	5.49	0.00	63.03
290.0	40.05	0.00	0.18	0.00	0.00	0.00	0.00	0.00	0.00	0.00	0.09	4.29	0.00	132.72
300.0	5.23	0.00	0.00	0.24	0.24	0.00	0.00	0.00	0.00	0.00	0.00	0.48	0.00	19.52
310.0	1.50	0.00	0.00	0.00	0.00	0.00	0.00	0.00	0.00	0.00	0.00	0.00	0.00	6.92
322.0	7.22	0.00	0.00	0.00	0.00	0.00	0.00	0.00	0.00	0.00	0.00	0.00	0.00	7.67
330.0	21.89	0.00	0.00	0.00	0.00	0.00	0.00	0.00	0.00	0.00	0.00	0.25	0.00	26.08
338.0	5.69	0.00	0.00	0.00	0.00	0.00	0.00	0.00	0.00	0.00	0.00	0.21	0.00	6.95
350.0	8.92	0.00	0.00	0.00	0.00	0.14	0.00	0.28	0.00	0.00	0.00	1.11	0.00	13.11
360.0	12.92	0.00	0.00	0.00	0.00	0.00	0.00	0.00	0.00	0.12	0.00	0.23	0.12	19.03
369.0	0.00	0.00	0.00	0.00	0.00	0.00	0.00	0.00	0.00	0.00	0.00	0.00	0.00	0.00
380.0	29.02	0.00	0.00	0.00	0.24	0.24	0.00	0.24	0.00	0.24	0.00	0.00	0.00	40.61
390.0	12.79	0.00	0.00	0.00	0.00	0.27	0.00	0.00	0.27	0.27	0.00	0.27	0.27	26.10
400.0	6.75	0.00	0.00	0.00	0.00	0.00	0.00	0.00	0.00	0.00	0.00	0.00	0.00	11.82
410.0	4.91	0.00	0.00	0.00	0.00	0.00	0.00	0.00	0.00	0.00	0.00	0.00	0.00	6.55
420.0	3.84	0.00	0.00	0.00	0.00	0.00	0.00	0.00	0.00	0.00	0.00	0.00	0.23	6.75
428.0	3.52	0.00	0.00	0.00	0.00	0.00	0.00	0.00	0.00	0.00	0.00	0.21	0.00	4.31
440.0	3.39	0.00	0.00	0.00	0.03	0.00	0.00	0.00	0.00	0.00	0.00	0.00	0.06	4.10
450.0	0.00	0.00	0.00	0.00	0.00	0.00	0.00	0.00	0.00	0.00	0.00	0.00	0.00	0.00
460.0	27.30	0.00	0.00	0.12	0.00	0.12	0.00	0.00	0.00	0.00	0.00	0.00	0.00	28.71
470.0	70.75	0.00	0.00	0.00	0.00	0.47	0.00	0.00	0.00	0.00	0.00	0.00	0.00	82.54
480.0	14.87	0.00	0.00	0.00	0.00	0.00	0.00	0.25	0.00	0.00	0.00	0.00	0.00	33.42
490.0	22.31	0.00	0.00	0.00	0.00	0.11	0.00	0.00	0.00	0.00	0.00	0.00	0.00	35.10
500.0	0.00	0.00	0.00	0.00	0.00	0.00	0.00	0.00	0.00	0.00	0.00	0.00	0.00	0.00
510.0	0.00	0.00	0.00	0.00	0.00	0.00	0.00	0.00	0.00	0.00	0.00	0.00	0.00	0.00
521.0	0.00	0.00	0.00	0.00	0.00	0.00	0.00	0.00	0.00	0.00	0.00	0.00	0.00	0.00
530.0	0.00	0.00	0.00	0.00	0.00	0.00	0.00	0.00	0.00	0.00	0.00	0.00	0.00	0.00
540.0	0.00	0.00	0.00	0.00	0.00	0.00	0.00	0.00	0.00	0.00	0.00	0.00	0.00	0.00
550.0	8.68	0.00	0.00	0.06	0.00	0.19	0.00	0.00	0.00	0.00	0.00	0.00	0.06	14.20
560.0	5.29	0.00	0.00	0.00	0.00	0.27	0.00	0.00	0.00	0.00	0.00	0.00	0.00	13.71
570.0	11.86	0.70	0.00	0.00	0.00	0.00	0.00	0.00	1.05	0.35	0.00	0.00	0.00	25.72

Appendix 8. Data from Core 23353 (Spec/g)

Depth [cm]	Age [ka]	DBD [g/ccm]	Dry Weight [g]	Isotope Event	LSR [cm/ka]	*Pyrgo rotalaria*	*Cibicidoides wuellerstorfi*	*Epistominella exigua*	*Quinqueloculina seminula*	*Elphidium* spp.	*Triloculina trihedrina*	*Cribrostomoides subglobosus*	agglutinated Tubes	*Ammobaculites agglutinans*	*Pullenia bulloides*	*Cassidulina teretis*
10.0	8.6			1.1												
15.0	9.43		20.96		6.00	0.00	0.38	0.00	0.00	0.57	1.15	17.37	0.62	0.00	1.34	1.15
27.0	11.43		25.00		6.00	0.00	19.68	0.00	0.00	0.16	0.00	8.36	0.72	0.00	0.00	12.80
35.0	12.77		36.34		6.00	0.00	0.00	0.00	0.00	0.00	0.00	0.74	0.94	0.00	0.00	0.00
40.0	13.6			Vo												
45.0	14.25		26.65		7.69	0.00	1.84	0.00	0.00	2.51	4.80	1.35	12.38	0.00	0.00	32.83
50.0	14.9			2.2												
55.0	17.93		30.02		1.65	0.00	0.67	0.00	0.03	0.13	7.19	0.03	7.09	0.00	0.00	74.75
65.0	23.98		26.08		1.65	0.00	0.12	0.00	0.88	2.45	20.90	0.73	17.14	0.00	0.00	90.72
70.0	27			3.1												
85.0	30.56		39.33		4.22	0.00	0.03	0.00	0.05	1.45	0.94	0.23	0.00	0.00	0.00	12.10
105.0	35.30		36.12		4.22	0.00	0.17	0.00	0.00	0.30	0.00	0.25	0.64	0.00	0.00	16.11
115.0	37.67		32.95		4.22	0.00	0.00	0.00	0.00	0.09	1.46	1.03	1.73	0.00	0.00	38.45
125.0	40.04		30.20		4.22	0.00	0.07	0.00	0.00	0.86	0.53	0.07	1.66	0.00	0.00	15.83
135.0	42.41		30.74		4.22	0.00	0.42	0.52	0.00	0.07	5.79	1.33	4.36	0.00	0.00	23.82
145.0	44.78		35.38		4.22	0.00	0.03	0.00	0.00	0.51	2.29	0.88	1.50	0.00	0.00	51.11
155.0	47.15		31.17		4.22	0.00	0.00	0.00	0.00	0.06	7.22	0.87	5.33	0.00	0.00	36.34
165.0	49.52		33.24		4.22	0.00	0.21	0.00	0.00	1.02	6.32	0.36	4.18	0.00	0.00	41.55
175.0	51.89		33.18		4.22	0.00	27.91	0.00	0.00	0.72	11.94	0.60	17.66	0.00	0.00	88.50
185.0	54.26		34.36		4.22	0.00	2.50	0.00	0.00	0.06	6.63	0.35	8.35	0.00	0.00	92.25
190.0	59			4.0												
205.0	62.78		42.11		2.05	0.00	23.99	0.00	0.00	0.00	7.60	4.27	8.79	0.00	0.00	37.43
210.0	71			5.0												
215.0	72.34		25.27		0.70	0.00	30.71	1.27	0.00	0.00	7.60	4.27	84.96	0.00	7.60	54.45
220.0	79.455			5.1												
225.0	82.22		27.46		1.81	0.00	2.73	0.00	0.00	0.04	0.00	1.13	15.37	0.00	1.60	4.22
235.0	87.76		28.44		1.81	0.00	35.58	0.00	0.00	2.25	7.88	0.77	34.49	0.00	0.00	41.65
240.0	90.525			5.2												
245.0	93.78		33.11		1.54	0.00	43.94	0.00	0.00	0.00	13.56	0.60	34.70	0.00	0.00	21.74
255.0	100.29		22.60		1.54	0.00	70.18	8.50	0.00	0.00	25.49	1.68	58.32	0.00	0.00	15.58
260.0	103.55			5.3												
265.0	107.17		28.41		1.38	0.00	24.95	0.00	0.00	0.00	4.50	3.13	87.81	0.00	0.00	47.30
270.0	110.79			5.4												
275.0	114.05		31.16		1.53	0.00	15.47	1.03	0.00	0.00	2.05	0.96	75.37	0.00	0.00	10.78
285.0	120.56		23.65		1.53	0.00	2.71	2.71	0.00	1.35	0.00	14.80	447.34	0.00	12.18	2.71
290.0	123.82			5.5												
295.0	125.36		24.86		3.25	0.00	12.87	0.00	0.00	0.00	0.00	5.63	178.50	0.00	0.00	0.00
305.0	128.44		42.53		3.25	0.00	0.21	0.00	0.00	0.12	0.00	0.07	0.16	0.00	0.00	1.13
315.0	131.51		26.56		3.25	0.00	0.08	0.00	0.00	0.08	4.25	0.00	13.37	0.00	0.00	29.68
335.0	137.67		24.14		3.25	0.00	0.21	6.63	0.00	0.08	5.43	0.00	6.13	0.00	0.00	44.48
345.0	140.74		34.60		3.25	0.00	0.35	0.00	0.00	0.98	3.70	0.06	2.28	0.00	0.00	27.67
350.0	141.33			6.3												
360.0	151.64		29.65		1.07	0.00	0.54	1.08	0.00	0.00	9.17	0.00	6.38	0.00	0.00	90.07
370.0	161.01		23.54		1.07	0.00	0.00	0.00	0.00	0.17	6.12	0.00	42.17	0.00	0.00	77.47
380.0	170.37		24.33		1.07	0.00	0.00	0.00	0.00	0.00	1.48	0.00	31.77	0.00	0.00	27.97
385.0	171.37			6.5												
390.0	179.73		28.89		3.66	0.00	0.55	0.00	0.00	0.00	4.46	0.00	1.00	0.00	0.00	35.37
400.0	182.46		29.72		3.66	0.00	0.00	0.00	0.00	0.27	1.08	1.08	2.46	0.00	0.00	8.61
405.0	183.3			6.6												
410.0	185.19		28.33		6.35	0.00	0.56	0.00	0.00	0.00	1.69	0.28	0.71	0.00	0.00	37.98
420.0	186.77		29.63		6.35	0.00	8.51	0.00	0.00	1.22	2.16	0.81	1.89	0.00	0.00	62.91
430.0	188.34		18.68		6.35	0.00	21.84	0.00	0.00	0.86	0.86	3.43	5.14	0.00	0.00	92.50
440.0	189.92		30.52		6.35	0.00	23.59	0.00	0.00	1.05	0.00	5.24	2.10	0.00	0.00	73.91
450.0	193.07		36.07	7.1	0.45	0.00	16.63	0.00	0.00	1.55	0.00	11.20	2.99	0.00	0.00	16.20
460.0	215.54		30.69	7.3	2.14	0.00	0.16	0.00	0.00	0.07	0.00	3.71	0.75	0.00	0.00	0.32
470.0	220.22		21.91		2.14	0.00	0.18	0.00	0.00	0.00	0.00	2.65	18.30	0.00	0.00	0.37
480.0	224.89		7.36		2.61	0.00	0.00	0.00	0.00	0.00	0.00	0.00	0.00	0.00	0.00	0.00
510.0	236.37		23.38		2.61	0.00	0.00	0.00	0.00	0.00	0.00	0.00	0.00	0.00	0.00	0.00
520.0	240.19		29.74	7.5	6.24	0.00	3.09	0.00	0.00	0.27	0.54	1.34	3.19	0.00	0.00	31.44
540.0	243.40		24.43		6.24	0.00	0.00	0.00	0.00	0.16	0.00	0.00	0.00	0.00	0.00	1.80
550.0	245.00		33.11	8.0	8.30	0.00	0.00	0.00	0.00	0.48	0.51	0.00	0.48	0.00	0.00	81.09
560.0	246.20		32.33		8.30	0.00	0.00	0.00	0.00	0.06	6.46	0.00	0.00	0.00	0.00	53.48
570.0	247.41		29.47		8.30	0.00	0.00	0.00	0.00	0.00	0.00	0.00	0.00	0.00	0.00	0.00
620.0	253.43		30.88	8.2	2.12	0.00	0.00	0.00	0.00	0.00	0.00	0.00	0.00	0.00	0.00	0.00
630.0	258.15		32.48		2.12	0.00	0.18	0.00	0.00	0.55	0.00	0.06	0.86	0.00	0.00	12.90
640.0	262.87		33.42		2.12	0.00	0.45	0.00	0.00	0.06	0.00	0.00	0.51	0.00	0.00	35.88
650.0	267.59		34.68		2.12	0.00	0.00	0.00	0.00	0.23	0.00	0.32	0.12	0.00	0.00	0.00
660.0	272.31		32.61		2.12	0.00	0.00	0.00	0.00	0.00	0.00	0.00	0.00	0.00	0.00	0.00
710.0	295.92		28.43		2.12	0.00	0.00	0.00	0.00	0.00	0.00	0.00	0.00	0.00	0.00	0.00
720.0	300.64		30.00		2.12	0.00	0.03	1.07	0.00	0.63	0.00	0.00	0.00	0.00	0.00	5.45
725.0	303			9.0												
730.0	308.14		36.81		0.97	0.00	0.58	1.09	0.00	1.30	0.22	0.00	0.00	0.00	0.00	10.05
740.0	318.43		33.77		0.97	0.00	0.00	0.00	0.00	0.00	0.00	0.00	0.00	0.00	0.00	0.00
770.0	339			10.0												
880.0	360.23		28.23		5.65	0.00	0.00	0.00	0.00	0.00	0.00	0.00	0.00	0.00	0.00	0.00
890.0	362.00		27.87	11.0	0.86	0.00	0.00	0.00	0.00	113.58	0.00	0.00	0.00	0.00	0.00	0.75
900.0	373.62		20.98		0.86	0.00	0.00	0.00	0.00	21.31	0.00	0.00	0.00	0.00	0.43	5.34
911.0	386.41		22.19		0.86	0.00	0.05	0.00	0.00	1.35	0.36	0.00	0.00	0.00	0.05	4.33
922.0	399.19		27.59		0.86	0.00	0.00	0.00	0.00	8.12	0.14	0.00	0.00	0.00	0.29	1.01
927.0	405.00		28.87	11.3	0.72	0.00	0.00	0.00	0.00	0.00	0.00	0.00	0.00	0.00	0.00	0.00

Appendix 8. continued

Depth [cm]	*Oridorsalis umbonatus*	*Globocassidulina subglobosa*	*Margoglina glabra*	*Dentalina pauperata*	*Siphotextularia rolshausenі*	*Cassidulina reniforme*	*Miliolinella sp.*	*Oolina hexagona*	*Cyclammina sp.*	*Parafissurina ovata*	*Lenticulina gibba*	*Eponides tumidulus*	*Lagena spp.*	Total [Spec./g]
10.0														
15.0	14.51	0.00	0.00	0.00	0.00	0.38	0.00	0.00	0.00	0.00	0.00	0.00	0.38	38.60
27.0	69.11	0.00	0.12	0.00	0.00	5.12	0.00	0.00	0.00	0.00	0.00	0.00	0.00	130.78
35.0	0.00	0.00	0.00	0.00	0.00	0.00	0.00	0.00	0.00	0.00	0.06	0.00	0.00	1.98
40.0														
45.0	31.44	0.00	0.04	0.00	4.20	0.60	0.00	0.60	0.04	0.11	0.04	1.20	0.04	96.01
50.0														
55.0	24.95	0.00	0.00	0.00	2.66	0.53	0.00	0.00	0.00	0.13	0.00	0.00	0.67	120.98
65.0	31.73	0.00	0.00	0.04	3.07	0.61	0.00	0.61	0.00	0.04	0.00	0.00	0.61	150.87
70.0														
85.0	6.94	0.00	0.00	0.00	0.00	0.41	0.00	0.00	0.00	0.03	0.00	0.00	0.00	22.35
105.0	6.01	0.00	0.00	0.03	0.00	0.22	0.00	0.22	0.00	0.06	0.00	0.00	0.22	24.25
115.0	32.11	0.00	0.00	0.03	0.00	0.49	0.00	0.00	0.00	0.03	0.00	0.49	0.49	76.50
125.0	23.94	0.00	0.00	0.03	0.00	0.53	0.00	0.00	0.00	0.36	0.00	0.00	0.26	44.67
135.0	60.22	0.00	0.00	0.07	0.00	1.04	0.00	0.00	0.00	0.16	0.03	0.52	0.52	99.95
145.0	51.14	0.00	0.03	0.00	0.00	2.26	0.00	0.00	0.00	0.14	0.00	0.45	0.45	111.86
155.0	37.09	0.00	0.00	0.03	0.00	2.05	0.00	0.00	0.00	0.06	0.00	1.03	0.00	91.43
165.0	33.49	0.00	0.06	0.00	0.00	0.00	0.00	0.00	0.00	0.18	0.06	0.48	0.00	88.48
175.0	45.09	0.00	0.03	0.03	0.00	1.93	0.00	0.00	0.00	1.93	1.93	0.00	0.00	200.32
185.0	21.71	0.00	0.03	0.09	0.00	0.00	0.00	0.00	0.00	0.93	0.00	0.00	0.93	104.15
190.0														
205.0	17.57	0.00	0.02	0.00	0.00	0.76	0.00	0.00	0.00	0.38	0.09	0.00	0.00	102.05
210.0														
215.0	43.06	0.00	0.12	0.08	0.00	2.53	0.00	0.00	0.00	3.84	0.00	0.00	0.00	242.38
220.0														
225.0	32.30	0.00	0.00	0.00	0.00	0.00	0.00	0.00	0.00	1.35	0.00	0.00	0.00	58.88
235.0	24.19	0.00	0.00	0.00	0.00	4.50	0.00	0.00	0.00	2.25	0.00	3.38	0.00	159.73
240.0														
245.0	46.87	0.00	0.03	0.00	0.00	0.00	0.00	0.00	0.00	0.00	0.00	1.93	0.00	189.96
255.0	48.15	0.00	0.00	0.00	0.00	0.00	0.00	0.00	0.00	8.50	0.00	0.00	0.00	260.46
260.0														
265.0	18.58	0.00	0.11	0.00	0.00	0.00	0.00	0.00	0.00	1.13	0.00	2.25	0.00	196.53
270.0														
275.0	18.48	0.00	0.06	0.03	0.00	0.00	0.00	0.00	0.00	1.28	0.03	0.00	0.00	125.82
285.0	24.36	0.00	0.00	0.00	0.00	0.00	0.00	0.00	0.00	0.00	0.08	0.00	2.71	521.78
290.0														
295.0	55.36	0.00	0.04	0.00	0.00	0.00	0.00	0.00	0.16	0.00	0.16	0.00	0.00	259.16
305.0	5.48	0.00	0.00	0.00	0.00	0.00	0.00	0.00	0.00	0.02	0.00	0.00	0.00	8.16
315.0	10.84	0.00	0.00	0.08	0.00	0.60	0.00	0.00	0.00	0.79	0.00	0.00	0.60	72.85
335.0	32.06	0.00	0.04	0.04	0.00	0.00	0.00	0.00	0.00	1.57	0.04	2.65	0.00	100.73
345.0	13.96	0.00	0.00	0.06	0.00	0.00	0.00	0.00	0.00	0.12	0.00	0.00	0.00	54.83
350.0														
360.0	25.64	0.00	0.00	0.00	0.00	0.54	0.00	1.08	0.00	0.27	0.00	0.54	0.00	138.06
370.0	21.41	0.00	0.04	0.17	0.00	0.00	0.00	0.00	0.00	0.00	0.04	0.00	0.68	150.99
380.0	25.81	0.00	0.00	0.00	0.00	0.66	0.00	0.00	0.00	0.16	0.00	0.00	0.00	98.22
385.0														
390.0	34.06	0.00	0.00	0.00	0.00	0.55	0.00	0.00	0.00	0.03	0.00	0.00	0.55	76.63
400.0	35.33	0.00	0.00	0.00	0.00	0.27	0.00	0.27	0.00	0.00	0.00	0.00	0.03	49.77
405.0														
410.0	59.57	0.00	0.00	0.00	0.00	0.00	0.00	0.00	0.00	0.00	0.14	0.00	0.56	102.07
420.0	113.81	0.00	0.00	0.00	0.00	0.00	0.00	0.00	0.00	0.14	0.14	0.00	1.08	196.56
430.0	100.64	0.00	0.00	0.00	0.00	0.00	0.00	0.00	0.00	0.00	0.00	0.00	0.00	237.24
440.0	106.94	0.00	0.00	0.00	0.00	0.00	0.00	0.00	0.00	0.26	0.26	0.00	1.05	220.69
450.0	53.78	0.00	0.00	0.00	0.00	0.00	0.00	0.00	0.00	0.00	0.00	0.00	0.00	117.00
460.0	1.89	0.00	0.00	0.00	0.00	0.00	0.00	0.00	0.00	0.00	0.00	0.00	0.00	7.07
470.0	0.00	0.00	0.00	0.00	0.00	0.00	0.00	0.00	0.00	0.00	0.00	0.00	0.00	21.50
480.0	0.00	0.00	0.00	0.00	0.00	0.00	0.00	0.00	0.00	0.00	0.00	0.00	0.00	0.00
510.0	0.00	0.00	0.00	0.00	0.00	0.00	0.00	0.00	0.00	0.00	0.00	0.00	0.00	0.00
520.0	40.11	0.00	0.00	0.03	0.00	0.00	0.00	0.00	0.00	0.00	0.00	0.00	0.00	81.67
540.0	14.41	0.00	0.00	0.00	0.00	0.00	0.00	0.00	0.00	0.00	0.00	0.00	0.16	17.19
550.0	54.63	0.00	0.00	0.06	0.00	0.48	0.00	0.00	0.00	0.00	0.00	0.00	0.00	164.01
560.0	80.95	0.00	0.00	0.00	0.00	0.99	0.00	0.00	0.00	0.00	0.06	0.00	0.49	146.00
570.0	0.00	0.00	0.00	0.00	0.00	0.00	0.00	0.00	0.00	0.00	0.00	0.00	0.00	0.00
620.0	0.00	0.00	0.00	0.00	0.00	0.00	0.00	0.00	0.00	0.00	0.00	0.00	0.00	0.00
630.0	27.58	0.03	0.00	0.03	0.00	0.00	0.00	0.00	0.00	0.00	0.00	0.00	0.00	41.44
640.0	39.32	0.00	0.00	0.03	0.00	0.00	0.00	0.24	0.00	0.00	0.00	0.00	0.00	77.44
650.0	39.67	0.03	0.00	0.03	0.00	0.00	0.00	0.00	0.00	0.00	0.00	0.00	0.12	40.51
660.0	0.00	0.00	0.00	0.00	0.00	0.00	0.00	0.00	0.00	0.00	0.00	0.00	0.00	0.00
710.0	0.00	0.00	0.00	0.00	0.00	0.00	0.00	0.00	0.00	0.00	0.00	0.00	0.00	0.00
720.0	47.47	0.03	0.00	0.03	0.00	0.00	0.00	0.00	0.00	0.00	0.03	0.00	0.00	56.40
725.0														
730.0	39.12	0.22	0.00	0.00	0.00	0.22	0.00	0.00	0.00	0.05	0.00	0.00	0.00	54.41
740.0	0.00	0.00	0.00	0.00	0.00	0.00	0.00	0.00	0.00	0.00	0.00	0.00	0.00	0.00
770.0														
880.0	0.00	0.00	0.00	0.00	0.00	0.00	0.00	0.00	0.00	0.00	0.00	0.00	0.00	0.00
890.0	19.52	0.00	0.00	0.00	0.00	0.00	0.00	0.00	0.00	0.00	0.00	0.00	0.00	134.50
900.0	8.39	1.95	0.00	0.05	0.00	0.38	0.00	0.00	0.00	0.00	0.00	0.00	0.00	45.05
911.0	5.05	0.36	0.00	0.05	0.00	0.72	0.00	0.00	0.00	0.00	0.00	0.00	0.00	13.02
922.0	6.67	1.45	0.00	0.00	0.00	0.14	0.00	0.00	0.00	0.00	0.00	0.00	0.00	17.83
927.0	0.00	0.00	0.00	0.00	0.00	0.00	0.00	0.00	0.00	0.00	0.00	0.00	0.00	0.00

Appendix 9. Data for Core 21852 (Spec/g)

Depth [cm]	Age [ka]	DBD [g/ccm]	Dry Weight [g]	O-Isotope Event	LSR [cm/ka]	*Pyrgo rotalaria*	*Cibicidoides wuellerstorfi*	*Epistominella exigua*	*Quinqueloculina seminula*	*Elphidium spp.*	*Triloculina tricarinata*	*Cribrostomoides subglobosus*	agglutinated Tubes	*Ammobaculites agglutinans*	*Psilonia bulloides*	*Cassidulina teretis*
60.0	26.50	0.55	42.01		1.76	0.00	0.00	0.00	0.00	0.33	0.33	0.00	0.00	0.00	0.00	28.23
70.0	26.80	1.00	45.25		1.76	0.00	0.00	0.00	0.00	0.66	0.00	0.00	0.00	0.00	0.00	46.60
78.0	27.00			3.1												
80.0	28.14	0.86	36.63		1.76	0.00	0.00	0.00	0.00	1.15	0.00	0.00	0.00	0.00	0.00	61.30
90.0	33.83	0.83	40.30		1.76	0.00	0.02	0.00	0.00	1.38	0.02	0.00	0.00	0.00	0.00	93.68
100.0	39.52	0.89	45.23		1.76	0.00	0.00	0.00	0.00	1.26	0.02	0.00	0.00	0.00	0.00	72.06
110.0	45.21	0.81	37.12		1.76	0.00	0.00	0.00	0.00	0.00	0.00	0.00	0.02	0.00	0.00	71.41
120.0	50.90	0.88	49.81		1.76	0.00	0.00	0.00	0.00	0.29	0.00	0.00	0.00	0.00	0.00	53.61
128.0	55.45			3.3												
130.0	57.40	0.87	44.45		1.02	0.00	0.00	1.25	0.00	0.50	0.00	0.00	0.00	0.00	0.00	4.25
138.0	65.22			4.2.2												
140.0	68.07	0.75	49.23		0.70	0.00	1.28	0.58	0.00	1.18	0.00	0.00	0.00	0.00	0.00	14.61
148.0	79.46			5.1												
151.0	81.12	1.10	26.97		1.81	0.00	27.60	0.00	0.00	0.00	0.00	1.39	2.06	0.00	4.55	376.00
156.0	83.89	1.01	39.52		1.81	0.00	7.41	0.68	0.00	1.98	0.00	0.00	0.00	0.00	1.98	116.41
165.0	88.83	0.89	37.29		1.81	0.00	3.54	0.00	0.00	0.79	0.05	0.00	0.00	0.00	0.00	47.52
168.0	90.53			5.2												
175.0	95.09	0.91	34.94		1.54	0.00	3.42	0.80	0.00	0.80	0.00	0.00	0.00	0.00	0.80	65.92
185.0	102.06	0.94	32.79		1.54	0.00	9.58	0.84	0.00	0.03	0.00	0.00	0.00	0.00	1.70	26.93
188.0	103.55			5.3												
195.0	108.62	0.90	36.41		1.38	0.00	9.57	0.00	0.00	0.00	0.00	0.00	0.00	0.00	0.00	34.64
198.0	110.79			5.4												
205.0	118.90	0.81	44.18		0.86	0.00	4.00	1.25	0.00	0.66	0.00	0.00	0.00	0.00	0.00	50.14
208.0	122.38			5.5.1												
215.0	123.29	0.77	36.06		7.62	0.00	10.32	4.02	0.00	0.05	0.00	0.00	0.00	0.00	0.00	119.15
218.0	123.58			5.5.2												
224.0	124.46	0.69	31.28		7.62	0.00	3.65	2.85	0.00	0.03	0.00	0.00	0.00	0.00	3.83	21.24
228.0	125.00			5.5.3												
233.0	127.53	0.71	28.90		1.98	0.00	0.00	0.13	0.00	0.00	0.00	0.00	0.00	0.00	0.26	0.65
243.0	132.53	0.82	29.53		1.98	0.00	0.00	0.12	0.00	3.41	0.00	0.00	0.00	0.00	0.00	1.77
248.0	135.10			6.2												
253.0	136.66	0.82	30.88		3.21	0.00	0.00	0.00	0.00	0.70	0.00	0.00	0.00	0.00	0.00	18.36
267.0	140.90	0.85	33.98		3.21	0.00	0.00	1.25	0.00	1.31	0.00	0.00	0.00	0.00	0.00	52.67
280.0	157.10	0.79	27.48	6.4	3.29	0.00	0.00	0.00	0.00	1.71	0.00	0.00	0.00	0.00	0.00	9.42
290.0	159.67	0.83	29.29		3.29	0.00	1.12	2.91	0.00	1.03	0.00	0.00	0.00	0.00	0.00	61.95
300.0	162.13	0.71	31.14		3.29	0.00	0.00	0.92	0.00	0.06	0.00	0.00	0.00	0.00	0.00	60.99
310.0	164.64	0.66	22.78		3.29	0.00	0.00	0.74	0.00	0.62	0.00	0.00	0.00	0.00	0.00	43.96
320.0	167.10	0.92	39.11		3.29	0.00	2.55	0.00	0.00	0.35	0.02	0.00	0.00	0.00	0.00	141.97
328.0	171.37			6.5												
330.0	173.88	0.90	35.16		1.20	0.00	0.07	0.38	0.00	2.20	0.00	0.00	0.00	0.00	0.00	33.57
336.0	179.55	0.96	36.92		5.68	0.00	0.00	0.00	0.00	1.02	0.00	0.00	0.00	0.00	0.00	1.54
344.0	180.96	0.90	39.94		5.68	0.00	0.00	0.00	0.00	0.00	0.00	0.00	0.00	0.00	0.00	0.00
350.0	182.02	0.90	48.89		5.68	0.00	0.00	0.00	0.00	0.00	0.00	0.00	0.00	0.00	0.00	0.00
353.0	182.55	0.90	48.15		5.68	0.00	0.00	0.00	0.00	0.00	0.00	0.00	0.00	0.00	0.00	0.00
365.0	184.66	0.88	38.67		5.68	0.00	0.00	0.00	0.00	0.00	0.00	0.00	0.00	0.00	0.00	0.00
368.0	186.00			7.0												
374.0	187.55	0.87	45.18		2.54	0.00	0.15	0.08	0.00	0.00	0.00	0.00	0.00	0.00	0.08	6.26
384.0	191.36	0.95	37.85		2.54	0.00	1.09	0.00	0.00	0.00	0.00	0.00	0.00	0.00	0.00	14.25
388.0	193.07			7.1												
394.0	195.12	0.92	38.10		2.93	0.00	0.00	0.00	0.00	0.05	0.00	0.00	0.00	0.00	0.03	0.15
404.0	200.05	0.80	41.29		2.93	0.00	0.05	0.00	0.00	0.14	0.00	0.00	0.00	0.00	0.00	0.00
410.0	200.57			7.2												
414.0	203.90	0.75	18.54		1.20	0.00	0.00	0.00	0.00	0.05	0.00	0.24	0.38	0.00	0.10	0.05
420.0	208.89	1.00	14.28		1.20	0.00	0.00	0.00	0.00	0.00	0.00	0.00	0.00	0.00	0.00	0.00
424.0	212.21	0.95	33.54		1.20	0.00	0.00	0.00	0.00	0.36	0.00	0.00	0.11	0.00	0.03	0.80
428.0	215.54			7.3												
436.0	225.51	0.92	33.04		0.80	0.00	0.00	0.00	0.00	0.36	0.00	0.00	0.00	0.00	0.00	36.18
438.0	228.00			7.4												
446.0	232.88	0.90	33.68		1.64	0.00	1.53	0.00	0.00	0.92	0.00	0.00	0.00	0.00	0.00	78.03
456.0	236.88	0.89	37.77		1.64	0.00	0.00	0.00	0.00	0.15	0.00	0.00	0.00	0.00	0.00	0.60
465.0	240.19			7.5												
466.0	240.64	0.99	41.14		17.79	0.00	0.00	0.00	0.00	0.00	0.00	0.00	0.00	0.00	0.00	0.00
476.0	243.20	1.03	33.48		17.79	0.00	0.00	0.00	0.00	0.00	0.00	0.00	0.00	0.00	0.00	0.00
488.0	242.44	1.00	43.26		17.79	0.00	0.00	0.00	0.00	0.00	0.00	0.00	0.00	0.00	0.00	0.00
498.0	242.44	0.94	38.59		17.79	0.00	0.00	0.00	0.00	0.00	0.00	0.00	0.00	0.00	0.00	0.00
508.0	243.00	0.76	32.35		17.79	0.00	0.00	0.00	0.00	0.00	0.00	0.00	0.00	0.00	0.00	0.00
521.0	243.79	0.82	36.96		17.79	0.00	0.02	0.00	0.00	0.21	0.00	0.00	0.00	0.00	0.00	0.19
531.0	0.25	1.09	48.94	8.0	5.33	0.00	0.00	0.00	0.00	0.00	0.00	0.00	0.00	0.00	0.00	0.00
541.0	248.19	1.03	38.08		5.33	0.00	0.00	0.00	0.00	0.00	0.00	0.00	0.00	0.00	0.00	1.04
551.0	248.31	1.00	43.63		5.33	0.00	0.00	0.00	0.00	0.00	0.00	0.00	0.00	0.00	0.00	0.00

Appendix 10. Data for Core 17730

Depth [cm]	Age [ka]	DBD [g/ccm]	Dry Weight [g]	AMS14C dates [ky]	LSR [cm/ka]	*Pyrgo rotalaria*	*Cibicidoides wuellerstorfi*	*Epistominella exigua*	*Quinqueloculina seminula*	*Elphidium* spp.	*Triloculina tricarinata*	*Cribrostomoides subglobosus*	agglutinated Tubes	*Ammobaculites agglutinans*	*Pullenia bulloides*	*Cassidulina lerchi*
10.0	1.79	0.63	6.30		8.77	0.48	76.03	12.70	0.00	0.00	19.05	6.51	0.00	13.33	0.00	0.00
20.0	2.93	0.65	6.52	2.93	8.77	4.60	40.03	68.71	0.00	0.00	0.15	6.75	0.31	5.37	0.00	0.00
30.0	4.07	0.60	6.01		8.77	8.15	58.90	3.99	0.00	0.00	11.48	12.48	0.00	11.98	0.00	0.00
40.0	5.41	0.57	5.72	5.41	8.40	19.06	53.85	0.00	0.00	0.00	32.87	5.07	0.00	6.99	0.00	0.00
50.0	6.40	0.59	5.92	6.4	11.98	15.20	52.53	0.00	0.00	0.00	4.22	7.60	0.00	8.11	0.00	0.00
60.0	7.24	0.64	6.45		11.98	11.32	56.12	0.00	0.00	0.00	0.00	11.16	0.00	0.00	0.00	0.00
70.0	8.07	0.58	5.78	8.07	28.57	7.27	35.29	0.00	0.00	0.00	13.84	5.19	0.00	0.00	0.00	0.00
80.0	8.42	0.58	5.82		28.57	0.00	22.68	0.00	0.00	0.00	4.81	6.53	0.00	0.00	0.00	0.00
90.0	8.77	0.60	6.02		28.57	0.00	1.50	0.00	0.00	0.00	0.17	0.00	0.00	0.00	0.00	0.00
100.0	9.12	0.52	5.16	9.12	6.04	0.00	8.14	0.00	0.00	0.00	1.55	0.00	0.00	0.00	0.00	0.00
105.0	9.95	0.61	6.05		6.04	0.00	120.33	0.00	0.00	0.00	1.32	0.00	0.00	0.00	0.00	0.00
110.0	10.78	0.83	8.32		6.04	1.80	1.56	0.00	0.00	0.72	0.00	0.00	0.00	0.00	0.00	0.00
112.5	11.19	0.83	8.32	11.19	6.94											
122.5	12.63	0.83	8.32	12.63	4.38											
125.0	13.20	0.88	8.80		4.38	0.00	1.48	0.00	0.00	0.23	0.00	0.00	0.00	0.00	0.00	0.00
130.0	14.34	0.90	9.04		4.38	0.00	0.00	0.00	0.00	0.88	0.00	0.00	0.00	0.00	0.00	0.22
140.0	16.63	0.92	9.18		4.38	0.00	0.11	0.00	0.00	0.33	0.00	0.00	0.00	0.00	0.00	0.00
145.0	17.77	0.91	9.10	17.77	10.00	0.00	0.11	0.00	0.00	0.33	1.76	0.11	3.85	0.00	0.00	0.00
147.5	18.02	0.91	9.05		10.00	0.00	0.00	0.00	0.00	1.44	0.00	0.00	0.77	0.00	0.00	0.00
150.0	18.27	0.90	9.01		10.00	0.11	0.00	0.00	0.00	0.89	0.11	0.33	2.22	0.00	0.00	0.00
152.5	18.52	0.90	8.99		10.00	0.00	0.00	0.00	0.33	0.11	0.22	0.11	10.57	0.00	0.00	0.00
155.0	18.77	0.90	8.97		10.00	0.00	0.00	0.00	0.11	0.78	0.11	0.00	2.23	0.00	0.00	0.00
157.5	19.02	0.90	8.96		10.00	0.22	0.22	0.00	0.00	0.89	0.00	0.22	1.79	0.00	0.00	0.11
160.0	19.27	0.89	8.94	19.27	6.21	0.11	0.00	0.00	0.00	0.56	0.22	0.00	0.22	0.00	0.00	0.45
162.5	19.67	0.91	9.11		6.21	0.00	0.00	0.00	0.00	0.66	1.54	0.00	5.16	0.00	0.00	0.00
165.0	20.08	0.92	9.18		6.21	0.11	0.00	0.00	0.00	0.33	0.33	0.00	0.54	0.00	0.00	0.00
167.5	20.48	0.93	9.26		6.21	0.22	0.00	0.00	0.00	0.54	0.97	0.11	4.43	0.00	0.00	0.00
170.0	20.88	0.93	9.32		6.21	0.64	0.00	0.00	0.00	0.32	0.11	0.97	2.47	0.00	0.00	0.32
172.5	21.28	0.89	8.90		6.21	0.45	0.22	0.00	0.00	1.46	1.12	0.56	5.96	0.00	0.00	0.11
175.0	21.69	0.85	8.50		6.21	0.47	0.00	0.00	0.00	0.82	0.35	0.24	2.94	0.00	0.00	0.12
177.5	22.09	0.82	8.20		6.21	0.49	0.00	0.00	0.00	0.61	0.00	0.00	0.00	0.00	0.00	0.37
180.0	22.49	0.81	8.07	22.49	5.43	0.12	0.00	0.00	0.00	0.37	1.12	0.12	0.00	0.00	0.00	0.00
182.5	22.95	0.82	8.20		5.43	0.00	0.00	0.00	0.00	0.49	0.37	0.12	1.46	0.00	0.00	0.00
185.0	23.41	0.86	8.60		5.43	0.00	0.00	0.00	0.00	1.40	0.35	0.12	3.14	0.00	0.00	0.12
187.5	23.87	0.90	9.00		5.43	0.22	0.00	0.00	0.44	0.11	0.67	0.78	10.00	0.00	0.00	0.00
190.0	24.33	0.93	9.31		5.43	1.50	0.00	0.00	0.00	0.75	0.32	0.32	1.07	0.00	0.00	0.11
192.5	24.79	0.94	9.40		5.43	0.11	0.64	0.00	0.00	0.74	0.43	1.70	0.43	0.00	0.00	0.21
195.0	25.25	0.95	9.45		5.43	0.11	0.85	0.00	0.00	1.48	0.00	0.11	0.21	0.00	0.00	0.32
197.5	25.71	0.96	9.56		5.43	0.00	0.10	0.00	0.00	1.46	0.10	0.00	0.00	0.00	0.00	0.10
200.0	26.18	0.96	9.64		5.43	0.00	0.10	0.00	0.00	1.45	0.00	0.00	1.04	0.00	0.00	0.21

Appendix 10. continued

Depth [cm]	*Oridorsalis umbonatus*	*Globocassidulina subglobosa*	*Margindulina glabra*	*Dentalina pauperata*	*Siphotextularia rolshausenii*	*Cassidulina reniforme*	*Miliolinella* sp.	*Oolina lineata*	*Cyclammina* sp.	*Parafissurina ovata*	*Lenticulina gibba*	*Eponides tumidulus*	*Lagena* spp.	Total [Spec./g]
10.0	94.44	0.00	0.00	0.00	0.00	1.27	0.00	0.00	0.00	0.63	0.00	1.90	0.00	226.51
20.0	55.21	0.00	0.00	0.00	0.00	1.38	0.00	0.00	0.00	0.15	0.00	2.30	0.31	185.12
30.0	41.26	0.00	0.00	0.00	0.00	2.66	0.00	0.00	0.00	0.17	0.00	0.67	0.00	151.75
40.0	77.62	0.00	0.00	0.00	0.00	4.20	0.00	0.00	0.00	0.17	0.00	1.40	1.40	203.32
50.0	66.89	0.68	0.00	0.00	0.00	4.73	0.00	0.00	0.00	0.34	0.00	2.70	0.84	166.39
60.0	68.53	0.00	0.00	0.00	0.00	3.10	0.00	0.00	0.00	3.41	0.00	2.48	1.40	158.76
70.0	73.70	0.17	2.94	0.00	0.00	5.54	0.00	0.35	0.00	0.00	0.00	1.38	1.38	148.10
80.0	109.28	0.00	0.00	0.00	0.00	7.90	0.00	0.00	0.00	0.00	0.00	0.69	0.00	156.87
90.0	119.10	0.00	0.00	0.00	0.00	0.83	0.00	0.00	0.00	0.17	0.00	0.00	0.00	122.59
100.0	80.62	0.00	0.00	0.00	0.00	2.71	0.00	0.00	0.00	0.00	0.00	0.00	0.00	93.60
105.0	55.70	0.00	7.27	0.17	0.00	0.66	0.00	0.00	0.00	0.00	0.00	3.97	3.31	193.06
110.0	19.71	0.00	0.00	0.00	0.00	1.44	0.00	0.00	0.00	0.00	0.00	0.24	0.00	25.48
112.5														
122.5														
125.0	52.27	0.00	0.00	0.00	0.00	0.45	0.00	0.00	0.00	0.00	0.00	1.14	0.00	55.91
130.0	6.64	0.00	0.00	0.00	0.00	0.66	0.00	0.00	0.00	0.00	0.00	0.22	0.00	8.63
140.0	0.65	0.00	0.00	0.00	0.98	0.11	0.00	0.00	0.00	0.00	0.00	0.44	0.00	2.61
145.0	0.88	0.00	0.00	0.00	6.92	0.22	0.00	0.00	0.00	0.33	0.22	0.66	0.00	15.82
147.5	0.33	0.00	0.00	0.00	2.65	0.11	0.00	0.00	0.00	0.00	0.00	0.55	0.00	5.86
150.0	1.11	0.00	0.00	0.00	6.55	0.00	0.00	0.00	0.00	0.00	0.11	0.00	0.00	11.43
152.5	0.44	0.00	0.00	0.00	4.45	0.11	0.00	0.00	0.00	0.11	0.00	0.00	0.00	17.24
155.0	0.78	0.00	0.00	0.00	5.02	0.00	0.00	0.00	0.00	0.11	0.00	0.00	0.00	9.14
157.5	0.89	0.00	0.00	0.00	1.90	0.45	0.00	0.00	0.11	0.11	0.00	0.00	0.11	7.81
160.0	0.89	0.00	0.00	0.00	3.58	0.00	0.00	0.00	0.00	0.00	0.00	0.00	0.22	7.49
162.5	0.55	0.00	0.00	0.00	9.77	0.22	0.00	0.00	0.00	0.11	0.00	0.00	0.11	18.22
165.0	0.65	0.11	0.00	0.11	18.63	0.00	0.00	0.00	0.00	0.22	0.00	0.00	0.00	21.02
167.5	0.76	0.00	0.00	0.00	3.67	0.00	0.00	0.00	0.00	0.22	0.00	0.00	0.00	11.02
170.0	0.64	0.00	0.00	0.00	3.97	0.21	0.00	0.00	0.00	0.00	0.00	0.32	0.00	10.30
172.5	0.34	0.00	0.00	0.00	4.61	0.79	0.00	0.00	0.00	0.11	0.00	0.34	0.00	16.63
175.0	0.71	0.00	0.00	0.00	3.06	0.35	0.00	0.00	0.00	0.24	0.00	0.00	0.00	9.53
177.5	0.73	0.00	0.00	0.00	2.93	0.49	0.00	0.00	0.00	0.12	0.00	0.00	0.00	6.10
180.0	1.49	0.00	0.00	0.00	0.74	0.74	0.00	0.00	0.00	0.00	0.00	0.00	0.37	5.20
182.5	0.24	0.00	0.00	0.00	0.24	0.37	0.00	0.00	0.00	0.00	0.00	0.00	0.12	3.78
185.0	0.47	0.00	0.00	0.00	0.12	0.35	0.00	0.00	0.00	0.12	0.00	0.00	0.00	6.16
187.5	0.78	0.00	0.00	0.00	4.44	0.22	0.00	0.11	0.00	0.11	0.00	0.00	0.11	18.22
190.0	0.86	0.00	0.00	0.00	7.30	0.00	0.00	0.00	0.00	0.11	0.00	0.00	0.00	12.46
192.5	0.74	0.00	0.00	0.00	6.06	0.00	0.00	0.00	0.00	0.11	0.00	0.00	0.00	11.49
195.0	0.74	0.00	0.00	0.00	3.39	1.38	0.00	0.00	0.00	0.21	0.00	0.00	0.00	9.63
197.5	0.10	0.00	0.00	0.00	1.05	1.05	0.00	0.00	0.00	0.00	0.00	0.00	0.00	4.18
200.0	0.52	0.00	0.00	0.00	0.00	0.93	0.00	0.00	0.00	0.00	0.00	0.00	0.10	4.36

Paleoceanography of the North Atlantic Ocean (68°-76°N) during the past 450 ky deduced from planktic foraminiferal assemblages and stable isotopes

HENNING A. BAUCH

GEOMAR - Research Center for Marine Geosciences, Wischhofstrasse 1-3, D-24148 Kiel, Germany

ABSTRACT

Polar and subpolar planktic foraminifera and the stable oxygen and carbon isotopes of *Neogloboquadrina pachyderma* (s) from the Nordic seas are analyzed for the time period since oxygen isotope Stage 12, with special emphasis on interglacial time slices Stages 11, 5e (Eemian), and 1 (Holocene).

A comparison of relative (%) and absolute test concentrations from two different size fractions reveals a complex downcore pattern for the morphogroup *N. pachyderma*. Ratios of small-sized *N. pachyderma* (s) to *N. pachyderma* (d) vary between Stage 11, the Eemian and the Holocene, due to changes in test concentrations of *N. pachyderma* (s) only. As revealed in the downcore records, both coiling varieties of *N. pachyderma* are somehow related to each other, but the use of percent data as surface water mass proxy appears to be limited. The most dominant subpolar species, *Turborotalita quinqueloba* and *Globigerina bulloides*, mainly occurred during the Holocene, the Eemian, and Stage 11. Both species are inversely related to *N. pachyderma* (s) in that their abundances steadily increased during all three interglacials. During these times, *G. bulloides* remained always restricted to the eastern area of the Nordic seas with dominant Atlantic water masses. In contrast *T. quinqueloba* exhibited a much wider distributional pattern.

From stable isotopes and faunal variability it is inferred that the entire Nordic seas was covered by sea-ice during the cold seasons in Stage 11 resulting in both, highest test concentrations of *N. pachyderma* (s) and highest $\delta^{13}C$ values observed throughout the past 450 ky. For the last two interglacials, oxygen isotope values and test concentrations of *T. quinqueloba* indicate that warmer surface waters must have prevailed in the western Iceland Sea in the Eemian compared with any time during the Holocene time interval.

INTRODUCTION

Recognizing variations of past water mass compositions has been a major issue for paleoceanographical and ultimately also for paleoclimatological interpretations. The climate over the past 600 ka has been dominated by strong fluctuations in northern hemisphere ice sheets (Tiedemann *et al.*, 1994). During times of retreat and advance of the ice sheets, modern-type circulation pattern evolved and/or deteriorated accordingly. The timing of these glacial-interglacial cycles, reflected in the oxygen isotope record as global ice volume effect, has been tied to variatons in solar radiation (e.g. Imbrie *et al.*, 1984; Martinson *et al.*, 1987). Based on the Milankovich theory, these orbitally induced changes (Hays *et al.*, 1976) have left their imprint on northern high-latitude sediments. The close vicinity of the Nordic seas (Norwegian, Greenland, and Iceland seas) to repeatedly glaciated landmasses makes this area a key region to monitor late Pleistocene water mass/climate relations, which become particularly apparent during the change

In: Hass, H.C. & Kaminski, M.A. (eds.) 1997. Contributions to the Micropaleontology and Paleoceanography of the Northern North Atlantic. *Grzybowski Foundation Special Publication*, no. 5, pp. 83-100

from a glacial to an interglacial climatic mode (Imbrie *et al.*, 1993). Previous faunal studies carried out in this region have shed some light on distributional patterns by assigning distinct species to belong to either a glacial or an interglacial fossil assemblage (e.g., Kellogg, 1984; Streeter *et al.*, 1982; Haake & Pflaumann, 1989). Kellogg (1976, 1977, 1980) first documented the strong climatic and oceanographic resemblance of the last interglacial optimum, isotope Stage 5e, with that of the Holocene and stated that only these periods where times of full interglacial conditions (i.e. Holocene-like) whereas the others were marked by cool or cold conditions with ice-cover. However, this statement is strongly dependant on discriminating between 'warm'- and 'cold'-water indicating species of planktic foraminifera. But these earlier interpretations were based on different methodologies, i.e. in terms of the lower limit of the used mesh size, which particularly during colder periods may not cover all of the 'warm' signal contained in the faunal record (Bauch, 1994a).

The purpose of this study is to show the temporal and spatial distribution of planktic foraminifera throughout the past 450 ky of glacial and interglacial change and to evaluate particularly the most prominent interglacials according to their oceanographic characteristics. It has been shown that of all interglacial phases during the past 450 ky, only the Holocene, Stage 5e and Stage 11 were prolonged times when the deposition of iceberg-rafted detritus (IRD) ceased in at least the southern Nordic seas (Birgisdottir, 1990; Baumann *et al.*, 1995). Core sections covering interglacial Stages 7 and 9 contain notable amounts of IRD in the Nordic seas (Henrich *et al.*, 1989). They, therefore, cannot be addressed as interglacials *sensu stricto*.

SURFACE WATER PROXIES

The modern surface water pattern of the Nordic seas may be characterized today by a threefold subdivision based on salinity variations and temperatures which decrease towards the north and the west (Swift, 1986). Incoming relatively warm and high saline Atlantic surface water (6-10°C, >35‰) that flows as the Norwegian Current (NC) along Norway's and Svalbard's shelf margin towards the north into the eastern Arctic Ocean basin comprises the Atlantic Domain (Fig. 1). The western part of the Nordic seas, made up of the Polar Domain, is marked by the outflow of the relatively cold and low saline water (<0°C, <34,4‰; Swift, 1986) of the East Greenland Current (EGC) from the Arctic Ocean. This water eventually leaves the Nordic seas via Denmark Strait into the North Atlantic. Polar and Atlantic domains are separated from each other by the Arctic Domain,

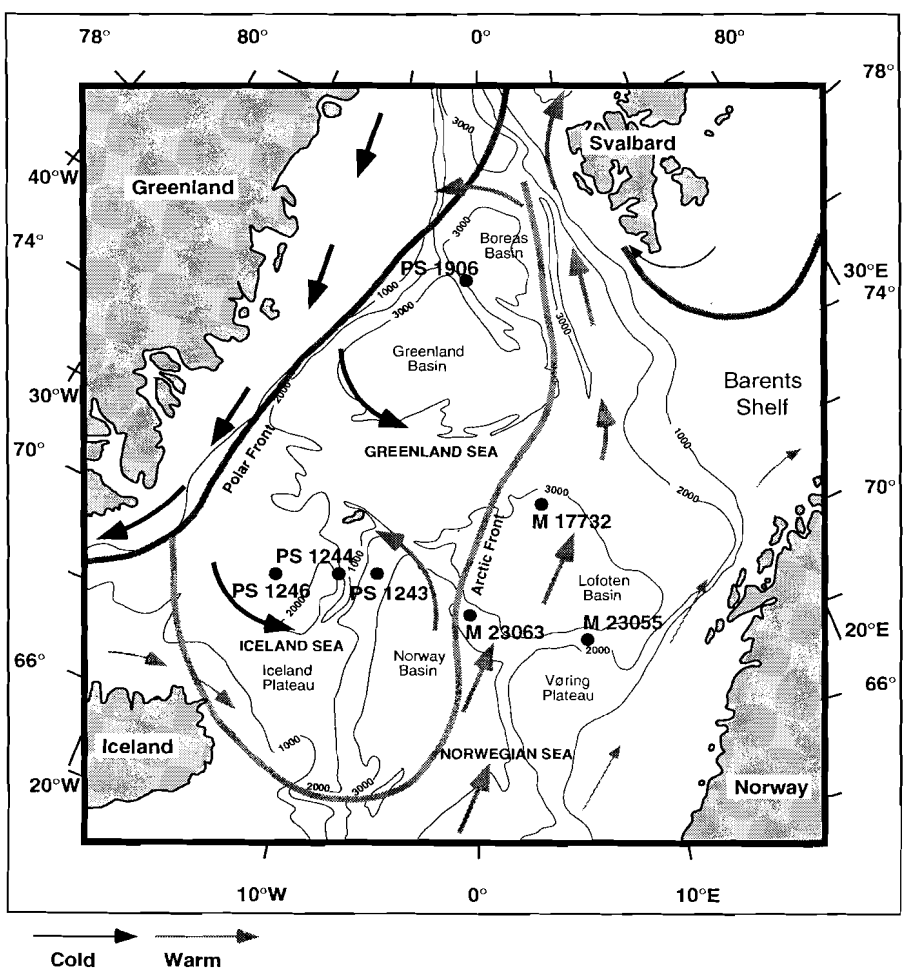


Figure 1. Overview of the modern distribution of main surface water masses in the Nordic seas.

Table 1. Geographical position, water depth, and modern surface water temperatures (adopted from Dietrich, 1969) of investigated core sites.

Site	Geogr. Position		Water Depth	Core Length	Modern Temp. °C
	Lat. (N)	Long.	(m)	(m)	Surface
M17732	71°36.8'	04°12.8'E	3103	5.93	8.0
M23055	68°25.4'	04°01.3'E	2311	6.67	9.5
M23063	68°45.0'	00°00.0'W	2299	9.18	8.5
PS1243	69°22.3'	06°32.1'W	2710	7.67	8
PS1244	69°22.0'	08°40.0'W	2162	6.68	7.5
PS1246	69°23.6'	12°52.1'W	1902	7.09	5.0
PS1906	76°50.1'	02°09.1'W	2939	6.53	3.5

which essentially is mixed water from the former two. Moreover, this domain is the main area of deep water formation in the Nordic seas and has two distinct oceanographic fronts on either side.

Various planktic faunal and floral investigations are instrumental in monitoring the variability of oceanic processes in the Nordic seas during glacial to interglacial time (e.g. Kellogg, 1980; Jansen & Bjørklund, 1985; Baumann & Matthiessen, 1992; Bauch, 1993). A particular marine microfossil assemblage can either serve as a direct indicator of the past surface water or can be utilized to estimate specific physical properties, e.g. temperature (Koç-Karpuz & Jansen, 1992). Within marine plankton assemblages, which are believed to be good recorders of present and past physical and chemical surface water changes, planktic foraminifera in particular represent a major component in the deposition of hemipelagic and pelagic sediments, resulting in high amounts of carbonate content in the sediments (Kellogg, 1975; Baumann *et al.*, 1993). Traditionally, all species that occur in upper Pleistocene or Holocene sediments in the North Atlantic may be assigned, according to their generally preferred latitudinal habitat, to a polar and a subpolar group (Kipp, 1976; Kennett & Srinivasan, 1983; Hemleben *et al.*, 1989), and consequently, to a glacial or interglacial group. In the Nordic seas left-coiled *Neogloboquadrina pachyderma* sinistral (s) is the main representative of the polar group. Although often regarded as the only true polar species, it is well known that *N. pachyderma* (s) is to some extent always accompanied by the right-coiled variety *N. pachyderma* dextral (d). The subpolar group is predominantly made up of *Turborotalita quinqueloba, Globigerina bulloides, Globigerinita glutinata, Gl. uvula* and depending on the water mass temperatures also of *N. pachyderma* (d). To a much lesser degree, even species from temperate or subtropical provenances do occasionally occur (Kellogg, 1984; Haake & Pflaumann, 1989). However, most of these species are rare and appear to be restricted to the Eemian time interval and the southeastern part of the Nordic seas where the influence of North Atlantic surface water is most dominant (Kellogg, 1980; Bauch, 1993). Stratigraphically, subpolar foraminifera occur in the Nordic seas mainly during interglacial times and are, therefore, indicative for the presence of warm Atlantic water. Because of its nearly continuous presence in both glacial and interglacial high-latitude sediments, the polar species *N. pachyderma* (s) is most commonly used for stable isotope analyses, thus providing the downcore stratigraphical framework.

MATERIALS AND METHODS

For this study six sites were chosen, which on a broad scale cover the main water masses of the Nordic seas (Fig. 1). Most of these cores are spliced together with box cores from the same site and originate from water depth ranging between ~1900-3100 m (Table 1). All cores were collected during cruises of the German research vessels RV *Polarstern* and RV *Meteor*.

Sampling of the cores was carried out as 1 cm thick slices at intervals of 5-10 cm for the long cores and usually every 2 cm for the box cores. All samples for faunal investigations were then dried, weighed, washed into >63 μm residues and later separated into different size fractions (63-125 μm, 125-250 μm, 250-500 μm, >500 μm). For counting the planktic fauna a mesh size range of 125-500 μm was considered. The use of the size fraction > 125 μm has proven to be a crucial issue for evaluating past oceanographic changes as planktic foraminiferal tests appear to be smaller in Nordic seas sediments than further south in the North Atlantic. Taking mesh size 150 μm as a lower limit, as recommended by CLIMAP Members (1976), may not give a fair reflection of relative species abundances. This in particular applies to the most abundant but relatively small-sized subpolar species in the Nordic seas, *Turborotalita quinqueloba*, which may bear important paleoceanographic implications for interpreting periods with changes in surface water properties (Bauch, 1994a; Hebbeln *et al.*, 1994).

Faunal counts were carried out separately on the 125-250 µm and 250-500 µm fractions. With this method the abundance variations of larger-sized species such as, e.g., *Globigerina bulloides* can be better expressed, which would otherwise appear to be statistically underestimated in terms of their paleoceanographic implication. Prior to quantifications each appropriate sample was split down by means of a microsplitter. Test concentrations are expressed as specimens per gram dry bulk sediment.

Stable isotope measurements were performed on the species *Neogloboquadrina pachyderma* sinistral (s) using a fully automated MAT 251 mass spectrometer (Leibniz Laboratory at Kiel University). To reduce the effects of stable isotope differences among morphotypes of this common species (Healy-Williams, 1992), 25-30 four-chambered, quadrate specimens from the 125-250 µm size fraction were picked. The stratigraphical framework of the cores is based on the correlation between stable isotope records given by *N. pachyderma* (s) and the SPECMAP time-scale with its assignment of oxygen isotope stages and substages (Imbrie *et al.*, 1984; Martinson *et al.*, 1987). Stage boundaries were always set along the decreasing or increasing slopes of the oxygen isotope curves and, where necessary, further aided by the faunal results.

RESULTS

Stable isotopes

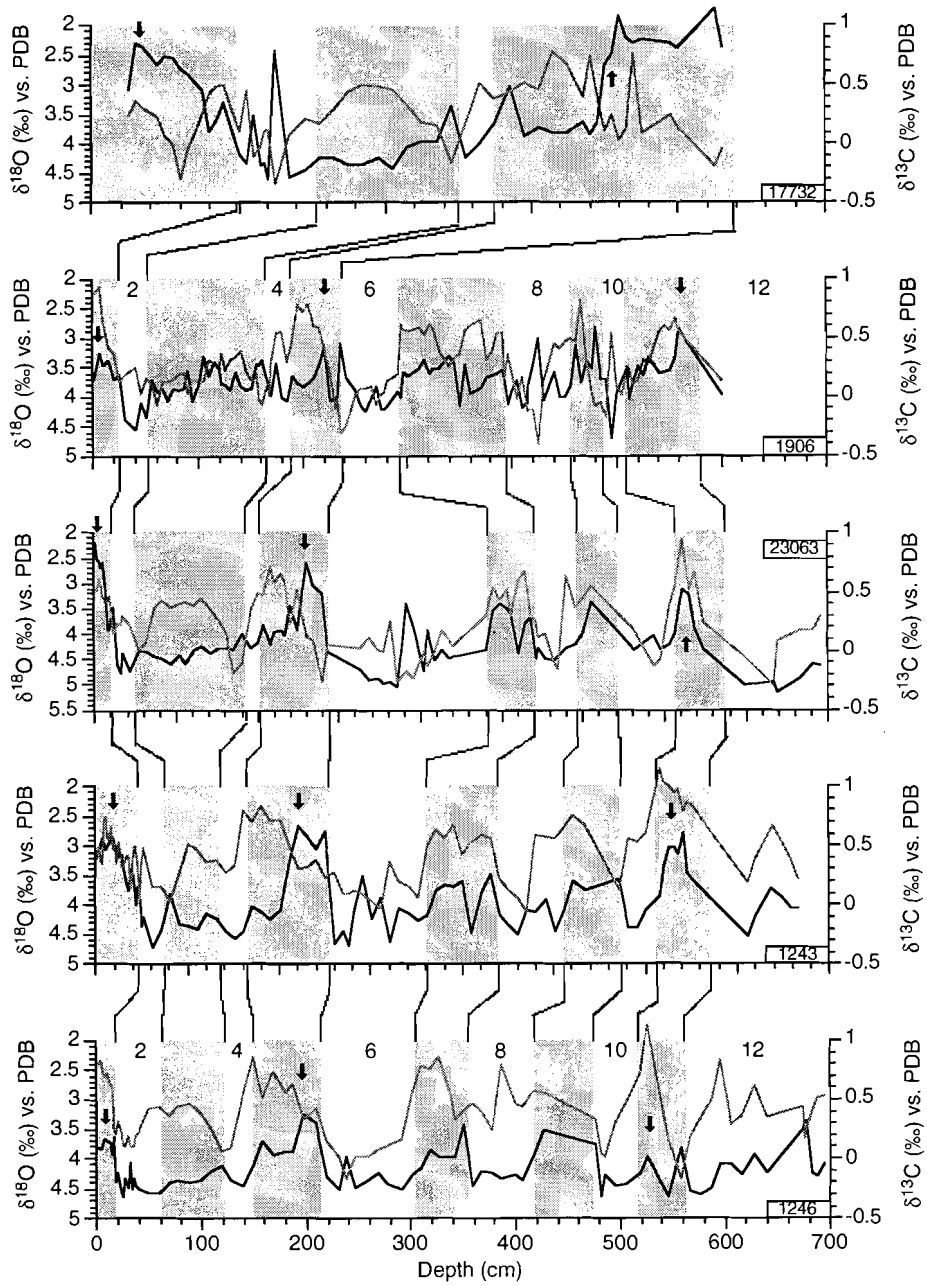
The stratigraphic control of the investigated sediment cores is based on both oxygen and carbon stable isotopes. This framework is further supported by the faunal results. Core PS1244 has no stable isotope record, but, as it will be shown in this study, it nevertheless has a good stratigraphical control due to faunal correlations with nearby Core PS1243. Furthermore, both cores correspond well in terms of $CaCO_3$ content (Birgisdottir, 1990). The isotope records date back to oxygen isotope Stage 12 for most cores (Fig. 2). Core M17732 extends stratigraphically down to approximately stage boundary 6/5 (Termination II). Despite the relatively low sample resolution, major features of the stable isotope records can be recognized in the cores. Interestingly, most often the carbon isotope record appears to be a more precise stratigraphical tool than the oxygen isotopes are. This in particular applies to Core PS1906 in which the oxygen record is rather difficult to interpret on its own below glacial Stage 2. Cores M23063 and PS1243, which today are most closely to the main flow path of Atlantic surface water, show best the typical changes that shaped environmental conditions during the past 5 glacial/interglacial cycles. However, apart from these common features, there are some significant characteristics which can be traced throughout the records and others which seem to vary laterally. In all cores the increase of $\delta^{13}C$ values after Stage 2 is always concurrent with a decrease in $\delta^{18}O$. Highest Holocene carbon values are very similar in most cores ranging between 0.7-0.9‰ - Core M17732 is lacking the uppermost ~4 ky (Weinelt, 1993). In comparison peak values of the oxygen isotopes show much larger deviations, essentially due to the effects of either temperature variations in the surface water and/or to an additional input of freshwater from melted icebergs (e.g. compare Cores PS1906 and PS1243), both leading to lower values. This finding appears to be in strong contrast to the carbon and oxygen values recorded during Stage 5. Surprisingly, the highest carbon values of similar magnitude recorded in the Holocene are not coeval with the lowest oxygen values of the last interglacial phase, which always appears during early Stage 5, that is Stage 5e (or the Eemian; Mangerud, 1989). Instead, the highest carbon values are noted much later during Stage 5, close to Stage 4, whereas Stage 5e values are indeed lower by about 0.5‰ in comparison to the Holocene.

Those parts in the cores which are assigned to Stage 11 show a very intriguing pattern in terms of the lateral distribution of stable isotopes. Cores M23063, PS1243, and PS1246 display their highest $\delta^{13}C$ values in Stage 11, but, whereas the oxygen values of about 3‰ indicate typically interglacial-like low values at the sites from the Norwegian Sea (Cores M23063 and PS1243), Core PS1246 from the western Iceland Sea records values close to 4‰. The $\delta^{13}C$ values in Core PS1906 during this time are lower in comparison to other stages of this core. But it should be noted that here the highest carbon values in Stage 11 slightly lag behind the lowest oxygen values. The same feature is also observed in Core PS1243, which for this time period seems to have the best sample resolution of all investigated cores. Despite the generally good stratigraphic agreement of Stage 11, there are some notable discrepancies among the cores concerning the proper position of the Stage 11/10 boundary, which could not be precisely determined with the present sample resolution.

In a previous study, the lowest part in Core PS1246 (~680 cm) has been assigned to Stage boundary 15/16 (Bauch, 1994b). This section is clearly not present in Cores PS1243 and M23063 and therefore it was not attempted to further subdivide this interval in Core PS1246.

Faunal distribution

It is beyond the scope of this study to discuss in detail any notable variation in faunal composition



Fiure 2. Glacial-interglacial stable oxygen (black curve) and carbon (grey curve) isotope records of the past 12 oxygen isotope stages analyzed on *N. pachyderma* (s) (approx. 450 ky). Arrows mark the peaks of the three most dominant interglacial phases. During these intervals test concentrations of planktic foraminifera were high and input of ice-rafted rock fragments by icebergs lowest, essentially indicating similar surface water conditions.

that might occur during, e.g., the Holocene section which of course could give valuable information on smaller-scaled oceanographic changes (Bauch & Weinelt, 1996); these Holocene to last glacial core sections were sampled in closer intervals than the older core sections and are therefore hardly comparable. But the way a full-interglacial subpolar assemblage evolved after a glacial maximum is illustrated in Fig. 3 for the Holocene and the last interglacial, the Eemian. Both, Holocene and Eemian faunal records show variations, however, the highest abundances of all interglacial-indicating species, i.e. subpolar species, are always noted during IRD-free sections only. Of all subpolar foraminifera in Core M23055 *T. quinqueloba* totals ~40% and is by far the most dominant species. The

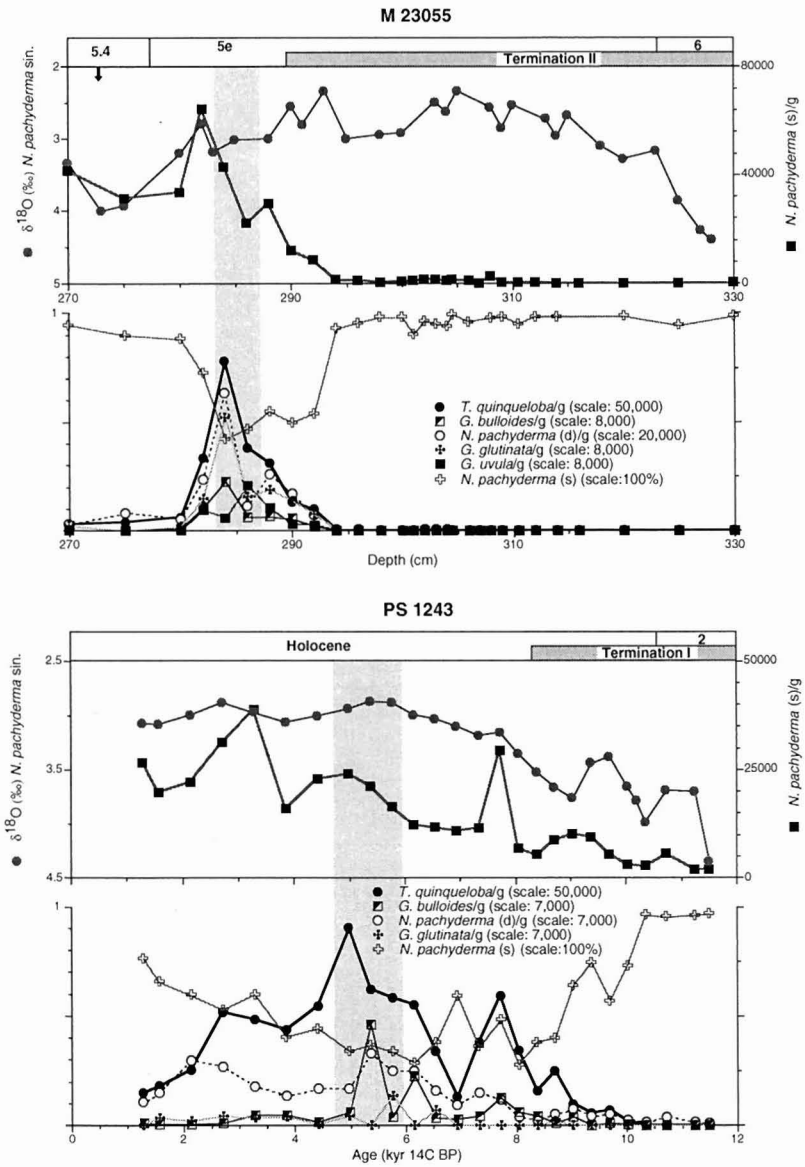


Figure 3. Distribution of the most dominant planktic foraminiferal species in the Holocene and across the last interglaciation, Stage 5e. The stratigraphy of Core PS1243 is based on radiocarbon ages (reservoir corrected by 400 years) and adopted from Bauch & Weinelt (1996). The duration of Termination I and II, i.e., the deglacial phase which preceded the Holocene and Stage 5e interglacial maximum, is deduced from the downcore distribution of ice-rafted rock fragments (adopted from Bauch *et al.*, 1996). The vertical shaded bars indicate the interglacial optimum in the Holocene and Stage 5e intervals when highest abundances of subpolar species are observed (numbers in parentheses refer to the top scale of the vertical axis).

remaining subpolar foraminifera only make up 18% of the assemblage altogether. If one compares the Eemian assemblage with that of the Holocene, then again all subpolar planktic foraminifera increase in test concentrations during the late deglaciation and, despite some obvious variability throughout the Holocene, reach their peaks between 6-5 ky BP (^{14}C) within the main phase of the hypsithermal with the highest Holocene temperatures (between 8-5 ky BP according to Nesje & Kvamme, 1991). *Turborotalita quinqueloba* once again dominates the subpolar fauna and moreover, makes up ~65% of the total assemblage during its peak at about 5 ky, whereas all other subpolar species do not even exceed 10% altogether. Although not shown here, but worth mentioning is the fact that the faunal species composition of the Holocene and Eemian sections is generally more diverse within the eastern cores from the Vøring Plateau and south of it, i.e. below the main track of Atlantic water (Bauch, 1993; Kellogg, 1980).

In the following section the glacial and interglacial distributional pattern of some of the more important species shown in Fig. 4a-f will be described for the time period since Stage 12.

Polar record

In this study the relative abundance of *N. pachyderma* (s) varies between 15-98% (Fig. 4a-f). Highest percentages are clearly related to typically glacial periods in all cores, whereas the lowest values are found in Cores M17732 and M23063 during the Holocene. Both of these sites are located below the modern track of warm Atlantic surface water. There is a clear signal of right coiling specimens between 30-40% in both size classes of Core M17732 during the Holocene. This is also seen in the Eemian section but with an enhanced relative dominance of the larger specimens over the smaller tests (17 to 40%). A similar pattern is noted in Core M23063 where larger specimens of *N. pachyderma* (d) dominate over smaller specimens during the Holocene but even more so during the Eemian. At the same time the relative abundance of *N. pachyderma* (s) in both cores is increased during the Eemian compared to the

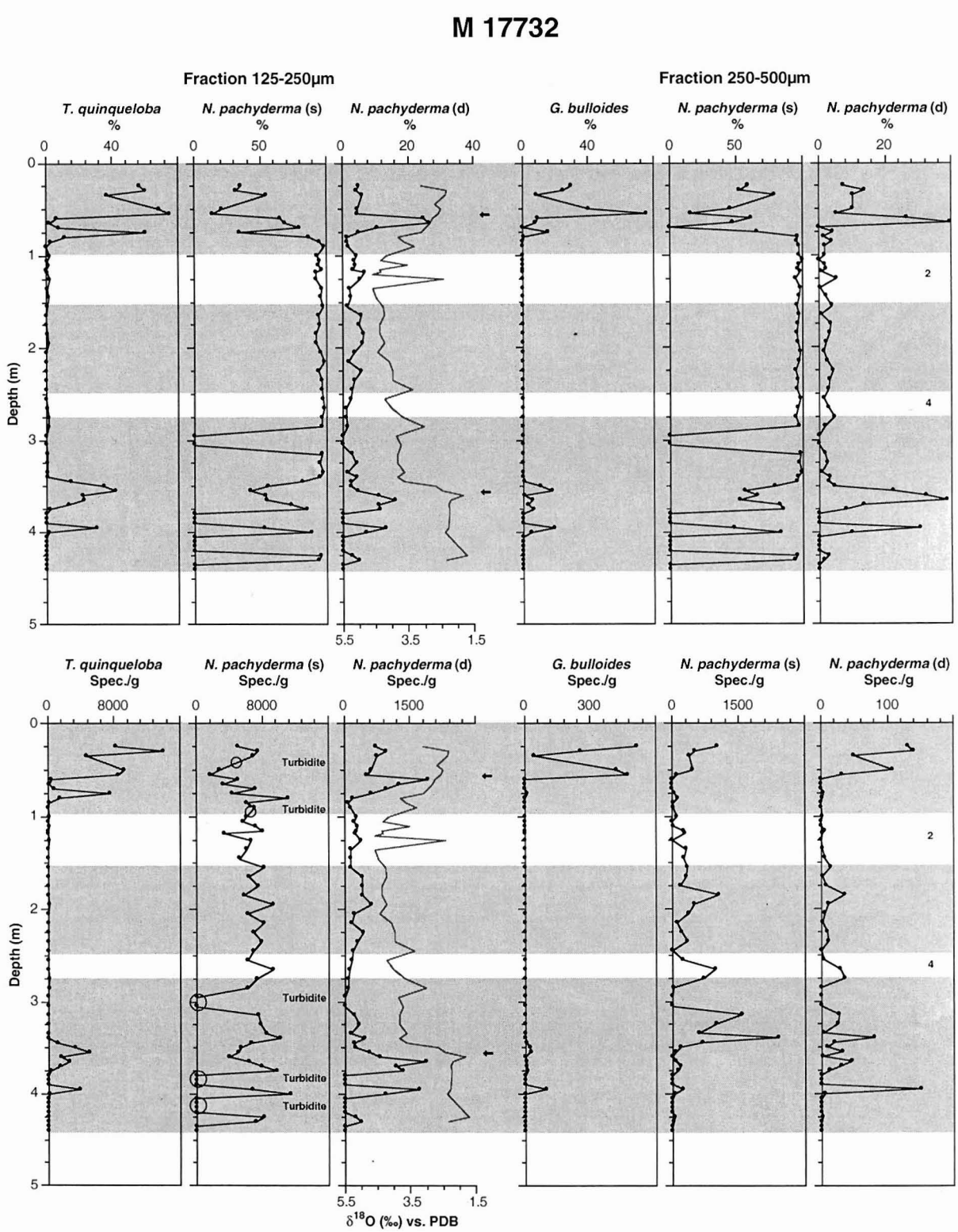


Figure 4a. Downcore variability of the dominant planktic foraminiferal species. Shown are the faunal results of the two size fractions 125-250 µm and 250-500 µm in comparison to planktic oxygen isotopes (grey curve) and relevant isotope stages. Arrows on oxygen isotope curves indicate the three most dominant interglacial phases.

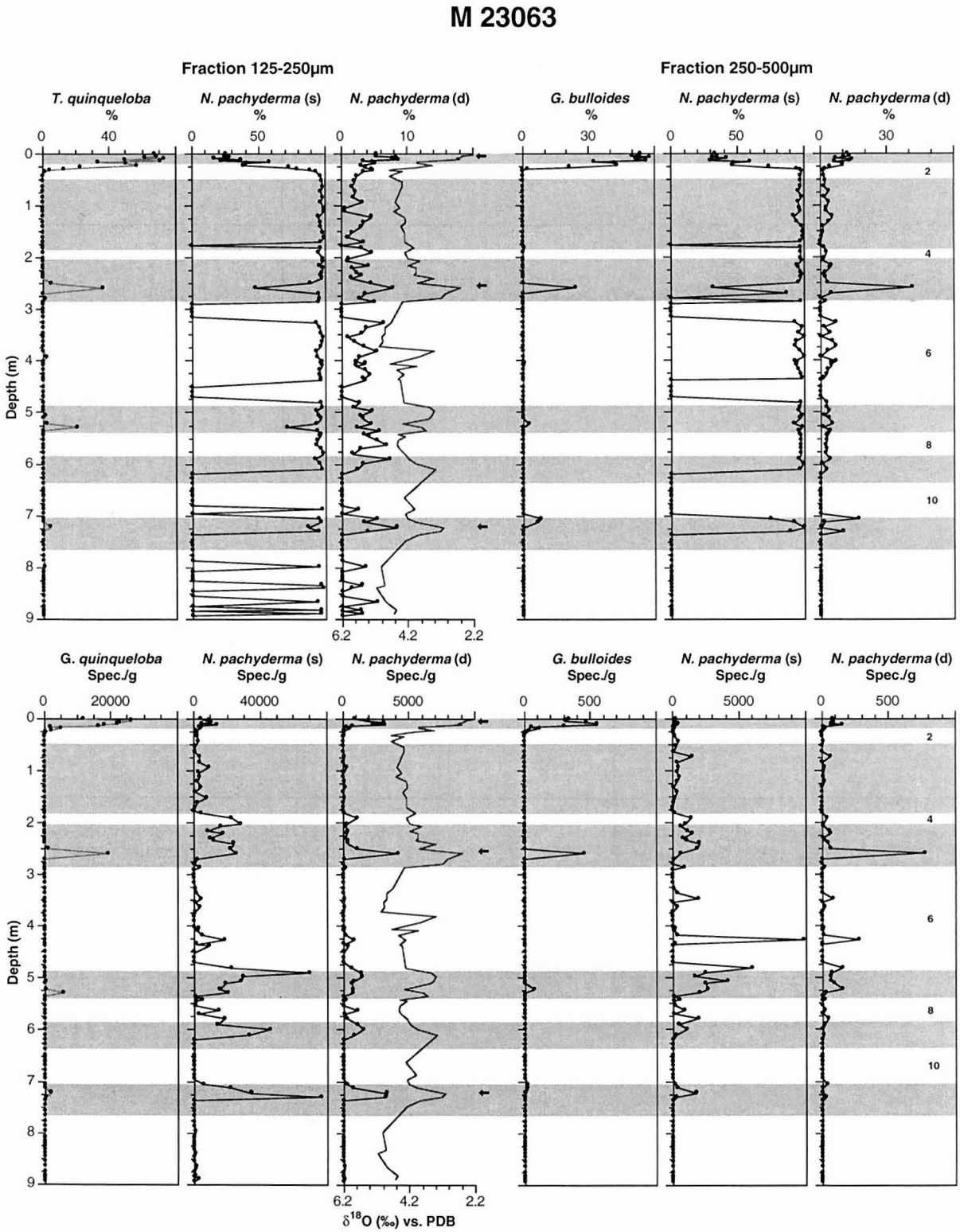


Figure 4b. Downcore variability of the dominant planktic foraminiferal species. Shown are the faunal results of the two size fractions 125-250 µm and 250-500 µm in comparison to planktic oxygen isotopes (grey curve) and relevant isotope stages. Arrows on oxygen isotope curves indicate the three most dominant interglacial phases.

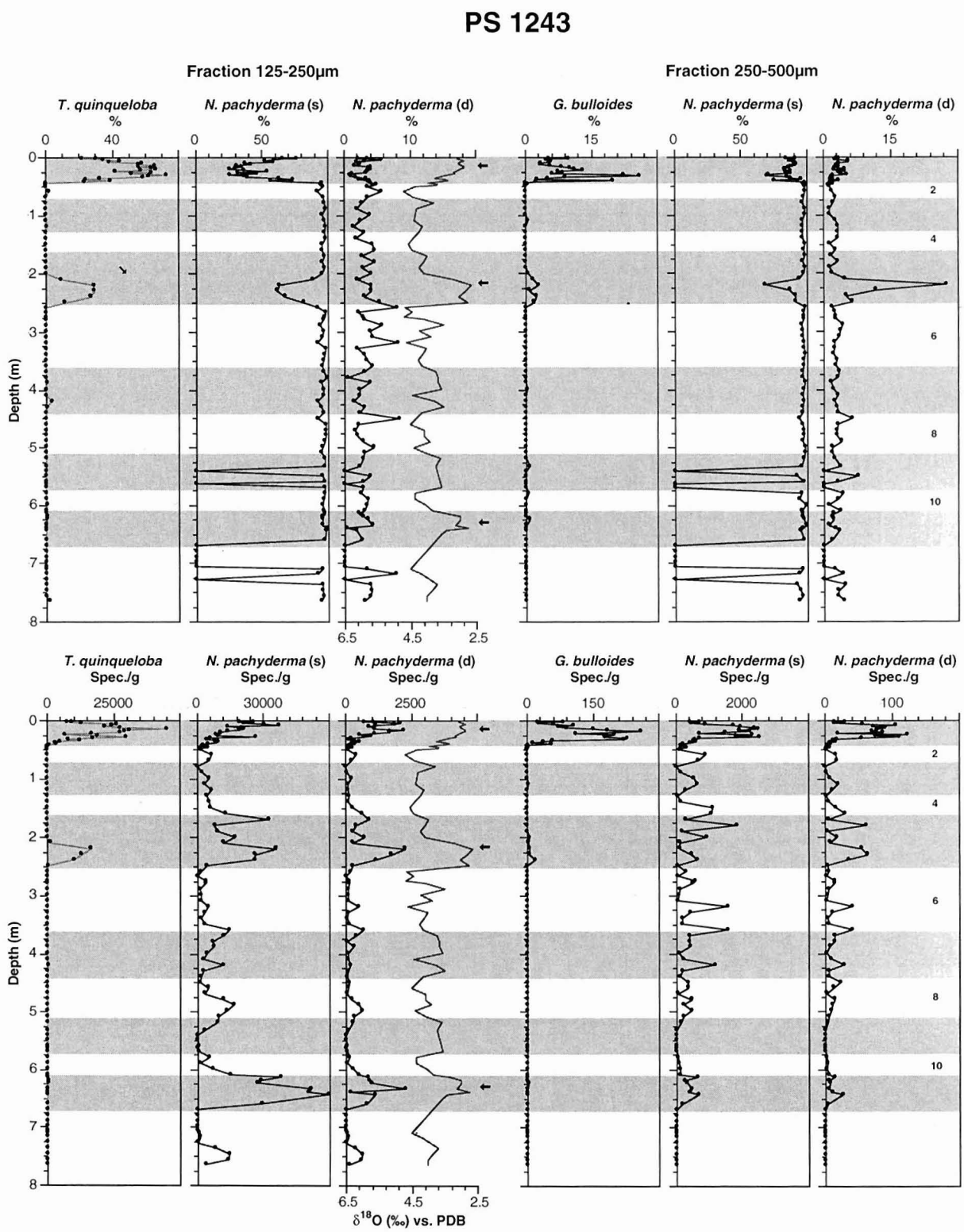
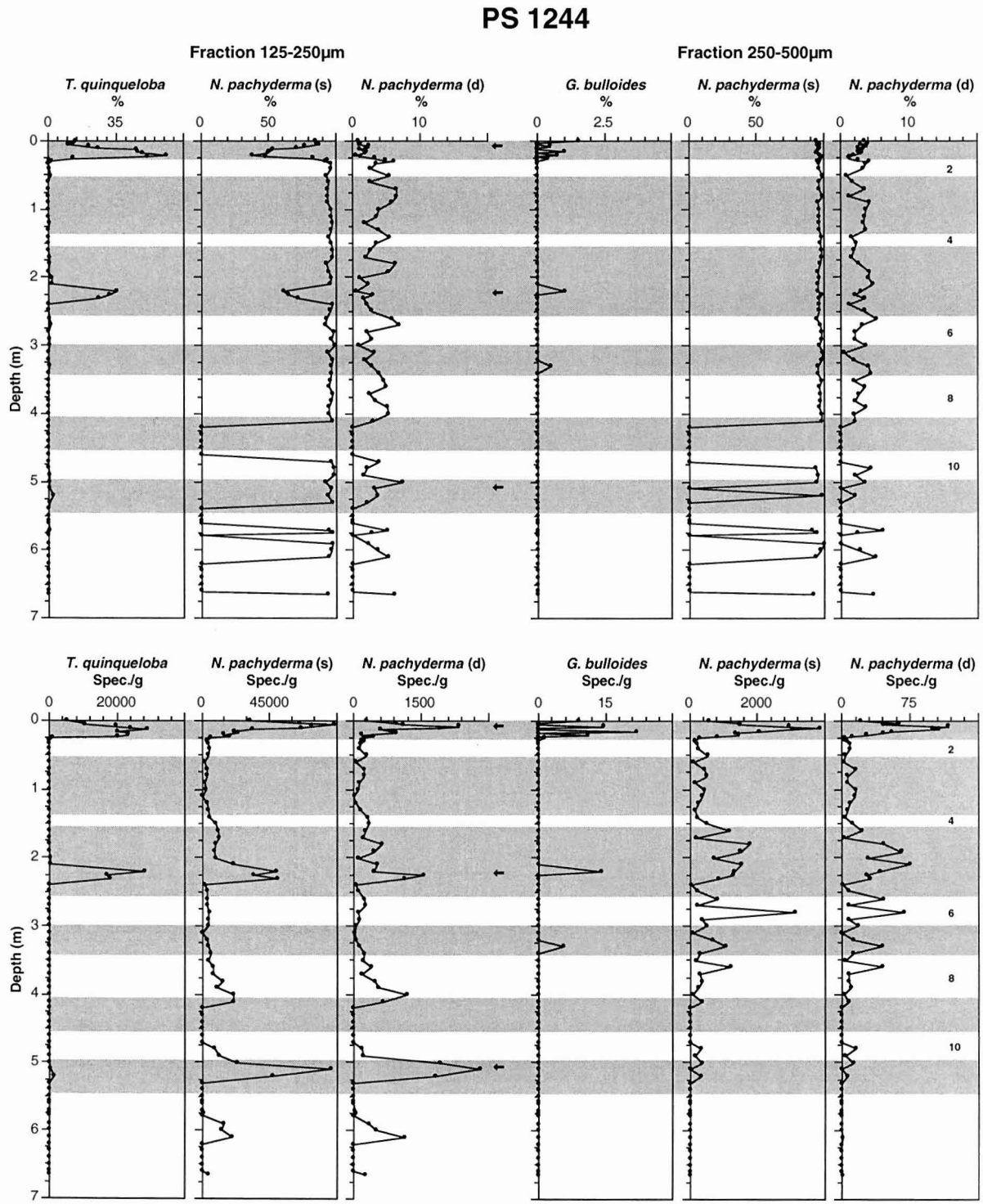


Figure 4c. Downcore variability of the dominant planktic foraminiferal species. Shown are the faunal results of the two size fractions 125-250 µm and 250-500 µm in comparison to planktic oxygen isotopes (grey curve) and relevant isotope stages. Arrows on oxygen isotope curves indicate the three most dominant interglacial phases.



Fiure 4d. Downcore variability of the dominant planktic foraminiferal species. Shown are the faunal results of the two size fractions 125-250 µm and 250-500 µm in comparison to planktic oxygen isotopes (grey curve) and relevant isotope stages. Arrows on oxygen isotope curves indicate the three most dominant interglacial phases.

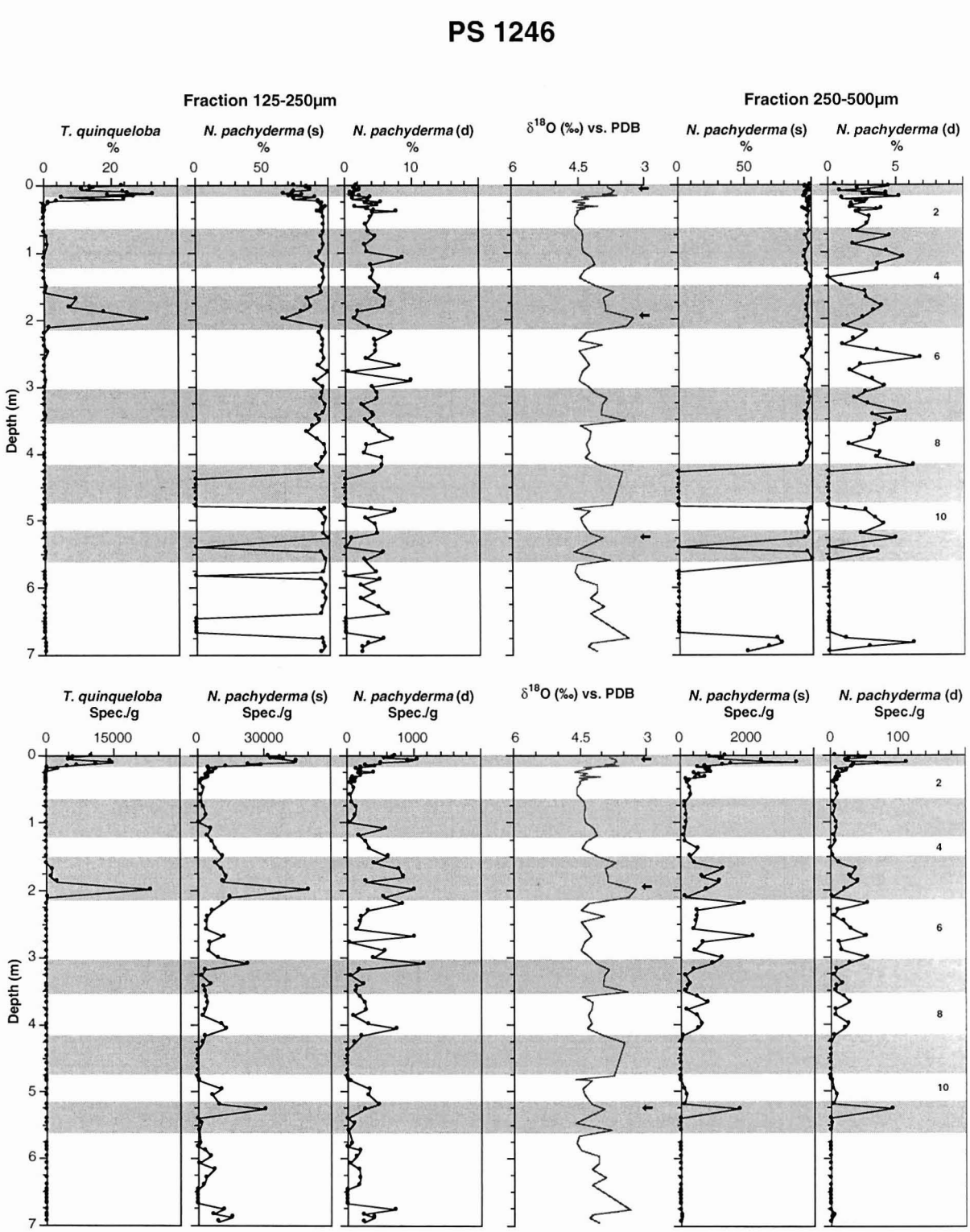


Figure 4e. Downcore variability of the dominant planktic foraminiferal species. Shown are the faunal results of the two size fractions 125-250 µm and 250-500 µm in comparison to planktic oxygen isotopes (grey curve) and relevant isotope stages. Arrows on oxygen isotope curves indicate the three most dominant interglacial phases.

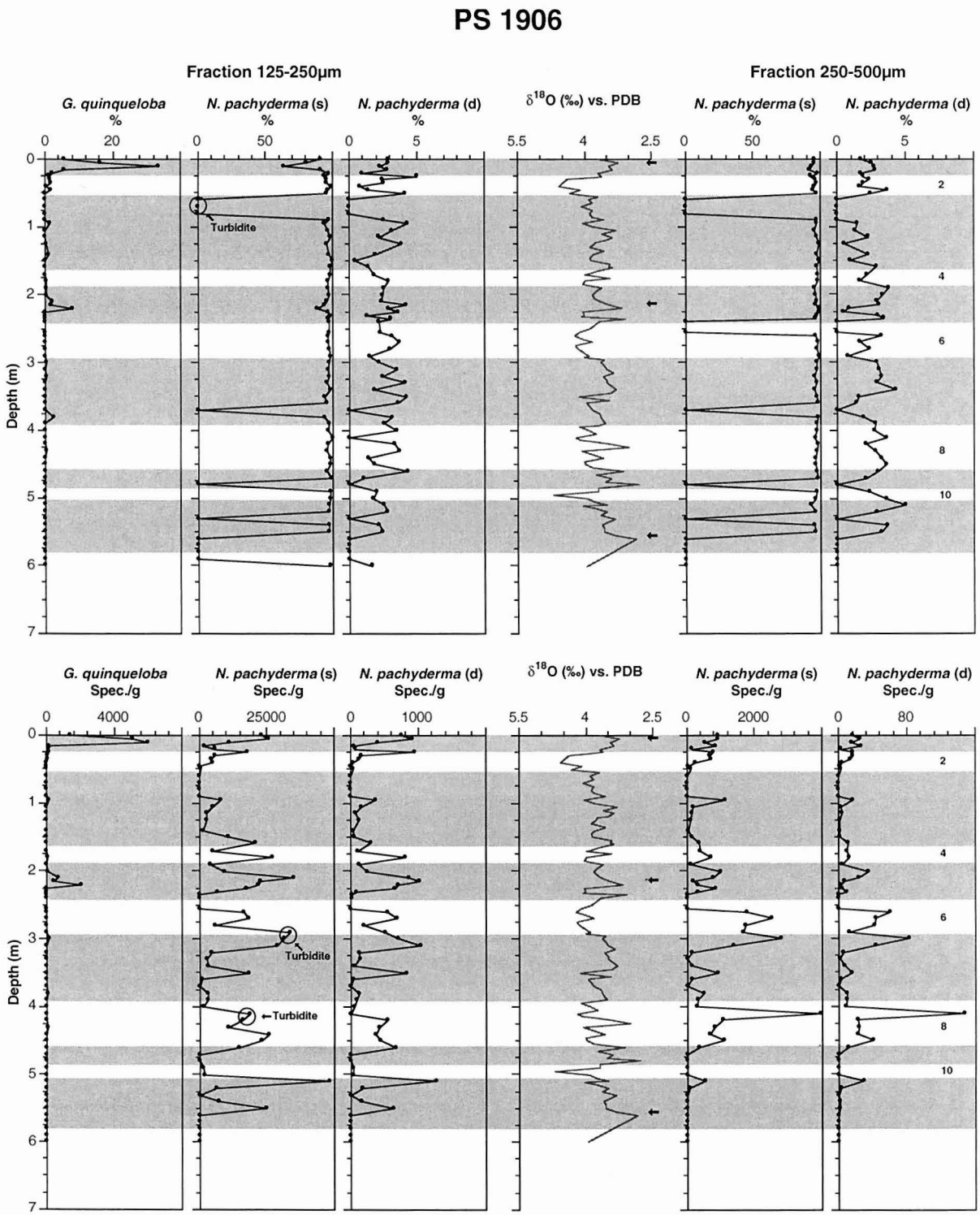


Figure 4f. Downcore variability of the dominant planktic foraminiferal species. Shown are the faunal results of the two size fractions 125-250 µm and 250-500 µm in comparison to planktic oxygen isotopes (grey curve) and relevant isotope stages. Arrows on oxygen isotope curves indicate the three most dominant interglacial phases.

Holocene. During the colder climate periods (Stages 3 and 4) *N. pachyderma* (s) is predominant. The further downcore record in Core M23063 reveals another notable drop in relative abundance of small-sized *N. pachyderma* (s) during early Stage 7 but with no response from the right coiling variety. This is only indicated in Stage 11 where *N. pachyderma* (d) records a slight increase.

If one compares relative abundances with test concentrations in Core M17732, the record of small-sized *N. pachyderma* (s) shows relatively constant values throughout, except for a significant decrease during the Eemian and the Holocene. In contrast *N. pachyderma* (d) indicates warm conditions during the Holocene and the Eemian whereas large-sized *N. pachyderma* (s) shows its peak abundances clearly after the Eemian (upper Stage 5) during Stage 4 and with one obvious increase in Stage 3. The test concentration record of small-sized *N. pachyderma* (s) and *N. pachyderma* (d) below Stage 5 is nearly coeval with major peaks in Stage 11, Stage 9 and late Stage 7 (Fig. 4b). Large-sized *N. pachyderma* (s) shows increased abundances during Stage 7, Stage 5, and with one minor spike in Stage 3. At this point it should be stressed that small-sized *N. pachyderma* (s) records highest test concentrations in Stage 11 (~80,000 tests) with a ratio to *N. pachyderma* (d) of about 24:1. Within the Eemian and the Holocene this ratio is 6:1 and 4:1, respectively. Obviously, this relation with a continuously decreasing dominance of *N. pachyderma* (s) over *N. pachyderma* (d) is caused solely by a reduction in test concentrations of *N. pachyderma* (s).

Overall, a similar pattern to that in Core M23063 is also recorded in Core PS1243 (Fig. 4c). This applies not only to the ratio of *N. pachyderma* (s) vs. *N. pachyderma* (d) in the small-size fraction but also to the major spike in relative abundance of large-sized *N. pachyderma* (d), which remains restricted to the Eemian time interval in all eastern cores (Fig. 4a-c). Further to the west, in Core PS1244 (Fig. 4d), the ratio between small-sized *N. pachyderma* (s) and *N. pachyderma* (d) is about 30:1 during all three major interglacials whereas in Core PS1246 (Fig. 4e) this relation varies between 40:1, 50:1, and 60:1 during the Holocene, Eemian and Stage 11, respectively. In both of these cores from the Iceland Plateau, the prominent spike in relative abundance of large-sized *N. pachyderma* (d) which is so dominant in the Eemian interval of the eastern cores, has totally vanished. The gradual decrease in predominance of *N. pachyderma* (s) over *N. pachyderma* (d) from Stage 11 through the Eemian down to the Holocene also remains in the foraminiferal record of Core PS1906 (Fig. 4f) with ratios of 40:1, 35:1, and 25:1, respectively. Although this site appears to be prone to turbidites which may have led to some size-sorted foraminiferal layers at core depth ~300 and ~415 cm (Hamich, 1991), the records from the Iceland Plateau indicate that the relative abundance of large-sized *N. pachyderma* (d) shows no major increase during the Eemian interval. Yet, it is noted from the test concentration record in these cores that both large-sized varieties reveal some variability thoughout Stages 7-5.

In summary, the following main features are observed:

- In all cores, both small-sized varieties of *N. pachyderma* are somehow related to each other during the last two interglacials in showing coeval records of test concentrations and relative abundances.
- On a one to one ratio based on interglacial test concentrations, the dominance of *N. pachyderma* (s) clearly decreases over *N. pachyderma* (d) from interglacial Stage 11, over Stage 5e, to the Holocene.
- A significant increase in relative abundance of the large-sized variety of *N. pachyderma* (d) is indicative for the Eemian interval only and is confined to cores from the modern Atlantic Domain.

Subpolar record

As already noted from the faunal distribution pattern in Fig. 3, true subpolar species increase during full interglacial conditions only after glacial conditions have vanished. Among this subpolar assemblage, *T. quinqueloba* and *G. bulloides* are the most dominant species due to high test concentrations per sample and/or size fraction. Accordingly, they have a strong interpretative basis and appear to be more suitable as paleoceanographic tools than the other species. Moreover, as will be shown, they also reveal a distinct lateral distribution in the Nordic seas.

The downcore faunal data for *T. quinqueloba* and *G. bulloides* are given in Fig. 4a-f alongside those of *N. pachyderma*. Both species show increased relative and test concentration abundances during interglacial phases. Taking the record from Core M23063 (Fig. 4b) as representative of the eastern Nordic seas, both species display steady increases in test concentrations since Stage 11, with the highest numbers recognized in the Holocene. Beside these records in Stage 11, the Eemian, and the Holocene, increased abundances are also observed during early Stage 7. Towards the west and onto the Iceland Plateau, (i.e. towards decreasing modern surface water temperatures), the distinct downcore pattern from Core M23063 displays some major changes (Fig. 4b-e). The subpolar record of Stage 11 is basically vanished west of Core PS1243. In comparison with Core M23063 the Eemian and Holocene abundance record of *G.*

bulloides is reduced by more than 50% in Core PS1243 and without significance in Core PS1244. If one follows the Eemian and Holocene pattern in each core from the east towards the west, the dominance of the subpolar species in the Holocene over that in the Eemian as revealed by the eastern cores (Fig 4a-c) is already reduced at site PS1244 and eventually is opposite in Core PS1246 (Fig. 4d-e). This is so despite the fact that much lower sample resolution were applied on these Eemian sections than on the Holocene core intervals. In relation to this finding, Core PS1906 with lowest modern surface water temperatures did not yield any subpolar specimens in Stage 11 at all and *G. bulloides* was encountered neither in the Eemian nor in the Holocene. However, based on the relation of the Eemian and Holocene abundance record of *T. quinqueloba* together with the oxygen isotope record, Core PS1906 appears to be similar to Core M23063.
In summary, the subpolar record is as follows:

- The stratigraphical occurrence of *T. quinqueloba* and *G. bulloides* is mainly tied to the Holocene, the Eemian, and Stage 11 with the least response in the latter interglacial.
- The spatial distribution pattern of *G. bulloides* is strongly water mass dependent, being confined to the area which is mostly influenced by Atlantic surface water.
- *Turborotalita quinqueloba* exhibits a wide distributional pattern in the Nordic seas, and is most dominant in the Holocene and Eemian intervals.
- Both *G. bulloides* and *T. quinqueloba* are inversely related to *N. pachyderma* (s) in that their abundances have steadily increased during all three main interglacials since Stage 11, whereas test concentrations of the polar species became reduced during the same time.

A similar change as observed in the faunal pattern of *T. quinqueloba* is recognized in the oxygen isotopes. Oxygen values of Stage 11 are always slightly higher than Eemian and Holocene values in most cores. Although maybe not very well represented in Cores M17732 and M23063 (the top in Core M17732 is missing and the actual Eemian peak in Core M23063 may not be completely sampled), many isotope records from the Norwegian Sea show similar planktic oxygen values during the Eemian and Holocene (Vogelsang, 1990). Taking this at face value there is a definite change in Core PS1246. Here, oxygen values in the Eemian are about 0.3‰ lower than in the Holocene.

PALEOCEANOGRAPHIC INTERPRETATION

Stage 11

In terms of terrestrial Pleistocene terminology, Sarnthein *et al.* (1986) and Shackleton (1987) correlated marine isotope Stage 11 with the Holsteinian warm phase. This is in contrast to studies by Sejrup & Knudsen (1993) who indicate ages which would place the Holsteinian into oxygen Stage 7 rather than into Stage 11. Regardless of this controversy, in Nordic seas sediments only oxygen Stage 11, Stage 5e and the Holocene represent prolonged time intervals which are barren of any IRD (e.g. Birgisdottir, 1990). This inevitably means that iceberg-melting was low in Stage 11 and hence, the chance that meltwater influenced the water mass circulation in the sense of Broecker & Denton (1989) must have been small also.

The lack of a proper subpolar planktic foraminiferal fauna with 'interglacial-type' abundances (i.e. Eemian or Holocene) is hard to reconcile with the present knowledge of typically glacial and interglacial water mass circulation in the N. Atlantic region. Based on the planktic foraminiferal distribution, it must be assumed (if at all) that the main mass of Atlantic surface water penetrated the Nordic seas as a strong eastern boundary current. Therefore, all cores used in this study would fall within a relatively cold water mass regime with polar imprint. Despite the fact that most areas of the Nordic seas were under strong influence of these polar water masses, a modern-like east to west and southeast to north temperature gradient obviously still existed. A decreasing temperature gradient towards Greenland with 'warm' species in the Norwegian Sea can also be inferred from coccolith studies (Bleil & Gard, 1989; Henrich & Baumann, 1994).

The large easterly expansion of polar surface water masses during Stage 11 may be also reflected in the planktic stable isotope records. Planktic carbon isotope records and their interpretations are much debated, because of a series of complicating factors. These arise from species-dependent 'vital effects' and depth-habitat changes, as well as global sea water $\delta^{13}C$ variations of total CO_2 due to gas exchange with the atmosphere in combination with local primary productivity in the surface water (e.g., Berger *et al.*, 1981). However, if it is still assumed that higher planktic carbon isotope values also reflect enhanced surface water ventilation to some degree (Labeyrie & Duplessy, 1985; Vogelsang, 1990), as it is the case with some benthic species (e.g., *Cibicidoides wuellerstorfi*), then the high carbon values observed in Stage 11 are due to the highest ventilation rate observed in these cores. Interestingly, a close modern analogue to these Stage 11 values is only noticed in Core PS1906. As this site is located near the Polar Front it not only has the lowest summer surface temperatures of all studied sites (Table 1), it is also strongly affected perennially by sea-ice cover (Thiede & Hempel, 1991). Recent data from this area with sea-ice cover

indicate a non-equilibrium state between atmosphere and surface water (Johannessen *et al.*, 1994). Holocene $\delta^{13}C$ values of *N. pachyderma* (s) which would match the values observed in Stage 11 are reported from surface sediments of the ice-covered Arctic Ocean (Spielhagen & Erlenkeuser, 1994). Therefore it appears unlikely that the very high $\delta^{13}C$ values in Stage 11 are caused by intense ventilation processes. This assumption is corroborated by a total lack of all epibenthic-living foraminifera, including *C. wuellerstorfi*, which is rather untypical for interglacials (Belanger & Streeter, 1980; Streeter *et al.*, 1982; Struck, 1992). Instead, the benthic foraminiferal assemblage is entirely composed of endobenthic-living species. Although the actual number of species is relatively high (Struck, this volume), an endobenthic assemblage is more typical for glacial rather than interglacial periods when thermohaline advection was reduced (Struck, 1995). In conclusion, it appears that the Nordic seas were covered by sea-ice most of the year, the summer season was relatively cold but ice-free, thus providing favourable conditions for *N. pachyderma* (s).

Stage 9-7

The paleoceanographic situation in Stages 9 to 8 was that relatively cold conditions must have prevailed since the planktic foraminiferal assemblage was made up of *N. pachyderma* only. A similar picture is given by coccolith data which indicate a minor inflow of warmer Atlantic surface water (Bleil & Gard, 1989; Baumann, 1990). Nevertheless, the benthic foraminiferal record for this time period shows high test concentration of *C. wuellerstorfi*, which indicates good ventilation of the water masses (Vogelsang, 1990; Struck, this volume). In general the situation did not change a great deal during Stage 7, except for the fact that there was an increase in warmer Atlantic surface water which influenced the eastern Nordic seas. This situation led to a slight increase of subpolar abundances at the beginning of Stage 7, whereas the upper part of Stage 7 is dominated by *N. pachyderma* again.

The general lack of warm water indicating species during Stages 9 and 7 in particular is in contrast to faunal data from the NE Atlantic (~55°N) where both oxygen isotope stages appear as typical interglacials (Ruddiman & McIntyre, 1976; Ruddiman *et al.*, 1986). This would mean that during these times a relatively steep temperature gradient between the Nordic seas and the NE Atlantic must have existed.

Eemian and Holocene

Based on a transfer function to calculate sea surface temperature estimates (SST), Kellogg (1980) reconstructed the paleoceanographic situation for the Eemian and Holocene time interval in great detail and concluded that these periods showed only minor differences. The work by Haake & Pflaumann (1989) essentially came to the same results. They also calculated SSTs which for the northern Norwegian Sea indicate slightly cooler SSTs in the Eemian than in the Holocene. With respect to the present study a simple evaluation of the test concentration record of *T. quinqueloba* is in absolute agreement with this statement. But in addition, this study has also shown that, if *T. quinqueloba* is taken as representative for peak interglacial conditions, then the conditions in the Iceland Sea were relatively warmer during the Eemian than during the Holocene. Moreover, this conclusion gains strong support from the oxygen isotope data which also would indicate this relation. Essentially this means that the east to west surface water temperature gradient was less steep in the Eemian compared to the Holocene, but that the southeast to north temperature decrease was maintained, possibly even reenforced.

PLANKTIC FORAMINIFERA AS PALEOCEANOGRAPHIC PROXY

In this study it was clearly indicated that using the same data base, relative and absolute abundances on their own may lead to different interpretations. This is probably best demonstrated using the different varieties of *N. pachyderma*. It has long been known that different coiling directions in *N. pachyderma* are somehow related to surface water temperatures (e.g. Ericson, 1959). Furthermore, it has been stated that the left coiling variety (s) makes up more than 95% of the assemblage in waters below ~5°C and that this variety has in general a preference for regions with water temperatures below 10°C (Bé & Tolderlund, 1971; Kellogg, 1980). But as yet, it is not known from a biophysiological point of view why even in the Arctic Ocean under most severe polar conditions, *N. pachyderma* (s) is always accompanied by some percentages of right coiling specimens (Carstens & Wefer, 1992). But despite the well known coiling ratios, *N. pachyderma* exhibits also a wide range of test morphologies (Kennett, 1968; Keller, 1978; Reynolds & Thunnell, 1986) among which changes in size have been applied as surface water proxy in previous studies (Malmgren & Kennett, 1978).

The cores from the Norwegian Sea have underlined the significance of relative abundances of *N. pachyderma* (d) for identifying an Atlantic-type water mass during the Eemian and the Holocene. But already in slightly cooler regions of the Nordic seas, relative abundances do not respond positively any more to these peak interglacial conditions. Interestingly, there still is a positive response in the

large-sized variety of *N. pachyderma* (d) but then only in the Eemian interval. This may imply that different test size varieties inhabit different water masses. *Neogloboquadrina pachyderma* (s) is known to show large differences in depth migration during its life cycle, ranging from below 100m to possibly two hundred meters depth for open water conditions (Hemleben *et al.*, 1989). It, therefore, reflects deeper water below the thermocline rather than the actual surface. But depending on the specific conditions, the upper depth limit in particular may be lower. During ice-covered seasons of the Fram Strait area and the Arctic Ocean, the depth range of *N. pachyderma* sin. seems to be related to a shallower habitat (Carstens & Wefer, 1992).

At those sites with cooler modern temperatures the downcore relative abundance of small-sized *N. pachyderma* (d) varies only on a minor scale almost regardless of glacial or interglacial climatic mode. Therefore, one should refrain from using *N. pachyderma* (d) as a proxy when it makes up less than 15-20% of the assemblage. Overall, the covarying downcore test concentration records of small-sized *N. pachyderma* indicates that the right and left coiling varieties are somehow related to each other, although with notable lags in peak interglacials (Fig. 3, 4a). On the other hand, the fact that ratios of *N. pachyderma* (s) to *N. pachyderma* (d) vary between Stage 11, the Eemian and the Holocene, due to changes in test concentrations of *N. pachyderma* (s) only, may suggest that both forms of the species have different ecological preferences. These may be related to the particular depth habitat and/or by a seasonal off-set in productivity (Reynolds & Thunell, 1986).

Among all subpolar species in the Nordic seas *T. quinqueloba* reflects best interglacial conditions marked by a Holocene-type thermohaline circulation. Furthermore, since this species contains symbionts, its habitat is restricted to the photic zone of the upper surface water, i.e., <100 m (Hemleben *et al.*, 1989). It has been demonstrated in detail that this comparatively small-sized species develops even smaller tests in cooler waters (Bauch, 1992). This is a crucial issue when evaluating the SST estimates based on foraminiferal counts as compiled by CLIMAP workers (1981) since these relied on the >150 µm mesh size. This may be the reason why the inferred relatively warm surface waters in the western Iceland Sea in Eemian times as noted in this study were not recognized previously (Kellogg, 1980).

When comparing all three major interglacials, Stages 11, 5e, and the Holocene, it is concluded that none of them are alike. Although environmental constraints such as low global ice volume and the lack of drifting icebergs were essentially the same during all of these intervals, the combined investigation of planktic stable isotope and foraminiferal assemblage data reveal major discrepancies in these surface water proxies. They were most likely induced by very different types of Atlantic water mass inflow, which led to the formation of temperature gradients which are not known from the modern Nordic seas. Thus, further detailed studies of the Eemian and Stage 11 should provide more insight into the system of Atlantic thermohaline circulation at high latitudes and help decipher the natural variability of this important climate mechanism.

ACKNOWLEDGEMENT

A large proportion of the data presented in this study were generated as part of "Project B2" of the *Sonderforschungsbereich 313* (publication No. 322) at Kiel University, which is funded by the *Deutsche Forschungsgemeinschaft*. Accordingly, I express my thanks to E. Vogelsang, A. Aichinger, L. Birgisdottir, A. Dettmer, and M. Weinelt who essentially provided most of the stable isotope data. I am also indebted to Helmut Erlenkeuser and his team at the Leibniz Laboratory of Kiel University for isotopically analyzing these samples and to valuable anonymous review comments.

REFERENCES

Bauch, H.A. 1992. Test size variation of planktic foraminifers as response to climatic changes. 4th International Conference on Paleoceanography (ICP), *GEOMAR Report*, **15**, 56.

Bauch, H.A. 1993. Planktische Foraminiferen im Europäischen Nordmeer - ihre Bedeutung für die paläozeanographische Interpretation während der letzten 600.000 Jahre. *Berichte aus dem Sonderforschungsbereich 313*, **40**, 1-108.

Bauch, H.A. 1994a. Significance of variability in *Turborotalita quinqueloba* (Natland) test size and abundance for paleoceanographic interpretations in the Norwegian-Greenland Sea. *Marine Geology*, **121**, 129-141.

Bauch, H.A. 1994b. *Beella megastoma* (Earland) in late Pleistocene Norwegian-Greenland Sea sediments: Stratigraphy and meltwater implication. *Journal of Foraminiferal Research*, **24**, 171-177.

Bauch, H.A. & Weinelt, M.S. 1997. Surface water changes in the Norwegian Sea during last deglacial and Holocene times. *Quaternary Science Reviews*, in press.

Bauch, H.A., Erlenkeuser, H., Grootes, P.M. & Jouzel, J. 1996. High latitude stratigraphic and paleoclimatic records of the last interglaciation: Implications from the Nordic seas. *Quaternary Research*, **46**, 260-269.

Baumann, K.-H., Lackschewitz, K.S., Erlenkeuser, H., Henrich, R. & Jünger, B. 1993. Late Quaternary calcium carbonate sedimentation and terrigenous input along the east Greenland continental margin. *Marine Geology*, **114**, 13-36.

Baumann, K.-H. & Matthiessen, J. 1992. Variations in surface water mass conditions in the Norwegian Sea: Evidence from Holocene coccolith and dinoflagellate cyst assemblages. *Marine Micropaleontology*, **20**, 129-146.

Baumann, K.-H., Lackschewitz, K.S., Mangerud, J., Spiel-

hagen, R.F., Wolf-Welling, T.C.W, Henrich, R. & Kassens, H. 1995. Reflections of Scandinavian ice sheet fluctuations in Norwegian Sea sediments during the past 150.000 years. *Quaternary Research*, **43**, 185-197.

Bé, A.W.H. & Tolderlund, D.S. 1971. Distribution and ecology of living planktonic foraminifera in surface waters of the Atlantic and Indian Oceans. *In:* Funnel, B.M. & Riedel, W.R. (eds.), *The Micropaleontology of the Oceans*, 105-149 Cambridge University Press, Cambridge.

Belanger, P.E. & Streeter, S.S. 1980. Distribution and ecology of benthic foraminifera in the Norwegian-Greenland Sea. *Marine Micropaleontology*, **5**, 401-428.

Berger, W.H., Bé, A.W.H. & Vincent, E. 1981. Oxygen and carbon isotopes in foraminifera. *Palaeogeography, Palaeoclimatology, Palaeoecology*, **33**, 277.

Birgisdottir, L. 1990. Die paläo-ozeanographische Entwicklung der Island See in den letzten 550.000 Jahren. *Berichte aus dem Sonderforschungsbereich 313*, **34**, 1-112.

Bleil, U. & Gard, G. 1989. Chronology and correlation of Quaternary magnetostratigraphy and nannofossil biostratigraphy in Norwegian-Greenland Sea sediments. *Geologische Rundschau*, **78**, 1173-1187.

Broecker, W.S. & Denton, G.H. 1989. The role of ocean-atmosphere reorganizations in glacial cycles. *Geochimica et Cosmochimica Acta*, **53**, 2465-2501.

Carstens, J. & Wefer, G. 1992. Recent distribution of planktonic foraminifera in the Nansen Basin, Arctic Ocean. *Deep-Sea Research*, **39**, 507-524.

CLIMAP Project Members 1976. The surface of the ice-age earths. *Science*, **191**, 1131-1137.

CLIMAP Project Members 1981. Seasonal reconstructions of the earth's surface at the last glacial maximum. *Geological Society America*, GSA Map Chart Series MC-36, Boulder, Colorado.

Dietrich, G. 1969. Atlas of the hydrography of the Northern North Atlantic Ocean. *Conseil International pour L'Exploration de la Mer Service Hydrographique*, 140 pp., Chalottenlund Slot, Denmark.

Ericson, D.B. 1959. Coiling direction of *Globigerina pachyderma* as a climatic index. *Science*, **130**, 219-220.

Haake, F.W. & Pflaumann, U. 1989. Late Pleistocene foraminiferal stratigraphy on the Vøring Plateau, Norwegian Sea. *Boreas*, **18**, 343-356.

Hamich, A., 1991. Sedimentologische Untersuchungen eines Kernes (GIK PS1906-2) der Grönlandsee, unpubl. MSc thesis, Kiel University, 78pp.

Hays, J.D., Imbrie, J. & Shackleton, N.J. 1976. Variations in the earth`s orbit: pacemaker of the Ice Ages. *Science*, **194**, 1121-1132.

Healy-Williams, N. 1992. Stable isotope differences among morphotypes of *Neogloboquadrina pachyderma* (Ehrenberg): implications for high-latitude palaeoceanographic studies. *Terra Nova*, **4**, 693-700.

Hebbeln, D., Dokken, T., Andersen, E.S., Hald, M. & Elverhoi, A. 1994. Moisture supply for northern ice-sheet growth during the Last Glacial Maximum. *Nature*, **370**, 357-360.

Hemleben, C., Spindler, M. & Anderson, O.R. 1989. *Modern planktonic foraminifera*. 363 pp., Springer Verlag, New York.

Henrich, R. & Baumann, K.-H. 1994. Evolution of the Norwegian current and the Scandinavian ice-sheets during the past 2.6 m.y.: evidence from ODP Leg 104 biogenic carbonate and terrigenous records. *Palaeogeography, Palaeoclimatology, Palaeoecology*, **108**, 75-94.

Imbrie, J., Berger, A., Boyle, E.A., Clemens, S.C., Duffy, A., Howard, W.R., Kukla, G., Kutzbach, J., Martinson, D.G., McIntyre, A., Mix, A.C., Molfino, B., Morley, J.J., Peterson, L.C., Pisias, N.G., Prell, W.L., Raymo, M.E., Shackleton, N.J. & Toggweiler, J.R. 1993. On the structure and origin of major glaciation cycles: 2. The 100,000-year cycle. *Paleoceanography*, **8**, 699-735.

Imbrie, J., Hays, J.D., Martinson, D.G., McIntyre, A., Mix, A.C., Morley, J.J., Pisias, N.G., Prell, W.L. & Shackleton, N.J. 1984. The orbital theory of Pleistocene climate: support from a revised chronology of the marine $\delta^{18}O$ record, *In*: Berger, A. et al. (eds.), Milankovitch and Climate, Part I, D. Reidel, Dordrecht, 269-305.

Jansen, E. & Bjørklund, K.R. 1985. Surface ocean circulation in the Norwegian Sea, 15,000 B.P. to present. *Boreas*, **14**, 243-257.

Johannessen, T., Jansen, E., Flatøy, A. & Ravelo, A. 1994. The relationship between surface water masses, oceanographic fronts and paleoclimatic proxies in surface sediments of the Greenland, Iceland, Norwegian Seas. *In:* Zahn, R., Kaminski, M.A. & Labeyrie, L. (eds.), *Carbon cycling in the glacial ocean: Constraints of the ocean's role in global change*, 61-85, Springer, Berlin.

Keller, G. 1978. Morphologic variation of *Neogloboquadrina pachyderma* (Ehrenberg) in sediments of the marginal and central Northeast Pacific Ocean and paleoclimatic interpretation. *Journal of Foraminiferal Research*, **8**, 208-224.

Kellogg, T.B. 1975. Late Quaternary climatic changes in the Norwegian-Greenland Sea. *In:* Bowling, S.A. & Weller, G. (eds.) *Climate of the Arctic*, 3-36, University of Fairbanks, Alaska.

Kellogg, T., Duplessy, J. & Shackleton, N. 1978. Planktonic foraminiferal and oxygen isotopic stratigraphy and paleoclimatology of Norwegian Sea deep-sea cores. *Boreas*, **7**, 61-73.

Kellogg, T.B. 1976. Late Quaternary climatic changes: Evidence from the deep-sea cores of Norwegian and Greenland Seas. *Geological Society of America Memoir*, **145**, 77-110.

Kellogg, T.B. 1977. Paleoclimatology and paleo-oceanography of the Norwegian and Greenland Seas: The last 450.000 years. *Marine Micropaleontology*, **2**, 235-249.

Kellogg, T.B. 1980. Paleoclimatology and paleoceanography of the Norwegian and Greenland Seas: Glacial-interglacial contrasts. *Boreas*, **9**, 115-137.

Kellogg, T.B. 1984. Paleoclimatic significance of subpolar foraminifera in high-latitude marine sediments. *Canadian Journal of Earth Science*, **21**, 189-193.

Kennett, J.P. & Srinivasan, M.S. 1983. *Neogene planktonic foraminifera*, 265 pp., Hutchinson Ross Publishing Company, Stroudsburg.

Kennett, J.P. 1968. Latitudinal variation in *Globigerina pachyderma* (Ehrenberg) in surface sediments of the south-west Pacific Ocean. Micropaleontology, **14**, 305-318.

Kipp, N.G. 1976. New transfer function for estimating past sea-surface conditions from sea-bed distribution of planktonic foraminiferal assemblages in the North Atlantic. *Geological Society of America Memoir*, **145**, 3-41.

Koç-Karpuz, N. & Jansen, E. 1992. A high-resolution diatom record of the last deglaciation from the SE Norwegian Sea; documentation of rapid climatic changes. *Paleoceanography*, **7**, 499-520.

Labeyrie, L.D. & Duplessy, J.-C. 1985. Changes in the oceanic (13)C/(12)C ratio during the last 140.000 years; high-latitude surface water records. *Palaeogeography, Palaeoclimatology, Palaeoecology*, **50**, 217-240.

Malmgren, B.A. & Kennett, J.P. 1978. Late Quaternary paleoclimatic applications of mean size variations in *Globigerina bulloides* D'Orbigny in the Southern Indian

Ocean. *Journal of Paleontology*, **52**, 1195-1207.

Mangerud, J. 1989. Correlation of the Eemian and the Weichselian with deep sea oxygen isotope stratigraphy. *Quaternary International*, **3/4**, 1-4.

Martinson, D.G., Pisias, N.G., Hays, J.D., Imbrie, J., Moore, T.C. & Shackleton, N.J. 1987. Age dating and the orbital theory of the Ice Ages: Development of a high-resolution 0 to 300.000 years chronostratigraphy. *Quaternary Research*, **27**, 1-29.

Nesje, A. & Kvamme, M. 1991. Holocene glacier and climate variations in western Norway: Evidence for early Holocene glacier demise and multiple Neoglacial events. *Geology*, **19**, 610-612.

Reynolds, L.A. & Thunell, R.C. 1986. Seasonal production and morphologic variation of *Neogloboquadrina pachyderma* (Ehrenberg) in the northeast Pacific. *Micropaleontology*, **32**, 1-18.

Ruddiman, W.F. & McIntyre, A. 1976. Northeast Atlantic paleoclimatic changes over the past 600,000 years. *Geological Society of America*, Memoir **145**, 111-146.

Ruddiman, W.F., Shackleton, N.J. & McIntyre, A. 1986. North Atlantic sea-surface temperatures for the last 1.1 million years. *In:* Summerhayes, C.P. & Shackleton, N.J., *North Atlantic paleoceanography*, Geological Society Special Publication, **21**, 155-173.

Sarnthein, M., Stremme, H.E. & Mangini, A. 1986. The Holstein interglaciation: time-stratigraphic position and correlation to stable-isotpe stratigraphy in deep-sea sediments. *Quaternary Research*, **26**, 283-298.

Sejrup, H.P. & Knudsen, K.L. 1993. Paleoenvironment and correlations of interglacial sediments in the North Sea. *Boreas*, **22**, 223-235.

Shackleton, N.J. 1987. Oxygen isotopes, ice volume and sea level. *Quaternary Science Reviews*, **6**, 183-190.

Spielhagen, R.F. & Erlenkeuser, H. 1993. Stable oxygen and carbon isotopes in planctic foraminifers from Arctic ocean surface sediments: Reflection of the low salinity surface water layer. *Marine Geology*, **119**, 227-250.

Streeter, S.S., Belanger, P.E., Kellogg, T.B. & Duplessy, J.-C. 1982. Late Pleistocene paleo-oceanography of the Norwegian-Greenland Sea: benthic foraminiferal evidence. *Quaternary Research*, **18**, 72-90.

Struck, U. 1992. Zur Paläo-Ökologie benthischer Foraminiferen im Europäischen Nordmeer während der letzten 600000 Jahre. *Berichte aus dem Sonderforschungsbereich 313*, **38**, 1-89.

Struck, U. 1995. Stepwise post-glacial migration of benthic foraminifera into the abyssal NE Norwegian Sea. *Marine Micropaleontology*, **26**, 207-213.

Swift, J. 1986. The Arctic Waters. In: Hurdle, B. (ed.), *The Nordic seas*, 129-151 Springer, New York.

Tiedemann, R., Sarnthein, M. & Shackleton, N.J. 1994. Astronomic timescale for the Pliocene Atlantic $\delta^{18}O$ and dust flux records of Ocean Drilling Program Site 659. *Paleoceanography*, **9**, 619-638.

Thiede, J. & Hempel, G. 1991. The expedition ARKTIS-VII/1 of RV 'POLARSTERN' in 1990. *Reports on Polar Research*, **80**, 1-137.

Vogelsang, E. 1990. Paläo-Ozeanographie des Europäischen Nordmeeres anhand stabiler Kohlenstoff- und Sauerstoffisotope. *Berichte aus dem Sonderforschungsbereich 313*, **23**, 1-137.

Weinelt, M.S. 1993. Veränderungen der Oberflächenzirkulation im Europäischen Nordmeer während der letzten 60.000 Jahre. *Berichte aus dem Sonderforschungsbereich 313*, **41**, 1-105.

Ocean. *Journal of Paleontology*, **52**, 1195-1207.

Mangerud, J. 1989. Correlation of the Eemian and the Weichselian with deep sea oxygen isotope stratigraphy. *Quaternary International*, **3/4**, 1-4.

Martinson, D.G., Pisias, N.G., Hays, J.D., Imbrie, J., Moore, T.C. & Shackleton, N.J. 1987. Age dating and the orbital theory of the Ice Ages: Development of a high-resolution 0 to 300.000 years chronostratigraphy. *Quaternary Research*, **27**, 1-29.

Nesje, A. & Kvamme, M. 1991. Holocene glacier and climate variations in western Norway: Evidence for early Holocene glacier demise and multiple Neoglacial events. *Geology*, **19**, 610-612.

Reynolds, L.A. & Thunell, R.C. 1986. Seasonal production and morphologic variation of *Neogloboquadrina pachyderma* (Ehrenberg) in the northeast Pacific. *Micropaleontology*, **32**, 1-18.

Ruddiman, W.F. & McIntyre, A. 1976. Northeast Atlantic paleoclimatic changes over the past 600,000 years. *Geological Society of America*, Memoir **145**, 111-146.

Ruddiman, W.F., Shackleton, N.J. & McIntyre, A. 1986. North Atlantic sea-surface temperatures for the last 1.1 million years. *In:* Summerhayes, C.P. & Shackleton, N.J., *North Atlantic paleoceanography*, Geological Society Special Publication, **21**, 155-173.

Sarnthein, M., Stremme, H.E. & Mangini, A. 1986. The Holstein interglaciation: time-stratigraphic position and correlation to stable-isotpe stratigraphy in deep-sea sediments. *Quaternary Research*, **26**, 283-298.

Sejrup, H.P. & Knudsen, K.L. 1993. Paleoenvironment and correlations of interglacial sediments in the North Sea. *Boreas*, **22**, 223-235.

Shackleton, N.J. 1987. Oxygen isotopes, ice volume and sea level. *Quaternary Science Reviews*, **6**, 183-190.

Spielhagen, R.F. & Erlenkeuser, H. 1993. Stable oxygen and carbon isotopes in planctic foraminifers from Arctic ocean surface sediments: Reflection of the low salinity surface water layer. *Marine Geology*, **119**, 227-250.

Streeter, S.S., Belanger, P.E., Kellogg, T.B. & Duplessy, J.-C. 1982. Late Pleistocene paleo-oceanography of the Norwegian-Greenland Sea: benthic foraminiferal evidence. *Quaternary Research*, **18**, 72-90.

Struck, U. 1992. Zur Paläo-Ökologie benthischer Foraminiferen im Europäischen Nordmeer während der letzten 600000 Jahre. *Berichte aus dem Sonderforschungsbereich 313*, **38**, 1-89.

Struck, U. 1995. Stepwise post-glacial migration of benthic foraminifera into the abyssal NE Norwegian Sea. *Marine Micropaleontology*, **26**, 207-213.

Swift, J. 1986. The Arctic Waters. In: Hurdle, B. (ed.), *The Nordic seas*, 129-151 Springer, New York.

Tiedemann, R., Sarnthein, M. & Shackleton, N.J. 1994. Astronomic timescale for the Pliocene Atlantic $\delta^{18}O$ and dust flux records of Ocean Drilling Program Site 659. *Paleoceanography*, **9**, 619-638.

Thiede, J. & Hempel, G. 1991. The expedition ARKTIS-VII/1 of RV 'POLARSTERN' in 1990. *Reports on Polar Research*, **80**, 1-137.

Vogelsang, E. 1990. Paläo-Ozeanographie des Europäischen Nordmeeres anhand stabiler Kohlenstoff- und Sauerstoffisotope. *Berichte aus dem Sonderforschungsbereich 313*, **23**, 1-137.

Weinelt, M.S. 1993. Veränderungen der Oberflächenzirkulation im Europäischen Nordmeer während der letzten 60.000 Jahre. *Berichte aus dem Sonderforschungsbereich 313*, **41**, 1-105.

The climate-sensitive Vesterisbanken area (central Greenland Sea): Depositional environment and paleoceanography during the past 250,000 years

MARTIN ANTONOW[1], PETER MARTIN GOLDSCHMIDT[2,3] and HELMUT ERLENKEUSER[2]

1. Freiberg University of Mining and Technology, Institute of Geology, Bernhard-von-Cotta-Str. 2, D–09596 Freiberg, Germany
2. SFB 313, University of Kiel, Heinrich-Hecht-Platz 10, D-24118 Kiel, Germany
3. present address: PCD, Eckernförder Str. 259, D-24119 Kiel, Germany

ABSTRACT

Sedimentological, micropaleontological and geochemical studies of sediment cores from the Vesterisbanken region were used to reconstruct the sedimentation pattern, depositional history and paleoceanography for this area over the last 250,000 years. The dating and correlation of the sediments were based on oxygen isotope stratigraphy and absolute ages.

The hemipelagic deposits near the Vesteris Seamount are characterised by biogenic, terrestrial and volcanogenic sediment input that varies through time. The area was influenced by sporadic turbidity currents and thermohaline-induced contour currents. Ice-rafted debris occurred nearly throughout the investigated time interval. Primary production was higher during interglacial periods. Filter-feeding epifauna (*C. wuellerstorfi*), an indicator of bottom currents, dominated in isotope stages 7 and 5.

During deglaciation (stage boundaries 8/7, 6/5 and 2/1, events 3.3 and 3.1), enormous meltwater input stabilised the water column, leading to periodic interruptions in deep water renewal. The influence of water masses from the Polar and Atlantic Domains in the Greenland Sea were very variable over time. The oceanic fronts in the Vesterisbanken area were always close together, allowing only a narrow Arctic Domain to exist.

Although the area is rather unique in relation to other parts of the Greenland Sea, climatic data can be compared favourably to the established Late Pleistocene/Holocene sedimentation pattern in the northern North Atlantic. Due to their good correlation to ice core records from Greenland and Antarctica, the Vesterisbanken sediments present a high-resolution picture of global climate change.

INTRODUCTION: THE VESTERIS SEAMOUNT IN THE GREENLAND SEA

The Greenland Sea is one of the few links between the Arctic Ocean and the northern North Atlantic. This area is remarkably sensitive to oceanographic and climatic changes because Polar and Atlantic water masses mix here. Morphologically, the Greenland Sea is framed by major fracture zones and ridges such as Knipovich and Mohns Ridges to the east and the Greenland continental slope/shelf to the west (Vogt, 1986). Tectonically, sea-floor spreading since the Paleocene led to a complex bathymetry and gave rise to strong basaltic volcanism that eventually generated the Vesteris Seamount (73°30'N, 9°10'W, Fig. 1). Vesterisbanken rises from the Greenland abyssal plain up to 133 m water depth (Johnson & Campsie, 1976), thus forming the only intra-plate volcano in the northern North Atlantic.

The goal of this investigation is to provide a reconstruction of the climatic development and the sedimentary environment of an area of the Greenland Basin that has been studied relatively little due to a thick ice cover limiting access. The

In: Hass, H.C. & Kaminski, M.A. (eds.) 1997. Contributions to the Micropaleontology and Paleoceanography of the North Atlantic. *Grzybowski Foundation Special Publication*, no. 5, pp. 101-118

central reasons and questions to be answered for this study are:

1. The determination of sedimentation in the Vesterisbanken area.
   - What depositional processes affected the study area?
   - Was there a temporal variation of different sedimentation patterns?
2. Paleoceanographic determination for the central Greenland Sea area.
   - Which paleo-surface water masses influenced the area around the Vesterisbanken and how variable is the position of the oceanic fronts?
   - When did meltwater pulses change the isotopic character of the Greenland Sea?
3. The integration of these results into the pattern of Late Pleistocene-Holocene sedimentation and paleoceanography of the Greenland-Iceland-Norwegian Seas.
   - Does the paleoceanographic development of the central Greenland Sea agree with that of other parts of the northern North Atlantic Ocean (e.g. the Norwegian and Iceland Seas)?
   - Did unique sedimentary or paleoceanographic events occur?
4. A comparison with global climate variations.
   - Can the marine climate information from the Vesterisbanken sediments be correlated with terrestrial signals from ice cores?
   - How do the changes in the central Greenland Sea fit into the global framework of climate changes?

RECENT CIRCULATION OF SURFACE AND DEEP WATERS

Surface waters

The modern hydrography of the Greenland Sea is dominated by water masses of the Arctic Domain that contrast with those from the Polar and Atlantic Domains (Figs. 1, 2). The region around the submarine Vesterisbanken mountain complex is mainly influenced by the East Greenland Current (EGC), which carries polar waters southwards. The Jan Mayen Current branches off from the EGC and moves southeastward, representing the southern flank of the cyclonic Greenland Sea Gyre (Figs. 1, 2). During winter, nearly the whole Greenland Sea is ice-covered, whereas the summer ice distribution retreats far to the west with strong interannual variations. Large amounts of sediment-laden Arctic sea ice are transported via Fram Strait into the Norwegian-Greenland Seas (Vinje & Finnekasa, 1986). Summer ice melting regionally produces surface salinities below 29‰ (Koltermann, 1987). Atlantic Intermediate Water (AIW) recirculating in parts of the Fram Strait beneath the polar

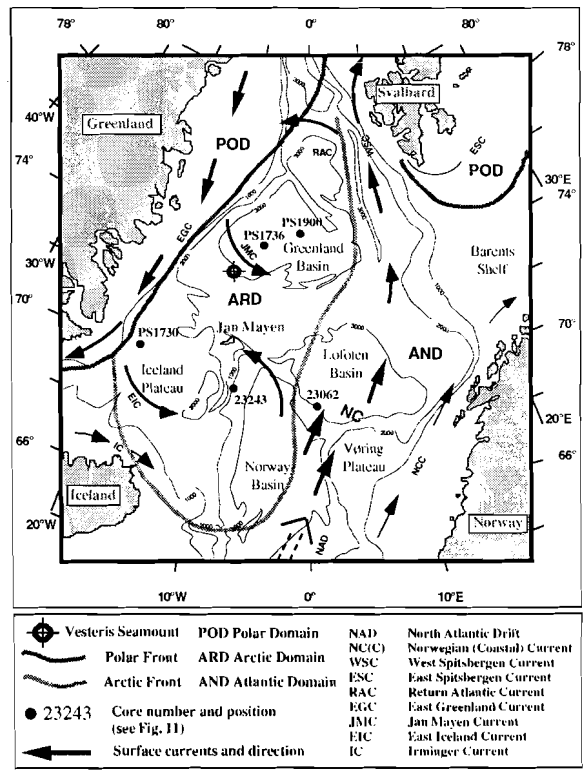


Figure 1. Recent surface circulation and different hydrographic regimes of the Greenland-Iceland-Norwegian Seas (from Jünger, 1994; modified after Paquette *et al.*, 1985; Johannessen, 1986; Bourke *et al.*, 1987; Dickson *et al.* 1988).

waters of the EGC represents the southward-flowing Return Atlantic Current (RAC, Paquette *et al.*, 1985).

Deep waters

Arctic Ocean Deep Water (AODW) enters the Greenland basin from the north. There it mixes with the Greenland Sea Deep Water (GSDW) that is formed due to surficial freezing processes: as a result of the genesis of sea-ice, the surface water masses cool down and reach a high density (salt enrichment). They therefore sink, following the convection of little "chimneys" (Aagaard *et al.*, 1985; Rudels, 1990). Depending on the stratification of the water column, these waters reach the bottom or stagnate as intermediate water masses (Fig. 2). The GSDW is assumed to cross the Mohns Ridge, moving southeast to the adjacent Lofoten Basin (Koltermann, 1987). Temporary Greenland Sea Deep Water renewal is described by Koltermann (1987) and Jünger (1994).

MATERIAL AND METHODS

During the expedition ARK VII/1 of the German ice-breaking research vessel *Polarstern*, short box cores (GKG) and long kastenlot cores (KAL) were

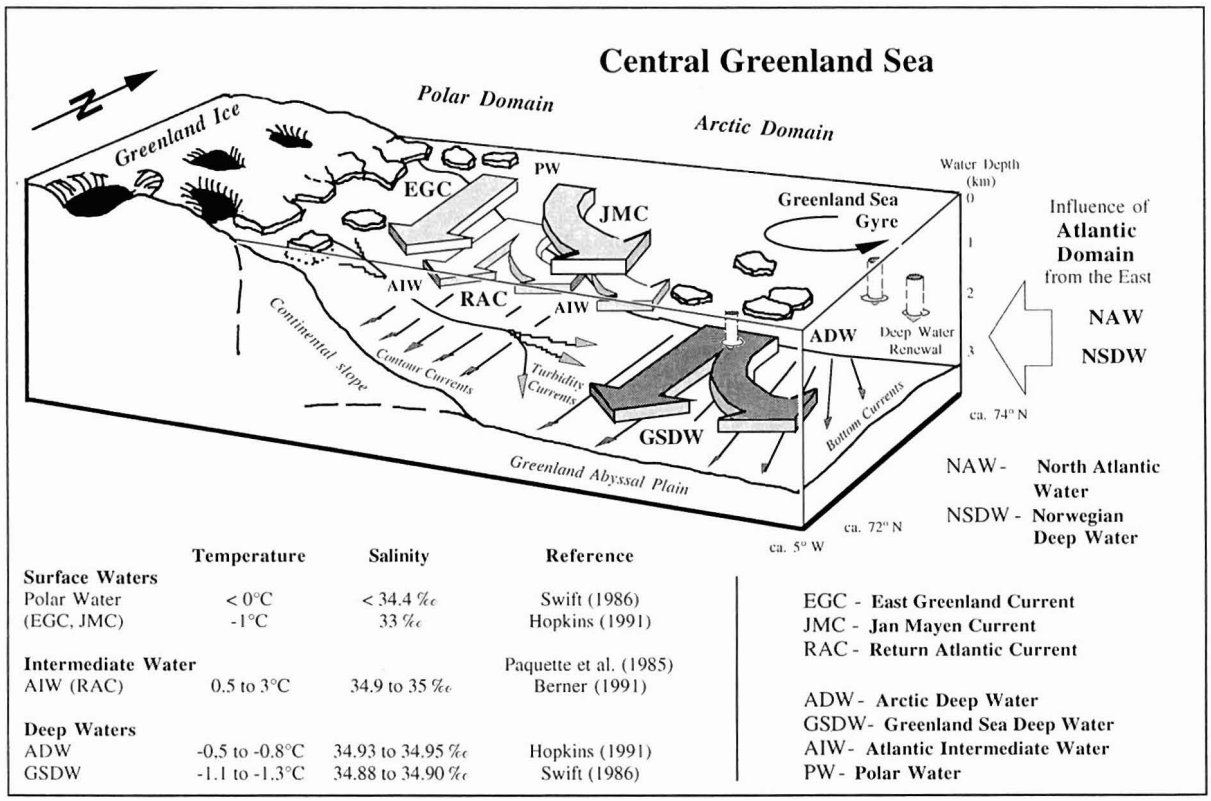


Figure 2. Recent oceanography of the Greenland Sea after several authors (see text).

recovered from the vicinity of the Vesteris Seamount (Thiede & Hempel, 1991). The present study investigates sedimentation processes at sites PS1878, PS1882, and PS1892 (Fig. 3, Table 1). To answer the questions raised in section 1, these sediment cores from the Greenland Sea were analysed in terms of sedimentology, micropaleontology and geochemistry. The sampling interval was 4 cm.

Granulometry

A combination of two size-dependent methods was used to determine the total grain size. The boundaries of the grain size subfractions are based on the Φ scale of Krumbein (1936).

The weighed sediment sample was wet-sieved to separate the fine (<63µm) and the coarse (>63µm) material. The coarse fraction was divided into five subfractions (63-125, 125-250, 250-500, 500-1000, >1000 µm) using standard sieves and an ATM Sonic Sifter™. The fine fraction was investigated using the Lumosed™ photosedimentometer (measuring range 1-63 µm). The photosedimentometer method is based on gravimetric sedimentation and is described by Staudinger *et al.* (1986). In comparison to conventional sediment decomposition (weight %) according to Atterberg (1912), this optical measuring method (volume %) offers very good reproduction (Syvitski, 1991).

Coarse fraction analysis

The analysis of the sediment composition of the two subfractions 125-250 µm and 250-500 µm was carried out according to the method of Sarnthein (1971). When the sample had more than ca. 400 particles per subfraction, a microsample splitter was used to generate representative subsamples. The presence and frequency of the coarse fraction analysis is represented in grain percent for each subfraction. A Zeiss GSZ microscope was used for the analyses.

Ca. 600-700 sediment particles were assigned to the following groups:

A terrigenous particles (quartz, rock fragments)
B volcanogenic particles (brown and transparent, porous and amorphous glass, volcanic fragments)
C benthic biogenic particles (foraminifera, sponge spicules)
D planktic biogenic particles (foraminifera, radiolaria, diatoms)
E authigenic particles (pyrite, aggregates)

The species and genus of benthic and planktic foraminifera were differentiated according to Bé (1977) and Thies (1991).

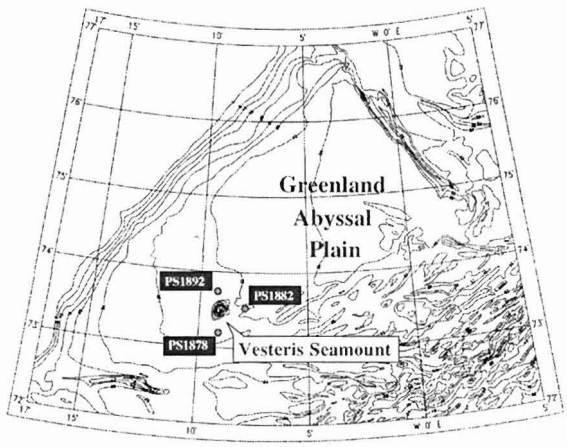


Figure 3. Bathymetry of the Greenland Basin and locations of the stations around Vesterisbanken.

Geochemistry ($CaCO_3$, TOC, S)

The total organic carbon (TOC) was determined photometrically using a Leco CS-125™ analysis system. An aliquot of each sample was decarbonated with 0.25n HCl and was also analysed. The difference of the measured values results in the anorganic carbon percentage, which leads to the carbon proportion when it is multiplied with a stochiometric factor (8.333). This assumes that the anorganic carbon percentage is actually present as $CaCO_3$. A "by-product" of the C/S analysis is the sulphur content of the sample. The preparation and analysis of samples using this method, as well as a discussion of arising errors, was described in detail by Wolf (1991). The Leco samples were made every 10 cm in the kastenlot cores and every 4-5 cm in the box cores. All geochemical measurements were carried out on both the total sample and the fine fraction (<63 µm). This allows estimates to be made regarding the input of both coccoliths (fine fraction) and planktic and benthic foraminifera (coarse fraction).

Table 1. Core locations (PS: Polarstern, GKG: boxcore, KAL: kastencore).

Core Number	Latitude (North)	Longitude (West)	Water Depth (m)	Recovery (cm)
PS1878-2 (GKG)	73° 15.10′	09° 00.94′	3038	40
PS1878-3 (KAL)	73° 15.33′	09° 00.74′	3048	469
PS1882-1 (GKG)	73° 35.52′	08° 23.80′	3169	12
PS1882-2 (KAL)	73° 35.96′	08° 19.29′	3175	650
PS1892-1 (GKG)	73° 44.05′	09° 37.52′	3125	18
PS1892-3 (KAL)	73° 44.06′	09° 41.17′	3002	436

Sedimentation and accumulation rates

According to the stratigraphy determined by the isotope dates (see following section), the samples between the isotope fixpoints can be dated using linear interpolation. Note, that several sediment sequences (turbidites) are not taken into account due to the sporadic sedimentation processes (Antonow, 1995). However, the assumptions of constant sedimentation and no compaction in the sediment core can lead to errors in the determined linear sedimentation rates (LSR). In order to take these factors into account, accumulation rates were calculated.

The dry bulk density (DBD) is calculated from the wet bulk density (WBD), the porosity (POR) and the density of seawater (1.025 $g \cdot cm^{-3}$ at 0°C) according to Ehrmann & Thiede (1985):

$$(1)\ DBD = WBD - (1.025 g \cdot cm^{-3} \cdot POR \cdot 10^{-2})$$

The DBD and the LSR are used to calculate the bulk accumulation rate (AR_{BULK}; van Andel *et al.*, 1975):

$$(2)\ AR_{BULK}\ [g \cdot cm^{-2} \cdot ky^{-1}] = DBD\ [g \cdot cm^{-3}] \cdot LSR\ [cm \cdot ky^{-1}]$$

The accumulation rates take sediment compaction into account with the assumptions that the pore space is totally filled with water and that no diagenetic effects occur (van Andel *et al.*, 1975; Thiede *et al.*, 1986).

To calculate the accumulation rate of individual parameters, their proportion to the total sediment is multiplied with AR_{BULK}:

$$(3)\ AR_{Parameter}\ [g \cdot cm^{-2} \cdot ky^{-1}] = Parameter\ [weight\text{-}\%] \cdot AR_{BULK}\ [g \cdot cm^{-2} \cdot ky^{-1}]$$

Accumulation rates of components in the coarse fraction uses the equation:

$$(4)\ AR_{Comp}\ [g \cdot cm^{-2} \cdot ky^{-1}] = Component\ [\%] \cdot AR_{>63\mu m}\ [g \cdot cm^{-2} \cdot ky^{-1}]$$

Wolf (1991) presented a detailed error analysis of results obtained with these equations.

STRATIGRAPHY

Absolute dating (^{14}C)

Four samples were dated using the AMS ^{14}C method. The required 1200-1300 specimens of *N. pachyderma* sin. were picked out of the 125-250 µm fraction and measured at the ETH Zürich (Institut für Mittelenergiephysik) according to the standard methods (see Kromer *et al.*, 1987). The measured ages were corrected according to Bard (1988), Bard *et al.* (1990) and Winn *et al.* (1991). The dates are listed in Table 2.

Analysis of stable isotopes ($\delta^{18}O$, $\delta^{13}C$)

Stable isotope analyses were carried out using 20-30 tests of *N. pachyderma* sin. (125-250 µm) per sample according to the method described by Duplessy (1978) and Ganssen (1983). The sampling interval was 4 cm. The isotope ratios $\delta^{18}O$ and $\delta^{13}C$ were measured by means of a Finnigan MAT 251 mass spectrometer at the C-14 Laboratory of the University of Kiel, Germany. The results were correlated to the PDB standard (Craig, 1957; Craig & Gordon, 1965). Statistical errors make up to 0.09‰ for $\delta^{18}O$ values and up to 0.04‰ for the $\delta^{13}C$ measurements (H. Erlenkeuser, pers. comm., 1994).

An oxygen isotope stratigraphy correlating the investigated sediment cores was established by Antonow (1995) by comparing the isotope data to the stratigraphy of Shackleton & Opdyke (1973, 1976), to the SPECMAP scale (Imbrie *et al.*, 1984; Martinson *et al.*, 1987) and to more recent results from sites in the Norwegian-Greenland Sea

Table 2. AMS ^{14}C ages of sediment samples.

Sediment core	Core depth, original (cm)	^{14}C age (ka)	^{14}C age corrected (ka)	Standard deviation (1Ó)
PS1878-3 (KAL)	280	28.530	28.130	330
PS1882-2 (KAL)	75	18.630	18.230	160
PS1882-2 (KAL)	350	40.610	40.210	1.020
PS1892-3 (KAL)	90	32.230	31.830	480

Table 3. Oxygen isotope stratigraphy and age/depth correlation of the sediment cores PS1878, PS1882, and PS1892 (note * markes ^{14}C ages).

Termination	$\partial^{18}O$ event	Age (ka)	Reference	Core depth PS1878 (cm)	Core depth PS1882 (cm)	Core depth PS1892 (cm)
End		9.000*	S	56	21	65
I	2.0	12.050	M	75	35	85
Beginning	2.2	14.900*	V	85	45	
	2.3	21.500	M	195	90	
	3.0	24.110	M	235	105	85
	3.1a	26.120*	W	250	115	
	3.1b(I)	30.840*	W	340		
	3.1b(II)	33.160*	W	365	180	
	3.1c	36.300*	W	380	210	
	3.1d	39.530*	W	405	240	
	3.31	50.210	M	435	305	
	3.33	55.450	M		345	105
	4.0	59.000	M		355	110
	4.2	65.000	I		375	130
	5.0	73.910	M		400	155
	5.1	79.250	M		410	160
	5.2	90.950	M		435	177
	5.3	99.380	M		465	190
	5.4	110.790	M		510	
End	5.51	122.560	M		538	200
II	6.0	129.840	M		570	223
Beginning	6.2	135.100	M		585	240
	6.3	142.280	M		610	260
	6.4	152.580	M		630	280
	6.5	175.050	M			290
	6.6	183.300	M			305
	7.0	189.610	M			325
	7.1	193.070	M			345
	7.2	200.570	M			360
	7.3	215.540	M			370
	7.4	224.890	M			380
End	7.5	240.190	M			405
III	8.0	244.180	M			420

V: Vogelsang (1990); **S:** Sarnthein *et al.* (1992); **W:** Weinelt (1993); **M:** Martinson *et al.* (1987); **I:** Imbrie *et al.* (1984)

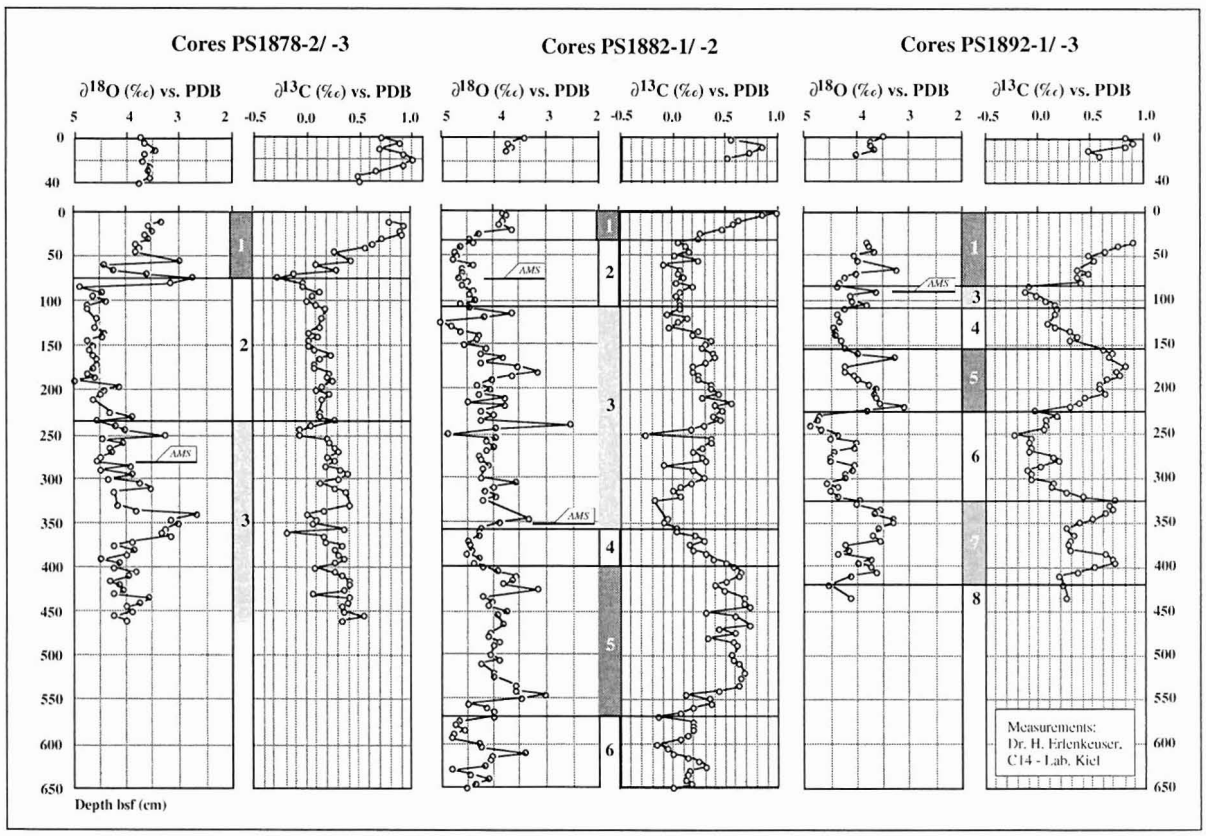


Figure 4. Stable isotope data ($\delta^{18}O$, $\delta^{13}C$) of *N. pachyderma* sin. versus depth of the cores PS1878, PS1882 and PS1892 (boxcore and kastencore). Oxygen isotope stages are marked.

(Vogelsang, 1990; Sarnthein *et al.*, 1992; Weinelt, 1993; Jünger, 1994).

Generally, the ratios of the stable isotopes $\delta^{18}O$ and $\delta^{13}C$ in the sediment cores presented in Fig. 4 are typical for middle/late Pleistocene to Holocene values in the Norwegian-Greenland Sea (Vogelsang, 1990; Weinelt, 1993; Jünger, 1994; Antonow, 1995, 1996; Nam *et al.*, 1995). The sedimentary record from the sites near Vesterisbanken represents the paleoceanographic history back to oxygen isotope Stage 8 (PS1892). Two of the cores (PS1878 and PS1882) contain high resolution records of Stages 2 and 3 (Fig. 4).

The oxygen isotope stratigraphy and age/depth correlation of sediment cores PS1878, PS1882 and PS1892 are presented in Table 3. The $\delta^{18}O$ stratigraphy was complemented by the four ^{14}C-AMS ages and a magnetostratigraphic framework (Antonow, 1995; Nowaczyk & Antonow in press).

Sedimentation and accumulation rates

In general, the linear sedimentation rates (LSR) of the Vesterisbanken cores vary between 0.4 and ca. 6 cm/ky. Since ca. 59 ka (Stage boundary 4/3), the LSR for the Vesterisbanken area have increased significantly (Table 4). The maximum amount is 10 cm/ky at the end of Stage 3. The Vesterisbanken LSR agree well with the values from the central Greenland Sea (Jünger, 1994) and with data from the east Greenland continental margin (Nam *et al.*, 1995; Nam, 1996) since isotope Stage 7. However,

Table 4. Mean linear sedimentation rates (LSR) since Stage 8.

Oxygen isotope stages	Duration (ky)	LSR PS1878 (cm/ky)	LSR PS1882 (cm/ky)	LSR PS1892 (cm/ky)
1	12.050	4.90	2.24	5.39
2	12.060	5.72	3.65	0.00*
3	34.890	3.17	3.75	0.72*
4	14.910		2.21	2.21
5	55.930		1.64	1.05
6	59.770		2.09	1.62
7	54.570			1.74
8	58.820			3.76 **

* Note: Low LSR are caused by erosion.
** Data available only for the last 4,000 years of Stage 8.

the Vesterisbanken LSR vary significantly since Stage 3.

Accumulation rates were calculated from the LSR (see section 3). These results are discussed in the following sections.

Vesterisbanken standard profile

The raw data sets for several segments of the sediment column had to be synthesised to characterise the overall sedimentation pattern and paleoceanography of the Vesterisbanken region (Fig. 5). The following core segments were used in the core synthesis: PS1878-2 (GKG), 0-40 cm: undisturbed surface and near-surface sediments; PS1878-3 (KAL), 45-435 cm: highest resolution of meltwater events in Stages 2 and 3; PS1882-2 (KAL), 310-535 cm: higher resolution of Stage 5 than in PS1892-3 (KAL); and PS1892-3 (KAL), >220 cm: con-

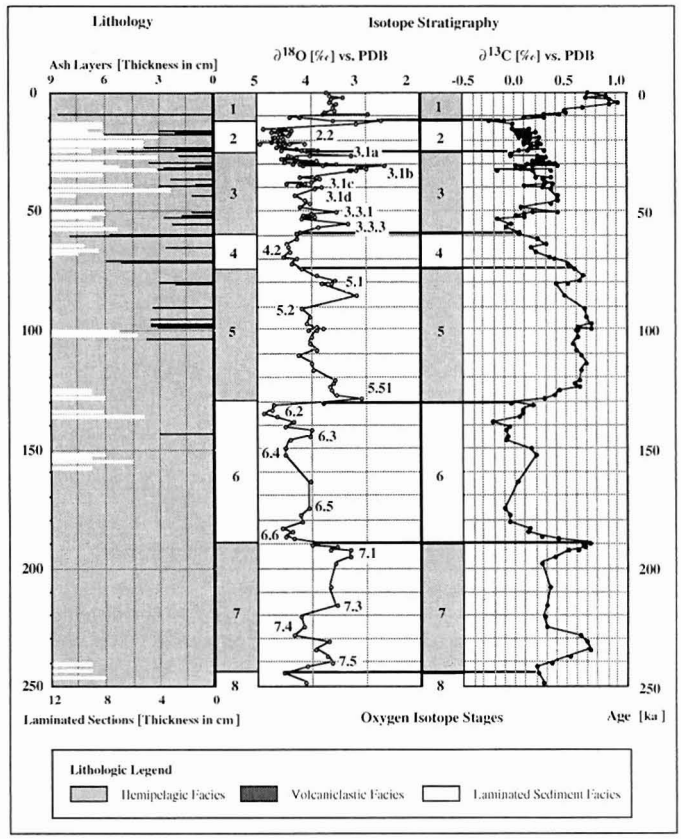


Figure 5. Standard profile of the Vesterisbanken region: Lithology and stable oxygen and carbon isotope records of *N. pachyderma* sin. during the past 250,000 years.

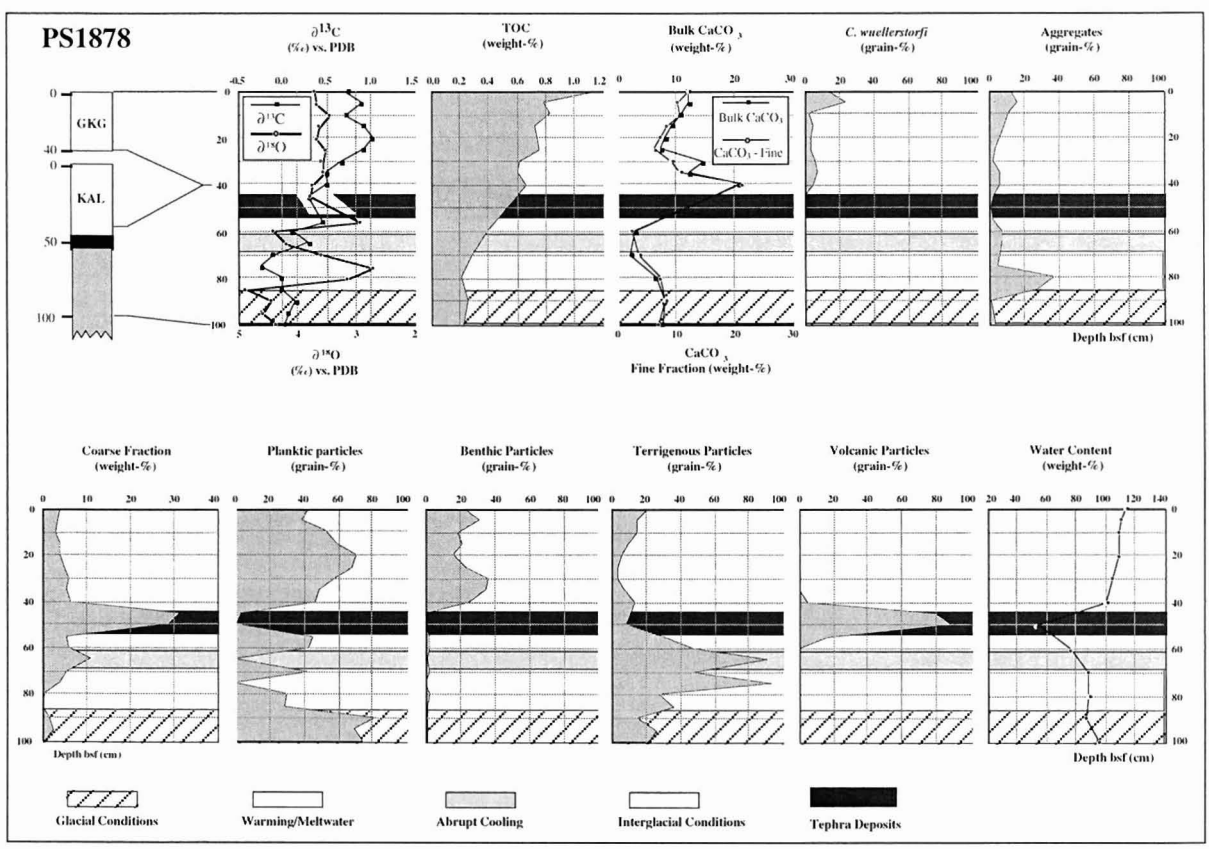


Figure 6. The variability of climatic and sedimentological records demonstrated by the example of a PS1878 sediment core section.

tinuous sedimentation and the maximum stratigraphic time period. Using this standard profile, it is possible to determine general trends of the changing environments in this area.

VARIATIONS OF CLIMATIC AND SEDIMENTOLOGIC SIGNALS: AN EXAMPLE OF A GLACIAL/INTERGLACIAL TRANSITION

The variations in the isotopic, geochemical and sedimentological signals indicate climatic trends that are important for correlating the cores and for determining sedimentological and paleoceanographical trends (for the complete data set and diagrams of all investigated parameters, see Antonow, 1995). An example of these variations and their implications is shown in the topmost metre of the sediment profile from Core PS1878 (Fig. 6). Due to the very similar trends for the isotopic and sedimentological signals in the short box core (GKG) and the long kastenlot core (KAL), the two can be combined to provide a single normalised core.

The lower portion of the section (100-85 cm, 16.3-14.9 ka) shows "heavy" $\delta^{18}O$ conditions (Fig. 6). Very low TOC and low carbonate contents indicate *glacial* conditions. The coarse fraction (>63 µm), which consists mainly of planktic foraminifera and terrigenous material (quartz and rock fragments), forms a relatively small part of the total sediment. Following the $\delta^{18}O$ maximum is a section (85-80 cm, 14.9-13.5 ka) with decreasing $\delta^{13}C$ conditions where the very small coarse fraction amount is primarily composed of sediment aggregates and terrigenous material.

Starting at ca. 80 cm (13.5 ka), the TOC content rises steadily. Drastically reduced $\delta^{18}O$ conditions correlate with increased terrigenous input, as is typical for *warming phases*, i.e. glacier melting events (Fig. 6). A short period of light oxygen isotope values is accompanied by increased terrigenous input (IRD), decreased biogenic input and a decrease in the $CaCO_3$ content. The rest of the core consists of large proportions of biogenic components (including benthic species). The increased TOC content, the high $\delta^{13}C$ conditions and the moderate $\delta^{18}O$ values are typical for *interglacial* conditions. Benthic filter-feeders (*C. wuellerstorfi*) also appear. A layer of tephra (volcanic glass) appears at 56-45 cm (9 ka); its coarse grains lead to losses in determining the water content (Fig. 6).

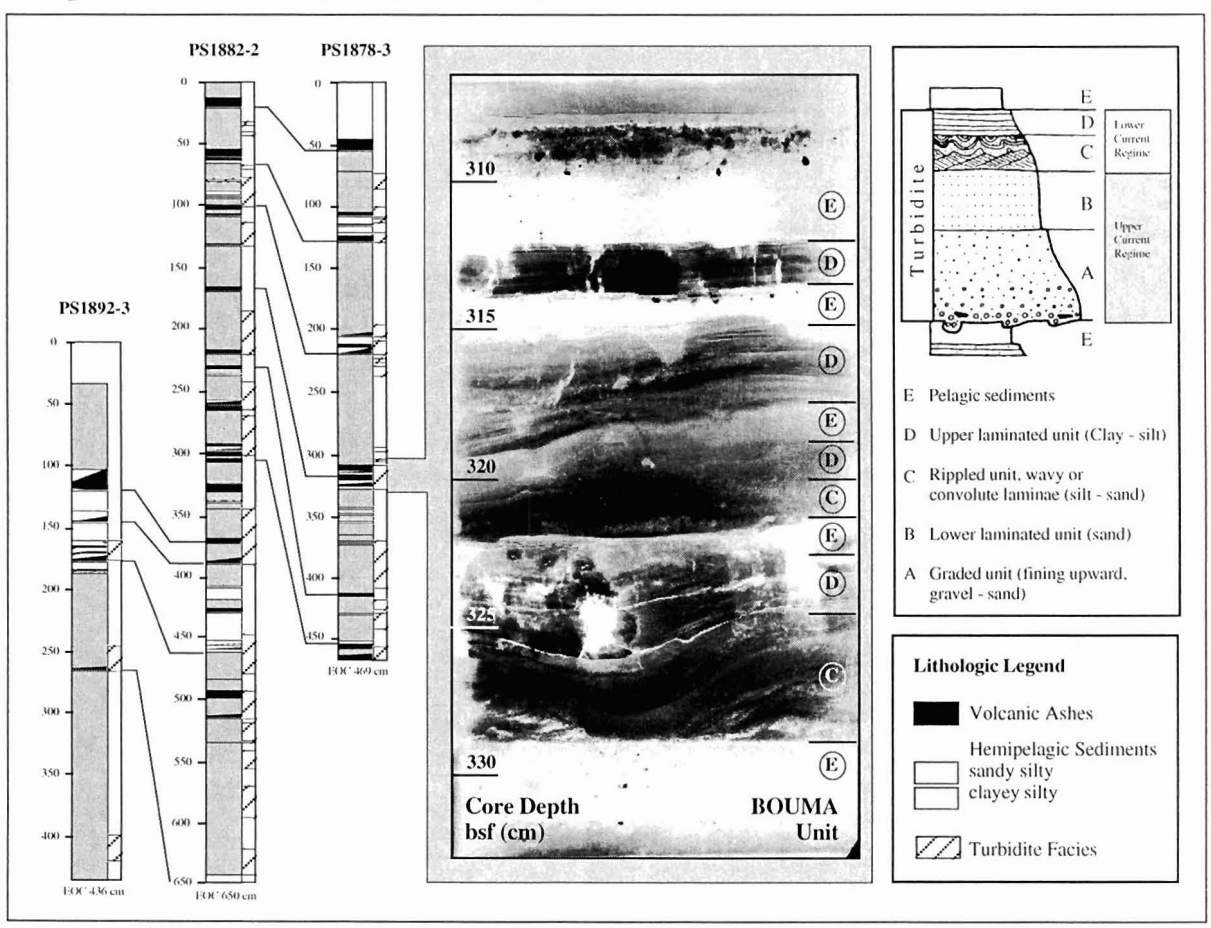


Figure 7. Lithology of the long sediment cores (kastencores). Volcanic ash cycles exhibit an influence of turbidity currents (turbidite units after Bouma 1962).

SEDIMENTARY PALEOENVIRONMENT

The Transpolar Drift transports large amounts of sediment-laden sea ice mainly from the Eurasian continental shelves across the North Pole to the Fram Strait, supplying mainly fine-grained ice-rafted detritus (IRD) to the northern North Atlantic Ocean floor (e.g. Wollenburg, 1993). During glacial eras, another source of IRD was iceberg calving of the Greenland, Scandinavian and Barents Sea Ice Sheets. Within the Greenland Sea, IRD is currently distributed by the southward-flowing East Greenland Current and the cyclonic Greenland Sea Gyre, the Jan Mayen Current and the Return Atlantic Current. IRD abundance in Pleistocene sediments documents the persistent climatic contrasts of severe polar conditions and iceberg melting in parts of the Greenland Sea and in the Fram Strait (Bischof, 1990; Spielhagen, 1991; Baumann *et al.*, 1994; Goldschmidt, 1994, *this volume*; Nam *et al.*, 1995). The input of IRD is discussed in detail in the following section.

All sediment cores are made up of grey, green and brown lithogenic hemipelagic muds in the grain size range of clay to sandy silty clay. The cores closest to Vesterisbanken are interrupted by successions of coarse-grained (>63 µm) black to fine-grained (<63 µm) olive green volcanic (basaltic) ash layers. These ash layers are composed of glass and rock fragments together with some crystalline components and can be classified as volcanoclastic turbidites (Fig. 7). They indicate an intensive Late Quaternary volcanic eruption phase since about 105 ka (Fig. 5). More detailed core descriptions of the cores are given in Thiede & Hempel (1991) and Antonow (1995).

Sedimentation in the area of Vesterisbanken was influenced by near-bottom currents (Michels, 1994; Antonow, 1995). There is a basic difference between gravitative and thermohaline current mechanisms in the marine environment. Gravitative current mechanisms create turbidites (Bouma, 1962) while thermohaline mechanisms induce bottom currents that follow bathymetric contours, leading to the deposition of contourites (Hollister & Heezen, 1972).

Deposits of both current mechanisms are evident in the study area (Antonow, 1995). The laminated sections of the investigated cores were usually interpreted as distal turbidites. But some of the investigated sediment characteristics (sorting, bio-

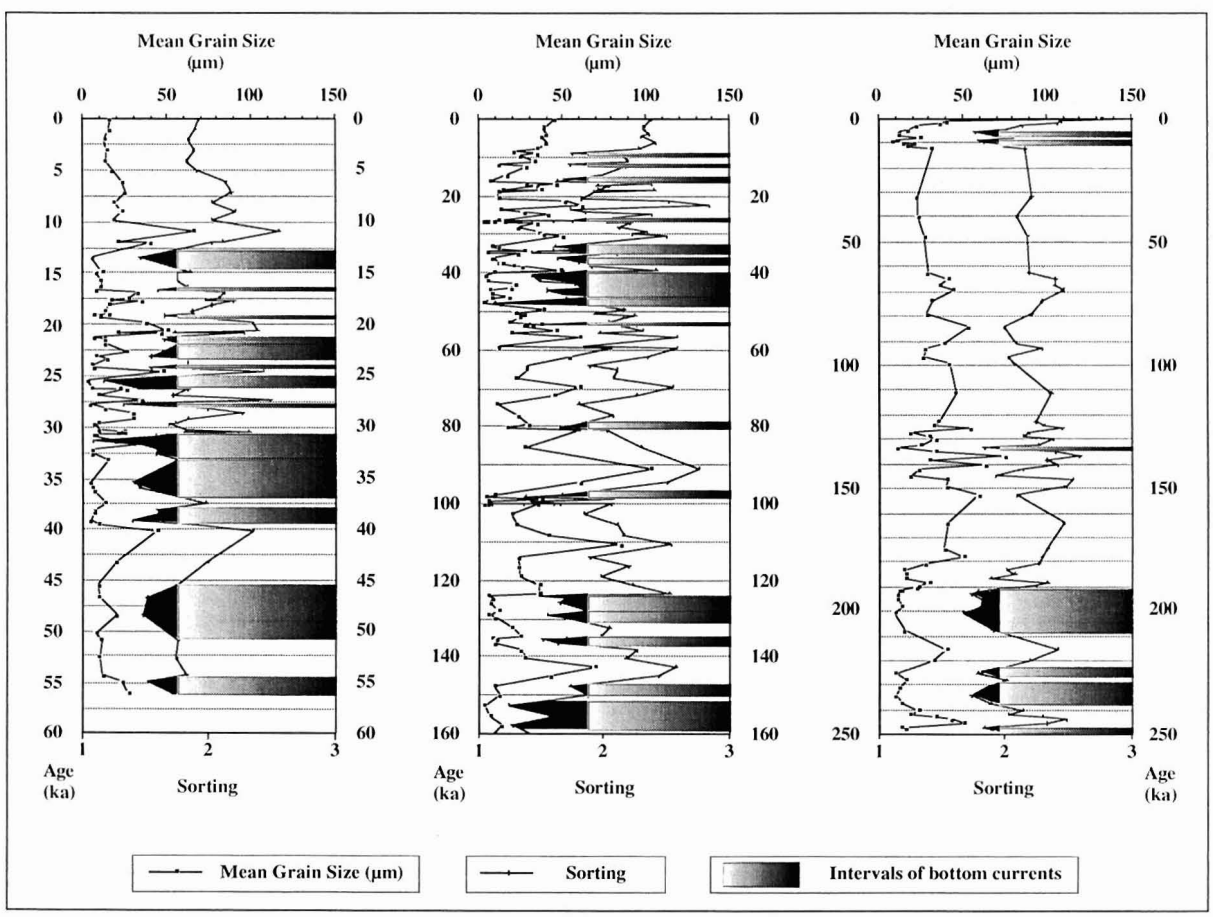


Figure 8. Sorting of sediments of the Vesterisbanken area as an indicator of bottom current influence during the past 250,000 years.

turbation, thickness, normal and inverse grading, lamination) are typical for contour currents (Bouma & Hollister, 1973; Hesse & Chough, 1980; Chough & Hesse, 1985).

Most episodic current events (turbidites) occur during cooler phases (Stage boundary 8/7, Events 6.4, 6.2, 4.2 and 2.2) or they occur during meltwater pulses during the entire Stage 3 (Figs. 5 and 8). There are intervals where the sediments are very well sorted (sorting values <2; see Friedman and Sanders, 1978). These well-sorted layers generally correlate with smaller grain sizes of the silt fraction (>10 µm, Fig. 8). During warmer times, thermohaline circulation is stable, resulting in an intense current influence by contour currents (Event 5.5, Figs. 5, 8).

Planktic and/or benthic fossils are rare in Greenland Sea sediments during glacial maxima (Baumann, 1990; Birgisdottir, 1991; Struck, 1992; Bauch, 1993; Jünger, 1994). But the local abundance of coccolithophorids documents that biogenic sediment input was never completely interrupted during glacial eras (Gard, 1987, 1988; Gard & Backman, 1990).

The carbonate production is related to the properties of water masses and sea-ice conditions (Kellogg, 1976, 1980). The Vesterisbanken area was very often controlled by the cold East Greenland Current and the sea-ice coverage within the last 250 ky. This resulted in a dominant occurrence of monospecific *N. pachyderma* sin. throughout time as also recorded at sites along the East Greenland continental margin (see Nam *et al.*, 1995; Stein *et al.*, 1996). Thus, the variation in calcium carbonate content reflects strong climate-induced changes in the inflow of warm Atlantic surface water masses

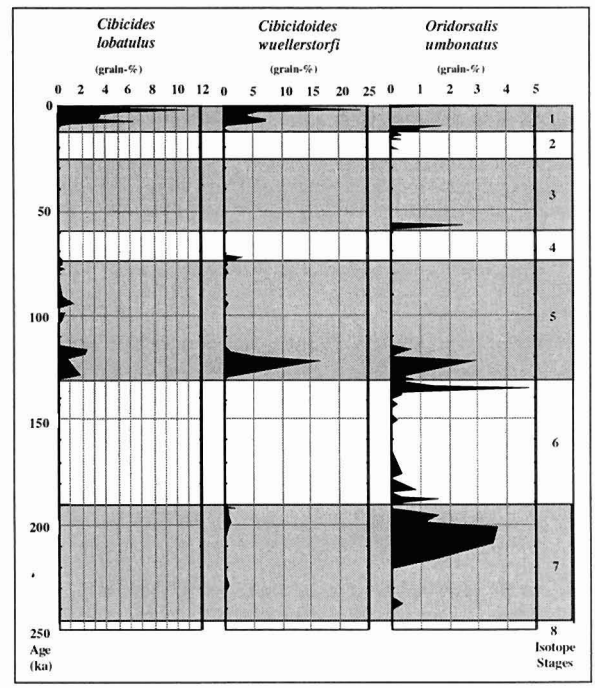


Figure 9. Occurrence of *C. lobatulus*, *C. wuellerstorfi* and *O. umbonatus* in the sediments of the Vesterisbanken area (standard profile) during the past 250,000 years.

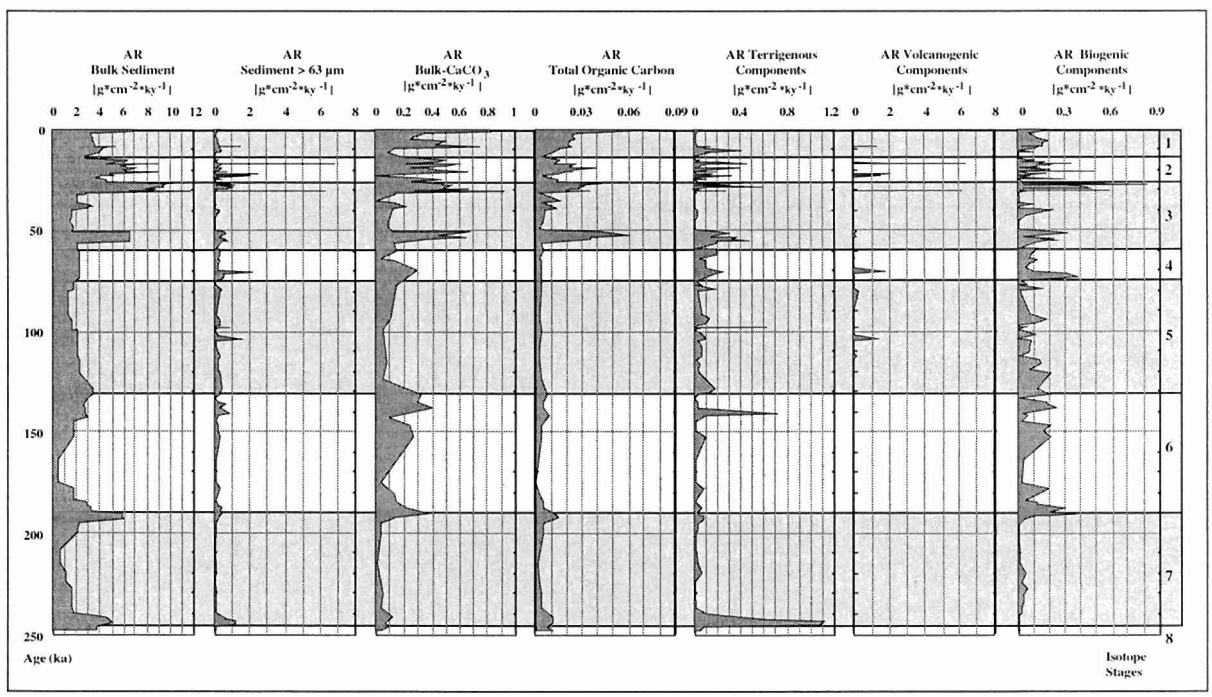


Figure 10. Accumulation rates (AR) of bulk sediment, the coarse fraction, the bulk carbonate and TOC contents, and AR of the terrigenous, volcanogenic and biogenic components of the Vesterisbanken region during the past 250,000 years.

and in paleoproductivity near the sea-ice edge (see Baumann *et al.*, 1993).

Of course, primary production is much higher during interglacial periods (Fig. 9). Suspension-feeding epifauna (*C. wuellerstorfi* , *O. umbonatus*), an indicator of bottom currents (Struck, 1992), dominate in parts of Stages 7, 5 and 1 (Fig. 9). The proportion of total organic carbon (0.2 to 0.3 weight % of bulk sediment) indicates "normal" (hemi)pelagic sedimentation in large parts of the abyssal Greenland Sea (Jünger, 1994; Antonow, 1995). The accumulation rates indicate varying depositional patterns in the Vesterisbanken area over the last 250 ky (Fig. 10).

PALEOCEANOGRAPHY OF THE VESTERISBANKEN AREA IN COMPARISION TO OTHER REGIONS OF THE GREENLAND-ICELAND-NORWEGIAN SEAS

Oxygen isotope signals in the Greenland-Iceland-Norwegian (GIN) Seas primarily display the interchange of temperate Atlantic waters with intermediate water masses of the Arctic Domain. Isotope signals in the Greenland Sea are less affected by temperature because they are mainly influenced by Polar water masses. Thus, the $\delta^{18}O$ variations in the Greenland Sea mainly reflect variations in the global ice volume (ice effect). Extremely low $\delta^{18}O$ values which strongly diverge from the ice effect ("mean seawater" signal according to Vogelsang (1990) in Fig. 11) were caused by strong melting events of the Greenland Ice Sheet (Vogelsang, 1990; Weinelt, 1993; Jünger, 1994; Nam *et al.*, 1995; Stein *et al.*, 1996).

Within the last 250,000 years, the paleoceanographic development of the central Greenland Sea was driven by the contrasting water masses of the Polar and the Arctic (influenced by Atlantic water masses) Domains as well as the resulting surface water circulation pattern (cyclonic Greenland Sea Gyre). A nearly continuous IRD signal in the sediments, even during moderate climate phases (such as Events 7.5, 7.3 and 7.1), is a sign of uninterrupted iceberg melting, underlining the relative proximity (and thus the climatic contrast) to the Polar Domain within the Greenland Sea. Phases of strong ice cover in the Greenland Sea during Event 7.4 are also seen in the Norwegian Sea. Weakened circulation is indicated by low carbonate values in Norwegian Sea sediments (Henrich *et al.*, 1989).

In Stage 6 (except for Event 6.5), broad expanses of the Norwegian Sea were under a permanent sea ice cover; isotope values (*N. pachyderma* sin.) indicate a significant shift to "heavy" values (Fig. 11). In the Greenland and Iceland Seas, on the other hand, the times of permanent sea ice cover were shorter. Large amounts of meltwater flowed into these seas from the instable Greenland Ice Sheet during Events 6.5 and 6.3 (Jünger, 1994; Antonow, 1995, 1996; Nam *et al.*, 1995).

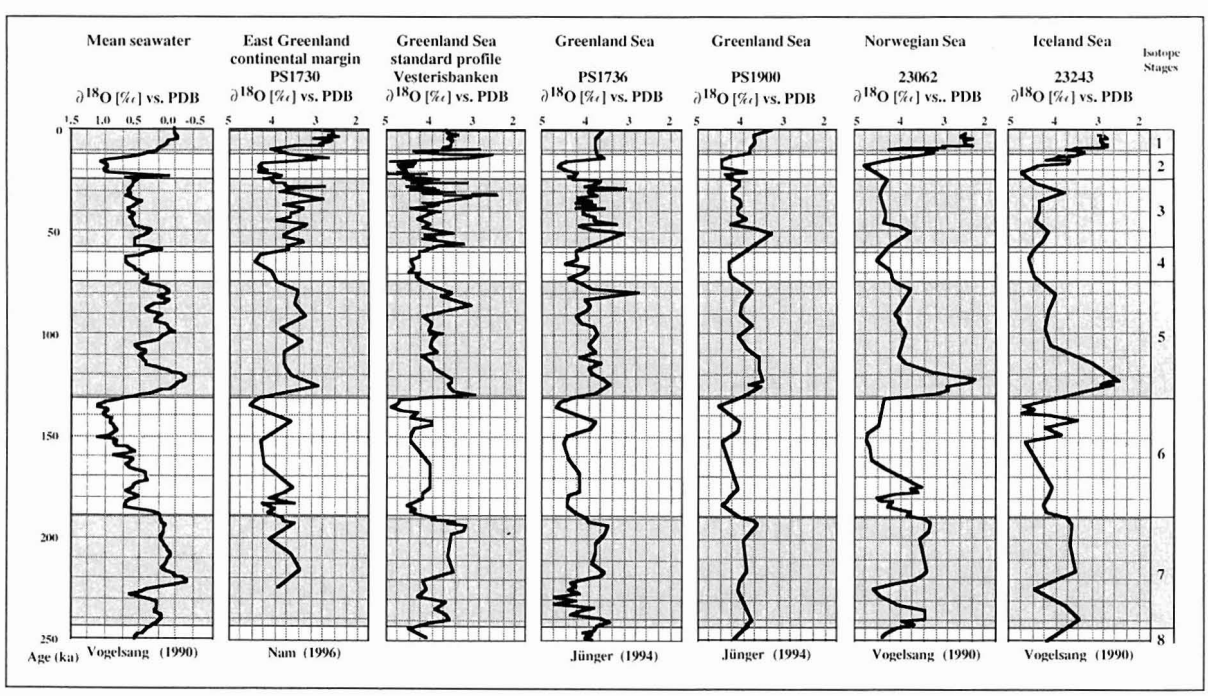


Figure 11. Oxygen isotope records of Vesterisbanken sediments in comparison to isotope records (*N. pachyderma sin.*) of cores from the Norwegian-Greenland Sea. Mean oxygen isotope ratios of seawater (ice effect) in the NGS related to Present after Vogelsang (1990).

At the start of Termination II, isotopically "light" meltwater again covered large areas of the GIN Seas (Fig. 11). The meltwater pulses were tremendous throughout these seas, leading to interruptions in convection (see Haake & Pflaumann, 1989). Isotopically "light" Atlantic Surface Water masses can be easily traced, especially in the Norwegian and Iceland Seas (Fig. 11). The intensive thermohaline surface water circulation increased the influence of temperate water masses in the Vesterisbanken area. The cores in the centre of the Greenland Sea Basin indicate very high rates of deep water renewal starting at Event 5.51; this is demonstrated by highly benthic $\delta^{13}C$ conditions (*O. umbonatus*; Jünger, 1994). Based on benthic oxygen isotope data, Birgisdottir (1991) and Bauch (1993) postulated a very low influence of Polar water masses in the Iceland Sea. As Stage 5 continued, the Norwegian Sea water masses showed relatively stable Atlantic Water influence, while in the central Greenland Sea alternating influences of water masses separated by the Arctic Front have been reported (Henrich *et al.*, 1989, 1992; Jünger, 1994; Antonow, 1995, 1996).

In Stage 4, high rates of terrigenous IRD input are seen not only in the Vesterisbanken area, but also in the Norwegian Sea (Henrich *et al.*, 1989), the Iceland Sea (Birgisdottir, 1991), the Greenland Sea (Hamich, 1991; Jünger, 1994), and the Fram Strait (Spielhagen, 1991; Hebbeln, 1992). This fact is in contrast to the situation near the east Greenland continental margin, where an IRD signal is distinctly reduced (Nam *et al.*, 1995; Stein *et al.*, 1996). The significant isotopic shift (by up to 0.25‰ $\delta^{18}O$, see Fig. 11) during Event 4.2 indicates contrasting oceanographic conditions within the central Greenland Sea (cores PS1900 and PS1736) and the Vesterisbanken area (Jünger, 1994; Antonow, 1995, 1996).

A reduced range of species (*N. pachyderma* is the only planktic species present) indicates severe paleo-ecologic conditions, as was the case throughout the GIN Seas during Stage 3 (see Kellogg, 1976, 1977, 1980; Bauch, 1993). The benthic fauna was also reduced: only *O. umbonatus* was present in significant amounts at the beginning of Stage 3. The isotope signals (Fig. 11) give evidence of early melting events that have been triggered by the weak inflow of warmer Atlantic water masses, as is recorded at the East Greenland continental margin (PS1730) as well as in the central Greenland Sea (cores PS1736, PS1900). Thus Stage 3, with its common, strong meltwater pulses and the constant alternation of ice-free surface waters and nearly complete ice cover, is an extremely variable, climatically sensitive period in the Greenland Sea (Fig. 11). During Stages 2 and 3 the sedimentation rates are much higher than those within other time intervals (Table 4). Winnowing and redeposition of fine sediment particles along the Greenland continental shelf, the slope and the adjacent Greenland basin by the EGC are likely to have occured (see also Mienert *et al.*, 1992; Nam *et al.*, 1995).

A drastic increase in the carbonate content (spread of biogenic production) at the beginning of Termination I can be seen in sediments throughout the GIN Seas (see Blaume, 1992; Henrich *et al.*, 1989; Koç Karpuz & Jansen, 1992). As in earlier

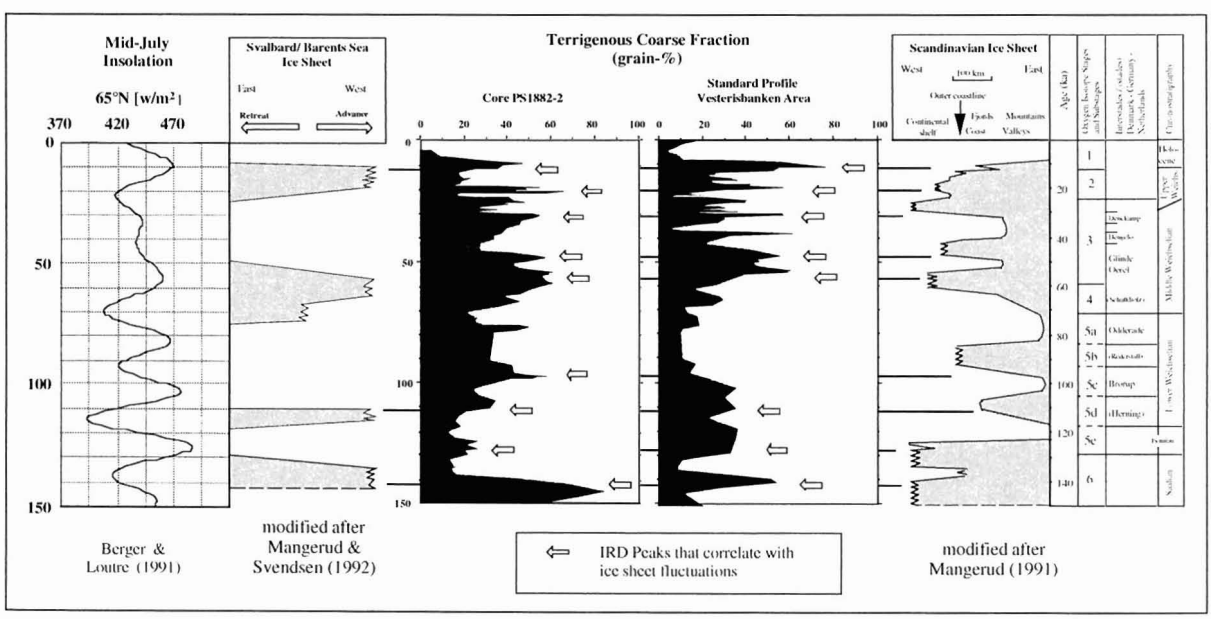


Figure 12. Ice-rafted debris (>125 µm) of the Vesterisbanken sediments in comparison with the extent of the Barents Sea and Scandinavian ice sheets.

episodes, the melting of the continental ice sheets resulted in meltwater input. As in the Norwegian Sea (Blaume, 1992), turbidity currents occurred at great depths in the Greenland Sea (Mienert *et al.*, 1993; Antonow, 1995).

MARINE VESTERISBANKEN RECORDS VS. TERRESTRIAL DATA: LAND-SEA CORRELATION

IRD records vs. oscillations of glaciers neighboring the northern North Atlantic

Variations in the input of terrigenous material (20-80 grain % IRD) can be seen in the Vesterisbanken sediment cores (Fig. 12). The terrigenous particles (>125 µm) consist mainly of monocrystalline (quartz, feldspar) and polycrystalline rock fragments (slate, volcanic fragments, sandstones and siltstones). Although their source areas cannot be precisely determined, it is likely that most of the rock fragments (excepting the volcanic fragments) come from Norway, Svalbard and the Barents Sea area (see Bischof, 1990; Baumann *et al.*, 1994; Goldschmidt, 1994, *this volume*). IRD originating in Greenland is generally carried southwards by the East Greenland Current (EGC) and would thus probably not be found in the study area. Spielhagen (1991) interpreted the flow and ice cover of the EGC as stable over (at least) the last 200,000 years.

Mangerud & Svendsen (1992) used a continental litho- and biostratigraphy for the last 140,000 years to reconstruct glacier oscillations in the Svalbard/Barents Sea area. Baumann *et al.* (1994) compared these terrestrial data with the marine IRD signal of cores from the northern Greenland Sea and found that the terrestrial data agreed well with the marine records.

The IRD signals of the Vesterisbanken sediments correlate well with both the data from Mangerud & Svendsen (1992) and with the reconstruction of fluctuations of the Scandinavian Ice Sheet of Mangerud (1991). The recent surface circulation pattern (Norwegian Current - Atlantic Return Current - EGC/Jan Mayen Current; Fig. 1) and the results of Spielhagen (1991) regarding the longevity of the EGC show that icebergs from the Norway/Svalbard area could have reached the central Greenland Sea in the last 250 ky. Nearly every time that the *continental* glaciers had reached beyond the continental shelf or were retreating from it, the *marine* IRD record shows a peak (Fig. 12). Glaciers become instable when passing the

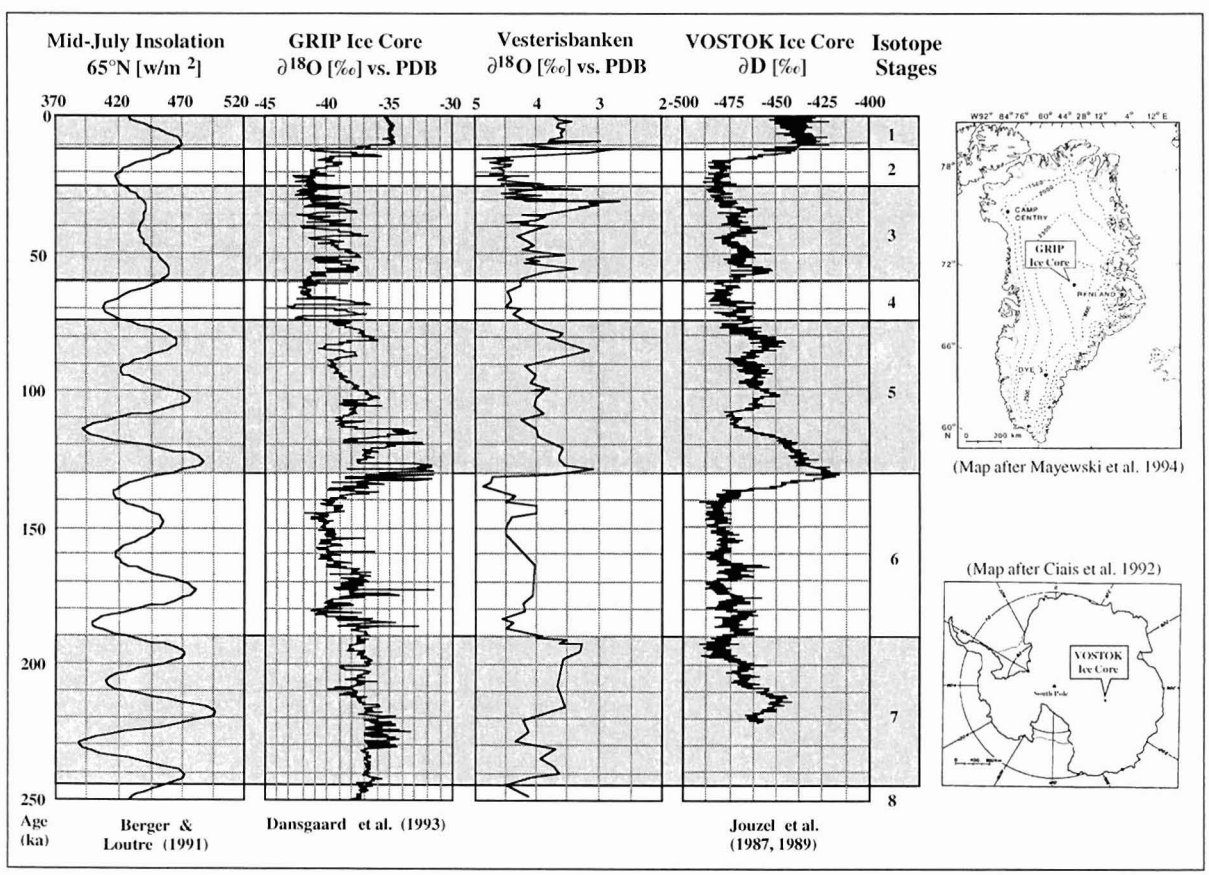


Figure 13. The oxygen isotope signal (*N. pachyderma* sin.) of the Vesterisbanken standard profile correlates with isotope data from Greenland (GRIP) and Antarctica (Vostok).

continental shelf, resulting in iceberg calving (see Heinrich, 1988), while glacier retreats with intense iceberg calving indicate the beginning of warming phases (see Baumann *et al.*, 1994; Goldschmidt, 1995; Nam *et al.*, 1995). In both cases, melting icebergs releasing their sediment load indicate the extension of glaciers beyond the continental shelf or the retreat therefrom. Although the marine signal varies from core to core, it is much more detailed and continous than the terrestrial signal.

However, IRD peaks in the study area do not have to indicate the existence of glaciers (Fig. 12). At certain times during Stages 5 and 3, the IRD signal must have been modified by iceberg-covered water masses of the Jan Mayen Current branching off of the EGC. *Local* melting processes in the Vesterisbanken area may also play a role.

Isotope signals (N. pachyderma) vs. ice core data

Data from the Greenland Ice Core Project (GRIP) document high-resolution series of temperature oscillations during the last 250,000 years (Dansgaard *et al.*, 1993). These so-called "Dansgaard-Oeschger cycles" are caused by changes in the $\delta^{18}O$ isotope ratios of the air masses above the Greenland ice sheet and correlate well with paleosurface water mass temperatures determined with *N. pachyderma* of North Atlantic sediment cores for the last 90,000 years (Bond *et al.*, 1993).

In general, the oxygen isotope data of the marine Vesterisbanken area are in good agreement with the terrestrial Greenland Ice Sheet isotopic record (Fig. 13). Extreme meltwater input reflects climatic fluctuations near Vesterisbanken during isotope Stages 6 and 3. Deviations of the climate records of the different sites are caused by regional influences within the Norwegian-Greenland Sea.

Orbital forcing of the documented Greenland Sea climate records is evident. "Light" isotope values result from more intensive insolation (Berger & Loutré, 1991) and coincide with the warm substages 7.5, 7.3, 7.1, 5.5, 5.1 and Termination I (Fig. 13).

The isotope record of the Vesterisbanken sediments corresponds better with the data from the Vostok ice core (Antarctica) than those derived from the Greenland ice core (GRIP), which is complicated by internal deformation of the ice older than ca. 100 ka towards the glacier's basal zone. The sediments around Vesterisbanken thus archive the *global* climatic record. The thermohaline circulation is strongly connected to climatic variations, which affects a rapid translation of the Polar Front and is well documented by the changing influence of different water masses. The sites around Vesterisbanken are situated in the narrow "battlefield" of oceanic frontiers and this makes it possible to correlate their isotope signals and the high-resolution ice core records to oceanic circulation

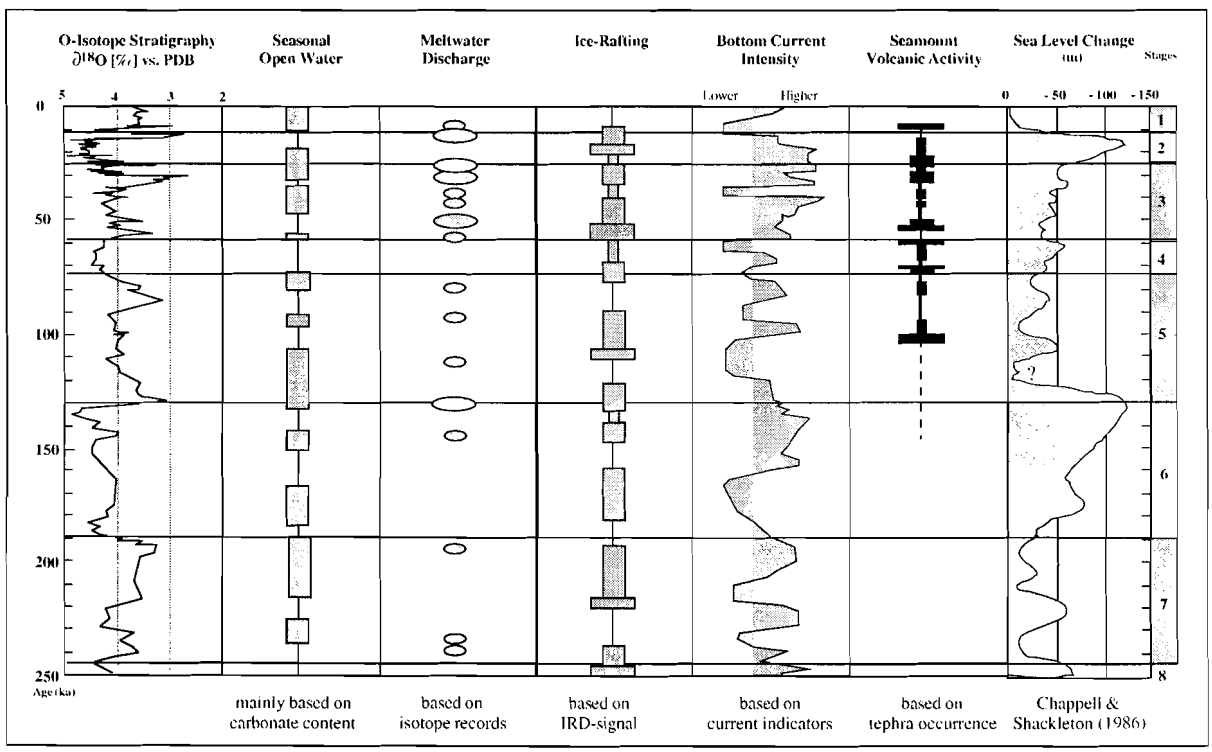


Figure 14. Synoptic overview of the environmental conditions of sedimentation in the Vesterisbanken area for the past 250,000 years. Sea level changes after Chappel & Shackleton (1986).

(see Zahn, 1994).

CONCLUSIONS

A general synthesis of the important sedimentation events and paleoceanographic determinations for the time since the end of Stage 8 is shown in Figure 14. The studies carried out on Vesterisbanken sediments indicate the following:

1. The paleo-environment within the studied time interval is very variable. The sediments result from varying formation and transport processes: sedimentation patterns dominated by terrigenous, biogenic and volcanogenic input alternate. Changes in the lithofacies usually occur due to climatic variations; these changes are related to transitions between the oxygen isotope stages and substages. Large-scale meltwater events occurred during Terminations (III, II and I) and during fluctuations during the entire Stages 3 and 2.
2. Hemipelagic sedimentation in the Vesterisbanken area was mainly current-controlled and indicates variable ice cover. In addition to biogenically dominated sedimentation patterns that were relatively constant over time, there were also time intervals in which episodic current-induced near-bottom particle transport was important. Particle deposition by suspension currents dominate over contour current processes.
3. Turbiditic volcanic sediments indicate episodes of volcanic activity at different times. Ca. 105 ka, intense volcanic activity occurred at Vesterisbanken. Eruptions occurred mainly when the sea level was high (Fig. 14). No volcanic activity took place since the beginning of the Holocene. It *appears* that the Vesterisbanken volcanic episodes were coupled to warming phases (crustal rebound due to ice sheets disappearing from neighboring land masses?).
4. Despite the modification of the depositional environment caused by the existence of Vesterisbanken, general paleoclimatic information can be gleaned from the sediments. The sedimentological and paleoceanographical data from this part of the central Greenland Sea can be integrated into the pattern of Late Quaternary sedimentation of the northern North Atlantic and present a picture of globally controlled climate changes.
5. The correlation between terrestrial glacier oscillations and marine IRD signals is very good. The climate record in the marine deposits using oxygen isotope data (*N. pachyderma* sin.) has a very good resolution in the Vesterisbanken area and agrees well with data from high-resolution ice cores from polar landmasses.

ACKNOWLEDGEMENTS

Many colleages and friends from the Geomar Research Center for Marine Geosciences and at the Special Research Project SFB 313 at Kiel University encouraged and helped us: Britta Jünger, Heidemarie Kassens, Henning Bauch, Helmut Beese, Frank Blaume, Andre Freiwald, Christian Hass, Jens Hölemann, Rüdiger Henrich, Harald Hommers, Klas Lackschewitz, Klaus Michels, Jürgen Mienert, Stefan Nees, Jan Rumohr, Robert Spielhagen, Jörn Thiede, Thomas Wagner, Hans-Joachim Wallrabe-Adams, and Rainer Zahn.
This paper benefitted from the review of Rüdiger Stein and the critical comments of Christian Hass. Thanks to Bernhard Fürst for technical assistance in the preparation of the manuscript. Financial support was given by the German Research Foundation sponsoring the Special Research Project SFB 313. This is SFB 313 publication number 304.

REFERENCES

Aagaard, K., Swift, J. & Carmack, E. 1985. Thermohaline circulation in the Arctic Mediterranean Seas. *Journal of Geophysical Research*, **90**, 4833-4846.

Antonow, M. 1995. Sedimentationsmuster um den Vesteris Seamount (zentrale Grönlandsee) in den letzten 250.000 Jahren. *GEOMAR Report*, **44**, 1-121.

Antonow, M. 1996. Spätquartäre Sedimentation im Gebiet von Vesterisbanken: Paläozeanographische und klimatische Ableitungen für die zentrale Grönlandsee. *Zentralblatt für Geologie und Paläontologie*, Teil I (1/2), 7-19.

Atterberg, A. 1912. Die mechanische Bodenanalyse und die Klassifikation der Böden Mittelschwedens. *Internationale Mitteilungen für Bodenkunde*, 1-314.

Bard, E. 1988. Correction of accelerator mass spectrometry ^{14}C ages measured in planktonic foraminifera: Paleoceanographic implications. *Paleoceanography*, **3**, 635-645.

Bard, E., Hamelin, B., Fairbanks, R.G. & Zindler, A. 1990. Calibration of the ^{14}C timescale over the past 30,000 years using mass spectrometric U-Th ages from Barbados corals. *Nature*, **345**, 241-243.

Bauch, H. 1993. Planktische Foraminiferen im Europäischen Nordmeer - ihre Bedeutung für die paläo-ozeanographische Interpretation während der letzten 600.000 Jahre. *Berichte aus dem Sonderforschungsbereich 313*, **40**, 1-108.

Baumann, K.-H. 1990. Veränderlichkeiten der Coccolithenflora des Europäischen Nordmeeres im Jungquartär. *Berichte aus dem Sonderforschungsbereich 313*, **22**, 1-146.

Baumann, K.-H., Lackschewitz, K.S., Spielhagen, R.F. & Henrich, R. 1993. Reflection of continental ice sheets in late Quaternary sediments from the Nordic Seas. *Zentralblatt für Geologie und Paläontologie*, Teil I, **7/8**, 897-912.

Baumann, K.-H., Lackschewitz, K.S., Mangerud, J., Spielhagen, R.F., Wolf-Welling, T.C.W., Henrich, R. & Kassens, H. 1994. Reflection of Scandinavian ice sheet fluctuations in Norwegian Sea sediments during the last 150,000 years. *Quaternary Research*, **43**, 185-197.

Bé, A.W. 1977. An ecological, zoographic and taxonomic review of recent planktonic foraminifera. *In:* Ramsay, A.T.S. (ed.), *Oceanic micropaleontology*, 1-100, Academic Press, London.

Berger, A. & Loutre, M.F. 1991. Insolation values for the climate of the last 10 million years. *Quaternary Science Review*, **10**, 297-317.

Birgisdottir, L. 1991. Die paläo-ozeanographische Entwicklung der Islandsee in den letzten 550.000 Jahren. *Berichte aus dem Sonderforschungsbereich 313*, **34**, 1-112.

Bischof, J. 1991. Dropstones im Europäischen Nordmeer-Indikatoren für Meeresströmungen in den letzten 300.000 Jahren. *Berichte aus dem Sonderforschungsbereich 313*, **30**, 1-127.

Blaume, F. 1992. Hochakkumulationsgebiete am norwegischen Kontinentalhang: Sedimentologische Abbilder Topographie-geführter Strömungsmuster. *Berichte aus dem Sonderforschungsbereich 313*, **36**, 1-150.

Bond, G.C., Broecker, W., Johnsen, S. & McManus, J. 1993. Correlations between climate records from North Atlantic sediments and Greenland ice. *Nature*, **365** (6442), 143-147.

Bouma, A.H. 1962. *Sedimentology of some flysch deposits. A graphic approach to facies interpretation*, 168 pp, Elsevier, Amsterdam.

Bouma, A.H. & Hollister, C.D. 1973. Deep ocean basin sedimentation. In: Middleton, G.V. & Bouma, A.H. (eds.), *Turbidites and deep water sedimentation*. SEPM short course, Anaheim, 79-118.

Bourke, R.H., Newton, J.L., Paquette, R.G. & Tunnicliffe, M.D. 1987. Circulation and water masses of the East Greenland shelf. *Journal of Geophysical Research.*, **92**, 6729-6740.

Chappel, J. & Shackleton, N.J. 1986. Oxygen isotopes and sea level. *Nature*, **324**, 137-140.

Chough, S.K. & Hesse, R. 1985. Contourites from Eirik ridge, south of Greenland. *Sedimentary Geology*, **41**, 185-199.

Ciais, P., Petit, J.R., Jouzel, J., Lorius, C., Barkov, N.I., Lipenkov, V. & Nikolajev, V. 1992. Evidence for an early Holocene climatic optimum in the Antarctic deep ice-core record. *Climate Dynamics*, **6**, 169-177.

Craig, H. 1957. Isotopic standards for carbon and oxygen and correction factors for mass-spectrometric analysis of carbon dioxide. *Geochimica and Cosmochimica Acta*, **12**, 1-133.

Craig, H. & Gordon, L.I. 1965. Deuterium and oxygen-18 variations in the ocean and the marine atmosphere. *In:* Tongiorgi, E. (ed.), *Stable isotopes in oceanographic studies and paleotemperatures*. Third SPOLETO conference on Nuclear Geology, Consilio Nazionale della Ricerche, Laboratorio di Geologia Nucleare, Pisa, 9-130.

Dansgaard, W., Johnsen, S.J., Clausen, H.B., Dahl-Jensen, D., Gundestrup, N.S., Hammer, C.U., Hvidberg, C.S., Steffensen, J.P., Sveinbjörnsdottir, A.E., Jouzel, J. & Bond, G. 1993. Evidence for general instability of past climate from a 250-kyr ice-core record. *Nature*, **364**, 218-220.

Dickson, R.R., Meincke, J., Malmberg, S.A. & Lee, A.J. 1988. The „great salinity anomaly" in the northern North Atlantic 1968-1982. *Progress in Oceanography*, **20**, 103-151.

Duplessy, J.-C. 1978. Isotope studies. *In:* Gribbin, J. (ed.), *Climatic change*, 46-67, Cambridge University Press, Cambridge.

Ehrmann, W.K. & Thiede, J. 1985. History of Mesozoic and Cenozoic sediment fluxes to the North Atlantic Ocean. *Contributions to Sedimentology*, **15**, 1-109.

Friedman, G.M. & Sanders, J.E. 1978. Principles of sedimentology, 211 pp, John Wiley & Sons, New York.

Ganssen, G. 1983. Dokumentation von küstennahem Auftrieb anhand stabiler Isotope in rezenten Foraminiferen vor Nordwest-Afrika. *Meteor-Forschungs-Ergebnisse*, **37C**, 1-46.

Gard, G. 1987. Late Quaternary calcareous nannofossil biostratigraphy and sedimentation patterns: Fram Strait, Arctica. *Paleoceanography*, **5**, 761-787.

Gard, G. 1988. Late Quaternary calcareous nannofossil biochronology and paleo-oceanography of Arctic and Subarctic Seas. *Medd. Stockholms Univ. Geol. Inst.*, **275**, 1-45.

Gard, G. & Backman, J. 1990. Synthesis of Arctic and Sub-Arctic coccolith biochronology and history of North Atlantic drift water influx during the last 500,000 years. *In:* Bleil, U. & Thiede, J. (eds.), *Geological history of the Polar Oceans: Arctic versus Antarctic*, 417-436, Kluwer Academic Publishers, Dordrecht.

Goldschmidt, P.M. 1994. The ice-rafting history in the Norwegian-Greenland Sea for the last two glacial/interglacial cycles. *Berichte aus dem Sonderforschungsbereich 313*, **50**, 1-103.

Goldschmidt, P.M. 1995. Accumulation rates of coarse-grained terrigenous sediment in the Norwegian-Greenland Sea: Signals of continental glaciation. *Marine Geology*, **128**, 137-151.

Goldschmidt, P.M. *this volume*. The ice-rafting history of coarse-grained sediments in the Norwegian-Greenland Sea for the last two glacial/interglacial cycles.

Haake, F.W. & Pflaumann, U. 1989. Late Pleistocene foraminiferal stratigraphy on the Vøring Plateau, Norwegian Sea. *Boreas*, **18**, 343-356.

Hamich, A. 1991. Sedimentologische Untersuchungen eines Kernes (GIK 21906-2) der Grönlandsee. unpubl. diploma thesis, Univ. Kiel, 78 pp.

Hebbeln, D. 1992. Weichselian glacial history of the Svalbard area: correlating the marine and terrestrial records. *Boreas*, **21**, 295-304.

Henrich, R., Kassens, H., Vogelsang, E. & Thiede, J. 1989. Sedimentary facies of glacial-interglacial cycles in the Norwegian Sea during the last 350 ka. *Marine Geology*, **86**, 283-319.

Henrich, R. 1992. Beckenanalyse des Europäischen Nordmeeres: Pelagische und glaziomarine Sedimenteinflüsse im Zeitraum 2.6 Ma bis Rezent. unpubl. habil. thesis, Univ. Kiel.

Hesse, R. & Chough, S.K. 1980. The Northwest Atlantic Mid-Ocean Channel of the Labrador Sea: II. Deposition of parallel laminated levee-muds from the viscous sublayer of low density turbidity currents. *Sedimentology*, **27**, 697-711.

Hollister, C.D. & Heezen, B.C. 1972. Geologic effects of ocean bottom currents. In: Gordon, A.L. (ed.), *Studies in physical oceanography - A tribute to Georg Wüst on his 80th birthday*, 37-66, Gordon and Breach, New York **2**.

Imbrie, J., Hays, J.D., Martinson, D.G., McIntyre, A., Mix, A.C., Morley, J.J., Pisias, N.G., Prell, W.L. & Shackleton, N.J. 1984. The orbital theory of Pleistocene climate: support from a revised chronology of the marine $\delta^{18}O$ record. *In:* Berger, A. et al. (eds.), Milankovitch and climate, Part 1, 269-305, Reidel, Dordrecht.

Johannessen, O.M. 1986. Brief overview of the physical oceanography. *In:* Hurdle, B.G. (ed.), *The Nordic Seas*, 103-127, Springer, New York.

Johnson, G.L. & Campsie, J. 1976. Morphology and structure of the western Jan Mayen Fracture Zone. *Norw. Polarinst. Arb.*, **1974**, 69-81.

Jouzel, J., Lorius, C., Petit, J.R., Genthon, C., Barkov, N.I., Kotlyakov, V.M. & Petrov, V.N. 1987. Vostok ice core: a continuous isotope temperature record over the last climatic cycle (160,000 years). *Nature*, **329**, 403-409.

Jouzel, J., Raisbeck, G., Benoist, J.P., Yiou, F., Lorius, C.,

Raynaud, D., Petit, J.R., Barkov, N.I., Korotkevitch, Y.S. & Kotlyakov, V.M. 1989. The Antarctic climate over the late Glacial period. *Quaternary Reserarch*, **31**, 135-150.

Jünger, B. 1994. Tiefenwassererneuerung in der Grönlandsee während der letzten 340.000 Jahre. *GEOMAR Report*, **35**, 1-103.

Kellogg, T.B. 1976. Late Quaternary climatic changes: evidence from deep-sea cores of Norwegian and Greenland Seas. In: Cline, R.M. & Hays, J.D. (eds.), Investigation of Late Quaternary paleoceanography and paleoclimatology. *Geological Society of America Memoir*, **145**, 77-110.

Kellogg, T.B. 1977. Paleoclimatology and paleo-oceanography of the Norwegian and Greenland Seas: The last 450,000 years. *Marine Micropaleontology*, **2**, 235-249.

Kellogg, T.B. 1980. Paleoclimatology and paleoceanography of the Norwegian and Greenland seas: glacial-interglacial contrasts. *Boreas*, **9**, 115-137.

Koç Karpuz, N. & Jansen, E. 1992. A high-resolution diatom record of the last deglaciation from the SE Norwegian Sea: documentation of rapid climatic changes. *Paleoceanography*, **7**, 499-520.

Koltermann, K.P. 1987. Die Tiefenzirkulation der Grönland-See als Folge des thermohalinen Systems des Europäischen Nordmeeres. unpubl. PhD thesis, Univ. Hamburg, 287 pp.

Krumbein, W.C. 1936. Application of logarithmic moments to size frequency distributions of sediments. *Journal of Sedimentary Petrology*, **6**, 35-47.

Mangerud, J. 1991. The last ice age in Scandinavia. *Striae*, **34**, 15-30.

Mangerud, J. & Svendsen, JI. 1992. The last interglacial-glacial period on Spitsbergen, Svalbard. *Quaternary Science Reviews*, **11**, 633-664.

Martinson, D.G., Pisias, N.G., Hays, J.D., Imbrie, J., Moore, T.C. & Shackleton, N.J. 1987. Age dating and the orbital theory of the Ice Ages: Development of a high-resolution 0 to 300,000 years chronostratigraphy. *Quaternary Research*, **27**, 1-29.

Mayewski, P.A., Wumkes, M., Klinck, J., Twickler, M.S., Putscher, J.S., Taylor, K.C., Gow, A.J., Waddington, E.D., Alley, R.B., Gibb, J.E., Grootes, P.M., Meese, D.A., Ram, M., Whalen, M. & Wilson, A.T. 1994. Record Drilling Depth Struck in Greenland. *EOS*, **75**, 113-124.

Michels, K. 1994. Strömungssortierung quartärer Sedimente des Europäischen Nordmeeres: Analyse von Sinkgeschwindigkeits-Verteilungen. *Berichte aus dem Sonderforschungsbereich 313*, **55**, 1-127.

Mienert, J., Kenyon, N.H., Thiede, J. & Hollender, F.-J. 1993. Polar continental margins: studies off East Greenland. *EOS*, **74**, 225.

Mienert, J., Andrews, J.T. & Milliman, J.D. 1992. The East Greenland continental margin (65°N) since the last deglaciation: Changes in seafloor properties and ocean circulation. *Marine Geology*, **106**, 217-238.

Nam, S.I. 1996. Late Quaternary glacial/interglacial changes in paleoclimate and paleoceanographic circulation along the East Greenland continental margin. unpubl. PhD thesis, Univ. Bremen.

Nam, S.I., Stein, R., Grobe, H. & Hubberten, H. 1995. Late Quaternary glacial-interglacial changes in sediment composition at the East Greenland continental margin and their paleoceanographic implications. *Maine Geology*, **122**, 243-262.

Nowaczyk, N.R. & Antonow, M. in press. Magnetostratigraphy of Greenland Sea Sediments I - Identification of the Mono Lake, Laschamp and Biwa I geomagnetic polarity events. *Geophysical Journal International*.

Paquette, R.G., Bourke, R.H., Newton, J.F. & Perdue, W. 1985. The East Greenland polar front in autumn. *Journal of Geophysical Research*, **90**, 4866-4882.

Rudels, B. 1990. Haline convection in the Greenland Sea. *Deep Sea Research*, **37**, 1491-1551.

Sarnthein, M. 1971. Oberflächensedimente im Persischen Golf und Golf von Oman II. Quantitative Komponentenanalyse der Grobfraktion. *„Meteor" Forsch.-Ergebn.*, **C5**, 1-113.

Sarnthein, M., Jansen, E., Arnold, M., Duplessy, J.C., Erlenkeuser, H., Flatøy, A., Veum, T., Vogelsang, E. & Weinelt, M.S. 1992. $\delta^{18}O$ time-slice reconstruction of meltwater anomalies at Termination I in the North Atlantic between 50 and 80°N. *In:* Bard, E. & Broecker, W.S. (eds.), *The last deglaciation: absolute and radiocarbon chronologies*, 183-200, Springer, Berlin.

Shackleton, N.J. & Opdyke, N.D. 1973. Oxygen isotope and paleomagnetic stratigraphy of Equatorial Pacific core V28-238: Oxygen isotope temperatures and ice volumes on a 10^5 year and 10^6 year scale. *Quaternary Research*, **3**, 39-55.

Shackleton, N.J. & Opdyke, N.D. 1976. Oxygen isotope and paleomagnetic stratigraphy of Pacific core V28-238 Late Pliocene to Latest Pleistocene. *Geological Society of America Memoir*, **145**, 449-464.

Spielhagen, R.F. 1991. Die Eisdrift in der Framstraße während der letzten 200.000 Jahre. *GEOMAR Report*, **4**, 1-133.

Spielhagen, R.F. & Thiede, J. 1994. Late Quaternary changes in the Arctic ocean ice cover. *Berichte zur Polarforschung*, **144**, 101-105.

Staudinger, G., Hangl, M. & Pechtl, P. 1986. Quick optical measurement of particle distribution in a sedimentation apparatus. *Particle Characteristics*, **3**, 158-162.

Stein, R., Grobe, H., Hubberten, H., Marienfeld, P. & Nam, S. 1993. Latest Pleistocene to Holocene changes in glaciomarine sedimentation in Scoresby Sund and along the adjacent East Greenland Continental Margin: Preliminary results. *Geo-Marine Letters*, **13**, 9-16.

Stein, R., Nam, S., Grobe, H. & Hubberten, H. 1996. Late Quaternary glacial history and short-term ice-rafted debris fluctuations along the East Greenland continental margin. In: Andrews, J.T., Austin, W.E.N., Bergsten, H. & Jennings, A.E. (eds.), Late Quaternary paleoceanography of the north Atlantic margins, 135-151, *Geological Society Special Publication*, **111**, London.

Stein, R., Nam, S., Schubert, C., Vogt, C., Fütterer, D. & Heinemeier, J. 1994. The last deglaciation event in the eastern central Arctic Ocean. *Science*, **264**, 692-696.

Struck, U. 1992. Zur Paläo-Ökologie benthischer Foraminiferen im Europäischen Nordmeer während der letzten 600.000 Jahre. *Berichte aus dem Sonderforschungsbereich 313*, **38**, 1-89.

Syvitski, J.P.M. 1991. *Principles, methods, and application of particle size analysis.* 368 pp, Cambridge University Press, Cambridge.

Thiede, J. & Hempel, G. (eds.) 1991. Die Expedition ARKTIS-VII/1 mit FS „Polarstern" 1990. *Berichte zur Polarforschung*, **80**, 1-137.

Thiede, J., Suess, E. & Müller, P.J. 1982. Late Quaternary fluxes of major sediment components to the sea floor of the northwest African continental slope. *In:* v. Rad, U. *et al.* (eds.), *Geology of the Northwest African continental margin*, 605-631, Springer, Berlin.

Thies, A. 1991. Die Benthos-Foraminiferen im Europäischen Nordmeer. *Berichte aus dem Sonderforschungsbereich 313*, **31**, 1-73.

Van Andel, T.H., Heath, G.R. & Moore, T.C. 1975.

Cenozoic history and paleoceanography of the central Equatorial Pacific. *Geological Society of America Memoir*, **143**, 134.

Vinje, T. & Finnekasa, Ö. 1986. The ice transport through the Fram Strait. *Norsk Polarinstitutt Skrifter*, **186**, 1-39.

Vogelsang, E. 1990. Paläo-Ozeanographie des Europäischen Nordmeeres an Hand stabiler Kohlenstoff- und Sauerstoffisotope. *Berichte aus dem Sonderforschungsbereich 313*, **23**, 1-136.

Vogt, P.R. 1986. Geophysical and geochemical signatures and plate tectonics. *In:* Hurdle, B.G. (ed.), *The Nordic Seas*, 413-662, Springer, Berlin.

Weinelt, M. 1993. Veränderungen der Oberflächenzirkulation im Europäischen Nordmeer während der letzten 60.000 Jahre - Hinweise aus stabilen Isotopen. *Berichte aus dem Sonderforschungsbereich 313*, **41**, 1-106.

Winn, K., Samthein, M. & Erlenkeuser, H. 1991. $\delta^{18}O$ stratigraphy and chronology of Kiel sediment cores from the East Atlantic. *Reports Geologisch-Paläontologisches Institut der Universität Kiel*, **45**, 99 pp.

Wollenburg, I. 1993. Sedimenttransport durch das arktische Meereis: Die rezente lithogene und biogene Materialfracht. *Berichte zur Polarforschung*, **127**, 1-159.

Wolf, T.C.W. 1991. Paläo-ozeanographisch-klimatische Entwicklung des Nördlichen Nordatlantiks seit dem späten Neogen. *GEOMAR Report*, **5**, 1-92.

Zahn, R. 1994. Core correlations. *Nature*, **371**, 289-290.

The ice-rafting history of coarse-grained sediments in the Norwegian-Greenland Sea for the last two glacial/interglacial cycles

PETER M. GOLDSCHMIDT

SFB 313, University of Kiel, Heinrich-Hecht-Platz 10, 24118 Kiel, Germany.

Present address: PCD, Eckernförder Str. 259, 24119 Kiel, Germany.

ABSTRACT

Using microscopic grain lithology analysis and factor analysis, the composition of coarse-grained sediments in the Norwegian-Greenland Sea (NGS) was investigated for the last two glacial/interglacial cycles (Oxygen Isotope Stages 6+5 and 2+1). These sediments can be classified into three facies: that dominated by quartz (QZF), that dominated by dark siltstones (DSF) and that dominated by biogenic material (BMF). The DSF occurs predominantly in NGS cores from Stage 6 and is thus a "strong glacial" facies. The main source for the DSF lies on Svalbard or east thereof; additional sources are the Norwegian continental shelf and north-eastern Greenland. The QZF dominates the sediment composition in Stage 2 and portions of Stages 5 and 1, as well as Terminations II and I; since the Weichselian (Stage 2) glaciation was much weaker than the Saale (Stage 6) glaciation, the QZF is considered to be a "weak glacial" and "deglacial" facies. Because the QZF consists of broken-down crystalline rocks, source areas could lie anywhere in the Arctic realm. The BMF dominates the sediments in most of Stages 5 and 1; it is therefore an "interglacial" facies signalling the lack of great terrigenous input.

A peak in the deposition of the DSF or of the QZF in the NGS generally occurs within 1000 years of the deposition of Heinrich layers further south in the North Atlantic Ocean. This, coupled with the fact that accumulation rates at the times of deposition of the Heinrich layers are generally increasing or high in the NGS, indicates that there is a possibility that sudden glacier surges and resulting iceberg calving events from the Scandinavian Ice Sheet occurred within 1000 years of those from the Laurentide Ice Sheet.

INTRODUCTION

The advent of polar palaeoceanography is generally marked with the expedition of Fritjof Nansen a century ago. Yet progress was slow until modern icebreaking technology allowed nuclear and conventionally powered icebreakers to reach as far as the North Pole (see Weber & Roots, 1990). The Earth's subpolar regions are extremely sensitive to variations in climate and are therefore ideal for investigating climate change.

This paper is concerned with the sediments that were deposited on the floor of the Norwegian-Greenland Sea (NGS) during the last two glacial/interglacial cycles. The sediments in this investigation are studied

- to identify ice-rafted debris within the sediments;
- to determine compositional differences in the lithology of the sediments in order to reconstruct ice drift patterns and trace sediments back to their source regions;
- to use the ice drift pattern reconstructions to determine spatial and temporal variations in oceanographic currents in the study area; and
- to compare the results gleaned from the investigation of ice-rafted debris to marine and continental records from other studies in order to derive a glaciation history of the circum-Arctic land areas and an ice-rafting history for the Norwegian-Greenland Sea.

This study is limited to the last two glacial/interglacial cycles (Oxygen Isotope Stages 6 and 5, ca. 190-ca. 60 ka, including Termination II, and Oxygen Isotope Stages 2 and 1, ca. 25 ka to present, including Termination I) in order to distinguish differences between strongly glacial and strongly interglacial climates (the boundaries for the stages were defined according to Imbrie *et al.*, 1984 and Martinson *et al.*, 1987). Most sediment cores taken in the Norwegian-Greenland Sea area are long

In: Hass, H.C. & Kaminski, M.A. (eds.) 1997. Contributions to the Micropaleontology and Paleoceanography of the Northern North Atlantic. *Grzybowski Foundation Special Publication*, no. 5, pp. 119-139

enough to contain these two cycles; thus a detailed record of several palaeoceanographic parameters exists for these two cycles, whereas previous glacial/interglacial cycles are not as well sampled. The cores analysed in this investigation have also been studied for several parameters including carbonate contents (Henrich, 1992), subpolar planktic and benthic foraminifers (Henrich, 1992), the chronological occurrence of sediment pellets (Goldschmidt, 1994), changes in organic geochemistry (Wagner, 1993; Wagner & Henrich, 1994), accumulation rates of coarse sediments (Goldschmidt, 1995) and bottom current velocities (Michels, 1994). Together with similar studies in the same geographic area (Bischof, 1991, 1994) as well as lithological investigations in neighbouring areas (e.g. Hebbeln, 1991; Kubisch, 1991; Spielhagen, 1991), it is hoped that the data from all these studies will contribute to an understanding of past eras of climate change with an eye toward comprehending the changes that are occurring today.

Introduction to the study area

The Norwegian-Greenland Sea is the only significant link between the Atlantic and Arctic Oceans. Presently surface currents in the NGS are marked by relatively warm water flowing from the Atlantic Ocean into the southern and eastern NGS and cold Arctic Water flowing into the northern and western NGS (Fig. 1).

The Norwegian Current brings the relatively warm North Atlantic Water (NAW; temperature 6-10°C, salinity 35.1-35.3‰) northwards off the Norwegian coast; the Norwegian Coastal Current (NCC) and the eastern portion of the NAW then flow along the northern coast of Norway (North Cape Current) and exit into the Barents Sea while the main portion of the NAW continues to flow northward in the West Spitsbergen Current to the Fram Strait; some of this NAW then flows into the Arctic Ocean, where it sinks due to an increase in density (Swift, 1986).

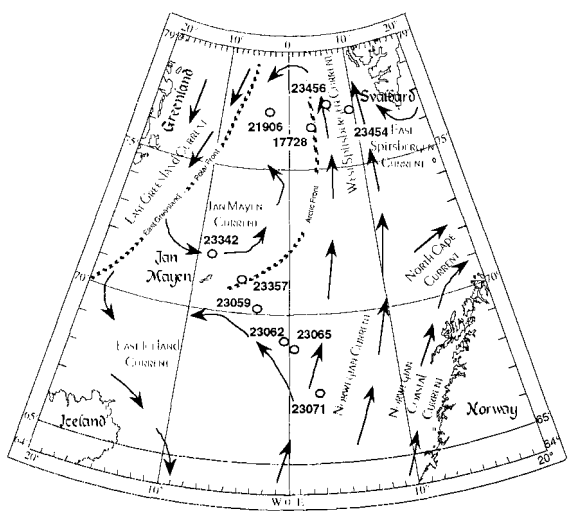


Figure 1 Modern surface currents in the Norwegian-Greenland Sea. Locations of cores investigated in this study are shown. After Henrich *et al.* (1995).

Cold water is discharged from the Arctic Ocean into the western NGS via the East Greenland Current (EGC; temperature <0°C, salinity 30-34‰). Water in the EGC can continue to flow southward into the Atlantic Ocean through Denmark Strait or curve eastward in the East Iceland or the Jan Mayen Currents. Water in the central NGS (the Arctic Surface Water) that results from the mixing of the cold EGC waters and the relatively warm NAW has a temperature of 0-4°C and a salinity of 34.6-34.9‰ (Swift, 1986).

The Norwegian-Greenland Sea and the Arctic Ocean differ from most of the world's other oceans because of the presence of a broad blanket of sea ice covering portions of them. This blanket serves not only to insulate the water from the atmosphere, but also provides a great concentration of salt where ice forms in the marginal seas (salt is left behind when seawater freezes) and of freshwater in areas of melting ice. In addition, the ice can be sediment-laden, providing coarser sediments a way of reaching the deep ocean basins in this area.

Ice-transported material

Sediments that have been transported by ice are usually called "ice-rafted detritus" (IRD). This does not, however, refer only to iceberg-rafted sediments, but also to those carried by sea ice. Differentiating sediments that have been dropped by melting icebergs from those that have been deposited by melting sea ice is not an easy task, yet it is important in the reconstruction of both palaeoclimates and of glacial advances and retreats. Due to the processes by which sediments are incorporated into glaciers vs. those through which sediments are entrained into sea ice, glacial (iceberg-deposited) sediments are usually considered to be coarser than those dropped by sea ice (see von Huene *et al.*, 1973; Hopkins & Herman, 1981; Spjeldnaes, 1981; Clark & Hanson, 1983; Goldschmidt *et al.*, 1992). Sediment grains coarser than 63 μm are usually considered to be ice-rafted (sea ice or icebergs; Mullen *et al.*, 1972, Watkins *et al.*, 1982), and grains >500 μm are considered to be iceberg-rafted (but see Emery, 1963). Several studies have used this 500 μm boundary to reconstruct past iceberg drift paths (e.g. Molnia, 1983; Bischof, 1991; Kubisch, 1991; Spielhagen, 1991; Elverhøi, 1992). But it must be kept in mind that, although it is less likely that coarse sediments are incorporated into (and later deposited by) sea ice than into icebergs and glaciers, this does not mean that it is impossible (see

Goldschmidt *et al.*, 1992). Many investigations in the Arctic have found coarse sediments on or in sea ice (e.g. Kane 1857; Tarr 1897; Herman, 1974; Wollenburg, 1991; Nürnberg *et al.*, 1994). However, in this paper it is assumed that coarse IRD found in sediment cores was deposited by melting icebergs.

MATERIAL AND METHODS

Determining the lithology of sediment samples

Sample selection

Cores selected for sampling of sediments for lithological studies are shown in Table 1 and Figure 1. The layout of the cores defines two transects, one running northwest-southeast across the central Norwegian-Greenland Sea and the other striking west-east between Greenland and southern Svalbard. These cores were chosen because their location can provide both detailed information for the transects themselves and general information for the Norwegian-Greenland Sea as a whole. Bioturbation in these cores is generally low for the investigated time period, allowing an increased accuracy for the dating of the cores. Furthermore, a large database for comparison already exists for most of these cores (Henrich *et al.*, 1989, 1995; Bischof *et al.*, 1990; Bischof, 1991, 1994; Henrich, 1992; Wagner, 1993; Michels, 1994; Wagner & Henrich, 1994; Goldschmidt, 1995); this makes it possible to correlate various parameters of the same cores and to refine palaeoceanographic interpretations. Two new, unstudied cores (23454 and 23456) were included to broaden the database for the northern transect.

Samples of ca. 1 cm thickness were taken from each of the cores on board ship. The sampling interval was 5-10 cm, which eventually led to a temporal resolution of up to ca. 200 years, depending on the sedimentation rate. The samples that were used in this investigation were taken from the beginning of Stage 6 (186-128 ka) to the end of Stage 5 (128-71 ka); additional samples document the transitions between Stages 7 and 6 and Stages 5 and 4. The same method was used for Stages 2 (24-13.6 ka) and 1 (13.6 ka-present); additional samples document the transition between Stages 3 and 2. Thus investigated samples had ages of ca. 190 to ca. 60 ka and ca. 25 to ca. 0 ka.

An approximately 2-5 cm^3 sample was used for carbonate measurements; these provided a preliminary stratigraphy. Sediment samples collected from the same depth as the carbonate samples were dried, weighed and washed in a hydrogen peroxide solution to disintegrate aggregates. The sediment mixture was then washed through a 63 µm sieve to separate the coarse from the fine fraction. The coarse fraction was then dried and weighed; the fine fraction was not used in this investigation and will not be further described.

After weighing, the coarse subsample was dry-sieved into the following fractions: 63-125 µm, 125-250 µm, 250-500 µm, 500-1000 µm and >1000 µm. These fractions were then weighed to determine the percentages of the weights of the various fractions in regard to the coarse and the total sample weights.

The lithology of ice-rafted sediment was determined by investigating two groups of sediment fractions: the 125-500 µm and the >500 µm fractions. Both fractions were analysed identically. At least 300 grains per fraction (equals >600 grains per sample) were examined under a reflecting light microscope. Occasionally the >500 µm fraction consisted of fewer than 300 grains; in this case all the existing grains were counted. Slight statistical errors may occur when there are fewer than 300 grains (see Watkins *et al.*, 1982). The grains were classified into 22 lithological classes plus one for biogenic grains (which consists almost exclusively of the shells of the planktic foraminifera *Neogloboquadrina pachyderma* sin.); these classes are shown in Table 2. A similar study (Bischof, 1991) found that a more detailed analysis (106 classes), while providing information about more specific rock types, could not be used in analysing spatial and temporal variations; the great number of classes made it impossible to make uniform correlations between

Table 1. Parameters concerning investigated cores

Core	Ship*	Cruise	Latitude	Longitude	Water Depth (m)	Recovery (m)
17728	M	XIII/2	76°31.2'N	03°57.5'E	2473	5.95
21906	P	VII/1	76°50'N	02°09'W	2939	6.52
23059	M	II/2	70°18.3'N	03°07.4'W	2281	6.22
23062	M	II/2	68°43.7'N	00°10.1'W	2244	7.00
23065	M	II/2	68°29.7'N	00°49.1'E	2802	7.85
23071	M	II/2	67°05.1'N	02°54.5'E	1308	8.05
23342	M	VII/5	71°38.2'N	08°26.7'W	1974	5.98
23357	M	VII/5	70°57.3'N	05°32.6'W	1736	5.26
23454	M	XXI/4	76°45.1'N	08°02.6'E	2144	3.61
23456	M	XXI/4	77°04.0'N	06°20.5'E	2182	6.34

*Ships: M = Meteor, P = Polarstern

cores in space and time.

After grain analysis had been completed, the grain percentages were subjected to factor analysis to determine the statistical significance of IRD facies over time. Factor analysis was done for the grain counts of the >125 µm fraction for each core. This was accomplished using the CABFAC program (Imbrie & Kipp, 1971; Klovan & Imbrie, 1971).

To determine the age of the samples, oxygen and carbon isotope ($\delta^{18}O$ and $\delta^{13}C$) measurements were performed on the 125-250 µm fraction of the planktic foraminifera *Neogloboquadrina pachyderma* sin. Analyses were done at the C-14 Laboratory at the University of Kiel using the procedures described by Winn *et al.* (1991). Isotopic events and stage boundaries were located using data of Imbrie *et al.* (1984) and Martinson *et al.* (1987). Cores without isotopic data were dated by comparing characteristic maxima and minima in carbonate content to the carbonate curves of cores with isotopic datings. The age data are presented in the Appendix.

Table 2. Lithologies investigated in this study.

quartz + feldspar	*chalk*
mica	*coal*
mafic minerals	*quartzite*
sandstone	*mica schist*
dark siltstone	*phyllite*
light siltstone	*crystalline schist*
red siltstone	*light crystalline rock*
spiculitic chert	*dark crystalline rock*
other chert	*red crystalline rock*
fossiliferous limestone	*green crystalline rock*
light limestone	*biogenic matter*
dark limestone	

Presentation of the data

The graphs of the factor analysis graphs require some explanation. Simple line graphs of the factor loadings (>0.700, the limit of statistical significance) vs. age resulted in up to 6 different lines crossing each other repeatedly; it was nearly impossible to distinguish the paths of all of the lines in a graph. Thus the portion of the lines that exceed a factor loading of 0.700 were covered with boxes of different patterns, resulting in an understandable presentation of the lithology data (see Fig. 2).

RESULTS

Composition of the investigated sediments

Figure 3 shows the occurrence of the IRD facies determined to be significant by factor analysis. There are 3 main IRD facies, consisting of:

- the **quartz facies (QZF)**, where quartz is the dominant IRD facies;
- the **dark siltstone facies (DSF)**, where dark silt-

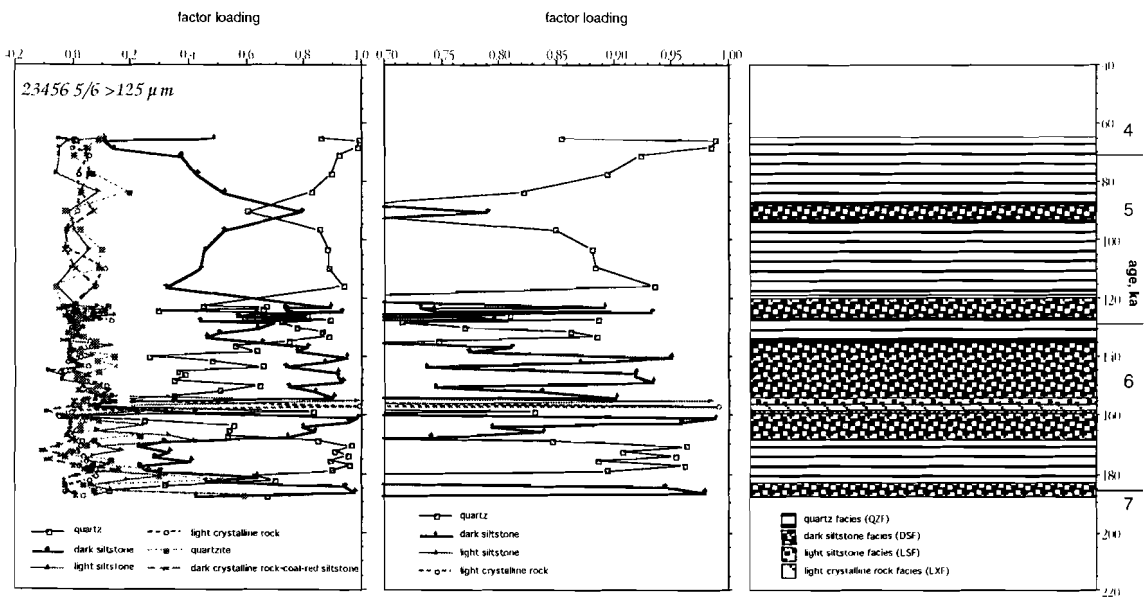


Figure 2. Process of presentation of results of factor analysis. Pure graphing results in the incomprehensible presentation at left. Restricting the results to factor loadings > 0.700 results in the presentation in the middle; this is better than that at left but is still difficult to understand. Covering the portion of the lines that exceed a factor loading of 0.700 with boxes of different patterns results in the understandable presentation at right.

stone is the dominant IRD facies; and
• the **biogenic material facies (BMF)**, where biogenic material dominates the sediments, indicating the *lack* of IRD.

Oxygen Isotope Stage 6
Northern transect. - The advent of Stage 6 can be seen as a dark siltstone facies (DSF) in the central cores of the northern transect (Fig. 3). An occurrence of the biogenic material facies (BMF) appears in the westernmost core (21906); the amount of terrestrial material is low enough in this core that biogenic material dominates during this period and, indeed, through nearly the entire core. At around 177-168 ka an influx of the quartz facies (QZF), interrupted briefly by a DSF, appears in all cores except 21906. Between 168 and 135 ka, cores 23454 and 17728 are dominated by alternating appearances of the QZF and the DSF while cores 23456 and 21906 apparently have too little terrestrial material and are thus dominated by the BMF. Toward the end of Stage 6 QZF deposition becomes predominant in all cores.

Souhern transect. - The BMF predominates in all cores for the Stage 7/6 transition in the southern transect. Greater amounts of terrigenous material begin to be deposited by 180 ka (178 ka in core 23342; Fig. 3). The QZF is deposited in all cores except 23062 (DSF) until about 173 ka. For the next 8 ky little terrigenous material is deposited except in core 23059 (QZF). The supply of terrigenous material gradually increases from east to west starting around 155 ka, so that the QZF is deposited in every core except the westernmost 23342 between 148 and 138 ka, including Event 6.3. Toward the end of Stage 6, the QZF was deposited in most cores while the DSF was deposited in core 23062. The QZF is the dominant facies for both transects in Termination II.

Oxygen Isotope Stage 5
Northern transect. - The QZF that was deposited toward the end of Stage 6 and in Termination II peters out during Event 5.5.3. After this time, nearly every core of the northern transect in Stage 5 has little terrigenous material; they are thus dominated by the biogenic matter facies (BMF). The northeasternmost core (23454), on the other hand, has more terrigenous sediment: rapid interlayering of the QZF and the DSF overwhelms the biogenic matter.

Southern transect. - The entire southern transect is dominated by the BMF for almost the entire Stage 5 (Fig. 3). The DSF does not appear at all here and the QZF appears only at 99-94 ka in core 23342. The near total dominance of biogenic matter nearly everywhere in the Norwegian-Greenland Sea (except in the core closest to Svalbard) demonstrates that ice-rafting was much less prevalent here than in Stage 6.

Oxygen Isotope Stage 2
Northern transect. - It can be seen that IRD deposition in the Stage 2 glaciation was much less intense than that in Stage 6 for both transects. The BMF is dominant in all but the westernmost core for most of Stage 2 in the northern transect (Fig. 3). Core 21906 consists of the DSF at the beginning of this Stage; a switch to the QZF occurs at about 18 ka. This QZF then becomes the dominant facies throughout the transect during Termination I.

Southern transect. - The facies deposited in the southern transect during Stage 2 are similar to those of Stage 6: the QZF dominates, there is interspersed BMF, and the DSF is absent (Fig. 3). The QZF covers the entire transect during the transition between Stages 3 and 2. The BMF is found at about 21.5-19 ka on both ends of the transect but not in the intervening cores. The QZF then covers most of the transect again between 18.5 and 13 ka; a small layer of BMF appears in core 23065 at ca. 17 ka.

Oxygen Isotope Stage 1
Northern transect. - At the beginning of Stage 1, QZF deposition occurs primarily in the western portion of the northern transect while DSF sediments are deposited mainly in the east (Fig. 3). The BMF appears asynchronously at ca. 11 ka in the west and ca. 6 ka in the east. The surficial sediments are made up of the BMF in every core.

Souhern transect. - QZF deposition is dominant in every core at the beginning of Stage 1 in the southern transect (Fig. 3). As is the case in the northern transect, the BMF appears asynchronously: the first appearance is at ca. 13 ka in cores 23059 and 23065, then at ca. 11 ka in cores 23342 and 23062 (the same time as in the western cores of the northern transect), with a final appearance at 9.5 ka in cores 23357 and 23071. As in the northern transect, the surficial sediments are made up of the BMF in every core.

DISCUSSION

Comparison of IRD facies with Norwegian-Greenland Sea lithofacies

In an attempt to categorise the sediments that occur in the Norwegian-Greenland Sea, Henrich (1992; Henrich et *al.*, 1995) presented a classification based on (1) carbonate content, (2) carbonate grain size, (3) terrestrial IRD content, (4) terrestrial IRD grain size, (5) the presence of planktic and benthic foraminifera as well as (6) the presence of sediment structures such as dropstones and bioturbation. In this classification are 8 lithofacies which point to differing depositional environments and the influence of various surface water masses:

• Lithofacies A and B3, rich in carbonate and poor in terrigenous matter, are currently being deposited beneath relatively warm Atlantic Water and in the transition to Arctic Surface Water. These lithofacies indicate that little floating ice existed in the NGS during their deposition in earlier periods. Lithofacies A and B3 are referred to as "warm water" lithofacies.

• Lithofacies B2, B1 and C represent the depositional environment beneath Arctic Surface Water and cold currents such as the modern East Greenland Current. Carbonate and terrigenous contents were somewhat lower and higher, respectively, than in lithofacies A and B3. Icebergs were common and sea ice cover dense at times. Lithofacies B2, B1 and C are referred to as "cool water" lithofacies.

• The diamictons of lithofacies D, E and F are related to high instabilities of tidewater glaciers which have advanced far out onto the outer continental shelf; large numbers of icebergs were released by retreating glaciers. Maximum amounts of the terrigenous coarse fraction and very low carbonate contents occur in these 3 lithofacies. These are referred to as "diamict" lithofacies.

Table 3 presents the sample depths (in cm) of the lithofacies in core 23071 determined by Henrich (1992). Also shown are the factor loadings determined by factor analysis for the quartz (QZF), dark siltstone (DSF) and biogenic matter facies (BMF) from this study. As can be seen in this example, lithofacies A and B3 are clearly dominated by the BMF. Lithofacies B1/B2 is also BMF-dominated, but the QZF is distinctly greater. The QZF rises to dominance in the C lithofacies and is clearly dominant in the diamict lithofacies D, E and F. (The table also indicates that four samples appear to be misidentified as C lithofacies by Henrich (1992); they are dominated by the BMF with QZF factor loadings of >0.300, and thus are more likely to belong to lithofacies B1/B2.) Taking this comparison into account, correlations between the IRD facies and the lithofacies of Henrich (1992; Fig. 4) are discussed below.

Oxygen Isotope Stage 6

The A and B3 lithofacies correlate well with the BMF in the penultimate glacial period. The B2/B1 lithofacies is usually made up of the QZF and DSF facies. The C lithofacies is dominated by the QZF and the BMF while the diamicts D, E and F are dominated by the QZF with subsidiary DSF and BMF.

Oxygen Isotope Stage 5

A positive correlation of the two "warm water"

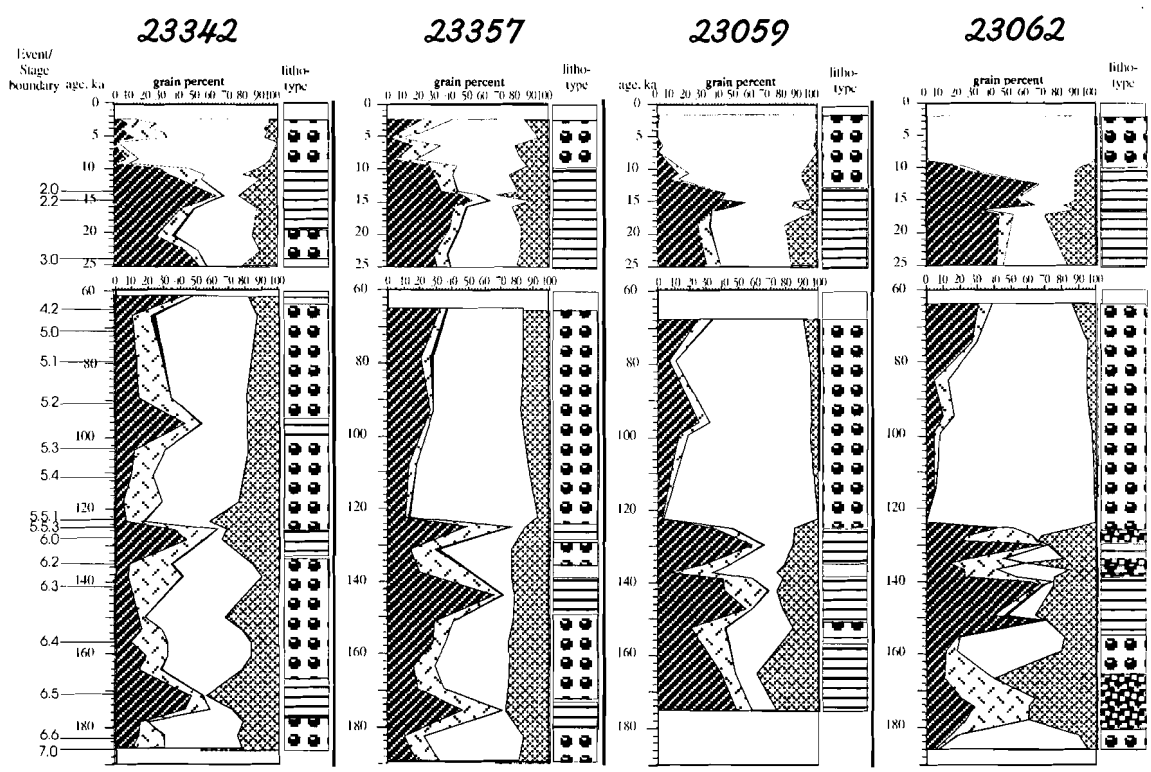


Figure 3. Results of the factor analysis of the >125 μm fraction for the cores examined in this study. The figure shows the occurrence of quartz, dark siltstone, chalk, coal, biogenic material and other terrigenous matter; to the right of each graph are the lithotypes resulting from factor analysis. Blank areas occur where factor analysis showed statistically insignificant results. Cores are displayed west to east. Legend to patterns on following page.

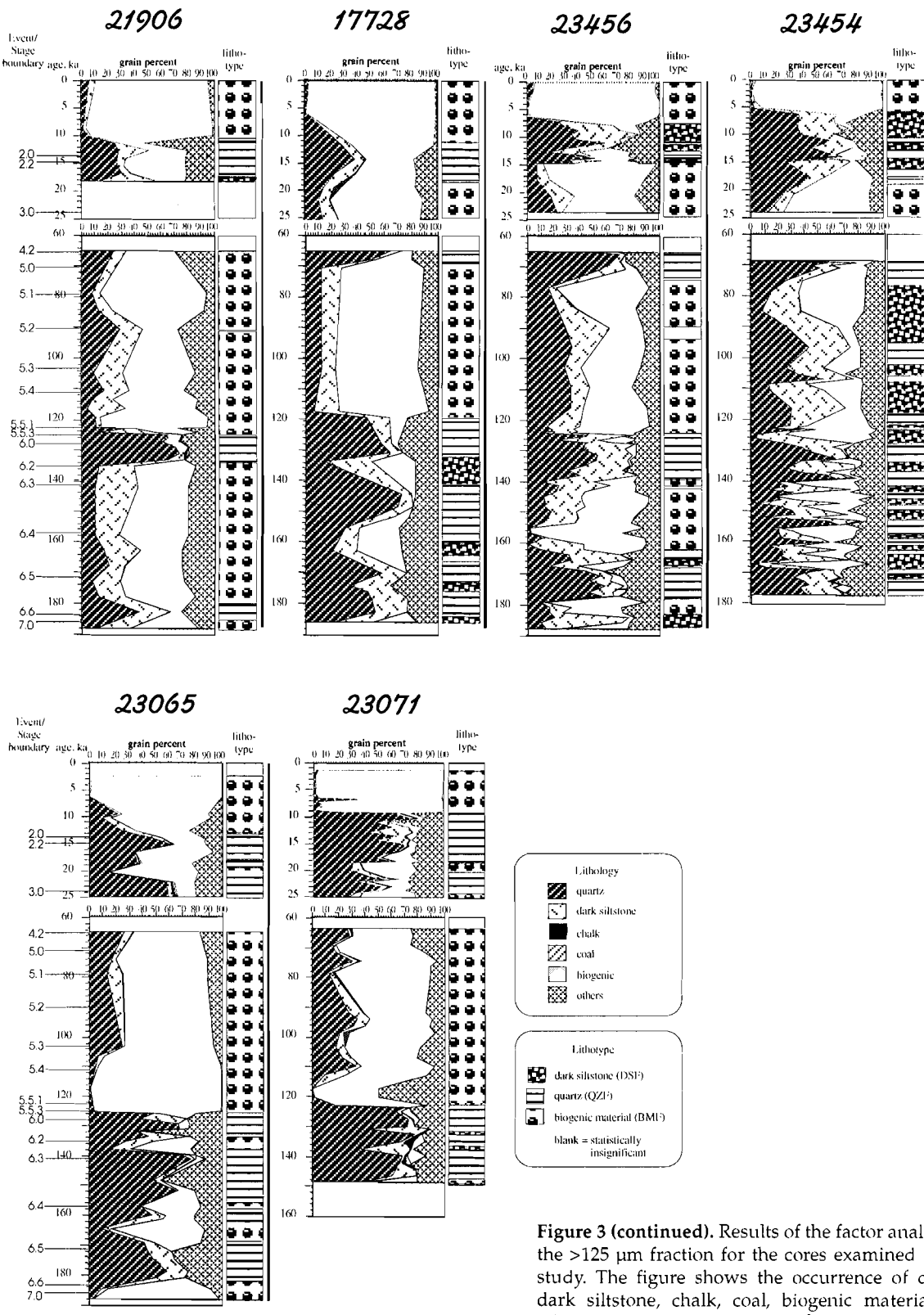


Figure 3 (continued). Results of the factor analysis of the >125 μm fraction for the cores examined in this study. The figure shows the occurrence of quartz, dark siltstone, chalk, coal, biogenic material and other terrigenous matter; to the right of each graph are the lithotypes resulting from factor analysis. Blank areas occur where factor analysis showed statistically insignificant results. Cores are displayed west to east.

Table 3. Example of comparison of IRD facies vs. lithofacies. Shown are the depths (in cm) of the occurrence of Henrich lithofacies (left column) vs. the factor loadings of the quartz (QZF), dark siltstone (DSF) and biogenic matter (BMF) facies for core 23071. Highest factor loading is shown in bold print.

A	QZF	DSF	BMF
520	.148	-.010	**.986**
530	.349	.025	**.934**
536	.184	.056	**.981**
544	.037	.021	**.997**
avg.=	.180	.023	**.974**
B3	**QZF**	**DSF**	**BMF**
596	.186	.106	**.968**
620	.023	.193	**.976**
634	-.134	-.034	**.988**
644	-.111	-.034	**.991**
avg.=	-.009	.058	**.981**
B1/B2	**QZF**	**DSF**	**BMF**
558	.380	.177	**.904**
567	.462	.126	**.872**
575	.412	.117	**.900**
584	.179	-.004	**.974**
596	.186	.106	**.968**
604	.301	.072	**.937**
610	.390	.022	**.912**
avg.=	.330	.088	**.924**
C	**QZF**	**DSF**	**BMF**
55	**.875**	.276	.387
63	**.892**	.266	.353
70	**.785**	.389	.402
80	**.824**	.354	.434
89	.542	**.791**	.279
94	**.873**	.274	.400
101	.675	**.686**	.259
106	**.894**	.259	.363
121	**.875**	.220	.428
130	**.815**	.235	.428
140	**.707**	.215	.672
151	**.799**	.212	.553
160	.366	.146	**.918**
170	.339	.199	**.917**
180	**.733**	.278	.609
184	**.824**	.299	.478
193	.498	.250	**.824**
221	**.755**	.259	.594
230	.406	.134	**.900**
avg.=	**.709**	.302	.537
DEF	**QZF**	**DSF**	**BMF**
113	**.910**	.234	.340
210	**.784**	.262	.560
748	**.959**	.227	.167
756	**.948**	.280	.144
avg.=	**.900**	.251	.303

lithofacies A and B3 with the BMF occurs in Stage 5. Core 23454 continues to show predominance of the DSF in these two lithofacies; this indicates both a greater supply of terrigenous material to this part of the Norwegian-Greenland Sea and a proximity to DSF source areas. The B2/B1 lithofacies is dominated by the QZF or the BMF. The two brief diamicts at the beginning of Stage 5 in cores 23357 and 23342 are QZF-dominated.

Oxygen Isotope Stage 2

The QZF dominates most of Stage 2; the DSF is greatly reduced compared to Stage 6. The DSF is only prominent in the B3 lithofacies in core 21906. The BMF can be seen in the B2/B1 and C lithofacies in other cores; since Stage 2 is a glacial era, the presence of the BMF in these lithofacies indicates that very low amounts of terrestrial material were deposited in these cores compared to the Stage 6 glaciation.

Oxygen Isotope Stage 1

The DSF continues to be uncommon in Stage 1; it is found only in the northeast (cores 23454 and 23456), implying that the northeastern DSF source was still being eroded by glaciers during the first half of Stage 1. The QZF predominates in the "cool" lithofacies C and B2/B1, but the presence of the BMF shows that relatively little terrigenous matter was being deposited. As usual, the "warmer" lithofacies A and B3 (affected by Atlantic waters) are BMF-dominated.

Summary of correlation of IRD facies with Henrich lithofacies

In general, the dark siltstone facies (DSF) appears much more frequently in Stages 6 and 5 (the penultimate glacial/interglacial cycle) than in Stages 2 and 1 (the last such cycle). The core with the greatest occurrences of this facies is core 23454, which lies off the coast of Svalbard. This implies that either Svalbard or the Barents Sea is the largest contributor of dark siltstones to the Norwegian-Greenland Sea. Furthermore, greater quantities of IRD in general and of the DSF in particular appear to have been transported from Svalbard or the Barents Sea in the penultimate glacial/interglacial cycle than in the later one.

Generally, the "warm water" lithofacies A and B3 are dominated by the biogenic matter facies (BMF). The DSF dominates in lithofacies B2/B1 and C. It does not figure strongly in the diamicts, which are usually dominated by the quartz facies (QZF). This is surprising, since the diamicts tend to be dark in colour, and it was assumed that this colouring comes from massive quantities of dark siltstones. Figure 5 shows that this does not appear to be the case. In this figure, the grain percentages

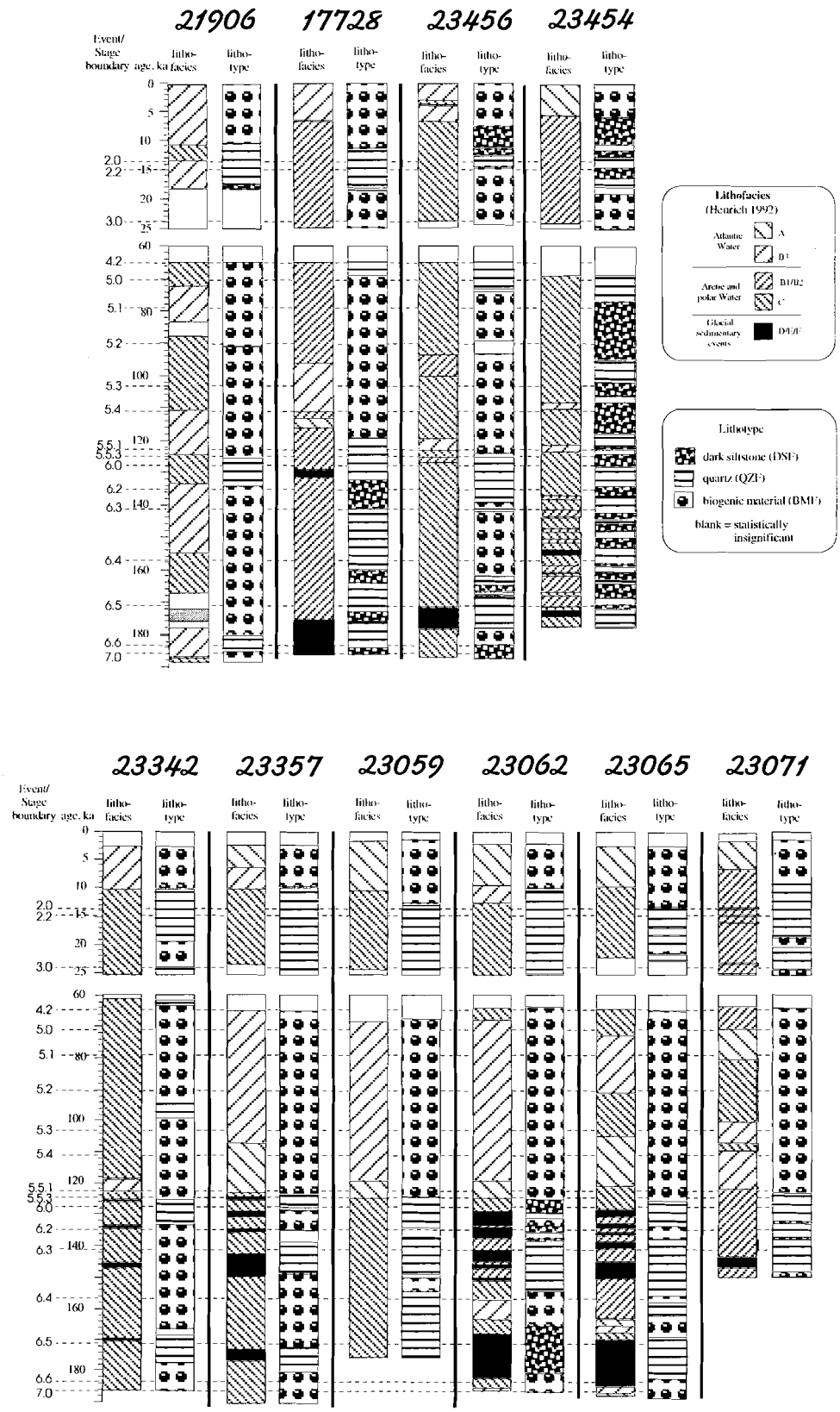


Figure 4. Comparison of Henrich lithofacies and IRD facies determined by factor analysis for the northern (top) and southern (bottom) transects.

of dark siltstones, chalk and coal are plotted against time and compared to the lithofacies of Henrich (1992). It can be seen that there are peaks in dark siltstone deposition during the deposition of the diamicts. It can also be seen, however, that (1) sometimes very few dark siltstones occur in the diamicts (e.g. core 23065, ca. 148 ka) and (2) peaks in dark siltstone deposition occur in other lithofacies. Sometimes these dark siltstone peaks are higher than the peaks in the diamicts (e.g. core 23071, diamict at 145 ka *vs.* dark siltstone peak at 139 ka).

Wagner (1993) found that the diamicts generally contain sediments with high total organic carbon (TOC) contents. While background TOC contents average about 0.20-0.30 weight percent (wt.%), diamicts have values of up to 1.04 wt.%. Results of the present study show that the same diamict samples determined by Wagner (1993) to have high TOC values have quartz:dark siltstone grain percent ratios of up to 20:1, averaging about 8:1. Although not all diamicts have TOC peaks, those that don't do not have a lower quartz:dark siltstone ratio than those that do. The coarser >500 µm fraction, however, has a quartz:dark siltstone grain percent ratio of up to ca. 1:2. This means that the coarser fraction contains a much higher proportion of dark siltstones; these may be the ones that account for the TOC peaks in the studies of Wagner (1993). Dark siltstones that were included during diamict deposition may thus be more TOC-rich or have larger grain sizes than dark siltstones deposited at other times; this may mean that the dark siltstones in the sediment that makes up diamicts originates in a different (high-TOC) source region than the dark siltstones from other lithofacies.

The distribution of the sediment lithology determined in this study and its relationship with the lithofacies determined by Henrich (1992) and with palaeoclimates can thus be summarised:

- The dark siltstone facies (DSF) is generally more frequent during glacials than in interglacials and also occurred more often in the penultimate glacial/interglacial cycle as opposed to the last one. The DSF can therefore be generally viewed as a "strong glacial" facies.
- The DSF is most prominent in the northern transect than in the southern.
- This appears to implicate Svalbard or regions east thereof as sources for the DSF.
- These land sources were supplemented by marine (continental shelf) sources during glacial times when glaciers advanced onto the continental shelves. The Barents Sea Shelf was probably another source for the DSF (see point above).
- The QZF facies was predominant during the Stage 2 glaciation, which was weaker than that of Stage 6. It was also deposited in both Terminations II and I. It can therefore be viewed as a "weak glacial" and "deglacial" facies.
- The BMF was deposited predominantly in interglacial periods, although it appears sporadically in glacial periods. It signals low amounts of terrigenous sedimentation and can be viewed as an "interglacial" facies.
- The "warm water" lithofacies A and B3 correlate with the biogenic matter facies (BMF).
- The "cool water" lithofacies B2/B1 correlate mostly with the DSF.
- The diamict lithofacies D, E and F usually correlate with the QZF, although

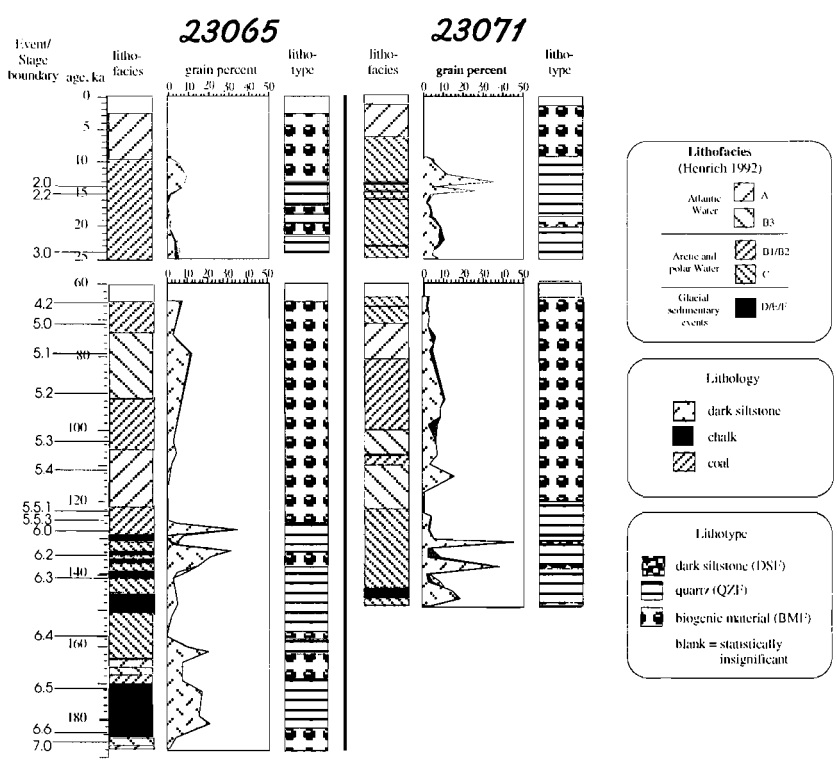


Figure 5: Comparison of Henrich lithofacies (left), makeup of the sediment according to the grain percentages of dark siltstone, chalk and coal (middle) and IRD facies determined through factor analysis (right) for cores 23065 and 23071.

there are some DSF diamicts. The DSF tends to show peaks in the diamicts but is still usually subordinate to quartz. The DSF lithofacies in the diamicts may contain rocks with higher TOC values than those in other lithofacies.

- The lithofacies defined by Henrich (1992) show some correlation with the IRD facies presented here. Any particular lithofacies can be divided into further subdivisions based on IRD facies. To do this would refine the ice-rafting history of any particular core but differences in the details would result in a reduced capability to correlate cores (see Bischof, 1991).

Correlation of IRD facies with accumulation rates

It would be interesting to know if there is a relationship between the IRD facies and the accumulation rates of coarse ice-rafted debris from the Norwegian-Greenland Sea (Goldschmidt, 1995); for instance, is the dark siltstone facies (DSF) associated with high accumulation rates? Or is this association affected by glacial/interglacial contrasts? The following discussion of Stages 6 and 5 compares the facies and the accumulation rate data (Fig. 6).

During the transition from the interglacial Stage 7 to the glacial Stage 6 (186 ka), accumulation rates (AR) were ca. 200 mg/cm^2/ky in the western NGS and ca. 200-450 mg/cm^2/ky in the northern and eastern NGS (Goldschmidt, 1995). The IRD facies indicate that the dark siltstone facies (DSF) was deposited only in the north at this time; the biogenic material facies (BMF) was deposited in the south. Thus, terrigenous matter, consisting of the DSF, was deposited in significant quantities only in the northern NGS. High ARs in the northern NGS correlate with this deposition of terrigenous matter. But the fact that the ARs in the eastern NGS were higher than those in the western NGS is not explained by the IRD facies. For Events 6.5-6.2 (171-135 ka) QZF is predominant in the high accumulation areas (up to 900 mg/cm^2/ky; Goldschmidt, 1994) of the southern transect, especially off the Norwegian coast, while the DSF dominates the high AR (up to 500 mg/cm^2/ky; Goldschmidt, 1994) sediments in the north.

During the first 5000 years of Stage 5 (128-123 ka) there were several high accumulation areas, notably off the coast of Norway (up to 700 mg/cm^2/ky; Goldschmidt, 1994) and south of Fram Strait (up to 1500 mg/cm^2/ky; Goldschmidt, 1994). The highest AR locations were almost invariably associated with the QZF. Supporting this is the fact that most of the diamict lithofacies, indicative of large-scale ice-calving events, are QZF-dominated. During the rest of Stage 5 accumulation rates were very low (<200 mg/cm^2/ky; Goldschmidt, 1995) and the BMF dominated in most areas.

There is no particular facies associated with the highest accumulation rates in the NGS; this varies with location, although the QZF does dominate

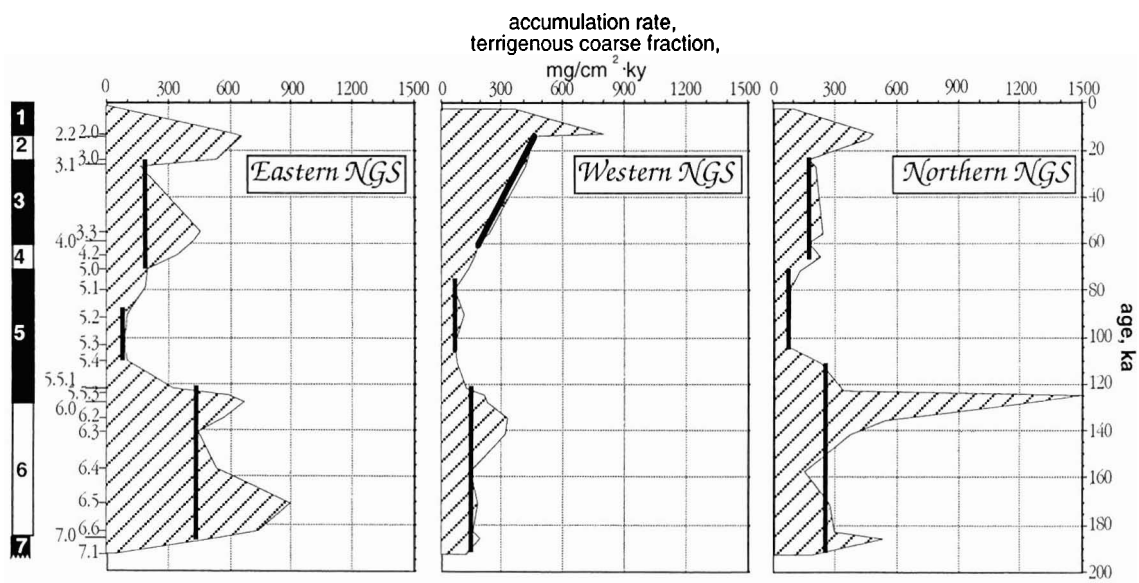


Figure 6. Histories of average accumulation rates of coarse terrigenous matter for Events 7.1-Present in the eastern, western and northern Norwegian-Greenland Sea. Accumulation rates from the eastern NGS include data from cores 23065 and 23071 (plus 3 additional cores); ARs from the western NGS include data from cores 23059, 23342 and 23357 (plus 7 additional cores); ARs from the northern NGS include data from cores 17728 and 21906 (plus 2 additional cores). Dark lines indicate approximate levels of background sedimentation. Modified from Goldschmidt (1995).

over the DSF during the Stage 6/5 deglaciation. An overall relationship, however, does exist between the presence of the biogenic material facies (BMF) and low IRD accumulation rates. A transition to the BMF from another facies would indicate a decrease in the deposition of terrestrial IRD while a transition from the BMF to another facies would indicate an increase in the deposition of terrestrial IRD.

Ice cover in the Norwegian-Greenland Sea over the last two glacial/interglacial cycles

Following is a brief discussion of the glacial history of the Norwegian-Greenland Sea and its surrounding continents over the past two glacial/interglacial cycles. Results gleaned from this study can be compared favourably with certain other investigations in the NGS area and unfavourably with others. These comparisons are discussed below.

Oxygen Isotope Stage 6

Accumulation rates were generally low (<400 mg/cm^2/ky; Goldschmidt, 1995) throughout the Norwegian-Greenland Sea during the transition between Stages 7 and 6. The biogenic matter facies (BMF) was dominant, indicating minimal ice-rafting. Coccolith evidence points to seasonal ice cover at this time; a brief warming episode occurred just before the start of Stage 6 (Baumann, 1990). The presence of the dark siltstone facies (DSF) in the northern NGS indicates melting icebergs from a possible glacier in the Barents Sea or on Svalbard.

Glaciers grew rapidly at the start of Stage 6, especially in Scandinavia, resulting in a peak (>600 mg/cm^2/ky; Goldschmidt, 1995) in accumulation rates (AR) in the eastern NGS. Dark siltstones were deposited in diamicts in the eastern NGS; these may have come from northward drifting icebergs from the Scandinavian Ice Sheet or from southward drifting icebergs from the Barents Sea Ice Sheet. Numerous authors have postulated that dark siltstones originate in the Barents Sea/eastern Svalbard region or further eastward (e.g. Hebbeln, 1991; Kubisch, 1991; Spielhagen, 1991; Kuhlemann *et al.*, 1993). Unfortunately, since dark siltstones crop out both in the Barents Sea and on the Norwegian continental slope, deciding between northward- or southward-oriented currents in the eastern NGS is impossible without more detailed analyses of the dark siltstones. Some investigators have found isotopic evidence that glacial currents flowed in a clockwise direction rather than the present anticlockwise pattern (Bischof *et al.*, 1990; Weinelt *et al.*, 1991, 1992; Sarnthein *et al.*, 1992). If currents were clockwise, a significant and long-lasting eddy would have to be imposed in the southern Fram Strait area to account for the dark siltstone facies in the northeasternmost cores. The clockwise reconstruction of Bischof *et al.* (1990) was based in part on the diminishing quantity of coal clasts in the >500 μm fraction from north to south in the eastern NGS. These coal clasts were considered to have come from more northern areas such as Franz Josef Land or the Siberian shelf. Wagner (1993) disputed this reconstruction based on the geochemical properties of coal samples from the NGS sea bottom in comparison with *in situ* coal from the Siberian shelf. It should be noted, however, that Wagner (1993) analysed only one sample from the Siberian Shelf; he also warned of the possible inaccuracy of using coal as a tracer because of its rather uniform geochemical properties throughout the Arctic realm. This leaves the questions of a Siberian origin for the coal from the NGS and of the possibility of a clockwise gyre during deglaciations still unanswered.

The presence of scattered chalk dropstones in the easternmost core (23071; Fig. 5; Henrich, 1992) indicates a northward drift from the North Sea area to the eastern NGS by around 175 ka and thus counterclockwise circulation. By this time, the quartz facies (QZF) had become the most dominant facies to be deposited in the NGS. Accumulation rates remained relatively high in the eastern and northern NGS. An increase in AR (>600 mg/cm^2/ky; Goldschmidt, 1994) occurred at 141 ka in the northern NGS, indicating an increase in the number of melting icebergs in this area. Based on the geochemical properties of dark siltstones in cores 23065 and 17728 and of *in situ* dark siltstones, Wagner (1993) reconstructed a westward and then southward ice drift from northern Norway and the Barents Sea. The AR evidence from the northern NGS does not appear to support the results of Wagner (1993).

The interpretation of relatively warm conditions during isotopic Events 6.5 and 6.3 (171 and 141 ka) is supported by the deposition of lithofacies A and the appearance of coccoliths in the Fram Strait (Hebbeln, 1991; Henrich, 1992). Although the climate was relatively warm for these parts of Stage 6, biogenic matter was not dominant, indicating that ice-rafting of terrigenous sediments was still strong at this time. Higher accumulation rates of coarse IRD (up to 900 mg/cm^2/ky; Goldschmidt, 1994) appear throughout the NGS during both events, indicating the increasing instability of ice margins and the melting of icebergs in the NGS. These increased ARs are supported by the increase in TOC-rich sediments (Wagner, 1993). The intervening Event 6.4 (157 ka) is marked by lower ARs (ca. 150-500 mg/cm^2/ky; Goldschmidt, 1994) throughout the NGS, indicating more stable ice margins and the reduced release of icebergs.

Oxygen Isotope Events 5.5.3-5.5.1

During the first 5000 years of the interglacial Stage

5 (Stage 5.5 = the Eemian; Mangerud *et al.*, 1979; Mangerud, 1989) accumulation rates (AR) were high (up to 1500 mg/cm^2/ky; Goldschmidt, 1995) in the northern and eastern NGS. During this time, the biogenic matter facies (BMF) began to dominate the sediments, indicating warmer climates and decreasing ice-rafting. By this time, warm Atlantic water had penetrated into the eastern NGS. This is supported by the deposition of the "warm water" lithofacies A and B3 in the NGS, by the deposition of the biogenic matter facies (BMF), by oxygen isotope records, by a strong peak in the amount of coccoliths and by the decrease in the TOC content of the sediments (Henrich *et al.*, 1989; Baumann, 1990; Henrich, 1992; Baumann *et al.*, 1993; Wagner, 1993).

Oxygen Isotope Events 5.4-5.0

The combination of low accumulation rates (<200 mg/cm^2/ky; Goldschmidt, 1995) and the dominance of the biogenic matter facies (BMF) indicate that the remainder of Stage 5 was relatively warm. It was not, however, as warm as during Event 5.5.1; this is supported by the decrease in deposition of carbonate sediments (Henrich, 1992). The NGS may have been at least seasonally covered with sea ice during portions of Stage 5 (Belanger, 1982; Hebbeln, 1991), but icebergs were rare. The dark siltstone facies (DSF) is more prominent in the northern NGS, indicating that the Svalbard/Barents Sea region was ice-covered at this time. Carbonate and biogenic data point to a brief warming of the NGS during Events 5.3 and 5.1 and cooling in Event 5.2 (103, 79 and 90 ka respectively; Baumann, 1990; Gard & Backman, 1990; Hebbeln, 1991; Henrich, 1992); TOC contents (Wagner, 1993) and accumulation rates for coarse IRD (Goldschmidt, 1995) are uniformly low at this time, hindering any interpretations of palaeoenvironments based on these data.

IRD accumulation rates began to increase (>200 mg/cm^2/ky; Goldschmidt, 1994) after Event 5.1 (79 ka). Carbonate evidence shows a relatively cool NGS; by this time the biogenic matter facies (BMF) had been replaced in some cores by the quartz facies (QZF).

Oxygen Isotope Stages 2 and 1

During Stage 2, ice sheets and sea ice became widespread for the last time. This is indicated by the combination of high accumulation rates (500-800 mg/cm^2/ky; Goldschmidt, 1994) and the general domination of the quartz (QZF) and, to a lesser degree, the dark siltstone facies (DSF) over the biogenic matter facies (BMF). A complete ice cover like that seen in the CLIMAP reconstruction (CLIMAP Project Members, 1976; Kellogg, 1980; Kellogg *et al.*, 1978) is unlikely due to the sedimentation rates in the NGS at this time; a complete ice cover would reduce sedimentation rates drastically. The Barents Sea, Svalbard and Scandinavian Ice Sheets all expanded to the continental shelf edge (Vorren *et al.*, 1984, 1988; Hald *et al.*, 1989; Haflidason & Sejrup, 1992; Baumann *et al.*, 1995).

The nearly continuous presence of chalk in core 23071 during Stage 2 points to a northward drift of icebergs in the eastern NGS and thus to an anticlockwise circulation pattern in the NGS as a whole. This chalk can be traced from the North Sea area northward along western Norway and up into the Fram Strait (Schacht, 1991; Spielhagen, 1991; Henrich, 1992).

Peaks in the accumulation rates of IRD can be seen between 26 and 12 ka in the Fram Strait (Hebbeln, 1991; Mangerud, 1992); these may be derived from the melting of icebergs from Svalbard. Most studies point to a rapid deglaciation of the Scandinavian and Barents Sea Ice Sheets around 15-13 ka (Ruddiman & McIntyre, 1981a and b; Vorren *et al.*, 1988; Hald *et al.*, 1989; Jones & Keigwin, 1989), although some investigators see some glacier melting at 18-22 ka (Grousset & Duplessy, 1983; Lehman *et al.*, 1991; H. Haflidason, pers. comm., 1993). Deglaciation was driven mainly by iceberg calving (Hughes, 1992). Svalbard may not have begun deglaciation before 10 ka (Hebbeln, 1992; Mangerud, 1992; Mangerud & Svendsen, 1992). This seems to be supported by the delayed appearance of the biogenic matter facies (BMF; ca. 5 ka vs. ca. 10 ka) in the northeastern NGS.

At ca. 15 ka, a rise in dark siltstones occurred in the eastern NGS (Figs. 4 and 5). Bischof (1991, 1994) found evidence of clastic sedimentary rock deposition (such as dark siltstones) for the eastern NGS at this time. Based on geochemical properties of the sediments, he attributed the origin of the sedimentary rock to the Barents Sea region, thus revealing a possible reversal in current directions in the eastern NGS. A complete change from anticlockwise to clockwise NGS circulation did not take place, however; currents in the western NGS continued to flow southward. In Figs. 4 and 5, it can be seen that chalk deposition comes to an abrupt halt at this time in core 23071; this may indicate that the heretofore prevailing northward flow of ice off Norway, carrying chalk from the North Sea region, suddenly was replaced by a southward flow which carried the siltstones from the Barents Sea. This may be a result of the deglaciation of the Barents Sea Ice Sheet (see also Sarnthein *et al.*, 1992).

A diamict deposited at 13.5-13.2 ka in core 23071 contains coal and chalk fragments (Henrich, 1992), indicating that the northward drift in the eastern NGS had reasserted itself by this time. High TOC values in the diamict appear to indicate

a source on the Norwegian continental shelf (Wagner, 1993).

Carbonate and diatom data indicate that the first intrusion of Atlantic Water occurred at 13-10 ka (Henrich, 1992; Koç Karpuz & Jansen, 1992). The biogenic matter facies (BMF) began to be deposited at ca. 12-10 ka (ca. 5 ka in the northeastern NGS), indicating a decrease in IRD and the return to warmer climates. The transition to Holocene climates after the Younger Dryas is marked by an increase in carbonate deposition and by the replacement of the C and B1 lithofacies by the A and B3 lithofacies 8-6 ka (Henrich, 1992). The deposition of modern coccoliths and diatoms began at about this time (Baumann, 1990; Baumann & Matthiessen, 1992). ARs of coarse IRD have generally been <200 mg/cm^2/ky for the last 5000 years (Goldschmidt, 1995).

Comparison to Heinrich events

In recent years much research has been devoted to "Heinrich layers" in the northern North Atlantic (Heinrich layers must not be confused with Henrich lithofacies). Heinrich layers appear to have been caused by massive discharges of icebergs from the Laurentide Ice Sheet in North America during at least the last ca. 70 ka. These layers are marked by peaks in terrestrial coarse IRD and in fossil detrital carbonate (Heinrich, 1988; Bond *et al.*, 1992a-c). It appears that they occurred when the Laurentide Ice Sheet, centred on the crystalline rocks of the Canadian Shield, advanced onto the softer carbonate rocks further eastward. The greater erodability of the carbonate rocks led to an increase in the velocity of the ice sheet and its consequent destabilisation. This brought about the calving of great numbers of icebergs and the precipitous retreat of the ice sheet (Alley & MacAyeal, 1994; MacAyeal, 1993). The icebergs carried glacial sediment into the northern North Atlantic Ocean (between latitudes 40-65°N); this sediment was deposited as far east as the Canary Islands off the northwest coast of Africa.

The origin of Heinrich layers and those of the diamict lithofacies D, E and F of Henrich (1992) are remarkably similar: both are assumed to have been caused by rapid disintegration of an ice sheet, the Laurentide for the Heinrich layers and the Scandinavian for Henrich lithofacies. Heinrich events occurred in the northern North Atlantic at ca. 69 (Heinrich layer 6 = H6), 52 (H5), 41 (H4), 28 (H3), 21 (H2) and 14.3 (H1) ka (Bond *et al.*, 1992c).

Only sediments with ages of 190-60 ka and 25-0 ka were analysed in the present study, so that correlations can be made only with layers H6, H2 and H1. Heinrich layers do *not* correlate well with the diamicts of Henrich (1992). In core 23071 a diamict occurs at 14.3 ka, the same time as H1 (see Henrich *et al.* (1995) for further discussion). No other diamicts have the same ages as Heinrich layers. But Table 4 lists some intriguing comparisons between Heinrich layers and the results of the present study. About 1000 years before the deposition of H6 a peak in the amount of dark siltstones occurred in the northern transect; 500 years later (500 years before H6) a quartz peak occurred. Similarly, peaks in dark siltstones occurred ca. 300 years before H1 while quartz peaks occurred ca. 1100 years before H2 and 200-300 years before H1. Peaks soon *after* the deposition of Heinrich layers are not as common: a dark siltstone peak appears 100 years after (essentially the same time as) H2 while a quartz peak occurs 200 years after the deposition of H1.

This, coupled with the fact that accumulation rates at the times of deposition of the Heinrich layers are generally increasing or high (see Table 4), indicates that there is some correlation between deposition of sediments in the Norwegian-Greenland Sea and of Heinrich layers further south. Specifically, it appears that a peak in the deposition of dark siltstones or of quartz in the NGS occurs within 1000 years of the deposition of Heinrich layers. This would indicate that sudden glacier surges and resulting iceberg calving events from the Scandinavian Ice Sheet occurred within 1000 years of those from the Laurentide Ice Sheet.

However, since the method used for dating the Norwegian-Greenland Sea cores is generally not more accurate than 1000 years (more accurate AMS dates exist only for Stages 1 and 2 in cores 23065

Table 4. Correlation of sediment characteristics from the Norwegian-Greenland Sea for the deposition times of Heinrich layers H6, H2 and H1.

	SOUTHERN TRANSECT			NORTHERN TRANSECT		
	H6 (69 ka)	**H2** (21 ka)	**H1** (14.3 ka)	**H6** (69 ka)	**H2** (21 ka)	**H1** (14.3 ka)
Lithotype	BMF	QZF	QZF	QZF	BMF	QZF
Accumulation Rate	increasing	high	high	increasing	low	high
qtz peak before	---	ca. 1100 y	ca. 300 y	ca. 500 y	---	ca. 200 y
qtz peak after	---	---	ca. 200 y	---	---	ca. 200 y
dss peak before	---	---	ca. 300 y	ca. 1000 y	---	ca. 300 y
dss peak after	---	---	---	---	ca. 100 y	---

and 23071), it cannot be resolved whether sedimentation peaks preceded, followed or occurred simultaneously with the deposition of Heinrich layers, only that they occurred within 1000 years of each other. Similar correlations between peaks in terrigenous IRD and Heinrich layers were observed in the Greenland Sea by Baumann *et al.* (1993).

CONCLUSIONS

- Coarse (>125 μm) sediments found on the floor of the Norwegian-Greenland Sea can be classified into three facies: that dominated by quartz (QZF), that dominated by dark siltstones (DSF) and that dominated by biogenic material (BMF). Other facies occur, but they do not cross the correlation coefficient = 0.7 boundary of statistical significance.
- The DSF occurs in Norwegian-Greenland Sea cores mainly in Stage 6 and is thus a "strong glacial" facies. The main source for the DSF appears to lie east and south of Svalbard; additional sources are the Norwegian continental shelf and northeastern Greenland. The QZF predominated the IRD in Stages 5.5 to 1; because the Stage 2 glaciation was much weaker than the previous one, the QZF is considered to be a "weak glacial" IRD facies; it is also a "deglacial" facies, being the predominant facies deposited during both Terminations II and I. Because the QZF consists of broken-down crystalline rocks, source areas could lie anywhere in the Arctic realm.
- Comparisons with IRD accumulation rates show that the presence of the BMF generally ties in with low accumulation rates. A transition to the BMF from another facies would therefore indicate a decrease in the deposition of terrestrial IRD while a transition from the BMF to another facies would indicate an increase in the deposition of terrestrial IRD.
- A one-to-one relationship between facies and the lithofacies of Henrich (1992) was not seen; rather, it was shown that most lithofacies consist of a variety of facies that correlate chronologically. An attempt to further subdivide the lithofacies according to the facies should not be made; although it would give more precise sedimentological data for any one core, correlation to neighbouring cores would prove difficult.
- Lithofacies A and B3, which are considered to be "warm water" facies, are dominated by the biogenic matter facies (BMF). The DSF occurs mainly in the lithofacies B2/B1 and C; it does not figure strongly in the diamicts, which are usually dominated by the quartz facies (QZF). Although peaks in dark siltstone deposition often occur during the deposition of the diamicts, quartz dominates over dark siltstones in almost every diamict by a factor of about 8 to 1. Yet the dark siltstones have enough total organic carbon to create the TOC peaks found by Wagner (1993) in the diamicts. These dark siltstones may occur mainly in the coarser (>500 μm) fractions.
- A peak in the deposition of dark siltstones or of quartz in the NGS generally occurs within 1000 years of Heinrich layers deposited further south in the North Atlantic Ocean. This, coupled with the fact that accumulation rates at the times of deposition of the Heinrich layers are generally increasing or high, indicates that there is a possibility that sudden glacier surges and resulting iceberg calving events from the Scandinavian Ice Sheet occurred within 1000 years of those from the Laurentide Ice Sheet.

ACKNOWLEDGEMENTS

I would like to thank Jörn Thiede for the allocation of the funds for this project and the advice throughout. Laboratory work was facilitated through the help of Katja Mellenthin, Birger Schlünz, Marion Wetzel and especially Susanne Schultz. An anonymous reviewer made useful comments on a previous version of this manuscript. This study was supported by a grant to the Sonderforschungsbereich 313 by the Deutsche Forschungsgemeinschaft. This is publication number 306 of the Sonderforschungsbereich 313, University of Kiel.

REFERENCES

Alley, R.B. & MacAyeal, D.R. Ice-rafted debris associated with binge/purge oscillations of the Laurentide ice sheet, *Paleoceanography*, **9**, 503-512.

Baumann, K.-H. 1990. Veränderlichkeit der Coccolithophoridenflora des Europäischen Nordmeeres im Jungquartär (Changes in the coccolithophorid flora of the Norwegian-Greenland Sea in the Late Quaternary). *Berichte aus dem Sonderforschungsbereich 313*, **22**, 1-146.

Baumann, K.-H., Lackschewitz, K.S., Erlenkeuser, H., Henrich, R. & Jünger, B. 1993. Late Quaternary calcium carbonate sedimentation and terrigenous input along the East Greenland continental margin. *Marine Geology*, **114**, 13-36.

Baumann, K.-H., Lackschewitz, K.S., Mangerud, J., Spielhagen, R.F., Wolf, T.C.W. & Henrich, R. 1995. Reflection of Scandinavian Ice Sheet fluctuations in Norwegian Sea sediments during the last 150,000 years. *Quaternary Research*, **43**, 185-197.

Baumann, K.-H. & Matthiessen, J. 1992. Variations in surface watermass conditions in the Norwegian Sea: Evidence from Holocene coccolith and dinoflagellate cyst assemblages. *Marine Micropaleontology*, **20**, 129-146.

Belanger, P.E. 1982. Paleo-oceanography of the Norwegian Sea during the last 130,000 years: Coccolithophorid and foraminiferal data. *Boreas*, **11**, 29-36.

Bischof, J. 1991. Dropstones im Europäischen Nordmeer: Indikatoren für Meeresströmungen in den letzten 300 000 Jahren (Dropstones in the Norwegian-Greenland Sea: Indicators for ocean currents in the last 300,000 years). *Berichte aus dem Sonderforschungs-*

bereich 313, **30**, 1-203.

Bischof, J. 1994. The decay of the Barents Ice Sheet as documented in nordic seas ice-rafted debris, *Marine Geology*, **117**, 35-55.

Bischof, J., Koch, J., Kubisch, M., Spielhagen, R.F. & Thiede, J. 1990. Nordic seas surface ice drift reconstructions- Evidence from ice rafted coal fragments during oxygen isotope stage 6. In: Dowdeswell, J.A. & Scourse, J.D. (eds.), *Glacimarine environments: Processes and sediments*, Geological Society Special Publication **53**, 235-251, London.

Bjørrlykke, K., Bue, B. & Elverhøi, A. 1987. Quaternary sediments in the northwestern part of the Barents Sea and their relation to the underlying Mesozoic bedrock. *Sedimentology*, **25**, 227-246.

Bond, G., Broecker, W., Lotti, R. & McManus, J. 1992a. Abrupt color changes in Isotope Stage 5 in North Atlantic deep sea cores: Implications for rapid change of climate-driven events. *In*: Kukla, G.J. & Went, E. (eds.), *Start of a glacial*, 185-205, Springer Verlag, Berlin.

Bond, G., Broecker, W.S., McManus, J. & Lotti, R. 1992b. Circulation changes on century and millennial time scales in the northern North Atlantic. *In:* Sarnthein, M., Thiede, J. and Zahn, R. (eds.), *Fourth International Conference on Paleoceanography, Program & Abstracts*, 72-73, Druckerei Fotosatz Nord, Kiel.

Bond, G., Heinrich, H., Broecker, W.S., Labeyrie, L., McManus, J., Andrews, J., Huon, S., Jantschik, T., Clasen, S., Simet, C., Tedesco, K., Klas, M., Bonani, G. & Ivy, S. 1992. Evidence for massive discharges of icebergs into the North Atlantic Ocean during the last glacial period. *Nature*, **360**, 245-249.

Bugge, T., Knarud, R. & Mørk, A. 1984. Bedrock geology on the mid-Norwegian continental shelf. *In:* Norwegian Petroleum Society (ed.), *Petroleum geology of the North European Margin*, 271-283, Graham & Trotman, London.

Churkin, M. Jr. & Trexler, J.H. Jr. 1981. Continental plates and accreted oceanic terranes in the Arctic. *In:* Nairn, A.E.M. (ed.), *The ocean basin and margins 5: The Arctic Ocean*, 1-20, Plenum Press, London.

Churkin, M. Jr., Soleimani, G., Carter , G. & Robinson, R. 1981. Geology of the Soviet Arctic: Kola Peninsula to Lena River. *In:* Nairn, A.E.M. (ed.), *The ocean basin and margins 5: The Arctic Ocean*, 331-375, Plenum Press, London.

Clark, D.L. & Hanson, A. 1983. Central Arctic Ocean sediment texture: A key to ice transport mechanisms. *In:* Molnia B.F. (ed.), *Glacial-marine sedimentation*, 301-330, Plenum Press, London.

CLIMAP Project Members 1976. The surface of the ice age Earth. *Science*, **191**, 1131-1137.

Dibner, V.D. & Krylova, N.M. 1965. Stratigraphic position and material composition of coal measures in Franz Josef Land. *International Geology Review*, **7**, 1030-1038.

Dowdeswell, E.K. 1988. The Cenozoic stratigraphy and tectonic development of the Barents Shelf. *In:* Harland, W.B. & Dowdeswell, E.K. (eds.), *Geological evolution of the Barents Shelf region*, 109-130, Graham and Trotman, London.

Edwards, M.B. 1975. Gravel fraction on the Spitsbergen Bank; NW Barents Shelf, *Norges Geologiske Undersøkelse*, **316**, 205-217.

Elverhøi, A. (ed.), 1992. *CLAMD Report (Correlation Land-Continental Margin-Deep Sea)*, Abstracts of the Polar North Atlantic Margins: Late Cenozoic Evolution (PONAM) Third Annual Workshop, 32 p.

Elverhøi, A. & Lauritzen, Ø. 1984. Bedrock geology of the northern Barents Sea (west of 35° E) as inferred from the overlying Quaternary deposits, *Norsk Polarinstitutt Skrifter*, **180**, 5-16.

Elverhøi, A. & Solheim, A. 1983. Surface sediment distribution, *Norsk Polarinstitutt Skrifter*, **179**, 3-23.

Emery, K.O. 1963. Organic transportation of marine sediments. *In:* Hill, M.N. (ed.), *The Sea* **3**, 776-789, Interscience Publishers, New York.

Frisch, T. & Trettin, H.P. 1991. Precambrian successions in the northernmost part of the Canadian Shield. *In:* Trettin, H.P. (ed.), *Geology of the Innuitian Orogen and Arctic Platform of Canada and Greenland*, Geology of Canada vol. **3**, Geol. Surv. Canada, pp. 103-108.

Funder, S. 1989. Introduction to the Quaternary geology of the ice-free areas and adjacent shelves of Greenland. *In:* Fulton, R.J. (ed.), *Quaternary geology of Canada and Greenland*, Geology of Canada vol. **1**, 744-749, Geol. Surv. Canada.

Gard, G. & Backman, J. 1990. Synthesis of arctic and subarctic coccolith biochronology and history of North Atlantic drift water influx during the last 500,000 years. *In:* Bleil, U. & Thiede, J. (eds.), *Geologic history of the polar oceans: Arctic versus Antarctic*, NATO ASI Series C, 499-518, Kluwer Academic Publishers, Amsterdam.

Goldschmidt, P.M. 1994. The ice-rafting history in the Norwegian-Greenland Sea for the last two glacial/interglacial cycles. *Berichte aus dem Sonderforschungsbereich 313*, **50**, 1-103.

Goldschmidt, P.M. 1995. Accumulation rates of coarse-grained terrigenous sediment in the Norwegian-Greenland Sea: Signals of continental glaciation. *Marine Geology*. **128**, 137-151.

Goldschmidt, P.M., Pfirman, S.L., Wollenburg, I. & Henrich, R. 1992. Origin of sediment pellets from the Arctic seafloor: Sea ice or icebergs?, *Deep-Sea Research*, **39**, S539-S565.

Grousset, F. & Duplessy, J.-C. 1983. Early deglaciation of the Greenland Sea during the last glacial to interglacial transition, *Marine Geology*, **52**, M11-M17.

Haflidason, H. & Sejrup, H.P. 1992, Paleotemperature and productivity variations in the Norwegian-Greenland Sea during the last 20 kyr: An east-west transect. *In:* Sarnthein, M., Thiede, J. & Zahn, R. (eds.), *Fourth International Conference on Paleoceanography, Program & Abstracts*, 134, Druckerei Fotosatz Nord, Kiel.

Hald, M., Danielsen, T.K. & Lorentzen, S. 1989. Late Pleistocene-Holocene benthic foraminiferal distribution in the southwestern Barents Sea: Paleoenvironmental implications, *Boreas*, **18**, 367-388.

Hancock, J.M. 1984. Cretaceous. *In:* Glennie, K.W. (ed.), *Introduction to the petroleum geology of the North Sea*, 133-150, Blackwell Science Publishing, Oxford.

Hebbeln, D. 1991. Spätquartäre Stratigraphie und Paläozeanographie in der Fram Straße (Late Quaternary stratigraphy and palaeoceanography in the Fram Strait), *Berichte aus dem Fachbereich Geowissenschaften der Universität Bremen*, **22**, 1-174.

Hebbeln, D. 1992. Weichselian glacial history of the Svalbard area: Correlating the marine and terrestrial records. *Boreas*, **21**, 295-304.

Heinrich, H. 1988. Origin and consequences of cyclic ice rafting in the northeast Atlantic Ocean during the past 130,000 years. *Quaternary Research*, **29**, 142-152.

Henrich, R. 1992. *Beckenanalyse des Europäischen Nordmeeres: Pelagische und glazionarine Sedimentflüsse im Zeitraum 2.6 Ma bis Rezent (Basin analysis of the Norwegian-Greenland Sea: Pelagic and glacionarine sediment influences in the period 2.6 Ma to Recent)*. 344p,

unpublished Habilitation thesis, Christian-Albrechts-Universität, Kiel.

Henrich, R., Kassens, H., Vogelsang, E. & Thiede, J. 1989. Sedimentary facies of glacial-interglacial cycles in the Norwegian Sea during the last 350 ka. *Marine Geology*, **86**, 282-319.

Henrich, R., Wagner, T., Goldschmidt, P. & Michels, K. 1995. Depositional regimes in the Norwegian-Greenland Sea: The last two glacial to interglacial transitions, *Geologische Rundschau*, **84**, 28-48.

Herman, Y. 1974. Arctic Ocean sediments, microfauna and the climatic record in Late Cenozoic time. *In:* Herman, Y. (ed.), *Marine geology and oceanography of the Arctic Seas*, 283-348, Springer-Verlag, New York.

Hodgson, D.A. 1989. Introduction to the Quaternary geology of the Queen Elizabeth Islands. *In:* Fulton, R.J. (ed.), *Quaternary geology of Canada and Greenland*, Geology of Canada vol. 1, 443-448, Geological Survey of Canada.

Hopkins, D.M. & Herman, Y. 1981. Ice-rafting, an indication of glaciation? (Reply). *Science*, **214**, 688.

von Huene, R., Larson, E. & Crouch, J. 1973. Preliminary study of ice-rafted erratics as indicators of glacial advances in the Gulf of Alaska. *In:* Kulm, L.D., von Huene, R. *et al.*, *Initial reports of the Deep Sea Drilling Project*, **18**, 835-842, U.S. Government Printing Office, Washington, D.C..

Hughes, T. 1992. Abrupt climatic change related to unstable ice-sheet dynamics: Toward a new paradigm. *Palaeogeography, Palaeoclimatology, Palaeoecology (Global and Planetary Change Section)*, **97**, 203-234.

Imbrie, J., Hays, J.D., Martinson, D.G., McIntyre, A., Mix, A.C., Morley, J.J., Pisias, N.G., Prell, W.L. & Shackleton, N.J. 1984. The orbital theory of Pleistocene climate: Support from a revised chronology of the marine $\delta^{18}O$ record. *In:* Berger A. *et al.* (eds.), *Milankovitch and climate*, 269-305, D. Reidel, Dordrecht.

Imbrie, J. & Kipp, N.G. 1971. A new micropaleontologic method for quantitative paleoclimatology: Application to a Late Pleistocene Caribbean core. *In:* Turekian, K.K. (ed.), *The late Cenozoic glacial ages*, 71-191, Yale University Press, New Haven.

Jones, G.A. & Keigwin, L.D. 1989. Evidence from Fram Strait (78°N) for early deglaciation. *Nature*, **336**, 56-59.

Kane, E.K. 1857. *Arctic explorations: The second Grinnell expedition in search of Sir John Franklin 1853, '54, '55.* Volume **2**, 464 p, Childs and Peterson, Philadelphia.

Kellogg, T.B. 1980. Paleoclimatology and paleoceanography of the Norwegian-Greenland Sea: Glacial-interglacial contrasts. *Boreas*, **9**, 115-137.

Kellogg, T.B., Duplessy, J.-C. & Shackleton, N.J. 1978. Planktonic foraminiferal and oxygen isotope stratigraphy and paleoclimatology of Norwegian Sea deep-sea cores. *Boreas*, **7**, 61-73.

Kelly, R.A. 1988. Jurassic through Cretaceous stratigraphy of the Barents shelf. *In:* Harland, W.B. & Dowdeswell, E.K. (eds.), *Geological evolution of the Barents Shelf region*, 109-130, Graham & Trotman, London.

Kent, D., Opdyke, N.D. & Ewing, M. 1971. Climate change in the North Pacific using ice-rafted detritus as a climatic indicator, *Geological Society of America Bulletin*, **82**, 2741-2754.

Klovan, J.E. & Imbrie, J. 1971. An algorithm and FORTRAN IV program for large-scale Q-mode factor analysis and calculation of factor scores. *Journal of the International Association of Mathematical Geology*, **3**, 61-77.

Koç Karpuz, N. & Jansen, E. 1992. A high-resolution diatom record of the last deglaciation from the SE Norwegian Sea: Documentation of rapid climate changes, *Paleoceanography*, **7**, 499-520.

Kubisch, M. 1991. Die Eisdrift im Arktischen Ozean während der letzten 250.000 Jahre (Ice drift in the Arctic Ocean during the last 250,000 years). *Geomar Report* **16**, 1-100 .

Kuhlemann, J., Lange, H. & Paetsch, H. 1993. Implications of a connection between clay mineral variations and coarse grained debris and lithology in the central Norwegian-Greenland Sea. *Marine Geology*, **114**, 1-11.

Lehman, S.J., Jones, G.A., Keigwin, L.D., Andersen, E.S., Butenko, G. & Østmo, S.R. 1991. Initiation of Fennoscandian ice-sheet retreat during the last deglaciation, *Nature*, **349**, 513-516.

MacAyeal, D.R. 1993. Growth/purge oscillations of the Laurentide ice sheet as a cause of the North Atlantic's Heinrich Events. *Paleoceanography*, **8**, 775-784.

Mangerud, J. 1989. Correlation of the Eemian and the Weichselian with deep sea oxygen isotope stratigraphy. *Quaternary International*, **3/4**, 1-4.

Mangerud, J. 1992. Glacial history of Europe through the last interglacial-glacial cycle, in Geirsdóttir, Á. *et al.* (eds.), *Abstracts*, **4**, 20. *Nordiska Geologiska Vintermötet.*

Mangerud, J., Sønstegaard, E. & Sejrup, H.-P. 1979. Correlation of the Eemian (interglacial) Stage and the deep-sea oxygen-isotope stratigraphy. *Nature*, **277**, 189-192.

Mangerud, J. & Svendsen, J.I. 1992. The last interglacial-glacial period on Spitsbergen, Svalbard. *Quaternary Science Reviews*, **11**, 633-664.

Martinson, D.G., Pisias, N.G., Hays, J.D., Imbrie, J., Moore, T.C. Jr. &, Shackleton, N.J. 1987. Age dating and the orbital theory of the ice ages: Development of a high-resolution 0 to 300,000-year chronostratigraphy. *Quaternary Research*, **27**, 1-29.

Michels, K. 1995. Strömungssortierung quartärer Sedimente des Europäischen Nordmeeres: Analyse von Sinkgeschwindigkeits-Verteilungen (Current sorting of Quaternary sediments in the Norwegian-Greenland Sea: Analysis of sinking velocity distributions). *Berichte aus dem Sonderforschungsbereich 313* **55**, 1-123.

Molnia, B.F. 1983. Distal glacial-marine sedimentation: Abundance, composition, and distribution of North Atlantic Ocean Pleistocene ice-rafted sediment. *In:* Molnia, B.F. (ed.), *Glacial-marine sedimentation*, 593-626, Plenum Press, London.

Mullen, R.E., Darby, D.A. & Clark, D.L. 1972. Significance of atmospheric dust and ice rafting for Arctic Ocean sedimentation. *Geological Society of America Bulletin*, **83**, 205-211.

Nürnberg, D., Wollenburg, I., Dethleff, D., Eicken, H., Kassens, H., Letzig, T., Reimnitz, E. & Thiede, J. 1994. Sediments in Arctic sea ice - implications for entrainment, transport and release. *Marine Geology*, **119**, 185-214.

Ruddiman, W.F. & McIntyre, A. 1981a. Oceanic mechanisms for amplification of the 23,000-year ice-volume cycle. *Science*, **212**, 617-627.

Ruddiman, W.F. & McIntyre, A. 1981b. The North Atlantic Ocean during the last deglaciation. *Palaeogeography, Palaeoclimatology, Palaeoecology*, **35**, 145-214.

Sarnthein, M., Jansen, E., Arnold, M., Duplessy, J.-C., Erlenkeuser, H., Flatøy, A., Veum, T., Vogelsang, E. & Weinelt, M.S. 1992. $\delta^{18}O$ time-slice reconstruction of meltwater anomalies at Termination I in the North Atlantic between 50 and 80°N. *In:* Bard, E. & Broecker

W.S. (eds.), *The last deglaciation: Absolute and radiocarbon chronologies*, NATO ASI Series 12, 183-200, Kluwer Academic Publishers, Amsterdam.

Schacht, R. 1991. *Palāo-ozeanographische Entwicklung des Gebietes der Grönland Fracture Zone während der vergangenen 350 ka (Palaeoceanographic development of the Greenland Fracture Zone region in the last 350 ky).* Master's Thesis, Christian-Albrechts-Universität, Kiel, 121pp..

Spielhagen, R. 1991. Die Eisdrift in der Framstraße während der letzten 200.000 Jahre (Ice drift in the Fram Strait during the last 200,000 years). *GEOMAR Report* **4**, 1-137.

Spjeldnaes, N. 1981. Ice-rafting, an indication of glaciation? (Discussion) *Science*, **214**, 687-688.

Swift, J.H. 1986. The Arctic waters. *In:* Hurdle, B.G. (ed.), *The Nordic Seas*, 129-153, Springer-Verlag, Berlin.

Tarr, R.S. 1897. The Arctic sea ice as a geological agent. *American Journal of Science*, **3**, 223-229.

Trettin, H.P. (ed.). 1991. *Geology of the Innuitian Orogen and Arctic Platform of Canada and Greenland*, Geology of Canada, vol. 3, Geological Survey of Canada, 569 pp.

Vorren, T.O., Hald, M. & Lebesbye, E. 1988. Late Cenozoic environments in the Barents Sea. *Paleoceanography*, **3**, 601-612.

Vorren, T.O., Hald, M. & Thomson, E. 1984. Quaternary sediments and environments on the continental shelf off northern Norway, *Marine Geology*, **57**, 229-257.

Wagner, T. 1993. Organisches Material in pelagischen Sedimenten: Glaziale/interglaziale Variationen im Europäischen Nordmeer (Organic material in pelagic sediments: Glacial/interglacial variations in the Norwegian-Greenland Sea). *Berichte aus dem Sonderforschungsbereich 313*, **42**, 1-138.

Wagner, T. & Henrich, R. 1994. Organo- and lithofacies of glacial/interglacial deposits of the Norwegian-Greenland Sea: Responses to paleoceanographic and paleoclimatic changes. *Marine Geology*, **120**, 335-364.

Watkins, N.D., Ledbetter, M.T. & Huang, T.C. 1982. Antarctic glacial history using spatial and temporal variations of ice-rafted debris in abyssal sediments of the Southern Ocean. *In:* Craddock, C. (ed.), *Antarctic geoscience*, 1013-1016, University of Wisconsin Press, Madison, WI.

Weber, J.R. & Roots, E.F. 1990. Historical background: Exploration, concepts and observations, In: Johnson, G.L. *et al.* (eds.), *The Arctic Ocean region*, Geological Society of America, 5-36, DNAG Vol. L, Boulder, CO.

Weinelt, M.S., Sarnthein, M., Arnold, M., Erlenkeuser, H. & Jansen, E. 1992. Meltwater episodes in the Norwegian-Greenland Sea during the last 60,000 years, In: Sarnthein, M., Thiede, J. and Zahn, R. (eds.), *Fourth International Conference on Paleoceanography, Program & Abstracts*, 287-298, Druckerei Fotosatz Nord, Kiel.

Weinelt, M.S., Sarnthein, M., Vogelsang, E. & Erlenkeuser, H. 1991. Early decay of the Barents Shelf ice sheet- spread of stable isotope signals across the eastern Norwegian Sea, *Norsk Geologisk Tidsskrift*, **71**, 137-140.

Winn, K., Sarnthein, M. & Erlenkeuser, H. 1991. $\partial^{18}O$ stratigraphy and chronology of Kiel sediment cores from the East Atlantic. *Berichte-Reports, Geologisch-Paläontologisches Institut der Universität Kiel*, **45**, 1-99.

Wollenburg, I. 1991. Sedimenttransport durch das arktische Meereis: Die rezente lithogene und biogene Materialfracht. *Berichte zur Polarforschung*, **127**, 1-150.

Appendix. Ages of samples examined in this study. Stars indicate short box cores that sample the surface sediments with less disruption than long gravity cores. Stratigraphic events (see Imbrie *et al.*, 1984 and Martinson *et al.*, 1987) are underlined.

17728 ages from Söding (1991)		**21906** ages from Hamich (1991)		**23059** ages from Vogelsang (1990)		**23062** ages from Vogelsang (1990)	
depth (cm)	age (ka)	depth (cm)	age (ka)	depth (cm)	age (ka)	depth (cm)	age (ka)
0	0.00	0	0.00	20	6.51	0.5*	2.09
5	6.00	5	8.60	40	15.84	3.5*	4.15
10	12.00	10	9.98	50	18.63	6.5*	6.20
15	14.41	15	11.35	70	24.21	9.5*	8.26
20	16.81	20	12.73	80	27.00	12.5*	8.98
25	19.22	25	14.11	90	30.32	15.0*	9.35
30	21.62	30	15.49			17.5*	9.72
45	29.86	35	16.86	140	46.89	21.0*	10.68
		40	18.24	150	50.21	24.0*	12.43
100	65.00	50	31.33	160	68.08	28.0*	14.25
105	68.00			174	79.25	30.5*	15.02
110	71.00	160	50.21	190	96.22	33.0*	15.63
130	103.50	165	57.61	196	99.38	36.0*	16.35
150	117.20	170	65.00	212	122.56	39.5*	17.20
155	119.60	175	79.25	220	125.19	80.0	27.00
165	128.00	180	85.10	228	129.59		
175	131.04	185	90.95	238	135.10	140	46.89
185	134.08	195	105.09	249	137.57	150	50.21
195	144.62	200	110.79	257	139.36	160	64.09
200	148.25	205	113.73	270	142.28	177	74.40
205	151.88	210	116.68	280	147.43	190	85.10
210	155.50	215	119.62	290	152.58	202	94.88
220	162.75	220	122.56	301	164.94	210	99.38
230	170.00	225	123.44	310	175.05	220	115.13
240	174.32	230	124.31	364	193.07	230	125.56
245	176.49	235	125.19			240	127.30
250	178.65	240	127.17			250	128.77
260	182.97	245	129.15			260	129.95
265	185.96	250	131.14			268	133.92
275	193.87	255	133.12			295	135.25
		260	135.10			304	137.01
		270	142.28			316	138.78
		280	157.64			328	140.10
		285	162.70			337	141.13
		290	167.76			344	149.25
		295	172.83			365	150.80
		300	177.89			369	155.06
		305	182.95			380	158.92
		310	188.01			390	166.66
		315	193.07			410	172.07
		320	200.57			424	174.40
						430	178.26
						440	182.13
						450	186.00
						460	195.33

Appendix. (cont.) Ages of samples examined in this study. Stars indicate short box cores that sample the surface sediments with less disruption than long gravity cores. Stratigraphic events (see Imbrie *et al.*, 1984 and Martinson *et al.*, 1987) are underlined.

23065 ages from Vogelsang (1990)		23071 ages from Vogelsang (1990)		23342 ages from Henrich (1992)		23357 ages from Henrich (1992)	
depth (cm)	**age (ka)**	**depth (cm)**	**age (ka)**	**depth (cm)**	**age (ka)**	**depth (cm)**	**age (ka)**
0.5*	2.55	0.5*	1.50	0*	2.50	0*	2.50
22.0	4.85	3.5*	2.57	3*	3.20	3*	4.53
6.5*	6.37	9.5*	4.72	6*	3.90	10	5.21
17.5*	9.72	12.5*	5.79	9*	4.60	6*	6.57
20.5*	10.45	15.5*	6.73	12*	5.30	9*	8.60
23.5*	12.55	18.0*	6.97	15*	6.00	12*	9.50
26.5*	14.09	21.0*	7.27	18*	8.60	15*	10.98
29.5*	15.16	23.5*	7.51	8	9.26	21*	13.60
32.5*	16.74	26.5*	7.80	21*	10.10	30*	14.03
36.5*	18.85	32.5*	8.39	25	10.88	48	14.90
39.5*	20.42	35.5*	8.69	30*	11.76	57	15.78
59.0	22.30	38.5*	8.98	45	14.25	67	19.22
77.0	29.30	41.5*	9.27	55	16.00	76	23.11
		55.0	9.62	75	20.40	85	27.00
140	54.03	63.0	10.40	85	22.60	90	30.56
150	59.12	70.0	11.08	95	24.80	100	37.67
162	65.22	80.0	12.06	105	27.00		
180	74.37	89.0	13.15			115	48.33
190	79.46	94.0	13.82	195	61.49	125	55.44
200	103.54	101.0	14.57	215	67.14	135	65.22
209	106.80	106.0	15.07	245	89.32	145	78.34
218	110.06	113.0	15.72	255	96.52	155	93.02
229	117.74	121.0	16.46	265	103.71	165	107.70
248	125.41	130.0	16.99	275	110.79	175	122.38
256	126.24	140.0	17.75	285	118.10	185	125.00
273	128.00	151.0	18.55	295	123.50	195	131.22
281	129.36	160.0	18.79	305	125.75	205	137.67
292	130.87	170.0	20.11	317	128.72	215	144.11
299	131.93	180.0	21.43	335	135.25	226	151.20
311	133.74	184.0	21.66	345	138.87	235	157.00
320	135.10	193.0	22.18	375	149.74	245	163.44
332	137.68	210.0	23.15	385	153.36	255	169.89
342	139.83	221.0	23.80	395	156.99	264	175.69
349	141.33	230.0	24.41	405	160.61	275	182.78
363	148.23	240.0	25.09	415	164.23	285	189.82
370	151.68	251.0	25.84	435	171.48	295	197.45
381	157.10	260.0	26.45	445	175.10	305	205.09
390	159.90	270.0	27.13	455	178.72		
395	161.45	274.0	27.41	465	182.35		
405	164.56	280.0	27.82	475	186.00		
420	169.22			485	191.59		
430	172.33	490	64.09	495	197.17		
437	174.50	499	66.53	505	202.76		
452	179.16	510	69.5				
458	181.03	520	72.21				
470	184.76	530	74.92				
480	187.86	536	76.54				
490	190.97	544	78.71				
500	194.08	558	92.00				
		567	94.37				
		575	96.48				
		584	98.85				
		596	103.77				
		604	107.28				
		610	109.91				
		620	113.27				
		634	117.6				
		644	120.7				
		654	123.09				
		660	123.87				
		670	125.19				
		680	127.67				
		690	130.15				
		694	131.14				
		701	132.87				
		710	135.10				
		722	138.07				
		730	140.05				
		738	142.19				
		743	143.45				
		748	144.68				
		756	146.74				
	End of core	763	148.55				

Appendix. (cont.) Ages of samples examined in this study. Stars indicate short box cores that sample the surface sediments with less disruption than long gravity cores. Stratigraphic events (see Imbrie *et al.*, 1984 and Martinson *et al.*, 1987) are underlined.

23454 ages from Goldschmidt (1994)		23454 (cont.)		23456 ages from Goldschmidt (1994)		23456 (cont.)	
depth (cm)	age (ka)	depth (cm)	age (ka)	depth (cm)	age (ka)	depth (cm)	age (ka)
0	0.00	400	126.50	0	0.00	405	123.00
5	1.23	405	128.00	5	0.80	410	123.62
10	2.47	410	129.15	10	1.60	415	124.25
15	3.71	415	130.30	15	2.40	420	124.88
20	4.94	420	131.45	20	3.20	425	125.50
25	6.18	425	132.60	25	4.00	430	126.12
30	7.72	430	133.75	30	4.80	435	126.75
35	8.65	435	134.90	35	5.60	440	127.38
40	9.89	440	136.05	40	6.40	445	128.00
45	11.13	445	137.20	45	7.20	450	129.70
50	12.36	450	138.35	50	8.00	455	131.41
55	13.60	455	139.50	55	8.80	460	133.12
60	13.82	460	140.66	60	9.60	465	134.82
65	14.03	465	141.81	65	10.40	470	136.53
70	14.25	470	142.96	70	11.20	475	138.24
75	14.47	475	144.11	75	12.00	480	139.94
80	14.68	480	145.26	80	12.80	485	141.64
85	14.90	485	146.41	85	13.60	490	143.35
90	17.72	490	147.56	90	13.74	495	145.06
95	20.95	495	148.71	95	13.88	500	146.76
100	23.98	500	149.86	100	14.03	505	148.47
105	27.00	505	151.01	105	14.18	510	150.18
110	28.06	510	152.16	110	14.32	515	151.88
115	29.13	515	153.31	115	14.46	520	153.59
120	30.20	520	154.46	120	14.61	525	155.30
		525	155.61	125	14.76	530	157.00
300	68.84	530	156.76	130	14.90	535	158.70
305	69.56	535	157.91	135	17.94	540	160.41
310	70.28	540	159.06	140	20.97	545	162.12
315	71.00	545	160.21	145	24.00	550	163.82
320	75.12	550	161.36	150	25.02	555	165.53
325	79.25	555	162.51	155	26.06	560	167.24
330	84.88	560	163.66			565	168.94
335	90.52	565	164.81	345	65.18	570	170.65
340	97.03	570	165.96	350	66.21	575	172.36
345	103.54	575	167.12	355	68.6	580	174.06
350	105.36	580	168.27	360	71.00	585	175.76
355	107.17	585	169.42	365	77.42	590	177.47
360	108.98	590	170.57	370	83.84	595	179.18
365	110.79	595	171.72	375	90.26	600	180.88
370	116.58	600	172.87	380	96.67	605	182.58
375	122.38	605	174.02	385	103.10	610	184.29
380	123.04	610	175.17	390	109.53	615	186.00
385	123.69	615	176.32	395	115.96	620	187.71
390	124.34	620	177.47	400	122.38	End of core	
395	125.00	End of core					

Late Pleistocene-Holocene productivity record of benthic foraminifera from the Iceland Plateau (Core PS1246-2)

ORAN P. COSTELLO[1] AND HENNING A. BAUCH[2]

[1]SFB 313, Universität Kiel, Heinrich-Hecht-Platz 10, D-24118 Kiel, Germany

[2]GEOMAR, Research Center for Marine Geosciences, Wischhofstr. 1-3, 24148 Kiel, Germany

ABSTRACT

Benthic foraminiferal assemblage patterns in Core PS 1246-2 from the Iceland Plateau are examined as they relate to annual productivity and seasonal productivity changes during the Late Pleistocene glacial (23,000-11,000 yrs B.P.), Younger Dryas cool period (11,000-10,000 yrs B.P.) and Holocene (10,000-2,900 yrs B.P.). Abundance fluctuations of *Cibicidoides wuellerstorfi*, a suspension-feeder, are used as the proxy for annual productivity, while fluctuations of the phytodetritus-exploiting species *Epistominella exigua*, *Eponides tumidulus* and *Globocassidulina subglobosa* are used as the indicators of seasonal productivity.

These records show seasonal productivity began to increase around 22,500 yrs B.P. and experienced three subsequent peaks in the glacial, while annual productivity increased around 16,000 yrs B.P. and shows only one peak in the glacial. The Younger Dryas shows a decrease in both seasonal and annual productivity records. Seasonal productivity in the early Holocene is much higher than during the glacial, yet appears more extreme. The Holocene record of annual productivity continues to show a strong general increase in intensity.

INTRODUCTION

The Iceland Plateau is an area which has experienced strong contrasting glacial-interglacial conditions, mainly as a function of its location in an area of the North Atlantic within close vicinity of Greenland ice sheets. Box Core PS 1246-2 (69°23.0'N, 12°55.0'W, 1861m water depth) is situated on the northern extent of the Iceland Plateau (Fig.1) and contains a Late Pleistocene glacial - Younger Dryas - early Holocene transition.

Supply of food is the deciding factor in controlling the abundance of benthic organisms, therefore both an increased organic flux (food source) from surface productivity (Altenbach & Sarnthein, 1989; Herguera & Berger, 1991; Struck, 1995) and the amount of organic carbon in the sediment (Lutze & Coulbourn, 1984) will affect the benthic foraminiferal fauna. Additionally, Herguera & Berger (1991) have determined a correlation of R=0.97 between benthic foraminiferal accumulation rates and organic carbon flux rates. This means that surface productivity (as indicated from organic carbon flux rates) linearly correlates with the benthic foraminiferal accumulation rates, confirming the finding of others that the fluctuating relative abundance or accumulation rates of benthic foraminiferal species can therefore be used as a proxy for surface water paleoproductivity (Altenbach & Sarnthein, 1989; Gooday, 1993; Smart *et al.*, 1994).

In this core, the suspension-feeding *Cibicidoides wuellerstorfi* (SCHWAGER, 1866) is used as the proxy for annual productivity (Lutze & Thiel, 1987; Altenbach & Sarnthein, 1989), as it is probably a long-living species (possibly several years, thus representative of the average annual productivity), fairly abundant and the distribution pattern is similar to the total benthic foraminiferal abundance curve from this core (Struck, 1992; this study).

Higher abundances of *Epistominella exigua* (BRADY, 1884), *Eponides tumidulus* (BRADY, 1884) and *Globocassidulina subglobosa* (BRADY, 1881) are used in this study to indicate periods of increased seasonal productivity, as modern specimens thrive in the phytodetritus falling on the sediment surface during periods of high surface productivity (Gooday, 1988). Such phytodetritus-exploiting foraminifera are regarded as opportunists, able to

In: Hass, H.C. & Kaminski, M.A. (eds.) 1997. Contributions to the Micropaleontology and Paleoceanography of the Northern North Atlantic. *Grzybowski Foundation Special Publication*, no. 5, pp. 141-148

rapidly grow and reproduce when presented with a sudden pulse of food, leading to the formation of large populations (Gooday, 1988; Graf, 1989; Gooday, 1993). Once the food source is exhausted the populations collapse, yet are able to "hibernate" until the next pulse of food (Gooday, 1988; Gooday, 1993; Smart *et al.*, 1994).

For any given year the trace of phytodetritus in the fossil record may fail to be preserved, however, the signal of increasing or decreasing phytodetritus inputs over many years should be. This would mean that inputs over significantly long periods of time would be recorded as peaks in phytodetritus-exploiting benthic foraminiferal species. The assumption of a foraminiferal abundance peak being representative of an average seasonal productivity over many years (or decades) holds true for the annual productivity peaks as well. This assumption is particularly true of Core PS 1246-2 which does not have high sedimentation rates (0.58-4.05 cm/kyear), necessarily meaning low temporal resolution.

It is a clear fact that habitat preferences of foraminifera are not rigidly set, but rather are able to tolerate fluctuating food availability and oxygen gradients (Gooday, 1993). Therefore, using the feeding habits of foraminifera more so than their respective living habitats, this study traces the changes in annual and seasonal productivity on the Iceland Plateau using indicative benthic foraminiferal species during the late glacial, Younger Dryas and Holocene. (The reader should remember this paper's use of "annual", and especially "seasonal", productivity are therefore loosely used terms).

METHODS

Foraminiferal Sampling

As pointed out by Schröder *et al.* (1987), some environmentally-significant foraminifera (for example the phytodetritus-exploiting species used in this study: *Epistominella exigua, Eponides tumidulus* and *Globocassidulina subglobosa*) are adequately represented in only the >63μm residues. Keeping this in mind, approximately 25cc of wet bulk sediment, in 1cm thick sediment slices, was wet sieved over a 63μm mesh and the retained sediment sample was dried and sieved into the following size fractions: 63-125μm, 125-250μm, 250-500μm, 500-1000μm and 1000-2000μm.

For a given sample, the entire foraminiferal population from each size fraction was picked and counted (or the statistically valid minimum number of 300 specimens if the sample was too large to be picked in its entirety). The data presented are based on the entire fraction >63μm.

Age Model Control

Ages used in this study are reservoir-corrected AMS ^{14}C years before present. The age of the surface (2,900 yrs B.P.) was determined by correlation of planktic foraminiferal abundance patterns with Core PS 1243 from the East Iceland Sea, which has a much higher sedimentation rate and radiocarbon age control (Bauch & Weinelt, in press). Correlation between these two cores has been done in order to aid the age control for Core PS 1246-2. A distinctive rhyolitic ash (18.5 cm core depth), undoubtedly the Vedde ash which identifies the Younger Dryas cool period, occurs at a depth stratigraphically-correlated to be 10,600 yrs B.P. (terrestrially dated; Mangerud *et al.*, 1984). The beginning of the Last Glacial Maximum (LGM) is given the age of 17,700 yrs B.P. (Sarnthein *et al.*, 1995) and is plotted based on linear interpolation of age data points. The end of the LGM (better identified in this core than the beginning) is indicated by the glacial maximum in the *Neogloboquadrina pachyderma* (sin) $\delta^{18}O$ record (see Fig. 5b(ii) this study; Bauch, 1994) and is given the age of 14,900 yrs B.P. (data from Vogelsang, 1990; age modi-

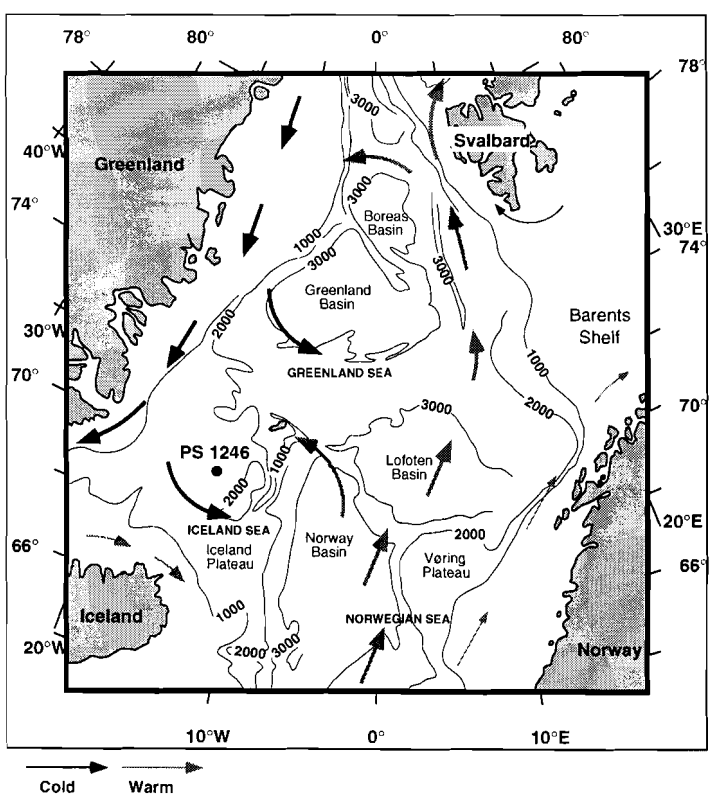


Figure 1. Locality map.

fied by Sarnthein *et al.*, 1992; Sarnthein *et al.*, 1995). The age of the bottom of the core, through correlations with Core PS 1243-2, has been assigned the age of 23,000 yrs B.P.. This age estimate is confirmed by the absence of an isotope Stage 3.1 melt water spike in the planktic $\delta^{18}O$ record and by the occurrence of *Siphotextularia rolshauseni* which also implies only isotope Stage 2 (Nees & Struck, 1994). Ages for the rest of the core were obtained by means of linear interpolation using the above four data points.

Calculation of Accumulation Rates

Foraminiferal counts were converted into individuals/gram (ind/g) using dry bulk sediment weight and, subsequently, into accumulation rates using the following formulas:

$$AR_{Bulk}(gcm\text{-}^{2}a^{-1}) = LSR(cma^{-1}) * DBD(gcm^{-1}) \quad (1)$$

$$indg^{-1} * AR_{Bulk}(gcm^{-2}a^{-1}) = INDAR(indcm^{-2}a^{-1}) \quad (2)$$

where:

AR_{Bulk} = bulk accumulation rate

a = years before present

LSR = linear sedimentation rate (partly modified from Bauch, 1993)

DBD = dry bulk density (linearly interpolated from Birgisdóttir, 1991)

$indg^{-1}$ = individuals/g (this study)

INDAR = individual accumulation rate

RESULTS

Only the environmentally significant species (those showing substantial fluctuations in abundance) are discussed in this study: *Cibicidoides wuellerstorfi*, *Epistominella exigua*, *Eponides tumidulus*, *Globocassidulina subglobosa* *Siphotextularia rolshauseni*, and *Stetsonia* spp.

General trends, as shown in Figure 2a(i), show larger numbers of foraminifera in the post-Younger Dryas and early Holocene portion of the core than during the glacial. *Stetsonia* spp. and *S. rolshauseni* are the only major exceptions. *Siphotextularia rolshauseni*, although not abundant in total number (Fig. 3d) or percent abundance (Fig. 2d), has an obvious preference for the glacial (Nees & Struck, 1994). *Stetsonia* spp. has only slightly higher total numbers (Fig. 3e) in the glacial (as compared to the

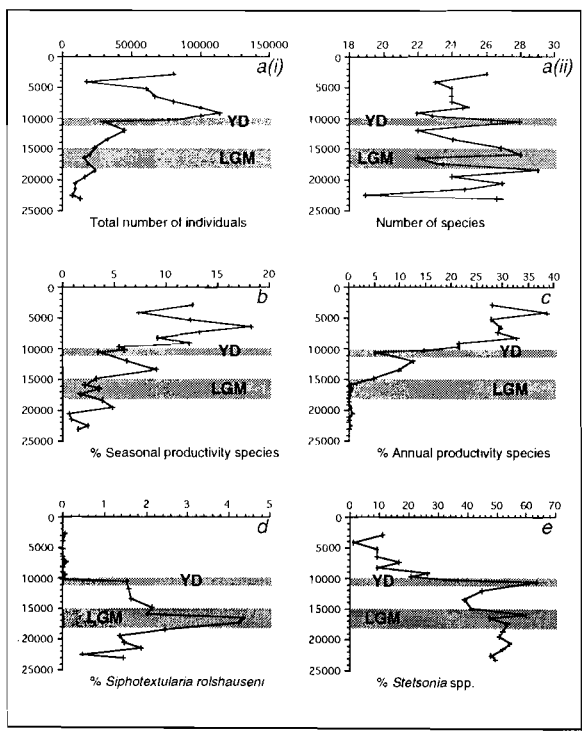


Figure 2. Percent abundances: (a(i)), total number of individuals (a(ii)) number of species, (b) % seasonal productivity species = % *Epistominella exigua*, % *Eponides tumidulus* and % *Globocassidulina subglobosa*, (c) % annual productivity species = % *Cibicidoides wuellerstorfi*, (d) % *Siphotextularia rolshauseni*, (e) % *Stetsonia* spp.. YD = Younger Dryas, LGM = Last Glacial Maximum. Vertical axis is age in ^{14}C years before present.

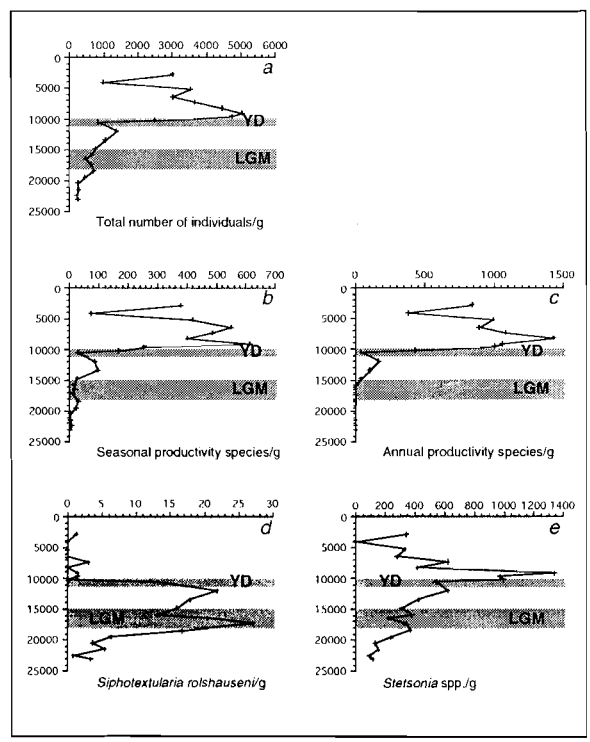


Figure 3. Individuals/g: (a) total number of individuals/g, (b) seasonal productivity species/g = *Epistominella exigua*/g, *Eponides tumidulus*/g and *Globocassidulina subglobosa*/g, (c) annual productivity species/g = *Cibicidoides wuellerstorfi*/g, (d) *Siphotextularia rolshauseni*/g, (e) *Stetsonia* spp./g. YD = Younger Dryas, LGM = Last Glacial Maximum. Vertical axis is age in ^{14}C years before present.

Holocene) yet, as the total number of foraminifera is lower in the glacial, the percent abundance of *Stetsonia* spp. (Fig. 2e) is markedly higher. This would suggest that *Stetsonia* spp. has an obvious preference for glacial environmental conditions, as the accumulation rates of *Stetsonia* spp. (Fig. 4e) show peaks clearly associated with the LGM and the Younger Dryas. The increased percent abundance of *Stetsonia* spp. during these times is in accordance with its dominance in modern Arctic Ocean deep sea foraminiferal faunas (Scott & Vilks, 1991).

There is a pre-Younger Dryas warming as shown by increased benthic and planktic foraminiferal abundances (Fig. 5a(i) and a(ii)). During the Younger Dryas a substantial drop in the size of the foraminiferal population is recognized.

Benthic foraminiferal accumulation rates generally mimic the trend of percent abundance (Fig. 4), more so than that of ind/g, and no major deviations from this trend are observed (compare Figs. 2 and 4). The accumulation rate data give a better indication of the absolute magnitude of productivity changes, showing the strong post-Younger Dryas peak in warming of surface waters and hence, in both annual and seasonal productivity.

Lower $\delta^{13}C$ values correspond to nutrient-rich waters, and higher values to nutrient-depleted waters. The $\delta^{13}C$ *C. wuellerstorfi* record (Fig. 5c(i)), shows a general increase in productivity from low glacial levels to the higher productivity levels of the Holocene. Additionally, it agrees well with the percent abundances of the annual (Fig. 2c) and seasonal (Fig. 2b) productivity-indicating species, i.e. the peaks in percent abundance positively correlate with lower $\delta^{13}C$ values. The general trend of the benthic $\delta^{13}C$ curve is coeval with that of the planktic $\delta^{13}C$ curve (Fig. 5b(ii)), further strengthening the relation of benthic foraminifera to surface productivity.

Heavier $\delta^{18}O$ values correspond to times of increased ice volume, necessarily inferring a colder climate, thus acting as a first-order proxy for paleotemperatures. The $\delta^{18}O$ benthic *C. wuellerstorfi* record (Fig. 5b(i)) generally corresponds with trends shown in the planktic *Neogloboquadrina pachyderma* (sin) $\delta^{18}O$ record (Fig. 5b(ii)), both suggesting colder times during peaks in productivity.

DISCUSSION

Late Pleistocene Glacial (23,000-11,000 yrs B.P.)

Glacial conditions are represented by total abun-

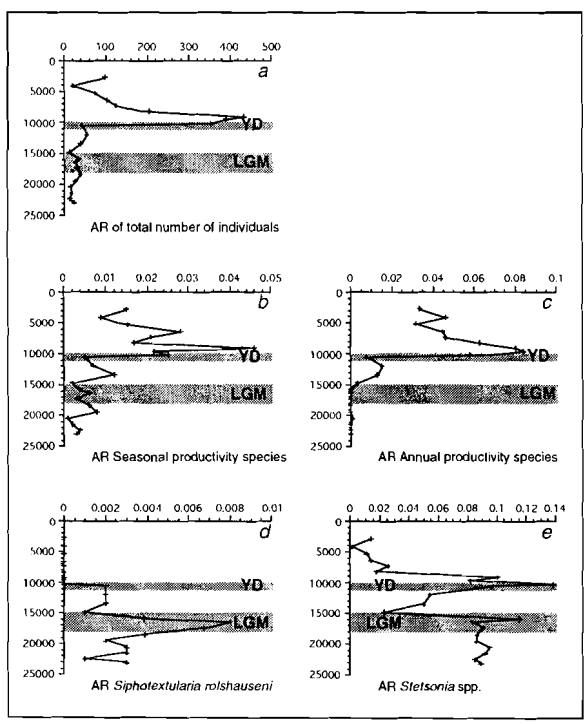


Figure 4. Accumulation rates (ind*cm^{-2}a^{-1}): (a) total individuals, (b) seasonal productivity species = *Epistominella exigua, Eponides tumidulus* and *Globocassidulina subglobosa*, (c) annual productivity species = *Cibicidoides wuellerstorfi*, (d) *Siphotextularia rolshauseni*, (e) *Stetsonia* spp.. YD = Younger Dryas, LGM = Last Glacial Maximum. Vertical axis is age in ^{14}C years before present.

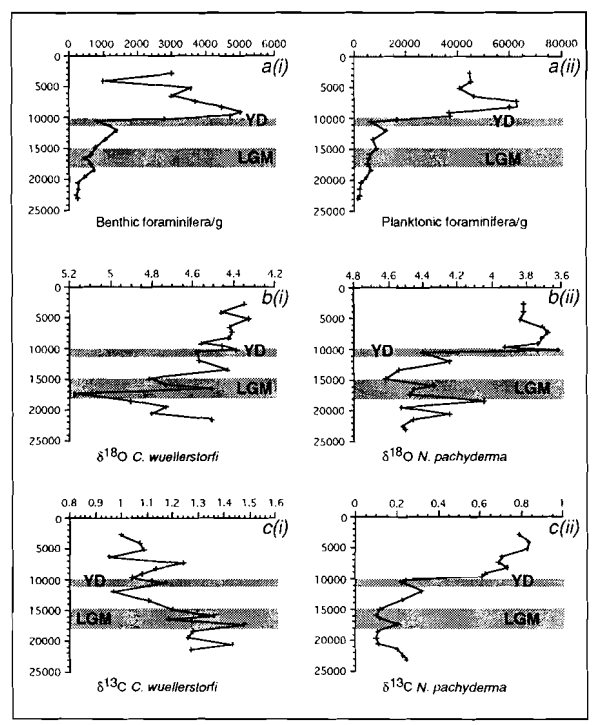


Figure 5. Stable isotopes: (a) benthic and planktonic foraminiferal abundances, (b) oxygen and (c) carbon stable isotope records of *Cibicidoides wuellerstorfi* and *Neogloboquadrina pachyderma* (s) (‰ vs. PDB). YD = Younger Dryas, LGM = Last Glacial Maximum. Vertical axis is age in ^{14}C years before present.

dances of about 1000 ind/g and species diversity ranging from 22 to 28 species (averaging around 26). *Siphotextularia rolshauseni* (characteristic of low organic carbon flux; Nees & Struck, 1994) ranges in abundance from 15 to 27 ind/g. This species reflects a strongly oligotrophic environment, which is supported by a near-absence (0.0125-0.25 ind/g) of high organic flux species (i.e. *Bolivina* sp., *Bulimina marginata*, *Brizalina* sp., *Pullenia bulloides* and *Uvigerina* spp.). Although *S. rolshauseni* does not constitute a large part of the foraminiferal population (1-4.5% in our core), it appears virtually only in the glacial, and strongly confirms to be stratigraphically useful in the Nordic Seas as an indicator of oxygen isotope Stage 2 (Struck & Nees, 1991; Nees & Struck, 1994). The percent abundance, ind/g and accumulation rate of *S. rolshauseni* all simultaneously reach a maximum around 16,500 yrs B.P..

Cibicidoides wuellerstorfi (used here as a first-order proxy for annual productivity) was virtually absent early in the glacial but, at approximately 16,000 yrs B.P., it began to gradually increase. In Core 1246-2, it reached its glacial peak of about 13% of the total foraminiferal population around 12,000 yrs B.P.. This peak is associated with peaks in both ind/g and accumulation rate.

Seasonal productivity, as recorded by phytodetritus species such as *Epistominella exigua*, *Eponides tumidulus* and *Globocassidulina subglobosa* (Gooday, 1993), shows small peaks around 22,500 yrs B.P., 19,000 yrs B.P., 16,500 yrs B.P. and the largest glacial peak at 13,500 yrs B.P..

Stetsonia spp. is undoubtedly the major constituent in the glacial foraminiferal assemblage (average of 52% and 300 ind/g). At 16,000 yrs B.P. *Stetsonia* spp. increases slightly in total numbers (400 ind/g) and has a much higher percent abundance (60%), accompanied by a sharp increase in the accumulation rate. Both annual and seasonal productivity trends are similar in degree of change but seasonal productivity begins to increase some 7,000 yrs B.P. earlier and is more of a gradual change than annual productivity trends. Seasonal productivity appeared to slowly increase at about 20,000 yrs B.P., reaching a small peak before decreasing in intensity during the LGM. Percentages of both seasonal and annual productivity-indicating species show an increase around 14,000-13,000 yrs B.P., possibly indicating prolonged sea-ice free conditions, as warming of the North Atlantic was underway at this time (Veum *et al.*, 1992). At approximately 12,000 yrs B.P., there is a near-minimum in species diversity (22 species) and a slight increase in total numbers (1400 ind/g). Indicated by an increase of *C. wuellerstorfi* from 10% to 13%, annual productivity has its maximum during the late glacial, and seasonal productivity (% phytodetritus species from 9% down to 6%) decreases at this time.

Younger Dryas (11,000-10,000 yrs B.P.)
A decrease in total numbers of individuals (850 ind/g), as well as a corresponding decrease in the total number of each individual species, occurred during the Younger Dryas. This is understandable, as there was a return to glacial conditions, with an associated decrease in temperature (Fig. 5b(i)) and productivity (Fig. 5c(i)). Oddly, there exists a near-maximum in species diversity (Fig. 2a(ii)), resembling the peak in species at 15,000 yrs B.P.. *Siphotextularia rolshauseni* comprises only 1.5% of the total population. Despite the low relative abundance, it maintains a glacial level, thereby indicating low organic carbon flux. The decrease in % *C. wuellerstorfi* as a suspension feeding species suggests a decrease in annual productivity (Fig. 2c), as well as a possible weakening of lateral advection of nutrients. This may be a manifestation of the slight decrease in NADW production in the Nordic Seas as suggested by Boyle & Rosener (1990). Seasonal productivity is also reduced during the Younger Dryas, as indicated by the lower percent abundance of phytodetritus species (Fig. 2b).

Most trends during the Younger Dryas seem to indicate environmental conditions similar to those indicated at 15,000 yrs B.P., during the last glacial. At both times, the total numbers of each species decrease and percent abundances are slightly lower. The lower percent abundances result from the relatively small decrease in total numbers of *S. rolshauseni* and especially *Stetsonia* spp. (Figs. 2e and 4e). In fact, this similarity between the Younger Dryas and conditions indicated at 15,000 yrs B.P. is evident in nearly all proxy indicators.

The abrupt decrease of *S. rolshauseni* at the end of the Younger Dryas may have resulted from a marked increase in organic carbon flux at this time which, in turn, may help explain the quick environmental recovery immediately following the Younger Dryas as shown by the sudden and dramatic increase in foraminiferal abundances.

Holocene (10,000-2,900 yrs B.P.)
Early Holocene conditions are represented by a post-Younger Dryas 4- fold increase (as compared to early- to mid-Younger Dryas levels) in total number of individuals (approximately 5000 ind/g) as well as a slight decrease in species diversity (average of about 24 species). Annual productivity, as indicated by % *C. wuellerstorfi*, increases rapidly from the Younger Dryas level to the early post-Younger Dryas level between 9,000 and 8,000 yrs B.P.. Seasonal productivity (% phytodetritus species) slightly decreases immediately after the

Younger Dryas, then increases to the Holocene average. Though seasonal productivity fluctuates, there appears to be a period of high (Fig. 2b with a maximum of 18% phytodetritus species abundance) seasonal productivity from 7,000 to 5,000 yrs B.P.. At 4,000 yrs B.P. there is a noticeably sharp decrease in the foraminiferal population, accompanied by a slight decrease in species diversity (Figs. 2a(i) and a(ii)). The relative abundance of *C. wuellerstorfi* is higher at this time, while all others decrease. This is interpreted not as an increase in annual productivity but, rather, as a change in environmental conditions that was detrimental to all species. As *C. wuellerstorfi* was the most numerous at the time (about 1000 ind/g), its higher percent abundance is a result of the greater loss to the remaining species.

CONCLUSIONS

Our study of benthic foraminifera (percent abundances, ind/g, and accumulation rates) support the following observations concerning late Pleistocene-Holocene productivity changes:

(1) During the glacial period (23,000 to 15,000 yrs B.P.) seasonal productivity increased some 7,000 yrs B.P. before any comparable increase in annual productivity. Seasonal productivity peaked at 22,500 yrs B.P., 19,000 yrs B.P., 16,500 yrs B.P. and 13,500 yrs B.P., while annual productivity had a peak at only 12,000 yrs B.P..

(2) The Younger Dryas is marked by a noticeable decrease in the total number of foraminifera and a near-maximum in species diversity. Foraminiferal evidence points to conditions similar to those present at 15,000 yrs B.P.. The abrupt decrease of *S. rolshauseni* at the end of the Younger Dryas possibly indicates a substantial increase in organic carbon flux, which may account for the post-Younger Dryas explosion in total numbers.

(3) Most species exhibit an abundance maximum during the early Holocene, reflecting highest seasonal productivity from 7,000 to 5,000 yrs B.P.. The major exception being *S. rolshauseni*, which almost disappeared. At 4,000 yrs B.P. there was a substantial change in environmental conditions on the Iceland Plateau, which caused total numbers to drastically decrease.

Acknowledgments

We are appreciative of the thorough and critical comments provided by an anonymous reviewer. This study was financed by the *Deutsche Forschungsgemeinschaft* (DFG) and is contribution No. 310 of the *Sonderforschungsbereich* 313 at Kiel University.

REFERENCES

Altenbach, A.V. & Sarnthein, M. 1989. Productivity record in benthic foraminifera. *In:* W.H. Berger, V.S. Smetacek & G. Wefer (eds.), *Productivity of the Ocean: Present and Past*, 255-269, John Wiley.

Bauch, H. 1993. Planktische Foraminiferen im Europäischen Nordmeer - ihre Bedeutung für die paläo-ozeanographische Interpretation während der letzten 600.000 Jahre. *Berichte aus dem Sonderforschungsbereich 313*, **40**, 1-108.

Bauch, H. 1994. Significance of variability in *Turborotalita quinqueloba* (Natland) test size and abundance for paleoceanographic interpretations in the Norwegian-Greenland Sea. *Marine Geology*, **121**, 129-141.

Bauch, H. & Weinelt, M. (in press). Surface water changes in the Norwegian Sea during last deglacial and Holocene times. *Quaternary Science Reviews.*

Birgisdóttir, L. 1991. Die paläo-ozeanographische Entwicklung der Islandsee in den letzten 550 000 Jahren. *Berichte aus demSonderforschungsbereich 313*, **34**, 1-186.

Boyle, E.A. & Rosener, P. 1990. Further evidence for a link between late Pleistocene North Atlantic surface temperatures and North Atlantic deep-water production. *Palaeogeography, Palaeoclimatology, Palaeoecology* (Global and Planetary Change Section), **89**, 113-124.

Gooday, A.J. 1988. A response by benthic foraminifera to the deposition of phytodetritus in the deep sea. *Nature*, **332**, 70-73.

Gooday, A.J. 1993. Deep-sea benthic foraminiferal species which exploit phytodetritus: Characteristic features and controls on distribution. *Marine Micropaleontology*, **22**, 187-205.

Graf, G. 1989. Benthic-pelagic coupling in a deep-sea benthic community. *Nature*, **341**, 437-439.

Herguera, J.C. & Berger, W.H. 1991. Paleoproductivity from benthic foraminifera abundance: Glacial to postglacial change in the west-equatorial Pacific. *Geology*, **19**, 1173-1176.

Lutze, G.F. & Coulbourn, W.T. 1984. Recent benthic foraminifera from the continental margin of northwest Africa: community structure and distribution. *Marine Micropaleontology*, **8**, 361-401.

Lutze, G.F. & Thiel, H. 1987. *Cibicidoides wuellerstorfi* and *Planulina ariminensis*, elevated epibenthic foraminifera. *Berichte aus dem Sonderforschungsbereich 313*, **6**, 17-30.

Mangerud, J., Lie, S.E., Furnes, H., Kristiansen, I.L. & Lomo, L. 1984. A Younger Dryas ash bed in western Norway, and its possible correlations with tephra in cores from the Norwegian Sea and the North Atlantic. *Quaternary Research*, **21**, 85-104.

Nees, S. & Struck, U. 1994. The biostratigraphic and paleoceanographic significance of *Siphotextularia rolshauseni* Phleger and Parker in Norwegian-Greenland Sea sediments. *Journal of Foraminiferal Research*, **24**, 233-240.

Sarnthein, M., Jansen, E., Duplessy, J.C., Erlenkeuser, H., Flatøy, A., Veum, T. Vogelsang, E. & Weinelt, M. 1992. $\delta^{18}O$ time-slice reconstructions of meltwater anomalies at Termination I in the North Atlantic between 50 and 80°N. *In:* E. Bard & W.S. Broecker (eds.), *The Last Deglaciation: Absolute and Radiocarbon Chronologies*, 183-200, NATO ASI Series, I, 2.

Sarnthein, M., Jansen, E., Weinelt, M. & 12 others. 1995. Variations in Atlantic surface ocean paleoceanography, 50°-80°N: A time-slice record of the last 30,000 years. *Paleoceanography*, **10**, 1063-1094.

Schröder, C.J., Scott, D.B. & Medioli, F.S. 1987. Can smaller benthic foraminifera be ignored in paleoenvironmental analysis? *Journal of Foraminiferal Research*, **17**, 101-105.

Scott, D.B. & Vilks, G. 1991. Benthonic foraminifera in the

surface sediments of the deep-sea Arctic Ocean. *Journal of Foraminiferal Research*, **21**, 20-38.

Smart, C.W., King, S.C., Gooday, A.J., Murray, J.W. & Thomas, E. 1994. A benthic foraminiferal proxy of pulsed organic matter paleofluxes. *Marine Micropaleontology*, **23**, 89-99.

Struck, U. 1995. Stepwise postglacial migration of benthic foraminifera into the abyssal northeastern Norwegian Sea. *Marine Micropaleontology*, **26**, 207-213.

Struck, U. & Nees, S. 1991, Die Stratigraphische Verbreitung von *Siphotextularia rolshauseni* (Phleger and Parker) in Sedimentkernen aus dem Europäischen Nordmeer. *Geologisches Jahrbuch*, **A128**, 243-249.

Veum, T., Jansen, E., Arnold, M., Beyer, I. & Duplessy, J.C. 1992. Water mass exchange between the North Atlantic and the Norwegian Sea during the past 28,000 years. *Nature*, **356**, 783-785.

Vogelsang, E. 1990. Paläo-Ozeanographie des Europäischen Nordmeeres an Hand stabiler Kohlenstoff- und Sauerstoffisotope. *Berichte aus dem Sonderforschungsbereich 313*, **23**, 1-136.

Appendix 1: SYSTEMATIC TAXONOMY

***Adercotryma glomerata* (BRADY 1878)**
Lituola glomerata BRADY, 1878, p. 433, Plate 20, Fig. 1

***Bolivina* spp.**

***Brizalina* spp.**

***Bulimina marginata* (D'ORBIGNY 1826)**
Bulimina marginata D'ORBIGNY, 1826, p. 269, Plate 12, Fig. 10-12
***Bulimina* spp.**

***Buliminoides williamsonianus* (BRADY 1881)**
***Bulimina williamsoniana* BRADY, 1881, p.56.**

***Cassidulina* spp.**

***Cassidulina laevigata* (D'ORBIGNY 1826)**
Cassidulina laevigata D'ORBIGNY, 1826, p. 282, Plate 15, Fig. 4-5

***Cibicides robertsonianus* (BRADY 1881)**
Truncatulina robertsoniana BRADY, 1881, p. 65

***Cibicides* spp.**

***Cibicidoides wuellerstorfi* (SCHWAGER 1866)**
Anomalina wuellerstorfi SCHWAGER, 1866, p. 258, Plate 7, Fig. 105, 107

***Cribrostomoides subglobosum* (SARS 1872)**
Lituola subglobosa SARS, 1872, p. 252

***Cyclammina* spp.**

***Dentalina pauperata* (D'ORBIGNY 1846)**
Dentalina pauperata D'ORBIGNY, 1846, p. 46, Plate 1, Fig. 57-58

***Dentalina* spp.**

***Elphidium* spp.**

***Epistominella exigua* (BRADY 1884)**
Pulvinulina exigua BRADY, 1884, p. 696, Plate 103, Fig. 13, 14

***Eponides tumidulus* (BRADY 1884)**
Truncatulina tumidulus BRADY, 1884, p. 666, Plate 95, Fig. 8

***Eponides* spp.**

***Fissurina* spp.**

***Fursenkoina fusiformis* (WILLIAMSON 1858)**
Bulimina pupoides var. *fusiformis* WILLIAMSON, 1858, p. 63, Plate 5, Fig. 129-130

***Globocassidulina subglobosa* (BRADY 1881)**
Cassidulina subglobosa BRADY, 1881, p. 60

***Glomospira gordialis* (JONES & PARKER 1860)**
Trochammina squamata JONES & PARKER var. *gordialis* JONES & PARKER, 1860, p. 304

***Gyroidina* spp.**

***Hormosina* spp. (infilled)**

***Islandiella norcrossi* (CUSHMAN 1988)**
Islandiella norcrossi (CUSHMAN) - Loeblich & Tappan, p. 506, Plate 559, Fig. 3-7

***Lagena* spp.**

***Lenticulina gibba* (D'ORBIGNY 1839)**
Cristellaria gibba D'ORBIGNY, 1839, p. 40, Plate 7, Fig. 20-21

***Marginulina glabra* (D'ORBIGNY 1826)**
Marginulina glabra D'ORBIGNY, 1826, p. 259, no. 6

***Neolenticulina peregrina* (SCHWAGER 1866)**
Cristellaria peregrina SCHWAGER, 1866, p. 245, Plate 7, Fig. 89

***Nonionellina labradorica* (DAWSON 1860)**
Nonionina labradorica DAWSON, 1860, p. 191, Fig. 4

***Nonionella* spp.**

***Oolina* spp.**

***Oridorsalis umbonatus* (REUSS 1851)**
Rotalina umbonata REUSS, 1851, p. 75, Plate 5, Fig. 35a-c

***Pullenia bulloides* (D'ORBIGNY 1846)**
Nonionina bulloides D'ORBIGNY, 1826, p. 293, Plate 5, Fig. 9-10

***Pyrgo rotalaria* (LOEBLICH & TAPPAN 1953)**
Pyrgo rotalaria LOEBLICH & TAPPAN, 1953, p. 47, Plate 6, Fig. 5-6

***Pyrgo* spp.**

***Quinqueloculina seminula* (LINNÉ 1758)**

Serpula seminulum LINNÉ, 1758, p. 786

***Quinqueloculina* spp.**

***Reophax nodulosa* (BRADY 1879)**
Reophax nodulosa BRADY, 1879, p. 52, Plate 1, Fig. 9

***Rhizammina algaeformis* (BRADY 1879)**
Rhizammina algaeformis BRADY, 1879, p. 39, Plate 4, Fig. 16-17

***Sigmoilopsis schlumbergeri* (BRADY 1884)**
Planispirina celata(Costa). - BRADY, 1884, p. 197, Plate 8, Fig. 1-4

***Siphotextularia rolshauseni* (PHLEGER & PARKER 1951)**
Siphotextularia rolshauseni PHLEGER & PARKER, 1951, p.4, Plate 1, Fig. 23, 24a-b

***Stetsonia* spp.**

***Subreophax guttifer* (BRADY 1881)**
Reophax guttifera BRADY, 1881, p. 49
***Textularia* spp.**

***Triloculina tricarinata* (D'ORBIGNY 1826)**
Triloculina tricarinata D'ORBIGNY, 1826, p. 299, Plate 7, Fig. 94

***Trochammina* spp.**

***Uvigerina* spp.**

agglutinated tube fragments (unidentified)

Dinoflagellate cyst records from the East Greenland continental margin during the last 15,000 years: Implications for paleoceanographic reconstructions

JENS MATTHIESSEN[1,2] and ASTRID BAUMANN[3]

1. Departement de Géologie et Océanographie, URA CNRS 197, Université de Bordeaux I, Avenue des Facultés, 33405 Talence Cedéx, France

2. present adress: Alfred Wegener Institute for Polar and Marine Research, P.O.Box 120161, D-27515 Bremerhaven, Germany

3. SFB 313, University of Kiel, Heinrich-Hecht-Platz 10, D-24118 Kiel, Germany

ABSTRACT

Late Weichselian and Holocene dinoflagellate cyst assemblages have been investigated at two stations situated close to the modern Polar Front at the continental margin off East Greenland. Both the concentrations of dinoflagellate cysts and the assemblage composition reflect changes in the surface water conditions, occurring in distinct steps during the past 15,000 years. Low concentrations of dinoflagellate cysts during Termination Ia suggest harsh environmental conditions, most probably caused by an extensive sea-ice cover and/or a high influx of low salinity meltwater. A surface water warming was recorded from 13,000 - 12,000 years BP, related to the inflow of warmer water from the North Atlantic into the western Norwegian-Greenland Sea. The interval between Terminations Ia and Ib was characterized by a strong seasonality with an extensive sea-ice cover in winter and relatively warm surface waters in summer. At the transition to the Holocene, a reorganisation of the hydrography resulted in surface water conditions characteristic for the Holocene with three well-defined major water masses and oceanographic fronts. The modern water mass conditions at both stations were established at the end of Termination Ib, around 6,400 to 6,800 years BP.

In general, the influence of colder surface waters was more pronounced at the location off Scoresby Sund throughout the Holocene. Arctic water had the strongest influence at both stations in the middle Holocene. A progressive cooling with an increase in sea-ice cover is time-transgressively recorded at both stations during the Holocene, indicating that the Polar Front moved to its present position or that branches of the zonal currents expanded from the East Greenland shelf eastward during the last 3,000 years.

INTRODUCTION

The surface waters of the Norwegian-Greenland Seas represent modifications and mixtures of two major water masses which enter from the Atlantic and the Arctic oceans, respectively (e.g. Swift, 1986). The Norwegian Atlantic Current (NAC) carries the relatively warm, saline Atlantic water along the Norwegian continental margin towards the Arctic Ocean and supplies the high northern latitudes with heat and moisture (Fig. 1). Smaller influxes of warmer water are provided by the Irminger Current (IC) and the Norwegian Coastal Current (NCC). The East Greenland Current (EGC) counteracts this warm water influence, transporting cold, low saline surface water and sea ice along the East Greenland shelf edge to the Denmark Strait. These boundary currents create two large cyclonic gyres in the central part of the Greenland and Iceland seas, resulting in the characteristic distribution of hydrographic fronts and surface water masses (Fig. 1).

These meridional and zonal hydrographic contrasts cause a distinct distribution of sea ice. The North Atlantic water (NAW) is usually free of sea ice throughout the year. The Arctic Water (AW) is characterized by a large seasonal and interannual

In: Hass, H.C. & Kaminski, M.A. (eds.) 1997. Contributions to the Micropaleontology and Paleoceanography of the Northern North Atlantic. *Grzybowski Foundation Special Publication*, no. 5, pp. 149-165

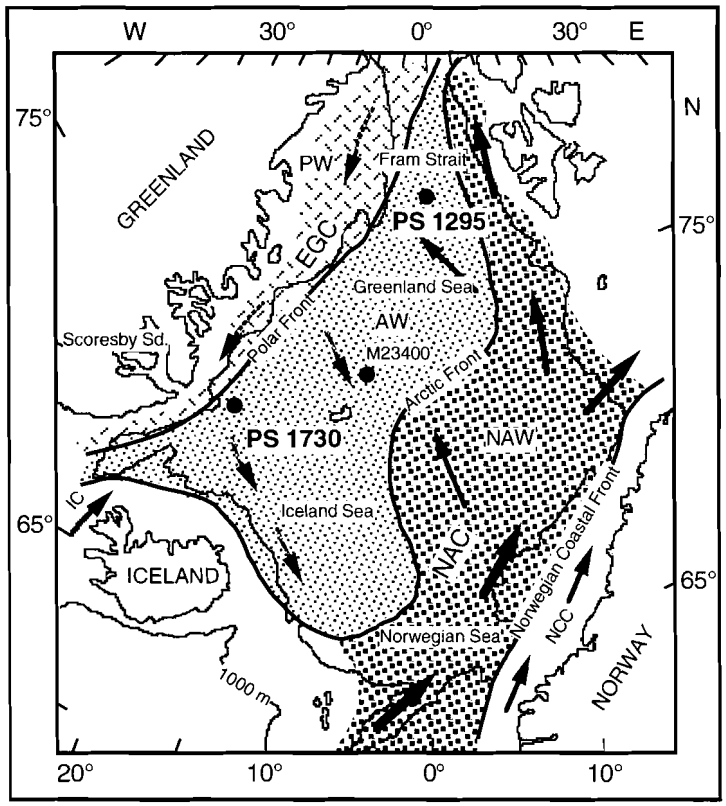


Figure 1. Schematic surface currents and distribution of surface water masses in the Norwegian-Greenland Sea. Abbreviations: PW = polar water masses; AW = arctic water masses; NAW = North Atlantic water masses; EGC = East Greenland Current; NAC = Norwegian Atlantic Current; NCC = Norwegian Coastal Current; IC = Irminger Current (after Dickson *et al.*, 1988; Johannessen, 1986; Swift, 1986).

variability in sea-ice cover especially in the winter, remaining free of sea ice in some years and being ice covered in other years. In contrast, the polar water (PW) is permanently covered by sea ice in winter (Vinje, 1977; Swift, 1986), whereas open conditions mainly prevail in the western Iceland Sea in summer.

Paleoceanographic investigations to date mainly focused on the Norwegian Sea because of the profound influence of the warm North Atlantic water on the past and present climate of Europe. The first inflow of relatively warmer water into the Norwegian Sea and the Fram Strait after Termination Ia forms a major datum in the late glacial and Holocene paleoceanography of the region (e.g. Jansen *et al.*, 1983; Jansen & Bjørklund, 1985; Koç Karpuz & Jansen, 1992; Lehman & Keigwin, 1992; Veum *et al.*, 1992; Koç *et al.*, 1993, 1996; Haflidason *et al.*, 1995; Hald *et al.*, 1996) which initiated the modern meridional Holocene type circulation (Sarnthein *et al.*, 1995). In contrast, upper Quaternary sediments underlying the colder water masses were investigated only in the past few years because of a previous lack of suitable sediment cores (e.g. Gard & Backman, 1990; Baumann *et al.*, 1993; Koç *et al.*, 1993; Stein *et al.*, 1994, 1996; Nam *et al.*, 1995; Antonow, 1995; Nam, 1996). Therefore, the influence of polar water has been widely ignored or considered a marginal phenomenon. It was quite recently realized that changes in the supply of fresh water from the Arctic Ocean via the EGC may considerably disturb the hydrological cycle in the Norwegian-Greenland Sea and the North Atlantic, resulting in changes in deep water convection (Aagaard & Carmack, 1989). The transport of sea ice and low saline surface water in the EGC through the Fram Strait is the largest contribution of fresh water to the Norwegian-Greenland Sea, of which only less than 3% flows into the convective gyres (Aagard & Carmack, 1989). If this influx increases annually by a factor of two, the deep convection would shut down. Sea-ice formation in the central Greenland and Iceland seas is also linked to the influx of low salinity, low density water from the EGC (Swift, 1986). Thus, past changes in the hydrography of the western Greenland and Iceland seas may have had a strong influence on the oceanography of the entire Norwegian-Greenland Sea.

Unfortunately, the variability of the present day oceanographic conditions is not adequately reflected in the distribution of planktic microfossils in the surface sediments from the Greenland and Iceland seas, and the reconstruction of paleoceanographic conditions is seriously hampered because of the sedimentary conditions. Calcareous microfossils are of restricted importance due to sparse occurrences and low diversity of assemblages, reflecting the harsh ecological conditions (e.g. Pflaumann, 1986; Eide 1990; Samtleben *et al.*, 1995b). Additionally, abiotic processes, in particular dissolution, alter the living communities of the calcareous and biosiliceous plankton, often leaving only a fragmentary record in recent and Holocene sediments (e.g. Samtleben *et al.*, 1995b).

Dinoflagellate cysts differ from calcareous and biosiliceous microfossils in being chemically more resistent to biochemical degradation and dissolution because their cyst wall is made of organic compounds. They are persistently present in recent sediments from the Norwegian-Greenland Sea, reflecting the summer conditions, and form distinct assemblages in upper Quaternary sedi-

ments (Matthiessen, 1991, 1995, 1996; Baumann & Matthiessen, 1992).

Therefore, dinoflagellate cysts assemblages have been investigated at two stations at the continental margin off East Greenland in order to reconstruct the evolution of surface waters during the last ca. 15,000 years which are today cold, relatively low saline and seasonally ice covered. The chronostratigraphy of both cores is well-constrained by means of stable oxygen isotopes and accelerator mass spectrometry dating (Jones & Keigwin, 1988; Nam *et al.*, 1995; Nam, 1996; Stein *et al.*, 1994, 1996). Previous investigations at both stations focused on reconstructing glacial-interglacial changes in the sedimentary environment (Letzig, 1995; Nam *et al.*, 1995; Nam, 1996; Stein *et al.*, 1994, 1996), whereas micropaleontological analyses were carried out only on Holocene coccolith and dinoflagellate cyst assemblages from core PS1295 (Matthiessen, 1991; Baumann & Matthiessen, 1992), and on planktic foraminifera from the gravity core of station PS1730 (Nam *et al.*, 1995; Nam, 1996).

In this study, special emphasis is placed on Termination I because previous paleoceanographic reconstructions suggested a time-transgressive inflow of North Atlantic surface water into the Norwegian Sea during the last deglaciation (Koç *et al.*, 1993; Hald *et al.*, 1996), reaching the southeastern Norwegian Sea from 13,500 to 13,000 years BP, the Fram Strait from 12,500 years BP and the western Iceland Sea after 9,000 to 8,000 years BP. A comparison of different planktic microfossil groups, however, showed that only dinoflagellate cysts are continuously present in the Greenland Sea during the past 11,000 years (Samtleben *et al.*, 1995b). Thus, dinoflagellate cysts may have a great potential to reconstruct the paleoceanography of cold, ice-covered regions. Additionally, the possible causes for differences between the dinoflagellate cyst and other planktic microfossil records are discussed because the continuous presence of dinoflagellate cysts has important implications for paleoecanographic reconstructions, which were previously based only on calcareous and siliceous microfossils.

MATERIAL & METHODS

The sediment cores from stations PS1295 and PS1730 were selected for this study because accelerator mass spectrometry radiocarbon dates (Table 1) and stable oxygen isotopes (Fig. 2) suggest that they provide continuous sections during the last ca. 15,000 years BP (Jones & Keigwin, 1988; Nam *et al.*, 1995; Nam, 1996; Stein *et al.*, 1994; 1996). Boxcore PS1295 (formerly referred to as PS21295-4 by Jones & Keigwin, 1988; 21295 by Baumann & Matthiessen, 1992) was collected in the southern Fram Strait (77°59.52′ N, 2°25.23′ E, 3112 m), while the boxcore (70°06.99′N, 17°41,66′W, 1622m) and the gravity core (70°07.19′ N, 17°42.06′ W, 1617m) from station PS1730 were taken in the western Iceland Sea (Fig. 1).

The upper Quaternary sediments of both cores consist of greyish brown silty clays to clayey silts with a variable degree of bioturbation (Letzig, 1995; Nam, 1996; Fig. 2). Samples were taken at variable intervals in order to get a resolution of approximately one sample per 1,000 years. An initial study on sediment core PS1295 revealed a distinct temporal variation in the composition of dinoflagellate cyst assemblages (Matthiessen, 1991) despite the low sedimentation rate (ca. 2 to 3 cm/ka; Jones & Keigwin 1988). Therefore, additional samples were analyzed from Termination I.

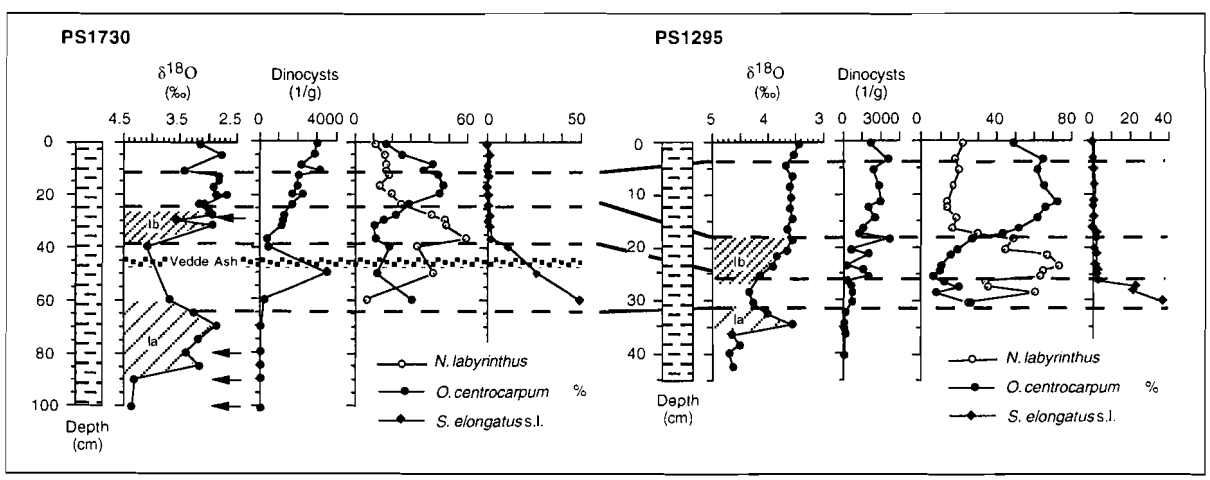


Figure 2. Correlation between the dinoflagellate cyst records of station PS1730 and PS1295. The distinct changes in the composition of the assemblages are marked with a dashed line. Arrows in the stable oxygen isotope record indicate AMS ages (Nam *et al.*, 1995), while all samples used for stable oxygen isotope analyses from PS1295 were dated (Jones & Keigwin, 1988).

Table 1. AMS dates of sediment cores.

Depth (cm)	Age (years BP)	Age Reservoir Corrected (years BP)
PS1295 (Jones & Keigwin, 1988)		
0.5	960± 60	520± 60
2.5	1,150±450	710±450
4.5	2,690± 70	2,250± 70
6.5	3,180± 80	2,740± 80
8.5	3,190± 70	2,750± 70
10.5	3,850± 60	3,410± 60
12.5	4,650± 80	4,210± 80
14.5	4,900± 70	4,460± 70
16.5	6,020± 60	5,580± 60
18.5	7,640± 80	7,200± 80
20.5	8,220± 90	7,780± 90
21.5	8,750±120	8,310±120
23.5	9,440± 90	9,000± 90
25.5	10,100±100	9,660±100
28.5	12,070±160	11,630±160
30.5	13,070±110	12,630±110
32.5	13,480±130	13,040±130
34.5	14,920±120	14,480±120
36.5	15,670±170	15,230±170
38.5	16,140±150	15,700±150
40	16,580±140	16,140±140
42.5	16,940±170	16,500±170
PS1730GC (Nam et al., 1995)		
20.0	8,460±110	7,910±110
35.0	Vedde Ash	10,310± 50
70.0	1,4870±140	14,320±140
80.0	16,820±150	16,270±150
90.0	19,150±190	18,600±190

Table 2. Taxonomic listing of species recovered.

Algidasphaeridium? *minutum* s.l.
(Harland & Reid, in Harland *et al.* 1980) Matsuoka & Bujak, 1988
Brigantedinium simplex
(Wall 1965) Reid 1977
Brigantedinium spp.
Reid 1974
Impagidinium? *pallidum*
Bujak 1984
Nematosphaeropsis labyrinthus
(Ostenfeld 1903) Reid 1974
Operculodinium centrocarpum
(Deflandre & Cookson 1955) Wall 1967
Spiniferites elongatus s.l.
Reid 1974
Spiniferites elongatus
Reid 1974
Spiniferites frigidus
Harland & Reid, in Harland *et al.* 1980
Spiniferites cf. *elongatus*
Harland & Sharp 1986
Spiniferites spp.
(Mantell 1850) Sarjeant 1970
Spiniferites bulloideus
(Deflandre & Cookson 1955) Sarjeant 1970
Spiniferites lazus
Reid 1974
Spiniferites membranaceus
(Rossignol 1964) Sarjeant 1970
Spiniferites mirabilis
(Rossignol 1963) Sarjeant 1970
Spiniferites ramosus
(Ehrenberg) Loeblich & Loeblich 1966

Other species
Ataxiodinium choanum
Reid 1974
Bitectatodinium tepikiense
Wilson 1973
Impagidinium spp.
Stover & Evitt 1978
Impagidinium sphaericum
(Wall 1967) Lentin & Williams 1981
Lingulodinium machaerophorum
(Deflandre & Cookson 1955) Wall 1967
Pentapharsodinium dalei
Indelicato & Loeblich 1986
Trinovantedinium capitatum
Reid 1977

The samples were processed with standard palynological methods which have been briefly described by Matthiessen (1995, 1996). Dinoflagellate cyst concentrations are calculated per gram dry sediment. The second set of samples from core PS1295 and all samples from the box and gravity core PS1730 were sieved with 6 µm mesh after each acid treatment, while 10 µm was used with the first set of samples from PS1295 (Matthiessen, 1991). The different mesh sizes do not pose any problems because the smallest Quaternary dinoflagellate cysts are usually larger than approximately 15 µm. The taxonomy follows principally Matthiessen (1991, 1995) who also illustrated the species shown in Figures 2 to 4. All species recovered are listed in Table 2.

Chronostratigraphy

Accelerator mass spectrometry ^{14}C dates on the planktic foraminiferal species *Neogloboquadrina pachyderma* (sin.) provides the basic chronostratigraphic framework for the sediment cores (Table 1). Boxcore PS1295 has a well constrained chronology because of 22 AMS dates (Jones & Keigwin, 1988). The gravity core from station PS1730 was

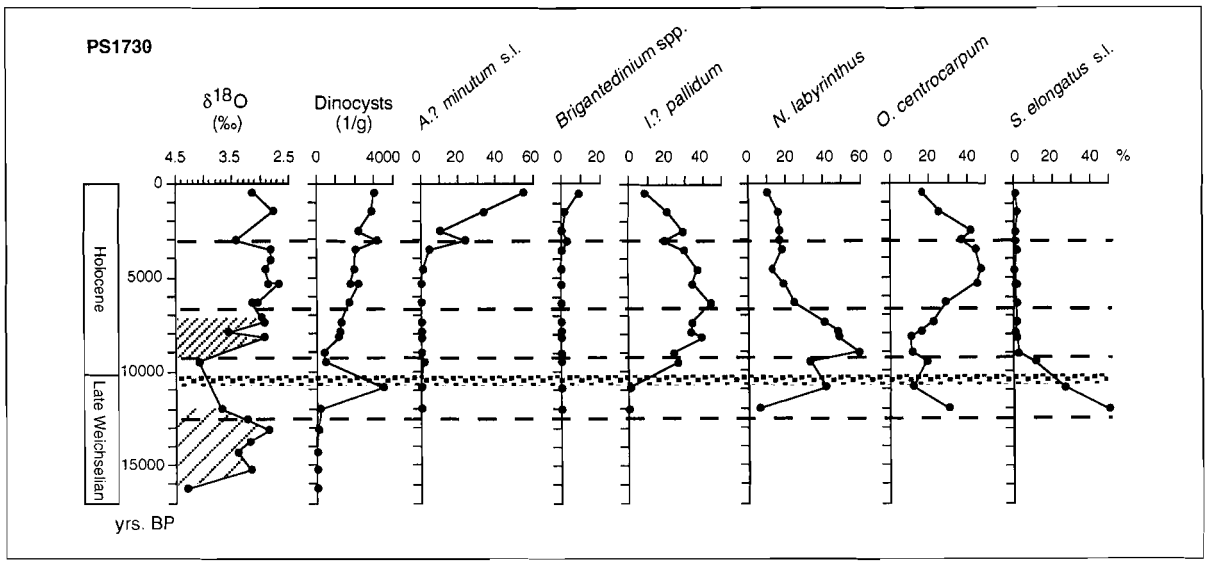


Figure 3. Dinoflagellate cyst record of selected species at station PS1730. The stable oxygen isotope stratigraphy and AMS dates are from Nam *et al.* (1995). The distinct changes in the composition of the assemblages are marked with a dashed line.

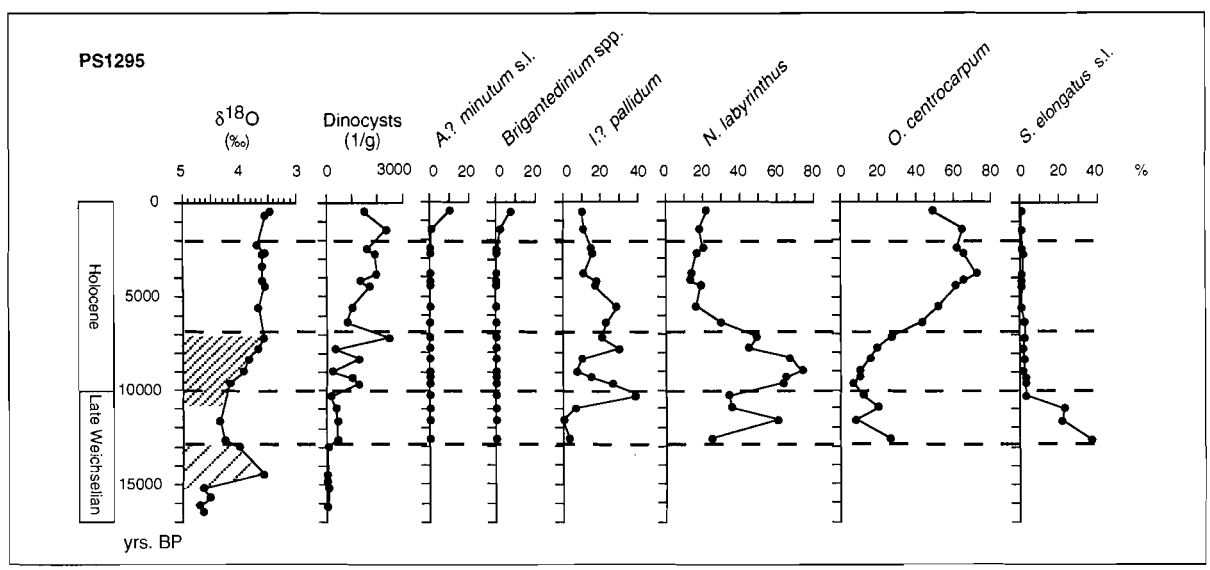


Figure 4. Dinoflagellate cyst record of selected species at station PS1295. The stable oxygen isotope stratigraphy and the AMS dates are from Jones & Keigwin (1988). The distinct changes in the composition of the assemblages are marked with a dashed line.

dated at four levels within the upper 100 cm (Nam *et al.*, 1995; Nam, 1996; Stein *et al.*, 1994, 1996). The ages have been reservoir corrected with 440 and 550 years, respectively (Tab. 2). Additionally, the Vedde Ash is a tephrachronological marker horizon at 35 cm core depth in gravity core PS1730 (Nam *et al.*, 1995; Fig. 2) which has been recently dated by AMS at 10,310 +/- 50 years B.P. (Birks *et al.*, 1996). Boxcore PS1730 was not dated. The age of the surface sediment from station PS1730 has been set at 500 years BP, in accordance with ages of surface sediments from the western Iceland and Greenland seas (Samtleben *et al.*, 1995b). All ages recorded in this study are conventional ^{14}C ages. Ages between the fix points were calculated assuming linear sedimentation rates. This chronostratigraphic framework is supported by the stable oxygen isotope stratigraphy of *Neogloboquadrina pachyderma* (sin.) which clearly shows Termination Ia and Ib (Figure 2; Jones & Keigwin, 1988; Nam *et al.*,

Table 3. Dinoflagellate cyst data from station PS1730. Note the different depth columns for the composite section, the box core (BC) and the gravity core (GC).

depth composite (cm)	depth BC	depth GC	age	cysts counted	cysts (1/g)	A.? minutum s.l.	Brigantedinium spp.	I.? pallidum	N. labyrinthus	O. centrocarpum	S. elongatus s.l.	Spiniferites spp. indet.	other cysts	dinocysts indet.
1	1		500	191	2960	54.5	8.9	8.4	10.5	16.2	0.5		0.5	0.5
5	5		1,522	412	2853	33.3	1.9	20.4	15.8	25.0	1.5	0.2	1.5	0.5
9	9		2,544	421	2146	10.5	0.5	28.5	16.9	41.6	0.7			1.4
11		1	3,055	299	3156	23.4	3.3	18.7	16.7	36.5	0.7	0.3		0.3
13	13		3,566	645	2020	4.3	0.3	29.0	18.0	44.0	1.1	0.5	0.6	2.2
17	17		4,588	511	1932	0.8		36.2	12.9	47.2	0.2		0.8	2.0
20	20		5,355	326	1717			33.4	18.7	44.8	1.2	0.6	0.3	0.9
20		10	5,355	168	2205			33.9	19.0	44.6	0.6		1.8	
24	24		6,377	231	1664			43.3	24.7	28.6	0.9		1.3	1.3
28	28		7,399	193	1244			33.7	40.4	21.8	1.6	0.5	1.0	1.0
30		20	7,910	169	1216			33.1	47.9	15.4	0.6	1.2	0.6	1.2
32	32		8,230	263	1145			38.8	48.3	10.3	1.5		0.4	0.8
37	37		9,030	166	372			23.5	59.0	10.8	2.4	1.8	1.2	1.2
40		30	9,513	142	414	1.4		26.1	33.1	18.3	11.3	8.5		1.4
50		40	10,883	662	3451			0.2	41.5	11.8	26.6	19.6	0.2	0.2
60		50	12,029	119	194				5.9	30.3	49.6	5.9	0.8	7.6
70		60	13,174	4	55									
80		70	14,320	4	21									
85		75	15,295	4	22									
90		80	16,270	0	0									
100		90	18,600	3	14									

1995; Nam, 1996; Stein *et al.*, 1994). The chronologic terminology of Mangerud *et al.* (1974) and Mangerud & Berglund (1978) has been used in Figures 3 to 6.

RESULTS

Dinoflagellate cyst stratigraphy

The sediment cores from both stations show a comparable development of the dinoflagellate cyst assemblages which is characterized by changes in percentage abundances of few species (Tables 3 and 4). In particular, the change in dominance from *Nematosphaeropsis labyrinthus* to *Operculodinium centrocarpum* provides an independent tool for stratigraphic correlation between the sediment cores and enables the construction of a composite section for station PS1730 (Tab. 3). The depth scale of the gravity core was corrected by +10 cm to obtain the best fit of the dinoflagellate cyst curves. In addition to the abundant taxa, other cyst species contribute usually less than 4% at both stations (Tables 3 and 4). These species are listed in Table 2. Usually, the diversity of the assemblages is higher in the samples from the Fram Strait. This is probably caused by the stronger influence of relatively warmer water on the hydrography.

Fluctuations in the concentrations and the percentage abundances of *O. centrocarpum*, *N. labyrinthus* and *Spiniferites elongatus* s.l. enable correlation of both sediment cores (Fig. 2). The concentrations continuously increase from the late Weichselian to the late Holocene. Concentrations are extremely low during Termination Ia, preventing the calculation of percentage abundances of individual taxa.

The changeover in dominance from *O. centrocarpum* to *N. labyinthus* has been recognized in several sediment cores from the Norwegian Sea (Matthiessen, 1991; Baumann & Matthiessen, 1992; Samtleben *et al.*, 1995b) and the eastern North Atlantic Ocean (Harland, 1994; Harland & Howe, 1995). The assemblages from the Greenland and Iceland seas (e.g. at station PS1730; Table 3) differ in having higher percentage abundances of *Impagidinium? pallidum* than the assemblages from the Norwegian Sea, and in showing a distinct increase of *Algidasphaeridium? minutum* s.l. and *Brigantedinium* spp. in the late Holocene.

The interval between Terminations Ia and Ib is dominated by species of *Spiniferites*, especially *S. elongatus* s.l., together with *N. labyrinthus*. *I.? pallidum* is almost absent in the late Weichselian, and *S. elongatus* s.l. increases downcore. The distinct increase of *I.? pallidum* at the transition to the Holocene has been observed in other sediment cores from the Iceland and Greenland seas (e.g. Samtleben *et al.*, 1995b) and thus may be a good marker for the onset of interglacial hydrographic conditions.

The distinct changes in the composition of the assemblages are approximately associated with the end of Termination Ia, the onset of Termination Ib and the end of Termination Ib. The significant

Table 4. Dinoflagellate cyst data from station PS1295.

depth (cm)	age	cyst counted	cysts (1/g)	A.? minutum s.l.	Brigantedinium spp.	I.? pallidum	N. labyrinthus	O. centrocarpum	S. elongatus s.l.	Spiniferites spp. indet.	other cysts	dinocysts indet.
0.5	520	443	1443	9.9	7.4	9.7	21.9	48.8	0.2	0.5	1.1	0.5
3.5	1,480	442	2355	0.7	2.3	11.1	17.9	64.7	0.5		2.7	0.2
5.5	2,495	1067	1574	0.3	0.5	15.3	20.0	61.6	0.9	0.7	0.5	0.4
8.5	2,750	652	1865			15.6	16.6	65.0	1.1	0.6	0.5	0.6
11.5	3,810	1048	1959		0.1	11.0	13.6	72.0	0.9	0.8	1.2	0.4
12.5	4,210	451	1310			18.0	13.1	65.4	0.4	0.4	1.8	0.9
14.5	4,460	811	1667			16.8	18.6	61.2	0.7	1.0	1.4	0.4
16.5	5,580	580	991			28.6	16.4	51.9	0.3	0.5	1.6	0.7
17.5	6,390	426	779			22.8	29.6	43.0	2.3	0.5	0.7	1.2
18.5	7,200	756	2446			20.4	48.7	26.7	2.1	1.5	0.5	0.1
20.5	7,780	279	343			29.4	44.4	19.0	1.1	1.8	3.2	1.1
21.5	8,310	383	1286			9.9	66.6	15.4	2.1	2.9	3.1	
23.5	9,000	138	203			7.2	73.2	10.1	1.4	1.4	4.3	2.2
24.5	9,330	219	988			15.1	64.4	9.6	2.7	3.7	0.5	4.1
25.5	9,660	980	1267			25.8	63.1	6.3	2.6	1.3	0.9	
26.5	10,317	103	153			41.7	34.0	11.7	2.9	4.9	1.0	3.9
27.5	10,974	322	384			6.8	35.1	19.9	22.7	15.5		
28.5	11,630	229	417				60.3	7.9	21.4	4.8	2.2	3.5
30.5	12,630	209	422			3.3	24.4	25.8	36.4	9.6		0.5
32.5	13,040	19	65									
34.5	14,480	18	45									
35.5	14,855	16	43									
36.5	15,230	31	88									
40.5	16,212	12	48									

decrease of *O. centrocarpum* in the latest Holocene is not clearly reflected in the stable oxygen isotope records. The major changes occur almost synchronously in both sediment cores proving the usefulness of dinoflagellate cysts as ecostratigraphic tools (Figs. 3 and 4). Stratigraphic datums are (1) 13,000 to 12,000 years BP at the end of Termination Ia, (2) around 10,000 years BP at the transition from the late glacial to the Holocene and (3) around 6,400 to 6,800 years BP at the end of Termination IB, whereas the change in the late Holocene occurred timetransgressively.

Ecology of species

The ecologic preferences are determined from the distribution in surface sediments in the North Atlantic Ocean and adjacent seas (Harland, 1983; Mudie, 1992; de Vernal *et al.*, 1994; Rochon & de Vernal, 1994; Matthiessen, 1995) and from sediment trap investigations in the Norwegian-Greenland Sea (Dale & Dale, 1992). The abundant dinoflagellate cyst species are arranged according to basic ecological preferences in Figures 3 and 4.

Algidasphaeridium minutum s. l. comprises morphotypes resembling the holotype (Harland & Reid in Harland *et al.*, 1980), and *A.? minutum* var. *cesare* (de Vernal *et al.*, 1989). It is a polar taxon (Dale & Dale, 1992; Mudie, 1992; Matthiessen, 1995), which is principally adapted to low sea-surface temperatures (<5°C), salinities less than ca. 33‰, and to a long seasonal sea-ice cover (de Vernal *et al.*, 1994). This species characterizes sediment assemblages underlying the polar surface water masses in the Norwegian-Greenland Sea (Matthiessen, 1995).

Brigantedinium species, which are commonly referred to as spherical brown protoperidinioid cysts, occur in polar to tropical regions (e.g. Wall *et al.*, 1977; Marret, 1994; Matthiessen, 1995; Biebow, 1995; Zonneveld, 1996). Most protoperidinioid cysts probably belong to heterotrophic dinoflagellates (Dale, 1983). It has been observed that several species feed on diatoms (Jacobsen & Andersen, 1986). Their presence may therefore be related to the occurrence of food organisms in the first instance and secondly to hydrographic parameters such as temperature and salinity (e.g. Dodge, 1994).

Usually, the orientation and preservation of these delicate cysts prevents identification of most specimens to species level. Therefore, it is only possible to assign specific assemblages to environments by considering the individual species in the assemblages, and not the percentage composition of the assemblage. Recent assemblages from polar to subpolar environments (Mudie & Short, 1985; Mudie, 1992; Rochon & de Vernal, 1994; Matthiessen, 1995) dominated by *Brigantedinium* contain usually two species, *B. simplex* and *B. cariacoense*. *Brigantedinium simplex* is the characteristic species

of polar environments (Dale, 1985; Matthiessen, 1991; 1995), and is abundant to dominant on the East Greenland shelf. In polar environments *Brigantedinium* species co-occur with *A.? minutum* s.l., while gonyaulacoid species such as *O. centrocarpum* and *S. elongatus* s.l. are rare to absent. In contrast, recent assemblages from warmer environments such as the permanent upwelling area off Peru contain several other species of *Brigantedinium* and additionally numerous spinose protoperidinioid species that are absent in polar environments (Wall *et al.*, 1977; Biebow, 1996). In the tropical eastern Atlantic, assemblages which are dominated by *Brigantedinium* spp. are characterized by gonyaulacoid species (mainly *Spiniferites*), while other spinose protoperidinioid species are usually rare (Marret, 1994).

In this study, only *Brigantedinium simplex* has been unequivocally identified, and counts have been included in *Brigantedinium* spp.. *Brigantedinium* species from polar and cold-temperate environments are adapted to a wide range of temperatures but obviously prefer sea-surface salinities lower than 33‰ and occur in regions with some months of sea-ice cover (de Vernal *et al.*, 1994). Thus, assemblages composed of both *A.? minutum* s.l. and *Brigantedinium* spp. characterize environments with low sea-surface temperatures and salinities, and a long seasonal extent of sea-ice cover (Mudie & Short, 1985; de Vernal *et al.*, 1994; Rochon & de Vernal, 1994; Matthiessen, 1995) such as the polar water masses in the Norwegian-Greenland Sea. Both species only occur in the latest Holocene of both sediment cores (Figures 3 and 4).

Impagidinium? pallidum is probably a bipolar species because it has been observed only in high northern (Mudie, 1992; Dale & Dale, 1992; de Vernal *et al.*, 1994; Matthiessen, 1995), and southern latitudes (Marret & de Vernal, in press). It requires similar summer temperatures as *A.? minutum* s.l. but has a higher minimum limit for sea-surface salinities (>25‰) and is found in regions with a somewhat lower extent of seasonal sea-ice cover (de Vernal *et al.*, 1994). It characterizes recent assemblages underlying the Arctic water masses of the Norwegian-Greenland Sea (Matthiessen, 1995). This species is abundant only in the Holocene, generally decreasing upwards in the cores. Thus, it is a good marker of the interglacial surface water conditions along the East Greenland continental margin.

The other species recorded in both sediment cores are characteristic of the relatively warmer waters found in the Norwegian Sea (e.g. Harland, 1983; Dale & Dale, 1992; Matthiessen, 1995). These species usually dominate the assemblages, and here, only the abundant species are considered.

Nematosphaeropsis labyrinthus and *Operculodinium centrocarpum* are two opportunistic cosmopolitan species (Wall *et al.*, 1977; Harland, 1983). *O. perculodinium centrocarpum* obviously tolerates a wider range in temperature and salinity conditions than *N. labyrinthus* (e.g. Dale, 1985; de Vernal *et al.*, 1994). This species is often a pioneer species in polar environments (Harland, 1983) and it is even adapted to brackish waters (Dale, 1988). The common to abundant occurrence of *N. labyrinthus* in sediments from the Norwegian-Greenland Sea and the Northeast Atlantic has been previously associated with a cold-temperate to subpolar outer neritic to oceanic preference (Matthiessen, 1991, 1995; Harland & Howe, 1995) but recently it has been shown that this species is also abundant to dominant in the tropical Arabian Sea (Zonneveld, 1996). Therefore, it may prefer higher sea surface temperatures than *O. centrocarpum*.

Spiniferites elongatus s.l. comprises a variety of morphotypes (Harland *et al.*, 1980; Harland, 1982; Harland & Sharp, 1986; Matthiessen, 1991, 1995) including *S. elongatus*, *S. frigidus* and intergrades. It prefers in contrast of *Spiniferites* spp. cold-temperate to polar conditions (Dale, 1983). *Spiniferites* spp. comprises all species other *S. elongatus* s.l. which have a preference for relatively warmer conditions (Tab. 2).

Spiniferites elongatus s.l. and *O. centrocarpum* form characteristic assemblages in subpolar environments. In Baffin Bay, these assemblages are associated with sea-surface temperatures around 2°C and reduced salinities around 32‰ (Mudie & Short, 1985; Rochon & de Vernal, 1994). Similar assemblages occur in the inner Barents Sea (Harland, 1982), where the surface waters are stratified in summer because of relatively high sea-surface temperatures (ca. 7° to 9° C) and sea-surface salinities lower than 34.7‰ (Midttun, 1989, 1990; Loeng, 1991). The Baffin Bay and the Barents Sea are characterized by some months of sea-ice cover (Vinje, 1983; Loeng, 1991; Middtun, 1989; Vinje & Kvambekk, 1991; Mudie & Short, 1985).

This compilation of the ecological preferences thus show that the predominant species, which are continuously present during the past 13,000 years are cosmopolitan forms, whereas the species which indicate specific ecological conditions are abundant during specific intervals (Figs. 3, 4).

DISCUSSION

Paleoceanographic interpretation

Termination Ia

Both stations show a period of extremely low Quaternary dinoflagellate cyst concentrations between 15,000 to ca. 13,000 years BP (Figures 3 and 4). The coeval shift in the stable oxygen isotope values is

probably caused by a significant decrease in surface water salinities owing to a strong freshwater discharge (Jones & Keigwin, 1988; Stein *et al.*, 1994, 1996). Termination Ia was characterized by a high input of meltwater into the entire Norwegian-Greenland Sea because of the decay of the major ice sheets (e.g. Hald *et al.*, 1996; Koç & Jansen, 1994; Stein *et al.*, 1994, 1996; Sarnthein *et al.*, 1995). In the Fram Strait, the retreat of the ice sheet from the outer shelf of Spitsbergen and the southern Barents Sea may have contributed to the increased meltwater discharge until ca. 13,000 to 12,500 years BP (Hald *et al.*, 1996; Elverhøi *et al.*, 1995; Polyak *et al.*, 1995). Stein *et al.* (1994) and Nam *et al.* (1995) attributed the light stable oxygen isotope values at station PS1730 off Scoresby Sund to fluctuations in the Greenland ice sheet. Additionally, changes in the inflow of low saline meltwater from the Arctic Ocean may have influenced the surface waters at both stations.

The low concentrations of dinoflagellate cysts may be explained by harsh living conditions for cyst forming dinoflagellates because of too low sea-surface salinities and/or an extensive sea-ice cover, resulting in a low production. The meltwater probably contained a high suspension load providing a difficult light regime which in addition to the low salinity caused a hostile environment for dinoflagellates.

Dinoflagellate cyst concentrations increased slightly between 13,000 and 12,000 years BP, corresponding to the end of Termination Ia (Figures 3 and 4). This event is well-dated in core PS1295, occurring between 13,000 to 12,600 years BP, while the lower temporal resolution of PS1730 hampers a more precise definition than 13,000 to 12,000 years BP. The presence of species which characterize relatively high surface water temperatures indicate that the initial warming occurred at the locations off Scoresby Sund and in the Fram Strait already at the end of Termination Ia. Previous investigations suggest that Atlantic waters flowed first into the southeastern Norwegian Sea around 13,500 years BP (e.g. Koç & Jansen, 1992, 1994; Lehman & Keigwin, 1992; Sarnthein *et al.*, 1995), reached the Barents shelf slope around 12,500 years BP (Hald *et al.*, 1996; Koç *et al.*, 1996) and the Iceland and Greenland Sea after 9,000 years BP (Koç *et al.*, 1993). The time-transgressive inflow along the Norwegian and Barents continental margins cannot be confirmed by the present study. Furthermore, the increase in dinoflagellate cyst concentrations in a sediment core from the Barents shelf slope is dated at 13,100 to 12,800 years BP (Baumann, A., unpubl. data), supporting that the initial warming occurred synchronously along the path of the Norwegian Atlantic Current. Time-slice reconstructions based on stable oxygen isotope records revealed that the Holocene style interglacial circulation mode persisted largely in the Norwegian-Greenland Sea over the last 12,800 years (Sarnthein *et al.*, 1995). In the adjacent North Atlantic, summer sea-surface temperatures increased already from 15,000 to 13,000 years BP (Duplessy *et al.*, 1992a,b; Koç *et al.*, 1996; Sarnthein *et al.*, 1995), suggesting that warmer water might have also flowed into the Norwegian and Iceland seas. Thus, it appears likely that warmer water reached almost synchronously the Fram Strait and the western Iceland Sea, but the question remains open as to whether the central Greenland and Iceland seas were also influenced by warmer water from 13,000 to 12,000 years BP.

In general, the continuous presence of dinoflagellate cysts suggest that the ocean climate evolved in accordance with the atmospheric climate. When the summer insolation increased in the high northern latitudes after the last glacial maximum (Berger, 1978), dinoflagellate cyst assemblages reflect the improving environmental conditions from 13,000 to 12,000 years BP.

Late Glacial

The composition of the dinoflagellate cyst assemblages varied in the late glacial but they are characterized by *S. elongatus* s.l., and an inverse relationship between *N. labyrinthus* and *O. centrocarpum*. These species indicate a stronger influence of relatively warmer water at both stations in summer but they occur today also in regions with some months of sea-ice cover (de Vernal *et al.*, 1994). The assemblages are somewhat comparable with recent assemblages from Baffin Bay (Mudie & Short, 1985; Rochon & de Vernal, 1994) and in particular the inner Barents Sea (Harland, 1982). The hydrography of both regions is characterized by the inflow of relatively warm water in summer mixing with cold polar water, causing a stratified upper water column. However, the assemblages from the continental margin of Greenland differ from these recent assemblages in having high proportions of *N. labyrinthus*. This can not be definitely explained yet but the ecological preferences of *N. labyrinthus* suggest that sea-surface temperatures and salinities were relatively higher when it was more abundant. The decrease of *S. elongatus* s.l. towards the Holocene may indicate an increase in sea-surface salinities. The late glacial surface water conditions at the East Greenland continental margin probably involved a strong seasonality. Low temperatures and a sea-ice cover may have prevailed in winter, whereas in summer the inflow of warmer water, the warming of the sea surface and the input of meltwater led to a stratified upper water column

which covered colder polar water.

Short-term input of meltwater from the margins of the retreating ice sheets close to the stations may have helped to maintain lower sea-surface salinities in summer. A second meltwater event started in the Fram Strait just after 13,000 years BP, when the ice retreated from the inner shelf to the coast of Spitsbergen but was interrupted by a short readvance around ca. 12,400 years BP (Elverhøi *et al.*, 1995). The Scoresby Sund glacier probably retreated after 13,000 years BP from the outer fjord system (Dowdeswell *et al.*, 1994) which is indicated by high sediment accumulation rates at station PS1730 between ca. 11,000 and 13,200 years BP (Nam *et al.*, 1995). Unfortunately, such events are not reflected in the stable oxygen isotope curves of stations PS1295 and PS1730 because of their low temporal resolution.

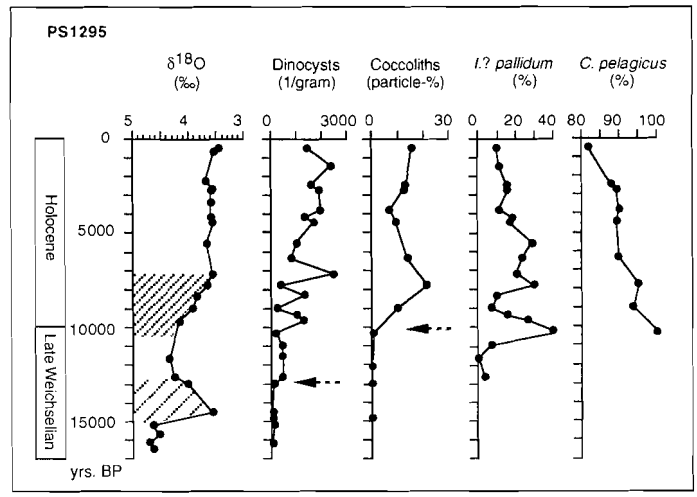


Figure 5. Comparison of dinoflagellate cyst and coccolith records of station PS1295. The arrows mark the first increase of dinoflagellate cyst concentrations and coccoliths at the end of Termination Ia and at the base of Termination Ib, respectively.

Previous investigations on diatoms and planktic foraminifera revealed a strong variability in the inflow of warmer water from the North Atlantic and in the hydrographic properties along the Norwegian continental margin between 13,000 and 10,000 years BP (Lehman & Keigwin, 1992; Koç & Jansen, 1992; Haflidason *et al.*, 1995; Koç *et al.*, 1996). This cannot be resolved at stations PS1730 and PS1295 because of low sample resolution and low sedimentation rates. However, fluctuations in the assemblages from core PS1295 might be associated with the Younger Dryas around 11,000 to 10,000 years BP (Figure 4). Peaks in the abundance of *N. labyrinthus* bracket the Younger Dryas. The peak in the abundance of *I.? pallidum* suggests that the sea surface was cooler in summer than before, and the sea-surface salinities increased during the Younger Dryas. Sarnthein *et al.* (1995) suggested that a strong seasonality prevailed in the Norwegian-Greenland Sea during the Younger Dryas with a closed sea-ice cover in winter, low surface water temperatures and sea-surface salinities in summer similar to modern values. According to their spatial reconstructions, colder waters extended to the east, but a narrow corridor was left open for Atlantic water inflow.

Holocene

Although the Holocene is considered to be a period of long-term stability in ocean climate without major evolutionary trends and/or important short-term events (e.g. Sarnthein *et al.*, 1995), the dinoflagellate cyst records from the East Greenland continental margin and other planktic microfossil records (e.g. Bauch & Weinelt, in press; Hald *et al.*, 1996; Koç *et al.*, 1993; Samtleben *et al.*, 1995b) suggest considerable changes in surface water mass properties and the position of oceanographic fronts.

Early Holocene: Termination Ib

The distinct increase of *I.? pallidum* and the strong decline of *S. elongatus* s.l. at the transition to the Holocene indicate that interglacial conditions were established along the East Greenland continental margin after 9,000 to 10,000 years BP. Because the distribution of *I.? pallidum* is today strongly related to the Arctic surface waters, the characteristic modern distribution of the surface water masses and oceanographic fronts did not exist before the Younger Dryas/Holocene transition. The onset of the Holocene conditions is clearly reflected in the coccolith abundances in the Fram Strait and Greenland Sea (e.g. Figure 5; Andruleit, 1995; Baumann, 1990; Baumann & Matthiessen, 1992; Samtleben *et al.*, 1995b) which strongly increase first after 9,000 years BP.

Termination Ib is characterized by fluctuations in the surface water temperatures which is reflected by a somewhat reciprocal relationship between *I.? pallidum* and *N. labyrinthus*. An abundance maximum of *N. labyrinthus* is found at both stations around 9,000 to 8,000 years BP bracketed by peaks of *I.? pallidum*. This reflects a short-term warming during a period of generally stronger influence of Arctic water.

The end of Termination Ib is marked by a changeover in dominance from *N. labyrinthus* to *O. centrocarpum*, suggesting that modern hydrographic conditions were established at the East Green-

land continental margin around 6,400 to 6,800 years BP (Figure 2). This event occurred slightly later in the Iceland and Greenland seas than the eastern Norwegian Sea (Samtleben *et al.*, 1995b; Baumann, A., unpubl. data) but this may be the result of the different temporal resolution and age control of the records.

Despite the major role of temperature as primary ecological factor, this pronounced change in the composition of the assemblages cannot be explained by the smooth long-term atmospheric temperature fluctuations during the middle Holocene alone. Both species are adapted to relatively warm sea-surface temperatures but *O. centrocarpum* tolerates a wider salinity range. Thus, the cause of change has to be found in the North Atlantic Drift-Norwegian Atlantic Current (NAC) system because the percentage abundances of *I.? pallidum* which is indicative of colder conditions does not change in the middle Holocene. Other ecological factors may have been involved, such as short-term surface water salinity changes. At the end of the postglacial sea-level rise (Fairbanks, 1989) a marked rise by ca. 6.5 m occurred within a few decades around 6,800 years BP (Blanchon & Shaw, 1995), probably resulting in short-term salinity reduction. Blanchon & Shaw (1995) correlate this rise event with a minimum in the stable oxygen isotope records from the Greenland ice sheet at ca. 7,300 years BP, indicating a cooling (Johnsen *et al.*, 1992; Dansgaard *et al.*, 1993; Taylor *et al.*, 1993). These events again occurred almost synchronously with a short-term climate cooling in coastal East Greenland dated at ca. 8,000 to 7,500 years BP (Björk *et al.*, 1994a; b). Additionally, the reorganisation of the surface water circulation along the Northwest European continental margin, in particular changes in the hydrographic properties of the Norwegian Coastal Current, has been proposed as possible causes (Baumann & Matthiessen, 1992; Bauch & Weinelt, in press). Thus, both a short-term input of freshwater and a cooling phase may have triggered the changes in the assemblages but the ultimate cause of this event can only be resolved, if marine records with a comparable temporal resolution as the sea level and ice core records are investigated.

Middle and late Holocene

The distribution of surface water masses remained relatively stable at both stations for approximately 3,000 to 4,000 years during the middle Holocene. The high percentage abundance of *I.? pallidum* document the strong influence of Arctic surface water on the hydrography in the Fram Strait and off Scoresby Sund until ca. 4,000 years BP. The dominance of *O. centrocarpum*, however, indicates that relatively warmer water from the Norwegian Sea continuously reached the continental margin off East Greenland during summer. The generally lower abundances of *I.? pallidum* in PS1295 indicate that the influence of relatively warmer Atlantic water was stronger at the location in the Fram Strait.

A decrease of *I.? pallidum* started at approximately 4,000 to 5,000 years BP, whereas *O. centrocarpum* decreases time-transgressively, at station PS1730 from approximately 2,500 years BP and at station PS1295 from approximately 4,000 years BP (Figures 3 and 4). Simultaneously, the distinct increase in polar species, especially *A.? minutum* s.l., suggests that branches of the East Greenland Current reached the sites and/or the Polar Front moved eastward. A stronger influence of colder, low saline surface water is recorded at station PS1730 from 3,000 years BP, and at station PS1295 from 1,500 years BP.

In principal, polar water did not influence the surface water at both stations before the late Holocene. During the major part of the Holocene Arctic water played a more important role, in addition to a variable inflow of relatively warmer North Atlantic water. The Polar Front was probably located to the west of both stations in the summer and the zonal advection of cold surface water was minimal. This interpretation generally agrees with the model of Polar Front movement of Koç *et al.* (1993). Koç *et al.* (1993) suggested that the Polar Front retreated to a position along northeastern Greenland until ca. 7,000 and the western Iceland Sea was under the influence of subarctic conditions. The Polar Front moved eastward from 5,000 years BP, reaching its modern position around 3,000 years BP.

Comparison of planktic microfossil records: Paleoceanographic implications

When comparing different planktic microfossil records from the same stations, strong differences in the temporal distributions are evident (Figures 5 and 6). Coccolith abundances first increased in sediment core PS1295 during Termination Ib, whereas dinoflagellate cysts increased their abundances from the end of Termination Ia (Figure 5; Baumann, 1990; Baumann & Matthiessen, 1992). Coccolith assemblages are compared to dinoflagellate cyst assemblages of lower diversity and are clearly dominated by *Coccolithus pelagicus* which contributes usually more than 80% to the assemblages (Baumann, 1990). Planktic foraminifer assemblages are almost monospecific in the 125 to 250 µm size fraction from gravity core PS1730 during the past 13,000 years consisting mainly of *Neogloboquadrina pachyderma* (sin.) (Nam *et al.*, 1995; Nam, 1996). In contrast, dinoflagellate cysts which

have been studied from the same sample intervals, show distinct changes in assemblage composition and are principally of higher diversity. Siliceous microfossils were not studied in the cores but a sediment core located ca. 20 miles to the west of station PS1730 is barren of radiolarians during the Holocene and Younger Dryas (Molina-Cruz, 1991).

The sediment core (M23400) is the only record from the Greenland and Iceland seas where organic-walled, calcareous and biosiliceous planktic microfossils have been investigated from the same sample intervals (Figure 6; Andruleit, 1995; Baumann, A. unpubl. data; Kohly, 1994; Schröder-Ritzrau, 1995; Samtleben *et al.*, 1995b). The differences in the Holocene records are striking, suggesting that records of single groups must be interpretated with caution. Dinoflagellate cysts are present from the base of the core. Coccoliths occur after 9,000 years BP, while diatoms and radiolarians are present only from ca. 2,000 years BP.

Comparison with previous studies show that these differences in the temporal distribution of the various groups has a strong impact on paleoceanographic reconstructions. Calcareous microfossils indicate that interglacial conditions were established almost synchronously in the whole Norwegian-Greenland Sea around 10,000 to 9,000 years BP. Coccoliths occur in most records at the transition to the Holocene (e.g. Andruleit, 1995; Baumann, 1990; Baumann & Matthiessen, 1992; Gard & Backman, 1990), while abundances of subpolar planktic foraminifers strongly increase at about the same time (e.g. Bauch, 1993; Hald *et al.*, 1996; Bauch & Weinelt, in press). In contrast, analyses of diatom assemblages from the Norwegian-Greenland Sea revealed a time-transgressive occurrence after Termination Ia (Koç *et al.*, 1993). Diatoms are present in the southeastern Norwegian Sea since 13,400 years BP, whereas they are only found from ca. 2,000 years BP in the Greenland Sea (Figure 6). The temporal distribution of radiolarians is principally comparable to that of diatoms (e.g. Molina-Cruz, 1991; Schröder-Ritzrau, 1995).

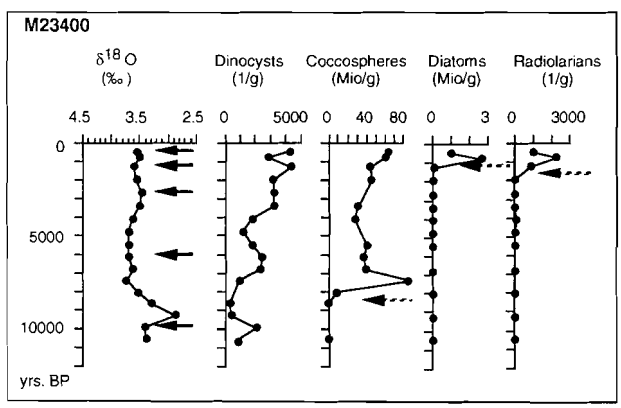


Figure 6. Comparison of dinoflagellate cyst, coccolith, diatom, and radiolarian records of station M23400 from the Greenland Sea (72°21.10'N, 007°48.40'W, 2630 m). The arrows in the individual records mark the first increase of concentrations (redrawn from Samtleben *et al.* (1995b) with additional AMS dates from Andruleit (1995)). Arrows in the stable oxygen isotope record indicate AMS dates.

Possible causes of variability in planktic microfossil records

There is evidence from actuopaleontological investigations that these inconsistencies can be attributed both to abiotic and to biotic processes (Andruleit, 1995; Kohly, 1994; Schröder-Ritzrau, 1995; Samtleben *et al.*, 1995b). Samtleben *et al.* (1995b) concluded that dissolution in the water column and in the sediment may considerably alter calcareous and biosiliceous microfossil records, causing sequences barren of biosiliceous microfossils even in Holocene sediments from the Greenland Sea. Abiotic processes obviously play a more important role for the occurrence of biosiliceous microfossils than for calcareous microfossils in upper Weichselian and Holocene sediments (cf. Figure 6).

The basic ecological requirements may additionally cause principal differences in the occurrence of planktic microfossils along the East Greenland continental margin both in upper Weichselian and Holocene sediments. The distribution of all plankton groups primarily depends on sea-surface temperatures, which is well demonstrated e.g. for the distribution of coccolithophores in the surface waters of the northern North Atlantic (Samtleben *et al.*, 1995a). Additionally, fossilizable coccolithophores, planktic foraminifers and radiolarians are generally considered marine plankton indicating that salinity is the second important ecologic factor. Few coccolithophore species only such as *Emiliania huxleyi*, tolerate sea-surface salinities as low as 20‰ (e.g. Bukry, 1974; Pankow, 1990), while *Neogloboquadrina pachyderma* (sin.) is the only planktic foraminifer which is adapted to a wide range of ecological conditions in the polar regions, in particular salinity fluctuations (e.g. Bauch & Weinelt, in press). Schröder-Ritzrau (1995) compiled information on salinity requirements of radiolarians showing that they may be not adapted to salinities below ca. 25‰. Low surface water salinities caused by e.g. deglacial meltwater discharge thus may be a limiting factor for these „marine" groups, resulting in the absence in the late Weichselian.

This may be true for coccolithophores which are autotrophic and live in the photic zone. *Coccolithus pelagicus* is the only polar to subpolar

species (Samtleben *et al.*, 1995a) preserved in the fossil record but it is absent in the Norwegian-Greenland Sea in glacial times when cold polar conditions can be anticipated (e.g. Baumann, 1990; Gard & Backman, 1990). The distribution in recent and Holocene sediments is somewhat comparable to that of the dinoflagellate cyst *Impagidinium? pallidum* (Samtleben *et al.*, 1995b, Fig. 14), suggesting that they might have similar ecological requirements. *I.? pallidum* is adapted to polar and subpolar environments and salinities larger than 25-28‰ (de Vernal *et al.*, 1994). *Coccolithus pelagicus* may tolerate temperatures as low as -1.7°C but it probably requires salinities exceeding 30‰ (Braarud, 1979). Therefore, an adverse combination of temperature and salinity might have caused the absence of *C. pelagicus* and *I.? pallidum* in upper Weichselian sediments.

In contrast to the phytoplankton, the zooplankton is able to migrate vertically in the water column, and foraminifers and radiolarians should thrive in deeper waters which are less affected by the rapid change in sea-surface conditions. However, species such as *Turborotalita quinqueloba*, which is an important subpolar planktic foraminifer in the Norwegian-Greenland Sea, contains symbionts restricting its depth habitat to the photic zone (e.g. Bauch, 1994). Additionally, it may require salinities higher than 30,5‰ (Carstens & Wefer, 1992). Therefore, its absence in the assemblages from the gravity core PS1730 may be either attributed to the absence of symbionts or a specific temperature/salinity relationship in surface waters. In contrast *N. pachyderma* (sin.) might have lived in colder, higher saline deeper waters, and dominated therefore the assemblages because of unfavourable living conditions for other surface dwelling species. The absence of radiolarians in the late Weichselian may be also attributed to too low sea-surface salinities for surface water species but the ecology of deep-dwelling species is insufficiently known in order to determine the ultimate cause of their absence (e.g. Schröder-Ritzrau, 1995).

In contrast to these planktic groups, diatoms are best-suited for palecological studies. They tolerate a wide range of temperature and salinity conditions, and are abundant in fresh to marine water (e.g. Pankow, 1990). Cyst forming dinoflagellates are the only other planktic group which replicates the salinity related distribution of diatoms (Wall *et al.*, 1977). Despite these comparable ecologic adaptions, diatoms are present only in upper Weichselian sediments from the Norwegian Sea, whereas dinoflagellate cysts are present in the entire Norwegian-Greenland Sea during this interval.

Again, ecologic causes cannot be completely ruled out to explain the different records of diatoms and dinoflagellate cysts. Dinoflagellates utilize a swimming strategy which is more suited for stratified systems, in contrast to diatoms which are adapted to a sinking strategy (Dale, 1983, 1986; Dale & Fjellså, 1994). Dinoflagellates may actively optimize their position in the surface water column to find optimal living conditions with respect to nutrients, light etc., while diatoms require some turbulence to remain in the photic zone. Thus, a stable upper water column in the summer season owing to strong temperature and salinity gradients, which is suggested by dinoflagellate cysts for the interval between Termination Ia and Ib, may provide difficult ecologic conditions to diatoms and result in a low production.

In contrast to biologic causes, the late Weichselian presence of dinoflagellate cysts can also be interpreted in terms of transport from adjacent oceans and shelves into the Norwegian-Greenland Sea (cf. Dale & Dale, 1992). The East Greenland shelf might be a source area but late glacial sequences are barren of Quaternary dinoflagellate cysts (Matthiessen, 1996). Considering other possible source areas this would involve long range transport from e.g. the northern North Atlantic, and the Iceland and Norwegian continental shelves. Although the dinoflagellate cyst record therefore might not reflect a living population, both indigenous occurrence and transport require the presence of currents which transport warmer water into the Norwegian-Greenland Sea. Reworking of older deposits can be ruled out with certainty because similar assemblages have not been recorded up to now from older deposits and it would require a widespread event in the entire ocean basin to explain the persistent distribution in regions which are far away from each other.

The presence of all plankton groups in the Norwegian-Greenland Sea from the transition of the Holocene suggests that the water masses then gained their modern physical properties, while the ocean chemistry still varied. Thus, biosiliceous microfossils are not adequately preserved in the Holocene sediments from the Greenland Sea.

CONCLUSIONS

Dinoflagellate cysts are continuously present along the East Greenland continental margin during the past 15,000 years. Distinct changes in the composition of the assemblages at two station occurred during certain time intervals.

1. The increase in concentrations and the composition of the assemblages indicate that warmer water reached the western Norwegian-Greenland Sea from 13,000 to 12,000 years BP when the Holocene type meridional circulation system was established (Sarnthein *et al.*, 1995). The surface waters

were free of sea ice during the summer and the upper water column was probably stratified owing to the surface water warming and the lowered sea-surface salinities. This marked environmental change is not reflected in the assemblages of other planktic microfossil groups from the same region. The specific ecological conditions and/or the lower fossilization potential of calcareous and biosiliceous microfossils may have caused this bias in the plankton records of the western Greenland and Iceland sea. Because of these differences, previous reconstructions based in particular on biosiliceous microfossil evidence suggest a later and/or time-transgressive incursion of relatively warmer water from the North Atlantic into the western Norwegian-Greenland Sea after Termination Ia.

2. At the transition to the Holocene the interglacial surface water hydrography with the characteristic distribution of surface water masses and oceanographic fronts was established. In the early Holocene, changes in the assemblage composition suggest fluctuations between warmer and cooler conditions. The end of Termination Ib is marked by a distinct change in dinoflagellate cyst assemblages which reflect the onset of the modern hydrographic conditions. Since the early Holocene dinoflagellate cysts and calcareous microfossils record the evolution of the ocean climate in the entire Norwegian-Greenland Sea while biosiliceous records are still variable in the Greenland and Iceland Sea suggesting that dissolution strongly altered the original signal.

3. The distribution of surface water masses varied considerably at both stations in the Fram Strait and off Scoresby Sund during the Holocene. Arctic surface waters strongly influenced the hydrography from the end of Termination Ib. The assemblages indicate a time-transgressive cooling at both stations. The polar front moved to its present position and/or branches of the colder zonal currents expanded eastward in the last 3,000 to 1,500 years.

ACKNOWLEDGEMENTS

We thank an anonymous referee for helpful comments. Ann E. Holbourn has thoroughly improved the English. This is publication No. 323 of the Sonderforschungsbereich 313 at Kiel University (Germany).

REFERENCES

Aagaard, K. & Carmack, E.C. 1989. The role of sea ice and other fresh water in the Arctic circulation. *Journal of Geophysical Research*, **94 (C10)**, 14,485-14,498.

Andruleit, H. 1995. Coccolithophoriden im Europäischen Nordmeer: Sedimentation und Akkumulation sowie ihre Entwicklung während der letzten 15000 Jahre. *Berichte aus dem Sonderforschungsbereich 313*, **59**, 1-110.

Antonow, M. 1995. Sedimentationsmuster um den Vesteris Seamount (zentrale Grönlandsee) in den letzten 250.000 Jahren. *Geomar Report*, **44**, 1-121.

Bauch, H. 1993. Planktische Foraminiferen im Europäischen Nordmeer - ihre Bedeutung für die paläo-ozeanographische Interpretation während der letzten 600.000 Jahre. *Berichte aus dem Sonderforschungsbereich 313*, **40**, 1-108.

Bauch, H.A. 1994. Significance of variability in *Turborotalita quinqueloba* (Natland) test size and abundance for paleoceanographic interpretations in the Norwegian-Greenland Sea. *Marine Geology*, **121**, 129-141.

Bauch, H.A., & Weinelt, M.S. in press. Surface water changes in the Norwegian Sea during last deglacial and Holocene times. *Quaternary Science Reviews*.

Baumann, K.-H. 1990. Veränderlichkeit der Coccolithophoridenflora des Europäischen Nordmeeres im Jungquartär. *Berichte aus dem Sonderforschungsbereich 313*, **22**, 1-146.

Baumann, K.-H., Lackschewitz, K.S., Erlenkeuser, H., Henrich, R., & Jünger, B. 1993. Late Quaternary calcium carbonate sedimentation and terrigenous input along the East Greenland continental margin. *Marine Geology*, **14**, 13-36.

Baumann, K.-H. & Matthiessen, J. 1992. Variations in surface water mass conditions in the Norwegian Sea: Evidence from Holocene coccolith and dinoflagellate cyst assemblages. *Marine Micropaleontology*, **20**, 129-146.

Berger, A. 1978. Long-term variations of caloric insolation resulting from the Earth's orbital elements. *Quaternary Research*, **9**, 139-167.

Biebow, N. 1996. Dinoflagellatenzysten als Indikatoren der spät- und postglazialen Entwicklung des Auftriebsgeschehens vor Peru. *Geomar Report*, **57**, 1-100.

Birks, H.H., Gulliksen, S., Haflidason, H., Mangerud, J. & Possnert, G. 1996. New radiocarbon dates for the Vedde Ash and Saksunarvatn Ash from Western Norway. *Quaternary Research*, **45**, 119-127.

Björck, S., Bennike, O., Ingólfsson, Ó., Barnekow, L. & Penney, D.N. 1994a: Lake Boksehandsken's earliest post-glacial sediments and their paleoenvironmental implications, Jameson Land, East Greenland. *Boreas*, **23**, 459-472.

Björck, S., Wohlfahrt, B., Bennike, O., Hjort, C. & Persson, T. 1994b: Revision of the Early Holocene lake sediment based chronology and event stratigraphy on Hochstetter Forland, NE Greenland. *Boreas*, **23**, 513-523.

Blanchon, P. & Shaw, J. 1995. Reef drowning during the last deglaciation: Evidence for catastrophic sea-level rise and ice-sheet collapse. *Geology*, **23 (1)**, 4-8.

Braarud, T. 1979. The temperature range of the non-motile stage of *Coccolithus pelagicus* in the North Atlantic region. *British Phycological Journal*, **14**, 349-352.

Bukry, D. 1974. Coccoliths as paleosalinity indicators - evidence from Black Sea. *In:* Degens, E.T. & Ross, D.A. (eds.) *The Black Sea - Geology, Chemistry and Biology* American Association of Petroleum Geologists, Memoir **20**, 353-363.

Carstens, J., & Wefer, G. 1992. Recent distribution of planktonic foraminifera in the Nansen Basin, Arctic Ocean. *Deep-Sea Research*, **39**, S507-S524.

Dale, B. 1983. Dinoflagellate resting cysts: „benthic plankton". *In:* Fryxell, G.A. (ed.) *Survival strategies of the algae*, 69-136, Cambridge University Press, Cambridge.

Dale, B. 1985. Dinoflagellate cyst analysis of Upper Quaternary sediments in core GIK 15530-4 from the Skagerrak. *Norsk Geologisk Tidsskrift*, **65**, 97-102.

Dale, B. 1986. Life cycle strategies of oceanic dinoflagellates. *Unesco technical papers in marine science*, **49**, 65-72.

Dale, B. 1988. Low salinity dinoflagellate cyst assemblages from Recent sediments of the Baltic region. 7th International Palynological Conference, University Queensland, Brisbane, Abstracts, 33.

Dale, A.L. & Dale, B. 1992. Dinoflagellate contributions to the sediment flux of the Nordic Seas. *In:* Honjo, S. (ed.) *Dinoflagellate Contributions to the Deep Sea*, Ocean Biocoenosis Series, **5**, 45-75.

Dale, B. & Fjellså, A. 1994. Dinoflagellate cysts as paleoproductivity indicators: state of the art, potential, and limits. *In:* Zahn, R., Pedersen, T.F., Kaminski, M.A. & Labeyrie, L. (eds.) *Carbon Cyling in the Glacial Oceans, Constraints on the Ocean's Role in Global Change*, NATO ASI Series I, **117**, 521-537, Springer Verlag, Berlin, Heidelberg, New York.

Dansgaard, W., Johnsen, S.J., Clausen, H.B., Dahl-Jensen, D., Gundestrup, N.S., Hammer, C.U., Hvidberg, C.S., Steffensen, J.P., Sveinbjörnsdottir, A.E., Jouzel, J. & Bond, G., 1993. Evidence for general instability of past climate from a 250-kyr ice-core record. *Nature*, **364**, 218-220.

de Vernal, A., Goyette, C. & Rodrigues, C.G. 1989. Contribution palynostratigraphique (dinokystes, pollen et spores) à la connaissance de la mer de Champlain: coupe de Saint-Césaire, Québec. *Canadian Journal of Earth Sciences*, **26 (12)**, 2450-2464.

de Vernal, A., Turon, J.-L. & Guiot, J. 1994. Dinoflagellate cyst distribution in high-latitude marine environments and quantitative reconstruction of sea-surface salinity, temperature, and seasonality. *Canadian Journal of Earth Sciences*, **31**, 48-62.

Dickson, R.R., Meincke, J., Malmberg, S.-A. & Lee, A.J. 1988. The "Great Salinity Anomaly" in the northern North Atlantic 1968-1982. *Progress in Oceanography*, **20**, 103-151.

Dodge, J.D. 1994. Biogeography of marine armoured dinoflagellates and dinocysts in the NE Atlantic and North Sea. *Review of Palaeobotany and Palynology*, **84**, 169-180.

Dowdeswell, J.A., Uenzelmann-Neben, G., Whittington, R.J. & Marienfeld, P. 1994. The late Quaternary sedimentary record in Scoresby Sund, East Greenland. *Boreas*, **23**, 294-310.

Duplessy, J.-C., Labeyrie, L., Arnold, M., Paterne, M., Duprat, J., & van Weering, Tj. C. E. 1992a. Changes in surface salinity of the North Atlantic Ocean during the last deglaciation. *Nature*, **358**, 485-487.

Duplessy, J.-C., Labeyrie, L., Juillet-Leclerc, A. & Duprat, J. 1992b. A new method to reconstruct sea surface salinity: Application to the North Atlantic Ocean during the Younger Dryas. Bard, E. & Broecker, W.S. (eds.) *The Last Deglaciation: Absolute and Radiocarbon Chronologies*. NATO ASI Series **I**, **2**, 201-217, Springer Verlag, Berlin, Heidelberg, New York.

Eide, L.K. (1990). Distribution of coccoliths in surface sediments in the Norwegian-Greenland Sea. *Marine Micropaleontology*, **16**, 65-75.

Elverhøi, A., Andersen, E.S., Dokken, T., Hebbeln, D., Spielhagen, R., Svendsen, J.I., Sørflaten, M., Rørnes, A., Hald, M. & Forsberg, C.F. 1995. The growth and decay of the late Weichselian ice sheet in western Svalbard and adjacent areas based on provenance studies of marine sediments. *Quaternary Research*, **44**, 303-316.

Fairbanks, R.G. 1989. A 17,000 year glacio-eustatic sea level record: influence of glacial melting rates on the Younger Dryas event and deep-ocean circulation. *Nature*, **342**, 637-642.

Gard, G., & Backman, J. 1990. Synthesis of Arctic and sub-Arctic coccolith biochronology and history of North Atlantic Drift influx during the last 500.000 years. *In:* Bleil, U. & Thiede, J. (eds.), *Geological History of the Polar Oceans: Arctic versus Antarctic*, 417-436, Kluwer Academic Publishers, Dordrecht.

Haflidason, H., Sejrup, H.P., Kristensen, D.K. & Johnsen, S. 1995. Coupled response of the late glacial climatic shifts of northwest Europe reflected in Greenland ice cores: Evidence from the northern North Sea. *Geology*, **23**, 1059-1062.

Hald, M., Dokken, T., & Hagen, S. 1996. Palaeoceanography on the European arctic margin during the last deglaciation. *In:* Andrews, J.T., Austin, W.E.N., Bergsten, H. & Jennings, A.E. (eds.), *Late Quaternary Palaeoceanography of the North Atlantic Margins*, 275-287, *Geological Society Special Publication*, **111**, The Alden Press, Oxford.

Harland, R. 1982. Recent dinoflagellate cyst assemblages from the southern Barents Sea. *Palynology*, **6**, 9-18.

Harland, R. 1983. Distribution maps of recent dinoflagellate cysts in bottom sediments from the North Atlantic Ocean and adjacent seas. *Palaeontology*, **26**, 321-387.

Harland, R. 1994. Dinoflagellate cysts from the glacial/postglacial transition in the northeast Atlantic Ocean. *Palaeontology*, **37**, 263-283.

Harland, R., & Howe, J.A. 1995. Dinoflagellate cysts and Holocene oceanography of the northeastern Atlantic Ocean. *The Holocene*, **5**, 220-228.

Harland, R., Reid, P.C., Dobell, P. & Norris, G. 1980. Recent and sub-Recent dinoflagellate cysts from the Beaufort Sea, Canadian Arctic. *Grana*, **19**, 211-225.

Harland, R. & Sharp, J. 1986. Elongate *Spiniferites* cysts from North Atlantic bottom sediments. *Palynology*, **10**, 25-34.

Jacobsen, D.M. & Anderson, D.M. 1986. Thecate heterotrophic dinoflagellates: Feeding behaviour and mechanisms. *Journal of Phycology*, **22**, 249-258.

Jansen, E., & Björklund, K. 1985. Surface ocean circulation in the Norwegian Sea, 15,000 BP to present. *Boreas*, **14**, 243-257.

Jansen, E., Sejrup, H.P., Fjæran, T., Hald, M., Holtedahl, H., & Skarbø, O. 1983. Late Weichselian paleoceanography of the southeastern Norwegian Sea. *Norsk Geologisk Tidsskrift*, **63**, 117-146.

Johannessen, O.M. 1986. Brief overview of the physical oceanography. In: Hurdle, B.G. (ed.) *The Nordic Seas*, 103-127, Springer Verlag, Berlin, Heidelberg, New York.

Johnsen, S.J., Clausen, H.B., Dansgaard, W., Fuhrer, K., Gundestrup, N.S., Hammer, C.U., Iversen, P., Jouzel, J., Stauffer, B. & Steffensen, J.P. 1992. Irregular glacial interstadials recorded in a new Greenland ice core. *Nature*, **359**, 311-313.

Jones, G.A. & Keigwin, L.D. 1988. Evidence from Fram Strait (78°N) for early deglaciation. *Nature*, **336**, 56-59.

Koç, N. & Jansen, E. 1994. Response of the high-latitude Northern Hemisphere to orbital climate forcing: Evidence from the Nordic Seas. *Geology*, **22**, 523-526.

Koç Karpuz, N. & Jansen, E. 1992. A high-resolution diatom record of the last deglaciation from the SE Norwegian Sea: Documentation of rapid climate changes. *Paleoceanography*, **7**, 499-520.

Koç, N., Jansen, E. & Haflidason, H. 1993. Paleoceanographic reconstructions of surface ocean conditions in the Greenland, Iceland and Norwegian seas through the last 14ka based on diatoms. *Quaternary Science Reviews*, **12**, 115-140.

Koç, N., Jansen, E., Hald, M., & Labeyrie, L. 1996. Late glacial-Holocene sea-surface temperatures and gradients between the North Atlantic and the Norwegian sea: implications for the Nordic heat pump. *In:* And-

rews, J.T., Austin, W.E.N., Bergsten, H. & Jennings, A.E. (eds.), *Late Quaternary Palaeoceanography of the North Atlantic Margins*, 177-185, *Geological Society Special Publication*, **111**, The Alden Press, Oxford.

Kohly, A. 1994. Aktuopaläontologische Untersuchungen zu Verbreitung und Vertikalfluß von Diatomeen sowie ihre räumliche und zeitliche Entwicklung im Jungquartär des Europäischen Nordmeeres. *Berichte aus dem Sonderforschungsbereich 313*, **49**,1-118.

Lehman, S.J. & Keigwin, L.D. 1992. Sudden changes in North Atlantic circulation during the last deglaciation. *Nature*, **356**, 757-762.

Letzig, T. 1995. Meereistransportiertes lithogenes Feinmaterial in spätquartären Tiefseesedimenten des zentralen östlichen Arktischen Ozeans und der Framstraße. *Berichte zur Polarforschung*, **162**, 1-98.

Loeng, H. 1991. Features of the physical oceanographic conditions of the Barents Sea. *In:* Sakshaug, E., Hopkins, C.C.E. and Øritsland, N.A. (eds.) *Proceedings of the Pro Mare Symposium on Polar Marine Ecology, Trondheim, 12-16 May 1990*, Polar Research, **10**, 5-18.

Mangerud, J., Andersen, S.T., Berglund, B.E. & Donner, J.J. 1974. Quaternary stratigraphy of Norden, a proposal for terminology and classification. *Boreas*, **3**, 109-128.

Mangerud, J. & Berglund, B.E. 1978. The subdivision of the Quaternary of Norden: a discussion. *Boreas*, **7**, 179-181.

Marret, F. 1994. Distribution of dinoflagellate cysts in recent marine sediments from the East Equatorial Atlantic (Gulf of Guinea). *Review of Palaeobotany and Palynology*, **84**, 1-22.

Marret, F., & de Vernal, A. *in press*. Dinoflagellate cyst distribution in surface sediments of the southern Indian Ocean. Marine Micropaleontology.

Matthiessen, J. 1991. Dinoflagellaten-Zysten im Spätquartär des Europäischen Nordmeeres: Palökologie und Paläo-Ozeanographie. *Geomar Report*, **7**, 1-104.

Matthiessen, J. 1995. Distribution patterns of dinoflagellate cysts and other organic-walled microfossils in recent Norwegian-Greenland Sea sediments. *Marine Micropaleontology*, **24**, 307-334.

Matthiessen, J. 1996. Dinoflagellate cyst evidence of Holocene environmental conditions off East Greenland. *Zentralblatt für Geologie und Paläontologie, Teil I*, 271-286.

Middtun, L. 1989. Climatic fluctuations in the Barents sea. *Rapport et Proces-verbaux de Réunion, Conseil permanent international a l'Exploration de la Mer*, **188**, 23-35.

Middtun, L. 1990. Surface temperatures of the Barents Sea. *Polar Research*, **8**, 11-16.

Molina-Cruz, A. 1991. Holocene palaeo-oceanography of the northern Iceland Sea, indicated by radiolaria and sponge spicules. *Journal of Quaternary Science*, **6**, 303-312.

Mudie, P.J. 1992. Circum-Arctic Quaternary and Neogene marine palynofloras: paleoecology and statistical analysis. *In:* Head, M.J. & Wrenn, J.H. (eds.) *Neogene and Quaternary Dinoflagellate Cysts and Acritarchs*, 347-390, Publishers Press, Salt Lake City.

Mudie, P.J. & Short, S.K. 1985. Marine palynology of Baffin Bay. *In:* Andrews, J.T. (ed.) *Quaternary Environments: Eastern Canadian Arctic, Baffin Bay, Western Greenland*, 263-307, Allen & Unwin, Boston.

Nam, S.-I. 1996. Late Quaternary glacial history and paleoceanographic reconstructions along the East Greenland continental margin: Evidence from high-resolution records of stable isotopes and ice-rafted debris. *unpublished PhD thesis, University Bremen*, 251pp.

Nam, S.-I., Stein, R., Grobe, H. & Hubberten, H. 1995. Late Quaternary glacial-interglacial changes in sediment composition at the East Greenland continental margin and their paleoceanographic implications. *Marine Geology*, **122**, 243-262.

Pankow, H. 1990. *Ostsee-Algenflora*, 648pp., Gustav Fischer Verlag, Jena.

Pflaumann, U., Duprat, J., Pujol, C., & Labeyrie, L. 1996. SIMMAX: A modern analog technique to deduce Atlantic sea surface temperatures from planktonic foraminifera in deep-sea sediments. *Paleoceanography*, **11**, 15-35.

Polyak, L., Lehman, S. J., Gataullin, V., & Timothy Jull, A. J. 1995. Two-step deglaciation of the southeastern Barents Sea. *Geology*, **23**, 567-571.

Rochon, A. & de Vernal, A. 1994. Palynomorph distribution in Recent sediments from the Labrador Sea. *Canadian Journal of Earth Sciences*, **31**, 115-127.

Samtleben, C, Baumann, K.-H., & Schröder-Ritzrau, A. 1995a. Distribution, composition and seasonal variation of coccolithophore communities in the northern North Atlantic. in: Flores, J.A. & Sierro, F.J. (eds.), 5th International Nannoplankton Association Conference Proceedings, 219-235.

Samtleben, C., Schäfer, P., Andruleit, H., Baumann, A., Baumann, K.-H., Kohly, A., Matthiessen, J. & Schröder-Ritzrau, A. 1995b. Plankton in the Norwegian-Greenland Sea: from living communities to sediment assemblages - an actualistic approach. *Geologische Rundschau*, **84**, 108-136.

Sarnthein, M., Jansen, E., Weinelt, M., Arnold, M., Duplessy, J.-C., Erlenkeuser, H., Flatøy, A., Johannessen, G., Johannessen, T., Jung, S., Koç, N., Labeyrie, L., Maslin, M., Pflaumann, U. & Schulz, H. 1995. Variations in Atlantic surface ocean paleoceanography, 50°-80°N: A time-slice record of the last 30,000 years. *Paleoceanography*, **10**, 1063-1094.

Schröder-Ritzrau, A. 1995. Aktuopaläontologische Untersuchung zu Verbreitung und Vertikalfluß von Radiolarien sowie ihre räumliche und zeitliche Entwicklung im Europäischen Nordmeer. *Berichte aus dem Sonderforschungsbereich 313*, **52**, 1-99.

Stein, R., Nam, S.-I., Grobe, H., & Hubberten, H. 1996. Late Quaternary glacial history and short-term ice-rafted debris fluctuations along the East Greenland continental margin. *In:* Andrews, J.T., Austin, W.E.N., Bergsten, H. & Jennings, A.E. (eds.), *Late Quaternary Palaeoceanography of the North Atlantic Margins*, 135-151, *Geological Society Special Publication*, **111**, The Alden Press, Oxford.

Stein, R., Nam, S.-I., Schubert, C., Vogt, C., Fütterer, D. & Heinemeier, J. 1994. The last deglaciation event in the eastern central Arctic Ocean. *Science*, **264**, 692-696.

Swift, J.H. 1986. The arctic waters. In: Hurdle, B.G. (ed.) *The Nordic Seas*. 129-153, Springer Verlag, Berlin, Heidelberg, New York.

Taylor, K.C., Lamorey, G.W., Doyle, G.A., Alley, R.B. Grootes, P.M., Mayewski, P.A., White, J.W.C. & Barlow, L.K. 1993. The 'flickering switch' of late Pleistocene climate change. *Nature*, **361**, 432-436.

Veum, T., Jansen, E., Arnold, M., Beyer, I. & Duplessy, J.-C. 1992. Water mass exchange between the North Atlantic and the Norwegian Sea during the past 28,000 years. *Nature*, **356**, 783-785.

Vinje, T.E. 1977. Sea ice conditions in the European sector of the marginal seas of the Arctic, 1966-1975. *Norsk Polarinstitutt Årbok*, **1975**, 163-174.

Vinje, T.E. 1983. Sea ice conditions in 1982. *Norsk Polarinstitutt Årbok*, **1982**, 49-53.

Vinje, T. & Kvambekk, Å.S. 1991. Barents Sea drift ice

characteristics. *In:* Sakshaug, E., Hopkins, C.C.E. and Øritsland, N.A. (eds.) *Proceedings of the Pro Mare Symposium on Polar Marine Ecology, Trondheim, 12-16 May 1990,* Polar Research **10**, 59-68.

Wall, D., Dale, B., Lohmann, G.P. & Smith, W.K. 1977. The environmental and climatic distribution of dinoflagellate cysts in modern marine sediments from regions in the North and South Atlantic Oceans and adjacent seas. *Marine Micropaleontology*, **2,** 121-200.

Zonneveld, K. 1996. Palaeoclimatic and palaeo-ecologic changes in the Eastern Mediterranean and Arabian Sea regions during the last deglaciation: a palynological approach to land-sea correlation. *Laboratory of Palaeobotony and Palynology, Contribution Series*, **3**, 1-199.

High-resolution benthic foraminiferal records of the last glacial termination in the northern North Atlantic

STEFAN NEES

GEOMAR - Research Center for Marine Geosciences, Wischhofstraße 1-3, D-24148 Kiel, Germany

ABSTRACT

Large oceanic changes occurred during the last transition from glacial to interglacial conditions (Termination I), which significantly affected pelagic and benthic environments. This study presents results of a quantitative investigation of benthic foraminifera at four sites distributed along a north-south transect across the northern North Atlantic with a high temporal resolution (± 200 years).

Benthic foraminifera are examined in samples (1-2 cm sampling intervals) from four long sediment cores located in the southern Fram Strait, the Greenland-Iceland-Norwegian Sea (GIN Sea), and the Rockall Plateau. The most prominent species of benthic foraminifera include *Oridorsalis umbonatus*, *Cibicidoides wuellerstorfi*, *Cassidulina* spp. group, *Pyrgo rotalaria*, *Globocassidulina subglobosa* and tubes of agglutinated taxa.

In each core, the climatic amelioration at Termination I is recorded to have occurred in two steps. A first INDAR maximum (**IND**ividuals **A**ccumulation **R**ate = ind/cm^2 ky; GIN Sea: average 3,000-6,000 ind/cm^2 ky, Rockall Plateau: average 150 ind/cm^2 ky) is followed by a period of lower values. A second maximum reveals slightly lower values than the older maximum. Interglacial INDAR values average 700 ind/cm^2 ky for the GIN Sea and 200 ind/cm^2 ky on the Rockall Plateau. This is roughly twice that of typical glacial values.

Meltwater events, identified by stable isotope data and sea-surface temperature reconstructions based on planktic foraminiferal transfer functions, are marked by an increase in endobenthic and opportunistic species. A decrease of reconstructed sea-surface temperatures appears synchronous with the relative INDAR minimum that occurs between the two INDAR maxima. The results indicate a close coupling of sea-surface processes to the benthic realm („pelagic-benthic coupling") with a longitudinally variable strength. The climate signal at the Rockall Plateau revealed by the fossil benthic foraminifera shows a lower amplitude than that of the GIN Sea. The second, younger INDAR maximum is characterized by an increased abundance of epibenthic species at all core locations, suggesting extended lateral bottom currents.

In comparison with various palaeo-climatological data sets, the variability of fossil benthic foraminiferal abundances in the GIN Sea show a distinct coherence with changes of atmospheric temperatures, sea-surface temperatures and the postglacial sea level rise. The variability of the benthic foraminiferal fauna is principally in phase with climate change events.

INTRODUCTION

Glacial terminations

The transitions from glacials to interglacials in the youngest part of the earth's history are major events in the development of the biosphere. With increasing geographical latitude, these „Terminations" forced massive and rapid reorganisations of the entire ecological system both on land and in the oceans. With respect to a geological timescale, climate changes happened in remarkably short periods of time, inducing a highly dynamic environmental impact (Jouzel *et al.*, 1987; Taylor *et al.*,

In: Hass, H.C. & Kaminski, M.A. (eds.) 1997. Contributions to the Micropaleontology and Paleoceanography of the Northern North Atlantic. *Grzybowski Foundation Special Publication*, no. **5**, pp. 167-197

1993; Alley *et al.*, 1996). These changes are recorded in environmentally sensitive tracers such as fossil benthic foraminiferal tests. Thus, the investigation of these fossils helps us understand the complex interactions between the atmosphere and the oceans.

Previous studies have shown that glacial-interglacial transitions are not continuous processes, but take place in several steps. The termination of the last glacial has been separated into Termination IA, IB (Duplessy *et al.*, 1981; Broecker *et al.*, 1988), and IC (Mix & Ruddiman, 1985). Terminations IA and IB are documented in most deep-sea $\delta^{18}O$ records (Berger *et al.*, 1987; Sarnthein & Tiedemann, 1990; Jansen & Veum, 1990; Winn *et al.*, 1991). However, the exact timing of these two steps still remains uncertain on a global scale and in high latitudes in particular (Ruddiman & Duplessy, 1985).

The Greenland-Iceland-Norwegian Sea (GIN Sea) is of major importance for the global oceanic circulation system (Figs. 1, 3). Surface water masses of Atlantic and Polar origin meet in this comparably small ocean basin and create one of the most important sources of oceanic deep water (Smethie *et al.*, 1986). The GIN Sea is, thus, an ideal region for studying past changes in the deep ocean (Thiede *et al.*, 1986) and the changes occurring during the last glacial/interglacial transition (Thiede *et al.*, 1985; Henrich, 1992).

Since 1985, the Special Research Project 313 („Sonderforschungsbereich 313" at Kiel University) has been involved in marine research of the northern North Atlantic. In collaboration with the micropalaeontology group at the Department of Geology, Kiel University, a substantial data set has been compiled for reconstructions of past climate changes. In particular the importance of Pleistocene fossil benthic and planktic foraminifera has been demonstrated in a variety of publications (Altenbach *et al.*, 1987; Hald & Vorren, 1987; Mackensen, 1987; Haake & Pflaumann, 1989; Linke, 1989; Nees, 1989; Heeger, 1990; Thies, 1991; Bauch, 1992; Struck, 1992; Altenbach, 1992; Nees & Struck, 1994; Struck, 1995; Bauch, 1996; Struck, *this volume*).

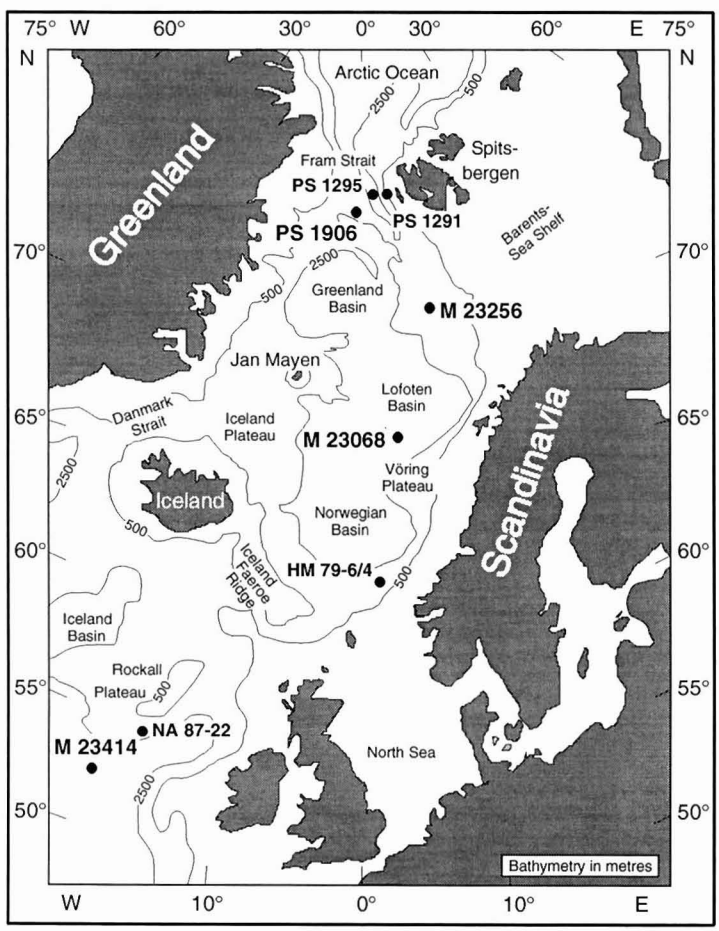


Figure 1. Physiography of the northeastern Atlantic Ocean and the Greenland-Iceland-Norwegian Sea (GIN Sea). This part of the ocean holds a key position in terms of deep-water exchange between the Arctic and the Atlantic Ocean. The core locations are marked with dots.

The precision of the climatic signal in benthic foraminiferal records

Accumulation rates of benthic foraminifera from deep-sea sediment cores reflect the oceanographic variability in the past (Mackensen, 1987). Although specific environmental preferences of benthic foraminifera are largely unknown (Murray, 1995; Jorissen *et al.*, 1995), they appear to be powerful tools for palaeoceanographic reconstructions (Altenbach, 1992; Fig. 2). Only recently the quantification of organic palaeo-flux rates has been realised using benthic foraminifera (Herguera & Berger, 1991; Herguera, 1992). Actuopalaeontological experiments with observations of living benthic foraminifera are also relatively new (Altenbach, 1985; Lutze & Altenbach, 1988; Altenbach *et al.*, 1993).

The use of a climatic signal preserved in fossil remains with a high temporal resolution is also relatively new. Past investigations in the GIN Sea are mainly descriptive and/or stratigraphic in character (Johnson, 1980; Haake & Pflaumann, 1989; Nees, 1989 and 1994). In this region, Struck

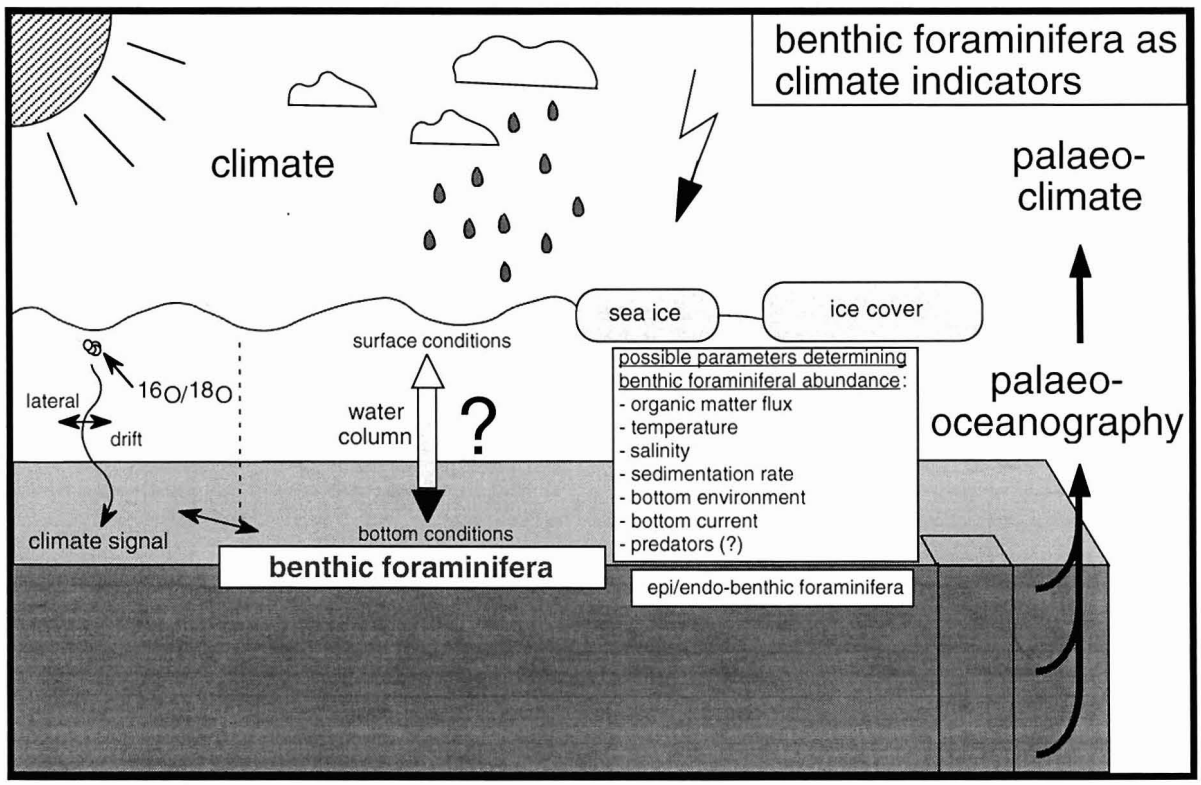


Figure 2. Accummulation rates of benthic foraminiferal assemblages and single species are useful indicators of past environmental changes. This figure illustrates the theoretical path of recording the „environmental signal" (as a secondary climatic signal), its preservation in the ocean sediment and its use as a tool for palaeoclimate reconstructions. With respect to their deep-sea environment, benthic foraminifera rarely receive a climatic-influenced signal as a primary signal, rather as secondary signals such as changes in organic fluxes (food) or changes in physio-chemical parameters of deep- and bottom water masses. Nevertheless, benthic foraminiferal abundances, together with proxies like stable isotope ratios in both planktic and benthic foraminiferal shells, preserve environmental conditions in a manner that allows palaeoclimatic and -oceanographic reconstructions.

(1992) has presented the hitherto most extensive data set of benthic foraminiferal taphocoenoses for the past 600 ky. This allowed him to detect a gradual recolonisation of the Norwegian Sea after the last and the penultimate glacial (Struck, 1995).

A striking feature that is clearly visible in almost all the quantitative benthic foraminiferal distributions is the distinct signal that occurs during dramatic climatic changes, such as glacial terminations (Struck, 1992). The large sampling intervals usually used, however, do not display such important events in greater detail. Stable oxygen isotope investigations have shown that high resolution sampling may reveal significant fluctuations in the climate signal (Weinelt, 1993).

These results give rise to the following questions:

- Does high resolution sampling of deep-sea sediment cores display the variability of benthic foraminiferal assemblages in greater detail, helping to increase the climatic information content of quantitative and qualitative data and subsequently allowing a more precise interpretation of the past variability of changes?
- What is the response of the benthic foraminiferal community to short termed events such as glacial/interglacial terminations?
- Do sea-surface events have an effect on the benthic foraminiferal community? What are the differences of the climatic signal in the benthic foraminifera in the GIN Sea compared to the Rockall Plateau?
- Is a correlation between the climatic signal of fossil benthic foraminifera and other climatic parameters possible?

In order to answer these questions, selected sediment cores from the northern North Atlantic are investigated in this study (Fig. 1). Characteristics of some indicative species, species assemblages, and their temporal variability is discussed. The relatively high temporal resolution of the samples (about 200 years) permits correlation with

other climate relevant data sets, and allows new insight into the palaeoclimatic „reconstruction potential" of fossil benthic foraminifera.

Oceanography of the northern North Atlantic

The northern North Atlantic plays a crucial role in the global ocean circulation as link between the Arctic and Atlantic Oceans. The surface circulation is characterized by warm Atlantic water masses intruding from the south along the Norwegian coast and cold Arctic water masses moving south east off the Greenland coast (Fig. 3). As a continuation of the Gulf Stream, the North Atlantic Current carries temperate and highly saline water masses over the Iceland-Faeroe Ridge into the eastern GIN Sea and forms the Atlantic Domain (Swift, 1986). The North Atlantic Current continues as the Norwegian Current to the Arctic Ocean. North of the Scandinavian landmass, a branch of the Norwegian Current diverges into the Barents Sea as the North Cape Current, and eventually produces deep water by cascading into the Arctic Ocean (Jones *et al.*, 1995).

The Transpolar Drift transports low salinity cold water masses from the Arctic Ocean as the East Greenland Current into the Greenland Sea to form the Polar Domain (Fig. 3). These water masses reach the North Atlantic via the Denmark Strait between Iceland and Greenland. The central part of the GIN Sea is characterised by two systems of mixing primary watermasses, and is named the Arctic Domain. The Arctic Front separates the Arctic from the Atlantic Domains, the Polar Front separates the Polar from the Arctic Domains (Fig. 3).

Surface waters in the Arctic Domain (Fig. 3) are cooled in winter by cold, easterly winds. Due to increased density, these waters sink, thus forming deep water. Together with sinking bottom water masses originating from the Barents Sea shelf (Midttun, 1985; Blindheim, 1989), these two major GIN Sea water masses form the Norwegian Sea Deep Water (NSDW) in the Norwegian Basin and the Lofoten Basin area, as well as the Greenland Sea Deep Water (GSDW) in the Greenland Basin area (Fig. 1). The GSDW is further fueled by highly saline cold Arctic Ocean Deep Water (AODW; Aagaard *et al.*, 1991; Rudels & Quadfasel, 1991) through the western parts of the Fram Strait. After convective mixing (Smethie *et al.*, 1986; Clarke *et al.*, 1990), it contributes to the Norwegian Sea Deep Water (NSDW; Swift & Koltermann, 1988). The NSDW is discussed as a possible source of deep water in the Arctic Ocean through the eastern Fram Strait (Jones *et al.*, 1995).

After approximately 30 years of turnover time [Smethie *et al.*, (1986); Heinze *et al.*, (1990) propose a maximum of 13 to 16 years] this oxygen-rich bottom water mass streams together with intermediate water masses as „overflow water" over the ridges that border the GIN Sea in the south (the Iceland-Faeroe Ridge and the

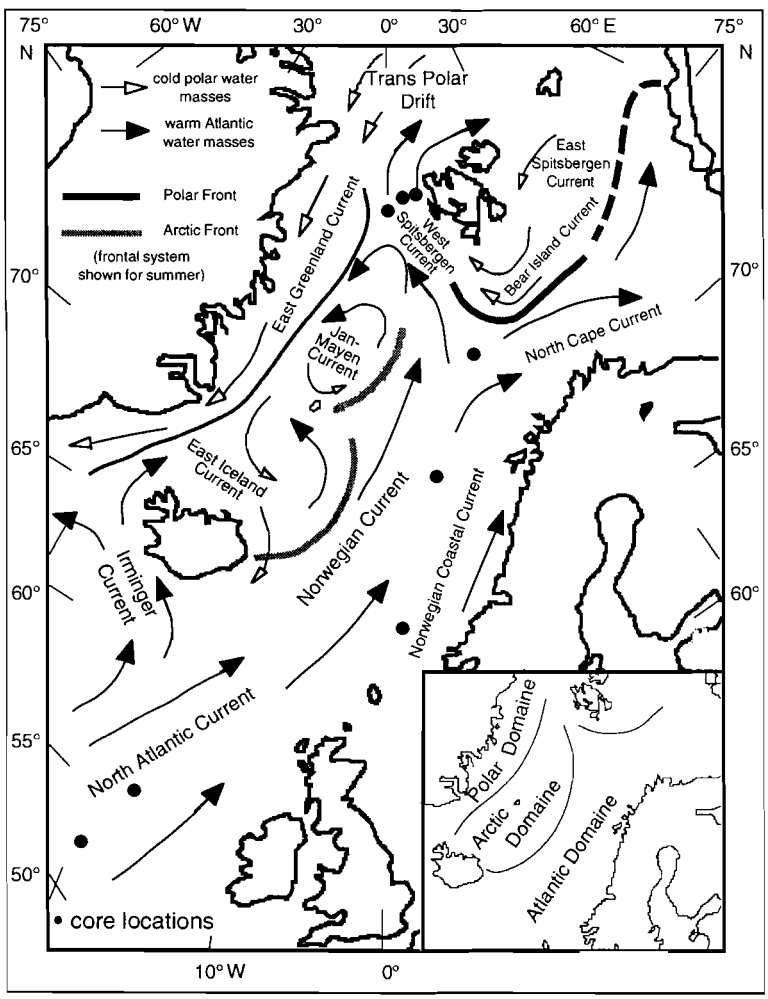


Figure 3. The modern surface circulation pattern of the northern North Atlantic (after Swift, 1986; Koltermann, 1987); core locations are marked with dots (labels see Fig. 1). The oceanographic frontal system in its summer situation (oceanographic domaines after Swift, 1986) is shown in the insert map.

Denmark Strait; Dickson *et al.*, 1990). Together with parts of the Mediterranean Outflow, these waters create the North Atlantic Deep Water (NADW) which ventilates, to a large extent, the world ocean (Broecker, 1987 and 1991).

MATERIAL AND METHODS

Core locations and core data are summarized in Table 1. The sediment cores were sampled either on board the research vessels or from archive material stored at the Department of Geology at Kiel University or the GEOMAR (Research Center for Marine Geosciences, Kiel). In order to cover Termination I, the cores were sampled from the sediment surface downwards until well into the glacial horizons in slices of 1 or 2 cm thickness and intervals of 1 or 2 cm (ca. 100 ml, see Fig. 4, „sample processing"). Long cores and box cores were linked using stable oxygen isotope stratigraphy. In the appendices and graphs, the arithmetic mean of the actual thickness of the sample slice is used.

The processing of sediment samples followed standard procedures (Fig. 4; Struck, 1992). By carefully washing the sediments, damage to arenaceous specimens was largely prevented (Linke, 1986). All sediment samples are therefore considered to be foraminiferally complete for microscopic analysis.

The benthic foraminifera were counted in two subfractions (125-250 µm and 250-2,000 µm). A minimum of 300 tests was counted to ensure statistical reliability. The width of the sample splitter is 2,000 µm, which limits the maximum size fraction.

The raw counts of benthic foraminiferal tests are related to the entire sample (specimens/sample) and further computed with the sample-specific dry weight data of the total sediment (specimens/dry weight). The resulting data set was further processed using physical property data of the sediment to obtain a quantitative benthic foraminiferal accumulation rate *sensu* van Andel *et al.* (1975) and Ehrmann & Thiede (1985). The results are expressed in INDAR (**IND**ividuals **A**ccumulation **R**ate *sensu* Struck 1992) following equation 1

(1)

$$\mathrm{INDAR}\left[\frac{\text{specimens}}{\mathrm{cm^2 \cdot ky}}\right] = \text{counts}\left[\frac{\text{specimens}}{\text{g (dry sed.)}}\right] \cdot \mathrm{LSR}\left[\frac{\mathrm{cm}}{\mathrm{ky}}\right] \cdot \mathrm{DBD}\left[\frac{\mathrm{g}}{\mathrm{cm^3}}\right]$$

LSR: linear sedimentation rate; DBD: dry bulk density.

(Fig. 5).

Dry bulk density data are provided by the following sources:

Core PS 1906: Kassens (unpublished data);

Core M 23256: Holler & Kassens (1989);

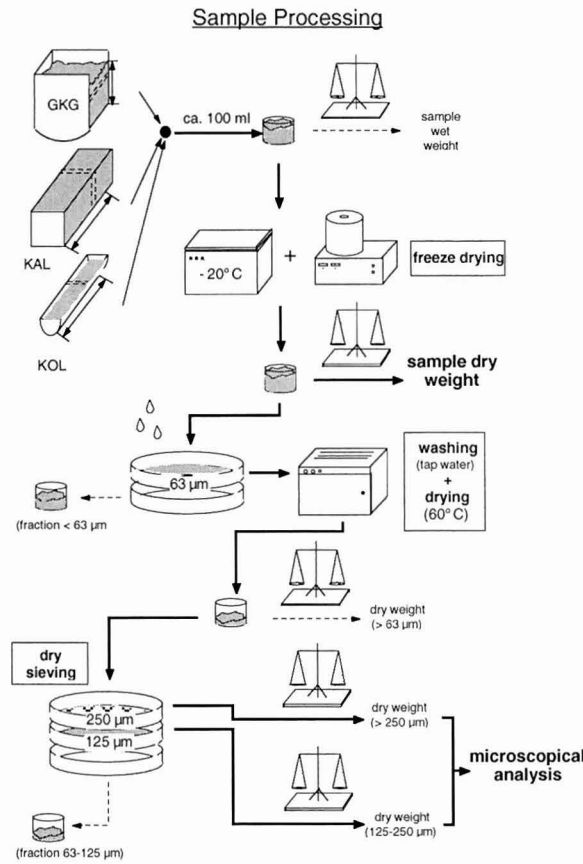


Figure 4. Schematic description of the sample processing technique. The fractionated sediment samples (125 - 250 µm and 250 - 2,000 µm) were analysed using a binocular microscope. Counting results were processed further (see Fig. 5).

Core M 23068: Kassens (1990);

Core M 23414: Jung (1996).

Linear sedimentation rates were calculated according to a newly interpreted stratigraphy. In order to compare all data, the percentages and INDAR are plotted versus age in years BP in all graphs of this paper.

STRATIGRAPHY

A large portion of the sediment core stratigraphy was done by other workers (see Appendix 1) using stable oxygen isotope analyses. However, additional stratigraphic work was necessary in all cores to meet the high-resolution objective of this study covering Termination I. At cores PS 1906, M 23256 and M 23068, additional material [*Neogloboquadrina pachyderma* (sin.)] was sampled for oxygen isotope analyses to cover gaps in the existing isotope records. Sample processing and preparation is described in Vogelsang (1990) and Weinelt (1993). The samples were analysed at the Department of

core number GIK/AWI	gear	core locations longitude	latitude	waterdepth (m)	total recovery (cm)	vessel	expedition	year
PS 1906 - 1	GKG	2° 9.00' W	76° 50.52' N	2,990	37	RV Polarstern	ARK VII/1	1990
PS 1906 - 2	KAL	2° 9.19' W	76° 50.18' N	2,939	652	"	"	"
M 23256 - 1	KOL	10° 56.60' E	73° 10.30' N	2,061	960*	RV Meteor	M 7/2	1988
M 23068 - 2	GKG	1° 30.15' E	67° 49.99' N	2,228	44	RV Meteor	M 2/2	1986
M 23068 - 3	KAL	1° 30.30' E	67° 50.06' N	2,231	760	"	"	"
M 23414 - 6	GKG	20° 17.40' W	53° 32.20' N	2,201	34	RV Meteor	M 17/2	1991
M 23414 - 9	KAL	20° 17.30' W	53° 32.20' N	2,196	908	"	"	"

GIK = Geological-Palaeontological Institute and Museum, University Kiel; GKG = box corer; KAL = Kasten corer; KOL = piston corer
AWI = Alfred-Wegener-Institute, Bremerhaven

Table 1. Station list and core data (M = RV METEOR; PS = RV POLARSTERN; data from: Thiede & Hempel, 1991; Hirschleber *et al.*, 1988; Gerlach *et al.*, 1986; Suess & Altenbach, 1992; * loss of sediment surface during core recovery).

Pure and Applied Nuclear Physics, Kiel University (Dr. H. Erlenkeuser) using a FINNIGAN MAT 251 mass spectrometer. All the collected data were included into an already existing data set (see Appendix 1 for reference and data sources). The oxygen and carbon isotope data for the last 30 ky from the four cores used in this study are displayed in Fig. 6. Interpretation of the extended stratigraphic data sets and new stratigraphic correlations (pers. comm. Sarnthein, Erlenkeuser and Weinelt, 1993) are listed in Appendix 1.

Age determinations between two isotopic events were calculated (interpolation/extrapolation) and their „^{14}C-ages" were converted to calendar years according to Bard *et al.* (1990). The entire data set, including interpretation, for Core M 23414 was taken from Jung (1996). Stable isotope analyses on material from this core was carried out using specimens of *Globigerina bulloides*. To ensure the best possible stratigraphic reliability the $\delta^{18}O$ data sets of all cores were tested by cross-correlation with the SPECMAP data set (Martinson *et al.*, 1987). This test is based on Milankovitch's theory that climatic cycles correlate with periodic cycles of the earths orbital parameters (Imbrie *et al.*, 1984). The analysis revealed good correlation for the 41 ky cycle in all cores. The 19 ky cycle in Core M 23256 and the 23 ky and 19 ky cycle in Core M 23068 correlated poorly; this is possibly due to interpretational problems for isotopic stages 3.1 to 5.3. (pers. comm. Struck, 1993).

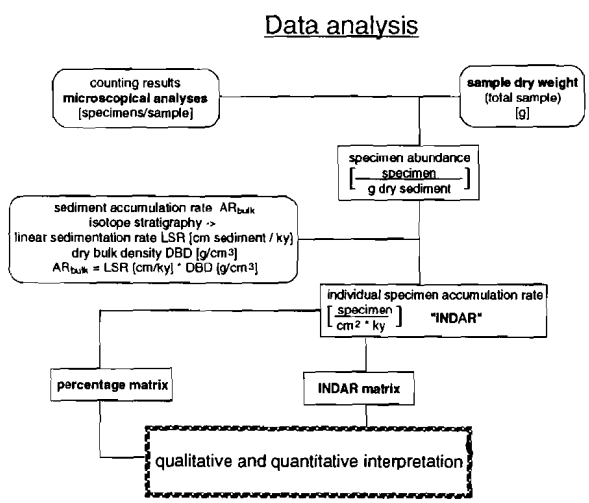


Figure 5: Data processing of the benthic foraminiferal test counts. This procedure, described in detail by Struck (1992), allows a quantitative review of test flux or benthic foraminiferal accumulation rates according to physical sediment and stratigraphic properties.

Based on the stratigraphy presented in Fig. 6 and individual ages calculated for each sample, age/depth graphs were produced and linear sedimentation rates were calculated (Fig. 7).

TAXONOMY

A total of 51 benthic foraminiferal species were taxonomically determined and counted. The most common taxa are listed in Table 2; a complete list of taxa is given in Appendix 2. Additionally, for the practical applications of this study, some species were summarized in four faunal groups on genus level. The taxonomy was controlled by use of micropalaeontological reference slides of the micropalaeontology group of the Department of Geology, Kiel University. Selected species were photographed using a CAMBRIDGE SCAN S2 at the SEM-Unit, The Australian National University, Canberra (Plate 1). The faunal groups include:

The *Cassidulina* sp. group

This group contains the species *C. laevigata* and *C. teretis*. A reliable differentiation of these species is only possible with excellent preservation (Mackensen & Hald, 1988). The description given by Tappan (1951) for *C. teretis* mentions the distinct umbilical plug and specific perforation of the test. These features might not be apparent on fossil specimens. *C. teretis*, described by Belanger & Streeter (1980), is interpreted as *C. laevigata* by Sejrup *et al.* (1981). *C. neoteretis* Seidenkrantz (1995) is believed to be the Recent and Subrecent representative of *C. teretis* and is included in the *Cassidulina* sp. group.

The *Elphidium* sp. group

All taxa belonging to the genus *Elphidium* are lumped together in a single group. They are not further

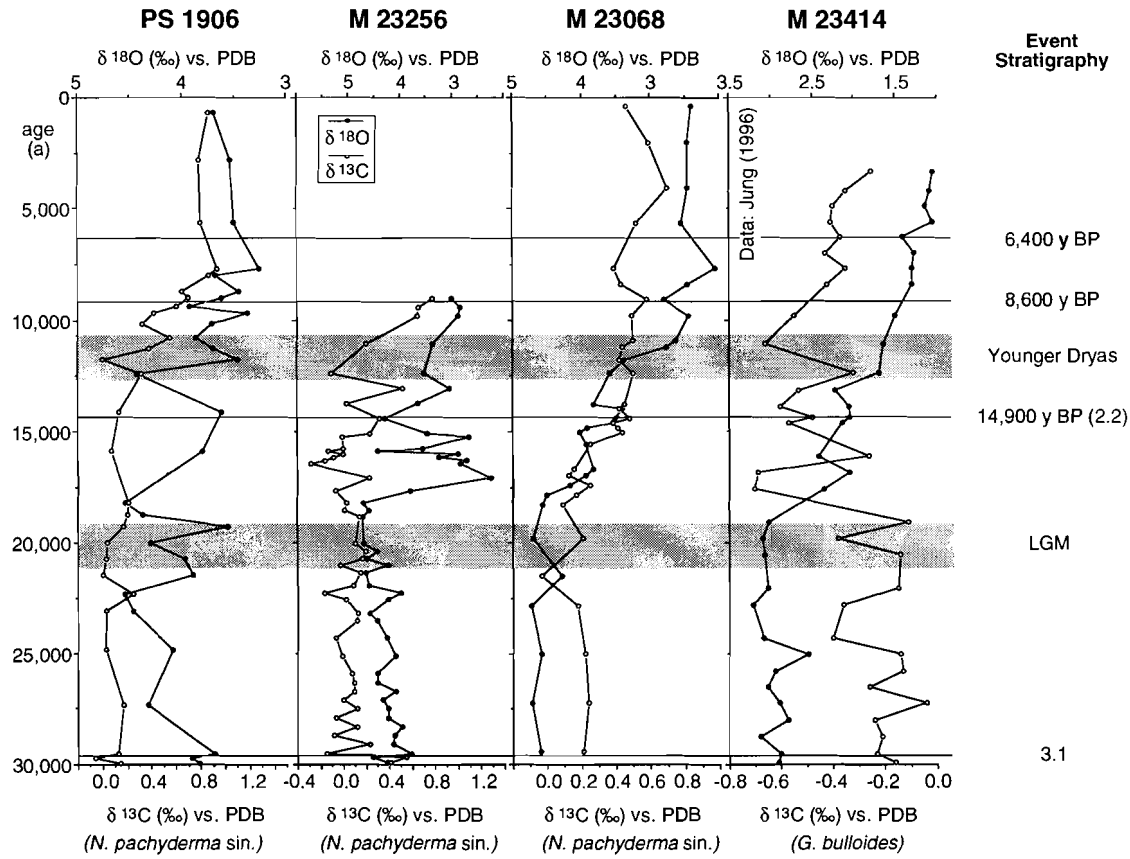


Figure 6. The $\delta^{18}O$ and $\delta^{13}C$ isotopic ratios for the last 30,000 years from cores used in this study. Single stratigraphic events and periods are marked by a stippled pattern or labels. The isotopic ratios were measured on shells of *Neogloboquadrina pachyderma* sin., except core M 23414 where *Globigerina bulloides* was used (includes data from Vogelsang, 1990; Hamich, 1991; Weinelt, 1993; Jung, 1996; see Appendix 1 for data and data sources, LGM = Last Glacial Maximum).

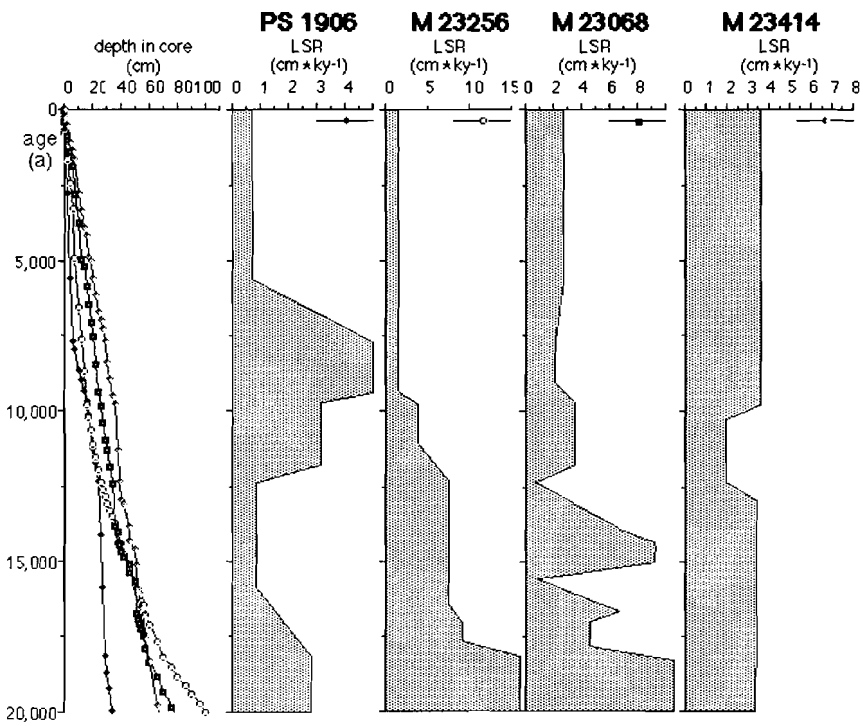


Figure 7. Age/depth control and linear sedimentation rates (LSR) according to the adjusted oxygen isotope stratigraphy. In the glacial section Core M 23256 shows an increased LSR.

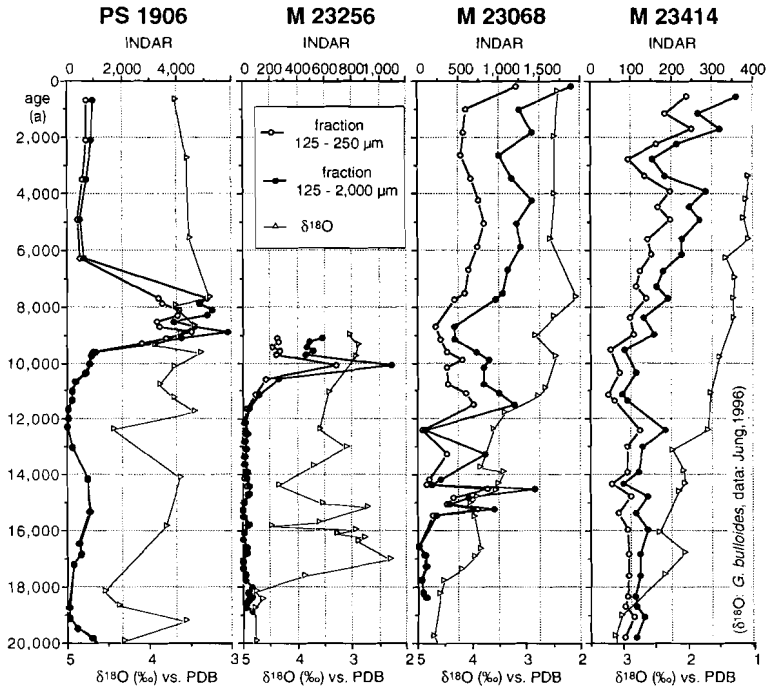


Figure 8. Benthic foraminiferal accumulation rates in the investigated cores of the last 20,000 y (INDAR = individual specimen accumulation rate; specimen * cm^{-2} * ky^{-1}). Filled circles mark the fraction 125 - 2,000 µm, open circles the fraction 125 - 250 µm and triangles the oxygen isotope ratios. The fine fraction dominates the assemblages of all cores. In core M 23414, the relation of the fractions is almost parallel throughout the entire core section.

taxonomically distinguished as they are interpreted as allochthonous faunal elements in deep-sea sediments (eg. Green, 1960; Lagoe, 1979, Murray, 1991).

The *Lagenida* sp. group

The species belonging to the genus *Lagena* appear in great variety but low numbers in the GIN sea (Struck, 1992). In this study, they are not taxonomically distinguished and are grouped together. The tests are usually hyaline and elongated. Spiny extensions and other individual features are often lost on fossil specimens.

The agglutinated tubes group

This group contains entire specimens and fragments of agglutinated tubes that are positively identified as benthic foraminifera. The tests of these species are rarely preserved completely; a taxonomic identification on a species level is mostly impossible. Counts of these fragments are therefore only semiquantitative. According to the extensive work by Thies (1991) using recent material, it is suspected that most of the specimens belong to the genera *Astorhiza* sp., *Rhabdammina* sp., *Saccorhiza* sp. and *Hyperammina* sp.

In general, the preservation of benthic foraminifera in this material is excellent. Corrosional features are rare; they occur only in single samples in glacial sediments and usually affect miliolid tests such as *Pyrgo rotalaria* or round the edges of fragile morphological features such as apertures. Massive carbonate dissolution (see Corliss & Honjo, 1981) is not observed. Textulariid species are usually found to be very well preserved. Possibly favoured by the outline of their tests (bi- and triserial and involute planispiral), these species can withstand the physical stress of sample processing.

RESULTS

Total benthic foraminiferal accumulation rates

In all cores the benthic foraminiferal assemblages are dominated by specimens found in the 125 to 250 µm fraction (Fig. 8). Between 20,000 and 9,600 y BP, the test size in Core PS 1906 shows little variation and is almost entirely dominated by the fraction < 125 µm. After a distinct accumulation minimum at 12,150 y BP (INDAR = 16), a maximum in foraminiferal accumulation occurs at 8,900 y BP with INDAR of 5,863. A younger maximum occurs around 8,000 y BP with INDAR of 5,282, followed by a decrease to INDAR of around 500 in most of the younger samples. In Core M 23256, benthic foraminifera between 18,820 to 11,100 y BP occur almost entirely in the 125-250 µm fraction. The INDAR range between 70 and 0. The INDAR reach a prominent maximum of 1,090 at 10,060 y BP. The total INDAR values for the youngest samples decrease to an average level of around 500 to 600. Due to loss of surface sediment during core recovery, samples younger than approximately 8,500 y BP are not available.

The abundance pattern of benthic foraminifera in Core M 23256 is repeated in Core M 23068. The INDAR in the samples prior to 15,550 y BP vary between 0 and 246. A distinct double maximum

occurs around 15,000 y BP, with maximum values of 1,400 INDAR at 14,500 y BP. From approximately 12,000 y BP to Present the samples show little variation in foraminiferal abundance, although the values increase up to 1,800 INDAR. A slight minimum occurs at about 9,000 y BP. Core M 23414 shows very little variation in its INDAR and the proportion between the two counted fractions. The INDAR increase continuously from 113 to 360 INDAR between 20,000 y BP and Present.

Individual species accumulation rates

The abundances of the most important benthic foraminiferal species (Tab. 2) are displayed for each core together with the individual percentage of the entire benthic foraminiferal assemblage (Figs. 8-12). The percentage data often reach very high values, particularly in the glacial samples. This is related to low INDAR and to low species numbers in these samples. In all cores, the individual species abundances vary , but show a pattern which can be related to glacial, interglacial and transitional environments.

In Core PS 1906 the INDAR show three ranges with maxima between 20,000 y BP and Recent (Fig. 9). The *Cassidulina* sp. group and *O. umbonatus* have maximum abundances of 220 and 610 INDAR between 19,000 and 20,000 y BP. At 16,800 y BP, *T. trihedra* shows a minor maximum that is accompanied by high percentages of this species. A further maximum range is dominated again by the *Cassidulina* sp. group and *O. umbonatus* with INDAR of 153 and 512, respectively, between 13,000 and 16,000 y BP. From 11,000 y BP onwards, the INDAR of almost any other species start to increase and

Table 2. Alphabetical listing of the most important species of benthic foraminifera found in the investigated sections of the sediment cores.

agglutinated group	*Globocassidulina subglobosa*
Bulimina marginata	*Cassidulina* sp. group
Cassidulina reniforme	*Elphidium* sp. group
Cibicides lobatulus	*Lagenida* sp. group
Cibicidoides wuellerstorfi	*Melonis barleeanum*
Cribrostomoides subglobosum	*Oridorsalis umbonatus*
Epistominella exigua	*Pyrgo rotalaria*
Eponides tumidulus	*Triloculina trihedra*

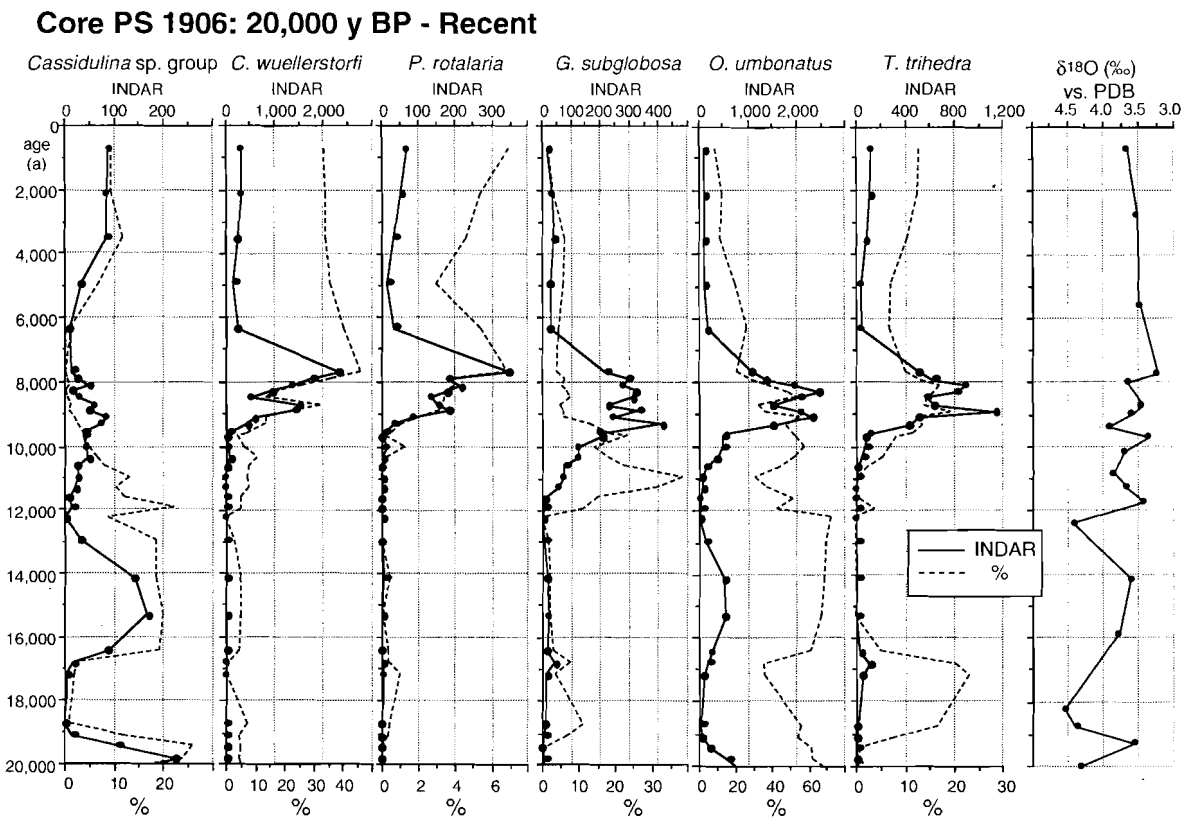


Figure 9. Abundance data of the most common benthic foraminifera in Core PS 1906 from 20,000 y BP to Recent (dashed line = percentages, solid line = INDAR). All species, except the *Cassidulina* sp. group, show a prominent maximum between 9,000 and 8,000 y BP. However, distinct maxima do not appear synchronously. *C. wuellerstorfi* and *P. rotalaria* reach maxima slightly later than the other species.

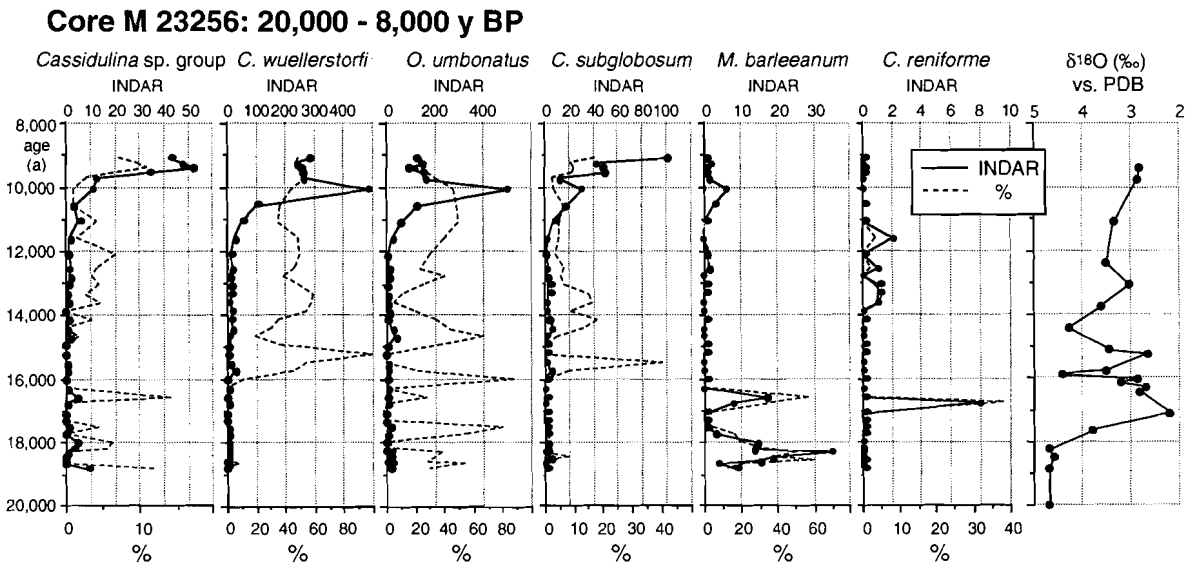


Figure 10. Benthic foraminiferal abundances of the most common species in Core M 23256 (dashed line = percentages, solid line = INDAR). The top sediment layers of this core were lost during core recovery.

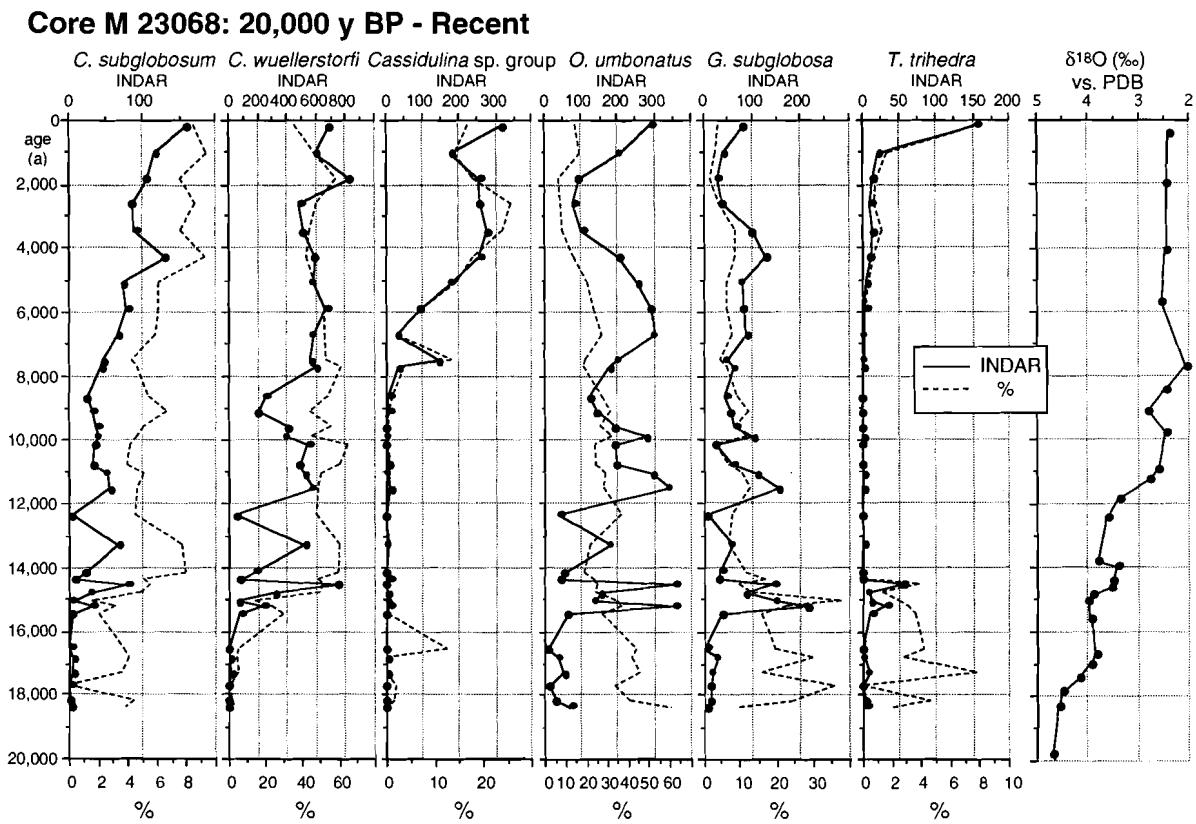


Figure 11. Benthic foraminiferal abundances of the most common species in Core M 23068 (dashed line = percentages, solid line = INDAR).

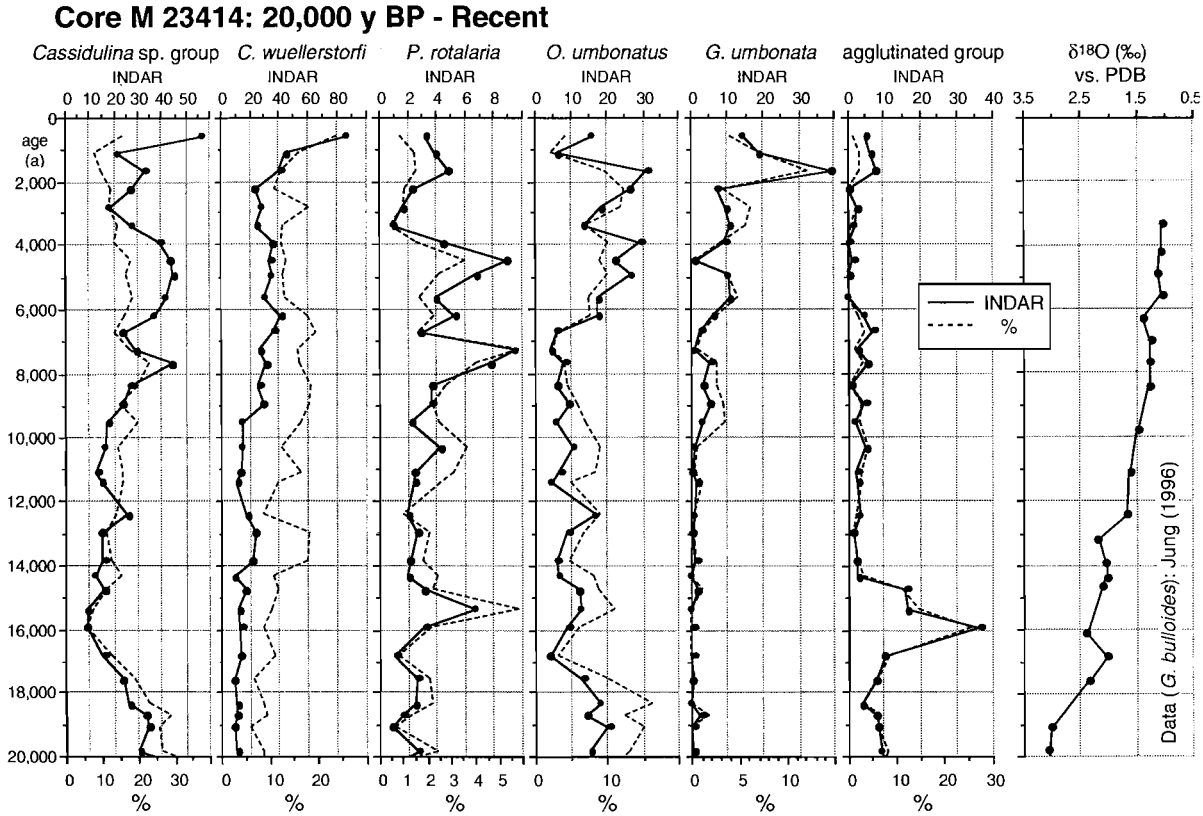


Figure 12. Benthic foraminiferal abundances of the most common species in Core M 23414 (dashed line = percentages, solid line = INDAR).

create a suite of abundance maxima up to ca. 7,000 y BP. *C. wuellerstorfi* and *O. umbonatus* show the highest INDAR with 2,398 and 2,443, respectively. At 7,720 y BP *C. wuellerstorfi* and *P. rotalaria* form a prominent peak. This maximum appears to be the youngest of the suite of high abundance maxima. *T. trihedra, G. subglobosa, O. umbonatus* and the *Cassidulina* sp. group show a maximum abundance shortly before 8,000 y BP. The younger samples reveal low INDAR and little variation in their benthic foraminiferal abundance.

The benthic foraminiferal abundance in Core M 23256 reveals two maxima (Fig. 10). The older maximum range between 19,000 and 16,000 y BP is dominated by *M. barleeanum* and the *Cassidulina* sp. group. These species reach maximum INDAR of 35 and 8, respectively. *Oridorsalis umbonatus* shows high percentages of the total assemblage but very low abundances during this time. A second interval with maximum values occurs between ca. 11,000 and 9,000 y BP, where most of the species reach highest abundances. A very prominent peak at 10,000 y BP shows *C. wuellerstorfi* and *O. umbonatus* with INDAR of 487 and 498. A younger prominent abundance peak at 9,400 y BP shows the INDAR of the *Cassidulina* sp. group (52) and the agglutinated foraminifer *C. subglobosum* (50). Younger sediments of these cores were lost during core recovery.

The benthic foraminiferal abundance in Core M 23068 shows a less distinct pattern than Cores M 23256 and PS 1906 (Fig. 11). The amplitude of INDAR in all species fluctuates less distinctly and most species, except *T. trihedra* and the *Cassidulina* sp. group, are present in all samples. A maximum abundance range occurs between 15,300 and 14,200 y BP. *C. wuellerstorfi* reaches a maximum INDAR of 772, *O. umbonatus* shows 403, *G. subglobosa* 218 and *C. subglobosum* reaches an INDAR of 83. A second maximum abundance range between 12,300 and 8,600 y BP is formed by the same species. Between 8,000 and 4,000 y BP, *O. umbonatus* and *C. wuellerstorfi* occur in slightly increased INDAR. The *Cassidulina* sp. group also occurs in slightly increased INDAR between 5,000 and 2,000 y BP.

The abundances of all species of benthic foraminifera in Core M 23414 show very little variation (Fig. 12). Along the entire investigated core section the INDAR of *O. umbonatus, G. umbonata* and agglutinated tubes only indicate a few ranges with increased values. *O. umbonatus* reveals increased

INDAR between 6,000 and 1,800 y BP with a maxium value of 31. *G. umbonata* shows a distinct INDAR maximum at 1,800 y BP of 39 and the agglutinated tubes occur in increased abundances between 18,000 and 14,000 y BP at a maximum value of 36.

DISCUSSION

The dynamic development of benthic foraminifera during a glacial/interglacial transition

High-resolution records of benthic foraminiferal abundances covering the last glacial termination indicate that the transition from glacial to interglacial conditions occurred in two steps. Bulk benthic foraminiferal accumulation rates in the 125-2,000 µm fraction reveal low values and little variations in glacial samples from all of the cores. Meltwater events or other regional phenomena, such as seasonal sea ice-free sea surfaces or temporary bottom currents, may be responsible for short-term INDAR peaks.

Benthic foraminiferal accumulation rates start to increase during the early termination of the last glacial between 12,500 y BP (Core M 23414 from the Rockall Plateau) and 9,500 y BP (Core PS 1906 from the southern Fram Strait). Within a period of roughly 1,500 years, the INDAR values of the total benthic foraminiferal fauna reach a distinct first maximum („older INDAR maximum"). This event lasts about 500 to 1,000 years. In Core M 23256 it corresponds with the Termination I B (10,400 to 9,900 y BP) described by Broecker *et al.* (1988). The enormous increase of INDAR with a steep gradient indicates an important turning point in the oceanic environment. *Cibicidoides wuellerstorfi* and *O. umbonatus* are the most common species forming this INDAR maximum. A comparable occurrence event is reported by Koç-Karpuz & Jansen (1992) in Core HM 79-6/4, located in the southeastern GIN Sea (Fig. 1). Reconstructed sea-surface temperatures indicate a decrease of 2° C within a period of at least 300 years between 10,100 and 9,600 y BP. The authors coined the term „Younger Dryas II" for this cold spell. Sea-surface temperature reconstructions by Schulz (1995) reveal similar results. The beginning of the sea-surface temperature decrease coincides chronologically with „meltwater event I B" (Fairbanks, 1989).

After this accumulation rate minimum a second peak in benthic foraminiferal accumulation occurs („younger INDAR maximum"), which is most distinct in Core PS 1906 (9,900-7,800 y BP). This event shows, in general, lower INDAR values than the older maximum, but a similar duration of 1,200 ± 500 years. The characteristic species are *C. wuellerstorfi*, *P. rotalaria*, *C. subglobosum*, *O. umbonatus* and *T. trihedra* appear in higher accumulation rates. This second, younger, peak indicates the beginning of the interglacial period and the return of the INDAR to a lower level with little variations. However, values remain two to ten times higher than the average glacial INDAR.

Do benthic foraminifera respond to „meltwater events" and changing sea-surface temperatures?

„Meltwater events" are short-term features, usually of limited extent, that can be traced by $\delta^{18}O$ values of planktic foraminiferal tests (Sarnthein *et al.*, 1992). An identification of true meltwater events is only possible with correlation to sea-surface temperature reconstructions (Weinelt, 1993; Schulz, 1995). These should not show a distinct warming of surface waters, as during the transition from a glacial to an interglacial, but the isotope record should have lighter $\delta^{18}O$ values. Reconstructed sea-surface temperatures by Schulz (1995) allowed the identification of such „meltwater events" in Cores M 23256 and M 23068 prior to the actual glacial termination (Figs. 13 a-d). In the southern Fram Strait (near Core PS 1906), a planktic oxygen isotope record from Core PS 1295 (Jones & Keigwin, 1988) is used to identify a possible meltwater event between 17,000 to 14,000 y BP (Fig. 13 a). A similar event occurs in Core PS 1291 (Fig. 1) located in the eastern Fram Strait (pers. comm. Spielhagen, 1996) and is also recognized in the eastern central Arctic Ocean (Stein *et al.*, 1994).

A minor increase of benthic foraminiferal INDAR values in the cores PS 1906, M 23256 and M 23058 reveals excellent temporal correspondence with identified „meltwater events". Periods of light oxygen isotope values correspond to increased accumulation rates of benthic foraminifera. Thus an environmental change with positive effects on the benthic foraminiferal fauna is suggested. The increased INDAR are formed almost entirely by the fraction 125-250 µm and species of the *Cassidulina* sp. group, *O. umbonatus* and agglutinated tubes, which also form the gradual increase of accumulation rates towards the „older maximum". Sparse but continuous occurrences of *O. umbonatus* in glacial material of GIN Sea cores are already described by Haake & Pflaumann (1989). The occurrence of tests of the *Elphidium* sp. group indicates winnowing and input of shelf sediments (Østby & Nagy, 1982).

The oxygen isotope peaks in Core M 23414 occur synchronously with SST maxima and are therefore interpreted as „warming events" rather than meltwater events (Fig. 13 d). This „warming" is evidence for the influence of warmer Atlantic waters (Ruddiman & McIntyre, 1973; Bard *et al.*, 1987), which do not have such a significant influence on the benthic foraminiferal fauna as is docu-

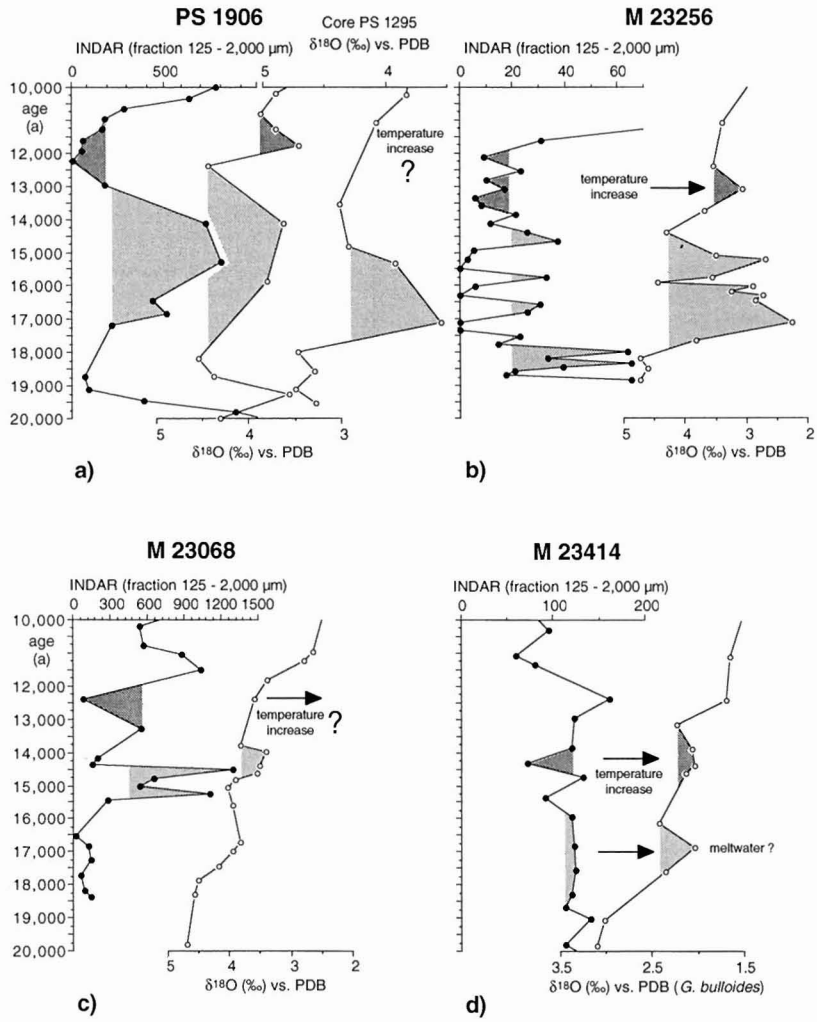


Figure 13 a-d. Accumulation rate maxima of benthic foraminifera occur parallel with shifts of planktic oxygen isotope ratios to lighter values in the period from ca. 17,000 to 14,000 y BP. This temporal coherence indicates a change of environment with positive effects for the abundance of benthic foraminifera (amelioriation of trophic situation?). These shifts are identified as „melt-water events". At all core locations, except Core PS 1906, reconstructed SSTs records do not parallel the oxygen isotope shifts. The oxygen isotope record of Core PS 1295 (Jones & Keigwin, 1988) from the eastern Fram Strait shows the same shape as Core 1906, whereas the younger isotope shift is probably lost due to a large sample spacing. Also, due to a low resolution, the oxygen isotope record in Core M 23068 does not show a younger shift towards lighter values, but an increase of SSTs.

mented at the northern core locations. Core NA 87-22, which is located near M 23414 (Fig. 1), shows parallel increases of salinity (Duplessy *et al.*, 1992) and hence supports this interpretation.

Reconstructed sea-surface temperatures are available for three core locations in this study (Schulz, 1995). These data are correlated with the benthic foraminiferal INDAR and can be related to the lateral influence of the North Atlantic Current and its continuation, the Norwegian Current (Figs. 14 a-c). The SSTs were calculated using the SIMMAX technique (Pflaumann *et al.*, 1996) and show a temporal gradient from south to north through the northern North Atlantic. The first shift to warmer SSTs occured at the Rockall Plateau around 13,400 y BP with 7° C and in the northeastern GIN Sea at 8,600 y BP at 5° C (Schulz, 1995). At the Rockall Plateau location (Core M 23414), the older INDAR maximum occurs synchronously with increased SSTs, whereas in the cores in the eastern GIN Sea (M 23068 and M 23256), INDAR suggest a temperature rise at 10,800 y BP and 10,000 y BP, respectively. Labeyrie *et al.* (1992) postulate that, in this period, the Norwegian Sea was „relatively warm" with salty surface water and cold, ventilated deep water. The later appearance of peaks towards the north is interpreted as indicative of the retreat of glacial ice cover of the GIN Sea (Nees *et al.*, subm.).

Apparently, the abundance of benthic foraminifera is closely related to sea-surface temperature changes. Warmer temperatures are likely to induce an increase of benthic foraminiferal accumulation rates. „Meltwater events" in contrast seem to have a similar effect, but with a considerably lower amplitude. Sediment trap and detailed interdisciplinary studies have already revealed a primary link between the sea surface and the benthic realm, the so-called „benthic-pelagic coupling" (Graf, 1989; Graf *et al.*, 1995). Increased primary production induces, within a period of few days, an increased nutrient flux and sedimentation of phytodetritus. This is detectable in the deep-sea (Graf, 1989; Asper *et al.*, 1992). In particular, some species of filtrating benthic foraminifera are well adapted to respond to pulses of organic matter

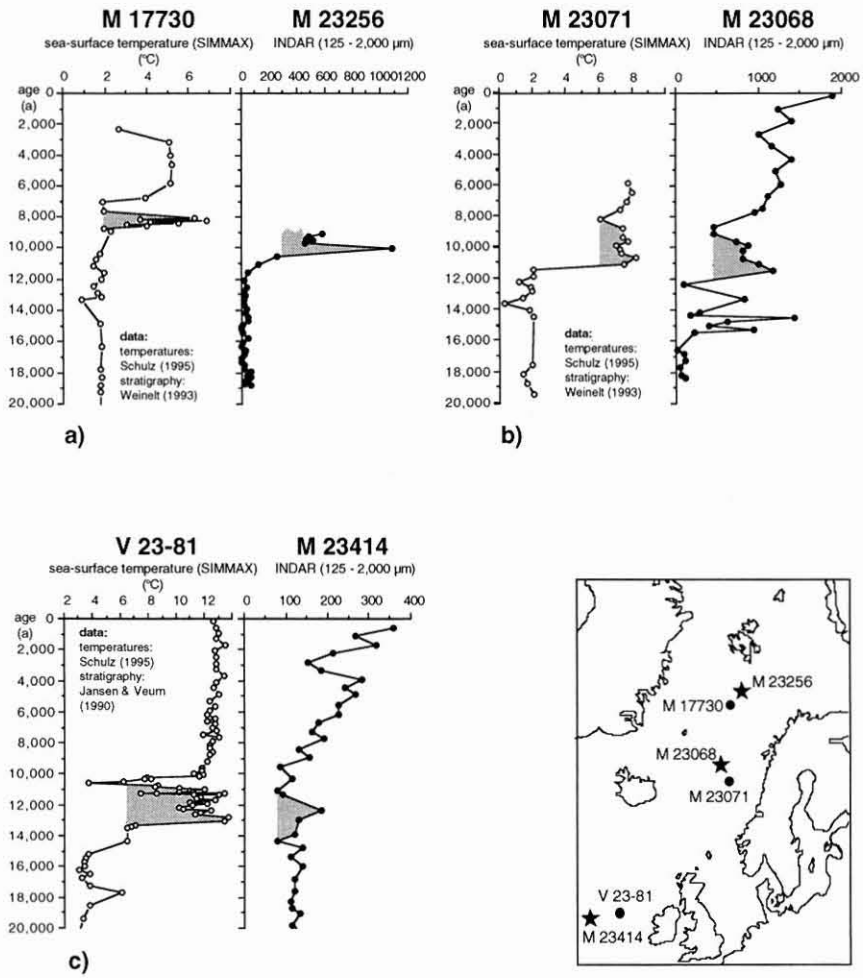


Figure 14 a-c. The benthic foraminiferal accumulation rates can be related to reconstructed sea-surface temperatures. Reconstructed SSTs are available for three core locations in the northern North Atlantic. In all cores, the benthic foraminiferal INDAR show a distinct maximum parallel to a postglacial rise of SSTs. While the INDAR and temperature rise occur synchronously at the Rockall Plateau location (Core M 23414); at the other locations a slight temporal shift occurs. This may be related to inaccuracies in the stratigraphic data of these cores.

input (Gooday, 1988; Gooday & Lambshead, 1989; Smart *et al.*, 1994). The synchronous increase of fossil benthic foraminiferal INDAR with the reconstructed SSTs implies a close link between the sea floor environment and changes of the sea surface.

Palaeoceanographical implications

Accumulation rates of benthic foraminifera clearly reflect oceanic changes in the GIN Sea since the last glacial. Low INDAR with little variation during oxygen isotope Stage 2 indicate a stable benthic environment with little input of organic matter. Kellogg (1980) suggested a year-round sea ice cover for the GIN Sea during the Last Glacial Maximum at 18,000 y BP. Extremely reduced primary production still produced a constant flux of organic matter into the deep-sea (Carey, 1987; Andersen, 1989). In particular, small species appear to respond instantly to minute environmental changes (Fig. 2) and, thus, may indicate variability in the sea ice cover. Short-term input of organic matter synchronous to meltwater events led to increased benthic foraminiferal accumulation rates. These maxima are mainly formed by endobenthic and opportunistic species. There is little sign of lateral advection in the GIN Sea during this period of time. But some occurrences of filtrating species indicate such an event in the eastern GIN Sea. Very low $\delta^{13}C$ values indicate limited exchange between the sea surface and the atmosphere and therefore a closed sea ice cover (Kellogg, 1980; Weinelt, 1993). From 12,400 y BP on Weinelt (1993) suggests the gradual development of an anti-estuarine circulation system with intrusions of warm Atlantic surface waters into the eastern parts of the GIN Sea. This might have created oceanographic conditions which have resulted in increased benthic foraminiferal INDAR. Furthermore the early decomposition of the Barents Sea ice cover by sea level rise (Jones & Keigwin, 1988) might be responsible for the increase of INDAR in the GIN Sea.

Prior to the „older maximum", the INDAR values show a gradual increase. This slow increase lasts up to 1,500 years and can be interpreted as an indicator of increasing flux of organic matter from the sea surface to the sea floor without lateral advection. It is possible that this gradual change results from seasonal advance and retreat of the sea

ice cover during the general retreat at the transition from glacial to interglacial. The first influence of warm Atlantic surface water that started to affect the southeastern GIN Sea (Jansen & Bjørklund, 1985) with the establishment of interglacial conditions might have induced the massive benthic foraminiferal INDAR maximum in all of the sediment cores. The increasing abundance of epibenthic species indicate an onset of deep-sea advection.

The following period of low accumulation rates is characterized by an icreased presence of agglutinated species. The INDAR of *C. wuellerstorfi* decreases in all cores prior to the massive increase leading to the second INDAR maximum. During this peak, epibenthic as well as endobenthic species reach high accumulation rates and therefore indicate ideal living conditions. This may be related to an optimized food supply. Under the gradually increasing influence of Atlantic water masses during the transitional phase, more nutrient-rich waters were transported northwards (Nürnberg, 1991). The abundance of epibenthic species indicate additional lateral advection in the deep-sea (Lutze & Thiel, 1989). The „return" of INDAR to a lower level after the younger maximum can not be related to a specific oceanographic event. Based on results of stable oxygen isotope analyses, the postglacial surface circulation in the GIN Sea seems to be stable since 9,000 y BP (Weinelt, 1993). It can be speculated that, in relation to organic matter flux rates, the trophic situation in the deep-sea has been debased due to variations in the zooplankton community during the early Holocene.

Changing climate at Termination I

The INDAR of 11 sediment cores are combined to a „stack" using data of Nees (1989) and Struck (1992) (Fig. 15). This curve represents the benthic foraminiferal accumulation rate in the eastern GIN Sea under the influence of the North Atlantic Current and Norwegian Current. The interpretation of this record, however, is limited to a transect from the Rockall Plateau through the eastern GIN Sea to the southern Fram Strait.

All parameters displayed in Fig. 15 show stable conditions between 20,000 and 16,000 y BP. Solar insolation increased slowly (Imbrie *et al.*, 1992) and reached a maximum at 11,000 y BP, some 2,500 years ahead of the INDAR maximum. Solar insolation is discussed as one of the most important factors influencing the earth's climate and oceanography (COHMAP, 1988; Crowley & Kim, 1992). The stack of benthic foraminiferal accumulation rates shows low values, slowly increasing, in glacial samples to ca. 10,500 y BP. The first step of a „deglacial warming" occured from 16,000 to ca. 11,000 y BP and is documented as a distinct sea-level rise (Fairbanks, 1989), higher SSTs (Schulz, 1995) and an increase in atmospheric temperatures calculated from Greenland (Mayewski *et al.*, 1993) and Antarctic ice cores (Jouzel *et al.*, 1993). Synchronous occurrence of oceanic and atmospheric changes in the North Atlantic region is documented by correlation of sediment core and ice core data (Haflidason *et al.*, 1995). The first step of transition from the last glacial to the present interglacial apparently had only little effect on the benthic foraminiferal accumulation rates. It is possible that climate-related oceanic changes on the sea surface did not increase productivity so that they affected deep-sea habitats by benthic-pelagic coupling.

A period of stagnancy in this warming trend occurs together with the insolation maximum between 13,000 and 11,000 y BP. This period is paralleled by changes in SSTs, sea level and INDAR of benthic foraminifera. A decrease of the sea level rise can be correlated with a decrease of atmospheric temperatures. This cold episode, the Younger Dryas, is well documented in all parameters, except the benthic foraminiferal INDAR. Apparently the deep-sea environment was affected to a lesser extent. Until this period, the benthic foraminiferal fauna was dominated by detritivore, endobenthic and opportunistic species, indicating stable and relatively calm conditions (Struck, 1995). Presumedly all organic matter that served as a major food source was delivered vertically. Studies on the organic components of the sediment in the eastern GIN Sea indicate an accumulation of very mature, terrigenous organic material during this period (Wagner & Henrich, 1994). This material is of low energetic value, but apparently seems to be favoured by endobenthic or opportunistic benthic foraminiferal species. Possibly a coupled process using the terrigenous input as a transporter of organic material from enhanced primary production has increased the organic matter flux rates and subsequent biological activity on the sea floor.

Between 10,000 and 8,000 y BP, SSTs (Schulz, 1995) and atmospheric temperatures (Jouzel *et al.*, 1993) form maxima. Solar insolation has passed its maximum. The melting of ice caps leads to sea level rise and the influence of the Norwegian Current in the eastern GIN Sea increases as well (Bauch, 1992). These changes seem to have an enormous effect on the benthic foraminiferal accumulation rates. INDAR reach a clear maximum around 8,500 y BP, parallel to the atmospheric temperatures reconstructed from the Vostok Ice Core (Jouzel *et al.*, 1993). The climatic conditions during this period created an evironment on the sea floor that apparently favoured the reproduction of benthic foraminifera. Planktic foraminifera and other zoo- and phytoplankton reach high accumulation rates

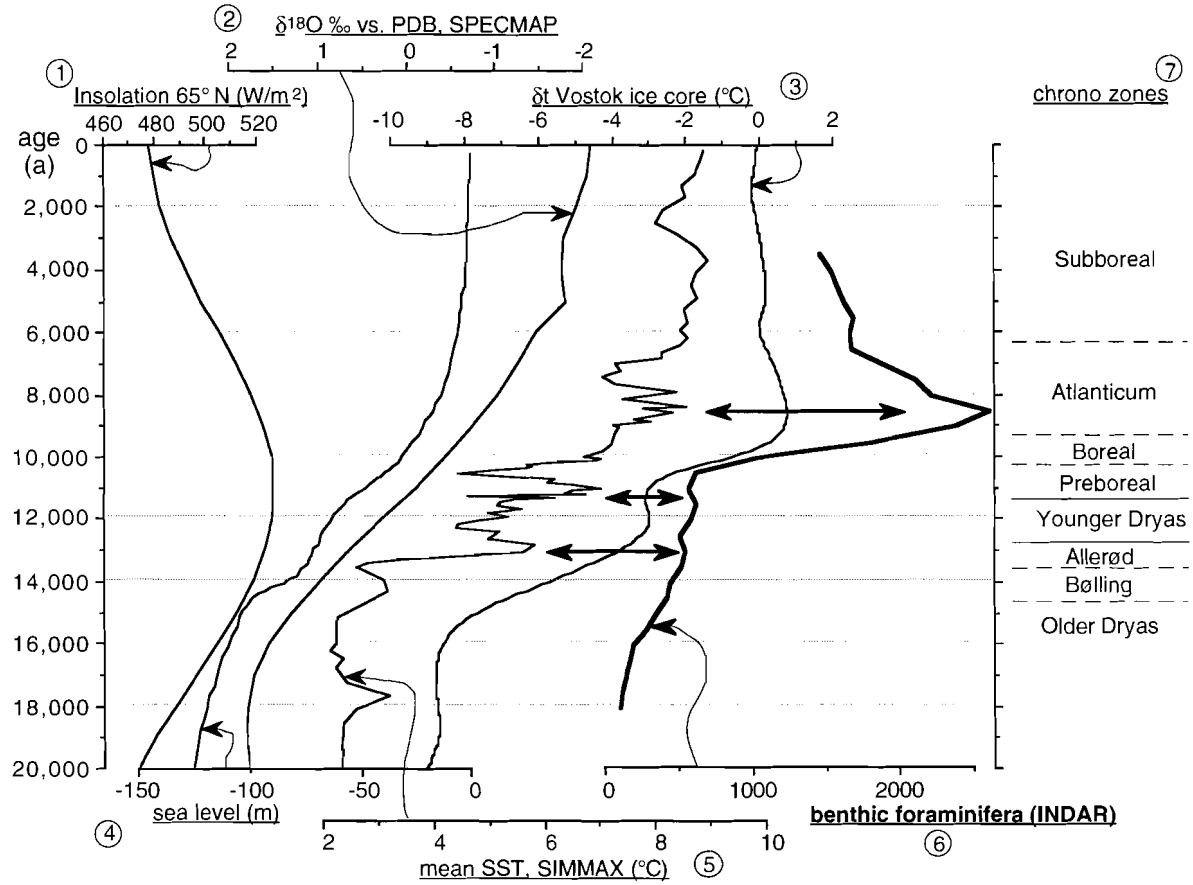


Figure 15. The stack of benthic foraminiferal INDAR of four cores along a transect through the GIN Sea can be correlated to various other regional and global climate records. The resulting maximum around 8,500 y BP occurs in a late phase of the transition from the last glacial to the present interglacial. It correlates well with a global sea level rise, a rise of sea-surface temperatures and a rise of atmospheric temperatures. Older SST warming peaks seem to have had little effect on benthic foraminiferal accumulation rates.

1: Insolation (Imbrie *et al.*, 1992).
2: SPECMAP (Martinson *et al.*, 1987).
3: Vostok Ice Core, temperature difference to the present mean (Jouzel *et al.*, 1993).
4: Sea level changes (Fairbanks, 1989).
5: Sea-surface temperatures (SST); this data set is computed as a stack from three cores located on the Rockall Plateau and the eastern GIN Sea (see Figs. 14 a-c; Schulz, 1995).
6: INDAR of benthic foraminifera, calculated as stack from 11 cores located at the Rockall Plateau and the central and eastern GIN Sea to the southern Fram Strait (data: this study; Nees, 1989; Struck, 1992).
7: Chrono zones (Mangerud *et al.*, 1974; Fairbanks, 1990).

synchronously (Baumann, 1990; Koç-Karpuz & Schrader, 1990; Matthießen, 1991; Bauch, 1992).

The mid-Holocene benthic foraminiferal assemblage is characterised by an increased portion of epibenthic species such as *C. wuellerstorfi*, *O. umbonatus* and *P. rotalaria*. The oceanography of the GIN Sea had changed significantly and shows great similarities with the present situation. Benthic foraminifera indicate greater activity of bottom currents and lateral advection. Despite only small changes in global atmospheric temperatures since 8,000 y BP (Dansgaard, 1987; Jouzel *et al.*, 1993; Johnsen *et al.*, 1992; Kerr, 1993) and insignificant changes in oceanography (Weinelt, 1993) the INDAR of benthic foraminifera decrease after the distinct maximum. An explanation of this maximum could possibly be the quick and optimised consumption of a short-term intensive pulse of organic matter by quickly responding and highly adapted species such as *C. wuellerstorfi*, *M. barleeanum* and *P. rotalaria* (Linke & Lutze, 1993). With the establishment of interglacial conditions, the abundance of benthic foraminifera finally stabilised, exceeding the glacial values of accumulation rates, but remained far below the peak values at Termination I.

CONCLUSIONS

High-resolution investigations of deep-sea benthic foraminifera enable detailed insight of climate-forced palaeoceanographic changes and distinguishes short-term events.

The transition from the last glacial to the present interglacial is documented in benthic foraminiferal accumulation rates as a noncontinuous signal. Glacials are characterized by low benthic foraminiferal accumulation rates. During the transitional phase, the values show two maxima with extremly high values. The present interglacial is characterized by higher accumulation rates than the glacial. However, they remain well below the peak values of the transitional phase.

Benthic foraminiferal accumulation rates reveal an excellent correlation with reconstructed SSTs. Meltwater events are synchronous with increased accumulation rates of endobenthic and opportunistic species of benthic foraminifera. This indicates the direct coupling of sea-surface processes with the deep-sea environment, which is more distinct in the GIN Sea than at the Rockall Plateau.

The correlation of benthic foraminiferal accumulation rates with other climate proxies yields a high temporal coherence with climate changes. The response in the deep sea seems on average to lag atmospheric changes.

ACKNOWLEDGEMENTS

The author gratefully acknowledges support, comments and discussion during this study by J. Thiede and A. Altenbach. Comments and critics in the very careful review of M.-S. Seidenkrantz and one anonymous referee are greatly appreciated and helped to improve the quality of the manuscript. Great cooperativeness and help during this study was provided by colleagues of the SFB 313 and GEOMAR in Kiel. Special thanks go to former and present members of the GEOMAR-Bungalow for the good spirits and a very special, happy-people research environment. H. Kassens (GEOMAR) kindly made unpublished dry-bulk-density data for Core PS 1906 available. Masters and crews of the research vessels *PVFS Polarstern* and *FS Meteor* were always helpful and supportive. Financial support for this study was provided by the Deutsche Forschungsgemeinschaft through the Sonderforschungsbereich 313 „Global Environmental Changes: The Northern North Atlantic". This is contribution No. 324 of the Sonderforschungsbereich 313.

REFERENCES

Aagaard, K., Fahrbach, E., Meincke, J. & Swift, J.H. 1991. Saline outflow from the Arctic Ocean: its contribution to the Deep Waters of the Greenland, Norwegian, and Iceland Seas. *Journal of Geophysical Research*, **96/C11**, 20.433-20.441.

Alley, R., Mayewski, P., Peel, D. & Stauffer, B. 1996. Twin ice cores from Greenland reveal history of climate change, more. *EOS*, **77**, 209-210.

Altenbach, A.V. 1985. *Die Biomasse der benthischen Foraminiferen - Auswertungen von „Meteor" - Expeditionen im östlichen Nordatlantik*. Unpubl. PhD. thesis, Geologisch-Paläontologisches Institut und Museum, Christian-Albrechts-Universität Kiel, 1-168 .

Altenbach, A.V. 1992. *Verteilungsmuster benthischer Foraminiferen im Arktischen Ozean und in glazialen und interglazialen Sedimenten des Europäischen Nordmeeres*. Unpubl. habilitation thesis, Christian-Albrechts-Universität Kiel, 1-111 p.

Altenbach, A.V., Heeger, T., Linke, P., Spindler, M. & Thies, A. 1993. *Miliolinella subrotunda* MONTAGU, a miliolid foraminifer building large detritic tubes for a temporary epibenthic lifestyle. *Marine Micropaleontology*, **20**, 293-301.

Altenbach, A.V., Lutze, G.F. & Weinholz, P. 1987. Beobachtungen an Benthos-Foraminiferen Teilprojekt A3. *Berichte aus dem Sonderforschungsbereich 313*, **6**, 1-86.

van Andel, T.H., Heath, G.R. & Moore, T.C. 1975. Cenozoic history and paleoceanography of the central equatorial Pacific. *Geological Society of America Memoirs*, **143**, 1-134.

Andersen, O.G.N. 1989. Primary production, chlorophyll, light, and nutrients beneath the Arctic sea ice. *In:* Herman, Y. (ed.) *The Arctic Seas*, 147-191, Reinhold van Nostrand, New York.

Asper, V.L., Deuser, W.G., Knauer, G.A. & Lohrenz, S.E. 1992. Rapid coupling of sinking particle fluxes between surface and deep ocean waters. *Nature*, **357**, 670-672.

Bard, E., Arnold, M., Maurice, P., Duprat, J., Moyes, J. & Duplessy, J.-C. 1987. Retreat velocity of the North Atlantic polar front during the last deglaciation determined by ^{14}C accelerator mass spectrometry. *Nature*, **328**, 791-794.

Bard, E., Hamelin, B., Fairbanks, R.G. & Zindler, A. 1990. Calibration of the ^{14}C timescale over the past 30,000 years using mass spectrometric U-Th ages from Barbados corals. *Nature*, **345**, 405-410.

Barker, R.W. 1960. Taxonomic Notes on the Species figured by H.B. Brady in his Report on the Foraminifera dredged by H.M.S. Challenger during the years 1873-1876. *Society of Economical Paleontologists and Mineralogists, Special Publication*, **9**, 238 pp.

Bauch, H.A. 1992. Planktische Foraminiferen im Europäischen Nordmeer - ihre Bedeutung für die paläo-ozeanographische Interpretation während der letzten 600.000 Jahre. *Berichte aus dem Sonderforschungsbereich 313*, **40**, 1-108.

Bauch, H.A. 1996. Monitoring Termination II at high latitude: anomalies in the planktic foraminiferal record. *Marine Geology*, **131**: 89-102.

Baumann, K.-H. 1990. Veränderlichkeit der Coccolithophoridenflora des Europäischen Nordmeeres. *Berichte aus dem Sonderforschungsbereich 313*, **22**, 1-146.

Belanger, P.E. & Streeter, S.S. 1980. Distribution and ecology of benthic foraminifera in the Norwegian-Greenland Sea. *Marine Micropaleontology*, **5**, 401-428.

Berger, W.H., Burke, S. & Vincent, E. 1987. Glacial-Holocene transition: climate pulsations and sporadic shutdown of NADW production. *In:* Berger, W.H. & Labeyrie, L.D. (eds.) *Abrupt Climatic Change*, 279-298, NATO ASI Series, **C 216**.

Blindheim, J. 1989. Cascading of Barents Sea bottom water into the Norwegian Sea. *Rapports et Procès-Ver-*

baux, Rèun. Cons. int. Explor. Mer, **188**, 49-58.

Brady, H.B. 1881. Notes on some of the Reticularian Rhizopoda of the „Challenger" Expedition. Part III. *Quaternary Journal of Microscopical Sciences*, **19**, 31-71.

Brady, H.B. 1884. Report on the Foraminifera dredged by *H.M.S. Challenger* during the years 1873-1876. *Reports of the Scientific Results of the Exploration Voyage, H.M.S. Challenger*, Zoology, **9**, 1-814.

Broecker, W.S. 1987. The biggest chill. *Natural History Magazine*, **97**, 74-82.

Broecker, W.S. 1991 The great ocean conveyor. *Oceanography*, **42**, 79-89.

Broecker, W.S., Andree, M., Wolfli, W., Oeschger, H., Bonani, G., Kennett, J. & Peteet, D. 1988. The chronology of the last deglaciation: implications to the cause of the Younger Dryas event. *Paleoceanography*, **3**, 1-19.

Carey, A.G. 1987. Particle flux beneath fast sea ice in the shallow southwest Beaufort Sea, Arctic Ocean. *Marine Ecological Progressive Series*, **40**, 247-257.

Chapman, F. & Parr, W.J. 1937. Foraminifera. Australasian Antarctic Expedition 1911-1914. *Scientific Reports Series*, C, **12**, 190 S.

Clarke, R.A., Swift, J.H., Reid, J.L. & Koltermann, K.P. 1990. The formation of Greenland Sea Deep Water: double diffusion or deep convection? *Deep-Sea Research*, **37/5**, 1385-1424.

COHMAP Members 1988. Climatic changes of the last 18,000 years: observations and model simulations. *Science*, **241**, 1043-1052.

Corliss, B.H. & Honjo, S. 1981. Dissolution of deep-sea benthonic foraminifera. *Micropaleonotology*, **27**, 356-378.

Crowley, J.T. & Kim, K.-Y. 1992. Complementary roles of orbital insolation and North Atlantic Deep Water during Late Pleistocene. *Paleoceanography*, **7**, 521-528.

Cushman, J.A. 1911. A monograph of the foraminifera of the North Pacific Ocean, Part II, Textulariidae. *Smithonian Institution of the U.S. National Museum, Bulletin*, **712**, 108 pp.

Cushman, J.A. 1922. Results of the Hudson Bay Expedition, 1920. I. The Foraminifera. *Contributions to Canadian Biology*, **1921**, 135-147.

Cushman, J.A. 1923. The Foraminifera of the Atlantic Ocean. Part IV: *Lagenidae*. *Smithonian Institution of the U.S. National Museum, Bulletin*, **1044**, 1-228.

Dansgaard, W. 1987. Ice core evidence of abrupt climatic changes. *In:* Berger, W.H. & Labeyrie, L.D. (eds.) *Abrupt Climatic Change*, 223-234, NATO ASI Series, **C 216**.

Dawson, J.W. 1879. On foraminifera from the Gulf and River St. Lawrence. *Canadian Naturalist and Quaterly Journal of Science*, **5**, 172-177.

Dickson, R.R., Gmitrowicz, E.M. & Watson, A.J. 1990. Deep-water renewal in the northern North Atlantic. *Nature*, **344**, 848-850.

Duplessy, J.C., Delibrias, G., Turon, J.C., Pujol, C. & Duprat, J. 1981. Deglacial warming of the Northeastern Atlantic Ocean: correlation with the paleoclimatic evolution of the European continent. *Palaeogeography, Palaeoclimatology, Palaeoecology*, **35**, 121-144.

Duplessy, J.C., Labeyrie, L., Arnold, M., Paterne, M., Duprat, J. & van Weering, T.C.E. 1992. Changes in surface salinity of the North Atlantic Ocean during the last deglaciation. *Nature*, **358**, 485-487.

Ehrmann, W. & Thiede, J. 1985. History of Mesozoic and Cenozoic sediment fluxes to the North Atlantic Ocean. *Contributions to Sedimentology*, **15**, 1-109.

Ellis, B.E. & Messina, A.R. 1940 - 1978. *Catalogue of Foraminifera*. New York, American Museum of Natural History.

Fairbanks, R.G. 1989. A 17,000-year glacio-eustatic sea level record: influence of glacial melting rates on the Younger Dryas event and deep-ocean circulation. *Nature*, **342**, 637-642.

Fairbanks, R.G. 1990. The age and origin of the „Younger Dryas climate event" in Greenland ice cores. *Paleoceanography*, **5**, 937-948.

Feyling-Hanssen, R.W. 1964. Late Quaternary deposits from the Oslofjord area. *Norges Geologisk Undersögelse*, **225**, 1-338.

Feyling-Hansen, R.W., Joergensen, J.A., Knudsen, K. L. & Andersen, A.-L. 1971. Late Quaternary Foraminifera from Vendsyssel, Denmark and Sandnes, Norway. *Bulletin of the Geological Society of Denmark*, **21**, 67-317.

Fichtel, L. von & Moll, J.P.C. 1798. *Microscopische und andere kleine Schalenthiere aus den Geschlechtern Argonaute und Schiffer*. Camesina, Wien. [fide Ellis & Messina]

Galloway, J.J. & Wissler, S.G. 1927. Pleistocene foraminifera from the Lomita Quarry, Palos Verdes Hills, California. *Journal of Paleontology*, **1**, 35-87.

Gerlach, S.A., Thiede, J., Graf, G. & Werner, F. 1986. Forschungsschiff METEOR, Reise 2 vom 19. Juni bis 16. Juli 1986. *Berichte aus dem Sonderforschungsbereich 313*, 4, 1-140.

Gooday, A.J. 1988. A response by benthic Foraminifera to the deposition of phytodetritus in the deep-sea. *Nature*, **332**, 70-73.

Gooday, A.J. & Lambshead, P.J.D. 1989. Influence of seasonally deposited phytodetritus on the benthic foraminiferal populations in the bathyal northeast Atlantic: the species response. *Marine Ecology Progress Series*, **58**, 53-67.

Gonzales-Donoso, J.M. & Linares, D. 1970. Datos sobre los foraminiferos del Tortonense de Alcala la Real. *Revista España de Micropaléontologia*, **23**, 235-242.

Graf, G. 1989. Benthic-pelagic coupling in a deep-sea benthic community. *Nature*, **341**, 437-43.

Graf, G., Gerlach, S.A., Linke, P., Queisser, W., Ritzrau, W., Scheltz, A., Thomsen, L., & Witte, U. 1995. Benthic-pelagic coupling in the Greenland-Norwegian Sea and its effect on the geological record. *Geologische Rundschau*, **841**, 49-58.

Green, E. 1960. Ecology of some arctic Foraminifera. *Micropaleontology*, **61**, 57-78.

Haake, F.W. 1962. Untersuchungen an der Foraminiferen-Fauna im Wattgebiet zwischen Langeoog und dem Festland. *Meyniana*, **12**, 25-64.

Haake, F.W. 1980. Benthische Foraminiferen in Oberflächen-Sedimenten und Kernen des Ostatlantiks vor Senegal/Gambia Westafrika. *Meteor Forschungs-Ergebnisse*, Reihe C, **32**, 1-29.

Haake, F.W. & Pflaumann, U. 1989. Late Pleistocene foraminiferal stratigraphy on the Voering Plateau, Norwegian Sea. *Boreas*, **18**, 343-356.

Haflidason, H., Sejrup, H.P., Kristensen, D.K. & Johnsen, S. 1995. Coupled response of the late glacial climatic shifts of northwest Europe reflected in Greenland ice cores: evidence from the northern North Sea. *Geology*, **23**, 1059-1062.

Hald, M. & Vorren, T. 1987. Foraminiferal stratigraphy and environment of Late Weichselian deposits on the continental shelf off Troms, Northern Norway. *Marine Micropaleontology*, **12**, 129-160.

Hamich, A. 1991. *Sedimentäre Untersuchungen eines Kernes (GIK 21906-2) der Grönlandsee*. Unpubl. diploma thesis, Geologisch-Paläontologisches Institut und Museum,

Univ. Kiel, 1-78.

Heeger, T. 1990. Elektronenmikroskopische Untersuchungen zur Ernährungsbiologie benthischer Foraminiferen. *Berichte aus dem Sonderforschungsbereich 313*, **21**, 1-139.

Heinze, C., Schlosser, P., Koltermann, K.P. & Meincke, J. 1990. A tracer study of the deep water renewal in the European polar seas. *Deep-Sea Research*, **37**, 1425-1453.

Henrich, R. 1992. *Beckenanalyse des Europäischen Nordmeeres: Pelagische und glaziomarine Sedimentflüsse im Zeitraum 2,6 Ma bis rezent.* - Unpubl. habilitation thesis, Christian-Albrechts-Universität Kiel, 1-345.

Herguera, J.C. 1992. Deep-sea benthic foraminifera and biogenic opal: Glacial to postglacial productivity changes in the western equatorial Pacific. *Marine Micropaleontology*, **19**, 79-98.

Herguera, J.C. & Berger, W.H. 1991. Paleoproductivity from benthic foraminifera abundance: glacial to postglacial change in west-equatorial Pacific. *Geology*, **19**, 1173-1176.

Heron-Allen, E. & Earland, A. 1930. The Foraminifera of the Plymouth district. I and II. *Royal Microscopical Society of London, Journal*, Series **3**, 161-199.

Hirschleber, H., Theilen, F., Balzer, W., von Bodungen, B. & Thiede, J. (eds.) 1988. Forschungsschiff METEOR, Reise 7 vom 1. Juni bis 28. September 1988. *Berichte aus dem Sonderforschungsbereich 313*, **10**, 1-358.

Höglund, H. 1947. Foraminifera in the Gullmar Fjord and the Skagerrak. *Zool. Bidrag Uppsala*, **26**, 1-328.

Holler, P. & Kassens, H. 1989. Sedimentphysikalische Eigenschaften aus dem Europäischen Nordmeer Datenreport F.S. Meteor, Reise 7. *Berichte aus dem Sonderforschungsbereich 313*, **15**, 1-61.

Imbrie, J., Boyle, E.A., Clemens, S.C., Duffy, A., Howard, W.R., Kukla, G., Kutzbach, J., Martinson, D.G., McIntyre, A., Mix, A.C., Molfino, B., Morley, J.J., Peterson, L.C., Pisias, N.G., Prell, W.L., Raymo, M.E., Shackleton, N.J. & Toggweiler, J.R. 1992. On the structure and origin of major glaciation cycles. 1. Linear responses to Milankovitch forcing. *Paleoceanography*, **7**, 701-738.

Imbrie, J., Hays, J.G., Martinson, D.G., McIntyre, A., Mix, A.C., Morley, J.J., Pisias, N.G.W., Prell, L. & Shackleton, N.J. 1984. The orbital theory of Pleistocene climates: Support from a revised chronology of the marine $\delta^{18}O$ record. *In:* Berger, A.L., Imbrie, J., Hays, J.G., Kukla, G. & Salzman, B. (eds.) *Milankovitch and Climate*, 269-305, Reidel, Hinham.

Jansen, E. & Bjørklund, K.R. 1985. Surface circulation in the Norwegian Sea, 15,000 B.P. to present. *Boreas*, **14**, 243-257.

Jansen, E. & Veum, T. 1990. Evidence for two-step deglaciation and its impact on North Atlantic deep water circulation. *Nature*, **343**, 612-616.

Johnsen, S.J., Clausen, H.B., Dansgaard, W., Fuhrer, K., Gundestrup, N., Hammer, C.U., Iversen, P., Jouzel, J., Stauffer, B. & Steffensen, J.P. 1992. Irregular glacial interstadials recorded in a new Greenland ice core. *Nature*, **359**, 311-313.

Johnson, R.F. 1980. *One-centimeter Stratigraphy in Foraminiferal Ooze: Theory and Practice.* Unpubl. PhD thesis, University of California, San Diego, Scripps Institution of Oceanography reference number 80-18, 1-202.

Jones, E.P., Rudels, B. & Anderson, L.G. 1995. Deep waters of the Arctic Ocean: origins and circulation. *Deep-Sea Research*, **425**, 737-760.

Jones, G.A. & Keigwin, L.D. 1988. Evidence from Fram Strait 78° N for early deglaciation. *Nature*, **336**, 56-59.

Jorissen, F.J.J. 1987. The distribution of benthic Foraminifera in the Adriatic Sea. *Marine Micropaleontology*, **12**, 21-48.

Jorissen, F.J.J., Stigter, H.C.. & Widmark, J.G.V. 1995. A conceptual model explaining benthic foraminiferal microhabitats. *Marine Micropaleontology*. **26**: 3-15.

Jouzel, J., Barkov, N.I., Barnola, J.M., Bender, M., Chapellaz, J., Genthon, C., Kotlyakov, V.M., Lipenkov, V., Lorius, C., Petit, J.R., Raynaud, D., Raisbeck, G., Ritz, C., Sowers, T., Stievenard, M., Yiou, F. & Yiou, P. 1993. Extending the Vostok ice-core record of palaeoclimate to the penultimate glacial record, *Nature*, **364**, 407-412.

Jouzel, J., Lorius, C., Merlivat, L. & Petit, J.-R. 1987. Abrupt climatic changes: the Antarctic ice record during the Late Pleistocene. *In:* Berger, W.H. & Labeyrie, L.D. (eds.) *Abrupt Climatic Change*, 235-246, NATO ASI Series, **C 216**.

Jung, S.J.A. 1996. Wassermassenaustausch zwischen NE-Atlantik und Nordmeer während der letzten 300.000 / 80.000 Jahre im Abbild stabiler O- und C-Isotope. *Berichte aus dem Sonderforschungsbereich 313*, **61**, 1-104.

Kassens, H. 1990. Verfestigte Sedimentlagen und seismische Reflektoren: Frühdiagenese und Paläo-Ozeanographie in der Norwegischen See. *Berichte aus dem Sonderforschungsbereich 313*, **24**, 1-117.

Kellogg, T.B. 1980. Paleoclimatology and paleo-oceanography of the Norwegian and Greenland seas: glacial-interglacial contrasts. *Boreas*, **9**, 115-137.

Kerr, R.A. 1993. How ice age climate got the shakes. *Science*, **260**, 890-892.

Koç-Karpuz, N.K. & Jansen, E. 1992. A high-resolution diatom record of the last deglaciation from the SE Norwegian Sea: documentation of rapid climatic changes. *Paleoceanography*, **7**, 499-520.

Koç-Karpuz, N.K. & Schrader, H. 1990. Surface sediment diatom distribution and Holocene paleotemperature variations in the Greenland, Iceland, and Norwegian Sea. *Paleoceanography*, **54**, 557-580.

Koltermann, K. 1987. *Die Tiefenzirkulation der Grönlandsee als Folge des thermohalinen Systems des Europäischen Nordmeeres.* Unpubl. PhD thesis, Universität Hamburg, 1-287.

Labeyrie, L.D., Duplessy, J.C., Duprat, J., Juillet-Leclerc, A., Moyes, J., Michel, E., Kallel, N. & Shackleton, N. 1992. Changes in the vertical structure of the North Atlantic Ocean between glacial and modern times. *Quaternary Science Review*, **11**, 401-413.

Lagoe, M.B. 1977. Recent benthic foraminifera from the Central Arctic Ocean. *Journal of Foraminiferal Research*, **72**, 106-129.

Lagoe, M.B. 1979. Recent benthonic foraminiferal biofacies in the Arctic Ocean. *Micropaleontology*, **25**, 214-224.

Larsen, A.R. 1982. Foraminifera from off the West Coast of Africa. *Atlantide Reports*, Copenhagen, **13**, 49-149.

Leroy, D.O. & Hodgkinson, K.A. 1975. Benthonic foraminifera and some pteropoda from a deep-water dredge sample, northern Gulf of Mexico. *Micropaleontology*, **214**, 420-447.

Linke, P. 1986. *Biomasse und Stoffwechsel-Leistungen benthischer Foraminiferen.* Unpubl. diploma thesis, Universität Kiel, 1-64.

Linke, P. 1989. Lebendbeobachtungen und Untersuchungen des Energiestoffwechsels benthischer Foraminiferen aus dem Europäischen Nordmeer. *Berichte aus dem Sonderforschungsbereich 313*, **18**, 1-123.

Linke, P. & Lutze, G.F. 1993. Microhabitat preferences of benthic foraminifera - a static concept or a dynamic adaption to optimize food acquisition? *Marine Micropaleontology*, **20**, 215-234.

Linné, C. von 1758. *Systema naturea*. **1**, ed. 10, Holmiae, Suecica, L. Salvii. [fide Ellis & Messina]

Loeblich, A.R. & Tappan, H. 1953. Studies of Arctic Foraminifera. *Smithonian Miscellaneous Collection*, **1217**, 1-150.

Loeblich, A.R. & Tappan, H. 1964. Sarcodina, chiefly „Thecamoebians" and Foraminiferida. *In:* Moore, R.C. (ed.) *Treatise on Invertebrate Paleontology*, 900 pp., Geological Society of America and University of Kansas Press, Kansas, Part C. Protista, **2**, I-II.

Loeblich, A.R. & Tappan, H. 1988. *Foraminiferal genera and their classification*, Van Norstrand Reinholdy, New York, 2 volumes, 970 pp.

Lohmann, G.P. 1978. Abyssal benthonic foraminifera as hydrographic indicators in the western South Atlantic. *Journal of Foraminiferal Research*, **8**, 6-34.

Luczkowska, E. 1974. Miliolidae Foraminiferida from the Miocene of Poland, Part II: biostratigraphy, palaeoecology and systematics. *Acta Paleontologica Polonica*, **191**, 1-176.

Lutze, G.F. 1979. Benthic foraminifers at Site 397: faunal fluctuations and ranges in the Quaternary. *Initial Reports of the DSDP*, **471**, 419-431.

Lutze, G.F. 1980. Depth distribution of benthic foraminifera on the continental margin off NW-Africa. *Meteor Forschungsergebnisse*, Reihe C, **32**, 31-80.

Lutze, G.F. & Altenbach, A.V. 1988. *Rupertina stabilis* WALLICH, a highly adapted suspension feeding foraminifer. *Meyniana*, **40**, 55-69.

Lutze, G.F. & Thiel, H. 1989. Epibenthic foraminifera from elevated microhabitats: *Cibicidoides wuellerstorfi* and *Planulina ariminensis*. *Journal of Foraminiferal Research*, **19**, 153-158.

Mackensen, A. 1987. Benthische Foraminiferen auf dem Island-Schottland Rücken: Umweltanzeiger an der Grenze zweier ozeanischer Räume. *Paläontologische Zeitschrift*, **613**, 149-179.

Mackensen, A. & Hald, M. 1988. *Cassidulina teretis* and *C. laevigata* d'ORBIGNY: their modern and Late Quaternary distribution in Northern Seas. *Journal of Foraminiferal Research*, **18**, 16-24.

Mangerud, J., Andersen, S.T., Berglund, B.E. & Donner, J.J. 1974. Quaternary stratigraphy of Norden, proposal for terminology and classification. *Boreas*, **3**, 109-128.

Martinson, D.G., Pisias, N.G., Hays, J.D.. Imbrie, J., Moore, T.C. & Shackleton, N.J. 1987. Age dating and the orbital theory of the ice ages: development of a high-resoltuion 0 to 300,000-year chronostratigraphy, *Quaternary Research*, **27**, 1-30.

Matthießen, J. 1991. Dinoflagellaten-Cysten im Spätquartär des Europäischen Nordmeeres: Palökologie und Paläo-Ozeanographie. *GEOMAR Report*, **7**, 1-104.

Mayewski, P.A., Meeker, L.D., Whitlow, S., Twickler, M.S., Morrison, M.C., Alley, R.B., Bloomfield, P. & Taylor, K. 1993. The atmosphere during the Younger Dryas. *Science*, **261**, 195-197.

Midttun, L. 1985. Formation of dense bottom water in the Barents Sea. *Deep-Sea Research*, **32**, 1233-1241.

Mix, A.C. & Ruddiman, W.F. 1985. Structure and timing of the last deglaciation: Oxygen isotope evidence. *Quaternary Science Reviews*, **4**, 59-108.

Murray, J.W. 1971. *An Atlas of Recent Foraminiferids*. 274 pp., Heineman Educational Books; London.

Murray, J.W. 1991. *Ecology and Palaecology of Benthic Foraminifera*. 397 pp., Longman Scientific & Technical, Harlow.

Murray, J.W. 1995. Microfossil indicators of ocean water masses, circulation and climate. *In:* Bosence, D.W.J. & Allison, P.A. (eds.) *Marine palaeoenvironmental analysis from fossils*, 245-264, The Geological Society, Publishing House, Bath.

Nees, S. 1989. *Biostratigraphie mit benthischen Foraminiferen im Europäischen Nordmeer für die letzten 350.000 Jahre*. Unpubl. diploma thesis, Institut für Paläontologie und Historische Geologie, Universität München, 1-42.

Nees, S. 1994. The benthic foraminiferal record of Late Quaternary glacial/interglacial cycles in core E 36-23, SE Tasman Plateau. *In:* van der Lingen, G.J., Swanson, K.M. & Muir, R.J. (eds.) *The Evolution of the Tasman Sea Basin. Proceedings of the Tasman Sea Conference, November 1992, Christchurch, New Zealand*, 203-214, Balkema Publishers, Rotterdam.

Nees, S. & Struck, U. 1994. The biostratigraphic and paleoceanographic significance of *Siphotextularia rolshauseni* (PHLEGER and PARKER) in Norwegian-Greenland Sea sediments. *Journal of Foraminiferal Research*. **24**, 233-240.

Nees, S., Altenbach, A.V. & Kassens, H. (subm.): A high resolution record of foraminiferal response induced by late Quaternary sea ice retreat in the Norwegian-Greenland Sea. *Geology*.

Nørvang, A. 1945. *The Zoology of Iceland, Foraminifera* **2/2**, 1-79, Copenhagen and Reykjavik, E. Munksgaard.

Nürnberg, D. 1991. Haupt- und Spurenelemente in Foraminiferengehäusen. Hinweise auf klimatische und ozeanographische Änderungen im nördlichen Nordatlantik während des Spätquartärs. *GEOMAR Report*, **8**, 1-117.

Oki, K. 1989. Ecological Analysis of Benthonic Foraminifera in Kagoshima Bay, South Kyushu, Japan. *South Pacific Study*, **101**, 1-191.

d'Orbigny, A.D. 1826. Tableau méthodique de la classe des Céphalopodes. *Ann. Sci. nat. Paris*, **ser. 1/7**, 245-314.

d'Orbigny, A.D. 1839. Foraminifères. *In:* de la Sagra, R. (ed.) *Histoire physique, politique et naturelle de l'Ile de Cuba*. P. XLVIII + 224, Paris, A. Bertrand.

d'Orbigny, A.D. 1846. *Foraminifères fossiles du Bassin Tertiaire de Vienna (Austriche)*. 1-312, Gide et Compe, Paris.

Parker, F.B. 1958. Eastern Mediterranean Foraminifera. *Reports of the Swedish Deep-Sea Expedition*, **8**, (Sediment Cores), 4, 219-285.

Parker, W.K. & Jones, T.R. 1865. On some Foraminifera from the North Atlantic and Arctic Oceans, including Davis Strait and Baffin's Bay. *Philosophical Transactions of the Royal Society of London*, **155**, 325-441.

Pflaumann, U., Duprat, J.C.P. & Labeyrie, L.D. 1996. SIMMAX: a modern analog technique to deduce Atlantic sea surface temperatures from planktonic foraminifera in deep-sea sediments. *Paleoceanography*, **111**, 15-35.

Phleger, F.B. 1952. Foraminifera in some sediment samples from the Greenland Arctic. *Contributions of the Cushman Foundation, Journal of Foraminiferal Research*, **32**, 80-89.

Phleger, F.B. 1964. Patterns of living benthonic foraminifera, Gulf of California. *Symposium on marine geology of the Gulf of California, Memoir*, **3**, 377-394.

Phleger, F.B. & Parker, F.L. 1951. Ecology of foraminifera, Northwest Gulf of Mexico, Part II, Foraminifera species. *Geological Society of America, Memoir*, **46**, 1-64.

Phleger, F.B., Parker, F.L. & Peirson, J.F. 1953. North Atlantic Foraminifera. *In:* Petterson, H. (ed.) *Reports of the Swedish Deep-Sea Expedition, Sediment cores from the North Atlantic Ocean*, **71**, 1-22.

Reuss, A.E. 1851. Ueber die fossilen Foraminiferen und Entromostraceen der Septarienthone der Umgegend von Berlin. *Zeitschrift der deutschen geologischen Gesellschaft*, **1**, 49-92.

Ruddiman, W.F. & McIntyre, A. 1973. Time-transgressive

deglacial retreat of polar waters from the North Atlantic. *Quaternary Research*, **3**, 117-130.

Ruddiman, W.F. & Duplessy, J.-C. 1985. Conference on the last deglaciation: timing and mechanism. *Quaternary Research*, **23**, 1-17.

Rudels, B. & Quadfasel, D. 1991. Convection and deep water formation in the Arctic Ocean - Greenland System. *Journal of Marine Systems*, **2**, 435-450.

Sarnthein, M., Jansen, E., Arnold, M., Duplessy, J.-C., Erlenkeuser, H., Flatoy, A., Veum, T., Vogelsang, E. & Weinelt, M.S. 1992. $\delta^{18}O$ Time-slice reconstruction of meltwater anomalies at Termination I in the North Atlantic between 50° and 80° N. *In:* Bard, E. & Broecker, W.S. (eds.) *The last deglaciation: absolute and radiocarbon chronologies*, 183-200, NATO ASI Series, Springer Verlag, Berlin, Heidelberg.

Sarnthein, M. & Tiedemann, R. 1990. Younger Dryas-style cooling events at glacial terminations I-VI at ODP Site 658: Associated benthic $\delta^{13}C$ anomalies constrain meltwater hypothesis. *Paleoceanography*, **5**, 1041-1055.

Sars, M. 1868. Fortsatte bemaerkninger over det dyriske livs udbredning i havets dybder. *Forhandlinger i Videnskasselskabet i Kristiania*, **1871**, 246-255.

Schiebel, R. 1992. Rezente benthische Foraminiferen in Sedimenten des Schelfes und oberen Kontinentalhanges im Golf von Guinea, Westafrika. *Berichte - Reports Geologisch-Paläontologisches Institut und Museum Universität Kiel*, **51**, 1-179.

Schultze, M.S. 1854. *Über den Organismuns der Polythalamien (Foraminiferen) nebst Bemerkungen über die Rhizopoden im Allgemeinen*. Leipzig, Engelmann. [fide Ellis & Messina]

Schulz, H. 1995. Sea-surface temperatures 10,000 years B.P. - consequences of the early Holocene insolation maximum. *Berichte - Reports Geologisch-Paläontologisches Institut und Museum Universität Kiel*, **73**,1-156.

Schwager, C. 1866. Fossile Foraminiferen von Kap Nicobar. Reise der österreichischen Fregatte *Novara* um die Erde in den Jahren 1857, 1858 und 1859 unter den Befehlen des Commodore B. von Wuellerstorf-Urbair, Geologischer Theil, **21** Geologische Beobachtungen, *Paläontologische Mitteilungen*, **2**, 187-268.

Scott, D.B. & Vilks, G. 1991. Benthic foraminifera in the surface sediments of the deep-sea Arctic Ocean. *Journal of Foraminiferal Research*, **201**, 20-39.

Seguenza, G. 1862. *Dei terreni Terziarii del distretto di Messin; Parte II - Descrizione dei foraminiferi monotalamici delle marne Mioceniche del distretto di Messina*. Messina, T. Capra. [fide Ellis & Messina]

Seidenkrantz, M.-S. 1995. *Cassidulina teretis* Tappan and *Cassidulina neoteretis* new species (Foraminifera): stratigraphic markers for deep sea and outer shelf areas. *Journal of Micropalaeontology*, **14**, 145-157.

Seiler, W.C. 1975. Tiefenverteilung benthischer Foraminiferen am portugiesischen Kontinentalhang. *Meteor Forschungsergebnisse*, Reihe C, **23**, 47-94.

Sejrup, H.P., Fjæran, T., Hald, M., Beck, L., Hagen, J., Miljeteig, I., Morvik, I. & Norvik, O. 1981. Benthonic foraminifera in surface samples from the Norwegian continental margin between 62° N and 65° N. *Journal of Foraminiferal Research*, **11**, 277-295.

Sejrup, H.P. &. Guilbault, J.P 1980. *Cassidulina reniforme* and *C. obtusa* Foraminifera, distribution and ecology. *Sarsia*, **65**, 79-85.

Silvestri, A. 1898. Foraminiferi pliocenici della Provincia di Siena; Parte II. *Accad. Pont. Nuovi Linecei Roma, Mem.*, **15**. [fide Ellis & Messina]

Silvestri, A. 1904. Richerche strutturali su alcune forme dei Trubi di Bonfornello (Palermo). *Accad. Pont. Nuovi Lincei Roma, Mem.*, **22**, 235-276.

Smart, C.W., King, S.C., Gooday, A.J., Murray, J.W., & Thomas, E. 1994. A benthic foraminiferal proxy of pulsed organic matter paleofluxes. *Marine Micropaleontology*, **23**, 89-99.

Smethie, W.M.jr., Ostlund, H.G. & Loosli, H.H. 1986. Ventilation of the deep Greenland and Norwegian sea: evidence from krypton-85, tritium, carbon-14 and argon-39. *Deep-Sea Research*, **33/5**, 675-703.

Stein, R., Nam, S.-I., Schubert, C., Vogt, C., Fütterer, D. & Heinemeier, J. 1994. The Last Deglaciation in the eastern central Arctic Ocean. *Science*, **264**, 692-696.

Stschedrina, Z.G. 1946. [New species of foraminifera from the Arctic Ocean - Transactions of the Arctic Scientific Research Institute, Northern Sea Route Board Drifting Expedition on the Icebraker „G. Sedov" in 1973 - 1940]. *Trudy Moscow - Leningrad* (Biology), **3**, 1-147 (*In Russian*).

Struck, U. 1992. Zur Paläo-Ökologie benthischer Foraminiferen im Europäischen Nordmeer während der letzten 600.000 Jahre. *Berichte aus dem Sonderforschungsbereich 313*, **38**, 1-129.

Struck, U. 1995. Stepwise postglacial migration of benthic foraminifera into the abyssal northeastern Norwegian Sea. *Marine Micropaleontology*, **261**, 207-231.

Struck, U. (*this volume*). Paleoecology of benthic foraminifera in the Norwegian-Greenland Sea during the past 500 ka.

Suess, E. & Altenbach, A.V. 1992. Europäisches Nordmeer, Reise Nr. 17, 15. Juli - 29. August 1991. *METEOR-Berichte, Universität Hamburg*, **92-3**, 1-164.

Swift, J.H. 1986. The Arctic Waters. *In:* Hurdle, B.G. (ed.) *The Nordic Seas*, 129-151, Springer Verlag, New York, Berlin, Heidelberg, Tokyo.

Swift, J.H. & Koltermann, K.P. 1988. The Origin of Norwegian Sea Deep Water. *Journal of Geophysical Research*, **93/C4**, 3563-3569.

Tappan, H. 1951. Northern Alaska index foraminifera. *Contributions from the Cushman Foundation for Foraminiferal Research*, **2**, 1-8.

Taylor, K.C., Lamorey, G.W., Doyle, G.A., Alley, R.B., Grootes, P.M., Mayewski, P.A., White, J.W.C. & Barlow, L.K. 1993. The „flickering switch" of late Pleistocene climate change. *Nature*, **361**, 432-436.

Thiede, J., Diesen, G.W., Knudsen, B.-E. & Snåre, T. 1986. Patterns of Cenozoic sedimentation in the Norwegian-Greenland Sea. *Marine Geology*, **69**, 323-352.

Thiede, J., Gerlach, S.A. & Wefer, G. 1985. Sedimentation im Europäischen Nordmeer, Organisation und Forschungsprogramm des Sonderforschungsbereichs für den Zeitraum 1985 - 1987. *Berichte aus dem Sonderforschungsbereich 313*, **1**, 1-110.

Thiede, J. & Hempel, G. (eds.) 1991. Die Expedition ARKTIS-VII/1 mit FS „POLARSTERN" 1990. *Berichte zur Polarforschung*, **80**, 1-137.

Thies, A. 1991. Die Benthos-Foraminiferen im Europäischen Nordmeer. *Berichte aus dem Sonderforschungsbereich 313*, **31**, 1-97.

Timm, S. 1992. Rezente Tiefsee-Benthosforaminiferen aus Oberflächensedimenten des Golfes von Guinea Westafrika - Taxonomie, Verbreitung, Ökologie und Korngrößenfraktionen. *Berichte - Reports Geologisch-Paläontologisches Institut und Museum Universität Kiel*, **59**, 1-192.

Todd, R. & Low, D. 1980. Foraminifera of the Kara and Greenland Seas. *Contributions on Paloeontology, Geological Survey Professional Papers*, **1070**, 1-30.

Todd, R. & Low, D. 1981. Marine Flora and Fauna of the

Northeastern U.S., Protozoa: Sarcodina benthic Foraminifera. *NOAA Technical Reports, NMFS Circular*, **439**, 1-51.

Vogelsang, E. 1990. Paläo-Ozeanographie des Europäischen Nordmeeres an Hand stabiler Kohlenstoff- und Sauerstoffisotope. *Berichte aus dem Sonderforschungsbereich 313*, **23**, 1-136.

Wagner, T., & Henrich, R. 1994. Organo- and lithofacies of glacial-interglacial deposits in the Norwegian-Greenland Sea: responses to paleoceanographic and paleoclimatic changes. *Marine Geology*, **120**, 335-364.

Walker, G. & Jacob, E. 1798. In Kanmacher, F. *Adams' essays on the microscope*. London, Dillon and Keating. [fide Ellis & Messina]

Wallich, G.C. 1877. On *Rupertina stabilis*, a new sessile foraminifer from the North Atlantic. *Annals and Magazine of Natural History*, ser. **4/19**, 501-504.

Weinelt, M.S. 1993. Schmelzwasserereignisse und klimatische Verstärkerimpulse im Europäischen Nordmeer während der letzten 60.000 Jahre - Hinweise aus hochauflösenden Isotopenkurven. *Berichte aus dem Sonderforschungsbereich 313*, **41**, 1-107.

Williamson, W.C. 1858. *On the Recent Foraminifera of Great Britain*. P. V-XX + 1-107, London.

Winn, K., Sarnthein, M. & Erlenkeuser, H. 1991. $\delta^{18}O$ Stratigraphy and chronology of Kiel sediment cores from the east Atlantic. *Berichte - Reports Geologisch-Paläontologisches Institut und Museum Universität Kiel*, **45**, 1-99.

Østby, K.L. & Nagy, J. 1982. Foraminiferal distribution in the western Barents Sea, Recent and Quaternary. *Polar Research*, **1**, 53-95.

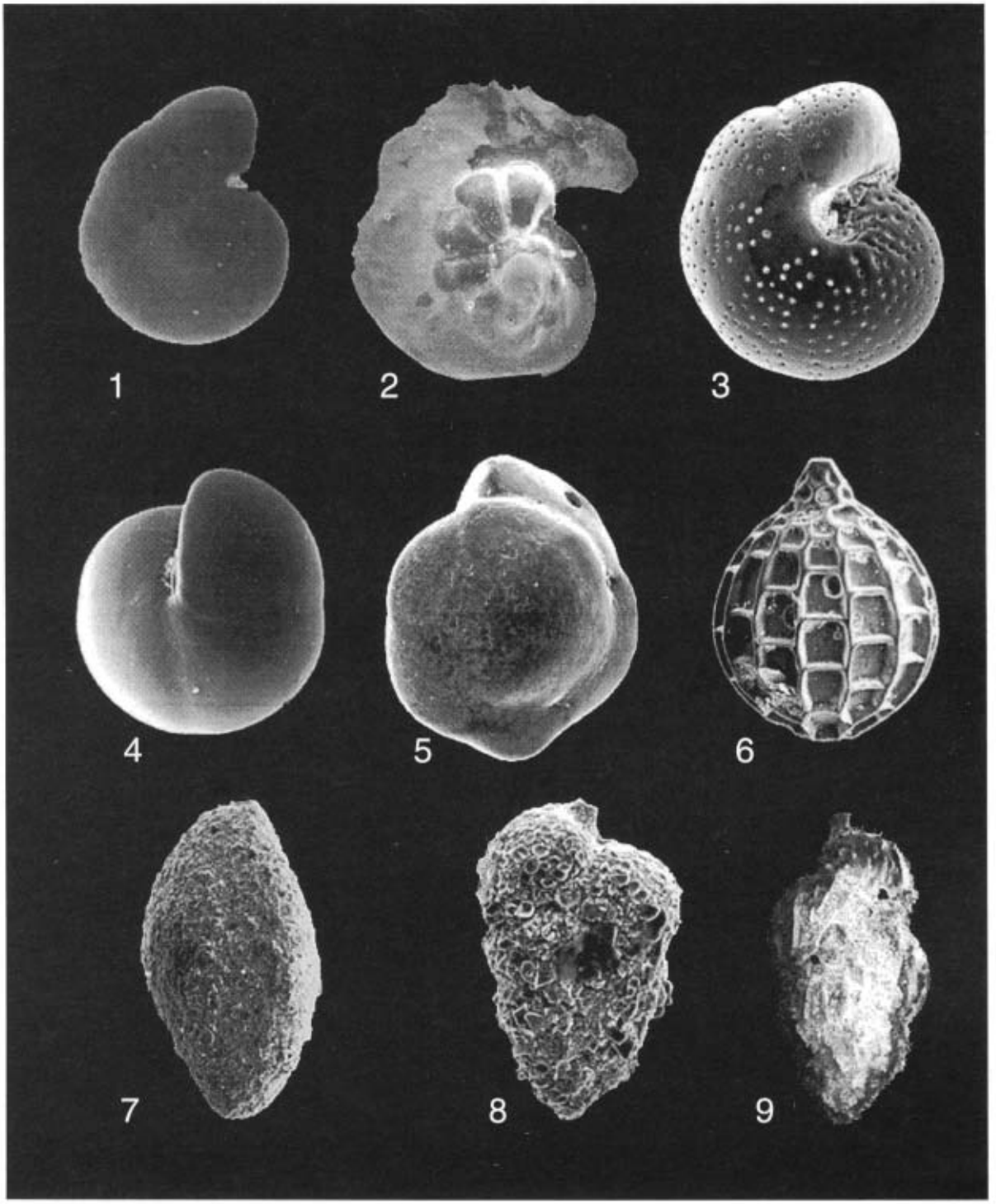


Plate 1. 1. *Gyroidina umbonata* M 23414-5.5, x 114. **2.** *Laticarinina pauperata* M 23414-7.5, x 48. **3.** *Melonis pompilioides* M 23414-1.5, x 132. **4.** *Pullenia bulloides* M 23414-17.5, x 128. **5.** *Oridorsalis umbonatus* PS 1906-4.5, x 161. **6.** *Oolina hexagona* PS 1906-0.5, x 154. **7.** *Sigmoilopsis schlumbergeri* M 23414-1.5, x 86. **8** *Siphotextularia rolshauseni* PS 1906-28.5, x 182. **9.** *Uvigerina peregrina* M 23414-3.5, x 74.

Appendix 2. Taxonomy and synonym list
The taxonomy follows micropalaeontological reference slides hosted at the Department of Micropalaeontology of the Institute of Geology, University of Kiel. The following synonym list records also the taxonomic literature used.

Ammobaculites agglutinans **(d'ORBIGNY)**
*1846 *Spirolina agglutinans* n. - d'ORBIGNY, p. 137, Plate 7 (10-12).
1960 *A. agglutinans* pars- BARKER, p. 66, Plate 32 (19-20 and 24-26).
1980 *A. agglutinans* - HAAKE, p. 7, Plate 1 (11).

Anomalina globulosa **CHAPMAN & PARR**
*1937 *A. globulosa* n. - CHAPMAN & PARR, p. 117, Plate 9 (27).
1971 *A. globulosa* - FEYLING-HANSSEN *et al.*, p. 258, Plate 9 (1-3).

Bolivina pseudoplicata **HERON-ALLEN & EARLAND**
*1930 *B. pseudoplicata* n. - HERON-ALLEN & EARLAND, p. 81, Plate 3 (36-40).
1971 *B. pseudoplicata* - FEYLING-HANSSEN *et al.*, p. 243, Plate 7 (16) and 18 (11).

Bolivinita quadrilatera **(SCHWAGER)**
*1866 *Textilaria quadrilatera* - n. SCHWAGER, p. 253.
1964 *B. quadrilatera* - LOEBLICH & TAPPAN, p. C 548, Plate 434 (1-3).

Buccella frigida **(CUSHMAN)**
*1922 *Pulvinulina frigida* n. - CUSHMANN, p. 12.
1971 *B. frigida* - FEYLING-HANSSEN *et al.*, p. 253, Plate 8 (12-14) and 19 (1).

Bulimina marginata **d'ORBIGNY**
*1826 *B. marginata* n. - d'ORBIGNY, Plate 12 (10-12).
1960 *B. marginata* - BARKER, Plate 51 (3-5).
1980 *B. marginata* - LUTZE, p. 41.

Bulimina striata **d'ORBIGNY**
*1826 *B. striata* n. - d'ORBIGNY, p. 269, nr. 2.
1971 *B. striata* - FEYLING-HANSSEN *et al.*, p. 236, Plate 6 (21).

Cassidulina laevigata **d'ORBIGNY**
*1826 *C. laevigata* n. - d'ORBIGNY, p. 282, Plate 15 (4-5).
1981 *C. laevigata* - SEJRUP *et al.*, p. 290, Plate 1 (5). (s. *Cassidulina* sp. group)

Cassidulina neoteretis **SEIDENKRANTZ**
*1995 *C. neoteretis* n. - SEIDENKRANTZ, p.148, pl. 1, figs. 1-6, pl. 2, figs. 1-14. (s. *Cassidulina* sp. group)

Cassidulina reniforme **NØRVANG**
*1945 *C. reniforme* n. - NØRVANG, p. 41, text fig. 6 e-h.
1980 *C. reniforme* - SEJRUP & GUILBAULT, p. 79-85, fig. 2.

Cassidulina teretis **TAPPAN**
*1951 *C. teretis* n. - TAPPAN, p. 7-8, pl. 1, fig. 30.
1988 *C. teretis* - MACKENSEN & HALD, p. 17, Plate 1 (8-15). (s. *Cassidulina* sp. group)

Cibicides fletscheri **GALLOWAY & WISSLER**
*1927 *C. fletscheri* n. - GALLOWAY & WISSLER, p. 49.
1980 *C. fletscheri* - LUTZE, Plate 12 (11).
1992 *C. teretis* - STRUCK, Plate 1 (7).

Cibicides lobatulus **(WALKER & JACOB)**
*1798 *C. lobatulus* n. - WALKER & JACOB, p. 642, Plate 14 (36).
1884 *Truncatulina lobatulus* - BRADY, p. 660, Plate 92 (10).
1952 *C. lobatulus* - PHLEGER, p. 83, Plate 14 (29).

Cibicidoides wuellerstorfi **(SCHWAGER)**
*1866 *Anomalina wuellerstorfi* n. - SCHWAGER, p. 258, Plate 7 (105, 107).
1978 *P. wuellerstorfi* - LOHMANN, p. 26, Plate 2 (1-4).
1979 *Cibicidoides wuellerstorfi* - LUTZE, p. 426, Plate 1 (5 a-b).

Cribrostomoides subglobosum **(SARS)**
*1868 *Lituola subglobosa* n. - SARS, p.248.
1964 *C. subglobosum* - LOEBLICH & TAPPAN, p. C225, Plate 136 (1, 2).
1981 *Alveolophragmium subglobosum* (SARS) - SEJRUP *et al.*, p. 290, Plate 1 (1).

Cyclogyra planorbis **(SCHULTZE)**
*1854 *Cornuspira planorbis* n. - SCHULTZE, p. 40.
1964 *C. planorbis* - LOEBLICH & TAPPAN, p. C 438, Plate 329 (1, 2).

Dentalina baggi **GALLOWAY & WISSLER**
*1927 *D. baggi* n. - GALLOWAY & WISSLER, p. 49, Plate 8 (14-15).
1953 *D. baggi* - LOEBLICH & TAPPAN, p. 54, Plate 9 (10-15).
1971 *D. baggi* - FEYLING-HANSSEN *et al.*, p. 199, Plate 3 (1).

Dentalina cuvieri **(d'ORBIGNY)**
*1826 *Nodosaria cuvieri* n. - d'ORBIGNY, p. 255.
1964 *D. cuvieri* - LOEBLICH & TAPPAN, p. C516, Plate 403 (3).
1989 *D. cuvieri* - NEES, p. 13, Plate 1 (6).

Dentalina frobisherensis **LOEBLICH & TAPPAN**
*1953 *D. frobisherensis* n. - LOEBLICH & TAPPAN, p. 55-56, Plate 10 (1-9).
1971 *D. frobisherensis* - FEYLING-HANSSEN *et al.*, p. 200, Plate 3 (2).

Dentalina pauperata **d'ORBIGNY**
*1846 *D. pauperata* n. - d'ORBIGNY, p. 46, Plate 1 (57-58).
1953 *D. pauperata* - LOEBLICH & TAPPAN, p. 54, Plate 9 (10-15).
1971 *D. pauperata* - FEYLING-HANSSEN *et al.*, p. 199, Plate 3 (1).

Eggerella bradyi **(CUSHMAN)**
*1911 *Verneulina bradyi* n. - CUSHMAN, p. 54, Plate 87.
1964 *E. bradyi* - LOEBLICH & TAPPAN, p. C275, Plate 186 (1).

Epistominella exigua **(BRADY)**
*1884 *Pulvinulia exigua* n. - BRADY, p. 696, Plate 103 (13-14).
1953 *E. exigua* - PHLEGER *et al.*, p. 43, Plate 9 (35-36).
1960 *E. exigua* - BARKER, Plate 103 (14).

Eponides tumidulus **(BRADY)**
*1884 *Truncatulina tumidula* n. - BRADY, p. 666, Plate 95 (8).
1951 *E. tumidulus* - PHLEGER & PARKER, p. 21, Plate 95 (8).
1992 *E. tumidulus* - TIMM, p. 56, Plate 7 (5 a-b).

Fissurina marginata **SEGUENZA**
*1862 *F. marginata* n. - SEGUENZA, p. 66, Plate 2 (27-28).
1981 *F. marginata* - TODD & LOW, p. 26, Plate 76 (73 a-c).

Fursenkoina fusiformis **(WILLIAMSON)**
*1858 *Bulimina pupoides*, var. *fusiformis* n. - WILLIAMSON, p. 63, Plate 5 (129-130).
1980 *F. fusiformis* - HAAKE, p. 14, Plate 3 (13-14).

Globocassidulina subglobosa **(BRADY)**
*1881 *Cassidulina subglobosa* n. - BRADY, p. 60.
1960 *C. subglobosa* - BARKER, Plate 54 (17).
1992 *G. subglobosa* - SCHIEBEL, p. 47, Plate 2 (14).

Gyroidina umbonata **(SILVESTRI)**
*1898 *Rotalia soldanii* d'ORBIGNY var. *umbonata* n. - SILVESTRI, p. 329, Plate 6 (14).
1958 *G.umbonata* - PARKER, p. 266, Plate 3 (19-20).
1975 *G.umbonata* - SEILER, p. 90, Plate 2 (27-28).

Laticarinina pauperata **(PARKER & JONES)**
*1865 *Pulvinulina repanda* var. *menardii* d'ORBIGNY subvar. *pauperata* n. - PARKER & JONES, p. 395, Plate 16 (50-51).
1953 *L. pauperata* - PHLEGER *et al.*, p. 49, Plate 11 (5-6).
1992 *L. pauperata* - TIMM, p. 58, Plate 7 (13).

Lenticulina gibba **(d'ORBIGNY)**
*1839 *Cristellaria gibba* n. - d'ORBIGNY, p. 40, Plate 7 (20-21).
1960 *L. gibba* - BARKER, p. 144, Plate 69 (8-9).

Marginulina glabra **d'ORBIGNY**
*1826 *M. glabra* n. - d'ORBIGNY, 259, fig. 55.
1923 *M. glabra* - CUSHMAN, p. 127, Plate 36 (5-6).
1992 *M. glabra* - STRUCK, p. 17, Plate 4 (7).

Melonis barleeanum **(WILLIAMSON)**
*1858 *Nonionina barleeana* n. - WILLIAMSON, p. 32, Plate 3 (68-69).
1981 *N. barleeanum* - SEJRUP *et al.*, p. 293, Plate 1 (12).
1987 *M. barleeanum* - JORISSEN, p. 42, Plate 4 (8).

Melonis pompilioides **(FICHTEL & MOLL)**
*1798 *Nautilus pompilioides* n. - FICHTEL & MOLL, p. 31.
1979 *M. pompilioides* - LUTZE, p. 428, Plate 2 (1 a-b).

Nodosaria subsoluta **CUSHMAN**
*1923 *N. subsoluta* n. - CUSHMAN, p. 74, Plate 13 (1).

Nonionellina labradorica **(DAWSON)**
*1879 *Nonionina labradorica* n. - DAWSON, ELLIS & MESSINA 1940, p. 14167.
1953 *N. labradorica* - LOEBLICH & TAPPAN, p. 86, Plate 17 (1-2).
1981 *N. labradorica* - SEJRUP *et al.*, p. 293, Plate 2 (5-6).

Nonionella auricula **HERON-ALLEN & EARLAND**
*1930 *N. auricula* n. - HERON-ALLEN & EARLAND, p. 192, Plate 5 (68-70).
1971 *N. auricula* - FEYLING-HANSSEN *et al.*, p. 265, Plate 10 (7-9).

Oolina hexagona **(WILLIAMSON)**
*1858 *Entosolenia squamosa (MONTAGU)*, var. *hexagona* n. - WILLIAMSON, p. 20, Plate 2 (23).
1953 *O. hexagona* - LOEBLICH & TAPPAN, p. 69, Plate 14 (1-2).
1971 *O. hexagona* - FEYLING-HANSSEN *et al.*, p. 224, Plate 17 (6).

Oridorsalis umbonatus **(REUSS)**
*1851 *Rotalina umbonata* n. - REUSS, p. 275, Plate 5 (35).
1981 *O. umbonatus* - SEIJRUP *et al.*, p. 293, Plate 2 (2-3).

Osangularia culter **(PARKER & JONES)**
*1865 *Planorbulina farcta* var. *ungeriana* (d'ORBIGNY) *culter* n. subvar. - PARKER & JONES, p. 421, Plate 19 (1).
1975 *O. culter* - LEROY & HODGKINSON, p. 436, Plate 9 (18).
1982 *O. culter* - LARSEN, p. 72, Plate 25 (1-2).

Parafissurina groenlandica **STSCHEDRINA**
*1946 *P. groenlandica* n. - STSCHEDRINA, p. 144, 147, Plate 4 (19).
1977 *P. groenlandica* - LAGOE, p. 125, Plate 3 (17).
1980 *P. groenlandica* - TODD & LOW, p. 24, Plate 2 (6 a-b).

Patellina corrugata **WILLIAMSON**
*1858 *P. corrugata* n. - WILLIAMSON, p. 46, Plate 3 (86-89).
1953 *P. corrugata* - LOEBLICH & TAPPAN, p. 114, Plate 21 (4, 5).
1988 *P. corrugata* - LOEBLICH & TAPPAN, p. 306, Plate 320 (7-14).

Pullenia bulloides **(d'ORBIGNY)**
*1826 *Noninina sphaeroides* n. - d'ORBIGNY, p. 293, fig. 1, 43.
1971 *P. bulloides* - FEYLING-HANSSEN *et al.*, p. 266, Plate 10 (13-14).
1981 *P. bulloides* - SEJRUP *et al.*, p. 293, Plate 2 (8).

Pullenia quinqueloba **(REUSS)**
*1851 *Nonionina quinqueloba* n. - REUSS, p. 71, Plate 5 (31 a-b).
1964 *P. quinqueloba* - PHLEGER, p. 383, Plate 3 (23).
1989 *P. quinqueloba* - OKI, p. 149, Plate 7 (a-c).

Pyrgo rotalaria **LOEBLICH & TAPPAN**
*1953 *P. rotalaria* n. - LOEBLICH & TAPPAN, p. 47-48, Plate 6 (5-6).
1980 *P. rotalaria* - TODD & LOW, p. 24, Plate 2 (20).
1991 *P. rotalaria* - THIES, p. 27, Plate 14 (4 a-c) and 15 (1-21).

Quinqueloculina pygmaea **REUSS**
*1851 *Q. pygmaea* n. - REUSS, p. 53.
1974 *Q. pygmaea* - LUCZKOWSKA, p. 60, Plate 27 (2).

Quinqueloculina seminula **(LINNÉ)**
*1758 *Serpula seminulum* n. - LINNÉ, p. 786, Plate 2 (1).
1962 *Q. seminula* - HAAKE, p. 31, Plate 1 (13-14).
1971 *Q. seminulum* - FEYLING-HANSSEN *et al.*, p. 194, Plate 1 (18-20).

Rupertina stabilis **WALLICH**
*1877 *R. stabilis* n. - WALLICH, p. 502.
1953 *R. stabilis* - PHLEGER et al, p. 50, Plate 11 (19).
1988 *R. stabilis* - LUTZE & ALTENBACH, p. 31-46, fig. 3-5.

Sigmoilopsis schlumbergeri **(SILVESTRI)**
*1904 *Sigmoilina schlumbergeri* n. - SILVESTRI, p. 267.
1960 *S. schlumbergeri* - BARKER, p. 16, Plate 8 (1-4).

Siphotextularia rolshauseni **PHLEGER & PARKER**
*1951 *S. rolshauseni* n. - PHLEGER & PARKER, p. 4, Plate 1 (23-24).
1992 *S. rolshauseni* - STRUCK, p. 21, Plate 2 (5-7).
1994 *S. rolshauseni* - NEES & STRUCK, p. 238, Plate 1.

Stetsonia horvathi **(GREEN)**
*1960 *S. horvathi* n. - GREEN, p. 72, Plate 1 (6).
1989 *S. horvathi* - NEES, p. 12, Plate 3 (4).
1991 *S. arctica* - SCOTT & VILKS, p. 35, Plate 3 (5-14).

Trifarina angulosa **(WILLIAMSON)**
1971 *T. angulosa* n. - MURRAY, p. 123, Plate 51.
1981 *T. angulosa* - SEJRUP *et al.*, p. 293, Plate 2 (10).
1992 *T. angulosa* - STRUCK, p. 21, Plate 5 (2).

Triloculina trihedra **LOEBLICH & TAPPAN**
*1953 *T. trihedra* n. - LOEBLICH & TAPPAN, p. 45, Plate 4 (10).
1960 *T. tricarinata* - BARKER, p. 6, Plate 3 (17 a-b).
1964 *T. tricarinata* - FEYLING-HANSSEN, p. 258, Plate 6 (7-8).

Uvigerina peregrina **CUSHMAN**
*1923 *U. peregrina* n. - CUSHMAN, p. 166, Plate 42 (7-10).
1947 *U. peregrina* - HÖGLUND, p. 279, Plate 23 (9), text Fig. 291-304.
1971 *U. peregrina* - FEYLING-HANSSEN *et al.*, p. 241, Plate 7 (9-11).

Faunal groups (s. main body of text):

Cassidulina sp. group
Elphidium sp. group
Lagenida sp. group
agglutinated tubes group

Appendix 3.1. Count data, fraction 125 - 2,000 µm, Core PS 1906 (specimens/gram dry sediment).

depth (cm)	age (y BP)	dry wt. (g)	agg. grp. *A. aggl.*	*B. trig.*	*B. stri.*	*C. flet.*	*C. loba.*	*C. plan.*	*C. reni.*	*C. subg.*	*C. wuel.*	*Cas.*	*E. tumi.* grp.	*Elp*	*F. fusi.* grp.
0.5	700	47.66	0.00	0.34	5.37	0.00	65.80	59.09	0.00	5.37	13.09	421.32	118.17	21.49	10.74	0.00
1.5	2,100	33.90	11.33	3.78	3.78	0.00	64.90	98.17	0.00	0.00	8.26	413.69	113.51	7.55	15.10	0.00
2.5	3,500	54.59	4.69	0.29	0.00	0.00	50.41	63.31	2.34	0.00	5.86	327.09	114.89	28.14	11.72	0.00
3.5	4,900	44.62	1.43	0.00	0.00	0.00	27.61	20.08	0.00	0.00	5.20	230.21	44.46	31.56	11.47	0.00
4.5	6,300	46.19	0.00	0.00	2.77	0.00	43.30	11.08	0.00	0.00	5.89	330.11	11.08	11.08	5.54	0.00
5.5	7,700	49.77	0.00	0.00	2.57	0.00	41.15	0.00	0.00	0.00	16.07	453.29	2.57	12.86	0.00	0.00
6.5	7,900	52.68	0.00	0.00	0.00	0.00	41.31	0.00	0.00	0.00	4.86	334.09	4.86	14.58	2.43	0.00
7.5	8,100	44.27	1.45	0.00	0.00	0.00	21.69	0.00	0.00	0.00	10.48	264.56	8.67	14.46	0.00	1.45
8.5	8,300	49.69	0.00	0.32	1.29	0.00	12.24	0.00	0.00	0.00	16.10	175.17	2.58	10.30	0.00	0.00
9.5	8,500	52.33	0.00	0.31	3.67	0.00	6.42	0.00	0.00	0.00	8.87	96.31	4.89	15.90	1.22	1.22
10.5	8,700	49.30	0.00	0.00	0.00	0.00	37.65	2.60	0.00	0.00	5.52	276.84	10.39	9.09	1.30	0.00
11.5	8,900	33.61	0.00	0.00	5.71	0.00	22.85	0.00	0.00	0.00	10.00	215.65	7.62	17.14	0.00	0.00
12.5	9,100	38.58	0.00	0.21	0.00	0.00	13.48	0.83	0.00	0.00	6.84	94.35	13.27	9.95	0.00	0.00
13.5	9,300	46.31	0.00	0.17	0.00	0.00	11.92	0.00	0.00	0.00	4.66	73.94	12.44	15.89	0.00	0.00
14.5	9,618	55.40	1.16	0.94	0.00	0.00	3.54	0.00	0.00	0.00	2.96	19.86	9.82	5.78	0.00	0.00
15.5	9,700	50.01	0.64	0.72	0.00	0.00	1.48	0.00	0.00	0.00	0.76	9.28	9.60	5.12	0.64	0.00
16.5	10,018	45.11	1.42	2.04	0.00	0.00	1.60	0.00	0.00	0.00	1.46	15.34	11.35	8.16	0.00	0.00
17.5	10,335	54.83	0.00	0.84	0.00	0.00	2.74	0.00	0.00	0.00	0.47	21.08	12.55	3.79	0.00	0.00
18.5	10,653	41.98	0.00	0.10	0.00	0.00	0.38	0.38	0.00	0.00	0.38	7.05	6.86	3.91	0.38	0.00
19.5	10,971	48.53	0.00	0.16	0.00	0.00	0.49	0.00	0.00	0.00	0.16	4.20	7.09	2.31	0.00	0.00
20.5	11,288	42.11	0.00	0.71	0.00	0.00	1.00	0.00	0.00	0.00	0.14	3.56	4.61	1.71	0.57	0.00
21.5	11,606	39.69	0.00	0.38	0.00	0.00	0.00	0.10	0.00	0.00	0.05	0.78	1.91	0.50	0.20	0.00
22.5	11,924	50.91	0.00	0.55	0.16	0.16	0.20	0.00	0.00	0.00	0.04	0.75	2.91	0.00	0.31	0.00
23.5	12,241	49.19	0.00	0.45	0.00	0.00	0.00	0.00	0.00	0.00	0.00	0.06	0.69	0.00	0.65	0.00
24.5	12,980	48.01	0.00	2.71	0.00	0.00	0.02	0.00	0.00	0.02	0.12	4.77	28.31	1.33	0.10	0.00
25.5	14,140	60.40	0.00	0.00	0.00	4.24	0.00	4.37	0.00	0.00	1.19	33.64	122.78	0.00	4.64	0.00
26.5	15,300	59.37	0.00	0.00	0.00	0.00	0.13	0.13	0.00	0.00	0.27	39.35	157.12	0.00	0.54	0.00
27.5	16,460	35.07	0.00	0.23	1.82	0.00	0.11	3.65	0.00	0.00	0.91	20.64	87.60	5.47	0.00	0.00
28.5	16,818	32.34	0.00	0.49	0.49	0.00	0.12	0.00	0.00	0.00	1.98	2.47	4.95	7.42	0.00	0.00
29.5	17,175	25.80	0.00	2.09	0.00	0.00	0.00	0.00	0.00	0.00	1.55	0.16	1.86	5.58	0.00	0.00
30.5	18,737	60.98	0.00	0.10	0.00	0.00	1.67	0.00	0.00	0.00	0.23	2.62	0.26	0.00	0.00	0.00
31.5	19,094	50.05	0.00	0.96	0.00	0.00	1.04	0.00	0.00	3.52	0.04	1.78	4.48	0.00	0.02	0.00
32.5	19,452	64.57	0.00	0.99	0.00	0.00	0.02	0.00	0.00	1.98	0.00	7.73	40.76	0.00	0.05	0.00
33.5	19,810	71.73	0.00	0.22	1.78	0.00	0.22	1.78	0.00	8.92	0.67	17.29	90.90	0.00	0.00	0.00
34.5	20,168	59.96	0.00	0.53	0.13	0.00	0.40	0.00	0.00	2.13	0.67	28.82	60.71	0.00	0.00	0.00
35.5	20,525	56.95	0.00	3.37	2.25	0.00	4.50	4.50	0.00	2.25	1.40	28.80	80.21	6.74	0.14	0.00
36.5	20,883	66.73	0.00	1.32	0.00	0.00	0.00	1.92	0.00	3.84	2.64	14.99	56.71	13.43	0.00	0.00
37.5	21,241	63.56	0.00	1.76	1.01	0.00	1.01	0.00	0.00	0.00	4.78	3.27	21.15	11.08	0.00	0.00
38.5	21,599	48.71	0.00	0.41	0.00	0.00	0.00	0.00	0.00	0.00	1.31	2.30	5.26	3.28	0.00	0.00
39.5	22,100	38.95	0.00	0.41	0.00	0.00	0.82	0.82	0.00	0.00	0.92	0.62	3.29	2.88	0.00	0.00
40.5	22,314	40.09	0.00	0.45	0.00	0.00	1.20	0.05	0.00	0.40	0.50	1.05	0.85	2.39	0.00	0.00
41.5	22,816	50.30	0.00	0.40	0.00	0.00	0.64	0.00	0.00	0.00	1.67	0.08	0.00	4.45	0.00	0.00
42.5	23,318	35.81	0.00	0.11	0.00	0.00	0.00	0.00	0.00	0.00	1.90	0.00	1.79	3.57	0.00	0.00

depth (cm)	*subg. L.*	*Lag. gibba*	grp. *M. barl.*	*N. subs. O. hexa.*	*O. umbo. P. corr.*	*P. rota. Q. semi.*	*S. arct. S. rols.*	*T. angu. T. trih.*	total
0.5	21.49	0.00	18.13	11.08	0.00	5.37	107.43	0.00	86.61	26.86	70.16	0.00	0.00	162.15	1,248.51
1.5	41.53	0.00	13.45	0.71	0.00	3.78	143.95	0.00	64.90	0.00	33.98	0.00	0.00	151.27	1,212.98
2.5	58.62	0.00	4.98	2.64	0.00	2.34	110.20	0.00	43.96	0.00	9.38	0.00	0.00	98.48	960.18
3.5	35.86	0.00	5.38	7.53	0.00	1.43	126.40	0.00	18.65	0.00	15.78	0.00	0.00	45.90	638.28
4.5	36.03	0.00	6.58	11.43	0.00	0.00	213.73	0.00	45.03	2.77	13.86	0.00	0.00	55.42	824.07
5.5	41.15	0.00	2.57	2.57	0.00	0.00	205.75	0.00	67.51	0.00	7.72	0.00	0.00	100.30	987.58
6.5	55.88	2.43	5.47	2.43	0.00	2.43	263.02	0.00	34.02	0.00	17.01	0.00	0.00	121.49	928.17
7.5	52.04	0.00	3.98	0.00	0.00	0.00	374.79	1.45	40.12	5.78	5.78	0.00	0.00	170.59	1,006.19
8.5	60.54	0.00	3.54	2.58	0.00	0.00	465.61	0.00	33.81	1.61	7.73	0.00	0.00	151.98	955.69
9.5	56.26	0.00	2.45	1.22	0.00	0.00	376.99	0.00	24.46	1.22	3.67	1.22	0.00	103.96	711.48
10.5	40.24	0.00	2.60	7.79	0.00	0.00	277.48	0.00	28.56	0.00	7.79	0.00	0.00	115.86	845.44
11.5	51.41	0.00	7.14	1.90	0.00	0.00	331.33	0.00	29.04	1.90	15.23	0.00	0.00	176.14	919.25
12.5	38.98	0.00	3.53	0.21	0.00	0.00	378.64	0.00	14.10	0.83	7.47	0.00	0.00	83.77	677.45
13.5	69.79	0.00	2.25	1.38	0.00	0.00	258.61	0.00	5.53	0.00	6.91	0.69	0.00	73.59	540.53
14.5	50.83	0.00	0.58	0.00	0.00	0.00	141.16	0.00	1.08	0.00	4.62	0.58	0.00	32.35	276.39
15.5	55.67	0.64	0.12	0.00	0.00	0.00	127.61	0.00	0.48	0.00	6.40	1.28	0.00	19.28	240.39
16.5	31.92	0.00	1.46	0.75	0.00	0.00	129.37	0.00	2.79	0.00	1.42	0.00	0.00	14.90	224.70
17.5	33.56	0.00	0.33	1.17	0.00	0.00	98.27	0.00	0.47	0.29	2.33	0.00	0.00	9.92	188.15
18.5	19.06	0.00	0.38	0.38	0.00	0.00	37.35	0.00	0.00	0.00	6.10	0.00	0.00	1.91	84.99
19.5	20.77	0.00	0.16	0.49	0.00	0.00	16.73	0.00	0.00	0.00	1.65	0.00	0.00	0.16	54.40
20.5	13.68	0.00	0.38	0.00	0.00	0.00	16.29	0.00	0.05	0.00	0.57	0.19	0.00	0.19	43.70
21.5	2.32	0.10	0.15	0.18	0.00	0.00	7.99	0.00	0.00	0.00	0.71	0.00	0.00	0.10	15.47
22.5	1.41	0.00	0.04	0.31	0.00	0.00	5.58	0.00	0.00	0.00	0.00	0.16	0.00	0.47	13.04
23.5	0.00	0.00	0.02	0.02	0.00	0.00	5.96	0.00	0.00	0.00	0.00	0.00	0.00	0.00	8.17
24.5	2.69	0.00	1.69	1.50	0.00	0.00	106.48	0.00	0.00	0.00	2.67	0.02	0.00	0.02	152.51
25.5	12.85	6.49	3.84	6.23	0.00	0.00	447.81	0.00	2.91	0.00	0.00	2.12	0.00	0.00	655.50
26.5	17.25	4.31	6.06	13.74	0.00	0.00	521.74	0.00	0.67	0.00	0.00	4.31	0.00	0.67	784.10
27.5	14.60	1.82	1.94	1.82	0.00	0.00	285.14	0.00	1.48	0.00	0.00	5.47	0.00	21.90	457.14
28.5	13.85	0.00	4.58	5.44	0.00	0.49	64.69	1.48	0.62	0.49	7.42	25.73	0.00	36.61	182.31
29.5	3.72	0.00	0.00	4.65	0.00	0.00	35.27	1.86	0.93	1.24	2.48	12.40	0.00	22.33	97.75
30.5	3.67	0.00	0.31	0.00	0.00	0.00	18.89	0.00	0.13	0.00	0.00	0.00	0.00	5.51	33.40
31.5	2.56	0.00	0.02	0.00	0.00	0.00	20.84	0.00	0.14	0.02	0.00	0.00	0.00	2.88	38.28
32.5	0.99	0.00	0.29	5.23	0.00	0.00	96.76	0.00	0.05	0.00	0.00	0.06	0.00	1.01	156.96
33.5	2.01	0.00	5.02	4.46	0.00	0.00	237.11	0.00	0.11	0.00	0.11	0.22	0.00	3.79	375.07
34.5	2.27	6.54	5.74	7.61	0.00	0.00	374.78	2.13	1.20	0.00	0.00	4.80	0.00	10.81	510.21
35.5	8.99	2.25	4.92	10.96	0.00	0.00	330.40	2.25	0.98	0.00	0.00	9.55	2.25	51.83	564.28
36.5	21.10	0.00	6.71	10.67	0.00	0.12	280.77	0.00	1.20	0.12	0.00	30.93	0.00	59.70	516.95
37.5	28.19	0.00	5.79	6.29	0.00	0.00	144.24	3.02	0.00	0.00	3.02	41.28	0.00	64.44	349.65
38.5	4.68	0.66	0.00	2.14	0.00	0.00	48.37	0.66	0.25	0.00	0.82	18.39	0.00	19.71	108.31
39.5	2.46	0.00	1.23	2.98	0.00	0.41	62.34	1.23	1.23	0.00	2.88	8.32	0.00	12.32	106.60
40.5	3.59	0.00	0.05	2.39	0.00	0.00	43.15	0.80	1.00	0.05	0.80	15.27	0.00	6.39	82.56
41.5	3.18	0.00	0.08	1.27	0.64	0.00	51.61	0.64	1.35	0.00	1.91	30.62	0.00	14.71	114.99
42.5	5.36	0.00	1.90	4.58	0.00	0.00	49.48	1.79	2.23	0.89	3.69	38.65	0.00	19.66	136.50

Appendix 3.2. Count data, fraction 125 - 2,000 µm, Core M 23256 (specimens/gram dry sediment).

depth	age	dry wt.	agg. grp.			C. loba.		C. subg.		Cas. grp.		E. exig.		Elp. grp.	G. subg
(cm)	(y BP)	(g)	A. aggl.		B. stri.		C. reni.		C. wuel.		D. paup.		E. tumi.		F. marg.
6	9.106	34,60	0,00	0,00	0,00	0,00	0,00	110,98	312,60	45,78	0,46	0,92	0,00	0,00	0,00	8,32
8	9.260	28,32	0,00	0,00	0,00	0,00	0,00	45,20	246,61	49,72	0,00	1,69	0,00	0,00	0,00	8,47
10	9.415	39,78	0,00	0,00	0,00	0,00	0,00	49,07	259,83	52,29	0,40	0,40	0,00	0,00	0,00	5,23
12	9.569	35,32	0,00	0,23	0,00	0,00	0,00	48,92	254,13	32,62	0,00	1,36	0,00	0,00	0,00	6,34
14	9.723	26,92	0,00	0,00	0,00	0,00	0,00	10,40	240,71	12,78	0,89	0,00	0,00	0,00	0,00	10,70
16	10.060	38,53	0,00	0,00	0,00	0,42	0,00	11,21	178,56	4,15	0,00	0,00	0,00	0,00	0,00	14,12
18	10.580	40,32	0,00	0,20	0,00	0,00	0,00	6,05	33,63	0,99	0,10	0,00	0,00	0,00	0,00	3,77
20	11.100	35,69	0,00	0,00	0,00	0,00	0,00	2,19	15,19	1,79	0,00	0,00	0,00	0,00	0,00	1,34
22	11.620	30,36	0,00	0,00	0,00	0,00	0,53	0,86	8,04	0,26	0,00	0,00	0,00	0,00	0,00	0,00
24	12.140	42,92	0,00	0,00	0,00	0,19	0,00	0,19	2,75	0,37	0,00	0,00	0,00	0,00	0,00	0,00
26	12.534	30,31	0,00	0,00	0,00	0,40	0,13	0,40	2,84	0,26	0,00	0,00	0,00	0,00	0,00	0,00
28	12.803	39,80	0,00	0,00	0,00	0,00	0,00	0,15	1,06	0,10	0,00	0,00	0,00	0,00	0,00	0,00
30	13.071	28,53	0,07	0,00	0,00	0,00	0,14	0,32	2,24	0,21	0,00	0,00	0,00	0,00	0,00	0,00
32	13.340	29,95	0,00	0,00	0,00	0,00	0,13	0,37	1,44	0,07	0,00	0,00	0,00	0,00	0,00	0,07
34	13.609	32,25	0,00	0,00	0,00	0,00	0,12	0,43	1,55	0,12	0,00	0,00	0,12	0,00	0,00	0,00
36	13.877	30,73	0,00	0,00	0,03	0,26	0,00	0,46	2,80	0,00	0,00	0,00	0,00	0,00	0,00	0,26
38	14.146	33,99	0,00	0,00	0,00	0,00	0,00	0,62	1,24	0,12	0,00	0,00	0,00	0,00	0,12	0,00
40	14.414	27,93	0,00	0,00	0,00	0,00	0,00	0,82	1,90	0,00	0,00	0,00	0,00	0,00	0,00	0,00
42	14.683	30,44	0,00	0,03	0,00	0,00	0,00	0,30	1,31	0,13	0,00	0,00	0,00	0,00	0,00	0,00
44	14.952	32,57	0,00	0,00	0,00	0,00	0,00	0,00	0,46	0,00	0,00	0,00	0,00	0,25	0,00	0,00
46	15.220	39,71	0,00	0,00	0,00	0,00	0,00	0,00	0,40	0,00	0,00	0,00	0,00	0,00	0,00	0,00
48	15.489	27,86	0,00	0,00	0,00	0,00	0,00	0,39	0,54	0,00	0,00	0,00	0,00	0,00	0,00	0,00
50	15.757	19,83	0,00	0,00	0,00	0,81	0,00	0,61	3,43	0,00	0,00	0,00	0,00	0,81	0,00	0,00
52	16.026	37,40	0,00	0,00	0,00	0,00	0,00	0,00	0,11	0,00	0,00	0,00	0,00	0,00	0,00	0,00
54	16.294	31,55	0,00	0,00	0,00	0,00	0,00	0,00	0,00	0,00	0,00	0,00	0,00	0,00	0,00	0,00
56	16.563	23,11	0,00	0,00	0,00	0,00	0,00	0,00	0,00	0,69	0,00	0,00	0,00	0,00	0,00	0,00
58	16.783	13,97	0,00	0,00	0,00	0,00	1,15	0,00	0,00	0,00	0,00	0,00	0,00	0,00	0,00	0,00
60	17.100	35,52	0,00	0,00	0,00	0,00	0,00	0,00	0,00	0,00	0,00	0,00	0,00	0,00	0,00	0,00
62	17.320	44,42	0,00	0,00	0,00	0,00	0,00	0,00	0,00	0,00	0,00	0,00	0,00	0,00	0,00	0,00
64	17.540	25,78	0,00	0,16	0,00	0,00	0,00	0,00	0,00	0,16	0,04	0,00	0,00	0,00	0,00	0,16
66	17.760	29,30	0,00	0,00	0,00	0,27	0,00	0,03	0,03	0,00	0,00	0,00	0,00	0,00	0,00	0,14
68	17.980	33,36	0,00	0,00	0,00	0,00	0,00	0,06	0,03	0,33	0,00	0,00	0,00	0,00	0,00	0,96
70	18.200	25,35	0,00	0,00	0,00	0,04	0,00	0,04	0,00	0,16	0,00	0,00	0,00	0,00	0,00	0,79
72	18.325	36,38	0,00	0,00	0,00	0,00	0,00	0,00	0,00	0,00	0,00	0,00	0,00	0,00	0,00	0,44
74	18.450	32,12	0,00	0,00	0,00	0,00	0,00	0,25	0,06	0,00	0,00	0,00	0,00	0,00	0,00	0,25
76	18.574	34,25	0,00	0,00	0,00	0,00	0,00	0,00	0,06	0,00	0,00	0,00	0,00	0,00	0,00	0,00
78	18.699	31,33	0,00	0,00	0,00	0,00	0,00	0,00	0,13	0,00	0,00	0,00	0,00	0,00	0,00	0,00
80	18.824	18,92	0,00	0,00	0,00	0,00	0,00	0,00	0,00	0,63	0,00	0,00	0,00	0,00	0,00	0,85

Appendix 3.2. *continued*

depth	Lag. grp.		N. labr.		P. bull.		P. quin.		S. arct.		T. trih.		total
(cm)	L. gibba		M. bari.		O. umbo.		P. groe.		P. rota.		S. rols.		U. pere.	
6	0,00	1,85	1,39	0,92	141,50	0,00	0,00	0,00	12,25	0,00	0,00	0,00	0,00	636,99
8	0,12	0,85	2,26	0,56	145,20	0,28	0,56	0,00	10,73	0,00	0,00	0,00	0,00	512,26
10	0,24	2,01	0,40	0,00	92,11	0,00	0,40	0,00	10,46	0,00	0,00	0,00	0,00	472,83
12	0,00	2,27	1,36	1,81	144,96	0,00	0,45	0,00	6,34	0,45	0,00	0,45	0,00	501,70
14	0,00	2,08	1,19	0,00	153,64	0,00	0,00	0,00	4,46	0,30	0,00	0,30	0,00	437,44
16	0,00	0,83	2,08	0,00	184,38	0,00	0,00	0,00	3,53	0,00	0,00	0,00	0,00	399,27
18	0,00	0,40	0,60	0,00	44,84	0,00	0,00	0,00	0,79	0,60	0,00	0,40	0,00	92,36
20	0,00	0,06	0,00	0,00	21,07	0,00	0,00	0,00	0,45	0,00	0,00	0,00	0,00	42,08
22	0,00	0,00	0,00	0,00	6,59	0,00	0,00	0,00	0,26	0,00	0,00	0,00	0,00	16,53
24	0,00	0,00	0,19	0,00	1,68	0,00	0,00	0,00	0,19	0,00	0,00	0,00	0,00	5,55
26	0,00	0,00	0,13	0,00	1,45	0,00	0,00	0,00	0,20	0,13	0,00	0,13	0,00	6,07
28	0,00	0,00	0,00	0,00	1,11	0,00	0,10	0,00	0,18	0,00	0,00	0,00	0,00	2,69
30	0,00	0,04	0,00	0,00	1,19	0,00	0,00	0,00	0,25	0,07	0,00	0,07	0,00	4,59
32	0,00	0,00	0,00	0,00	0,27	0,00	0,00	0,00	0,10	0,00	0,00	0,00	0,00	2,44
34	0,00	0,00	0,00	0,00	0,12	0,00	0,00	0,00	0,19	0,00	0,00	0,00	0,00	2,67
36	0,00	0,00	0,03	0,00	1,04	0,00	0,00	0,00	0,33	0,00	0,00	0,00	0,00	5,21
38	0,00	0,00	0,00	0,00	1,18	0,00	0,00	0,00	0,21	0,00	0,00	0,00	0,00	3,47
40	0,00	0,00	0,00	0,14	2,72	0,00	0,00	0,00	0,32	0,29	0,00	0,00	0,00	6,19
42	0,00	0,00	0,00	0,00	4,57	0,00	0,00	0,20	0,13	0,26	0,00	0,00	0,00	6,93
44	0,00	0,00	0,00	0,00	0,49	0,00	0,00	0,06	0,00	0,00	0,00	0,00	0,00	1,26
46	0,00	0,00	0,00	0,00	0,00	0,00	0,00	0,00	0,00	0,00	0,00	0,00	0,00	0,40
48	0,00	0,00	0,00	0,00	0,00	0,00	0,00	0,00	0,04	0,00	0,00	0,00	0,00	0,97
50	0,00	0,00	0,00	0,00	1,61	0,00	0,00	0,00	0,20	0,00	0,00	0,00	0,00	7,46
52	0,00	0,00	0,00	0,00	0,86	0,00	0,00	0,00	0,00	0,00	0,00	0,00	0,00	0,96
54	0,00	0,00	0,00	0,00	0,00	0,00	0,00	0,00	0,00	0,00	0,00	0,00	0,00	0,00
56	0,03	0,00	2,77	0,00	1,38	0,00	0,00	0,00	0,00	0,00	0,00	0,00	0,00	4,88
58	0,12	0,00	1,15	0,57	0,00	0,00	0,00	0,00	0,00	0,00	0,00	0,00	0,00	2,98
60	0,00	0,00	0,00	0,00	0,00	0,00	0,00	0,00	0,00	0,00	0,00	0,00	0,00	0,00
62	0,00	0,00	0,00	0,00	0,00	0,00	0,00	0,00	0,00	0,00	0,00	0,00	0,00	0,00
64	0,00	0,00	0,16	0,00	2,83	0,00	0,00	0,00	0,00	0,00	0,00	0,00	0,00	3,49
66	0,01	0,00	0,38	0,00	1,30	0,00	0,00	0,00	0,00	0,14	0,00	0,00	0,00	2,30
68	0,01	0,12	1,02	0,00	0,03	0,00	0,00	0,00	0,00	0,24	1,23	1,20	0,00	5,23
70	0,00	0,16	0,91	0,00	0,16	0,00	0,00	0,00	0,00	0,04	0,32	0,16	0,00	2,76
72	0,00	0,05	2,36	0,00	1,81	0,00	0,00	0,00	0,00	0,00	0,00	0,00	0,00	4,67
74	0,00	0,06	1,12	0,00	1,00	0,00	0,00	0,00	0,00	0,00	0,00	0,25	0,00	2,99
76	0,00	0,06	0,99	0,00	0,47	0,00	0,00	0,00	0,00	0,00	0,00	0,00	0,06	1,64
78	0,00	0,00	0,32	0,00	0,83	0,00	0,00	0,00	0,00	0,00	0,00	0,26	0,00	1,53
80	0,00	0,05	0,63	0,00	1,53	0,00	0,00	0,00	0,00	0,85	0,42	0,21	0,00	5,18

Appendix 3.3. Count data, fraction 125 - 2,000 µm, Core M 23068 (specimens/gram dry sediment).

depth (cm)	age (y BP)	dry wt. (g)	*A. aggl.*	*A. glob.* agg.	*B. marg.* grp.	*C. subg.*	*C. wuel.*	*Cas.*	*D. baggi* grp.	*D. cuvi.*	*D. frob.*	*D. paup.*	*E. tumi.*	*Elp.*	*F. fusi.* grp.	*F. marg.*
0,5	202	14,97	6,41	1,74	8,55	0,00	105,93	453,38	210,79	0,00	0,00	0,00	0,67	8,55	0,00	2,14	0,00
2,5	1.014	14,49	0,00	0,00	0,00	0,00	75,85	380,43	112,84	0,35	0,00	0,00	1,38	7,73	0,00	4,42	0,00
4,5	1.825	12,27	3,26	0,00	1,30	0,00	67,15	520,90	159,73	0,00	0,00	0,00	3,26	5,87	0,00	0,00	0,00
6,5	2.636	18,24	0,00	0,66	0,88	0,00	53,52	300,71	159,68	0,00	0,00	0,44	0,66	2,19	0,00	0,00	0,00
8,5	3.447	16,38	0,00	0,00	0,12	0,00	54,27	313,35	172,27	0,24	0,00	0,00	0,24	1,40	0,00	0,00	0,00
10,5	4.258	14,82	0,00	7,02	0,00	0,00	79,82	363,70	156,01	0,00	0,00	0,54	0,00	1,42	0,00	0,00	0,00
12,5	5.069	19,55	0,00	2,40	0,00	0,00	45,43	354,31	110,51	0,61	0,00	0,00	0,00	1,74	0,00	0,00	0,00
14,5	5.880	18,33	2,02	3,27	0,00	0,00	47,19	410,37	57,61	0,00	0,00	0,00	0,00	0,65	0,00	0,00	0,00
16,5	6.692	20,11	4,77	5,57	0,00	0,00	39,97	356,98	17,50	0,00	0,00	0,20	0,00	0,00	0,00	0,00	0,00
18,5	7.501	15,92	5,02	3,27	0,00	0,00	34,79	432,73	109,41	0,00	0,00	0,38	1,13	1,32	0,00	0,00	3,01
20,5	7.750	17,44	1,84	3,21	0,46	0,00	32,69	444,39	25,70	0,00	0,00	0,00	0,00	0,00	0,00	0,00	0,00
22,5	8.684	16,13	0,00	1,36	0,12	0,00	18,35	187,00	3,72	0,00	0,00	0,00	0,00	0,00	0,00	0,00	0,00
23,5	9.139	14,84	0,00	2,97	3,24	0,00	22,92	152,75	2,16	0,00	0,00	0,00	0,00	0,00	0,00	0,00	0,00
24,5	9.604	14,29	0,00	1,12	1,12	0,00	17,08	187,01	0,56	0,00	0,00	0,00	0,00	0,00	0,00	0,00	0,00
25,5	9.893	16,23	0,49	2,71	4,07	0,00	18,24	181,38	1,48	0,00	0,12	0,00	0,00	0,00	0,00	0,49	0,00
26,5	10.182	11,20	0,00	0,89	0,54	0,00	15,18	235,74	0,71	0,00	0,00	0,00	0,36	0,00	0,00	0,00	0,00
28,5	10.767	17,65	0,00	0,91	0,11	0,00	14,16	214,24	2,95	0,00	0,00	0,00	0,23	0,45	0,00	0,45	0,00
29,5	11.057	19,33	0,00	0,62	0,41	0,00	21,11	212,16	2,48	0,00	0,00	0,00	0,00	0,00	0,00	0,00	0,00
30,5	11.499	19,53	0,00	3,07	0,31	0,00	21,92	233,51	3,07	0,00	0,00	0,00	0,20	0,00	0,00	0,00	0,00
32,5	12.384	20,50	0,00	0,68	0,39	0,00	8,78	95,32	0,00	0,00	0,00	0,00	0,20	0,00	0,00	0,00	0,00
34,5	13.269	16,35	0,00	1,28	0,00	0,00	14,31	113,33	0,98	0,00	0,00	0,31	0,49	0,00	0,00	0,00	0,00
36,5	14.154	18,90	0,00	0,21	0,00	0,00	4,71	34,76	0,00	0,00	0,00	0,00	0,00	0,00	0,00	0,00	0,00
38,5	14.371	29,12	0,00	0,00	0,00	0,00	1,30	12,46	0,55	0,00	0,00	0,00	0,00	0,00	0,00	0,00	0,00
39,8	14.506	30,00	0,00	0,00	0,00	0,27	10,87	102,67	0,00	0,00	0,00	0,00	0,07	0,00	1,07	0,00	0,13
42,5	14.804	31,47	0,00	0,00	0,06	0,51	3,91	39,85	0,00	0,00	0,00	0,51	0,00	0,00	0,13	0,00	0,06
44,5	15.021	32,36	0,00	0,00	0,09	0,59	0,80	7,14	0,00	0,00	0,00	0,25	0,06	0,00	0,15	0,00	0,12
46,5	15.238	32,64	0,49	0,00	0,18	0,98	3,62	26,59	0,49	0,00	0,00	0,06	0,00	0,00	0,92	0,00	0,12
48,5	15.455	33,62	0,00	0,00	1,73	0,54	0,54	7,97	0,06	0,00	0,12	0,06	0,00	0,00	0,06	0,00	0,06
50,5	16.536	35,38	0,00	0,00	0,51	0,23	0,62	0,93	2,04	0,00	0,00	0,00	0,00	0,00	0,00	0,00	0,00
52,5	16.836	39,20	0,20	0,00	0,94	0,51	0,59	0,74	0,00	0,00	0,00	0,00	0,00	0,00	0,00	0,00	0,00
54,5	17.269	40,79	0,83	0,00	0,96	0,12	0,91	1,40	0,00	0,00	0,00	0,00	0,02	0,78	0,05	0,00	0,12
56,5	17.703	39,50	0,20	0,00	0,30	0,03	0,00	0,10	0,20	0,00	0,00	0,00	0,00	0,61	0,20	0,00	0,00
58,5	18.181	33,71	0,03	0,00	0,50	0,24	0,68	0,27	0,24	0,00	0,00	0,00	0,00	0,95	0,00	0,00	0,06
60,5	18.370	38,78	0,00	0,00	0,31	0,00	0,41	0,31	0,03	0,00	0,00	0,00	0,00	0,41	0,05	0,00	0,15

Appendix 3.3. *continued*

depth (cm)	*G. subg.*	*G. umbo.*	*L. gibba*	*Lag.*	*M. barl.* grp.	*M. glab.*	*N. labr.*	*O. umbo.*	*P. groe.*	*P. rota.*	*Q. pygm.*	*Q. semi.*	*S. arct.*	*S. rols.*	*S. schl.*	*T. trih.*	total
0,5	53,83	0,00	0,00	15,90	0,00	0,00	4,27	190,22	0,00	51,56	2,14	0,00	29,92	0,00	0,00	101,52	1.247,53
2,5	25,54	0,00	0,00	15,46	0,00	0,00	3,31	135,83	0,00	23,74	0,00	0,00	4,42	0,00	0,00	13,18	804,47
4,5	16,95	0,00	0,00	9,78	0,00	0,00	2,61	59,98	0,00	24,77	0,00	0,00	2,61	0,00	0,00	9,13	887,30
6,5	24,46	0,00	0,00	7,68	0,00	0,44	5,70	47,38	0,00	8,99	0,88	0,00	5,70	0,00	0,00	4,83	624,77
8,5	62,51	0,00	0,00	9,16	0,00	0,00	7,39	59,70	0,00	13,74	1,71	0,00	6,04	0,00	0,00	9,40	711,56
10,5	78,61	0,00	0,00	7,42	0,00	0,00	5,87	124,56	0,00	19,84	0,61	0,00	8,64	0,00	0,00	6,61	860,66
12,5	48,81	0,00	0,00	4,50	0,00	0,00	2,61	154,72	0,00	13,10	0,20	0,00	3,27	0,00	0,00	2,66	744,90
14,5	51,66	0,00	0,00	4,20	0,22	0,00	1,69	180,52	0,00	11,13	0,05	0,00	3,27	0,00	0,00	1,53	775,40
16,5	53,30	0,00	0,00	3,23	0,15	0,00	0,65	185,35	0,00	6,96	0,15	0,00	1,59	0,00	0,00	0,80	677,17
18,5	37,56	0,00	0,00	2,07	0,00	0,00	0,00	152,74	0,00	8,10	0,00	0,00	12,06	0,00	0,00	1,00	804,61
20,5	47,83	0,00	0,00	1,09	0,69	0,00	0,46	131,23	0,00	6,77	0,00	0,00	21,11	0,00	0,00	0,00	717,46
22,5	32,24	0,00	0,00	0,74	0,56	0,00	0,00	93,50	0,00	3,10	0,00	0,00	0,99	0,00	0,00	0,00	341,70
23,5	41,12	0,00	0,00	2,43	2,16	0,00	0,00	106,24	0,00	4,85	0,00	0,00	0,00	0,00	0,00	0,00	340,82
24,5	29,12	0,00	0,00	0,00	1,96	0,00	0,00	87,63	0,00	2,38	0,00	0,00	4,48	0,00	0,00	0,00	332,45
25,5	46,21	0,00	0,00	0,00	4,44	0,00	0,00	126,18	0,00	5,05	0,00	0,00	2,96	0,00	0,00	0,00	393,81
26,5	11,07	0,00	0,00	0,89	3,57	0,00	0,00	86,44	0,00	4,29	0,00	0,00	0,00	0,00	0,00	0,00	359,67
28,5	24,92	0,00	0,00	1,13	3,63	0,00	0,00	85,65	0,00	7,14	0,00	0,00	0,45	0,00	0,00	0,00	356,43
29,5	44,71	0,00	0,00	0,41	1,66	0,00	0,00	123,36	0,00	9,94	0,00	0,00	0,00	0,00	0,00	0,00	416,87
30,5	61,66	0,00	0,00	0,82	5,74	0,00	0,00	136,83	0,00	4,30	0,00	0,00	2,46	0,00	0,00	0,00	473,88
32,5	15,02	0,00	0,00	0,00	1,56	0,00	0,00	73,37	0,00	1,17	0,00	0,00	0,00	0,00	0,00	0,00	196,49
34,5	12,72	0,00	0,00	0,00	0,00	0,00	0,00	40,12	0,00	0,49	0,00	0,00	0,00	0,00	0,00	0,00	184,03
36,5	6,77	0,00	0,00	0,00	0,85	0,00	0,00	11,00	0,00	0,26	0,00	0,00	0,00	0,00	0,00	0,00	58,57
38,5	4,40	0,00	0,00	0,00	0,55	0,00	0,00	6,04	0,00	0,07	0,00	0,00	0,00	0,00	0,00	0,00	25,37
39,8	19,47	1,60	0,00	0,00	0,07	0,00	0,00	49,40	0,00	2,13	0,00	0,00	2,67	0,00	0,00	7,73	198,13
42,5	10,68	0,00	0,51	0,00	1,02	0,00	0,00	19,38	0,00	0,10	0,00	0,00	2,03	0,00	0,00	1,02	79,76
44,5	18,79	0,25	0,00	0,25	0,74	0,00	0,00	17,40	0,00	0,12	0,00	0,00	1,48	0,00	0,00	1,24	49,47
46,5	25,98	0,98	0,06	0,49	0,55	0,00	0,00	42,22	0,00	2,02	0,00	0,00	3,43	0,49	0,00	3,49	113,17
48,5	4,28	0,48	0,06	0,00	0,00	0,00	0,06	7,32	0,00	0,89	0,00	0,00	0,95	0,00	0,48	0,95	26,59
50,5	3,17	0,23	0,00	0,03	0,25	0,00	0,00	7,24	0,00	0,06	0,00	0,00	0,23	0,00	0,06	0,68	16,25
52,5	4,29	0,00	0,00	0,00	0,26	0,00	0,05	5,92	0,00	0,23	0,00	0,00	0,00	0,00	0,10	0,41	14,23
54,5	3,95	0,39	0,00	0,02	0,81	0,00	0,00	11,38	0,00	0,61	0,00	0,02	0,00	0,00	0,49	1,96	24,83
56,5	3,44	0,00	0,20	0,00	0,66	0,00	0,03	3,24	0,00	0,15	0,00	0,00	0,00	0,20	0,00	0,00	9,57
58,5	3,80	0,00	0,00	0,00	0,95	0,00	0,00	6,23	0,24	0,21	0,00	0,00	0,00	0,24	0,00	0,71	15,34
60,5	1,06	0,00	0,23	0,00	0,64	0,00	0,00	6,40	0,00	0,08	0,00	0,00	0,00	0,21	0,05	0,21	10,55

Appendix 3.4. Count data, fraction 125 - 2,000 µm, Core M 23414 (specimens/gram dry sediment).

depth (cm)	age (y BP)	dry wt. (g)	A. glob. A. aggl.	B. marg. agg. grp.	B. marg. B. pdp.	B. quad. B. strl.	C. fiel. C. loba.	C. reni. C. subg.	C. wuel. Cas. grp.	D. beggl. D. cuvl.	D. frob.
1.5	560	46.75	0.00 0.00	2.05 1.37	0.00	4.11 0.00	4.11 0.00	0.00 0.68	37.65 24.64	0.00 0.00	0.00
3.5	1.120	24.31	1.32 0.00	2.63 1.65	0.00	5.27 0.00	2.63 0.00	0.00 6.25	18.43 9.21	0.00 0.00	0.00
5.5	1.680	39.49	1.62 0.00	3.24 0.00	3.24	3.24 0.41	8.10 2.03	0.00 2.03	16.61 13.37	0.00 0.00	0.00
7.5	2.240	41.28	0.39 0.00	0.19 0.78	1.55	2.33 0.00	6.78 0.58	0.00 1.55	9.50 11.05	0.00 0.00	0.78
9.5	2.800	37.81	0.21 0.00	1.06 1.69	0.85	0.00 0.00	4.44 0.63	0.85 1.27	11.21 7.41	0.00 0.00	0.00
11.5	3.360	42.99	0.00 0.00	0.74 0.00	0.74	4.47 0.00	5.95 0.74	0.74 0.74	9.30 10.79	0.74 0.00	0.00
13.5	3.920	32.70	0.00 0.24	0.00 0.98	0.00	1.96 0.24	5.87 1.22	0.00 7.83	13.46 14.68	0.73 0.00	0.24
15.5	4.480	41.83	0.00 0.00	0.38 0.77	0.00	0.77 0.57	12.24 0.19	0.00 2.49	12.05 16.07	0.19 0.00	0.19
17.5	4.900	50.86	0.16 0.00	0.16 1.26	1.89	0.00 0.00	5.66 0.31	0.00 3.15	12.90 16.52	0.79 0.00	0.00
19.5	5.600	54.86	0.00 0.00	0.00 0.58	0.00	0.00 0.00	5.83 0.58	0.58 1.75	11.08 15.75	0.00 0.00	0.00
21.5	6.160	37.00	0.00 0.00	1.73 0.86	0.86	0.00 0.00	8.00 0.22	0.00 0.22	15.35 13.84	0.00 0.00	0.00
23.5	6.720	59.01	0.00 0.00	2.44 0.54	0.00	0.00 0.00	2.44 1.90	0.00 1.63	13.01 8.95	0.00 0.00	0.00
25.5	7.280	51.56	0.00 0.00	0.93 0.62	0.00	1.24 0.00	3.26 0.78	0.00 1.55	9.15 10.24	0.00 0.47	0.00
27.5	7.700	55.62	0.00 0.00	2.16 0.58	0.58	0.00 0.00	1.87 0.29	0.58 1.01	11.36 16.25	0.00 0.00	0.14
29.5	8.400	29.07	0.00 0.00	0.25 0.61	0.00	0.50 0.18	2.45 0.06	0.00 0.41	9.69 10.45	0.06 0.06	0.28
31.5	8.960	26.52	0.00 0.00	1.71 0.06	0.45	0.30 0.11	2.52 0.58	0.39 1.14	11.18 9.23	0.34 0.00	0.11
33.5	9.520	30.59	0.00 0.00	1.54 0.79	0.00	0.00 0.07	1.07 0.58	1.25 1.46	9.73 11.91	0.32 0.11	0.00
35.5	10.320	57.68	0.00 0.00	3.27 1.36	0.00	0.36 0.00	0.84 0.21	4.36 2.20	9.85 11.58	0.00 0.00	0.12
37	11.100	42.13	0.00 0.00	1.52 0.95	0.00	0.00 0.19	0.95 0.95	3.04 1.71	8.92 8.54	0.38 0.00	0.00
39	11.360	45.10	0.00 0.00	1.77 0.89	0.00	0.71 0.00	0.71 0.71	3.19 1.95	7.10 9.93	0.00 0.00	0.35
41	12.400	32.09	0.00 0.00	1.25 0.25	0.00	0.00 0.00	0.50 0.25	2.49 1.25	6.23 9.72	0.00 0.00	0.00
43	12.990	36.97	0.00 0.00	0.54 0.87	0.00	0.00 0.00	2.16 0.00	1.30 0.00	8.66 5.41	0.43 0.00	0.00
45	13.875	43.69	0.00 0.00	0.73 0.18	0.00	1.10 0.00	0.55 0.27	1.10 0.00	6.32 4.49	0.00 0.00	0.00
47	14.318	36.41	0.00 0.00	0.88 0.22	0.00	0.00 0.00	0.44 0.00	0.44 0.44	2.86 4.17	0.22 0.00	0.00
49	14.760	41.01	0.00 0.00	5.27 0.20	0.00	0.00 0.00	0.78 0.78	0.78 0.39	5.56 5.36	0.49 0.00	0.00
51	15.350	43.14	0.00 0.00	5.56 0.74	0.00	0.00 0.00	0.00 0.37	0.74 0.93	3.89 2.97	0.37 0.00	0.00
53	15.940	40.59	0.00 0.00	11.63 0.39	0.00	0.00 0.00	1.18 0.79	0.39 1.18	3.94 2.76	0.39 0.00	0.00
55	16.825	44.68	0.00 0.00	3.76 0.72	0.36	0.00 0.00	0.72 0.00	1.43 0.90	4.83 5.55	1.43 0.00	0.00
57	17.563	34.83	0.00 0.00	2.76 0.23	0.00	0.00 0.00	0.00 1.03	0.46 1.49	2.99 8.50	0.92 0.00	0.00
59	18.300	38.09	0.00 0.00	1.47 0.00	0.00	0.00 0.00	0.53 0.32	0.00 0.74	3.78 9.77	0.42 0.00	0.00
61	18.674	38.89	0.00 0.00	3.09 0.00	0.00	0.00 0.00	0.00 1.44	0.00 0.62	4.32 13.37	0.41 0.00	0.00
63	19.047	33.25	0.00 0.00	3.37 0.00	0.00	0.00 0.00	1.44 0.60	0.00 1.20	3.25 13.83	0.00 0.00	0.00
65	19.793	42.05	0.00 0.00	3.52 0.00	0.00	0.00 0.00	0.38 0.48	0.00 0.86	3.71 11.51	0.38 0.00	0.00
67	20.241	35.84	0.00 0.00	3.91 0.00	0.00	0.00 0.00	0.45 0.56	0.00 0.89	4.69 17.75	0.00 0.00	0.00
69	20.689	33.02	0.00 0.00	3.39 0.00	0.00	0.24 0.00	0.00 0.00	0.00 0.48	4.72 18.90	0.00 0.00	0.00

Appendix 3.4. *continued*

depth (cm)	E. brad. D. paup.	E. tumi. E. exig.	E. tumi. Elp. grp.	F. fusi. F. marg.	G. subg. G. umbo.	L. gibba L. paup.	Lag. grp. M. barl.	M. glab. M. pomp.	N. auri. N. labr.
1,5	0,00 6,16	2,05 1,37	0,00	0,00 6,84	1,37 6,16	2,74	0,00 4,11	3,42	0,68 4,11	1,37	1,37
3,5	0,00 1,32	1,32 0,00	0,00	0,00 7,90	1,32 7,90	0,00	0,00 3,62	2,63	0,00 2,63	0,00	0,00
5,5	0,41 3,65	1,62 0,00	0,00	0,00 0,00	3,24 16,21	0,00	0,00 3,24	10,53	0,00 2,43	3,24	0,00
7,5	0,00 0,97	1,55 0,00	0,00	0,00 5,43	1,55 2,91	0,00	1,16 1,16	3,68	0,00 2,71	0,78	0,00
9,5	0,00 1,27	0,00 0,21	0,00	1,69 0,85	0,85 3,81	0,00	0,85 2,75	1,48	0,00 1,06	0,00	0,00
11,5	0,00 1,86	2,98 1,49	0,00	0,00 1,49	2,23 4,09	0,00	0,00 2,23	1,49	0,00 0,00	0,00	0,74
13,5	0,00 2,69	5,87 0,00	0,00	0,98 2,94	3,18 3,43	0,00	0,24 7,09	7,58	0,00 0,49	0,00	0,98
15,5	0,00 4,21	5,36 0,00	0,00	0,00 0,77	0,19 0,38	0,77	0,19 0,96	2,49	0,77 1,53	2,30	0,00
17,5	0,00 3,78	9,44 0,00	0,00	0,00 1,89	0,63 3,78	0,63	0,16 3,15	3,78	0,00 1,89	1,26	0,63
19,5	0,00 4,08	6,42 0,00	0,00	0,58 2,33	0,58 4,08	0,58	0,00 2,04	4,96	0,00 1,46	0,58	0,00
21,5	0,00 7,14	6,92 0,00	0,00	0,86 3,46	0,86 2,16	0,00	0,00 1,73	2,16	0,43 1,08	0,86	0,00
23,5	0,00 0,81	4,34 0,00	0,00	0,54 2,17	1,63 0,81	0,00	0,00 2,71	2,71	0,00 2,98	1,08	2,17
25,5	0,00 4,50	3,72 0,00	0,00	0,62 1,86	0,62 0,31	0,00	0,16 1,24	4,50	0,00 0,16	1,24	0,00
27,5	0,00 2,88	4,60 0,58	0,00	0,58 2,88	0,00 1,87	0,00	0,00 1,01	4,17	0,00 0,00	1,15	0,00
29,5	0,00 2,49	3,64 0,61	0,00	0,50 0,44	0,78 1,33	0,44	0,22 1,24	2,56	0,00 1,44	0,00	0,06
31,5	0,00 4,08	4,87 0,00	0,00	0,39 1,79	0,50 2,09	0,39	0,00 2,16	2,65	0,00 0,39	0,70	0,06
33,5	0,00 2,44	3,36 0,26	0,00	0,26 0,47	1,20 2,13	0,00	0,06 4,27	3,59	0,00 0,77	0,00	0,00
35,5	0,00 3,02	6,27 1,19	0,36	1,19 1,32	1,74 0,48	0,00	0,24 2,81	3,00	0,00 0,86	0,00	0,00
37	0,00 1,33	3,80 0,00	0,00	2,28 0,76	0,19 0,19	0,38	0,00 0,95	4,18	0,00 1,14	0,00	0,00
39	0,00 2,13	5,32 0,00	0,00	0,18 1,42	0,89 0,71	0,00	0,00 4,26	3,37	0,00 0,53	0,71	0,18
41	0,00 3,24	7,98 0,00	0,00	1,00 1,00	1,25 0,25	0,50	0,00 4,74	6,73	0,00 0,25	1,00	0,00
43	0,00 0,65	5,63 0,87	0,00	0,54 1,30	0,43 0,11	0,87	0,00 1,51	3,90	0,00 0,11	0,43	0,00
45	0,00 1,10	2,93 0,00	0,00	0,00 2,56	1,10 0,18	0,00	0,00 2,47	2,66	0,00 0,18	0,37	0,00
47	0,00 0,66	0,44 0,44	0,00	0,00 2,20	0,00 0,00	0,00	0,00 1,32	3,52	0,00 0,44	0,00	0,00
49	0,10 1,27	5,66 1,17	0,00	0,00 1,56	0,78 0,59	0,00	0,00 0,78	4,00	0,00 0,39	0,39	0,00
51	0,37 1,11	3,15 1,11	0,00	0,37 0,74	0,00 0,00	0,00	0,00 0,37	3,89	0,00 0,00	0,74	0,00
53	0,00 0,39	4,93 0,39	0,00	0,39 0,39	2,76 0,00	0,39	0,00 0,00	1,77	0,00 0,59	0,00	0,00
55	0,00 0,54	5,19 0,36	0,00	0,00 1,43	1,07 0,00	0,90	0,00 0,72	2,15	0,00 0,00	0,00	0,00
57	0,00 0,00	3,10 1,03	0,00	0,00 1,38	0,46 0,11	0,92	0,00 0,57	3,45	0,00 0,46	0,46	0,00
59	0,00 0,74	0,74 0,42	0,00	0,00 2,52	0,42 0,00	0,42	0,00 1,79	1,37	0,00 0,11	0,00	0,00
61	0,00 0,62	1,85 1,23	0,41	0,41 1,23	0,41 0,82	0,62	0,00 1,23	0,62	0,00 0,21	0,00	0,00
63	0,00 0,24	0,36 0,48	0,00	0,48 0,00	1,68 0,00	0,48	0,00 1,92	2,17	0,00 0,24	0,48	0,00
65	0,00 0,38	0,38 0,76	0,00	0,38 1,52	2,28 0,10	0,38	0,00 0,57	1,81	0,00 0,95	0,00	0,38
67	0,00 0,11	0,45 0,45	0,00	1,34 1,79	1,45 0,00	0,00	0,00 1,90	0,78	0,00 0,45	0,00	0,00
69	0,00 0,36	0,48 0,97	0,00	0,48 0,97	0,97 0,00	0,00	0,00 0,97	0,00	0,00 0,24	0,00	0,00

Appendix 3.4. *continued*

depth (cm)	N. subs.	O. cult.	O. hexa.	O. umbo.	P. bull.	P. groe.	P. quin.	P. rota.	Q. pygm.	Q. semi.	R. stab.	S. rois.	S. schl.	T. trih.	U. pere.	total
1,5	0,00	6,84	0,00	6,84	0,68	0,00	7,53	1,37	0,68	0,68	0,00	0,00	8,21	6,84	0,00	156,06
3,5	0,99	5,27	1,32	2,63	3,95	0,00	6,91	1,65	0,00	0,33	0,00	1,32	5,92	2,63	3,95	112,88
5,5	0,00	1,62	4,86	12,97	1,62	0,00	4,05	2,03	0,00	0,41	0,00	0,00	3,65	0,41	2,03	132,08
7,5	0,00	6,20	0,00	10,85	3,29	0,00	0,39	0,97	0,00	0,00	0,19	0,00	3,68	0,78	3,10	86,82
9,5	0,00	1,69	0,00	7,41	1,48	0,00	0,85	0,63	0,00	0,21	0,00	0,85	1,69	0,00	2,12	61,36
11,5	0,00	0,74	1,49	5,21	1,49	0,00	5,58	0,37	0,00	0,00	0,00	0,00	4,09	0,00	0,00	72,58
13,5	0,00	0,98	0,00	11,01	1,22	1,96	1,22	1,71	0,00	0,73	0,00	0,00	4,16	0,98	0,98	107,89
15,5	0,00	0,77	0,00	8,22	2,68	1,53	2,49	3,25	0,00	0,77	0,00	0,00	2,87	0,77	0,19	89,31
17,5	0,00	1,89	0,00	10,07	4,09	0,00	2,20	2,52	0,00	0,79	0,00	0,63	2,36	0,63	0,63	99,57
19,5	0,00	1,17	0,00	6,42	1,75	0,00	1,46	1,46	0,00	1,46	0,00	0,58	6,12	0,00	0,29	84,58
21,5	0,00	1,73	0,00	6,49	0,00	0,00	2,16	1,95	0,00	0,00	0,00	0,00	2,59	0,86	0,00	84,54
23,5	0,00	1,63	0,00	2,17	1,08	0,00	0,81	1,08	0,00	0,54	0,00	0,54	4,34	1,08	0,00	66,16
25,5	0,00	0,62	0,00	1,40	1,24	0,00	1,24	3,41	0,00	0,78	0,00	0,62	1,40	0,00	0,00	57,87
27,5	0,00	0,58	0,58	2,88	1,73	0,14	1,29	2,88	0,00	0,00	0,00	0,58	3,88	1,15	0,00	70,19
29,5	0,00	0,77	0,22	2,38	0,88	0,00	1,72	1,45	0,00	0,00	0,00	0,00	2,51	0,66	0,63	51,95
31,5	0,00	1,79	0,30	3,60	1,36	0,30	1,71	1,38	0,00	0,09	0,04	0,39	1,80	0,04	0,11	61,12
33,5	0,00	0,89	0,00	4,08	0,63	0,00	1,07	1,48	0,00	0,17	0,00	0,26	2,11	0,89	0,11	59,31
35,5	0,00	2,58	0,00	7,27	1,50	0,00	1,14	2,87	0,00	0,42	0,12	0,00	4,79	0,95	0,24	78,54
37	0,00	0,38	0,00	4,56	0,95	0,00	2,28	1,71	0,00	0,38	0,00	0,38	0,95	0,38	0,00	54,31
39	0,00	2,13	0,00	3,19	1,24	0,00	1,60	1,60	0,00	0,71	0,00	0,00	3,90	0,35	0,00	61,73
41	0,00	0,00	0,00	6,48	1,75	0,75	3,49	0,75	0,50	0,00	0,00	0,50	4,99	1,50	0,50	71,05
43	0,00	1,30	0,00	3,14	0,65	0,00	1,41	0,97	0,43	0,00	0,00	0,43	2,81	0,00	0,00	46,85
45	0,00	0,37	0,00	1,65	1,10	0,09	0,73	0,64	0,00	0,00	0,00	0,73	1,46	0,00	0,00	35,07
47	0,00	0,44	0,00	2,20	2,20	0,22	1,54	0,66	0,00	0,22	0,00	0,00	0,66	0,00	0,00	26,81
49	0,00	0,78	0,39	4,10	1,95	0,00	0,39	1,07	0,00	0,39	0,00	0,39	1,37	0,00	0,00	47,11
51	0,00	0,37	0,00	4,27	1,11	0,00	0,37	2,23	0,00	0,00	0,00	0,00	2,04	0,00	0,00	37,83
53	0,00	0,00	0,39	2,76	2,76	0,00	0,79	0,99	0,00	0,39	0,00	0,39	1,38	0,79	0,00	45,33
55	0,00	0,00	0,00	1,43	5,19	0,00	1,43	0,36	0,00	0,36	0,00	0,36	2,33	0,72	0,00	44,23
57	0,00	0,46	0,46	4,48	4,71	0,00	0,46	0,92	0,00	0,11	0,00	0,00	1,95	0,00	0,00	43,87
59	0,00	1,26	0,00	6,83	1,89	0,00	2,10	0,95	0,00	0,63	0,00	0,00	2,73	0,00	0,00	41,90
61	0,00	0,00	0,00	5,76	3,91	0,41	0,00	0,62	0,00	1,03	0,00	0,00	1,44	0,00	0,00	46,08
63	0,00	1,68	0,00	8,18	2,05	0,60	3,37	0,36	0,00	2,05	0,00	0,00	2,29	0,48	0,12	53,41
65	0,00	0,76	0,00	5,71	0,38	0,00	1,90	1,05	0,00	0,67	0,00	0,76	1,05	0,00	0,00	43,00
67	0,00	0,45	0,00	6,14	2,90	0,00	1,79	0,45	0,00	1,00	0,00	0,45	2,57	0,00	0,00	52,68
69	0,00	0,48	0,12	7,63	2,91	0,00	1,70	1,09	0,00	0,73	0,00	0,00	0,61	0,48	0,12	49,06

The benthic foraminiferal response to late Holocene climate change over northern Europe

H. CHRISTIAN HASS

GEOMAR - Research Center for Marine Geosciences, Wischhofstraße 1-3, D-24148 Kiel, Germany

Present address: SFB 313, Kiel University, Heinrich-Hecht-Platz 10, 24118 Kiel, Germany

ABSTRACT

Calcareous benthic foraminifera from four cores from the southern flank of the Skagerrak (NE North Sea) were investigated in order to estimate the response of this fossil group to climate fluctuations during the upper part of the Holocene. Q-mode factor analyses were carried out for the most abundant taxa.

The results reveal *C. laevigata, H. balthica, M. barleeanus, G. turgida, B. marginata,* and *U. peregrina* as most common/important taxa. In the upper part of all cores *B. skagerrakensis* shows a significant increase and dominates the foraminifer fauna in cores from greater water depth. The data suggest no direct relation between the fluctuations of foraminifer assemblages and climate change. However, climate forced fluctuations in the strength of the water-circulation caused considerable changes in the foraminifer assemblages. Three major assemblages were used for environmental analysis: *H. balthica* dominated assemblages were identified as indicators for stagnant conditions. They characterize the oldest core sections, most probably the Holocene climate optimum. *Cassidulina laevigata* assemblages seem to indicate increasing current strength, a process that is often associated with deteriorating climatic conditions. *Brizalina skagerrakensis* appears to have a certain relation to unstable water masses, and probably a tolerance for increasing polution of the North Sea since the advent of modern industrialization.

INTRODUCTION

There is currently considerable debate about the present and future development of the earth's climate. While most climate modelers agree in that there will be a remarkable warming in the near future, the regional effect of global warming still is a major issue of discussion.

During the later part of the Holocene at least Northern Europe witnessed various minor climatic changes known as the Little Ice Age or the Medieval Warm Period which had tremendous effect on ecology and human society (Lamb, 1995; Schönwiese, 1994). Understanding of the consequences of such climate fluctuations is of highest importance since they mirror conditions which we are about to face in forthcoming years. A great number of investigations, including ice-core and tree-ring analyses in the first place, are presently concerned with late Holocene climate variations. The marine record, however, often suffers from bad resolution yet it is not obvious whether the benthos is reacting to minor climate change at all.

The Skagerrak is well known as the sink for suspended matter from the North Sea (Van Weering *et al.*, 1993). Major currents keep fine material in suspension until it is deposited where currents decelerate in the Skagerrak (Van Weering, 1981). In addition, great amounts of bedload sediment enter the Skagerrak area every year. The total amount of sediment being transported annually into the Skagerrak was estimated at 28.4 Mt (Van Weering *et al.*, 1987). Due to this high sediment accumulation some areas in the Skagerrak bear virtually complete geological records for the Holocene at very high resolution (e.g. Hass, 1996; Conradsen & Heier-Nielsen, 1995; Stabell &

In: Hass, H.C. & Kaminski, M.A. (eds.) 1997. Contributions to the Micropaleontology and Paleoceanography of the Northern North Atlantic. *Grzybowski Foundation Special Publication*, no. 5, pp. 199-216

Thiede, 1985; Jørgensen *et al*, 1981). Sediment cores chosen for the present study provide undisturbed records of the past 1-4 millennia with sedimentation rates ranging between 0.4 and 54 mm/yr which are well suited for high resolution paleoclimate studies of the late Holocene.

Previous investigations of these cores (granulometry, $\delta^{18}O$; Hass, 1993, 1996) revealed a distinct climate signal through a coupled atmospheric-hydrographic system, in which changing mean wind speed and direction are most likely to strengthen or weaken the water-mass circulation in the Skagerrak. The present study investigates the response of the calcareous benthic foraminifera to climate fluctuations basically through the past ca. 2,000 years. Although not much is known about the ecologic preferences of benthic foraminifera they are among the most powerful tools in stratigraphy. Recent studies (e.g. Alve & Murray, 1995; Altenbach, 1992; Murray, 1991) once more point out the close relationship between benthic foraminifer assemblages and the conditions of the surrounding water masses. The North Sea in general and the Skagerrak in particular appear to be well suited to study benthic foraminifer ecology as there are narrow zones of changing conditions due to the influence of changing water masses (see e.g. Alve & Murray, 1995; Conradsen *et al.*, 1994; Seidenkrantz, 1993; Corliss & Van Weering, 1993; Qvale & Van Weering, 1985; Nagy & Qvale, 1985; Van Weering & Qvale, 1983; Jørgensen *et al.*, 1981; Thiede *et al.*, 1981; Kihle, 1971; Lange, 1956). Thus, many different environments can be sampled in a very small area.

THE SKAGERRAK

The Skagerrak is a deep glacio-erosive sedimentary basin (>700 m water depth) between the epicontinental North and Baltic Seas bordering SW Sweden, S Norway, and N Denmark (Fig. 1). As a result of the Pleistocene glacier's general SW flow direction, the cross-section through the basin is asymmetrical, with a steep northern flank and a smooth, convex southern flank (von Haugwitz & Wong, 1993). Davies (1980) attributes higher current speed over the S flank and lower current speed over the N flank, as measured during JONSDAP '76, to the asymetry of the basin.

Oceanography

Water-mass exchange in the Skagerrak generally runs counter-clockwise, guided by a prominent current system (Fig. 1). It is fueled by the Jutland Currents which transport water masses from the southern North Sea, the South Trench Current that adds northern North Sea and Atlantic waters, and the Baltic Current that enters the Skagerrak

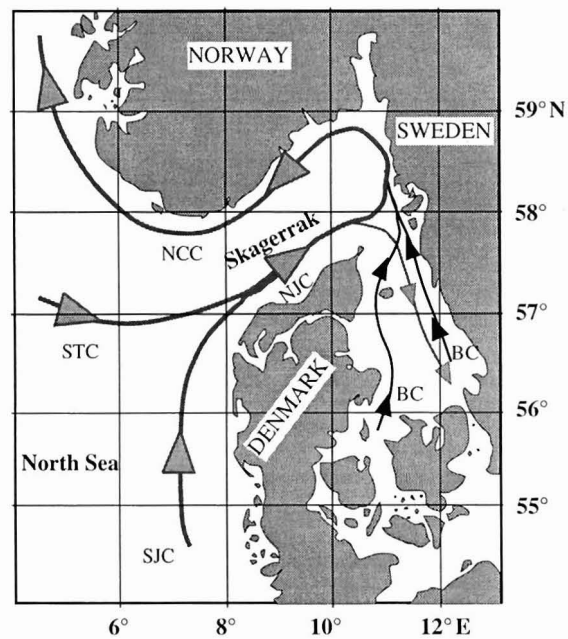


Figure 1. General circulation pattern of the Skagerrak (after Svansson, 1975 and Nordberg, 1989). SJC = South Jutland Current, NJC = North Jutland Current, STC = South Trench Current, BC = Baltic Current; NCC = Norwegian Coastal Current.

through the Kattegat, adding brackish Baltic Sea water into the westernmost part of the Skagerrak (Svansson, 1975). Furthermore, there is a deep counter current flowing through the Norwegian Trough into the deep Skagerrak. Its surface is marked by the 35 PSU isohaline (Dahl, 1978).

Surface currents change direction in the western Skagerrak and eventually leave the Skagerrak as the Norwegian Coastal Current which follows the southern Norwegian coast line. The bottom currents generally follow this cyclonic circulation pattern. Thus, inflowing water is generally constrained to the southern flank of the Skagerrak, whereas the outflow takes place over the northern flank (Larsson & Rodhe, 1979; Svansson, 1975; Figs. 1 and 2).

Ljøen (1981) differentiated 3 different water masses involved in the Skagerrak water-mass circulation: North Sea water (salinity 34-34.95 PSU), Atlantic water (salinity >34.95 PSU) and Skagerrak water (salinity <34 PSU). According to Rodhe (1987) salinity changes can be neglected below 250 m water depth (σ<0.1 PSU). Likewise, temperatures are more or less stable between 5 and 7° C below 250 m (Fonselius, 1989).

Sedimentation and climate development

There are few areas in the Skagerrak where erosion

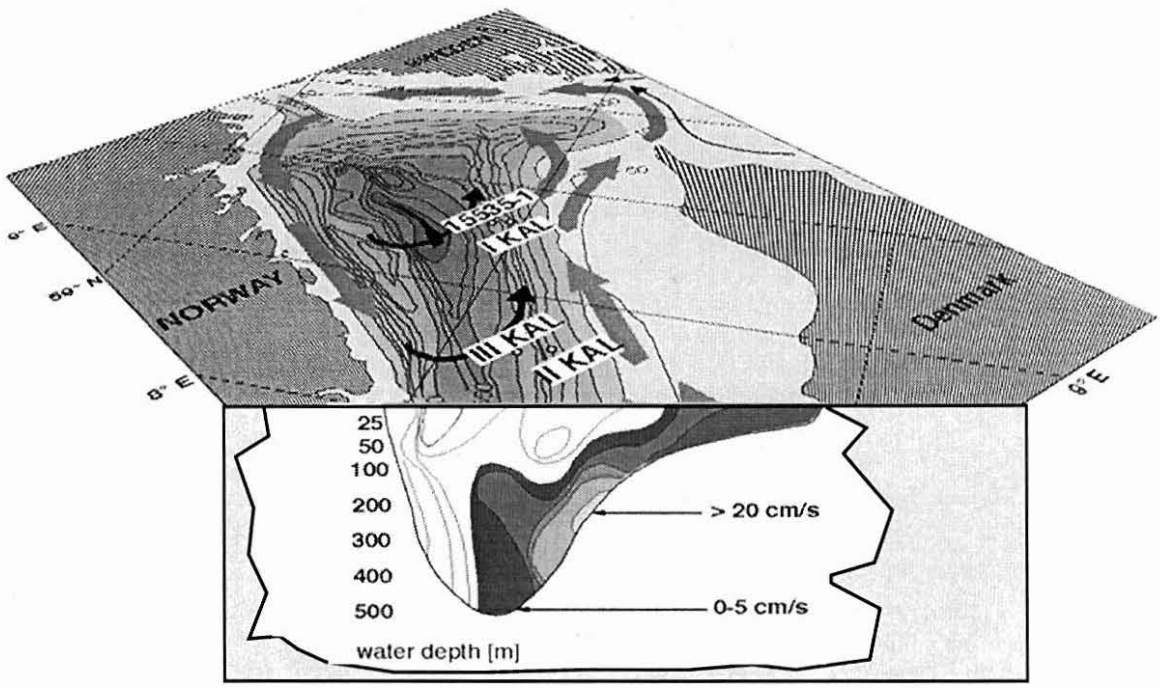


Figure 2. Perspective map of the Skagerrak including directions of surface-currents, core locations (I, II, III KAL and 15535-1), and a current-speed profile (Hanstholm-Kristiansand, winter situation 1977, redrawn after Rodhe, 1979).

outweighs accumulation. These areas are situated on the southern flank under the influence of the Jutland Current. In these areas Quaternary tills and even Mesozoic strata crop out, blown free of sediment by intensive bottom current action (Salge & Wong, 1988; Van Weering, 1981; Sellevoll & Aalstad, 1971).

In places where sedimentation takes place (which includes most of the Skagerrak) sedimentation rates are generally high (Hass, 1996; Van Weering, 1987; Erlenkeuser & Pederstad, 1984). Extremely high sedimentation rates, especially in the eastern Skagerrak, are due to strong current activity, which transports high quantities of suspension load over the southern flank of the Skagerrak. Great amounts of bedload and suspended sediment carried by strong currents are deposited in the eastern and inner Skagerrak, where currents decelerate and dump large quantities of sediment. Sedimentation rates over the northern flank are significantly lower because of the generally lower current speed.

The Skagerrak is situated in the climate sensitive, boreal area well under the influence of the northern hemisphere main westerly wind stream. A close relation between the atmospheric and oceanic circulations has been suggested by various oceanographers (e.g. Fonselius, 1989; Rodhe, 1987). Hass (1993, 1996) was able to show a relation between the effects of atmospheric forcing on the Skagerrak water-mass circulation and the sedimentary record of the past 3,000-4,000 years (see also Hass & Kaminski, 1994). It appears that increased current speed is induced during periods of probable stormy zonal (W to E) atmospheric circulation patterns over the North Atlantic and North Sea leading to a general coarsening of the sediment, and increased sedimentation rates at least in the eastern Skagerrak. Such events were most frequent during colder periods.

Warmer phases, however, are characterized by calmer meridional to zonal atmospheric circulation patterns which are likely to cause water mass circulation to slow down. Thus, during warmer periods less sediment is transported over the southern flank. Due to the lower current speed, a proportion of the sediment is able to settle further to the West, resulting in decreased sedimentation rates in the eastern and central Skagerrak. The granulometric composition also suggests a fining of the sediments as coarser grains can no longer be transported.

During the later part of the Holocene various climate periods affected the North Atlantic-North Sea region, which likewise had a significant influence on the Skagerrak system (basically derived from granulometric and stable isotope analyses). The following climate periods are compiled after Lamb, 1995, 1977; Schönwiese, 1994, 1979; Fairbridge, 1987, and the results of previous work on the cores presently studied (Hass, 1996). The

Subboreal climate optimum (until ca. 1300-1200 BC) and the Subatlantic climate deterioration (until ca. 300 BC) appear to have left only indistinct traces in the sediments of the Skagerrak, whereas the Roman climate optimum and a colder period between ca. 400 and 700 AD are sufficiently documented. The subsequent Medieval Warm Period is characterized by generally lower sedimentation rates and finer sediments, which point to calm atmospheric conditions over the area; slightly increased water temperatures are suggested by the stable isotope record. The onset of the Little Ice Age has been set between 1300 and 1400 AD. There are three distinct intervals of the Little Ice Age, the first and last being stormy and rough, whereas the middle phase was likely to have been calm but exceptionally cold.

The magnitude of atmospheric forcing mainly from strong westerly winds has been related to the movement and position of the North Atlantic cyclone tracks (to the south during cold phases, to the north during warm phases. See e.g. Lamb, 1969). Around 1900 AD at the termination of the Little Ice Age the cyclone track zone moved back beyond the northern limits of the Skagerrak system, signalling the beginning of the Modern Climate Optimum.

MATERIAL AND METHODS

In 1991 three long cores (4.5-8 m) were taken from the southern flank of the Skagerrak during a cruise of RV „Planet" (see Tab. 1 and Figs. 1 and 2 for details). One additional core (15535-1), taken 1980 on board the RV „Poseidon", was chosen to complete the core material. At least one box core was taken from each station in order to obtain undisturbed surface samples.

Table 1. Background information on the cores used for this study.

Core (RV)	Position	Water depth [m]	Core length [cm]	Corer
15535-1 (Po)	58°04.90'N 9°37.00'E	428	800	KL
15535-2 (Po)	58°04.90'N 9°37.00'E	427	70	RL
V GKG (Pl)	58°04.55'N 9°37.21'E	422	34	GKG
I KAL (Pl)	58°02.03'N 9°37.15'E	320	507	KAL
I GKG (Pl)	58°02. 3'N 9°37.15'E	320	46	GKG
II KAL (Pl)	57°46.4'N 8°42.7'E	245	539	KAL
II GKG (Pl)	57°46.4'N 8°42.7'E	245	28	GKG
III KAL (Pl)	57°50.3'N 8°42.4'E	450	485	KAL
III GKG (Pl)	57°50.3'N 8°42.4'E	450	40	GKG

The cores were opened, described, photographed and sub-sampled onboard (except for Core 15535-1). Surface samples (approximately 1 cm thick) were taken directly from the box cores. Further subsamples (0.7 cm wide; in 4 and 8 cm intervals, respectively) were taken in the laboratory later on for granulometric analyses. Once the granulometric analyses (via settling tubes) were completed the residual coarse fractions were used for further micropaleontologic analyses.

A total of 322 samples were micropaleontologically analyzed. The coarse fractions were dry-sieved into 4 fractions (ϕ 4-1) using a sonic sifter. Each of the fractions 125-250 µm (ϕ 3-2), 250-500 µm (ϕ 2-1), and >500 µm ($<\phi$ 1) were split to an appropriate size using a micro-splitter and then separately analyzed. In each of the fractions an average of 250 to 300 specimens of benthic foraminifera were identified and counted. If there were fewer than 250 specimens, the entire fraction was analyzed. The data from single fractions of each sample were then recombined for further analyses. Percentages given in the following refer to percent of the total foraminiferal fauna (fraction >125µm).

Q-mode factor analyses were carried out using the program MacCabfac (Imbrie & Kipp, 1971; Klovan & Imbrie, 1971). Two different types of analysis were run: (A) an overall analysis with all cores stacked to one data set, and (B) separate analyses of each individual core (however, not including the corresponding box cores). Run (A) provides basic information for a comparison of the benthic foraminifer assemblages from all cores. The large data set, however, blurs individual differences between assemblages in individual cores. In order to elucidate these core-specific differences and to control run (A), run (B) was carried out. For the factor analysis, frequency percentages of the most common 25 foraminiferal taxa (run (A)) and the most common taxa in the individual cores (run(B)) were used. Run (A) factors will be referred to as „O-factors" (overall factors), run (B) factors as „I-factors" (individual factors). For run (A) the program was configurated to 6 factors; for run (B) it was set to 4 factors.

AGE DETERMINATIONS

Age determinations for the past 3,000-4,000 years were carried out using the advanced ^{210}Pb method described by Erlenkeuser & Pederstad (1984), Erlenkeuser (1985), and Hass (1996). The results of the age dating procedure are thoroughly described by Hass (1996). Fig. 3a and 3b depict simplified age/depth relations for the cores studied. They

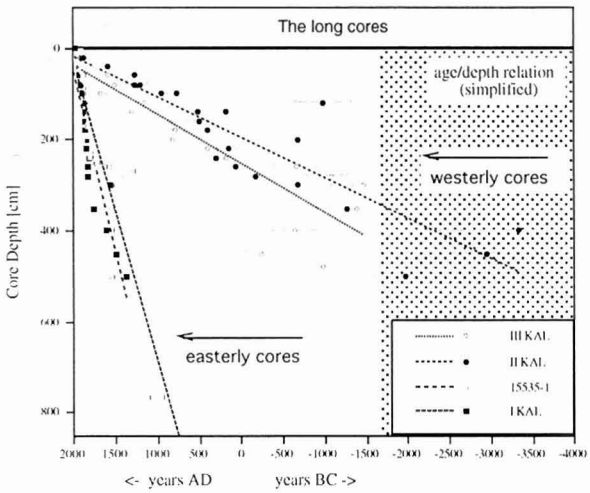


Figure 3a. Simplified age/depth relation for the long easterly (15535-1, I KAL) and the westerly (II, III KAL) cores. For more details see Hass (in press). Shaded area marks dating limit. Note strong differences in general sediment accumulation between easterly and westerly cores. (^{210}Pb-measurements: C14 Laboratory, Kiel).

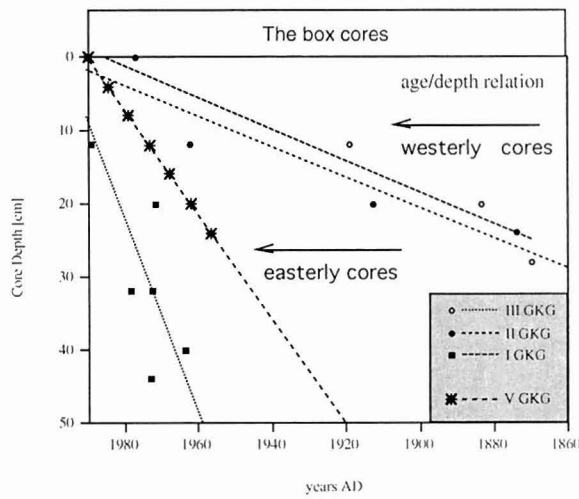


Figure 3b. Simplified age/depth relation for the long easterly (15535-1, I KAL) and the westerly (II, III KAL) cores. For more details see Hass (in press). Shaded area marks dating limit. Note strong differences in general sediment accumulation between easterly and westerly cores. (^{210}Pb-measurements: C14 Laboratory, Kiel).

show the remarkable difference in sediment accumulation between the easterly (high) and the westerly (low) stations.

TAXONOMY

For this study ca. 50 taxa of more than 130 taxa

Table 2. The most important foraminifer species, including references used for identification

***Brizalina skagerrakensis* (Qvale & Nigam, 1985)**
as *Bolivina skagerrakensis* in Qvale & Nigam (1985)
Pl. 1, Fig. 1-11, Pl. 2, Fig. 1-10 in Qvale & Nigam (1985).
Pl. 7, Fig. 17 in Feyling-Hanssen *et al.* (1971) (as *Bolivina* cf. *Bolivina robusta* Brady).

***Bulimina marginata* d'Orbigny, 1826**
Pl. 6, Fig. 17-20 in Feyling-Hanssen *et al.* (1971).
Pl. 14, Fig. 12 in Gabel (1971).

***Cassidulina laevigata* d'Orbigny, 1826**
Pl. 7, Fig. 20-21 in Feyling-Hanssen *et al.* (1971).
Pl. 17, Fig. 7-9 in Gabel (1971).

***Cassidulina reniforme* Nørvang, 1945**
Pl. 1, Fig. 7 in Hald & Vorren (1987).

***Cassidulina* spp. group: see text.**

***Cibicides lobatulus* (Walker & Jacob, 1798)**
Pl. 9, Fig. 9-14 in Feyling-Hanssen *et al.* (1971).
Pl. 18, Fig. 32-34 in Gabel, (1971).

***Elphidium excavatum* Terquem, 1875**
Pl. 11, Fig. 10-13 (as *E.clavatum* Cushman) in Feyling-Hanssen *et al.* (1971).
Pl. 13, Fig. 10-11 (as *Cribrononion excavatum* Terquem) in Gabel (1971).

***Elphidium* spp. group: see text.**

***Fissurina* spp.: *Lagena*spp.-*Fissurina* spp.-*Parafissurina* spp. group, see text)**

***Globobulimina turgida* (Bailey, 1851)**
Pl. 6, Fig. 23 in Feyling-Hanssen *et al.* (1971).
Pl. 14, Fig. 21 in Gabel (1971).

***Hyalinea balthica* (Schroeter, 1783)**
Pl. 9, Fig. 7-8 in Feyling-Hanssen *et al.* (1971).
Pl. 18, Fig. 22-23 in Gabel (1971).
Pl. 18, Fig. 24-29 (as „*H. aberrante* Mutationen") in Gabel (1971).

***Islandiella helenae* Feyling-Hanssen & Buzas, 1976**
Fig. 1-4 in Feyling-Hanssen & Buzas (1976).
Pl. 17, Fig. 25-26 in Gabel (1971) (as *Cassidulina teretis* Tappan).

***Lagena* spp.: *Lagena* spp.-*Fissurina* spp.-*Parafissurina* spp. group, see text.**

***Melonis barleeanum* (Wiliamson, 1858)**
as *Melonis barleeanus* in Seidenkrantz & Knudsen (1993)
Pl. 4, Fig. 6 in Struck (1992)
Pl. 9, Fig. 15-18 (as *Nonion barleeanum* Williamson) in Feyling-Hanssen *et al.* (1971).

***Nonion labradoricum* (Dawson, 1860)**
Pl. 10, Fig. 1-2 in Feyling-Hanssen *et al.* (1971).

***Parafissurina* spp.: *Lagena* spp.-*Fissurina* spp.-*Parafissurina* spp. group, see text.**

***Planorbulina mediterranensis* d'Orbigny, 1826**
Pl. 4, Fig. 1 in Schiebel (1991).
Pl. 19, Fig. 18-20 in Gabel (1971).

***Pullenia bulloides* (d'Orbigny, 1826)**
Pl. 10, Fig. 13-14 in Feyling-Hanssen *et al.* (1971).
Pl. 17, Fig. 39-40 in Gabel (1971).

***Pullenia subcarinata* (d'Orbigny, 1839)**
Pl. 18, Fig. 7-8 in Feyling-Hanssen *et al.* (1964).
Pl. 17, Fig. 37-38 in Gabel (1971).

***Quinqueloculina* spp.**

***Rosalina williamsoni* d'Orbigny, 1826**
Pl. 16, Fig. 12-14 in Gabel (1971).

***Stainforthia fusiformis* (Williamson, 1858)**
Pl. 14, Fig. 15-18 (as*Virgulina fusiformis* Williamson) in Feyling-Hanssen (1964).

***Trifarina fluens* (Todd, 1947)**
Pl. 7, Fig. 12-15 in Feyling-Hanssen *et al.* (1971).
Pl. 15, Fig. 17-18 in Gabel (1971).

***Triloculina* spp.**

***Uvigerina peregrina* Cushman, 1923**
Pl. 7, Fig. 9-11 in Feyling-Hanssen *et al.* (1971)
Pl. 15, Fig. 27-29 in Feyling-Hanssen (1964).

Qvale & van Weering (1983) identified in samples from all over the Skagerrak were identified. The following list comprises the most important species, including references used for identification.

Specimens of *Stainforthia fusiformis* were often found to be sticking together in chains and clusters of different number and size glued by organic material. It was often impossible to separate them, thus counts of *Stainforthia fusiformis* may be partly incorrect or incomplete.

According to previous studies (e.g. Nagy & Qvale, 1985; Van Weering 1982; Lange, 1956; Alve & Nagy, 1990; Jørgensen *et al.*, 1981) many taxa are not relevant for paleoclimatic investigations. Furthermore, low percentage values of single rare taxa (close to 0, or even 0 in various samples) are likely to distort the results of the factor analysis. It was, therefore, attempted to group some of the taxa in order to prepare suitable data matrices. Although they mostly do, the taxa within these groups do not necessarily have ecologic or taxonomic connection. The following groups were formed:

The *Islandiella helenae - Cassidulina* spp. group
This cassidulinid-group is composed of *Cassidulina laevigata*, which dominates the group with an average percentage of 98%. *Islandiella helenae* (=*Cassidulina teretis* before 1976), *C. crassa*, and *C. reniforme* are present in insignificant numbers, thus, they were combined into the *Islandiella helenae - Cassidulina* spp. group. Studies of Nagy & Qvale (1985), Van Weering (1982), and others suggest that within the time period studied in this paper the Arctic species *Islandiella helenae*, *C. crassa*, and *C. reniforme* are very rare to absent in sediments of the Skagerrak.

The *Elphidium* spp. group
The *Elphidium* spp. group is dominated by *Elphidium excavatum*. Other *Elphidium* species occur sporadically, but do not represent a significant portion of this group.

The planktic foraminifer group
Due to their very small numbers, planktic foraminifera were not further determined.

The agglutinated foraminifer group
Agglutinated foraminifera were only poorly preserved, thus, the remains were partly indeterminable (see also Hass, *this volume*).

The *Lagena* spp.-*Fissurina* spp.-*Parafissurina* spp. group
This group was actually composed of 3 groups (*Lagena* spp., *Fissurina* spp., and *Parafissurina* spp.) which all showed very low percentages. The species were not further determined.

The *Triloculina-Quinqueloculina* group
Only in very few samples of the entire data set *Triloculina* spp. and *Quinqueloculina* spp. together made up slightly more than 2%. Since both genera mostly occurred together, the *Triloculina-Quinqueloculina* group was established.

RESULTS

Benthic foraminifera form the major part of benthic life in the Skagerrak. Only the most important foraminiferal taxa will be discussed here. These make up between 100% (maximum) and 94% (minimum) of the total benthic foraminifer fauna. In the following the characterizing species or group is underlined.

After convention the statistical level of confidence for correlation analyses is at 0.5 (correlation coefficient) (Backhaus *et al.* 1990). In order to obtain a clearer overview this value was raised by 0.2, thus the following figures (4 and 5) only show factor loadings >0.7. The results of the O-factor analysis are compared to the results of the I-factor analyses vs. core depth for each of the cores.

Overall factor analysis (run A)

Six factors were calculated which together account for 96% of the total variance (Figs. 4 and 5). Nine taxa clearly show increased factor values and determine the factors that can here be regarded as foraminiferal assemblages. As they are not „Assemblage Zones" according to the biostratigraphic definition, they are herein called „Foraminiferal Factor Units" following Alve (1991).

- ***O-factor 1*** (38% of total variance) is characterized by the Cassidulina spp. group (in the following as *C. laevigata*) alone. This O-factor reveals high loadings at the westerly stations (dominating II KAL and the surface of II GKG; clear-cut sections within III KAL). Within Core I KAL O-factor 1 only explains a small amount of the samples whereas it is meaningless for Core 15535-1.
- ***O-factor 2*** (23% of total variance) is characterized by *H. balthica*, and further by *B. marginata* and *M. barleeanus*., and to a lesser extend by *P. bulloides*. O-factor 2 shows clear-cut zones within cores from greater water depth (15535-1, III KAL). This factor is of significance for none of the shallower cores (with one exception all factor loadings remain <0.6).
- ***O-factor 3*** (15% of total variance) is clearly characterized by *G. turgida*. Subordinate species are *M. barleeanus* and the agglutinated foraminifera group. O-factor 3 is significant for a few samples of

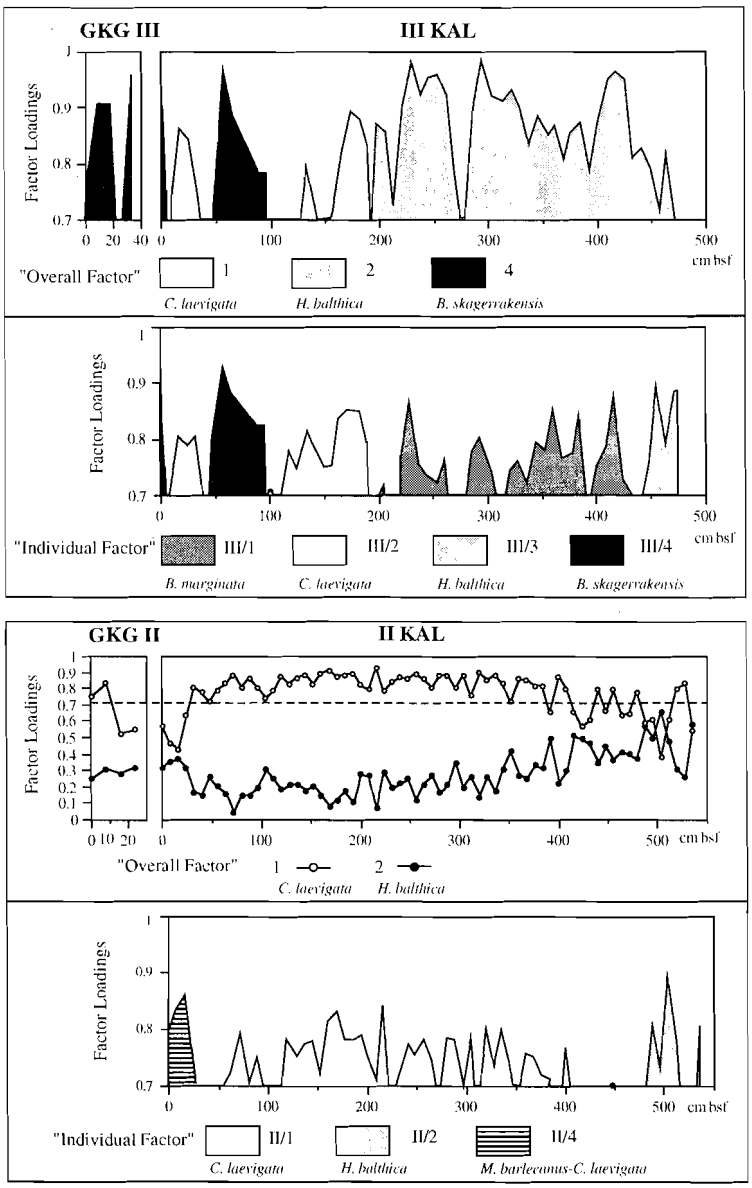


Figure 4. Diagram of relevant factors of the westerly cores GKG III, III KAL, GKG II, and II KAL ("overall" and "individual" factor analysis). The characterizing species for each factor is indicated. For a clearer overview only significant Varimax factor loadings >0.7 vs. core depth are depicted. Due to technical reasons Varimax factor loadings of I-factors III/2 and III/3 have been multiplied by -1 (see text).

the easterly cores (I KAL, 15535-1) as well as for the surface sample of I GKG. It is meaningless for the westerly cores (II KAL, III KAL).

- *O-factor 4* explains only 11% of the total variance, however, it reveals clear-cut zones especially within the cores from greater water depth (III KAL, 15535-1). It is solely characterized by *B. skagerrakensis*. O-factor 4 is meaningless for Core II KAL but it determines the dominant species in Cores GKG III and V.

- *O-factors* 5 (7% of total variance) and 6 (1 % of total variance) are not significant for any of the cores. They do, however, substantiate the 4-factor model used for run (B).

Individual factor analyses (run B)

Core 15535-1 (referred to as: I-factor 15/#, Fig. 5)

Factors calculated for Core 15535-1 account for 94% of the total variance.

- *I-factor 15/1* (45% of total variance) is characterized by *C. laevigata* and *H. balthica*. It is significant between 800 and 244 cm core depth.
- *I-factor 15/2* (24% of total variance) is characterized by *M. barleeanus* and *H. balthica*. This factor only shows a clear-cut zone around 200 cm core depth. There are few single samples with increased I-factor 15/2 loadings throughout the core.
- *I-factor 15/3* (11% of total variance) contains *G. turgida* and the agglutinated foraminifera group. This factor shows dominance only around 100 cm core depth. *H. balthica* reveals slight anti-correlation.
- *I-factor 15/4* (15% of total variance) corresponds to O-factor 4 (*B. skagerrakensis*). It shows high factor loadings around 600 and <100 cm core depth.

Core I KAL (referred to as: I-factor I/#, Fig. 5)

Factors calculated for Core I KAL account for 98% of the total variance. Unless otherwise stated, the factors cannot be assigned to distinct zones or sections within the core because factor loadings show strong fluctuations from sample to sample.

- *I-factor I/1* (37% of total variance) corresponds to O-factor 1 (*C. laevigata*).
- *I-factor I/2* (24% of total variance) is characterized by *M. barleeanus*, *R. williamsoni*, *C. lobatulus*, and *Elphidium*.
- *I-factor I/3* (27% of total variance) is solely characterized by *G. turgida*.
- *I-factor I/4* (8% of total variance) contains *B. skagerrakensis* and as secondary species *H. balthica*. This factor shows high loadings within the upper 40 cm of the core.

Core II KAL (referred to as: I-factor II/#, Fig. 4)
Factors calculated for Core II KAL account for 96% of the total variance.

- *I-factor II/1* (46% of total variance) is characterized by *C. laevigata* and reveals slight anti-correlation to *M. barleeanus*. It is significant between 400 and 60 cm core depth.
- *I-factor II/2* (29% of total variance) is characterized by *H. balthica*, *U. peregrina*, and *B. marginata*. It shows increased factor loadings from the bottom of the core up to ca. 480 cm core depth.
- *I-factor II/3* explains less than 1% of the total variance and is thus meaningless.
- *I-factor II/4* (22% of total variance) contains *M. barleeanus*, and *C. laevigata* as characterizing species; *H. balthica* is weakly anti-correlated. This factor is dominant from 40 cm core depth to the core top.

Core III KAL (referred to as: I-factor III/#, Fig. 4)
Factors calculated for Core III KAL explain 97% of the total variance.

- *I-factor III/1* (37% of total variance) is dominated by *B. marginata*, *M. barleeanus*, and *P. bulloides*. This factor charactrizes the section between 430 and 220 cm core depth.
- *I-factor III/2* (29% of total variance) shows high negative factor scores for *C. laevigata* and low positive scores for *B. skagerrakensis*. Since all factor loadings are negative *C. laevigata* can be regarded as the dominant species whereas *B. skagerrakensis* is weakly anti-correlated. This factor is significant from 190 to 100 cm and from 40 to 8 cm core depth.
- *I-factor III/3* (17% of total variance) is dominated by *H. balthica*, whereas *M. barleeanus* is weakly anti-correlated (see I-factor III/2). This factor is significant from the core bottom to 440 cm core depth.
- *I-factor III/4* (14% of total variance) corresponds to O-factor 4 (*B. skagerrakensis*). It shows high loadings between 100 and 40 cm core depth and from 8 cm to the core top.

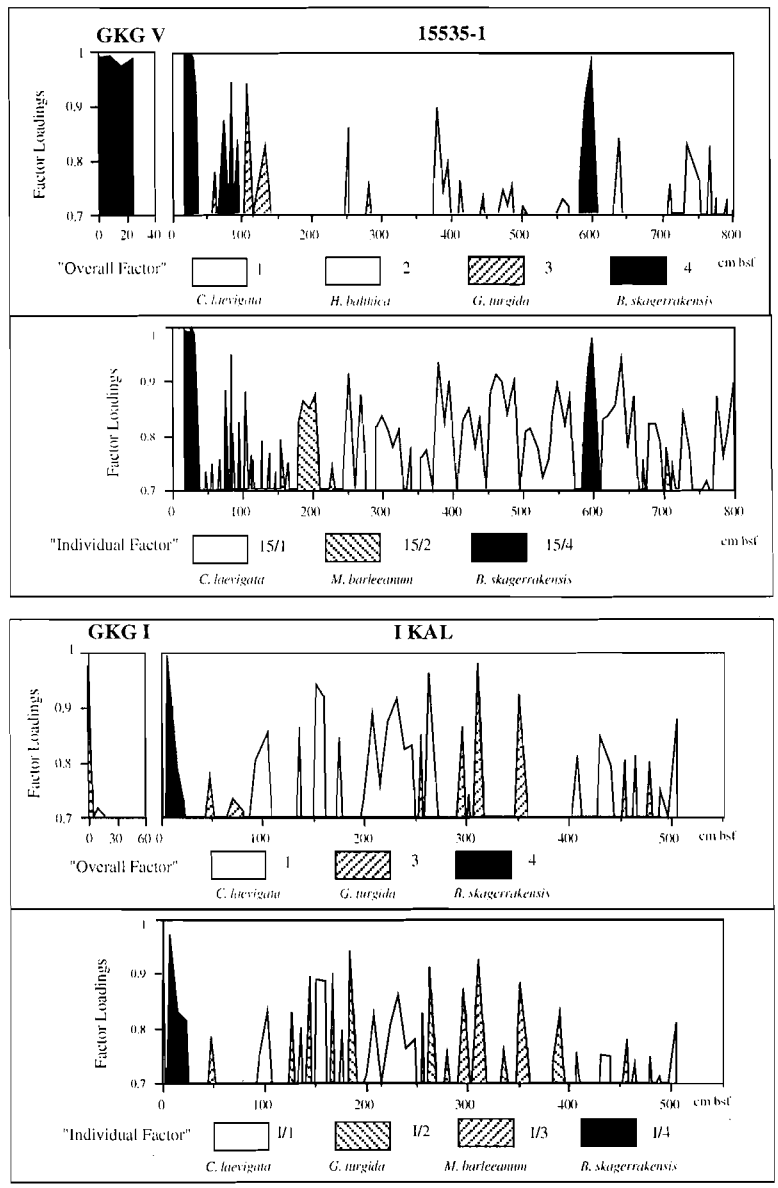


Figure 5. Diagram of relevant factors of the easterly cores GKG I, I KAL, GKG V, and 15535-1 ("overall" and "individual" factor analysis). The characterizing species for each factor is indicated. For a clearer overview only significant Varimax factor loadings >0.7 vs. core depth are depicted.

It appears that the sediment cores partly reveal quite different assemblages according to their location (I-factor analyses). Factor analysis of the entire data set (O-factor analysis), however, is able to discover similarities between the different cores.

Surface and near-surface samples of the GKGs reveal significantly increased amounts of agglutinated foraminifera. Quantitative down-core decreases of this group are explained by poor resistence of the tests (see also Moodley *et al.*, 1993). This is substantiated by down-core increasing

amounts of broken tests accompanied by a down-core decrease in the size of the fragments. Thus, the GKGs were not included in the I-factor analyses.

BENTHIC FORAMINIFERA AS PALEO-ENVIRONMENTAL INDICATORS

The following sections will deal mainly with interpretations based on the factor analyses (Fig. 6,7). The significance of factor analyses or principal component analyses for micropaleontologic studies have been demonstrated by Imbrie & Kipp (1971) and Klovan & Imbrie (1971) in general, related to Skagerrak benthic foraminifera by e.g. Van Weering & Qvale (1983), Alve & Nagy (1990), Conradsen *et al.* (1994) and Seidenkrantz (1992, 1993).

The oldest core sections

Within the deepest sediment core, III KAL, that most probably includes the oldest deposits of this study, a factor characterized by *H. balthica* (I-factor III/3, Fig. 4) characterizes the section from its base until 450 cm core depth (Fig. 8). Stable isotopes in this zone may suggest increased temperatures and probably decreased ventilation (see also Hass, 1996). A similar *H. balthica* factor unit can be found at the base of Core II KAL (I-factor II/2, Fig. 4). These sections are not well resolved by the O-factor analysis. Both factors include increased factor scores of low oxygen conditions tolerant species like *B. marginata* (Murray, 1991; Alve, 1990; Bandy *et al.*, 1964, 1965; I-factor III/3, Fig. 4) and *U. peregrina* (Streeter & Shackleton, 1979; Schnitker, 1979, 1980; I-factors III/3, II/2, Fig. 4), and are characterized by *H. balthica* which is a boreallusitanian species which may suggest an amelioration of the climate (Nagy & Qvale, 1985). Both factors are interpreted here as indicators for increased temperatures and stagnant oxygen conditions.

Van Weering & Qvale (1983) found a *B. marginata-H. balthica* assemblage („factor 4") in Skagerrak sediments which appeared to have a relation to bottom currents. *H. balthica* was found to occur mostly at intermediate water depths. *B. marginata* occurred most frequently in relatively shallow waters, whereas *U. peregrina* seemed to prefer greater water depth, as it was found to replace deep-water assemblage of the inner Skagerrak, which was dominated by *B. skagerrakensis* (as *B.* cf. *B. robusta* in Van Weering & Qvale, 1983) where the amount of oxygen in the water decreases along the Norwegian Trench to the West and the North. Thus, at least *B. marginata* and *U. peregrina* may stand for decreased oxygen content.

Alve & Nagy (1990), working on cores from the Oslo Fjord, described a similar assemblage (*Bulimina marginata-Verneuilinoides media* assemblage) which is dominated by *B. marginata* (*H. balthica* ranking third); however, in this area it characterizes the transitional fjord water mass between 25 and 90m water depth. The deep water mass in the Oslo Fjord is characterized by a *B. skagerrakensis-Nonion barleeanus* assemblage.

Investigating Eemian sediments from the Anholt III deep borehole, Seidenkrantz (1993b) explained the dominance and increasing amounts, respectively, of *H. balthica* and *B. marginata* as likely representing oxygen depletion.

Nagy & Qvale (1985) who studied benthic foraminifera in Core 15530-4 from the western Skagerrak (Stabell & Thiede, 1985) also found a similar assemblage. After their interpretation the *H. balthica* assemblage belongs to the Atlantic period, thus, basically indicating a climate amelioration.

Thus, in agreement with results and interpretations of cited studies and taking into account the age determinations carried out for cores II and III KAL, the sections dominated by a *H. balthica* assemblage may at least represent the later part of the Atlantic climate optimum when calm and warm atmospheric conditions prevailed.

Cassidulina laevigata documents changes in water-mass circulation

Changes in foraminifer assemblages above the previously described *H. balthica* factor unit within Cores II and III KAL are likely to document drastic changes in ecologic conditions (Fig. 4). Oxygen isotopes suggest slightly decreasing temperatures (or/and a salinity increase) (Hass, 1996; see also Figs. 8,9). Both cores show a very slight coarsening of the sediment which may be interpreted as an increase in bottom current strength (Hass, 1993; see also Figs. 8,9). Corresponding changes in the environment are mirrored by O-factor 2 within Core III KAL. Among the 3 species with high factor scores, *H. balthica* now is less significant, wheras I-factor III/1 points to *B. marginata* (Fig. 6) (which also is a component of the *H. balthica* assemblage in Core II KAL) and *M. barleeanus* as the characterizing species. O-factor 2 remains dominant within Core III KAL until the age-dated section around 700 AD (ca. 190 cm core depth).

In contrast, the changes that affected Core II KAL from 400 cm (probably intensifying current strength and coarsening of the sediment; Hass, 1996) lead to the establishment of an assemblage clearly dominated by *C. laevigata*: O-factor 1 and I-factor II/1, respectively (Figs. 6, 9). The assemblage which characterizes O-factor 1, thus, may indicate ecologic conditions under a slightly intensifying water-mass circulation.

O-factor 1 (*C. laevigata*) replaces O-factor 2 (*B.*

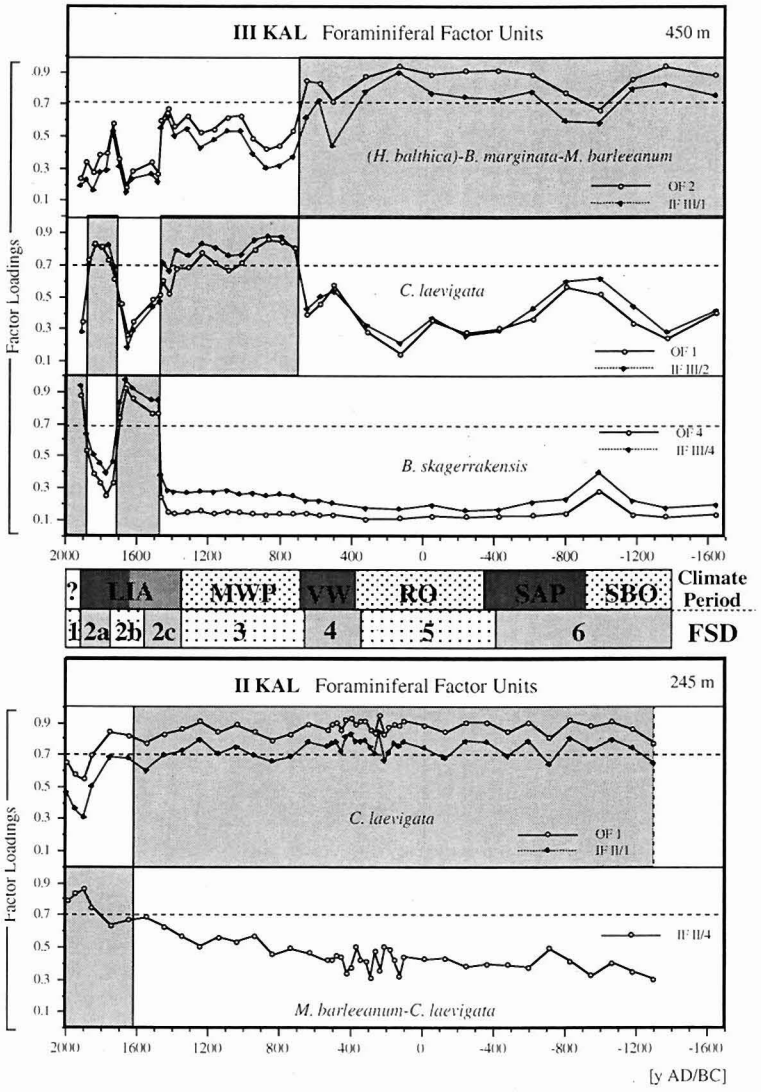


Figure 6. Cores II and III KAL: selected varimax factor loadings of the „overall" (OF) and „individual" (IF) factor analysis vs. years AD/BC in regard to climate periods and lithofacies (FSD; see also Figs. 8 and 9. For more detail on lithofacies refer to Hass, 1996). Climate period abbreviations (see also Figs. 7-11): AO = Atlantic Climate Optimum; SBO = Subboreal climate optimum; SAP = Subantlantic climate deterioration („pessimum'); RO = Roman climate optimum; VW = Climate Deterioration of the period of the migration of the Germanic tribes („Pessimum der Völkerwanderungszeit" after Schönwiese 1979); MWP = Medieval Warm Period; LIA = Little Ice Age.

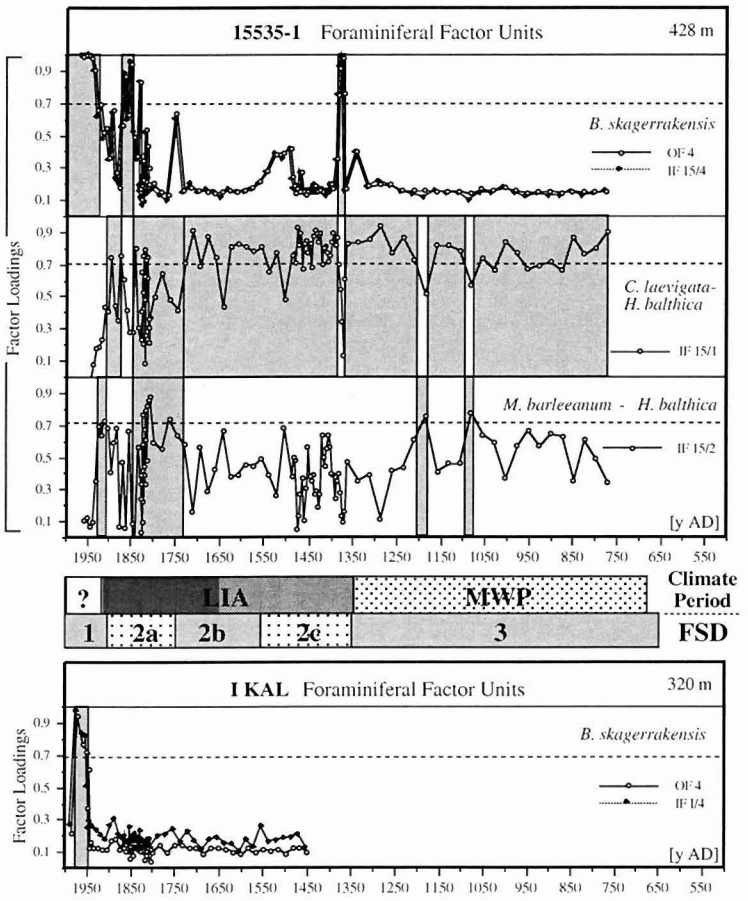


Figure 7. Cores I and 15535-1: selected varimax factor loadings of the „overall" (OF) and „individual" (IF) factor analysis vs. years AD/BC in regard to climate periods and lithofacies (FSD; see also Figs. 8 and 9. For more detail on lithofacies refer to Hass, 1996). For abbreviations of climate periods see Fig. 6.

marginata) rapidly within Core III KAL around 700 AD. During the Period between 600 and 700 AD all investigated parameters suggest a significant environmental change: sediments abruptly begin to coarsen, whereas the oxygen isotopes decrease to Medieval Warm Period minimum values (Hass, 1996; see also Fig. 8). Core II KAL, which suggests similar changes, appears to be dominated by O-factor 1 (*C. laevigata* showing high factor loadings) already from 400 cm core depth. This factor remains dominant until the 14th century AD. I-factor II/4, however, shows that *M. barleeanus* becomes more important from 600-700 AD. At the onset of the Little Ice Age *M. barleeanus* starts to become significant at the cost of *C. laevigata* (I-factor II/4, Fig. 6).

Apparently O-factor 1 and the corresponding I-factors can be interpreted as a 'current-indicative' factor. The *Cassidulina laevigata* assemblage seems to have expanded down-slope from at least the shallow Core II KAL to the deeper Core III KAL. A slight increase in current strength appears to have led to a change from a *H. balthica* assemblage to a *B. marginata* dominated assemblage at Station III KAL (Fig. 8). Another hydrographic shift then caused the dominance of a *C. laevigata* assemblage, replacing the *H. balthica-B. marginata* assemblage subsequently around 600-700 AD. Individual percentage data show that a *'H. balthica-B. marginata-C. laevigata'* succession is also present in Core II KAL during the probable manifestation of the first increase in water-mass circulation in the Skagerrak (II KAL: core base until ca. 400 cm, Fig. 9). Although not mentioned, a similar succession can be seen in Nagy & Qvale (1985: Fig. 1).

Seidenkrantz (1993) explains a recent/subrecent change from *H. balthica* to *B. marginata* as a result of increased organic carbon content and oxygen depletion due to anthropogenic polution. This cannot be the reason for the succession during the Atlantic/Subboreal, though. More likely it is steered by a gradual change of the environment and/or competition between species. It seems, however, after studies of Alve (1994), Conradsen *et al.* (1994), and others that a succession via *C. laevigata* to either a *E. excavatum* assemblage in case of a more or less natural intensification of the water-mass circulation, or to a *S. fusiformis* assemblage in case of intensification of the circulation *and* a certain level of oxygen depletion (most probably caused by anthropogenic pollution) is possible. Since neither a fall of the sea level nor a permanent change in salinity could have triggered the change, a slight intensification of the bottom currents must have led to the establishment of conditions favorable for foraminifera of the shallower areas to dwell in deeper areas of the Skagerrak.

There seems to be no doubt that *C. laevigata* assemblages occur most frequently in turbulent or at least strongly current-influenced environments and on coarser grained substrate than is normally found in the deeper areas of the Skagerrak (see Conradsen *et al.*, 1994). This assemblage is mostly situated in the transitional zone between two water masses, thus under unstable oceanographic conditions (see Nagy & Qvale, 1985; Van Weering & Qvale, 1983). Since a change of the environment seems to have taken place from the shallower into the deeper Skagerrak as well as from the West to the East (i.e. from the higher to the lower energy zone) in order to provide conditions suitable for a *C. laevigata* assemblage a general increase in bottom current strength can be inferred. As a further point *Elphidium* spp. shows an increase in Core II KAL and a very slight increase in Core 15535-1. Two cores studied by Jørgensen *et al.* (1981) reveal a similar pattern (see Figs. 13 and 14 by Jørgensen *et al.*, 1981).

It can thus be inferred that bottom current energy was increasing at least from the later part of the Atlantic until at least the Medieval Warm Period including a phase of rapid increase around 600-700 AD. Foraminiferal data suggest that the high energy zone migrated down-slope most likely in a northwesterly direction. Hass (1996) came to a similar interpretation while studying stable isotopes and granulometry of the same cores used in the present study.

The easterly cores: alternating ecologic conditions?

Within sediment Core 15535-1 *H. balthica* and *C. laevigata* assemblages seem to be mixed (I-factor 15/1, Figs. 5,7). This is also suggested by fluctuating but generally high loadings of O-factors 1 and 2 which may be caused by alternating ecologic conditions due to fluctuating current strength. During the last phase of the Little Ice Age, which has been interpreted as a phase of strongly increased current speed (Hass, 1996; Hass & Kaminski, 1994; see also Fig. 11) all individual factors apper to have fluctuated.

Core I KAL shows small scale fluctuations within the corresponding period just like Core 15535-1 (Figs. 5,7). This is also reflected by the I-factors. Thus, rapidly changing bottom current strengths are suggested, leading to likewise rapid changes in ecologic conditions. Results show, however, that especially *C. laevigata* and *M. barleeanus* have increased in number during the phase of stronger current activity of FSD 2a (Fig. 10; see also Core II KAL, Fig. 9).

1300 AD until Present: *B. skagerrakensis* „conquers" the area

Assemblages with high abundances of *C. laevigata* or with *C. laevigata* as the dominant species (O-factor 1: indicative for intensified current strength) occur mainly where higher current speed is suggested (see Hass, 1996). High loadings of this factor are interrupted when *Brizalina skagerrakensis* (O-factor 4) appears in the sediments. *B. skagerrakensis* is principally (in very small amounts) present throughout the cores from deeper water (15535-1, III KAL, Figs. 8, 11). However, it is not before 1300-1400 AD that this species increases dramatically up to 60%, but only to decrease again until the mid-19th century AD, when another acme occurs (Core 15535-1, Figs. 7, 11). Until the end of the 19th century AD *B. skagerrakensis* again decreases but only to dominate the benthic foraminifer fauna with more than 70% from the mid-20th century AD onwards (Fig. 11).

Within Core III KAL (Fig. 8) *B. skagerrakensis* shows less variability, probably because of the lower temporal resolution. It does not exceed 50%; the first maximum appears ca. 100 years later than it occurs in Core 15535-1. Between 1700 and 1900 AD *B. skagerrakensis* decreases down to 5%. From ca. 1900 AD the corresponding O-factor increases again to high factor loadings and remains dominant until the top of the core (Fig. 6). *B. skagerrakensis* shows a strong increase in all examined cores at the beginning of the 20th century AD except in Core II KAL, which is the shallowest core. However, even in this core the amount of *B. skagerrakensis* increases threefold but it never exceeds 7% (9% in GKG II) (Fig. 9). All cores are characterized by a strong increase of *B. skagerrakensis* although it does not dominate the foraminifer fauna in the shallow cores.

The sudden first increase of *B. skagerrakensis* can be related to the first increase in current strength during the initial phase of the Little Ice Age (FSD 2c). At least Core 15535-1 suggests the second *B. skagerrakensis* increase is related to the last phase of the Little Ice Age (FSD 2a, Fig. 7). Both phases were characterized as being strongly influenced by the atmospheric forced intensification of the Skagerrak circulation system. The younger maxima, including the successive 'conquest' cannot easily be explained. There may be a relation to increasing anthropogenic pollution of the North Sea since the advent of industrialization. Aside from possible reasons such as changing hydrographic conditions or the quality of the TOC, it seems that the trend to increase has not yet finished.

WHAT CONTROLS THE DYNAMICS OF FORAMINIFER ASSEMBLAGES IN THE SKAGERRAK?

Due to the strong variability of ecologic conditions,

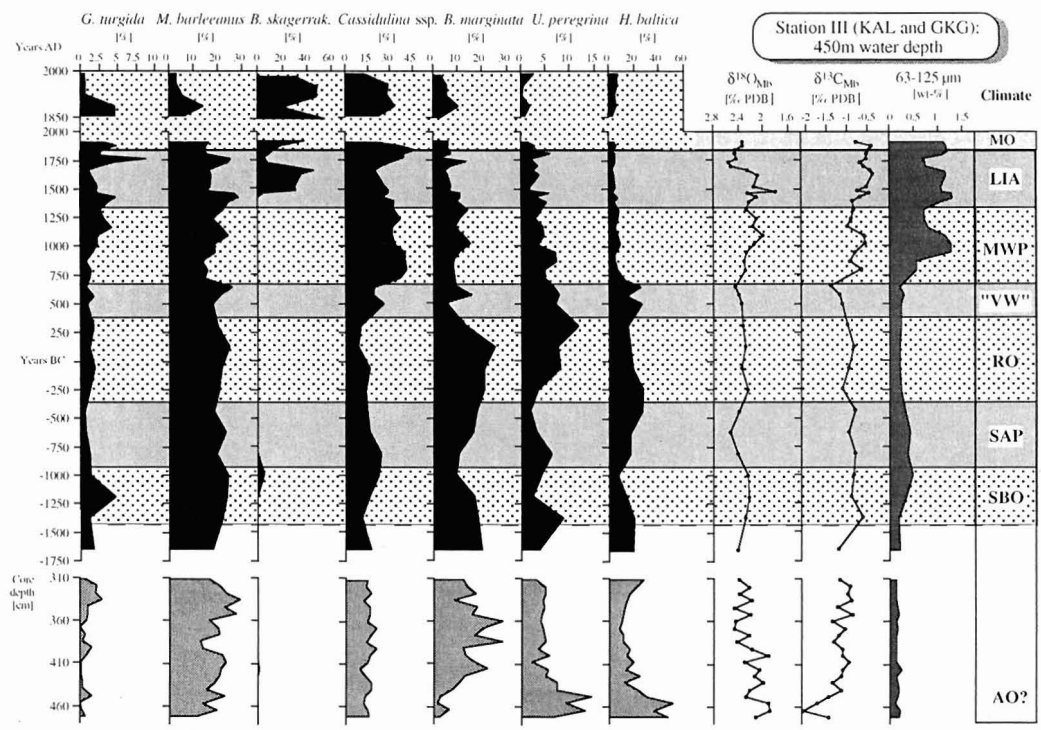


Figure 8. Selected benthic foraminifer species (Gt = *Globobulimina turgida*), $\delta^{18}O$, $\delta^{13}C$, and indicative grain-size class (see Hass & Kaminski, 1994) from Cores 15535-1 and GKG V. The uppermost part of the figure refers to the surface samples (boxcorer GKG V), the lower part refers to the long core (15535-1). ($\delta^{18}O$ and $\delta^{13}C$ measurements: C14 Laboratory, Kiel).

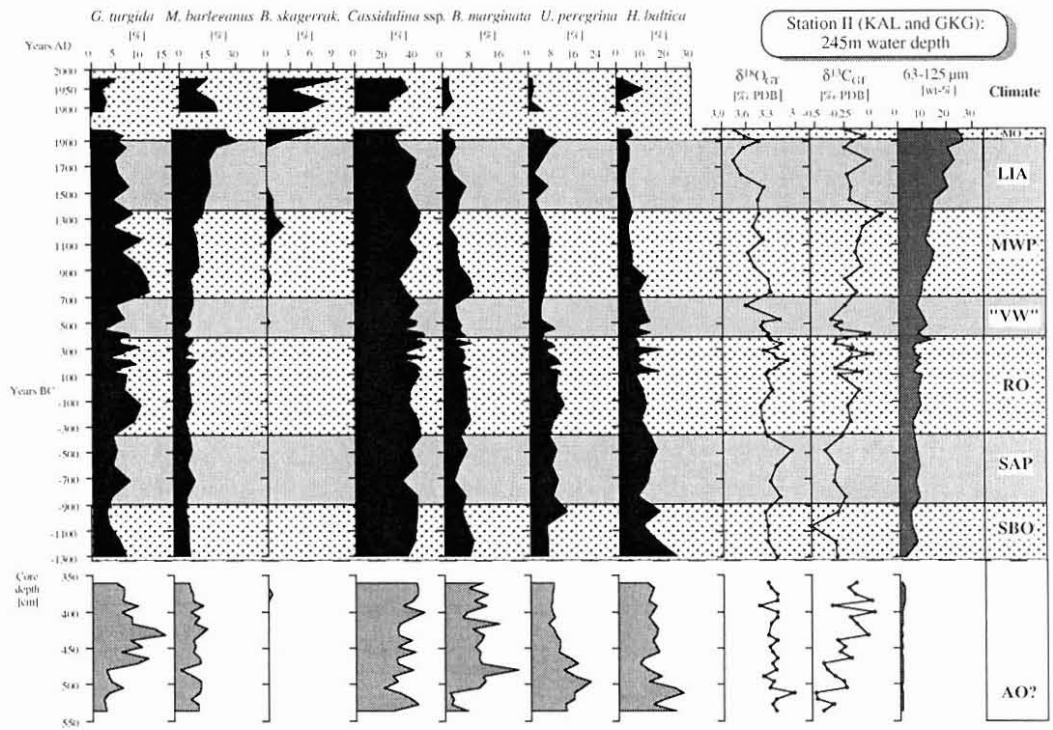


Figure 9. Selected benthic foraminifer species (Gt = *Globobulimina turgida*), $\delta^{18}O$, $\delta^{13}C$, and indicative grain-size class (see Hass & Kaminski, 1994) from Cores II KAL and GKG II. Note different vertical scales („years AD/BC" where age determination have been carried out and „cm" where no age determinations were available). The uppermost part of the figure refers to the surface samples (boxcorer GKG II), the lower part refers to the long core (II KAL). ($\delta^{18}O$ and $\delta^{13}C$ measurements: C14 Laboratory, Kiel).

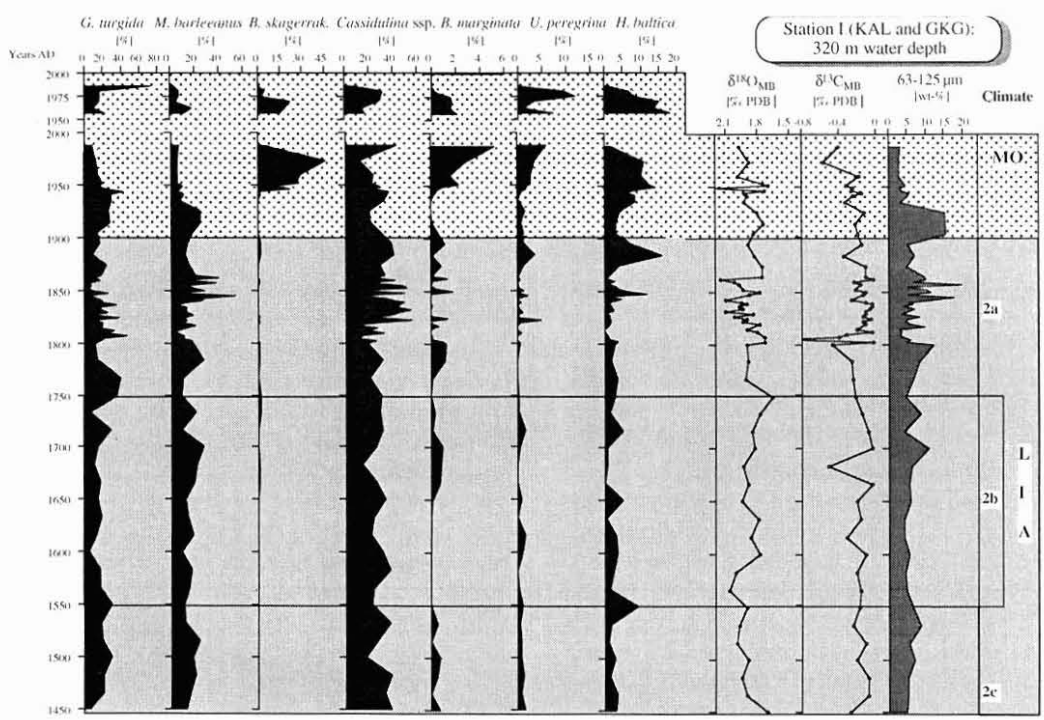


Figure 10. Selected benthic foraminifer species (Mb = *Melonis barleeanus*), $\delta^{18}O$, $\delta^{13}C$, and indicative grain-size class (see Hass & Kaminski, 1994) from Cores I KAL and GKG I. The uppermost part of the figure refers to the surface samples (boxcorer GKG I), the lower part refers to the long core (I KAL). ($\delta^{18}O$ and $\delta^{13}C$ measurements: C14 Laboratory, Kiel).

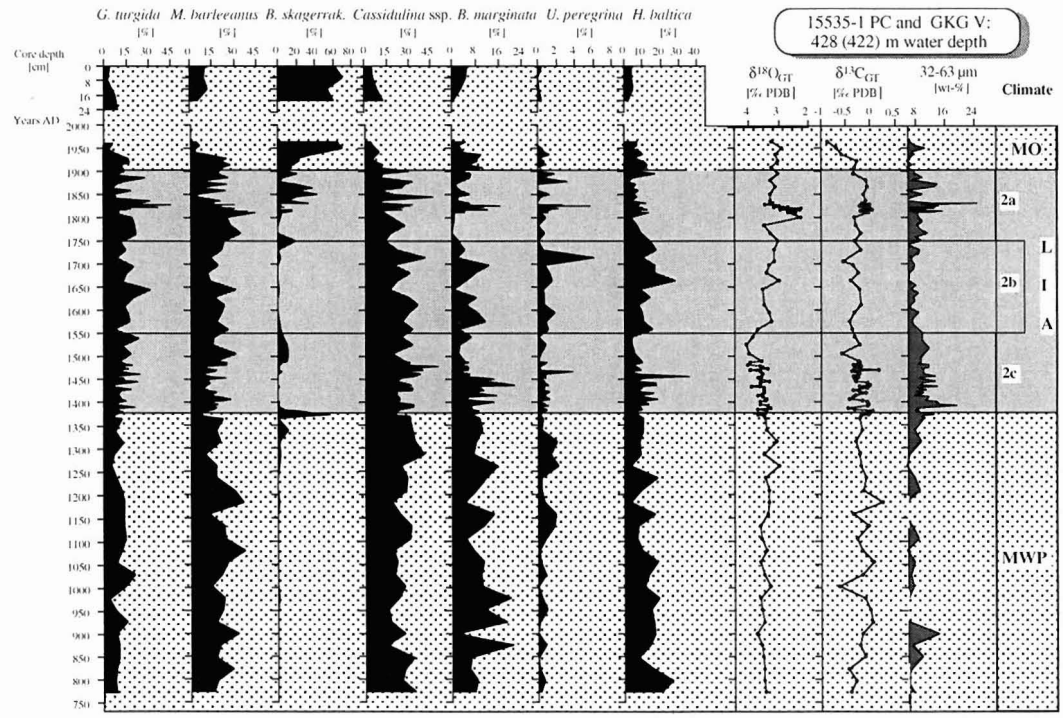


Figure 11. Selected benthic foraminifer species (Mb = *Melonis barleeanus*), $\delta^{18}O$, $\delta^{13}C$, and indicative grain-size class (see Hass & Kaminski, 1994) from Cores I KAL and GKG I. The uppermost part of the figure refers to the surface samples (boxcorer GKG I), the lower part refers to the long core (I KAL). ($\delta^{18}O$ and $\delta^{13}C$ measurements: C14 Laboratory, Kiel).

results of investigations on the continental slope and in the deep sea cannot directly be related to shallow-water foraminifer assemblages (Corliss & Van Weering, 1993; see also Qvale *et al.*, 1984). Shallow-water environments often provide extreme habitats which are not comparable to the deep sea. Direct interpretation from assemblages to the prevailing ecologic conditions are therefore difficult or impossible in shallower, current controlled environments. Corliss & Van Weering (1993) consider the differences in the habitats of benthic foraminifera from the Skagerrak and the continental slope off Nova Scotia (Corliss & Emerson, 1990) to be related to the effect of water depths and to micro-habitats affected by different grades of bioturbation.

Dynamics of the bottom currents

The dependency of foraminifer assemblages on oceanographic parameters within the Skagerrak has been outlined by e.g. Conradsen *et al.* (1994), and Van Weering & Qvale (1993). Such a dependency can be substantiated by the results of the present study. It can be concluded that despite the spacial proximity of the core locations there is a significant heterogeneity in the foraminifer assemblages, which can be attributed to the dynamics of the bottom current circulation.

It could be shown that a persistant intensification of the bottom currents lead to the establishment of a *C. laevigata* dominated assemblage replacing a *H. balthica* assemblage in the lower part of Core II KAL. Probably synchronously, *M. barleeanus* established itself at the deeper location of Core III KAL. A similar zone was not outlined but is evident from the data of Nagy & Qvale (1985: Fig. 1, p. 108). Investigations of „Core 2" (Jørgensen *et al.*, 1981), and P78-4 (Van Weering, 1982) suggest similarities as well.

Present day observations of surface assemblages of the Skagerrak (e.g. Conradsen *et al.*, 1994; Van Weering & Qvale, 1983) cannot easily be related to fossil assemblages, as the huge abundance of *B. skagerrakensis* during the past 500-1,000 years strongly affects the percentage distribution. However, at least „Factor 3" (Van Weering & Qvale, 1983), which identifies a *C. laevigata* assemblage, shows a strong maximum on the southern flank of the Skagerrak, an area which is basically characterized by a coarser substrate. In zones where slower currents lead to a finer grained substrate, assemblages such as „Factor 4" (*B. marginata-H. balthica assemblage*) are dominant (Van Weering & Qvale, 1983). The interpretation of the *C. laevigata* assemblage as 'current indicative' as well as its expansion down slope, thereby replacing firstly *H. balthica* and later on (600-700 AD) also *B. marginata* assemblages in the course of

intensifying currents, can thus be substantiated.

Mackensen & Hald (1988) describe a weak preference by *C. laevigata* for sandy substrates in the North Sea. Further east, in the Skagerrak, Conradsen *et al.* (1994) found a *C. laevigata* assemblage on sandy to fine grained substrate and under rather high current velocities (see also Seidenkrantz, 1992). It is not evident, however, whether *C. laevigata* prefers a coarser substrate or the conditions which characterize shallower (i.e. 100-400m) water depths, such as generally higher current velocities with higher standard deviations leading then to coarser substrate. A preference of *H. balthica* for coarser substrate, as suggested by Pujos (1972, Golf de Gascogne), is not evident from the Skagerrak. However, a preference for certain sediment types is often secondary, as the prime cause for foraminifera living on a given substrate is the availability of food (Graf, 1989; Lutze *et al.*, 1983). The changes in foraminiferal assemblages within Core III KAL during the intensification of water-mass circulation, thus, are likely to mirror changes in the availability of food and probably changes in ventilation of the bottom water mass, which generally favor smaller foraminifer forms like *C. laevigata* (Perez-Cruz & Costillo, 1990).

It appears that between ca. 600 and 700 AD a general displacement of the average situation of the current core by some 100 m down-slope the southern flank of the Skagerrak has taken place. Correspondingly, the biotopes including the associated foraminifer assemblages joined that downslope movement. Slightly increasing amounts of *E. excavatum* which forms the dominant species in the shallow-water assemblage (Van Weering & Qvale, 1983) in Cores II and III KAL (see also Jørgensen *et al.*, 1981) suggest that the shallow water assemblages may also have slightly expanded downslope.

Brizalina skagerrakensis: indicator for stable conditions?

O-factor 4 (characterized by *B. skagerrakensis*) which loads high in all of the surface samples of the four analyzed cores, except for the shallow water Core II KAL (*B. skagerrakensis* is also increasing in this core, however, remains at low percentage), is similar to „Factor 1" (Van Weering & Qvale, 1983) and an assemblage described by Conradsen *et al.* (1994) (see also Nagy & Qvale, 1985; Qvale & Van Weering, 1985; Van Weering, 1982a; Jørgensen *et al.*, 1981; Lange, 1956). The main area of distribution of *B. skagerrakensis* is below 200 m water depth. The immigration of *B. skagerrakensis* is thought to have taken place between 2000 BP (Lange, 1956) and 1000 BP (Jørgensen *et al.*, 1981). Results of the present work, however, suggest that this species occurred already much earlier in very small amounts. Despite this, a pronounced maximum was established not earlier than at the beginning of the Little Ice Age. The establishment of this maximum takes place during the start of a period of generally unstable conditions. The circulation energy was already increased through a „hydrographic jump" around 600-700 AD. Superimposed on this, a further atmospherically forced increase in current speed during the Little Ice Age may have finally produced conditions that were favorable for *B. skagerrakensis* to invade the southern flank of the Skagerrak. Thus, the established consensus that *B. skagerrakensis* indicated stable hydrographic conditions or at least a stable bottom water mass in the Skagerrak (Conradsen *et al.*, 1994; Nagy & Qvale, 1985; Qvale & Van Weering, 1985; Van Weering, 1985) cannot be confirmed by all means. The steady occupation even of the shallower areas of the Skagerrak (Core II KAL, 245 m), that are rather prone to stronger hydrodynamic variability appears to be contradictive to this view. The occurrence of *B. skagerrakensis* under stable conditions in the Oslo Fjord (Alve & Nagy, 1990; Thiede *et al.*, 1981; Risdal, 1964) may thus not be primarily caused by stable hydrodynamic conditions. The present study, however, is not able to elucidate the causes that have supported the extreme fluctuations of *B. skagerrakensis* during the past ca. 500 years (varying between 1 and 70%).

Most likely there is a relation between the latest increase of *B. skagerrakensis* and anthropogenic pollution since the advent of the industrialized era. Earlier spikes may be favored by current speed fluctuations, thus a preference of *B. skagerrakensis* for unstable conditions. Although a relation between the Little Ice Age climate deterioration and the distribution of *B. skagerrakensis* seems to exist, there is - as for the entire benthic foraminifer fauna of the Skagerrak - no striking evidence for a climatic response during the latest part of the Holocene.

CONCLUSIONS: FORAMINIFER ASSEMBLAGES IN THE SKAGERRAK AND CLIMATE FLUCTUATIONS

The investigations suggest that fluctuations in benthic foraminiferal assemblages are principally caused by long-term energy changes in the water mass circulation system. These changes, however, appear to be only indirectly caused by climate change. Pronounced climate fluctuations, such as the Medieval Warm Period or the Little Ice Age, affected the system only periodically through atmospherically forced alterations of the water mass circulation strength, whereas the general circulation regime (refering e.g. to the energy increase

around AD 700) is more probably depending on large scale oceanographic processes elsewhere.

The primary effect of e.g. the Medieval Warm Period (i.e. warming) is obviously not reflected by the benthic foraminifer fauna as there seems to be no obvious correlation between the stable oxygen isotopes (as a major indicator for temperatures) and the benthic foraminifer assemblages. It was the rapid hydrographic change to a higher energy level producing conditions similar to those of earlier cooler climate phases that finally supported *C. laevigata*. Under normal conditions of a warm period one would have expected a *H. balthica* assemblage to become dominant just like what possibly happened during the Holocene Optimum. During the Little Ice Age, however, one would have expected the *C. laevigata* assemblage to become even stronger as strong westerly winds increased the current energy above the level that was already present. Instead, *B. skagerrakensis* invades the area, most likely supported by strong currents or the effects resulting therefrom. Decreased current energy during the Little Ice Age maximum may then have supported the *C. laevigata* assemblage again whereas *B. skagerrakensis* nearly completely disappeared. *B. skagerrakensis* occurs again in very high amounts at the end of the Little Ice Age probably supported by a combination of increased currents and increasing pollution. Thus, it can be concluded that changes in the composition of foraminifer assemblages are directly related to the dynamics of the Skagerrak circulation system.

Although the mentioned climate phases were the result of substantial changes in the atmospheric circulation (e.g. Lamb, 1979, 1969), that resulted in significant fluctuations of the climate aspects, they did not lead to significant changes in the benthic foraminifer fauna other than as a reaction to the displacement of the average position of the current core over the southern flank of the Skagerrak. Thus, strong fluctuations in the amount of *B. skagerrakensis* are most likely caused by fluctuations of the Jutland Current and its bottom current counterpart, respectively. Part of the dynamics within the foraminiferal assemblages from the beginning of the Little Ice Age is probably linked to „competition" between *B. skagerrakensis* and *C. laevigata* dominated assemblages (see also Van Weering & Qvale, 1983), suggesting limiting ecologic conditions for either of them. There is, however, some evidence that current energy fluctuations also lead to fluctuations in the availability and quality of food which is one of the major aspects influencing benthic foraminifer assemblages (Altenbach, 1992). Not enough is known, though, about the food and nutrient preferences of the individual species involved.

The strong increase of *B. skagerrakensis* from the beginning of the 20th century AD may be supported by anthropogenic pollution of the North Sea since the advent of modern industry in the area.

ACKNOWLEDGEMENTS

The author acknowledges the kind help of H. Erlenkeuser who carried out the age determinations and stable isotope analyses. I thank K.L. Knudsen and E. Alve for valuable comments. A. Holbourn is thanked for improving the English version. I wish to thank Capt. von Bredow and the crew of RV „Planet" for help and teamwork during a cruise in November 1991. This study was supported by a research grant of the European Commission and was carried out at GEOMAR and University College London. This is contribution no. 325 of the Sonderforschungsbereich 313 (Special Research Project) of the University of Kiel.

REFERENCES

Altenbach, A.V. 1992. Verbreitungsmuster benthischer Foraminiferen im Arktischen Ozean und in glazialen und interglazialen Sedimenten des Europäischen Nordmeeres. Habilitationsschrift, Mathematisch-Naturwissenschaftliche Fakultät, Christian-Albrechts-Universität zu Kiel, 95 pp.

Alve, E. 1994. Opportunistic features of the foraminifer *Stainforthia fusiformis* (Williamson): evidence from Frierfjord, Norway. *Journal of Micropaleontology*, **13**, 24.

Alve, E. & Murray, J.W. 1995. Benthic foraminiferal distribution and abundance changes in Skagerrak surface sediments: 1937 (Höglund) and 1992/93 data compared. *Marine Micropaleontology*, **25**, 269-288.

Alve, E. & Nagy, J. 1990. Main features of foraminiferal distribution reflecting estuarine hydrography in Oslo Fjord. *Marine Micropaleontology*, **16**, 181-206.

Backhaus, K., Erichson, B., Plinke, W. & Weiber, R. 1990. *Multivariate Analysenmethoden*, Springer, 416 pp.

Bandy, O.L., Ingle, J.C. & Resig, J. M. 1964. Foraminiferal trends, Laguna Beach outfall area, California. *Limnologica et Oceanographica*, **9**, 112-123.

Bandy, O.L., Ingle, J.C. & Resig, J. M. 1965. Foraminiferal trends in the Hyperion outfall area, California. *Limnologica et Oceanographica*, **10**, 314-322.

Conradsen, K. 1993. Recent benthic foraminifera in the southern Kattegat, Scandinavia: distributional pattern and controlling parameters. *Boreas*, **22**, 367-382.

Conradsen, K., Bergsten, H., Knudsen, K.-L., Nordberg, K. & Seidenkrantz, M.-S. 1994. Recent benthic foraminiferal distribution in the Kattegat and the Skagerrak, Scandinavia. *Cushman Foundation Special Publication*, **32**, 53-68.

Conradsen, K. & Heier-Nielsen, S. 1995. Holocene paleoceanography and paleoenvironments of the Skagerrak-Kattegat, Scandinavia. *Paleoceanography*, **10**, 801-813.

Corliss, B.H. & Emerson, S. 1990. Distribution of Rose Bengal stained deep-sea benthic foraminifera from the Nova Scotian continental margin and the Gulf of Maine. *Deep-Sea Research*, **37**, 381-400.

Corliss, B.H. & Van Weering, T. C. E. 1993. Living (stained) benthic foraminifera within surficial sediments of the Skagerrak. *Marine Geology*, **111**, 323-336.

Dahl, G.E. 1978. On the existence of a deep countercurrent to the Norwegian Coastal Current in the Skagerrak. *Tellus*, **30**, 552-556.

Davies, A.M. 1980. Application of numerical models to the computation of the wind induced circulation of the North Sea during JONSDAP '76. *„Meteor" Forschungsergebnisse*, **22**, 53-68.

Erlenkeuser, H. 1985. Distribution of ^{210}Pb with depth in core GIK 15530-4 from the Skagerrak. *Norsk Geologisk Tidsskrift*, **65**, 27-34.

Erlenkeuser, H. & Pederstad, K. 1984. Recent sediment accumulation in Skagerrak as depicted by ^{210}Pb-dating. *Norsk Geologisk Tidsskrift*, **64**, 135-152.

Fairbridge, R.W. 1987. Climatic variation, historical record. *In:* Oliver, J. E. & Fairbridge, R. W. (eds.), *The encyclopedia of climatology*, Van Nordstrand Reinhold Company, 93-305.

Feyling-Hanssen, R.W. 1964. Foraminifera in Late Quaternary deposits from the Oslofjord area. *Norges Geologiske Undersøkelse*, **225**, 1-383.

Feyling-Hanssen, R.W. & Buzas, M.A. 1976. Emendation of *Cassidulina* and *Islandiella helenae* new species. *Journal of Foraminiferal Research*, **6**, 154-158.

Feyling-Hanssen, R.W., Joergensen, J.A., Knudsen, K.L. & Andersen, A.-L.L. 1971. Late Quaternary Foraminifera from Vendysyyel, Denmark and Sandnes, Norway. *Bulletin of the Geological Society of Denmark*, **21**, 67-317.

Fonselius, S. (1989) Hydrographic variabilities in the Skagerrak surface water. *ICES, C.M. 1989, Session Q.*

Gabel, B. 1971. Die Foraminiferen der Nordsee. *Helgoländer wissenschaftliche Meeresuntersuchungen*, **22**, 1-65.

Graf, G. 1989. Benthic-pelagic coupling in a deep-sea benthic community. *Nature*, **341**, 437-439.

Hald, M. & Vorren, T. 1987. Foraminiferal stratigraphy and environment of Late Weichselian deposits on the continental shelf off Troms, Northern Norway. *Marine Micropaleontology*, **12**, 129-160.

Hass, H.C. 1993. Depositional processes under changing climate: Upper subatlantic granulometric records from the Skagerrak (NE-North Sea). *Marine Geology*, **111**, 361-378.

Hass, H.C. 1994. Sedimentologische und mikropaläontologische Untersuchungen zur Entwicklung des Skagerraks im Spätholozän. *GEOMAR Report*, **34**, 115.

Hass, H.C. 1996. Northern Europe climate variations during Late Holocene: evidence from marine Skagerrak. *Palaeogeography, Palaeoclimatology, Palaeoecology*, **123**, 121-145.

Hass, H.C. & Kaminski, M.A. 1994. Change in atmospheric and ocean circulation reflected in North Sea sediments during late Holocene. *Zentralblatt für Geologie und Paläontologie Teil I*, **1/2**, 51-65.

Imbrie, J. & Kipp, N.G. 1971. A new micropaleontologic method for quantitative paleoclimatology: application to a late Pleistocene Caribbean core. *In:* Turekian, K. K. (ed.), *The late Cenozoic glacial ages*, Vol. 3, pp. 71-181, Yale University Press.

Jørgensen, P., Erlenkeuser, H., Lange, H., Nagy, J., Rumohr, J. & Werner, F. 1981. Sedimentological and stratigraphical studies of two cores from the Skagerrak. *In:* Nio, S.D., Schüttenhelm, R.T E. & van Weering, T.C.E. (eds.), *Holocene marine sedimentation in the North Sea basin*, Special Publication of the International Association of Sedimentologists, **5**, 397-414.

Kihle, R. 1971. Foraminifera in five sediment cores across the Norwegian channel south of Mandal. *Norsk Geologisk Tidsskrift*, **51**, 261-286.

Klovan, J.E. & Imbrie, J. 1971. An algorithm and FORTRAN IV program for large-scale Q-mode factor analyses and calculation of factor scores. *Journal of the International Association of Mathematical Geologists*, **3**, 61-77.

Lamb, H.H. 1969. Climatic fluctuations. *In:* Landsberg, H. E. (ed.), *General Climatology (ed. H. Flohn)*, Vol. 2, Elsevier, 173-263.

Lamb, H.H. 1977. *Climatic history and the future*, Methuen, 835 pp.

Lamb, H.H. 1979. Climatic variation and changes in the wind and ocean circulation: the Little Ice Age in the Northeast Atlantic. *Quaternary Research*, **11**, 1-20.

Lamb, H.H. 1995. *Climate, history and the modern world. Second edition*, Routledge, 433 pp.

Lange, W. 1956. Grundproben aus Skagerrak und Kattegat, mikrofaunistisch und sedimentpetrographisch untersucht. *Meyniana*, **5**, 51-86.

Larsson, A. M. & Rodhe, J. 1979. Hydrographical and chemical oceanography in the Skagerrak 1975-1977. *Göteborg University Oceanographic Institute Reports*, **29**, 1-39.

Ljøen, R. 1981. Seasonal variations in inflow of different water masses to the Skagerrak. *In:* Sætre, R. & Mork, M. (eds.), *The Norwegian Coastal Current*, Vol. I, University of Bergen, 357-370.

Lutze, G.F., Mackensen, A. & Wefer, G. 1983. Foraminiferen der Kieler Bucht: 2. Salinitätsansprüche von *Eggerella scabra* (Williamson). *Meyniana*, **35**, 55-56.

Moodley, L., Troelstra, S. R. & Van Weering, T. C. E. 1993. Benthic foraminiferal response to environmental change in the Skagerrak, northeastern North Sea. *Sarsia*, **78**, 129-139.

Nagy, J. & Qvale, G. 1985. Benthic foraminifers in upper quaternary Skagerrak deposits. *Norsk Geologisk Tidsskrift*, **65**, 107-113.

Nordberg, K. 1989. Sea floor deposits, paleoecology and paleoceanography in the Kattegat during the later part of the Holocene. *Geologiska Institutionen*, **A65** (dissertation), 1-205.

Perez-Cruz, L.L. & Machain-Castillo, M.L. 1990. Benthic foraminifera of the oxygen minimum zone, continental shelf of the Gulf of Tehuantepec, Mexico. *Journal of Foraminiferal Research*, **20**, 312-325.

Pujos, M. 1972. Repartition des biocenoses de Foraminifères benthiques sur le Plateau continental du Golfe de Gascogne à l'Ouest de l'Embouchure de la Gironde. *Revista Español Micropaleontol.*, **IV**, 141-156.

Qvale, G., Markussen, B. & Thiede, J. 1984. Benthic foraminifera in fjords: response to watermasses. *Norsk Geologisk Tidsskrift*, **64**, 235-249.

Qvale, G. & Nigam, R. 1985. *Bolivina skagerrakensis*, a new name for *Bolivina* cf. *B. robusta*, with notes on its ecology and distribution. *Journal of Foraminiferal Research*, **15**, 6-12.

Qvale, G. & Van Weering, T.C.E. 1985. Relationship of surface sediments and benthic foraminiferal distribution patterns in the Norwegian Channel (northern North Sea). *Marine Micropaleontology*, **9**, 469-488.

Risdal, D. 1964. Foraminiferfaunaensrelasjon til dybdeforholdene i Oslo-fjorden, med en diskusjon av de senkvartaere foraminifersoner. *Norges Geologiske Undersøkelse*, **226**, 1-142.

Rodhe, J. 1987. The large-scale circulation in the Skagerrak; interpretation of some observations. *Tellus*, **39**, 245-253.

Salge, U. & Wong, H.K. 1988. The Skagerrak: A depo-environment for recent sediments in the North Sea. *In:* Kempe, S., Liebezeit, G., Detlefsen, V. & Harms, U.

(eds.), *Biogeochemistry and distribution of suspended matter in the North Sea and implications to fisheries biology, Mitteilungen des Geologisch-Paläontologischen Institutes der Universität Hamburg*, **65**, 367-380.

Schiebel, R. 1992. Rezente benthische Foraminiferen in Sedimenten des Schelfes und oberen Kontinentalhangs im Golf von Guinea (Westafrika). *Berichte - Reports, Geologisch-Paläontologisches Institut der Universität Kiel*, **51**, 179 pp.

Schnitker, D. 1979. The deep waters of the western North Atlantic during the past 24000 years and the re-initiation of the Western Boundary Undercurrent. *Marine Micropaleontology*, **4**, 265-280.

Schnitker, D. 1980. Loss of calcareous microfossils from sediments through gypsum formation. *Marine Geology*, **36**, 35-44.

Schönwiese, C.-D. 1979. *Klimaschwankungen*, Springer, 181 pp.

Schönwiese, C.-D. 1994. *Klimatologie*, Verlag Eugen Ulmer, 436 pp.

Seidenkrantz, M.-S. 1993. Benthic foraminiferal and stable isotope evidence for a „Younger Dryas-style" cold spell at the Saalian-Eemian transition, Denmark. *Palaeogeography, Palaeoclimatology, Palaeoecology*, **102**, 103-120.

Seidenkrantz, M.-S. 1993. Subrecent changes in the foraminiferal distribution in the Kattegat and the Skagerrak, Scandinavia: anthropogenic influence and natural causes. *Boreas*, **22**, 383-395.

Seidenkrantz, M.-S. & Knudsen, K.-L. 1993. Middle Weichselian to Holocene palaeoecology in the eastern Kattegat, Scandinavia: foraminifera, ostracods and 14C measurements. *Boreas*, **22**, 299-310.

Seidenkrantz, M.-S. 1992. Recent benthic foraminiferal provinces in the Kattegat and Skagerrak and indication of diminished oxygen conditions. *In:* Dennegård, B. & Kuijpers, A. (eds.), *Marine Geological Environmental Investigations in the Skagerrak and Northern Kattegat*, University of Göteborg, Department of Marine Geology, **7**, 1-12.

Sellevoll, M.A. & Aalstad, I. 1971. Magnetic measurements and seismic profiling in the Skagerrak. *Marine Geophysical Research*, **1**, 284-302.

Stabell, B. & Thiede, J. (1985) Upper Quaternary marine Skagerrak (NE North Sea) deposits; stratigraphy and depositional environment. *Norsk Geologisk Tidsskrift*, **65**, 1-149.

Streeter, S.S. & Shackleton, N.J. 1979. Paleocirculation of the deep North Atlantic: 150,000-year record of benthic foraminifera and oxygen-18. *Science*, **203**, 168-171.

Struck, U. 1992. Zur Paläo-Ökologie benthischer Foraminiferen im Europäischen Nordmeer während der letzten 600.000 Jahre. *Berichte aus dem Sonderforschungsbereich 313*, **38**, 1-89.

Svansson, A. 1975. Physical and chemical oceanography in the Skagerrak and the Kattegatt. 1. Open sea conditions. *Fishery Board Sweden, Institute for Marine Research Reports*, **1**, 1-88.

Thiede, J., Qvale, G., Skarbø, O. & Strand, J.E. 1981. Benthonic foraminiferal distributions in a southern fjord system: a reevaluation of Oslo Fjord data. *In:* Nio, S.D., Schüttenhelm, R.T.E. & van Weering, T.C.E. (eds.), *Holocene marine sedimentation in the North Sea basin*, Special Publication of the International Association of Sedimentologists, **5**, 469-495.

Van Weering, T.C.E. 1981. Recent sediments and sediment transport in the northern North Sea: surface sediments of the Skagerrak. *In:* Nio, D., Schüttenhelm, R.T.E. & Van Weering, T.C.E. (eds.), *Holocene marine sedimentation in the North Sea Basin*, Special Publication of the International Association of Sedimentologists, **5**, 335-359.

Van Weering, T.C.E. 1982. Recent sediments and sediment transport in the northern North Sea; piston cores from the Skagerrak. *Proceedings of the KNAW, Series B*, **85**, 155-201.

Van Weering, T.C.E., Berger, G. W. & Kalf, J. 1987. Recent sediment accumulation in the Skagerrak, northeastern Skagerrak. *Netherlands Journal for Sea Research*, **21**, 177-189.

Van Weering, T.C.E., Berger, G.W. & Okkels, E. 1993. Sediment Transport, resuspension and accumulation rates in the northeastern Skagerrak. *Marine Geology*, **111**, 269-285.

Van Weering, T.C.E. & Qvale, G. 1983. Recent sediments and foraminiferal distribution in the Skagerrak, northeastern North Sea. *Marine Geology*, **52**, 75-99.

Von Haugwitz, W.R. & Wong, H.K. 1993. Multiple Pleistocene ice advances into the Skagerrak: a detailed seismic stratigraphy from high resolution seismic profiles. *Marine Geology*, **111**, 189-207.

Recent and subrecent agglutinated foraminifers in four box cores from the Skagerrak (NE North Sea)

H. CHRISTIAN HASS

Department of Geological Sciences, University College London, Gower Street, London WC1E 6BT, UK

Present address: SFB 313, Kiel University, Heinrich-Hecht-Platz 10, 24118 Kiel, Germany

ABSTRACT

Agglutinated foraminifers from 4 box cores spanning the past ca. 140 years (maximum) taken from the southern flank of the Skagerrak (NE North Sea) were studied. Fourtyseven species were identified, among them *Liebusella goesi*, *Eggerelloides* spp., *Rhabdammina discreta*, and *Haplophragmoides bradyi* are the most common. The two more westerly locations reveal significantly higher amounts of agglutinated foraminifers, which may be caused by a better supply of suitable food provided by east headed bottom currents. Extremely high sedimentation rates and a higher degree of pollution suggest environmental stress that may be one reason for lower amounts of agglutinated foraminifers at the two more easterly stations close to the Skagerrak deep. Increasing numbers of specimens within the present century suggests a combination of instability of the tests and ecological controls.

INTRODUCTION

„Agglutinated foraminifera belong to the most widely distributed and abundant groups of marine meiofaunna *in some environments* (e.g. salt marshes, deep sea)." That is how the editors of the special publication on paleoecology, biostratigraphy paleoceanography and taxonomy of agglutinated foraminifera (Hemleben *et al.*, 1990) start the preface of their book. Indeed, the restriction (here in italics, above) to only some environments promoted this foraminifer group as an unpopular one. Recent efforts, however, namely through the IWAF (International Workshop on Agglutinated Foraminifera) meetings and proceedings, however, succeeded in establishing a forum, that exclusively deals with agglutinated foraminifers.

Numerous investigations of benthic foraminifers from the Skagerrak have been carried out through the past 50 years (e.g. Knudsen *et al.*, 1996 a, b; Alve & Murray, 1995, Conradsen *et al.*, 1994; Seidenkrantz, 1993; Alve & Nagy, 1986; Nagy & Qvale, 1985; Van Weering & Qvale, 1983; Jørgensen *et al.*, 1981; Höglund, 1947; see also Hass, *this volume*), however, mostly, the agglutinated foraminifers have not enjoyed a great deal of attention as sometimes the poor resistability of their tests results in disintegration in a short time period in some environments. This study exclusively investigates the agglutinated foraminifer fauna of four box cores from the Skagerrak with regard to the physical environment, and with regard to the apparent strong increase of agglutinated foraminifers during the present century.

OCEANOGRAPHY AND SEDIMENTS

The Skagerrak forms the deepest part of the Norwegian Trough that stretches in a northerly direction along the Norwegian coastline. It consists of a number of different sedimentary environments, characterized by current-energy related grain-size distributions and assemblage zones of calcareous benthic foraminifers (see references above).

Generally, the water mass circulation is counterclockwise (Svansson, 1975) (Fig.1). The southern flank of the Skagerrak is affected by the Jutland Current that transports North Sea water masses into the Skagerrak. According to the dominant wind conditions the Jutland Current largely varies in flow energy (Hass, 1996; Fonselius, 1989; Rodhe, 1987; Davies, 1980). Bottom current speed may vary between 0 and 15-20 cm/s on average (Rodhe, 1987). In the inner Skagerrak water masses turn around and eventually leave the Skagerrak as the Norwegian Coastal Current. A deep counter current to the Norwegian Coastal Current injects sa-

In: Hass, H.C. & Kaminski, M.A. (eds.) 1997. Contributions to the Micropaleontology and Paleoceanography of the Northern North Atlantic. *Grzybowski Foundation Special Publication*, no. 5, pp. 217-226

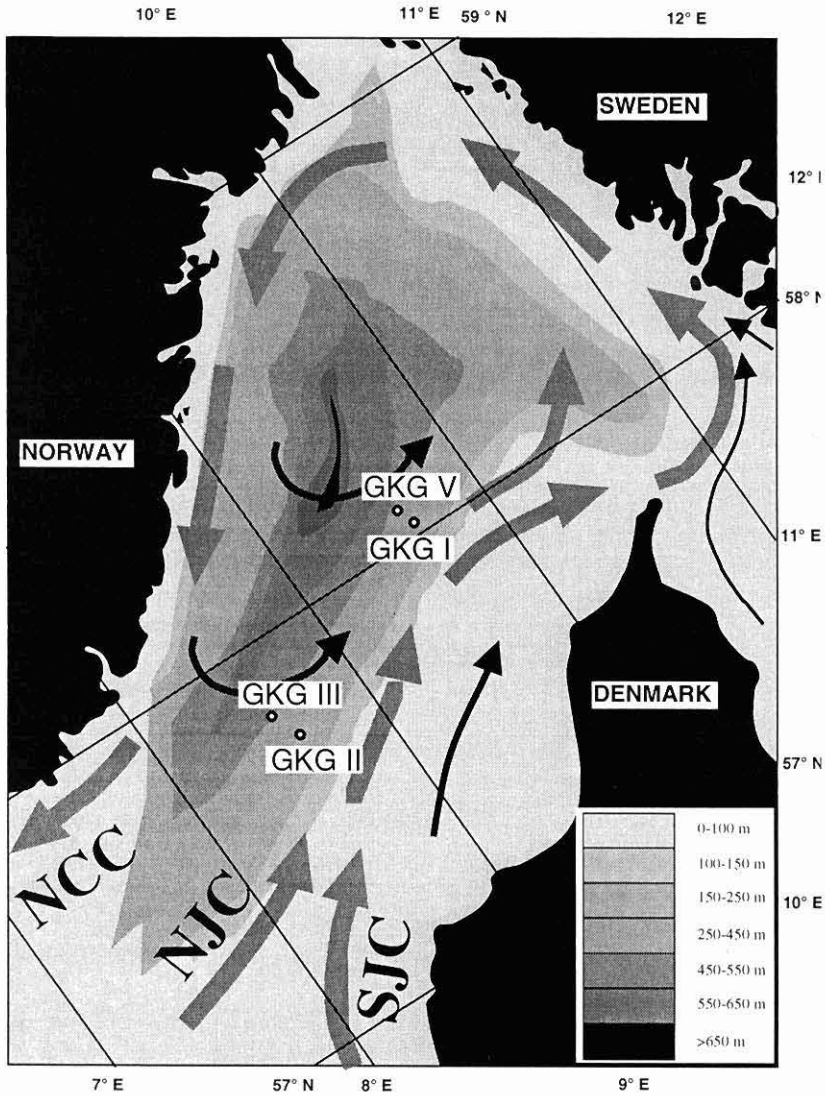


Figure 1. Bathymetry (continents in black, water depths in shades of gray), general surface circulation pattern (after Svansson, 1975) and core locations (GKG I, II, III, V). SJC = South Jutland Current; NJC = North Jutland Current; NCC = Norwegian Coastal Current (after Nordberg, 1989).

line Atlantic water into the Skagerrak deep (Dahl, 1978).

At the depths that are of interest for this study, seasonal influences are minor (Corliss & Van Weering, 1993). Temperatures may vary between 4 and 7°C (Larsson & Rodhe, 1979; Fonselius, 1989), but remain usually around 6°C. Salinities show little variation around 35 PSU (Lee, 1980). TOC values range between 1.3 and 3% (Hass, 1994); oxygen saturation is good throughout (Svansson, 1975). The sediments suggest a series of environments characterized by different current strengths. Sediments range from silty clay with about 57 weight% of clay at the deepest location (GKG III, 450 m) to to silty sand with about 26 weight% of sand at the shallowest location (GKG II, 245 m). Equally different appear the sedimentation rates, that vary between 2 and 10 mm/yr (Hass, 1994).

The Skagerrak basin is affected by environmental pollution that began with the onset of modern industrialization during the last century. Especially heavy metals (Cr, Pb, Cu, Co, Mn) show a clear increase (Müller & Irion, 1984; Erlenkeuser & Pederstad, 1984).

MATERIAL AND METHODS

In November 1991 four box cores were taken from the southern flank of the Skagerrak during a cruise of RV „Planet" (GKG I, II, III, V; see Tab. 1). In the following, Cores GKG II and III will be addressed as the „westerly cores", Cores GKG I and V are termed the „easterly cores".

Bulk density measurements (4cm intervals) were carried out using syringe samples that were taken aboard the research vessel during the cruise. The cores were subsampled using 50 cm plastic liners which were

Table 1. Background information on the cores used for this study.

Core (RV)	Position	Water depth [m]	Recovery [cm]	Corer
V GKG (Pl)	58°04.55'N 9°37.21'E	422	34	GKG
V GKG (Pl)	58°02. 3'N 9°37.15'E	320	46	GKG
V GKG (Pl)	57°46.4'N 8°42.7'E	245	28	GKG
V GKG (Pl)	57°50.3'N 8°42.4'E	450	40	GKG

GKG = Large Box Core (30 x 30 x 50 cm)
(Pl) = RV "Planet"

then sliced into 0.7 cm slabs every 4 cm (Core GKG I: 8 cm intervals). After freeze-drying the samples were washed through a 63 µm standard sieve. Then the dried coarse fraction was further fractionated into the usual fractions 63-125 µm, 125-250 µm, 250-500 µm, and >500 µm using a sonic-sifter. Agglutinated foraminifers were picked and counted in 3 fractions: 125-250 µm, 250-500 µm, and >500 µm. Where possible, at least 300 specimens in each sample were counted. If there were less than 300 individuals, the entire sample was counted. Fragments of agglutinated foraminifers were counted whenever the fragment was unequivocally the larger part of an agglutinated test. Very small fragments were generally not counted. In the following quantitative data are always rounded to the nearest integer value.

Age determinations were carried out by means of the excess ^{210}Pb method (for sample preparation and chemical treatments see Erlenkeuser & Pederstad, 1984). All measurements were taken by and at the C14-Laboratory of the Institute for Pure and Applied Nuclear Physics, Kiel University. There are no age determinations for Core GKG V. It was assumed that sedimentation rates have not significantly changed during the past 30-40 years, thus sedimentation rates for the upper part of a long core from the same location were applied, and age data calculated (Core 15535-1: see Hass, 1996).

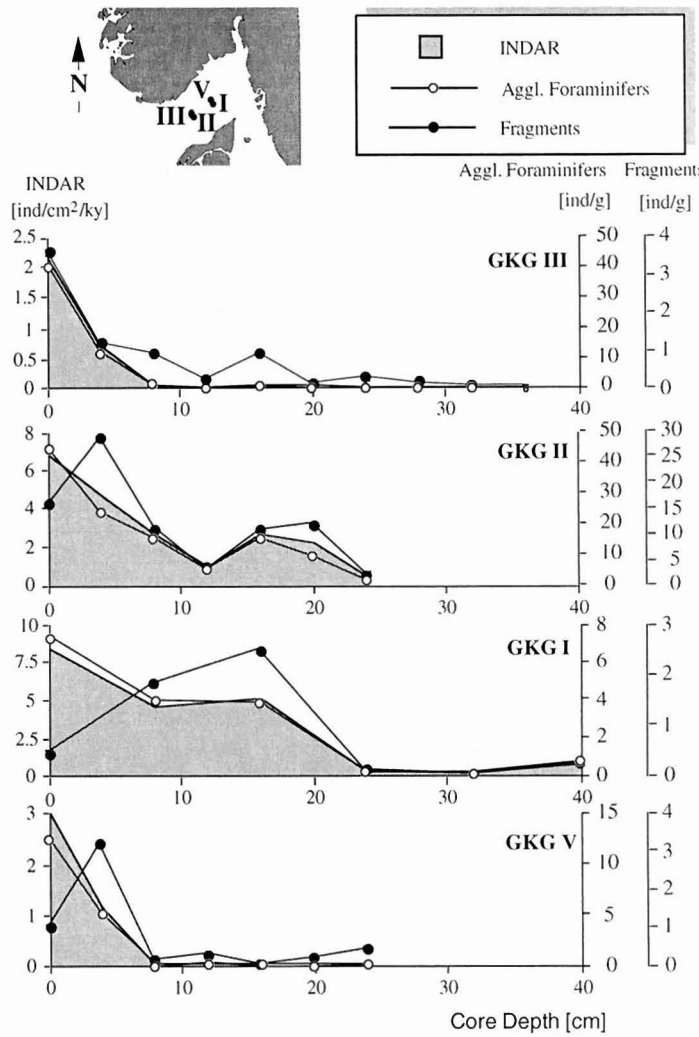


Figure 2. Agglutinated foraminifers per cm^2 and per year (INDAR), agglutinated foraminifers per gram dry sediment (ind/g) and counted fragments versus core depth.

Individual accumulation rates (INDAR) were calculated by multiplying dry bulk density data, linear sedimentation rate, and quantitative foraminifer data according to Ehrmann & Thiede (1985) and Struck (1992; see also Nees, *this volume*; Hass, *this volume*).

Various further analyses (stable isotopes, calcareous foraminifers, $CaCO_3$, TOC) were carried out using sediments from the same cores used for this study (Hass, 1994, 1996, *this volume*).

RESULTS

Total abundance of agglutinated foraminifers

Highest abundances of agglutinated foraminifers were found throughout the cores in the topmost samples. The westerly stations reveal between 3 and 5 times as many individuals within the topmost samples than the easterly stations (Fig. 2). Westerly Core GKG III shows about 41 individuals per gram dry sediment (Ind/g), whereas Core GKG II shows up to 45 Ind/g. Easterly Core GKG V reveals about 12.5 Ind/g; Core I GKG shows even less (7.5 Ind/g).

INDAR („individuals per square centimeter and per year" in the following as ind·cm^{-2}·y^{-1}), however, show more balanced values. These are likely to depend more on water depth (Fig. 2): GKG II (245 m) shows highest values at 6.8 ind·cm^{-2}·y^{-1}, GKG I (320 m) records 8.4 ind·cm^{-2}·y^{-1}, GKG V (427 m) shows 2.9 ind·cm^{-2}·y^{-1}, and GKG III (460 m) reaches only 2.1 ind·cm^{-2}·y^{-1}. INDARs strongly depend on the calculated linear sedimentation rates (LSR, Fig. 3) which may be biased by different degrees of compaction, as the sediments dealt with in this study are very young. Because of different hydrographic regimes and likewise diffe-

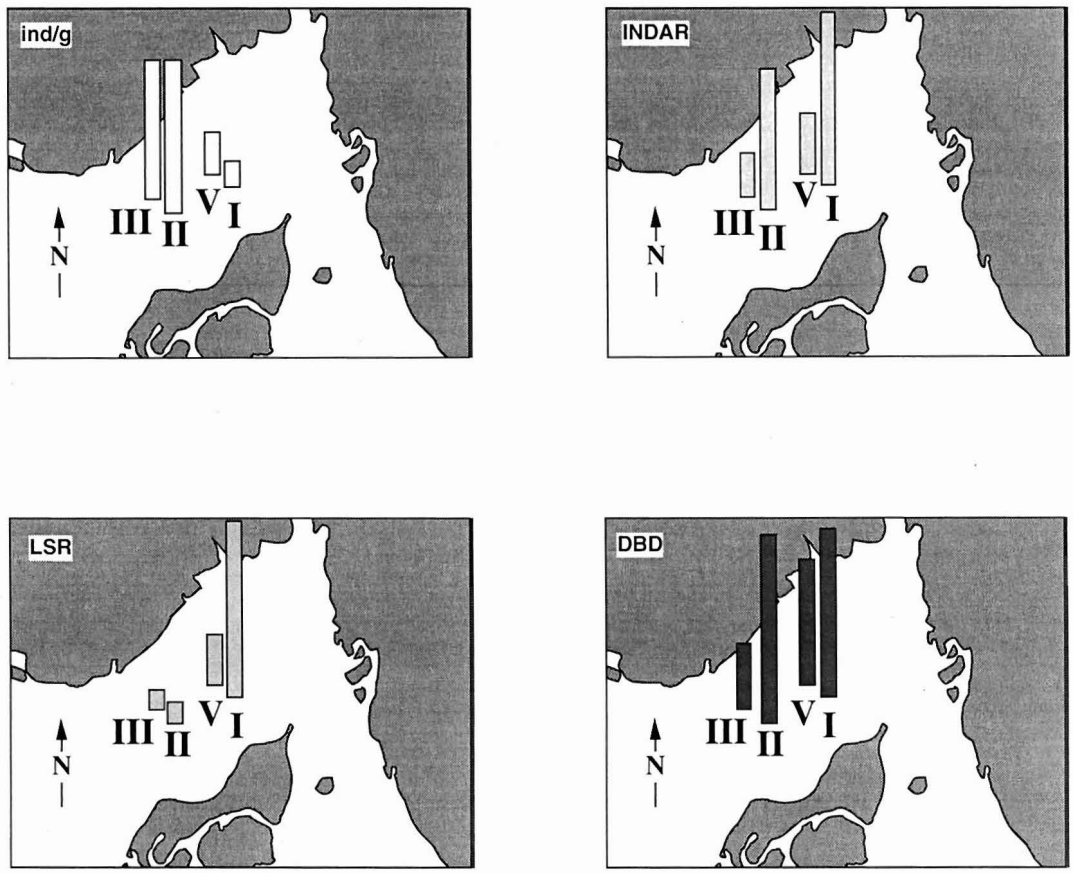


Figure 3. Measured and calculated data from surface sample of the four cores: agglutinated foraminifers per gram dry sediment (ind/g); agglutinated foraminifers per cm^2 and year (INDAR); linear sedimentation rate (LSR); dry bulk density (DBD).

rent grain size distributions, the dry bulk density data is different in all four cores as well (Fig. 3). All of these variables may have a considerable influence on the INDARs. Thus, in the following discussion, the main emphasis will be placed on the parameter „Ind/g" that appears to be less biased by the physical properties of the sediment (although strongly influenced by the sedimentation rate).

All four cores show a marked downcore trend towards a decreasing abundance of agglutinated foraminifers. Figure 2 depicts INDAR and „Ind/g" values of the bulk agglutinated foraminifer fauna for the four box cores. Westerly Core GKG II carries the maximum number of agglutinated foraminifers of all cores with approximately 2.5 Ind/g within the lowermost sample (24 cm core depth). The remaining cores show values below 0.02 Ind/g. These trends are paralleled by INDAR values. Compared to the calcareous benthic foraminifer fauna (% agglutinated foraminifers of the bulk benthic foraminifer fauna), percentages are heterogenous: Core GKG III starts at about 34% and decreases downcore to 0.008%; Core GKG II starts at 3.2% and finishes with 0.2% at the bottom of the core. The easterly cores show more similarities: Core GKG V starts at 11% and decreases to 0.16%, whereas GKG I decreases from approximately 7% down to 5.8%. Only in Core GKG I the calcareous foraminifers reveal a similar downcore decreasing trend.

Species distributions: the surface samples

Fourty-seven agglutinated foraminifer species were identified (see Appendix 1). About 15 species accounted for more than 5% or totalled to more than 0.2 Ind/g (> 0.5 Ind/g in Core GKG II). Only 5 agglutinated species appeared to be characteristic for the cores investigated.

Since there is a rapid decrease in the number of individuals downcore, species distributions expressed in percent are likely to loose competence from the top to the bottom of the cores (see Fig. 4: bulk agglutinated foraminifer data is included).

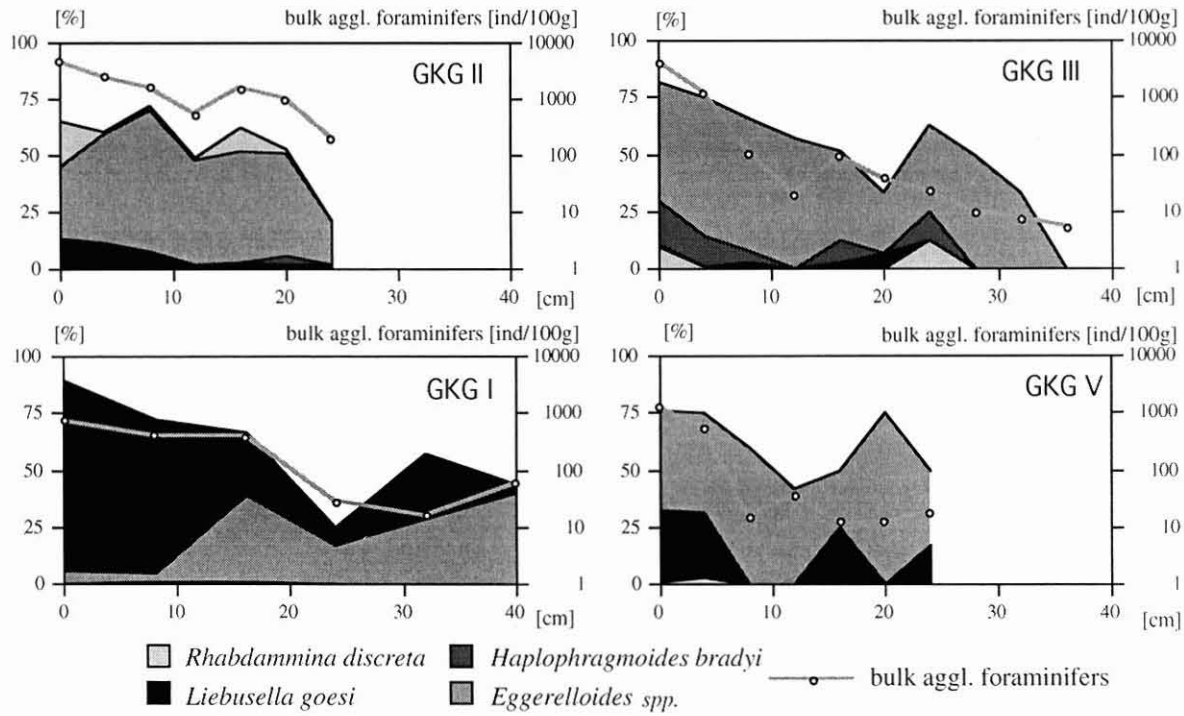


Figure 4. The most important species (in %) versus core depth, and the total amount of agglutinated foraminifers (ind/100g).

Thus, in this chapter main emphasis will be placed on the surface samples.

The characteristic, and thus most abundant species are *L. goesi*, *Eggerelloides* spp., *H. bradyi*, and *R. discreta* (Fig. 4). Core GKG I, the shallower of the easterly cores, reveals an assemblage that is strongly dominated by *L. goesi* accounting for 83% of the agglutinated foraminifer fauna (>0.6 Ind/g). In the deeper easterly core (GKG V) *Eggerelloides* spp. (44%, 5.50 Ind/g) and *L. goesi* (30%, 3.8 Ind/g) dominate the fauna. In the westerly cores *L. goesi* is of less importance. The shallower core GKG II shows only 13% (5.6 Ind/g) *L. goesi*, whereas *Eggerelloides* spp. amounts to 32% (14.4 Ind/g). *R. discreta* shows 20% (8.8 Ind/g). In the deeper westerly core GKG III, *L. goesi* remains below 1%. In this core the dominant species are *Eggerelloides* spp. (53%, 21.4 Ind/g), *H. bradyi* (20%, 7.9 Ind/g), and *R. discreta* (10%, 4.0 Ind/g).

Downcore changes in species distribution

Downcore changes in agglutinated foraminifer species are expressed in terms of quantity rather than in terms of percentages as the number of individuals rapidly decreases to values beyond a reasonable interpretation of percentages (see previous sections). Figure 4 shows the percentage distribution of the agglutinated foraminifers in comparison with the bulk number of agglutinated foraminifers as the strong decrease in quantity makes a quantitative graph unreadable.

Easterly Core GKG V shows no significant change in the characteristic species core depth. Although *L. goesi* decreases to zero within the upper 8 cm of the core, no other species takes its place in a significant quantity. The decrease of *Eggerelloides* spp. parallels the decrease of the entire agglutinated foraminiferal assemblage, thus, it is present from the top to the bottom of the core. The shallower easterly Core GKG I reveals a decrease of *L. goesi* parallel to the decrease of the entire benthic foraminifer assemblage (including the agglutinated foraminifers); *Eggerelloides* spp. shows strong changes, but is present throughout the core.

The shallower westerly Core GKG II shows relatively high numbers of *Eggerelloides* spp. throughout the core, whereas *R. discreta* seems to be present in significant numbers only in the topmost sample and to a lesser extent at 16 cm core depth where the entire agglutinated foraminfer assemblage shows a short-term increase. *Liebusella goesi* steadily decreases in number from top to bottom of the core, also showing a slight increase at 16 cm core depth. The deeper westerly Core GKG III reveals the most significant decrease in the number of agglutinated foraminifers of the four cores analyzed. It drops from more than 40 to less than 0.2 Ind/g within the upper 12 cm. There is a very slight increase at 16 cm core depth mirroring Core

GKG II. *Eggerelloides* spp. parallels the decreasing trend of the entire agglutinated foraminifer fauna. *Haplophragmoides bradyi* drops from 7.9 Ind/g to 5 within the upper 8 cm of the core. *Rhabdammina discreta* is is only present at 0.06 Ind/g at 4 cm and disappears at 8 cm core depth.

ENVIRONMENTAL PROPERTIES

What controls quantitative differences between easterly and westerly stations?

According to the abundance data, the westerly stations show more than 300% more individuals of agglutinated foraminifera than the easterly stations. Both areas are also characterized by strongly different sedimentation rates (Fig. 3). According to the INDAR, both shallower cores yield more than 100% higher values than the two deeper cores.

Thus, most likely the differences between the four cores from the southern flank of the Skagerrak are not entirely the result of dilution through different sedimentation/accumulation rates.

In terms of grain sizes, Cores GKG V and III, and GKG I and II are comparable, more or less reflecting the average strengths of the bottom currents and the INDAR results. TOC, taken as an indicator for the supply of food, however, does not show any dependence on water depth: GKG I: 2.67%; GKG V: 2.48% GKG II: 2.03%; GKG III: 2.62% (surface samples). With regard to the calcareous benthic foraminifer fauna, there also appear to be similarities that are more related to water depth than to the juxtoposition of the location (e.g. strong *Brizalina skagerrakensis* assemblages in both deeper Cores GKG V and III, but differing assemblages in the shallower cores) (Hass, *this volume*). Winnowing may be a reasonable interpretation for highest abundances of foraminifers in core GKG II, however, grain size distributions do not back up this interpretation for core GKG I.

Various possibilities may account for the differences in abundance (here: „ind/g") of agglutinated foraminifers between the agglutinated foraminifer faunas of the easterly and the westerly stations: The quality of the TOC (i. e. the food supply) may vary. Anton *et al.* (1983) and Liebezeit (1988) point out that up to 89% of the TOC is refractory in nature and, thus, not suitable as food for benthic foraminifers, although they might benefit from the associated bacteria (Alve & Murray, submitted). Van Weering *et al* (1987) suggest the TOC may be of allochthonous origin; Anton *et al.* (1993) were not able to clearly determine the portions of terrestrial and marine origin of the organic material. The fraction of TOC that may serve as a potential food source for benthic foraminifers thus decreases down to 0.20-0.27%. Given the quantity of the bulk foraminifer fauna (GKG I: 101 ind/g; GKG II: 1359 ind/g; GKG III: 104 ind/g; GKG V: 94 ind/g), the TOC content of the sediments turns out to be a crucial environmental factor in the sediments investigated for this study. As most of the organic carbon is considered to be allochthonous, the portion that arrives at the easterly stations has to be transported a longer way and may be more affected by oxydization and consumption, thus reducing both quantity and quality for marine benthic life. The calcareous portion of the benthic foraminifers shows numbers of individuals per gram dry sediment (see above) in all cores except GKG II that are similar to each other, hence the calcareous foraminifers might have advantages when competing with the agglutinated foraminifers for food.

The extreme sedimentation rates at the easterly stations may produce some additional stress for the agglutinated foraminifer fauna that results in a lower number of individuals. Agglutinated foraminifers may have a general disadvantage in areas of very high sedimentation rates when compared to the calcareous foraminifers, as their tests do not posses wall pores, which may limit oxygen uptake (Murray, 1991). Thus, the infaunal forms may have to constantly move to escape the oxygen depleted zones in the sediment, these may be as shallow as 0.5 cm core depth in places (Bakker & Helder, 1993).

Geochemical investigations of Kuijpers *et al.* (1993) reveal pathways and concentrations of heavy metals over the study area, that might provide further suggestions for the differences between the easterly and the westerly core locations on the southern flank of the Skagerrak. They showed that concentrations of Hg, Cu, Zn and most likely Pb as well significantly increase from west to east. Mercury, Cu, and Zn contents of the sediment surface appear to increase by 100% from the westerly to the easterly stations. Although absolute values are not exceptionally high, it can be speculated that heavy metal pollution adds further environmental stress to the easterly stations.

Although it is not yet entirely clear which environmental factor is the dominant controlling factor, it appears that the easterly core locations are probably more affected by environmental stress than the westerly stations. This may account for significantly lower abundance of agglutinated foraminifers at these stations.

The recent abundance increase of agglutinated foraminifers

Quantitative analyses carried out for this study support the findings of Alve & Murray (1995) and Alve (in press), showing generally balanced amounts of agglutinated foraminifers during the past 200 years and a marked increase from the

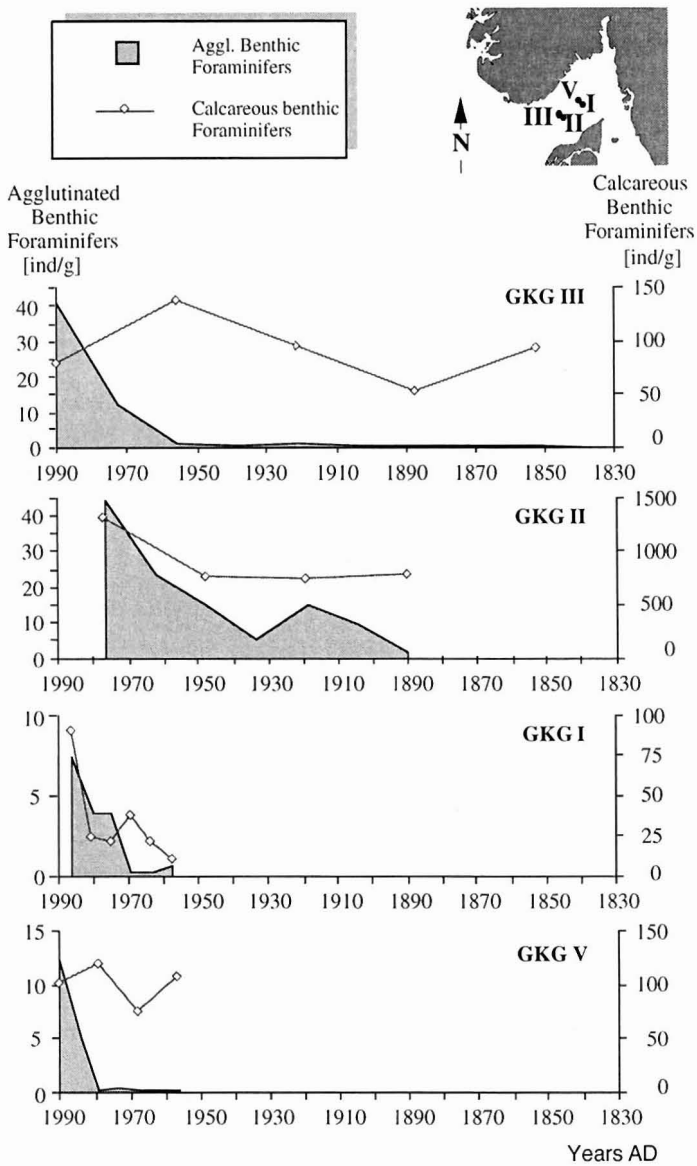


Figure 5. Agglutinated foraminifers and calcareous foraminifers (both ind/g) versus years AD.

early 1970's (Fig. 5). It is apparant, however, that this increase is more marked than that found in the cores of the study of Alve & Murray (op. cit.). This latter effect may be due to different preparation techniques.

The recent increase in agglutinated foraminifers is not paralleled by any of the other variables measured ($\delta^{18}O$, $\delta^{13}C$, $CaCO_3$, TOC, grain size, calcareous benthic foraminifers, etc; see Hass, 1994). Thus, the increase can be inferred to be either the result of a physical or chemical change of the water masses that is not affecting the other parameters analyzed, or it may be a taphonomic effect. Counts of the fragments of the agglutinated foraminifer tests yield trends similar to the complete tests (Fig. 2). This should be significantly different if a large portion of the agglutinated tests were broken or disintegrated in the lower part of the box cores.

A quantitative plot of the agglutinated foraminifers versus depth reveals that a prominent increase in numbers of tests starts basically at approximately 10 cm. The shallow cores GKG I and II show a significant increase at the deeper depth of approximately 24 cm. As there are similar depth-features in cores of strongly different sedimentation rates, these results suggest, that the recent increase may at least partly be controlled by burial depth rather than by external parameters.

Alve (in press), working on cores from the deep Skagerrak basin, could show that not only the quantity but also the species distribution of the agglutinated foraminifer fauna has changed over the past 20-30 years (strong increase of *T. pusillus* and *Saccammina* sp.). As stated in previous chapters, no significant change could be found in the four cores analyzed in this study, however, these are from shallower areas of the Skagerrak than those studied by Alve (op. cit.).

Species distributions

Not much is known about the ecologic preferences of agglutinated foraminifers from the study area. *Eggerelloides* and *L. goesi* dominate the assemblages of all cores. Whereas *Eggerelloides* is of minor importance in Core GKG I, *L. goesi* shows high abundance in both easterly cores. *L. goesi* is of less importance within the cores from the westerly area.

More interestingly, *R. discreta* accounts here for 10 and 20%, respectively. Alve & Murray (submitted) point out that tubular agglutinated foraminifers such as *Rhabdammina* generally suggest a higher food supply because of their relatively high biomass volume. Thus, it may be substantiated that food supply is greater towards the west than at the easterly stations, although this is not reflected by the TOC contents of the sediments.

In addition, the deeper westerly station additionally reveals *H. bradyi*, a species that is not important in any of the other cores. *H. bradyi* and *Eggerelloides* are also among the most frequent agglutinated taxa elsewhere in the deep Skagerrak (see Alve, in press); they mark the upper part of the

stable deep water and the lower part of the transitional water layer, respectively, in the Oslo Fjord (Alve & Nagy, 1990). Thus, *H. bradyi* may account for the conditions, that characterize the Skagerrak deep water, such as more stable conditions and the increased influence of Atlantic water. Since one major difference between location III and the three other stations is lower current speed (Hass, 1996; Rodhe, 1987), *H. bradyi* may as well be indicating a weaker current circulation.

It is possible that, along with other shelf species, *E. scabrus* has been transported in from shelf areas of the Skagerrak, probably originating from the southern North Sea (Alve & Murray, submitted), as only very rarely living specimens have been found outside the shelf area of the Danish slope in the Skagerrak. *Eggerelloides medius*, however, is common, especially in the deeper Skagerrak (Alve & Murray, submitted), a fact that is reflected by the depth dependence of *Eggerelloides* in the sediments investigated for this study.

There is no hint to current strengths sufficient to transport noticable amounts of foraminifers into the deeper Skagerrak (e.g. Rodhe, 1987). Slight downslope transport (creeping) of sediment cannot be excluded, but significant transport would have affected all foraminifers, which is not the case (see also Hass, *this volume*), and terrigenous material of the appropriate equivalent grain size as well. Thus, resedimentation of benthic foraminifers is unlikely at least at the deeper two stations investigated here (GKG III, V).

SUMMARY AND CONCLUSIONS

Four box cores from the southern flank of the Skagerrak covering the past 30-150 years revealed remarkable differences in quality and quantity of the agglutinated foraminifer fauna. Of up to 47 taxa, the four most common are considered to yield information on environmental properties (*L. goesi*, *Eggerelloides*, *R. discreta* and *H. bradyi*).

Generally, the two more westerly locations yield higher ammounts („ind/g") of agglutinated foraminifers than two more easterly locations. The supply of food in combination with the hydrographic regime is the most likely control over these differences. The water mass circulation over the southern flank of the Skagerrak runs from west to east, thus the westerly locations most likely receive a greater amount of more suitable food for foraminifers than the easterly locations. This is not only reflected in the number of agglutinated foraminifers per gram sediment but also in the species distribution. *Rhabdammina discreta*, a suspension feeding tube-shaped agglutinated foraminifer, is characterized by a higher volume of biomass. This foraminifer is abundant in sediments from the westerly locations, whereas it is rare at the easterly locations.

Downcore, the number of specimens in all cores decrease in a manner that suggests a combination of instability of the tests and ecological controls.

ACKNOWLEDGEMENTS

I am gratefull to M. Kaminski (UCL, London) and E. Alve (University of Oslo) who provided many helpful comments. I thank H. Erlenkeuser (C14 Laboratory, Kiel University) for ^{210}Pb analyses. This study was supported by a HCM grant of the European Commission; it is contribution no. 326 of the Sonderforschungsbereich 313 (Special Research Project) of the University of Kiel.

REFERENCES

Alve, E. (in press). Benthic foraminiferal evidence of environmental change in the Skagerrak over the last six decades. *Norges Geologiske Undersøkelse.*

Alve, E. & Murray, J.W. (submitted). Inferences on high fertility and transport from benthic foraminiferal studies in the Skagerrak, North Sea. *Marine Micropaleontology.*

Alve, E. & Murray, J.W. (in press). Benthic foraminiferal distribution and abundance changes in Skagerrak surface sediments: 1937 (Höglund) and 1992/93 data compared. *Marine Micropaleontology.*

Alve, E. & Murray, J.W. 1995. Experiments to determine the origin and paleoenvironmental significance of agglutinated foraminiferal assemblages. *In:* Kaminski, M.A., Geroch, S. & Gasinski, M.A. (eds.), *Proceedings of the Fourth International Workshop on Agglutinated Foraminifera*, Grzybowski Foundation Special Publication, **3**, 1-11.

Alve, E. & Nagy, J. 1990. Main features of foraminiferal distribution reflecting estuarine hydrography in Oslo Fjord. *Marine Micropaleontology*, **16**, 181-206.

Alve, E. & Nagy, J. 1986. Estuarine foraminiferal distribution in Sandebukta, a branch of the Oslo Fjord. *Journal of Foraminiferal Research*, **16**, 261-284.

Anton, K.K., Liebezeit, G., Rudolph, C. & Wirth, H. 1993. Origin, accumulation and distribution of organic carbon in the Skagerrak. *Marine Geology*, **111**, 287-297.

Bakker, J.F. & Helder, W. 1993. Skagerrak (northeastern North Sea) oxygen microprofiles and porewater chemistry in sediments. *Marine Geology*, **111**, 299-321.

Bender, H. 1989. Gehäuseaufbau, Gehäusegenese und Biologie agglutinierter Foraminiferen (Sarcodina: Textulariina). *Jahrbuch Geologische Bundesanstalt*, **132**, 259-347.

Bender, H. 1995. Test structure and classification in agglutinated foraminifera. *In:* Kaminski, M.A., Geroch, S. & Gasinski, M.A. (eds.), *Proceedings of the Fourth International Workshop on Agglutinated Foraminifera*, Grzybowski Foundation Special Publication, **3**, 27-70.

Conradsen, K., Bergsten, H., Knudsen, K.-L., Nordberg, K. & Seidenkrantz, M.-S. 1994. Recent benthic foraminiferal distribution in the Kattegat and the Skagerrak, Scandinavia, *Cushman Foundation Special Publication*, **32**, 53-68.

Corliss, B.H. & Van Weering, T.C.E. 1993. Living (stained) benthic foraminifera within surficial sediments of the Skagerrak. *Marine Geology*, **111**, 323-

336.

Dahl, G.E. 1978. On the existence of a deep countercurrent to the Norwegian Coastal Current in the Skagerrak. *Tellus*, **30**, 552-556.

Davies, A.M. 1980. Application of numerical models to the computation of the wind induced circulation of the North Sea during JONSDAP '76. *„Meteor" Forschungsergebnisse*, **22**, 53-68.

Ehrmann, W. & Thiede, J. 1985. History of Mesozoic and Cenozoic sediment fluxes to the North Atlantic Ocean. *Contributions to Sedimentology*, **15**, 1-109.

Erlenkeuser, H. & Pederstad, K. 1984. Recent sediment accumulation in Skagerrak as depicted by 210Pb-dating. *Norsk Geologisk Tidskrift*, **64**, 135-152.

Feyling-Hanssen, R.W. 1964. Foraminifera in Late Quaternary deposits from the Oslofjord area. *Norges Geologiske Undersøkelse*, **225**, 1-383.

Feyling-Hanssen, R.W., Joergensen, J.A., Knudsen, K.L. & Andersen, A.-L.L. 1971. Late Quaternary Foraminifera from Vendysyyel, Denmark and Sandnes, Norway. *Bulletin of the Geological Society of Denmark*, **21**, 67-317.

Fonselius, S. 1989. Hydrographic variabilities in the Skagerrak surface water. *ICES*, C.M. 1989, Session Q.

Gabel, B. 1971. Die Foraminiferen der Nordsee. *Helgoländer wissenschaftliche Meeresuntersuchungen*, **22**, 1-65.

Hass, H.C. 1994. Sedimentologische und mikropaläontologische Untersuchungen zur Entwicklung des Skagerraks im Spätholozän. *GEOMAR Report*, **34**, 115.

Hass, H.C. 1996. Northern Europe climate variations during Late Holocene: evidence from marine Skagerrak. *Palaeogeography, Palaeoclimatology, Palaeoecology*, **123**, 121-145.

Hemleben, C., Kaminski, M.A., Kuhnt, W. & Scott, D.B. (eds.) 1990. *Paleoecology, biostratigraphy, paleoceanography and taxonomy of agglutinated foraminifera*, NATO ASI Series C-327, 1017pp., Kluwer Academic Publishers.

Höglund, H. 1947. Foraminifera of the Gullmar Fjord and the Skagerrak. *Zoologiska Bidrag från Uppsala*, **26**, 0-328.

Jones, R.W. 1994. *The Challenger foraminifera*, 150pp., Oxford University Press.

Jørgensen, P., Erlenkeuser, H., Lange, H., Nagy, J., Rumohr, J. & Werner, F. 1981. Sedimentological and stratigraphical studies of two cores from the Skagerrak. *In:* Nio, S.D., Schüttenhelm, R.T.E. & Van Weering, T.C.E. (eds.), *Holocene marine sedimentation in the North Sea basin*, Special Publication of the International Association of Sedimentologists, **5**, 397-414.

Knudsen, K.-L., Conradsen, K., Heier-Nielsen, S. & Seidenkrantz, M.-S. 1996. Paleoenvironments in the Skagerrak-Kattegat in the eastern North Sea during the last deglaciation. *Boreas*, **25**, *in press*.

Knudsen, K.-L., Conradsen, K., Heier-Nielsen, S. & Seidenkrantz, M.-S. 1996. Quaternary paleoceanography in northern Denmark: a review of results from the Skagen cores. *Bulletin of the Geological Society of Denmark*, **43**, *in press*.

Kuijpers, A., Dennegård, B., Albinsson, Y. & Jensen, A. 1993. Sediment transport pathways in the Skagerrak and Kattegat as indicated by sediment Chernobyl radioactivity and heavy metal concentrations. *Marine Geology*, **111**, 231-244.

Kuijpers, A., Dennegård, B., Troelstra, S.R., Albinsson, Y., Gustafsson, O., Jensen, A., Schwarz, U., Svensson, R. & Christvall, A. 1989. *Areal distribution patterns of heavy metals, radionuclides and benthic foraminifera in surface sediments of the northern Kattegat and adjacent Skagerrak*, University of Göteborg, Dept. of Marine Geology, Report **6**.

Larsson, A.M. & Rodhe, J. 1979. Hydrographical and chemical oceanography in the Skagerrak 1975-1977. *Göteborg University, Oceanography Institute Reports*, **29**, 1-39.

Lee, A.J. 1980. North Sea: physical oceanography. *In:* Banner, F.T., Collins, M.B. & Massie, K.S. (eds.), *The sea bed and the sea in motion: II. Physical and chemical oceanography, and physical resources*, 467-495, Elsevier.

Liebezeit, G. 1988 Early diagenesis of carbohydrates in the marine environment; II, Composition and origin of carbohydrates in Skagerrak sediments. *Proceedings of the 13th international meeting on Organic Geochemistry, Milan, Italy, 1988.*

Loeblich, A.R. & Tappan, H. 1987. *Foraminiferal genera and their classification*, Vol. 1, 970 pp, Vol. 2, 212 pp, Van Nostrand Reinhold Company, New York.

Moodley, L., Troelstra, S.R. & Van Weering, T.C.E. 1993. Benthic foraminiferal response to environmental change in the Skagerrak, northeastern North Sea. *Sarsia*, **78**, 129-139.

Müller, G. & Irion, G. 1984. Chronology of heavy metal contamination in sediments from the Skagerrak (North Sea). *In:* Degens, E.T., Krumbein, W.E. & Prashnowsky, A.A. (eds.), *Ein Nord-Süd Profil; Zentraleuropa-Mittelmeerraum-Afrika*, Mitteilungen aus dem Geologisch Palaeontologischen Institut der Universität Hamburg, **56**, 413-421.

Murray, J.W. 1991. *Ecology and Palaeoecology of Benthic Foraminifera*, 397 pp., Longman Scientific & Technical.

Nagy, J. & Qvale, G. 1985. Benthic foraminifers in upper quaternary Skagerrak deposits. *Norsk Geologisk Tidskrift*, **65**, 107-113.

Nigam, R., Qvale, G. & Thiede, J. 1984 Foraminiferal distribution of post-glacial Quaternary sediments in a core from the Skagerrak, NE-North Sea. Paper presented at the X Indian colloquium on micropaleontology and stratigraphy, 1984.

Nordberg, K. 1989. Sea floor deposits, paleoecology and paleoceanography in the Kattegat during the later part of the Holocene. *Geologiska Institutionen*, **A65** (dissertation), 1-205.

Rodhe, J. 1987. The large-scale circulation in the Skagerrak; interpretation of some observations. *Tellus*, **39**, 245-253.

Schröder, C. J. 1986. Deep water arenaceous foraminifera in the Northwest Atlantic Ocean. *Canadian Technical Reports on Hydrography and Ocean Sciences*, **71**, 1-191.

Seidenkrantz, M.-S. 1993. Subrecent changes in the foraminiferal distribution in the Kattegat and the Skagerrak, Scandinavia: anthropogenic influence and natural causes. *Boreas*, **22**, 383-395.

Seidenkrantz, M.S. 1992. Recent benthic foraminiferal provinces in the Kattegat and Skagerrak and indication of diminished oxygen conditions. *In:* Dennegård, B. & Kuijpers, A. (eds.), *Marine Geological Environmental Investigations in the Skagerrak and Northern Kattegat*, 1-12, University of Göteborg, Dept. of Marine Geology Reports, **7**.

Struck, U. 1992. Zur Paläo-Ökologie benthischer Foraminiferen im Europäischen Nordmeer während der letzten 600 000 Jahre. *Berichte aus dem Sonderforschungsbereich 313*, **38**, 1-89.

Svansson, A. 1975. Physical and chemical oceanography in the Skagerrak and the Kattegatt. 1. Open sea conditions. *Fishery Board Sweden, Institute for Marine Research Reports*, **1**, 1-88.

Thiede, J. 1985. Planctonic foraminifers in upper quaternary Skagerrak sediments. *In:* Stabell, B. & Thiede, J.

(eds.), *Upper Quaternary marine Skagerrak (NE North Sea) deposits; stratigraphy and depositional environment*, Norsk Geologisk Tidsskrift, **65**, 115-118.

Van Weering, T.C.E., Berger, G.W. & Kalf, J. 1987. Recent sediment accumulation in the Skagerrak, northeastern Skagerrak. *Netherlands Journal of Sea Research*, **21**, 177-189.

Van Weering, T.C.E. & Qvale, G. 1983. Recent sediments and foraminiferal distribution in the Skagerrak, northeastern North Sea. *Marine Geology*, **52**, 75-99.

APPENDIX : Taxonomy

A total of 47 species could be identified. Although it was attempted to determine the agglutinated foraminifers to the species level, some could not sufficiently be determined. Thus, in the text, references are occasionally only to the genus level.

Adercotryma glomeratum (Brady, 1878)
Plate 4, Fig. 19 in Bender (1995);
Plate 67, Figs. 1-3 in Loeblich & Tappan (1988);
Plate 3, Figs. 22-23 in Gabel 1971 (as *Adercotryma glomerata*).
Ammodiscus sp.
Ammolagena clavata (Jones & Parker, 1860)
Plate 41, Figs. 12-16 in Jones (1994);
Plate 2, Fig. 9 in Bender (1995);
Plate 36, Fig. 16 in Loeblich & Tappan (1988);
Plate 3, Figs. 16-17 in Gabel (1971)
Bathysiphon filiformis (Sars, 1872)
Plate 13, Fig. 2 in Loeblich & Tappan (1988);
Plate 26, Figs. 17-20 in Jones (1994).
Bigenerina nodosaria (d'Orbigny, 1826)
Plate 7, Fig. 1 in Bender (1995);
Plate 191, Figs. 1-2 in Loeblich & Tappan (1988);
Plate 46, Figs. 46-48 in Gabel, 1971.
Cribrostomoides kosterensis (Höglund, 1974)
Plate 4, Figs. 5-6 in Gabel (1971).
Cribrostomoides subglobosus (Cushman, 1910)
Plate 5, Fig. 2 in Bender (1995);
Plate 1, Figs. 1-4 in Jones *et al.* (1993) (as *Cribrostomoides subglobosus* forma *subglobosus* [Cushman, 1910]);
Plate 4, Figs. 1-2 in Gabel (1971) (as *Cribrostomoides subglobosum* [Sars]).
Cribrostomoides wiesneri Parr, 1950
Plate 3, Figs. 36-37 in Gabel (1971).
Cribrostomoides sp.
Crithionina sp.
Dorothia sp.
Eggerelloides scabrus (Williamson, 1858)
Plate 1, Figs 6-7 in Alve & Murray (1995);
Plate 47, Figs. 15-17 in Jones *et al.* (1995) (as *Eggerelloides scaber* [Williamson]);
Plate 189, Figs. 5-7 in Loeblich & Tappan (1988).
Eggerelloides medius (Höglund, 1947)
Plate 1, Figs 6-7 in Alve & Murray (1995).
Eratidus foliaceus (Brady, 1884)
Plate 59, Figs. 1-3 in Loeblich & Tappan (1988).
Glomospira charoides (Jones & Parker, 1860)
Plate 3, Fig. 1 in Bender (1995);
Plate 3, Figs. 13-15 in Gabel (1971).
Haplophragmoides bradyi (Robertson, 1893)
Plate 1, Figs. 10-11 in Alve & Murray (1995);
Plate 3, Figs. 30-31 in Gabel (1971).
Haplophragmoides sphaeriloculus Cushman, 1910
Plate 17, Figs. 5-7 in Schröder (1986).
Hyperammina cylindrica Parr, 1950
Plate 23, Fig. 4, 7 in Jones (1994).
Hyperammina laevigata Wright, 1891
Plate 16, Fig. 6 in Bender (1989);
Plate 23, Figs. 9-10 in Jones (1994).
Hyperammina sp.
Lagenammina sp.
Liebusella goesi Höglund, 1947
Plate 14, Figs. 4-8 in Höglund (1947);
Plate 6, Fig. 4 in Bender (1995) (as *L.? goesi*);
Plate 5, Figs. 20-21 in Gabel (1971).
Liebusella sp.
Morulaeplecta bulbosa (?)
Psammosphaera fusca Schulze, 1875
Plate 4, Figs. 9-14 in Höglund (1947);
Plate 1, Fig. 14 in Bender (1995).
Quinqueloculina agglutinans d'Orbigny, 1839
Plate 7, Fig.16 in Bender (1995).
Recurvoides sp.
Reophax difflugiformis Brady, 1879
Plate 3, Fig. 9 in Bender (1995) (as *R.* cf. *R. difflugiformis*);
Reophax fusiformis (Williamson, 1858)
Plate , Fig. 1 in Bender (1995).
Reophax micacea Earland, 1934
Plate 4, Fig. 3 in Bender (1995);
Plate 1, Figs 20-21 in Alve & Murray (1995).
Reophax regularis Björkholmen
Plate 9, Figs. 11-12 in Höglund (1947).
Reophax scorpiurus Montfort, 1808
Plate 9, Figs. 9-10 in Höglund (1947);
Plate 4, Fig. 5 in Bender (1995);
Reophax subfusiformis Earland, 1933
Plate 9, Figs. 1-4 in Höglund (1947).
Reophax sp.
Rhabdammina discreta Brady, 1884
Plate 1, Figs. 6-7 in Höglund (1947).
Rhabdammina linearis Brady, 1879
Plate 1, Figs. 1-5 in Höglund (1947);
Plate 20, Fig. 1 in Gabel (1971).
***Rhabdammina* sp.**
***Saccammina* sp.**
Saccammina sphaerica Brady, 1871
Plate 4, Figs. 15-17 in Höglund (1947);
Plate 3, Fig. 2 in Gabel (1971).
***Spiroplectammina* sp.**
Textularia conica d'Orbigny, 1839
Plate 17, Fig. 17 in Bender (1989);
***Textularia* sp.**
***Tritaxis* sp.**
Trochamminopsis pusillus (Höglund, 1947)
Plate 1, Figs 24-25 in Alve & Murray (1995).
***Trochammina* sp.**
***Veleroninoides* sp.**
Verneuilina advena Cushman, 1910
Plate 13, Fig. 11 in Höglund (1947).

Spatial and temporal dynamics of coccolithophore communities during low production phases in the Norwegian-Greenland Sea

KARL-HEINZ BAUMANN[1], HARALD ANDRULEIT[2], ANDREA SCHRÖDER-RITZRAU[3] and CHRISTIAN SAMTLEBEN[4]

1. FB Geowissenschaften, Univ. Bremen, Postfach 330440, D-28334 Bremen, Germany
2. SFB 313, University of Kiel, Heinrich-Hecht-Platz 10, D-24118 Kiel, Germany
3. GEOMAR - Research Center for Marine Geosciences, Wischhofstr. 1-3, D-24148 Kiel, Germany
4. Geolog.-Paläontolog. Inst., University of Kiel, Olshausenstr. 40, D-24118 Kiel, Germany

ABSTRACT

The present investigation was initiated to report on species compositions and dynamics in the Norwegian-Greenland Sea during low production phases in spring and early summer. Thus, the distribution patterns of living coccolithophores during June to July, 1990, February and May, 1991, and March to April, 1995 were investigated. In general, the seasonal development of the phytoplankton started after the yearly dark period and coccolithophores increased in abundance when the water column was more stratified and both temperatures and insolation increased. Cell densities reached a maximum of 207×10^3 coccospheres/l in the southeastern part of the studied area. However, these high cell densities probably resulted from „old" populations, drifted to the Norwegian-Greenland Sea from the North Atlantic. Some of the collected samples did not contain any coccolithophores.

In total, 15 coccolithophore species were identified. The diversity was generally higher in the eastern part of the Norwegian-Greenland Sea and to the west the coccolithophore communities often were monospecific. *Emiliania huxleyi* is the dominant species, but *Calciopappus caudatus* and *Algirosphaera robusta* also considerably contribute to the communities. High cell densities of *C. caudatus* were interpreted as the result of a bloom or more probably close to bloom conditions during the general low productive period. In addition, many of the *E. huxleyi* coccoliths from the surface waters of the southeastern Norwegian-Greenland Sea were heavily corroded. These specimens may have drifted within the Atlantic water for a longer time.

INTRODUCTION

Coccolithophores are a major group of marine, unicellular phytoplankton. They form external calcified plates with a complex ornamentation, which cover the cell surface. These coccoliths form an important part of the fine fraction of deep-sea sediments and therefore are extensively used in biostratigraphic, paleoecologic, and paleoceanographic studies (e.g. McIntyre & Bé, 1967; Geitzenauer *et al.*, 1976; Roth & Coulborn, 1982; Gard, 1988; Crux & van Heck, 1989; Baumann, 1990; Baumann & Matthiessen, 1992). Many studies on recent calcareous nannoplankton in the northern Atlantic Ocean are predominantly taxonomic (e.g. Halldal & Markali, 1954, 1955; Gaarder & Markali, 1956; Gaarder & Heimdal, 1977; Heimdal & Gaarder, 1980, 1981; Kleijne, 1991; Knappertsbusch, 1993). In addition, much of the earlier plankton work from our study area in the Norwegian-Greenland Sea only included microscopic examinations of the netplankton, while the smaller nannoplankton has often been overlooked. However, a number of investigations concerning the dynamics and ecology of calcareous nannoplankton in northern North Atlantic have recently been published (e.g. Samtleben & Schröder, 1992; Knappertsbusch & Brummer, 1995; Samtleben *et al.*, 1995a). About 20 different coccolithophore species have so far been

In: Hass, H.C. & Kaminski, M.A. (eds.) 1997. Contributions to the Micropaleontology and Paleoceanography of the Northern North Atlantic. *Grzybowski Foundation Special Publication*, no. 5, pp. 227-243

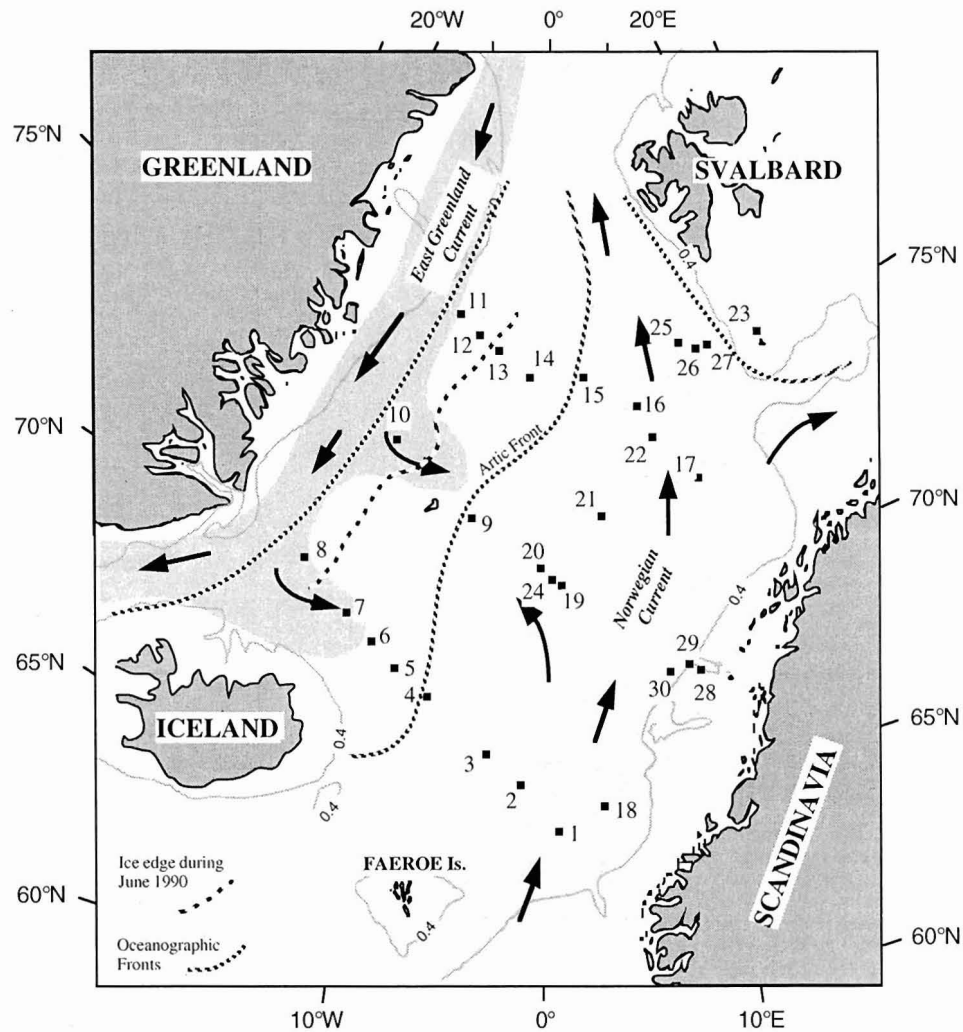


Figure 1. Map of the Norwegian-Greenland Sea including surface current pattern, oceanographic fronts, ice edge during June 1990 (from Thiede & Hempel, 1991), and locations (squares) of the plankton samples.

identified in the Norwegian-Greenland Sea (e.g. Halldal & Markali, 1955; Samtleben & Schröder, 1992; Samtleben *et al.*, 1995a). The communities with the highest diversities are found in the area of the Norwegian Current. To the north and to the west species numbers gradually decrease and only three species are found on the Greenland shelf (Samtleben & Schröder, 1992).

The Norwegian-Greenland Sea is an area of strong east to west hydrographic gradients (Fig. 1). The present surface current system on the eastern side of the Norwegian-Greenland Sea is dominated by the Norwegian Current, a relatively warm (6°-10°C), saline (>35‰) branch of the North Atlantic Drift flowing northward into the Arctic Ocean (Swift, 1986). On the western side the East-Greenland Current carries cold (<0°C), less saline (30-34‰) polar water southward along the East Greenland coast. Between these two main currents mixed Arctic surface water is formed in two large gyres (Jan Mayen Current and East-Iceland Current) (Johannessen, 1986). The close juxtaposition of warm and cold water masses results in the formation of distinct oceanographic fronts (Fig. 1).

The Norwegian-Greenland Sea is also characterized by strong seasonal changes which are mainly controlled by cycles of insolation, water temperature, and ice cover. These seasonal changes result in distinct variations of the biological productivity (Bathmann *et al.*, 1990; Bauerfeind *et al.*, 1994; von Bodungen *et al.*, 1995). Long-term records of vertical coccolithophore flux in the Nor-

wegian-Greenland Sea demonstrated strong seasonality with peak fluxes during summer and autumn. A less distinct but still recognizable coccolith flux was observed during spring and early summer (Samtleben & Bickert, 1990; Andruleit, *in press*). However, the distribution of living coccolithophore communities during this time of the year was hitherto poorly known in the Norwegian-Greenland Sea. Thus, this study was initiated to report on species compositions and dynamics during low production phases in spring and early summer. The present investigation is part of an extensive actualistic study of the plankton community, settling assemblages, and development of late Quaternary assemblages in the Norwegian-Greenland Sea (Samtleben *et al.*, 1995b).

MATERIAL AND METHODS

The investigated plankton samples were collected in different years since 1990 during spring and early summer in the entire Norwegian-Greenland Sea and are part of an on-going sampling project on coccolithophores in this region. A total of 76 plankton samples from 30 stations (Fig. 1) have been studied and are listed in Appendix 1 together with the geographical and hydrological data for each location.

The main portion of plankton samples was collected during PRV „Polarstern" Cruise ARK VII/1 (Thiede & Hempel, 1991) between June 12th and July 8th in 1990. Sampling took place along two transects extending from the central Norwegian Sea to the continental margin of Greenland, crossing the major surface water mass boundaries (Fig. 1). The ice edge was crossed by PRV „Polarstern" several times during ARK VII/1 (Thiede & Hempel, 1991). Thus, samples of the stations 8, 10, 11, and 12 are from below the ice cover. Ice concentra-

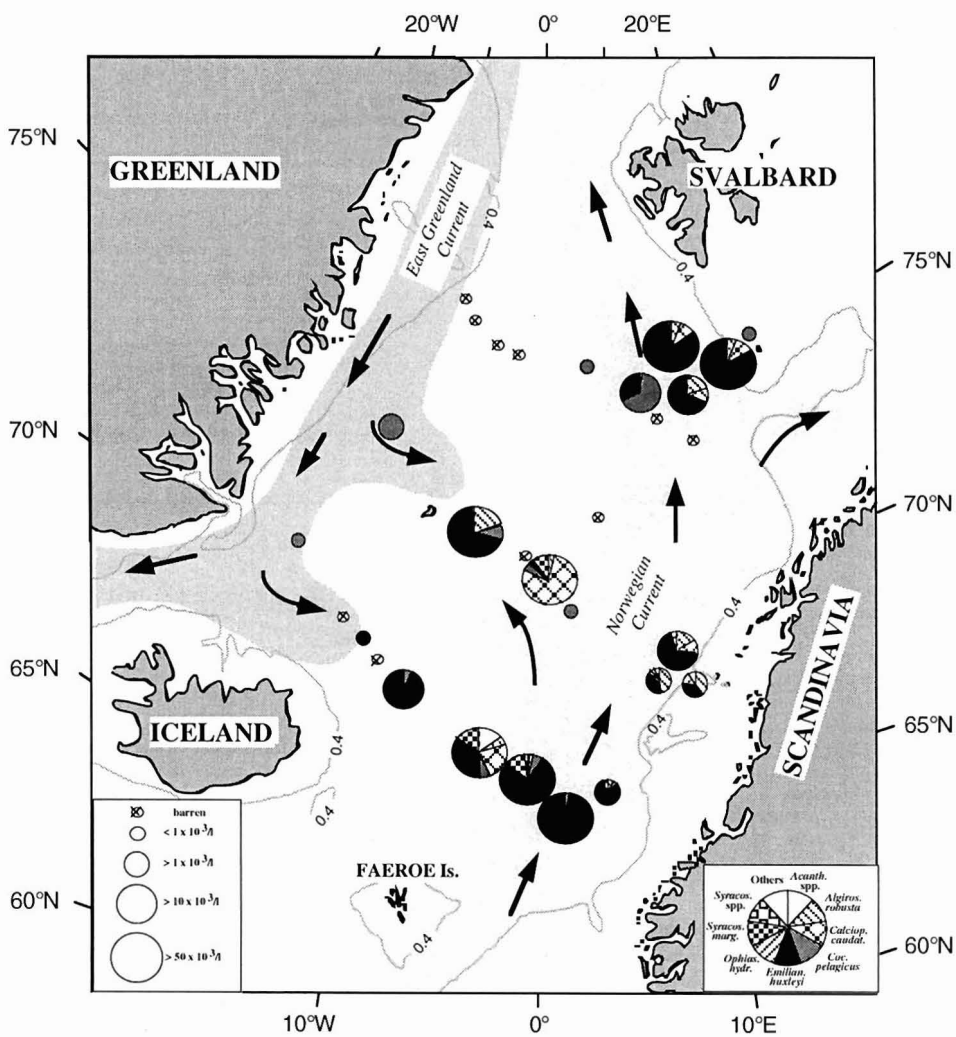


Figure 2. Cell densities and species compositions of coccolithophore communities during low production periods in spring and early summer in the Norwegian-Greenland Sea.

tions ranged from 1/10 to 9/10, but generally were about 5/10. The dominant ice type seen was 2.5m to 3.5m-thick multiyear ice, while firstyear ice was uncommon. Additional water samples were taken during a „Valdivia" Cruise in the central and northern Norwegian Sea between May 20th and 27th in 1991, and during two „Poseidon" Cruises in the eastern and northern Norwegian Sea from February 22nd to 27th 1991 and March 25th to April 6th 1995 (Appendix 1).

Generally, samples were taken in 5l Niskin bottles with a Rosette-sampler. Dependent on CTD-profiles, water was collected at the surface, above (7m-30m) and below (10m-40m) thermocline, and at around 100m water depth at each station. Additional surface water samples from 10m depth were obtained with the ship's seawater pump (Stations 1, 4, 5, 6, and 7).

The water samples were immediately filtered on board through Millipore filters (47 mm diameter, 0.45 µm pore size) by means of a vacuum pump. Without further washing, rinsing or chemical conservation the filters were dried at 40-60°C for at least four hours. The filters were then stored in plastic Petri dishes, and kept permanently dry in closed boxes with silica gel.

Coccolithophore cell densities were determined with a scanning electron microscope (SEM) at 10 KV. For that purpose, a small piece was cut from the dried filter, fixed on an SEM stub, and then coated with carbon and gold. The number of individuals and the species composition were determined by identifying and counting coccospheres on measured transects (1-2 mm^2) at a magnification of 2000x. A specimen which appeared to be a perfect or nearly perfect coccosphere was counted as one individual. Isolated coccoliths were not included in this study. For species identification the publications of Gaarder & Heimdal (1977), Okada & McIntyre (1977), Nishida (1979), Norris (1984), Samtleben & Schröder (1992), and Jordan & Kleijne (1994) were used.

RESULTS

Coccolithophore cell densities and species compositions

The standing crop varied from $207x10^3$ coccospheres/l at station 2 to below $1x10^3$ coccospheres/l at several stations (Appendix 1). Some of the collected samples did not contain any coccolithophores (Fig. 2). In particular, samples from the western part of the study area were characterized by very low cell densities (consistently $<2.5x10^3$ coccospheres/l) or were even barren. Medium (1 to $50x10^3$ coccospheres/l) to high ($>50x10^3$ coccospheres/l) cell densities were found only in surface water samples from the eastern Norwegian Sea which were influenced by temperate water of the Norwegian Current. This general distribution of cell densities was independent of the time of sampling; for example stations 11 to 14 from the northwestern Greenland Sea were taken during early July and were barren of coccolithophores, whereas

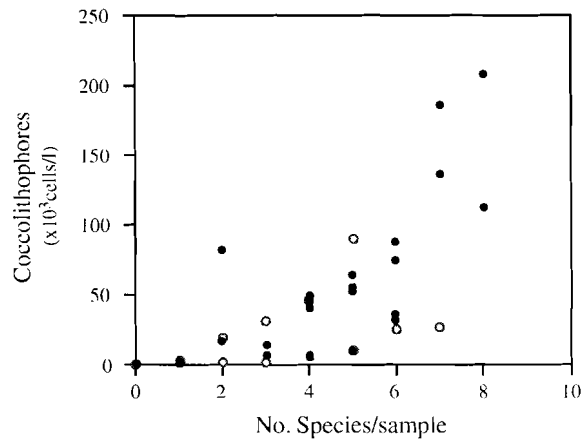


Figure 3. Numbers of species per sample plotted against cell density (black dots = 0-25m water depth, open circles = >25m water depth).

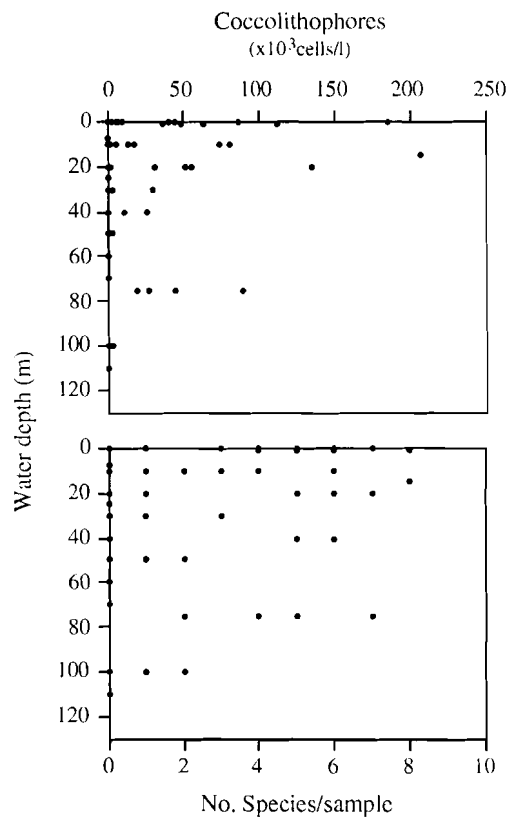


Figure 4. Cell densities and numbers of species per sample plotted against water depth.

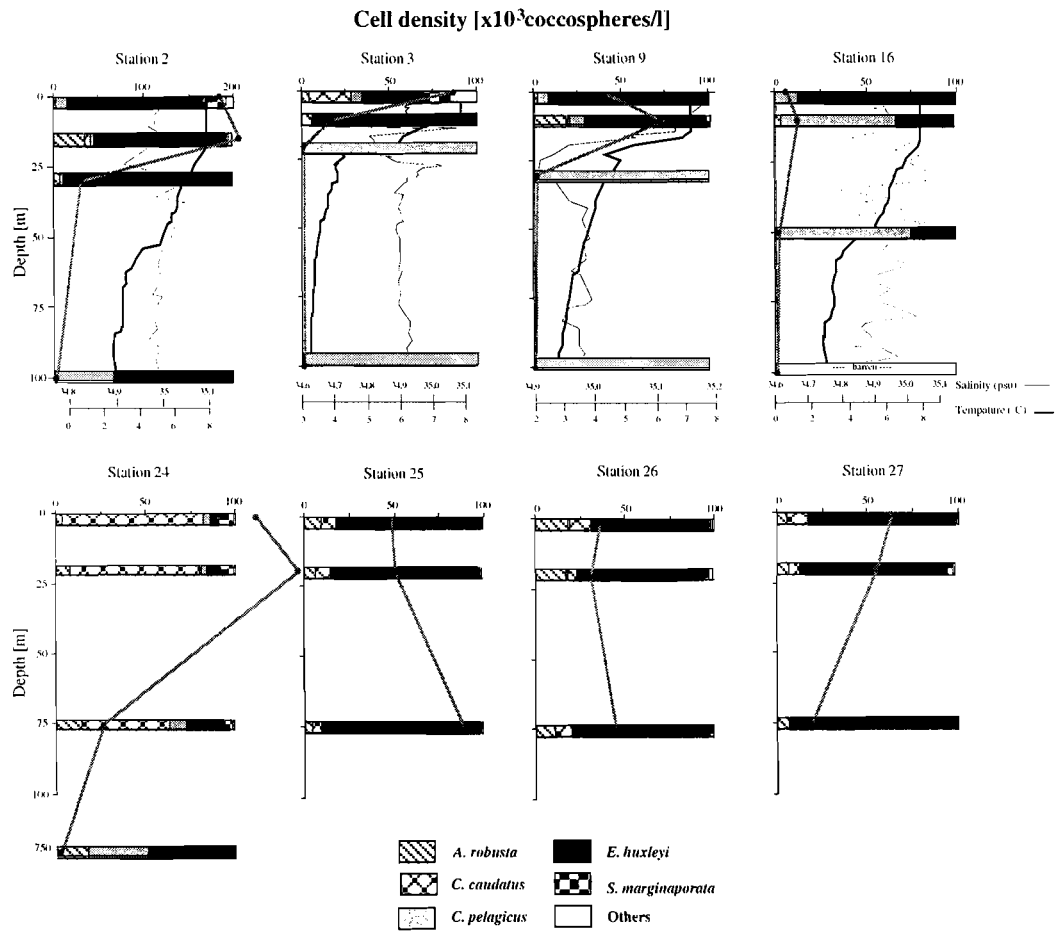


Figure 5. Vertical distribution of coccolithophore communities from stations which have at least three samples containing coccolithophores. Salinity and temperature data for stations 2, 3, 9, and 16 are from CTD-measurements.

stations 28 to 30, taken earlier in the year during late March and early April, already exhibited medium cell densities.

Overall, a total of 15 coccolithophore species was identified during the present study (Appendix 2; Plates 1, 2). The number of species generally increased with increasing cell numbers (Fig. 3). The diversity was generally higher in the eastern part of the study area and coincides with the highest cell densities. To the west the coccolithophore communities were often monospecific.

The main component of the coccolithophore flora in surface waters was *Emiliania huxleyi*. This species almost always dominated the communities when medium to high cell densities occurred, accounting for approximately 70% of most of the sample communities. An exception was station 24 where *Calciopappus caudatus* dominated the coccolithophore community with high cell densities of about $100x10^3$ coccospheres/l. Other species such as *Algirosphaera robusta*, *Acanthoica quattrospina*, *Ophiaster hydroideus*, and *Syracosphaera marginaporata*, were also well represented during the non-production phases but neither reached high cell densities nor dominated the communities. *Coccolithus pelagicus*, found in both the non-motile stage and the *Crystallolithus hyalinus* stage (motile phase), was the most frequently occurring species but was important only at station 16 with $8x10^3$ coccospheres/l. This species frequently was characteristic of very low diversity to monospecific communities, especially in the western part of the study area.

Sixteen of the 30 subsurface samples (> 20m water depth) yielded coccosphere communities with nine species (Appendix 1). Cell densities were highest in the uppermost 20m of the water column and decreased towards greater depth, whereas the number of species did not show equivalent changes (Fig. 4). Cell densities and species compositions

of all stations with at least three sampling depths which were not barren are depicted in Figure 5.

At all locations the communities in a mixed water layer above a thermocline were characterized by a relatively high similarity in species composition. At stations 2, 3, 9, and 16 the temperature and salinity values (Fig. 5) indicated the transition between two different water layers. Above this stratification, diverse communities with highest cell densities prevailed, often dominated by *E. huxleyi*. In contrast, in the range of the thermocline and especially below it *C. pelagicus* dominated the low diversity to monospecific communities with very low cell densities. At stations 24-27 no clear thermocline was observed and, thus, abundances and species composition were relatively similar to each other at all depths. *E. huxleyi* was the most dominant species in all of the samples at stations 25-27, whereas at station 24, *Calciopappus caudatus* dominated the coccolithophore flora. In addition, a strong decrease in cell density with increasing water depth was observed at the latter station.

Many of the June-July 1991-samples (from PRV Polarstern ARKVII/1-cruise) also contain a significant number of siliceous organisms, including diatoms and some silicoflagellates. A bloom of *Thalassiotrix longissima* was observed over the eastern Iceland Plateau; and west of Jan Mayen high concentrations of *Rhizosolenia* spp. occurred (see also Thiede & Hempel, 1991). However, most of the samples of the westernmost stations were free of siliceous organisms as well as of coccolithophores.

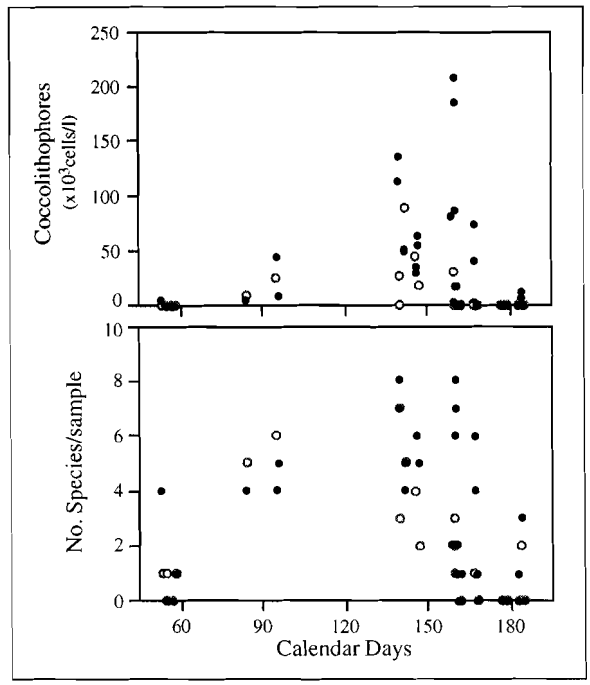


Figure 6. Cell densities and numbers of species per sample plotted against calendar days (black dots = 0-25m water depth, open circles = >25m water depth). Note that cell densities >150*10^3 cells/l probably resulted from drifted „old" *E. huxleyi* populations.

Corrosion of coccolithophores

The presence of highly corroded and/or dissolved coccospheres and, especially, coccoliths was a significant result of this investigation. Remarkably, corroded specimens were found only in the June-July 1991 samples within the temperate Norwegian Current. In addition, only coccoliths of *Emiliania huxleyi* were affected by this feature. Other delicate-structured forms such as *Calciopappus caudatus*, *Acanthoica quattrospina* did not show any signs of corrosion or dissolution. All samples also contained a relatively high number of intact *E. huxleyi* specimens. Nevertheless, more than approximately 70% of the *E. huxleyi* coccospheres in the plankton samples from surface and subsurface waters of the Norwegian Current (Stations 1, 2, 3, 4, and 16) were collapsed and many of them had an opening, possibly a pylome (Plate 2, Fig. 6).

All coccospheres seemed to have their normal shape, and only the coccoliths show a high degree of corrosion. Usually, all coccoliths on a coccosphere were affected. However, the proximal shield of the coccoliths was not or less affected by this phenomenon, and differentiation of boundaries between single proximal shields was often impossible. The T-shaped elements of the distal shields were not connected to each other at the periphery and mostly their arrangement was totally disturbed. Often, single elements were heavily or totally dissolved. The elements of the central opening either were fused together without building the normal central grid or were absent (Plate 2). In addition, incomplete shields in the central area of the specimens (Plate 2, Fig. 3, 6) are probably organic and not fused calcitic elements.

DISCUSSION

Variation in coccolithophore cell densities and community dynamics

The observed coccolithophore communities are part of a recurrent seasonal cycle of communities in the Norwegian-Greenland Sea. However, the production phases and the development of coccolithophore blooms are highly variable in space and time (Samtleben & Schröder, 1992; Samtleben *et al.*, 1995a). Also, the composition and species numbers within the Norwegian Current may vary considerably from year to year. Sakshaug *et al.* (1981) found small-scale and short-term horizontal and vertical variations in standing crop of the coccolithophore flora off northern Norway in 1975 and 1976. However, generally the main production phase of coc-

colithophores in the Norwegian-Greenland Sea shifts from the southeast to the northwest during summer (Samtleben & Schröder, 1992; Samtleben *et al.*, 1995a). While south of Iceland the first blooms occur during May/June, a high cell density is observed in the region of the Vøring Plateau during July, in the Barents Sea during August, and west of Jan Mayen not before September. In the present study, the limiting influence of low temperatures to coccolithophore thriving is clearly depicted by overall low cell densities and many barren samples during spring and early summer. This is, further supported by absence or very low cell densities of coccolithophores recorded at the westernmost stations which, at least partly, were within the ice cover. The increase in coccolithophore production during spring and early summer is also indicated by a general increase in cell numbers in the investigated samples (Fig. 6). This holds true even when considering that a high portion of *Emiliania huxleyi*, the main component of the community, may not be part of the coccolithophore standing crop of this region. The heavily corroded specimens most probably were the result of a plankton bloom which occurred in the North Atlantic either in fall of the previous year or in early spring and were drifted to this region by the North Atlantic Drift (see discussion below).

It is obvious that, even during low production phases in spring coccolithophore communities may exhibit a relatively high variability in both species diversity and species composition, although low cell densities prevailed during February to April (Fig. 6). Cell densities, in contrast, drastically increased in waters above about 5°C (Fig. 7). In addition, medium to high cell densities are only reached in the eastern part of the Norwegian-Greenland Sea, in an area influenced by temperate surface waters of the Norwegian Current, whereas relatively high cell concentrations in late summer were previously recorded in close proximity to the East Greenland Current (Samtleben & Schröder, 1992; Samtleben *et al.*, 1995a). Therefore, during spring and early summer

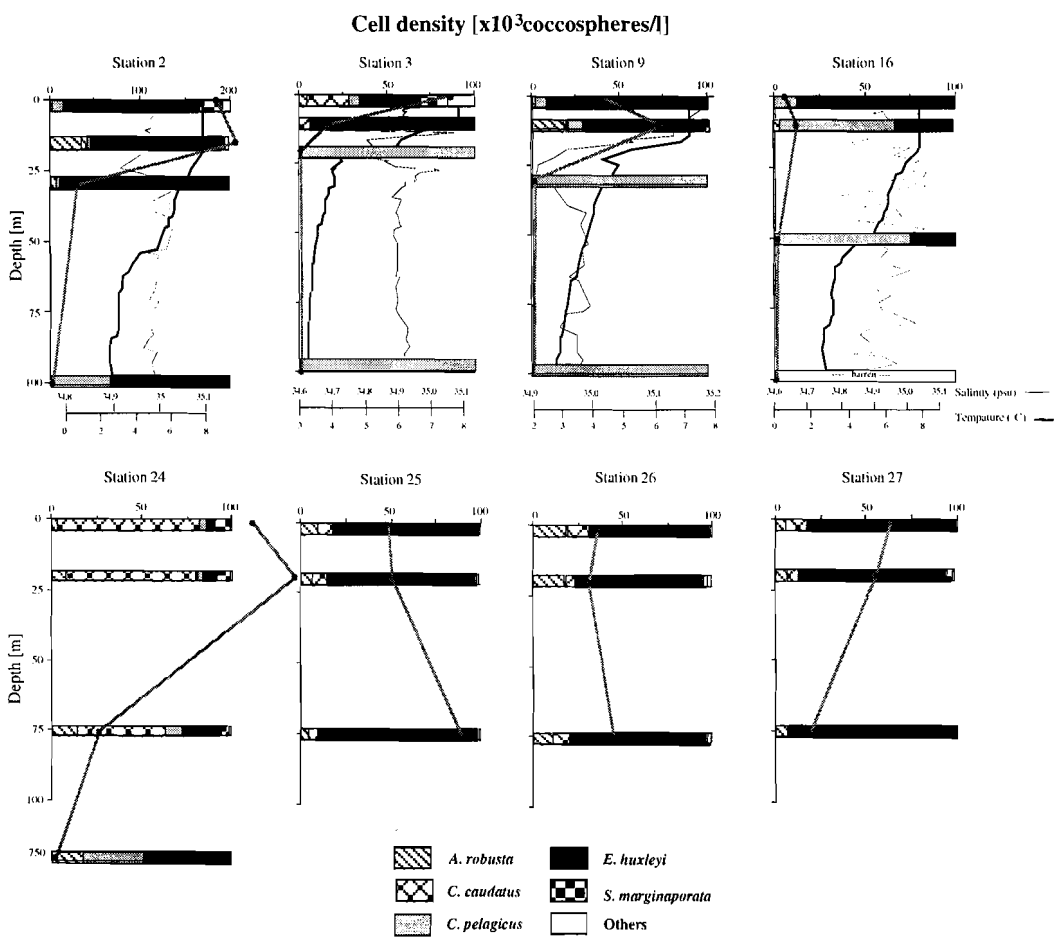


Figure 7. Cell densities and numbers of species per sample plotted against both temperature and salinity.

the oceanic fronts, such as the Arctic Front, divide the Norwegian-Greenland Sea into distinct areas of coccolithophore habitats. In the western part, which mainly coincides with the Artic water masses, only low diversity to monospecific communites were observed, whereas in the eastern part high cell densities with high diversities were already present. In contrast, in late summer during the main production phases the oceanic frontal systems probably lose their boundary function and high cell densities, especially of *E. huxleyi*, occur in the entire study area (Samtleben *et al.*, 1995b).

In general, the low standing crop as well as the increase in cell density during the period February-June corresponds well with previous findings of Halldal (1953), Braarud *et al.* (1958), Smayda (1958), Samtleben & Schröder (1992), and Samtleben *et al.* (1995a). They all reported that coccolithophores play a very subordinate role in the Norwegian-Greenland Sea before summer. Diatoms make up the bulk of the phytoplankton, but usually with small populations before May (e.g. Halldal, 1953). In the present study, this is supported by significant number of diatoms which were observed over the eastern Iceland Plateau and west of Jan Mayen during June 1990 (see Thiede & Hempel, 1991). In contrast, investigations have recorded large amounts of coccolithophores in the entire Norwegian-Greenland Sea during summer (Samtleben *et al.*, 1995a). Thereby, abundances of single species changed spatially and temporally, and strong summer blooms occurred.

Species distribution and composition

The overall species number of the investigated coccolithophore communities is only slightly lower than the total of about 25 previously described living species in the Norwegian-Greenland Sea (Halldal & Markali, 1955; Braarud *et al.*, 1958; Smayda, 1958; Ramsfjell, 1960; Sakshaug *et al.*, 1981; Samtleben & Schröder, 1992; Samtleben *et al.*, 1995a, b). This indicates that the communities of spring and early summer are already represented by typical species compositions of this area. Thus, not changes in diversity but the proportions of species seem to be the main characteristic of the high northern coccolithophore communities. This holds true especially for *Anthosphaera robusta* and *Syracosphaera marginaporata*. These two species were present in most samples which were not barren, but never reached dominant portions of the communities. However, both species are dominant members both of deep-living communities and post-bloom communities respectively in late summer and autumn (Samtleben *et al.*, 1995a).

Changes in composition and cell density of the coccolithophore community during the study period are, at least in part, dominated by changes in the abundance of *Emiliania huxleyi*. This species is by far the most abundant coccolithophore species in the investigated water samples. Moreover, it is the most important and ubiquitous species in todays world oceans. Gigantic blooms which mainly consist of *E. huxleyi* are regularly observed during early summer in the subpolar North Atlantic and the adjacent Norwegian-Greenland Sea (e.g., Holligan *et al.*, 1983, 1993; Samtleben *et al.*, 1995a). In our study, cell densities were considerably lower than previously described from this area, especially during February - April. *Emiliania huxleyi* is dominant mainly in the surface layers (<30m water depth) and, with the exception of stations 25-27, its abundance drops drastically at the thermocline. The presence of relatively high cell numbers in the subsurface samples at 75m in May 1991 (Stations 25-27, see Fig. 5) seems to indicate that this species has lived deeper in the photic zone. However, coccolith production in *E. huxleyi* is light-dependent (Westbroek *et al.*, 1989) and, thus, these high cell numbers below thermocline depth are most probably due to repopulations, introduced from the south via the Norwegian Current. In addition, the relatively high cell densities recorded in the southernmost Norwegian-Greenland Sea were probably not part of the increase in late spring/early summer *E. huxleyi* production, but rather the result of a supply from outside the Norwegian-Greenland Sea.

The large differences in the numbers of *E. huxleyi* between spring and summer are probably due to several factors. This species is dominant in water masses depleted in nutrients (Okada & Honjo, 1975; Kleijne, 1990) while diatom growth is favoured by nitrate dominated water masses (Probyn, 1993). In addition, it has been shown that *E. huxleyi* becomes abundant when the water column becomes stratified (Brand, 1994). Stable water masses further increases the growth rate of *E. huxleyi*, which is higher than those of other coccolithophore species (Brand, 1982). Therefore, this species seems to have a much higher reproduction rate than other coccolithophores.

Calciopappus caudatus was also commonly observed in our samples. This species reached medium high cell densities at station 3, and exceptionally high cell densities at station 24 which had not previously been found in the Norwegian-Greenland Sea. Samtleben & Schröder (1992) observed *C. caudatus* in abundances below $10x10^3$ cells/l evenly distributed in the surface water masses of the Norwegian-Greenland Sea. Thus, we assume that the high coccolithophore cell densities, especially at station 24, were the result of a *C. caudatus* bloom or probably close to bloom conditions

during the general low productive period. Previous observations have already shown that this species can be a prominent coccolithophore in the Norwegian Sea as early as May and June (Ramsfjell, 1960; Paasche & Rom, 1962; Schei, 1975). Large populations were observed when the water temperature was only 4-6°C, although *C. caudatus* was also present at most of the localities in the warmer Atlantic water of the Norwegian-Greenland Sea. Early blooms of other species comparable to those of *C. caudatus* are not reported from this area, but have been observed in the subpolar North Atlantic south of Iceland (Knappertsbusch & Brummer, 1995). There are, however, reports of blooms of *C. caudatus* from Norwegian fjords, where large quantities were observed in both early and late summer (Schei, 1975).

Coccolithus pelagicus, which is today regarded as a cold-water adapted species (Braarud, 1979), had a high abundance in the investigated samples but did not exhibit generally higher cell densities in comparison to the summer communities (Samtleben & Schröder, 1992; Samtleben *et al.* 1995a, 1995b). *C. pelagicus* is observed with medium cell densities only in one sample (station 16), despite of being the dominant species of the poor to monospecific communities. This species seems to be a „survivor" species, i.e. it is still found at locations were other species are missing due to a too harsh environment. In the western part of the study area, where *C. pelagicus* is the most commonly found species at all depths, in many cases temperature seems to be the limiting factor. In contrast, in the eastern part *C. pelagicus* seems to dominate the communities below the thermocline. Most of the other species again were influenced by decreasing temperatures but also by reduced insolation.

There are several stations (e.g. 17 to 22) with relatively high temperatures of more than 4°C which are characterized by very low cell densities or even the absence of coccolithophores (Appendix 1, Fig. 7). These stations, located in the northeastern part of the study area, should have been permanently influenced by coccolithophore communities via the northern prolongation of the North Atlantic Drift. However, this is not the case and, therefore, temperature does not seem to be the only reason for the absence of living coccolithophores in the surface waters of the northern Norwegian-Greenland Sea. These stations were sampled in February 1991 which was the earliest time in the year of all sampling. Therefore, it becomes obvious that coccolithophores are at their limits for living probably due to low insolation intensities and not only due to low temperature. The seasonal development of the phytoplankton started after the yearly dark period and coccolithophores increased in abundance when the water column was more stratified.

Corrosion of coccolithophores and coccoliths

Many of the coccolithophores (> 70%!) from the southernmost stations were highly corroded (Plate 2). However, only coccoliths of *Emiliania huxleyi* were affected and corroded specimens in the surface samples always co-occurred with intact cells. This feature may be the result of either dissolution (Schneidermann, 1977) or of malformation, which is the incomplete formation of single coccoliths (Kleijne, 1990). Malformed coccoliths were mostly described from marginal and inland seas during several seasons (Okada & Honjo, 1975; Kleijne, 1990). Young & Westbroek (1991) recently described that malformed *E. huxleyi* coccoliths commonly occurred in late stationary phase cultures, and in cultures held in artificial sea water. Thus, they concluded that a depletion in trace nutrients might be responsible for the observed malformation.

However, the recorded *E. huxleyi* specimen are not identical to the malformed coccoliths described by Okada & Honjo (1975) and Kleijne (1990). Malformation is not observed in this study, but many of the specimens from the surface waters simply were heavily dissolved. Dissolution of coccoliths in the near-surface waters has not been widely reported from the open Norwegian-Greenland Sea, but was described recently from Norwegian fjord populations (Young, 1994). Thus, it seems likely that the observed specimens drifted within the Atlantic water for a longer time and, therefore, these specimens most probably were supplied to this region from outside the Norwegian-Greenland Sea via the North Atlantic Drift. A wide range of altered morphotypes caused by different degrees of dissolution have been reported from surface sediments (Burns, 1977). It is interesting to note that a dissolution feature typical for sediment samples can be seen in the plankton samples from the Norwegian-Greenland Sea (Plate 2, Figs. 3, 4). The difference between dissolution morphotypes usually seen in surface sediments and that of plankton samples has been discussed by Young (1994). He concluded that the collapsed coccolith pattern may be the result of early dissolution, when there is still a large amount of organic matter surrounding the coccoliths.

In addition, many of the dissolved coccospheres have an opening (Plate 2), which may probably be a pylome. Young (1994, Fig. 6A) also found coccospheres of collapsed coccoliths which do have holes and described this feature as collapsed structures. This is probably the case in many, but not in all of our samples. Although a

phenomenon like a pylome in *E. huxleyi* has not been described earlier, this species is known to have several life phases (Klaveness, 1972). Besides the common coccolith-bearing cells, naked cells lacking conspicuous extracellular scales or coccoliths are commonly found in laboratory cultures (e.g. Wilbur & Watabe, 1963; Klaveness, 1972). It is also known that motile life stages alternate with non-motile stages. Possibly, these cells document a change in the life phase of an *E. huxleyi* population. However, the primary mode of reproduction in coccolithophores is asexual binary fission and each daughter cell gets about half the coccoliths of the former coccosphere (Brand, 1994). Another possibility would therefore be that this population has been grazed by small heterotrophic organisms. At least, whether this or the release of a single daughter cell accounts for the cells openings cannot be confirmed from the present material.

CONCLUSIONS

The spatial and temporal distribution of spring to early summer coccolithophore communities in the surface and subsurface waters of the Norwegian-Greenland Sea has shown considerable variability in both cell numbers and species composition. In contrast, changes in diversity do not seem to be the main characteristic features of high northern coccolithophore communities. Relatively high species numbers are already present early in spring although cell densities are still low.

Overall, a total of 15 living species is recorded from the Norwegian-Greenland Sea samples, all known from this area. Coccolithophore standing crop and species diversity are highest in the eastern part of the study area, influenced by the warm Atlantic surface water. In the western part of the Norwegian-Greenland Sea communities often were monospecific and characterized by very low cell numbers. The seasonal development of the phytoplankton started after the yearly dark period and coccolithophores increased in abundance when the water column was more stratified and both temperatures and insolation increased.

Emiliania huxleyi is the dominant species, but *Calciopappus caudatus* and *Algirosphaera robusta* also contribute significantly to the communities. High cell densities, of *C. caudatus* were interpreted as the result of bloom or more probably close to bloom conditions during the general low productive period. In addition, many of the *E. huxleyi* coccoliths from the surface waters of the southeastern Norwegian-Greenland Sea were heavily dissolved. It seems likely that they drifted within the Atlantic water for a long time and, therefore, these specimens may have been supplied to this region from outside the Norwegian-Greenland Sea via the North Atlantic Drift.

ACKNOWLEDGEMENTS

We are grateful to Jeremy Young who made valuable suggestions on the manuscript. The officers and crews of the research vessels PRV Polarstern, RV Valdivia, and RV Poseidon are thanked for their excellent help during expeditions. U. Jacobi carefully collected water samples during the RV Valdivia cruise. U. Schuldt and W. Reimann provided invaluable technical support. This study was part of the Special Research Projekt 313 (contribution no. 298) which was funded by the German Science Foundation.

REFERENCES

Andruleit, H. 1995. Coccolithophoriden im Europäischen Nordmeer: Sedimentation und Akkumulation; sowie ihre Entwicklung während der letzten 15000 Jahre. *Berichte aus dem Sonderforschungsbereich 313*, **59**, 1-110.

Andruleit, H. *in press*. Coccolithophore fluxes in the Norwegian-Greenland Sea: Seasonality and assemblage alterations. *Marine Micropaleontology*.

Bathmann, U.V., Peinert, R., Noji, T.T. & von Bodungen, B. 1990. Pelagic origin and fate of sedimenting particles in the Norwegian Sea. *Progresses in Oceanography*, **24**, 117-125.

Bauerfeind, E., v. Bodungen, B., Arndt, K. & Koeve, W. 1994. Particle flux, and composition of sedimenting matter in the Greenland Sea. *Journal of Marine Systems*, **5**, 411-423.

Baumann, K.-H. 1990. Veränderlichkeit der Coccolithophoridenfauna des Europäischen Nordmeeres im Jungquartär. *Berichte aus dem Sonderforschungsbereich 313*, Univ. Kiel, **22**, 1-146.

Baumann, K.-H. & Matthiessen, J. 1992. Variations in surface water mass conditions in the Norwegian Sea: Evidence from Holocene coccolith and dinoflagellate cyst assemblages. *Marine Micropaleontology*, **20**, 129-146.

v. Bodungen, B., Antia, A., Bauerfeind, E., Haupt, O., Koeve, W., Machado, E., Peeken, I., Peinert, R., Reitmeier, S., Thomsen, C., Voss, M., Wunsch, M., Zeller, U. & Zeitzschel, B. 1995. Pelagic processes and vertical flux of particles: an overview of a long-term comparative study in the Norwegian and Greenland Sea. *Geologische Rundschau*, **84**, 11-27.

Braarud, T. 1979. The temperature range of the non-motile stage of *Coccolithus pelagicus* in the North Atlantic region. *British Phycology Journal*, **14**, 349-352.

Braarud, T., Gaarder, K.R. & Nordli, O. 1958. Seasonal changes in the phytoplankton at various points off the Norwegian west coast. *Fiskeridirektoratets Skrifter, Serie Havundersøkelser*, **XII**, 1-48.

Brand, L.E. 1982. Genetic variability and spatial patterns of genetic differentiation in the reproductive rates of the marine coccolithophores *Emiliania huxleyi* and *Gephyrocapsa oceanica*. *Limnology and Oceanography*, **27**, 236-245.

Brand, L.E. 1994. Physiological ecology of marine coccolithophores. *In:* Winter, A. & Siesser, W.G. (eds.), *Coccolithophores*, 39-49, Cambridge University Press.

Burns, D.A. 1977. Phenotypes and dissolution morphotypes of the genus *Gephyrocapsa* Kamptner and *Emiliania huxleyi* (Lohmann). *New Zealand's Journal of Geology and Geophysics*, **20**, 143-155

Crux, J.A. & Heck, S.E. van 1989. Nannofossils and their applications. *Proceedings of the INA Conference, London 1987*, 356, Ellis Horwood Ltd., Chichester.

Gaarder, K.R. & Markali, J. 1956. On the coccolithophore *Crystallolithus hyalinus* n. gen., n. sp.. *Nytt Magasin for Botanikk*, **5**, 1-5.

Gaarder, K.R. & Heimdal, B.R. 1977. A revision of the genus *Syracosphaera* Lohmann (Coccolithineae). *„Meteor" Forschungs-Ergebnisse*, **D 24**, 54-71.

Gard, G. 1988. Late Quaternary calcareous nannofossil biozonation, chronology and paleo-oceanography in areas north of the Faeroe-Iceland Ridge. *Quaternary Science Reviews*, **7**, 65-78.

Geitzenauer, K.R., Roche, M.B. & McIntyre, A. 1976. Modern Pacific coccolith assemblages: derivation and application to late Pleistocene paleotemperature analysis. *In*: Cline, R.M. & Hays, J.D. (eds.), Investigation of Late Quaternary Paleoceanography and Paleoclimatology, *Geological Society of America Memoir*, **145**, 423-448.

Halldal, P. 1953. Phytoplankton investigations from Weather Ship M in the Norwegian Sea, 1948-49. Norske Videnskab-Akademi i Oslo, *Havundersøklser Skrifter*, **38**, 1-91.

Halldal, P. & Markali, J. 1954. Morphology and microstructure of coccoliths studied in the electron microscope. Observations on *Anthosphaera robusta* and *Calyptrosphaera papillifera*. *Nytt Magasin for Botanikk*, **2**, 117-121.

Halldal, P. & Markali, J. 1955. Electron microscope studies on coccolithophores from the Norwegian Sea, the Gulf Stream and the Mediterranean. *Avhandlinger Utgitt av det Norske Videnskab-Akademi i Oslo*, **1**, 1-30.

Heimdal, B.R. & Gaarder, K.R. 1980. Coccolithophores from the northern part of the eastern Central Atlantic. I. Holococcolithophores. *„Meteor" Forschungs-Ergebnisse*, **D 32**, 1-14.

Heimdal, B.R. & Gaarder, K.R. 1981. Coccolithophores from the northern part of the eastern Central Atlantic. II. Heterococcolithophores. *„Meteor" Forschungs-Ergebnisse*, **D 33**, 37-69.

Holligan, P.M., Viollier, M., Harbour, P., Camus, P. & Champagne-Philippe, M. 1983. Satellite and ship studies of coccolithophore production along a continental shelf edge. *Nature*, **304**, 339-342.

Holligan, P.M., Fernandez, E., Aiken, J., Balch, W.M., Boyd, P., Burkill, P.H., Finch, M., Groom, S.B., Maslin, M., Müller, K., Purdie, D.A., Robinson, C., Trees, C.C., Turner, S.M. & van der Wal, P. 1993. A biogeochemical study of the coccolithophore *Emiliania huxleyi* in the North Atlantic. *Global Biogeochemical Cycles*, **7**, 879-900.

Johannessen, O.M. 1986. Brief overview of the physical oceanography. *In*: Hurdle, B.G. (ed.), *The Nordic Seas*, 103-127, Springer-Verlag, New York, Berlin, Heidelberg, Tokyo.

Jordan, R. & Kleijne, A. 1994. A classification system of living coccolithophores. *In:* Winter, A. & Siesser, W.G. (eds.), *Coccolithophores*, 83-105, Cambridge University Press, Cambridge.

Klaveness, D. 1972. *Coccolithus huxleyi* (Lohmann) Kamptner II. The flagellate cell, aberrant cell types, vegetative propagation and life cycles. *British Phycological Journal*, **7**, 309-318.

Klejne, A. 1990. Distribution and malformation of extant calcareous nannoplankton in the Indonesian Seas. *Marine Micropaleontology*, **16**, 293-316.

Klejne, A. 1991. Holococcolithophores from the Indian Ocean, Red Sea, Mediterranean Sea and North Atlantic Ocean. *Marine Micropaleontology*, **17**, 1-76.

Knappertsbusch, M. 1993. *Syracosphaera norioticus* sp. nov., and *S. marginaporata* sp. nov., (Syracosphaeraceae, Prymnesiophyta), new coccolithophores from the Mediterranean Sea and North Atlantic Ocean. *Journal of Micropalaeontology*, **12**, 71-76.

Knappertsbusch, M. & Brummer, G.-J. 1995. A sediment trap investigation of sinking coccolithophores in the North Atlantic. *Deep-Sea Research*, **42**, 1083-1109.

McIntyre, A. & Bé, A.W.H. 1967. Modern coccolithophoreae of the Atlantic Ocean - I. Placoliths and Cyrtoliths. *Deep-Sea Research*, **14**, 561-597.

Nishida, S. 1979. Atlas of Pacific nannoplanktons. *News of Osaka Micropaleontologists*, Special Paper, **3**, 1-31.

Norris, R.E. 1984. Indian Ocean nannoplankton. I, Rhabdosphaeraceae (Prymnesiophyceae) with a review of extant taxa. *Journal of Phycology*, **20**, 27-41.

Okada, H. & Honjo, S. 1973. The distribution of oceanic coccolithophores in the Pacific. *Deep-Sea Research*, **20**, 355-374.

Okada, H. & Honjo, S. 1975. Distribution of coccolithophores in marginal seas along the western Pacific Ocean and in the Red Sea. *Marine Biology*, **31**, 271-285.

Okada, H. & McIntyre, A. 1977. Modern coccolithophores in the western North Atlantic Ocean. *Micropaleontology*, **23**, 1-55.

Paasche, E. & Rom, A.-M. 1962. On the phytoplankton vegetation of the Norwegian Sea in May 1958. *Nytt Magasin for Botanikk*, **9**, 33-60.

Probyn, T.A. 1993. The inorganic nitrogen nutrition of the phytoplankton in the southern Benguela: new production, phytoplankton size and implication for pelagic food web. *South African Journal of Marine Sciences*, **12**, 411-420.

Ramsfjell, E. 1960. Phytoplankton distribution in the Norwegian Sea in June, 1952 and 1953. *Fiskeridirektoratets Skrifter, Serie Havundersøkelser*, **XII**, 1-39.

Roth, P.H. & Coulborn, W.T. 1982. Floral and solution patterns of coccoliths in surface sediments of the North Pacific. *Marine Micropaleontology*, **7**, 1-52.

Sakshaug, E., Myklestad, S., Andresen, K., Hegseth, E.N. & Jörgensen, L. 1981. Phytoplankton off the Møre Coast in 1975-1979: distribution, species composition, chemical composition and conditions for growth. *In*: Saetre, R. & Mork, M. (eds.), *The Norwegian Coastal Current*, 681-711, University of Bergen, Geilo.

Samtleben, C. & Bickert, T. 1990. Coccoliths in sediment traps from the Norwegian Sea. *Marine Micropaleontology*, **16**, 39-64.

Samtleben, C. & Schröder, A. 1992. Living coccolithophore communities in the Norwegian-Greenland Sea and their record in sediments. *Marine Micropaleontology*, **19**, 333-354.

Samtleben, C., Baumann, K.-H. & Schröder-Ritzrau, A. 1995a. Distribution, composition and seasonal variation of coccolithophore communities in the northern North Atlantic. *In*: J. A. Flores & F.J. Sierro (eds.), *5th INA Conference, Proceedings*, 219-235.

Samtleben, C., Schäfer, P., Andruleit, H., Baumann, A., Baumann, K.-H., Kohly, A., Matthiessen, J. & Schröder-Ritzrau, A.: `Synpal´ Working Group 1995b. Plankton in the Norwegian-Greenland Sea: from living communities to sediment assemblages - an actualistic approach. *Geologische Rundschau*, **84**, 108-136.

Schei, B. 1975. Coccolithophorid distribution and ecology in coastal waters of North Norway. *Norwegian Journal of Botany*, **22**, 217-225.

Schneidermann, N. 1977. Selective dissolution of recent coccoliths in the Atlantic Ocean. *In:* Ramsay, A.T.S.

(ed.), *Oceanic Micropaleontology* 2, 1009-1052, Academic Press.

Smayda, T.J. 1958. Phytoplankton studies around Jan Mayen Island March-April, 1955. *Nytt Magasin for Botanikk*, **6**, 75-96.

Swift, J.H. 1986. The Arctic waters. *In*: Hurdle, B.G. (ed): *The Nordic Seas*, 129-153, Springer-Verlag, New York, Berlin, Heidelberg, Tokyo.

Thiede, J. & Hempel, G. 1991. The Expedition ARKTIS-VII/1 of RV „Polarstern" in 1990. *Berichte zur Polarforschung*, **80**, 1-136.

Westbroek, P., Young, J.R. & Linschooten, K. 1989. Coccolith production (biomineralization) in the marine alga *Emiliania huxleyi*. *Journal of Protozoology*, **36**, 368-373.

Wilbur, K.M. & Watabe, N. 1963. Experimental studies on calcifications in molluscs and the alga *Coccolithus huxleyi*. *Annales of the New York Academic Sciences*, **109**, 82-112.

Young, J.R. 1994. Variation in *Emiliania huxleyi* coccolith morphology in samples from the Norwegian EHUX experiment. *Sarsia*, **79**, 417-425.

Young, J.R. & Westbroek, P. 1991. Genotypic variation in the coccolithophore species *Emilinia huxleyi*. *Marine Micropaleontology*, **18**, 5-23.

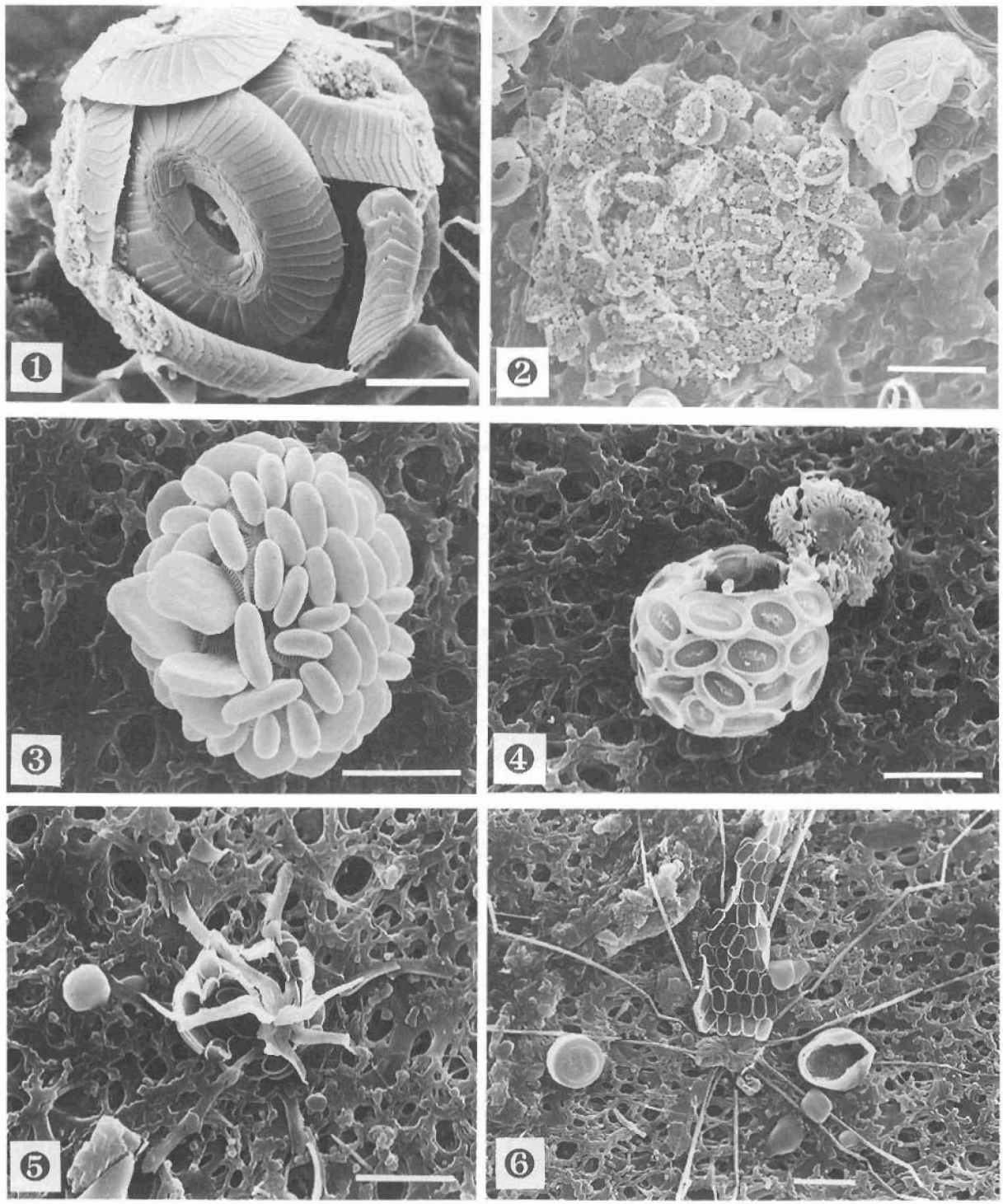


Plate 1. (Bar = 4µm). 1. *Coccolithus pelagicus* (Wallich) Schiller, Station 43, 0m; 2. *Crystallolithus hyalinus* (Gaarder & Markali and *Syracosphaera marginaporata* Knappertsbusch, Station 2, 0m ; 3. *Algirosphaera robusta* (Lohmann) Norris, Station 30, 0m; 4. *Syracosphaera borealis* Okada & McIntyre, Station 30, 40m; 5. *Ophiaster hydroideus* (Lohmann) Lohmann, Station 30, 40m; 6. *Calciopappus caudatus* Gaarder & Ramsfjell, Station 30, 40m.

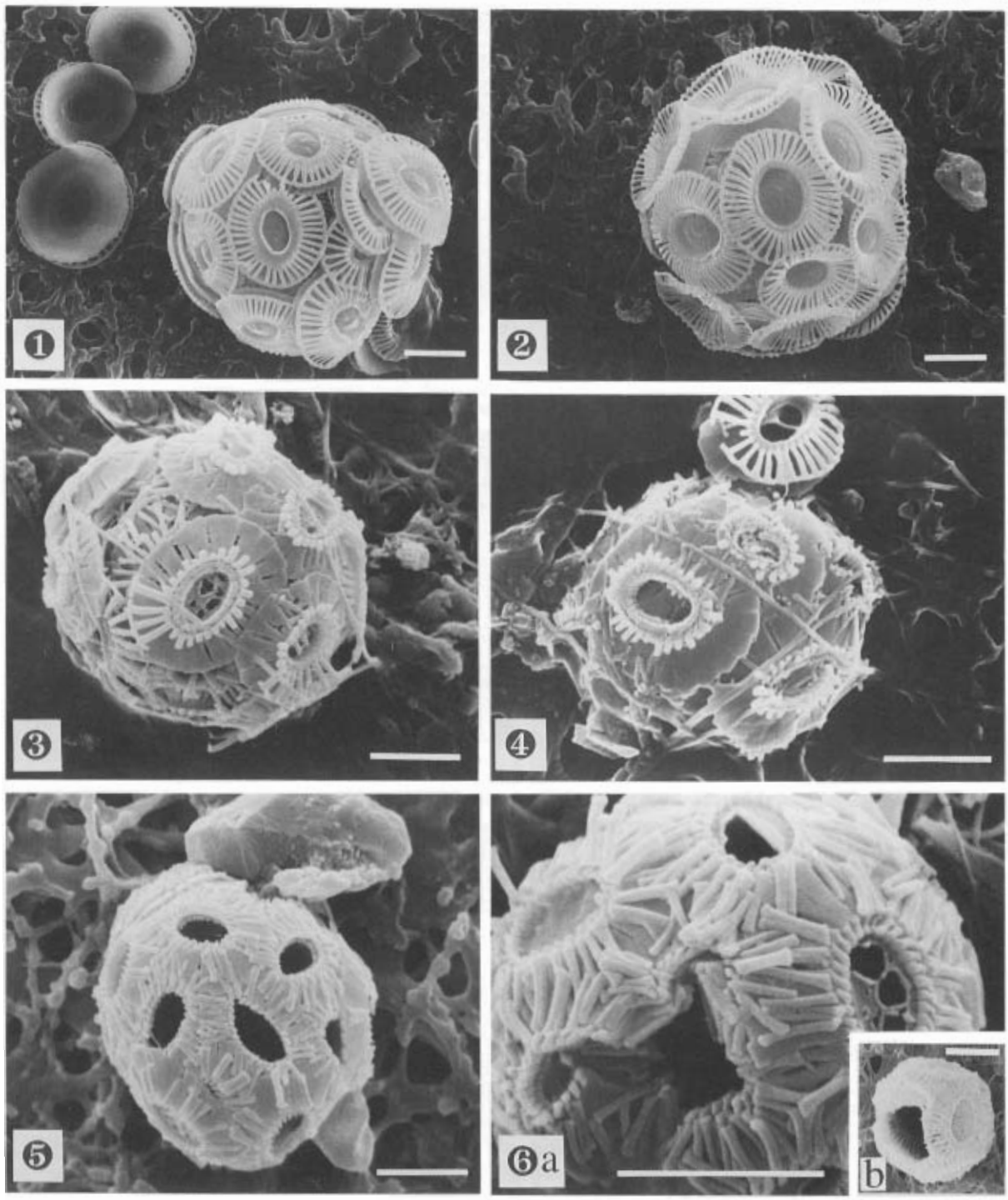


Plate 2. (Bar = 4µm). 1-6. *Emiliania huxleyi* (Lohmann) Hay & Mohler. 1. Normal coccosphere, Type A (Young & Westbroek, 1991); Station 30, 0 m; 2. Normal coccosphere, Station 30, 0 m; 3. Coccosphere with corroded coccoliths, Station 2, 15 m; 4. Coccosphere with heavily corroded coccoliths and all individual elements are dissolved, Station 2, 15 m; 5. Coccosphere with severely corroded coccoliths and totally disturbed arrangement of the distal shield elements, Station 3, 10 m; 6. Coccospheres with corroded coccoliths and an opening; a) Station 2, 15 m; b) Station 3, 10 m.

Appendix 1. Station list with temperatures, salinities, and coccolitophore densities of all investigated samples (cruises: PS-Polarstern, Pos-Poseidon, V-Valdivia; x=no data)

No.	Station	Date	Geogr.	Position	Sample Depth (m)	Temp. (°C)	Sal. (ppt)	Volume (l)	Coccospheres (bulk)	*Acanth. acule.*	*Acanth. quattro.*	*Algiros. robusta*
1	PS-A	12.06.90	63 45.8 N	00 20.7 E	10	9.3	35.11	1.0	80640	-	-	-
2	PS-2	13.06.90	65 00.0 N	00 59.8 W	0	8.4	34.99	1,5	184760	2510	1260	2510
					15	7.5	34.98	2.0	207380	1260	1260	35190
					30	6.5	34.97	2.0	29900	-	-	1150
					100	4.4	34.95	2.0	1470	-	-	-
3	PS-3	13.06.90	65 29.9 N	03 59.9 W	0	7.9	34.99	1.5	86730	-	13200	3770
					10	7.4	34.85	1.5	16940	-	-	-
					20	5.0	34.83	2.0	420	-	-	-
					100	3.7	34.87	2.0	830	-	-	-
4	PS-C	14.06.90	66 39.9 N	8 00.2 W	10	5.3	34.74	1.5	16480	-	-	-
5	PS-D	14.06.90	67 27.1 N	9 37.7 W	10	4.6	34.67	2.0	-	-	-	-
6	PS-E	14.06.90	67 59.0 N	10 50.6 W	10	5.2	34.72	3.0	100	-	-	-
7	PS-F	14.06.90	68 41.1 N	12 35.2 W	10	5.1	34.72	2.0	-	-	-	-
8	PS-6	15.06.90	69 28.0 N	16 32.2 W	0	0.8	33.15	1.25	-	-	-	-
					10	0.4	33.70	0.55	470	-	-	-
					20	-0.8	34.25	0.6	510	-	-	-
					50	-0.5	34.76	2.0	-	-	-	-
9	PS-43	20.06.90	70 45.0 N	5 30.0 W	0	7.3	35.09	2.0	39900	-	-	950
					10	7.1	35.10	2.0	73330	-	-	13970
					30	4.4	34.95	2.0	2420	-	-	-
					100	3.0	34.95	2.0	730	-	-	-
10	PS-47	21.06.90	72 33.0 N	12 15.1 W	0	1.9	33.10	2.0	1460	-	-	-
					10	1.3	34.15	2.0	-	-	-	-
					40	-0.3	34.45	2.0	-	-	-	-
11	PS-69	30.06.90	75 50.0 N	8 11.0 W	0	-0.7	32.39	2.0	-	-	-	-
					30	-0.5	34.25	2.0	-	-	-	-
					110	2.4	34.90	2.0	-	-	-	-
12	PS-70	30.06.90	75 25.0 N	7 20.0 W	0	-0.1	32.37	2.0	-	-	-	-
					30	2.2	34.86	2.0	-	-	-	-
					70	1.7	34.92	2.0	-	-	-	-
13	PS-73	1.07.90	74 59.8 N	4 59.5 W	0	2.2	33.32	2.0	-	-	-	-
					20	-0.5	34.50	2.0	-	-	-	-
					60	-0.8	34.77	2.0	-	-	-	-
14	PS-75	2.07.90	74 32.0 N	2 19.3 W	0	2.2	34.50	1.25	-	-	-	-
					20	-0.8	34.66	2.0	-	-	-	-
					100	-1.4	34.82	2.0	-	-	-	-
15	PS-87	6.07.90	74 35.9 N	2 59.9 E	0	2.9	34.68	2.0	630	-	-	-
					7	1.9	35.09	2.0	-	-	-	-
					25	0.0	34.74	2.0	-	-	-	-
16	PS-89	7.07.90	73 58.0 N	7 40.0 E	0	7.8	34.99	2.0	6110	-	-	-
					10	7.3	35.01	2.0	12650	-	-	370
					50	5.9	34.83	2.0	1420	-	-	-
					100	1.8	34.83	2.0	-	-	-	-
17	PS-90	8.07.90	72 15.1 N	11 00.2 E	0	9.4	34.86	2.0	-	-	-	-
					10	7.6	34.97	2.0	-	-	-	-
					40	6.7	35.11	2.0	-	-	-	-
18	Pos/181-20	22.02.91	64 35N	3 30E	10	7.6	x	4.0	4800	-	-	300
					50	7.6	x	4.0	900	-	-	-
19	Pos/181-20	24.02.91	69 55.6N	0 11.1E	10	4.0	x	4.0	0	-	-	-
					50	4.0	x	4.0	300	-	-	-
20	Pos/181-20	24.02.91	70 14.5N	0 14W	10	4.6	x	4.0	0	-	-	-
					50	4.6	x	4.0	0	-	-	-
21	Pos/181-21	26.02.91	71 38.3N	4 13.4E	10	4.55	x	4.0	0	-	-	-
					50	4.53	x	4.0	0	-	-	-
22	Pos/181-21	26.02.91	73 12.7N	8 21.4E	10	4.4	x	4.0	0	-	-	-
					50	3.9	x	4.0	0	-	-	-
23	Pos/181-21	27.02.91	74 52N	18 59.9E	10	x	x	4.0	300	-	-	-
					50	x	x	2.0	600	-	-	-
24	V-1	20.05.91	69 58N	0 09E	1	5.3	35.05	2.0	112000	-	510	3580
					20	5.1	35.06	2.0	135260	-	1230	10450
					75	4.8	35.07	2.0	26420	-	-	3720
					750	1.86	34.9	2.0	2030	-	-	350
25	V-3	22.05.91	75 15N	12 52E	1	x	x	2.0	48200	-	-	4610
					20	x	x	2.0	50890	-	-	3260
					75	x	x	2.0	89470	-	1110	3310
26	V-4	26.05.91	75 00N	14 42E	1	x	x	2.0	35640	-	390	6590
					20	x	x	2.0	30290	-	350	5280
					75	x	x	2.0	44720	-	-	4820
27	V-5	27.05.91	74 47N	13 52E	1	x	x	2.0	63710	-	-	3500
					20	x	x	2.0	55030	-	-	3500
					75	x	x	2.0	18430	-	-	1290
28	Pos/205-18	25.03.95	67 10.9N	9 16.9E	0	6.15	34.93	2.0	5420	-	-	2090
					40	6.65	35.36	2.0	9690	-	-	3630
29	Pos/205-20	5.04.95	67 24.5N	8 41.8E	0	6.49	35.56	2.0	43590	-	-	7130
					40	6.51	35.58	2.0	24490	-	-	9430
30	Pos/205-21	6.04.95	67 07.9N	7 20.3E	0	6.76	35.39	2.0	8770	-	-	4160

Appendix 1. (cont.) Station list with temperatures, salinities, and coccolitophore densities of all investigated samples (cruises: PS-Polarstern, Pos-Poseidon, V-Valdivia; x=no data)

No.	*Alisph. unic.*	*Calciop. caudat.*	*Coc. pelagic.*	*Cryst. hyalinus*	*Emilian. huxleyi*	*Gephyr. muell.*	*Ophias. hydr.*	*Pappos. sp.*	*Syracos. borealis*	*Syracos. marg.*	*Syracos. med.*	*Syracos. mol.*	*Syracos.* spp.
1	-	-	1910	-	78730	-	-	-	-	-	-	-	-
2	-	-	-	12570	139510	-	-	-	3770	22620	-	-	-
	-	7540	-	3770	154600	-	-	-	2510	1260	-	-	-
	-	-	580	-	28180	-	-	-	-	-	-	-	-
	-	-	490	-	980	-	-	-	-	-	-	-	-
3	-	20470	-	5660	30170	-	-	-	-	13200	-	-	-
	-	1060	-	-	15880	-	-	-	-	-	-	-	-
	-	-	420	-	-	-	-	-	-	-	-	-	-
	-	-	830	-	-	-	-	-	-	-	-	-	-
4	-	-	1180	-	15300	-	-	-	-	-	-	-	-
5	-	-	-	-	-	-	-	-	-	-	-	-	-
6	-	-	-	-	100	-	-	-	-	-	-	-	-
7	-	-	-	-	-	-	-	-	-	-	-	-	-
8	-	-	-	-	-	-	-	-	-	-	-	-	-
	-	-	-	470	-	-	-	-	-	-	-	-	-
	-	-	-	510	-	-	-	-	-	-	-	-	-
	-	-	-	-	-	-	-	-	-	-	-	-	-
9	-	-	2220	320	36420	-	-	-	-	-	-	-	-
	-	700	4890	2100	50280	-	-	-	-	1400	-	-	-
	-	-	2420	-	-	-	-	-	-	-	-	-	-
	-	-	730	-	-	-	-	-	-	-	-	-	-
10	-	-	1460	-	-	-	-	-	-	-	-	-	-
	-	-	-	-	-	-	-	-	-	-	-	-	-
	-	-	-	-	-	-	-	-	-	-	-	-	-
11	-	-	-	-	-	-	-	-	-	-	-	-	-
	-	-	-	-	-	-	-	-	-	-	-	-	-
	-	-	-	-	-	-	-	-	-	-	-	-	-
12	-	-	-	-	-	-	-	-	-	-	-	-	-
	-	-	-	-	-	-	-	-	-	-	-	-	-
	-	-	-	-	-	-	-	-	-	-	-	-	-
13	-	-	-	-	-	-	-	-	-	-	-	-	-
	-	-	-	-	-	-	-	-	-	-	-	-	-
	-	-	-	-	-	-	-	-	-	-	-	-	-
14	-	-	-	-	-	-	-	-	-	-	-	-	-
	-	-	-	-	-	-	-	-	-	-	-	-	-
	-	-	-	-	-	-	-	-	-	-	-	-	-
15	-	-	630	-	-	-	-	-	-	-	-	-	-
	-	-	-	-	-	-	-	-	-	-	-	-	-
	-	-	-	-	-	-	-	-	-	-	-	-	-
16	-	-	380	380	5350	-	-	-	-	-	-	-	-
	-	-	8190	-	4090	-	-	-	-	-	-	-	-
	-	-	1070	-	360	-	-	-	-	-	-	-	-
	-	-	-	-	-	-	-	-	-	-	-	-	-
17	-	-	-	-	-	-	-	-	-	-	-	-	-
	-	-	-	-	-	-	-	-	-	-	-	-	-
	-	-	-	-	-	-	-	-	-	-	-	-	-
18	-	-	300	-	3900	-	-	-	-	-	300	-	-
	-	-	900	-	-	-	-	-	-	-	-	-	-
19	-	-	-	-	-	-	-	-	-	-	-	-	-
	-	-	300	-	-	-	-	-	-	-	-	-	-
20	-	-	-	-	-	-	-	-	-	-	-	-	-
	-	-	-	-	-	-	-	-	-	-	-	-	-
21	-	-	-	-	-	-	-	-	-	-	-	-	-
	-	-	-	-	-	-	-	-	-	-	-	-	-
22	-	-	-	-	-	-	-	-	-	-	-	-	-
	-	-	-	-	-	-	-	-	-	-	-	-	-
23	-	-	300	-	-	-	-	-	-	-	-	-	-
	-	-	600	-	-	-	-	-	-	-	-	-	-
24	-	87450	1020	4600	4090	-	-	-	-	10230	-	-	510
	-	98980	1840	2460	9220	-	-	-	-	11070	-	-	-
	-	13020	1490	1120	5580	370	-	-	-	1120	-	-	-
	-	-	700	-	980	-	-	-	-	-	-	-	-
25	-	3900	-	-	39340	-	-	-	-	350	-	-	-
	-	4240	-	-	42410	-	330	-	-	650	-	-	-
	-	5160	370	-	79530	-	-	-	-	-	-	-	-
26	-	4260	90	-	23630	-	-	-	-	390	-	-	-
	350	1760	-	-	21840	-	-	-	-	704	-	-	-
	-	3950	-	-	35080	-	-	-	-	880	-	-	-
27	-	6990	-	390	52050	-	-	-	-	390	-	-	-
	-	3820	-	-	44710	-	760	-	-	1910	-	-	-
	-	-	-	-	17140	-	-	-	-	-	-	-	-
28	-	-	-	-	2090	-	830	420	-	-	-	-	-
	-	610	-	-	3630	-	1210	-	-	610	-	-	-
29	-	4750	-	-	29330	-	2380	-	-	-	-	-	-
	-	3140	-	-	8770	-	1050	-	1050	1050	-	-	-
30	-	-	-	-	3230	-	460	-	-	460	-	460	-

Appendix 2. List of observed species.

Species name	Illustration in this paper
Acanthoica aculeata Kamptner	
Acanthoica quattrospina Lohmann	
Algirosphaera robusta (Lohmann) Norris	Plate 1, Fig. 3
Alisphaera unicornis Okada & McIntyre	
Calciopappus caudatus Gaarder & Ramsfjell	Plate 1, Fig. 6
Coccolithus pelagicus (Wallich) Schiller	Plate 1, Fig. 1
**Crystallolithus hyalinus* Gaarder & Markalli	Plate 1, Fig. 2
Emiliania huxleyi (Lohmann) Hay & Mohler	Plate 2, Fig. 1-6
Gephyrocapsa muellerae Bréhéret	
Ophiaster hydroideus (Lohmann) Lohmann	Plate 1, Fig. 5
Papposphaera sp.	
Syracosphaera borealis Okada & McIntyre	Plate 1, Fig. 4
Syracosphaera marginaporata Knappertsbusch	Plate 1, Fig. 2
Syracosphaera mediterranea Lohmann	
Syracosphaera molischii Schiller	
Syracosphaera spp.	

* This motile phase of *C. pelagicus* was counted separately.

Seasonality in microhabitats of rose bengal stained deep-sea benthic foraminifera from the New Jersey continental margin

MICHAEL A. KAMINSKI[1], AMAL M. AL HASSAWI[2], and WOLFGANG KUHNT[3]

1. Research School of Geological & Geophysical Sciences, UCL, Gower Street, London WC1E 6BT, UK
2. Department of Anatomy & Developmental Biology, UCL, Gower Street, London WC1E 6BT, UK
3. Institut und Museum für Geologie und Paläontologie, CAU, Olshausenstr. 40, D-24118 Kiel, Germany

ABSTRACT

Analysis of Rose Bengal stained calcareous benthic foraminifera in a box core taken at a water depth of 3098 m on the New Jersey continental margin in late February (before the spring phytoplankton bloom) reveals important differences in the vertical distribution of taxa when compared with the post-bloom data of Corliss (1985) from a nearby station. Winter populations display a large subsurface peak in the foraminiferal population and consist of „deep infaunal" forms such as *Globobulimina* and *Melonis*, whereas the late summer populations sampled by Corliss consist largely of „epifaunal" taxa such as *Hoeglundina* and *Cibicidoides*. The near lack of live „epifaunal" forms in winter may be attributed to low seasonal food supply and the cumulative effects of predation at the sediment surface. In the absence of the „epifaunal morphogroup", infaunal taxa such as *Melonis* rise to occupy the shallow subsurface habitat (0-4 cm depth). Alternatively, low winter populations of epifaunal forms may be part of a natural seasonal phase in their life cycle, as observed in some shallow-water foraminifera.

INTRODUCTION

Benthic foraminifera display enormous ecological adaptability, and constitute more than half of the total meiofaunal biomass in the deep sea (Shirayama, 1984). However, precious little is known about the population dynamics of deep-sea taxa. In a series of papers, Corliss and co-workers have determined that individual foraminiferal morphogroups occupy microhabitats that are vertically partitioned with respect to the sediment/water interface and pointed out the relationship between vertical stratification and the shape of the foraminiferal test (Corliss, 1985; Corliss & Emerson, 1988; Rathburn & Corliss, 1994). In a subsequent study, a positive correlation was observed between the proportion of infaunal morphogroups and the flux of organic matter to the sea floor (Corliss & Chen, 1988). However, the flux of organic matter to the ocean floor (especially phytodetritus) is seasonal, and the benthic foraminiferal populations have been documented to react quickly to seasonal fluctuations in food supply (Gooday, 1988). If benthic populations in the deep sea are limited by the amount of available food as numerous studies suggest, it is therefore reasonable to propose that both populations and habitat preferences of benthic foraminifera may change in response to the seasonal cycles of food flux.

The foraminiferal data originally presented by Corliss (1985) was collected in September 1980, and provides a snapshot of the population structure sampled after the marine phytoplankton bloom. In this study, we document the distribution of Rose Bengal stained calcareous benthic foraminifera from the upper 15 cm of sediments in a boxcore from the New Jersey continental margin. The boxcore was collected in late February, 1990, which is before the spring phytoplankton bloom. Therefore, if the vertical distribution of benthic foraminiferal morphotypes within sediment displays seasonality, we ought to observe differences between samples collected before and after the spring bloom. To achieve this goal, we compare our data set with that of Corliss (1985).

In: Hass, H.C. & Kaminski, M.A. (eds.) 1997. Contributions to the Micropaleontology and Paleoceanography of the Northern North Atlantic. *Grzybowski Foundation Special Publication*, no. 5, pp. 245-248

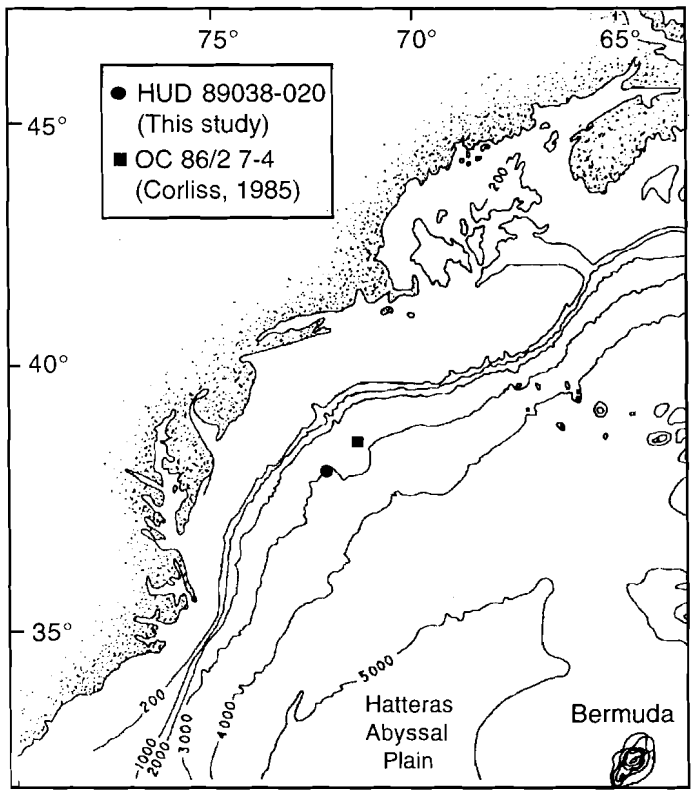


Figure 1. Location of CSS Hudson Boxcore 89038-020 and the station studied by Corliss (1985) in the northwest Atlantic. Base map modified from Corliss & Emerson (1988).

MATERIAL AND METHODS

Boxcore 89038 - 020 examined in this study was collected on board the CSS Hudson at 37°31.23'N, 72°00.97'W from a water depth of 3098 m on the New Jersey continental margin off Atlantic City (figure 1). This depth is within 100 m of the boxcore (38°12.9'N, 71°30.4'W; 3000 m depth) that Corliss sampled in 1980 for his classic study of benthic foraminiferal microhabitats (Corliss, 1985). The lithology of Boxcore 89038 - 020 consisted of 6 cm of brown homogeneous soft clay underlain by 4-5 cm of light brown clay. A distinct color change associated with a major change in redox conditions is observed at 10 cm depth. Below 10 cm the sediment consists of olive gray stiff clay with mottling by bioturbating organisms. The sediment in the core was subdivided on board ship, and slices (one cm thick) from one of the subcores were taken from the sediment/water interface to a depth of 20 cm. Each 75-cm^3 subsample was preserved in a buffered formalin solution. In the laboratory, samples were gently washed over a 63 μm sieve, and preserved in a 50% methanol solution. Samples were treated with Rose Bengal (a protein-specific stain) to highlight organisms that were alive at the time of collection. All stained foraminifera were picked from the >150 μm fraction to ensure that our data and results are directly comparable to those of Corliss (1985). We counted only the calcareous benthic foraminifera with bright red-stained protoplasm. Agglutinated foraminifera were ignored for the purpose of this comparison. We noticed that many stained foraminifera contained protoplasm that did not fully occupy the test. In many cases the final chamber or chambers were empty. These specimens were counted as live, but the data were recorded separately. Some deep-sea benthic foraminifera have been observed to double their protoplasm mass within three days of being fed (Altenbach, 1992), indicating that benthic foraminifera can survive extended periods with little food. The foraminiferal census data are presented in Table 1.

RESULTS

At our station the dominant species group was represented by *Globobulimina* spp. and *Chilostomella oolina* (Schwager) which accounted for a broad subsurface peak in the foraminiferal fauna between 5 and 10 cm below the sediment/water interface. However, these forms did occur in lower numbers to the base of the studied depth interval at 15 cm. Both *Globobulimina* and *Chilostomella* were identified by Corliss (1985) as deep infaunal deposit feeders, preferring a habitat deeper than 5 cm on the New Jersey margin. The second most abundant species in the winter population is *Melonis barleeanum* (Williamson) which was found mainly within the upper four centimeters, but may extend to a depth of 10 cm. However, the specimens occurring below 3 cm mainly contained partial protoplasm

Table 1. Benthic foraminiferal census data in Core 89038-20. Depth is in cm. Numbers indicate specimens with full protoplasm – specimens with partial protoplasm.

Species/depth in core:	0-1	1-2	2-3	3-4	4-5	5-6	6-7	7-8	8-9	9-10	10-11	11-12	12-13	13-14	14-15
Full–Partial Protoplasm:	F–P	F–P	F–P	F–P	F–P	F–P	F–P	F–P	F–P	F–P	F–P	F–P	F–P	F–P	F–P
Cibicidoides kullenbergi								0–1							
Cibicidoides wuellerstorfii													0–1		
Cibicidoides bradyi									0–1						
Chilostomella oolina						2–4	1–7	6–4	4–7	0–6		0–2	0–3	0–6	1–6
Fissurina spp.							0–2	0–2	0–1	0–1		0–2			
Globobulimina auriculata								2–3	0–3	0–1		0–1	0–1		
Globobulimina sp. A					0–3	0–11	0–9	4–1	0–10	0–7			0–1	0–1	
Globobulimina affinis						0–6	2–1	0–3		2–5				0–2	0–1
Hoeglundina elegans														0–1	
Melonis barleeanum	11–0	10–0	7–1	0–6	1–2	1–5	0–4	0–4	0–4	0–2					
Oridorsalis spp.									1–0						
Pullenia subcarinata	1–0		2–0												
Pullenia osloensis			1–0												
Prygo spp.					0–1					0–1				2–0	
Quinqueloculina spp.							0–1		1–0						
Quadrimorphina		1–0													

and may have been in a stressed or dormant state owing to the seasonal lack of food. In Corliss' late summer data, *M. barleeanum* occupied an intermediate depth habitat of between 1 and 5 cm. Surprisingly, stained specimens of epifaunal taxa such as *Hoeglundina elegans*, *Cibicidoides wuellerstorfi*, and *Cibicidoides* spp. were absent from the uppermost centimeter of the sediment column, although their dead tests were common at this site. Single stained individuals of *Hoeglundina elegans*, *Oridorsalis* spp., *Cibicidoides wuellerstorfi*, *C. kullenbergi*, and *C. bradyi* were present in the subsurface, and most specimens contained protoplasm that only partially occupied the test. This is in marked contrast to the summer populations which were dominated by *Hoeglundina elegans*, *Oridorsalis*, and *Cibicidoides wuellerstorfi*.

DISCUSSION & CONCLUSIONS

Comparison of our winter samples with the summer data collected by Corliss (1985) reveals large differences in both the population structure and the microhabitat preference of lower bathyal benthic foraminifera (figure 2). The late summer foraminiferal populations sampled by Corliss were dominated by epifaunal forms. Some of the smaller epifaunal foraminifera may be opportunistic taxa whose life cycle is linked to the seasonal supply of phytoplankton detritus. Following the spring phytoplankton bloom in the North Atlantic, a number of species of calcareous benthic foraminifera apparently reproduce and rapidly invade the fluffy layer of detritus that arrives at the sea floor (Gooday, 1993). However, by winter this ephemeral food source has been exhausted, and the epifaunal benthic foraminiferal population apparently collapses. There may be several reasons (or a combination of reasons) why the numbers of epifaunal benthics are lower in winter at our station. One cause for the drastically lowered populations may be predation. In the absence of abundant food, there would low population growth, and predation pressure would tend to further reduce the number of foraminifera. A number of grazing metazoans, such as holothurians, gastropods and polychetes, are known to ingest benthic foraminifera (Lipps, 1983). Another explanation for low numbers of winter epifaunal taxa is the possibility of a natural seasonality in the life cycle of deep-sea benthic foraminifera, as observed in some shallow-water foraminiferal species. Our data suggest that, in the absence of epifaunal taxa, the shallow infaunal species *M. barleeanum* rises through the sediment column to occupy the surface layer. This species has also been observed to occupy the sediment surface in the Norwegian Sea during winter, whereas at other times in the year it was found at a depth of 3-4 cm (Lutze, 1987).

The deep infaunal taxa appear to be less sensitive to seasonal fluctuations in food supply than

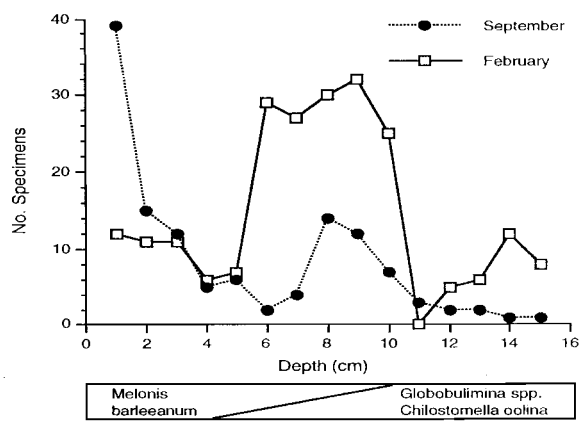


Figure 2. Seasonality of benthic foraminiferal populations in the upper 15 cm of sediments from box cores collected at water depths of ca. 3000 m on the New Jersey margin. February data (this study) is measured in no. specimens/75 cm^3. September data is measured in no. specimens/g dry sand fraction, and is taken from Corliss (1985).

taxa that have a preferred epifaunal or shallow infaunal mode of life. After the spring bloom, the organic carbon from the phytodetritus is removed from the sediment surface by surface grazing metazoans and deposited in their burrows (Aller & Aller, 1986). This resource may serve as a food for

bacteria and ultimately for infaunal detritivores such as benthic foraminifera during the winter season. Increasing preservation of organic matter and high numbers of bacteria are often found in association with the subsurface redox boundary. This level was observed at 10 cm depth in Core 89038-20 and is associated with a strong subsurface peak in *Globobulimina*, a form known to ingest bacteria and associated sediment particles (Goldstein & Corliss, 1994). A less pronounced subsurface peak in benthic foraminiferal numbers is also evident in Corliss' summer data. This may indicate that the redox boundary is seasonally stable and provides a constant source of food for the deep infaunal detritivores.

We believe our observation of strong seasonality among cosmopolitan deep-water benthic foraminifera has important repercussions for interpretations of benthic foraminiferal biogeography (because most studies of live populations are based on samples collected during the summer months) as well as for studies of Cenozoic palaeoceanography based on the isotopic composition of foraminiferal calcite (which use taxa that are representative of water-column conditions present during only a fraction of the year). The deep sea environment must be sampled at a much higher temporal resolution before we can fully understand the life cycle of these deep sea organisms. Once the relation of seasonal microhabitats and life-cycles of deep-water benthic foraminifera are more firmly established, benthic populations may prove to be a sensitive monitor of the seasonal carbon flux to the seafloor.

ACKNOWLEDGEMENTS

W. Kuhnt thanks the Captain & crew of the CSS Hudson and Dr. K. Moran for the opportunity to participate on cruise no. 89038. Amal Al Hassawi acknowledges support of a postgraduate studentship from the Kuwait Public Authority for Higher Education & Training at UCL. We thank A. Altenbach, B.H. Corliss, A.E.L Holbourn, A.R. Lord, and J. Wollenburg for reading an early draft of this manuscript.

REFERENCES

Aller, J.Y. & Aller, R.C. 1986. Evidence for localized enhancement of biological activity associated with tube and burrow structures in deep-sea sediments at the HEBBLE Site, western North Atlantic. *Deep-Sea Research*, **33**, 755-790.

Altenbach, A.V. 1992. Short term processes in benthic foraminifera. *Marine Micropaleontology*, **19**, 119-129.

Corliss, B.H. 1985. Microhabitats of benthic foraminifera within deep-sea sediments. *Nature*, **314**, 435-438.

Corliss, B.H. & Chen, C. 1988. Morphotype patterns of Norwegian Sea deep-sea benthic foraminifera and ecological implications. *Geology*, **16**, 716-719.

Corliss, B.H. & Emerson, S. 1990. Distribution of Rose Bengal stained benthic foraminifera from the Nova Scotia continental margin and Gulf of Maine. *Deep-Sea Research*, **37**, 381-400.

Goldstein, S.T. & Corliss, B.H. 1994. Deposit feeding in selected deep-sea and shallow-water benthic foraminifera. *Deep-Sea Research*, **41**, 229-241.

Gooday, A.J. 1988. A response by benthic foraminifera to the deposition of phytodetritus in the deep sea. *Nature*, **332**, 70-73.

Gooday, A.J. 1993. Deep-sea benthic foraminiferal species which exploit phytodetritus: Characteristic features and controls on distribution. *Marine Micropaleontology*, **22**, 187-205.

Lipps, J.H. 1983. Biotic interactions in benthic foraminifera. *in:* Tevesz, M.J.S. & McCall, P.L. (Eds.) *Biotic interactions in Recent and Fossil benthic communities*, 331-376, Plenum Publishing Co.

Lutze, G.F. 1987. Benthische Foraminiferen: Vertikale Verteilung in den obersten Sedimentlagen und Probleme bei der Entnahme von Standard Proben. *Berichte aus dem Sonderforschungsbereich 313*, **6**, 79-89.

Rathburn, A.E. & Corliss, B.H. 1994. The ecology of living (stained) deep-sea benthic foraminifera from the Sulu Sea. *Paleoceanography*, **9**, 87-150.

Shirayama, Y. 1984. Vertical distribution of meiobenthos in the sediment profile in bathyal, abyssal, and hadal deep sea systems of the western Pacific. *Oceanologica Acta*, **7**, 113-121.

Psamminopelta gradsteini n.sp., a new species of Paleogene deep-water agglutinated foraminifera from the northern North Atlantic and Polish Outer Carpathians

MICHAEL A. KAMINSKI[1] and STANISŁAW GEROCH[2]

1. Research School of Geological & Geophysical Sciences, UCL, Gower Street, London WC1E 6BT, UK

2. Institute of Geological Sciences, Jagiellonian University, ul. Oleandry 2a, 30-063 Krakow, Poland. (deceased).[1]

ABSTRACT

We describe the new species *Psamminopelta gradsteini* Kaminski and Geroch, n. sp. from green shales of Eocene age from the Labrador Sea, Norwegian Sea, and the Silesian Unit of the Polish Outer Carpathians. The species is characterised by its small, gracile test and numerous evolute whorls. The more or less synchronous appearance of *Psamminopelta gradsteini* n.sp. in middle to late Eocene green shales in three geographically separated areas means that the species is probably cosmopolitan, and is a useful stratigraphical index species in the abyssal area of the Atlantic and Tethys oceans.

INTRODUCTION

The deep water agglutinated foraminifera (DWAF) are widely distributed in oceanic sediments deposited beneath the Carbonate Compensation Depth throughout the world ocean. Although some faunal endemism may admittedly exist in semi-isolated oceanic basins such as the North Sea (e.g. Gradstein & Kaminski, 1989), as a general rule most DWAF species are cosmopolitan in distribution. This particularly applies to the faunas of the abyssal plains.

On various occasions over the years, the authors of this study have carried out direct comparisons of DWAF assemblages from classic localities in the Atlantic and Carpathian regions for the purpose of establishing a standardised taxonomic framework for biostratigraphical studies. Our earlier comparative studies have shown, for example, that a number of species described from the Paleogene of Trinidad by Cushman and co-workers in the 1930's and 1940's are identical with those first described from the Carpathian flysch by Grzybowski and co-workers at the turn of the 19th/20th centuries (Kaminski *et al.* 1988; Kaminski & Geroch, 1993). In another instance, a species newly found in Trinidad by the first author also turned up in samples from the Polish Carpathians (Kaminski & Geroch, 1987). It would appear that the faunal links between the Atlantic Ocean and the Carpathian flysch basins were indeed strong, at least until the Oligocene when Alpine tectonic movements severed the connections between the two areas.

The purpose of this note is to assign formal taxonomic status to yet another new species of cosmopolitan DWAF that has been found in the Eocene of the northern North Atlantic and Carpathi-

[1] Prof. Stan Geroch visited the GEOMAR bungalow in the spring of 1991 to carry out comparative studies of microfossils with the first author. At this time, the matter of the new *Psamminopelta* was discussed, and Prof. Geroch contributed photographs of specimens of the species from the Carpathian flysch. We again discussed this species in 1992 - 1993 while we were carrying out our revision of the Paleogene species from the Grzybowski Collection (Kaminski & Geroch, 1993). Although the idea carrying out more taxonomic work was discussed and a preliminary description of the species was written at that time, Prof. Geroch's death in 1995 precluded him from taking part in the actual writing of this paper. However, photographs of the Carpathian specimens used in this paper were made by him. Because of his initial contribution to this paper he is included here as the co-author.

In: Hass, H.C. & Kaminski, M.A. (eds.) 1997. Contributions to the Micropaleontology and Paleoceanography of the Northern North Atlantic. *Grzybowski Foundation Special Publication*, no. 5, pp. 249-252

an deep sea basins. The species has been reported previously under various names, notably in four (possibly five) different studies of Paleogene DWAF from DSDP and ODP localities in the Labrador Sea and Norwegian Sea. The species may have also been observed by Grzybowski (1901) from the Paleocene of the Magura Unit of the Carpathians, but as specimen is not preserved in the collections we cannot be certain of the synonymy. We therefore propose the new name *Psamminopelta gradsteini* n.sp. and provide a formal description of the species.

SYSTEMATIC TAXONOMY

Family RZEHAKINIDAE Cushman, 1933

Genus *Psamminopelta* Tappan, 1957

Psamminopelta differs from *Rzehakina* in having flat sides and in the absence of any wall thickening over the flat sides of the test. Loeblich & Tappan (1987) reported the stratigraphic distribution of the genus as Cretaceous. Reports of this genus in the Norwegian Sea extend its known stratigraphic range to the Miocene.

Psamminopelta gradsteini Kaminski & Geroch, n. sp.

Textfigure 1; Plate 1, figs. 1-9.

aff. *Ammodiscus polygyrus* (abnormal).—Grzybowski, 1901, pl. 8, fig. 27.

aff. *Spirolocammina lamposa* (Hussey).—Verdenius & van Hinte, 1983, p. 192, pl. 4, figs. 19, 20.

Spirosigmoilinella compressa Matsunaga.—Miller *et al.*, 1982, p. 20, pl. 2, fig. 5; —Kaminski *et al.*, 1989. pl. 5, fig. 6.

Psamminopelta sp. Kaminski *et al.* 1990. pl. 4, figs. 3,4.

Diagnosis: A gracile species of *Psamminopelta* with a thin wall and a concave initial part.

Type Specimen: Currently housed in the first author's collection at University College London. Holotype and paratypes will be deposited in the micropalaeontology collections of the Natural History Museum, London.

Type Level: Upper Eocene.

Type Locality: ODP Site 647, Southern Labrador Sea. Holotype is from Sample 647A-45R-1, 14-17cm.

Diagnostic Features: Test small, wholly planispiral, flat or weakly biconcave, evolute, with two chambers per whorl. Proloculus is minute. Chambers increase in diameter slowly, and do not overlap preceeding whorls. Specimens consist of as many as eight sets of whorls, and have a poorly developed spiral suture. Periphery is rounded. Aperture is an eccentric slit at the end of a produced neck.

Size: Specimens from ODP Site 647 are up to 0.6 mm in length, 0.28 mm in width.

Derivation of Name: In honour of Dr. Felix M. Gradstein (Saga Petroleum), who was co-author of three of the ODP papers that originally reported this species under various names. Also in recognition of his long-standing work on the systematics and biostratigraphy of DWAF from the northern North Atlantic region.

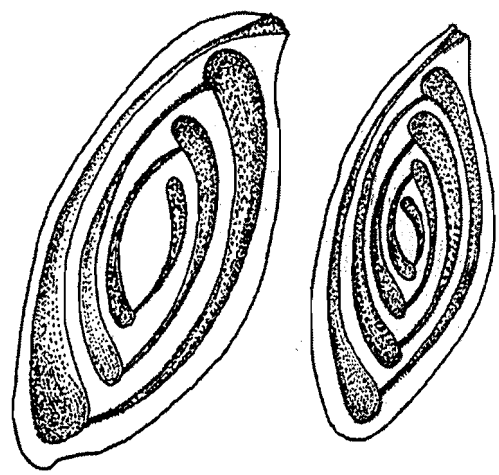


Figure 1. Internal structure of *Psamminopelta gradsteini* n.sp., drawn from transmitted light photographs. Specimens from the upper Eocene of Biecz, Poland, magnification ca. x160.

Observed Occurrences: This species may have been seen by J. Grzybowski in the Paleogene of the Gorlice region of the Carpathians. The specimen illustrated by Grzybowski (1901) as *„Ammodiscus polygyrus* (abnormal)" in his plate 8, fig. 27 is certainly reminiscent of our species. However, this specimen is not preserved in the collection, and has no formal status. Miller *et al.* (1982) reported this form as *Spirosigmoilinella compressa* from the upper middle Eocene to upper Eocene of DSDP Site 112 in the Labrador Sea. Verdenius & van Hinte (1983) illustrated specimens as *Spirolocammina lamposa* from DSDP Hole 338 which probably fit the description of *Psamminopelta gradsteini* n.sp. Osterman & Spiegler (*in press*) illustrated a specimen as *S. compressa* from the Miocene at Site 909, west of Spitsbergen.

We observed *Psamminopelta gradsteini* n.sp. in

the upper middle Eocene to lower Oligocene at Sites 112 and 647 in the southern Labrador Sea (Kaminski *et al.*, 1989), in the upper Eocene to Oligocene at ODP Site 643 in the Norwegian-Greenland Sea (Kaminski *et al.*, 1990), and in middle to upper Eocene (A. latus Zone) green claystones of the Silesian Unit of the Polish Carpathians, in Biecz, Poland.

Known Stratigraphic Range: upper middle Eocene to ?lower Miocene. The first occurrence of this species is a useful biostratigraphic datum in the upper middle Eocene in the deep Labrador Sea and Norwegian Sea.

Bathymetry: lower bathyal to abyssal.

Remarks: One of us (MAK) originally believed this form to represent one of the alternate generations of *S. compressa*, and therefore included it together with the latter species in data from ODP Site 647 (Kaminski *et al.*, 1989). However, after closer examination of material from both the Labrador and Norwegian-Greenland Sea, we have been unable to find any individuals of this species with spirosigmoiline initial coiling. Moreover, at both localities, the first occurrence of this form occurs lower in the stratigraphic section than that of the typical *S. compressa* Matsunaga. There is also a paleobathymetrical separation between *S. compressa* and *P. gradsteini* n.sp. in the North Sea region. *Psamminopelta gradsteini* n.sp. is rare in the North Sea, and is only observed in the deepest parts of the basin and at the abyssal ODP sites, whereas *S. compressa* is widely distributed. *Psamminopelta gradsteini* n.sp. occurs in low numbers in the middle to upper Eocene (Ammodiscus latus Zone) of the Silesian basin of the Polish Carpathians, but in this area *S. compressa* has not been observed. Based on the above observations, we now believe it is necessary to separate this species from *S. compressa*.

Although some specimens may be slightly assymetrical, others are almost perfectly symmetrical. The species therefore cannot be placed in the genus *Spirolocammina* Earland, 1934. (*Spirolocammina* is a strongly sigmoidal modern genus described from the Antarctic seas).

Psamminopelta gradsteini n.sp. is most similar in morphology to Paleocene specimens of *Rzehakina minima* from the Central North Sea. The major differences can be found in the nature of the initial portion of the test. *Rzehakina minima* has a larger proloculus than *Psamminopelta gradsteini* n.sp. Topotype specimens of*R. minima* from Lizard Springs are broader and thicker, and have perfectly flat lateral sides, whereas *Psamminopelta gradsteini* n.sp. is biconcave. Many specimens of *Psamminopelta gradsteini* n.sp. have broken centers, indicating that the proloculus and first whorls must have been extremely thin-walled. Schröder-Adams & McNeil (1994) described the new species *Psamminopelta arca* from the Oligocene Kugmallit sequence in the Beaufort-Mackenzie Basin. This species differs in its thicker test and more rounded outline.

Acknowledgements
We thank Jaroslaw Migacz for help with the figures and Dennis Grieg (Chevron, USA) for assistance with the SEM work. Jenö Nagy reviewed the paper. This is contribution no. 57 of the Deep-Water Agglutinated Foraminiferal Project.

References:

Gradstein, F.M., & Kaminski, M.A. 1989. Taxonomy and biostratigraphy of new and emended species of Cenozoic deep-water agglutinated foraminifera from the Labrador and North Seas. *Micropaleontology*, **35**, 72-92.

Grzybowski, J. 1901. Otwornice warstw inoceramowych okolicy Gorlic. *Rozprawy Wydzialu Matematyczno-przyrodniczego, Akademia Umiejetnosci w Krakowie, serya 2*, **41**, 219-286.

Kaminski, M.A. & Geroch, S. 1987. Two new species of *Phenacophragma* from the Paleogene of Trinidad and Poland. *Micropaleontology*, **33**, 185-188.

Kaminski, M.A. & Geroch, S. 1993. A revision of foraminiferal species in the Grzybowski Collection. *In:* Kaminski, M.A., Geroch, S. and Kaminski, D. (eds.), *The Origins of Applied Micropaleontology: The School of Jozef Grzybowski*, Grzybowski Foundation Special Publication no. 1. Alden Press, Oxford, 239-323.

Kaminski, M.A., Gradstein, F.M., Berggren, W.A., Geroch, S. & Beckmann, J.P. 1988. Flysch-type agglutinated foraminiferal assemblages from Trinidad: Taxonomy, Stratigraphy and Paleobathymetry. Proceedings of the Second Workshop on Agglutinated Foraminifera, Vienna 1986, *Abhandlungen der Geologischen Bundesanstalt*, **41**, 155-228.

Kaminski, M.A., Gradstein, F.M. & Berggren, W.A. 1989. Paleogene benthic foraminiferal stratigraphy and paleoecology at Site 647, Southern Labrador Sea. *In:* Arthur, M.A., Srivastava, S., et al. *Init. Repts. ODP Leg 105.*

Kaminski, M.A., Gradstein, F.M., Goll, R.M., & Grieg, D. 1990. Biostratigraphy and paleoecology of deep-water agglutinated foraminifera at ODP Ste 643, Norwegian-Greenland Sea. *In*: Hemleben, C., Kaminski, M.A., Kuhnt, W., and Scott, D.B. (eds.), *Paleoecology, Biostratigraphy, Paleoceanography and Taxonomy of Agglutinated Foraminifera*, NATO ASI Series, Kluwer Acad. Publ. 345-386.

Loeblich, A.R., & Tappan, H. 1988. *Foraminiferal genera and their classification.* - Van Nostrand Reinhold Co., 970 pp.

Miller, K.G., Gradstein, F.M. & Berggren, W.A. 1982. Late Cretaceous to early Tertiary agglutinated benthic foraminifera in the Labrador Sea. *Micropaleontology*, **28**, 1-30.

Osterman, L.E. & Spiegler, D. *in press.* Agglutinated benthic foraminiferal biostratigraphy of the Ocean Drilling Program (ODP) Sites 909 and 913, northern North Atlantic. *ODP Scientific Results*, **151**.

Schröder-Adams, C.J. & McNeil, D.H. 1994. New paleoenvironmentally important species of agglutinated foraminifera from the Oligocene and Miocene of the Beaufort Sea, Arctic Canada. *Journal of Foraminiferal Research*, **24**, 178-190.

Verdenius, J.G. & van Hinte, J.E. 1983. Central Norwegian-Greenland Sea: Tertiary arenaceous foraminifera, biostratigraphy and environment. Proceedings of the First Workshop on Arenenaceous Foraminifera, 7-9 Sept. 1981. *Continental Shelf Institute Publication*, **108**, 173-224.

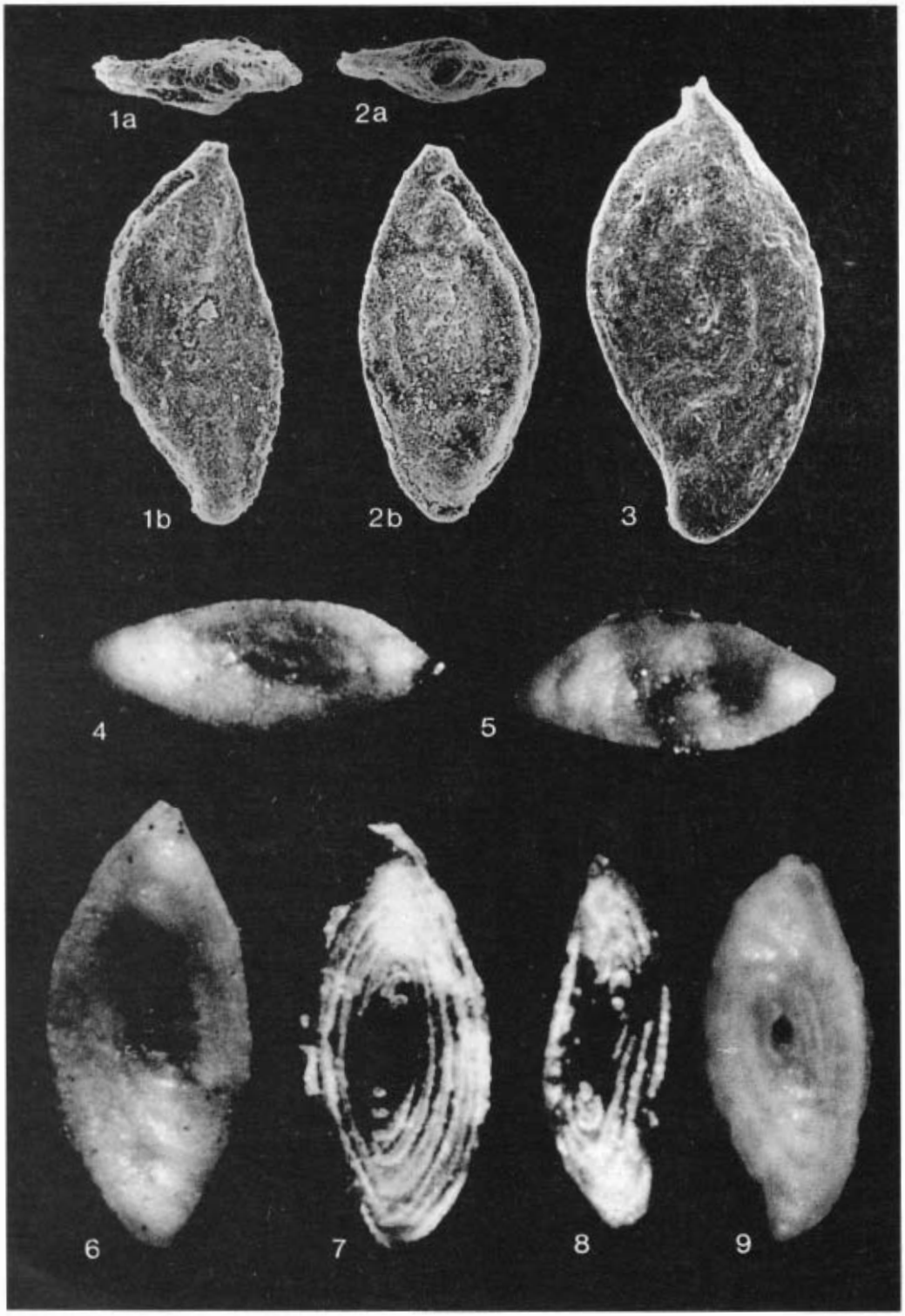


Plate 1. *Psamminopelta gradsteini* n.sp.
Fig. 1a,b. Oligocene, ODP Site 643, Norwegian Sea, Sample 643A-44R-5, 79-84 cm, x145.
Fig. 2a,b. Oligocene, ODP Site 643, Norwegian Sea, Sample 643A-44R-5, 79-84 cm, x145.
Fig. 3. Upper Eocene, ODP Site 647, Labrador Sea, Sample 647A-36R-4, 49-52 cm, x175.
Fig. 4-6. Upper Middle Eocene, ODP Site 647, Labrador Sea, Sample 647A-45R-1, 14-17 cm, 4,5, Paratypes, 6, Holotype, x132.
Fig. 7-8. Upper Middle Eocene, ODP Site 647, Labrador Sea, Sample 647A-45R-2, 20-24 cm, x142.
Fig. 9. Upper Eocene, Silesian Unit of the Polish Carpathians near Biecz Poland. x140

Wurstkammer specimens of the planktic foraminifer *Neogloboquadrina pachyderma* (sinistral): A new morphotype from the Arctic Ocean and the Weddell Sea

HARALD HOMMERS

GEOMAR - Research Center for Marine Geosciences, Wischhofstraße 1-3, D-24148 Kiel, Germany

ABSTRACT

From two cores of the central Arctic Ocean and the Southern Ocean (Weddell Sea) a new morphotype of the planktic foraminifer *Neogloboquadrina pachyderma* (sinistral) (Ehrenberg) with "sausage" shaped final chambers (i.e. "Wurstkammer") is described. A comparison of these morphotypes in the two polar regions shows significant differences in shape and frequency during the last 70,000 years in the central Arctic Ocean and during the last 140,000 years in the Weddell Sea. In the central Arctic Ocean the frequency of wurstkammer specimens can be correlated to that of the so-called kummerform specimens during the last 70,000 years; this correlation cannot be seen in a core from the Weddell Sea. The wurstkammer and kummerform specimens are interpreted as being end-members of a morphological progressional line. The abnormal chamber growth is probably an adaption to various environmental stress conditions found in the two polar regions during the last 70,000 in the Arctic and 140,000 years in the Antarctic, but the reasons for this abnormality are not yet fully understood.

INTRODUCTION

In this study, a new morphotype of the planktic foraminifer *Neogloboquadrina pachyderma* (sinistral) (Ehrenberg) is described and its occurences in the central Arctic (Fig. 1) and the South Atlantic Ocean (Weddell Sea, Fig. 2) is compared. The last chambers of these specimens are „sausage" shaped („Wurstkammer" = sausage chamber), especially in Core PS2185, or are more inflated (in Core PS1388).

Earlier studies concentrated mainly on the integration of the planktic foraminifer species *N. pachyderma* (sin.) within the total planktic foraminifer taxa. Since the 1970's several workers have studied the paleoceanographic and ecological parameters of this polar species, such as the evaluation of coiling directions and of frequency distributions (Kennett, 1968, Keller, 1978).

In the 1980's, research on the recent distribution of planktic foraminifers in the water column was strengthened by plankton tow and sediment trap experiments, especially in the Pacific Ocean (Arikawa, 1983, Reynolds & Thunell, 1986).

During the 1990's, detailed studies of the vertical and horizontal distribution of *N. pachyderma* in the water column of the Arctic Ocean (Carstens & Wefer, 1992) and the South Atlantic (Donner & Wefer, 1994, Berberich, 1996) have been carried out. Several tropical and subtropical planktic foraminifer species (i.e. *Globigerinoides sacculifer, Globigerinella siphonifera* and *Orbulina universa*) have been successfully cultured under varying laboratory conditions (e.g. temperature, salinity, food) (Hemleben *et al.*, 1987, Hemleben *et al.*, 1989, Bijma *et al.*, 1990, Bijma *et al.*, 1992). Studies of *N. pachyderma* in the Weddell Sea have focused on its distribution and abundance in the water column with and without sea ice cover, and on the occurence of living specimens of *N. pachyderma* in the Weddell Sea ice (Spindler & Dieckmann, 1986, Spindler *et al.*, 1990, Dieckmann *et al.*, 1991, Berberich, 1996). Culture experiments to demonstrate the special adaption of *N. pachyderma* to high salinities in Antarctic sea ice have been carried out by Spindler (1996).

MATERIAL & METHODS

Samples of two sediment cores were examined: Core PS2185 in the central Arctic Ocean (Lomonosov Ridge, core location 87°32.0'N 144°22.9'E, 1051 m water depth, Fig. 1) and Core PS1388 in the eastern Weddell Sea (core location

In: Hass, H. C. & Kaminski, M. A. (eds.) 1997. Contributions to the Micropaleontology and Paleoceanography of the Northern North Atlantic. *Grzybowski Foundation Special Publication*, no. 5, pp. 253-262

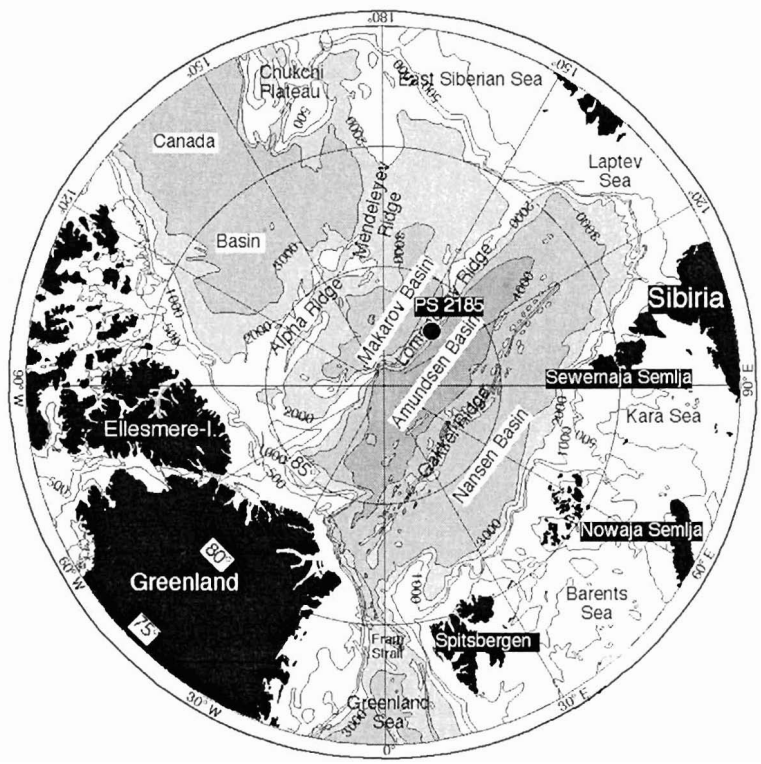


Figure 1. Core location of Core PS2185 in the central Arctic Ocean (Lomonosov-Ridge).

69°02.0′S; 5°55.0′W, 2526 m water depth, Fig. 2). Core PS2185 was recovered during the Arktis-VIII/3 expedition of RV „Polarstern" (Fütterer, 1992) and Core PS1388 during the Antarktis- IV/3 expedition (Fütterer, 1987).

All samples were wet-sieved over a 63 µm mesh-size sieve and later dry-sieved. The coarse fraction was dry-sieved into the subfractions 63-125, 125-250 and 250-500 µm. The wurstkammer and kummerform specimens were counted in the 250-500 µm fraction and calculated for the total sample (specimens per gram dry sediment). Simultaneously the wurstkammer specimens were picked for SEM-analysis. Ongoing work shows that only few specimens of *N. pachyderma* (sin.) with wurstkammer-shaped chambers occur in the subfraction 125-250 µm.

A wurstkammer is defined as one of the last chambers of *N. pachyderma* (sin.) which is, in contrast to a kummerform chamber, normally two to three times more elongated than the previous chamber. They are normally „sausage" shaped with a width/length ratio of 0.25 - 0.50. These wurstkammers usually grow at an angle of 90° to the trochospiral growth direction and overlap earlier chambers.

This study covers the last 70,000 years including isotope Stages 4 to 1 in Core PS2185 (Arctic Ocean, Fig. 3) and the last 140,000 years spanning isotope Stages 6 to 1 in Core PS1388 (Weddell

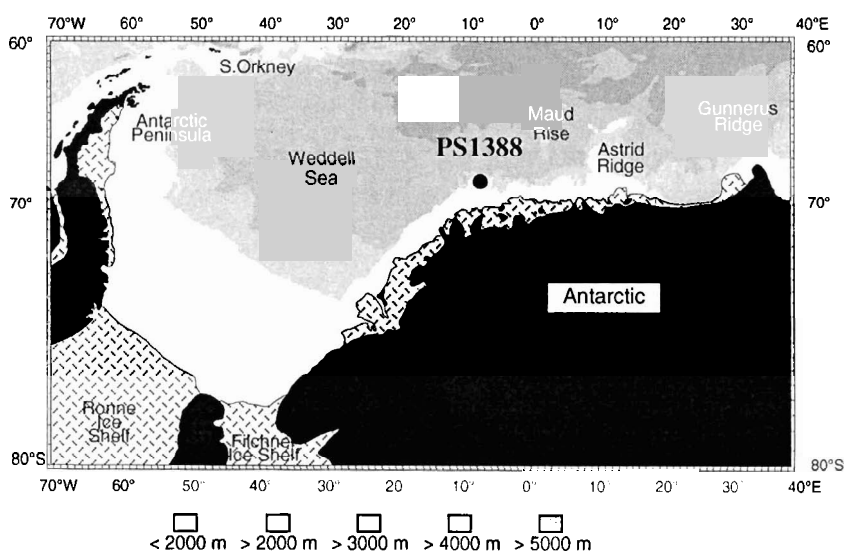


Figure 2. Core location of Core PS1388 in the eastern Weddell Sea.

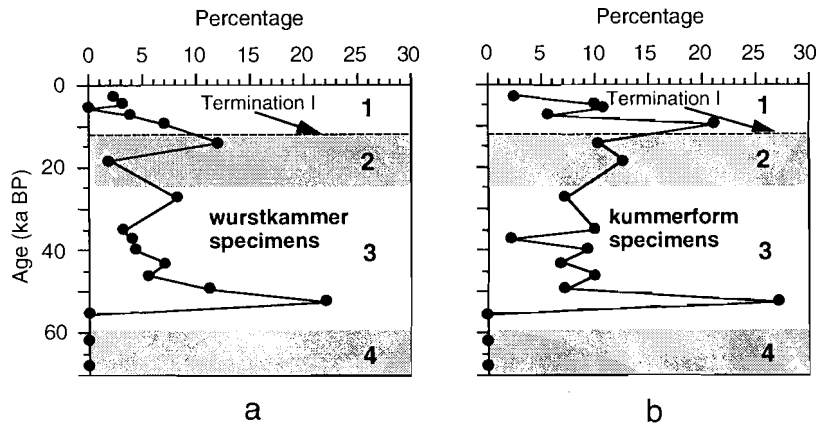


Figure 3a,b.. Percentages of wurstkammer and kummerform specimens of *Neogloboquadrina pachyderma* (sin.) of total *N. pachyderma* (sin.) specimens in the fraction 250-500 µm in Core PS2185, central Arctic Ocean (oxygen isotope Stages 4 to 1).

Sea, Fig. 4). Of special interest are the morphological and faunal changes in the wurstkammer specimens during the glacial/interglacial transitions 6/5 (Termination II) and 2/1 (Termination I). These time spans are recorded in Core PS1388 through stable oxygen isotope data, but between 52-24 ka B.P. no samples are available (Figs. 4, 6, 7b, 8b). Samples in Core PS2185 cover the last 70,000 years dated through AMS-ages and stable oxygen isotope data (Nørgaard-Pedersen, 1996). The stratigraphical basement of Core PS1388 (Weddell Sea) used in this study, is the *N. pachyderma* (sin.) $\delta^{18}O$ curve, carried out by Grobe *et al.* (1990) and Grobe & Mackensen (1992). The stratigraphic fix points are in accordance with Martinson *et al.* (1987).

RESULTS

Morphological results of the wurstkammer specimens (interpretation of SEM-photographs)

The scanning electron microscope photographs (Plates 1 and 2) show abnormal shell growth (i.e. „Wurstkammer" specimens) in comparison to normal shell growth. Here the „Wurstkammer" morphotypes are defined as *N. pachyderma* (sin.) specimens with abnormally elongated last chambers. In these specimens the final chambers are not normally arranged in a trochospire. The wurstkammers appear to grow at an angle of 90° to the normal growth direction, thus overlapping the spiral and umbilical parts of the test in the form of a „sausage". Usually only one chamber is formed as a wurstkammer, but occasionally two or more wurstkammers can be seen in one specimen. In this case the last wurstkammer is larger in size and more elongated than the others (Plate 1: Fig. IV).

In the two polar regions morphologically different types of wurstkammer specimens can be found:

a) In samples from the central Arctic Ocean (Core PS2185) relatively long wurstkammers dominate (Plate 1: Fig. Ia, Ib, III, IV). These chambers can be up to three times larger than the penultimate chamber. The very wide aperture of the wurstkammer specimens in comparison to normal specimens of *N. pachyderma* (sin.) is another important characteristic feature (Plate 1: Fig. Ib, III).

b) Many wurstkammer specimens in the Weddell Sea (Core PS1388) differ in shape from those of the Arctic Ocean: The wurstkammers formed here are more inflated as they have a lower length/width ratio than the wurstkammers from Core PS2185 (Plate 2: Fig. IIIa, IVb).

In addition to the *N. pachyderma* wurstkammer specimens with large terminal chambers, samples also contain specimens with rudimentary last chambers, so called kummerform-specimens (Berger, 1969; Olsson, 1973) (Plate 2: Fig. II). Berger (1969) first described these specimens: he defined kummerforms as specimens with a smaller or equal-sized final chamber as the penultimate one. In exceptional cases kummerkammers and wurstkammers occur in the same specimen: Here the last chamber is formed as a kummerkammer whereas the penultimate and antepenultimate chambers are formed as wurstkammers (Plate 1: Fig. IV).

Quantitative analysis of wurstkammer/kummerform *N. pachyderma* (sin.) specimens in the subfraction 250-500 µm

In the sediment samples of Core PS2185 the maximum frequency of wurstkammer specimens is found at the beginning of oxygen isotope Stage 3 (up to 22% of the total *N. pachyderma* specimens in the subfraction 250-500 µm) and at Termination I (up to about 12%, Fig. 3a). The lowest frequencies of wurstkammer specimens appear in Termination II (about 0%), in Stage 2 (about 2%) and in the Holocene (up to 3%) (Fig. 3a). Highest numbers of kummerform specimens occur at the same time as the wurstkammer specimens, i.e. at the beginning of Stage 3 (27% frequency) and at Termination I (21%). Frequency minima occur at stage boundary 4/3, in the middle part of Stage 3 and in the upper Holocene (Fig. 3b).

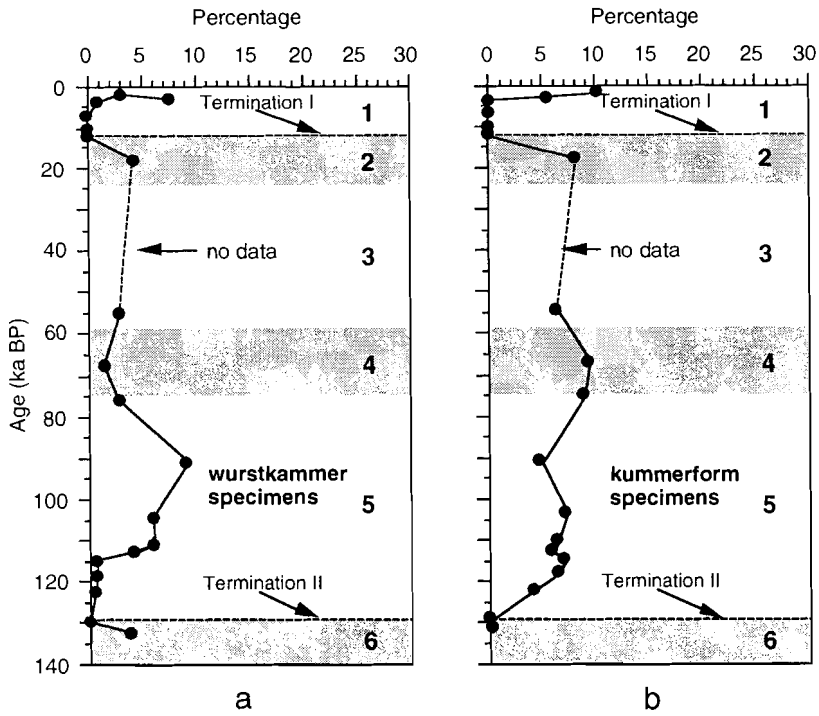


Figure 4a,b. Percentages of wurstkammer and kummerform specimens of *Neogloboquadrina pachyderma* (sin.) of total *N. pachyderma* (sin.) in the fraction 250-500 µm in Core PS1388, eastern Weddell Sea (oxygen isotope Stages 6 to 1).

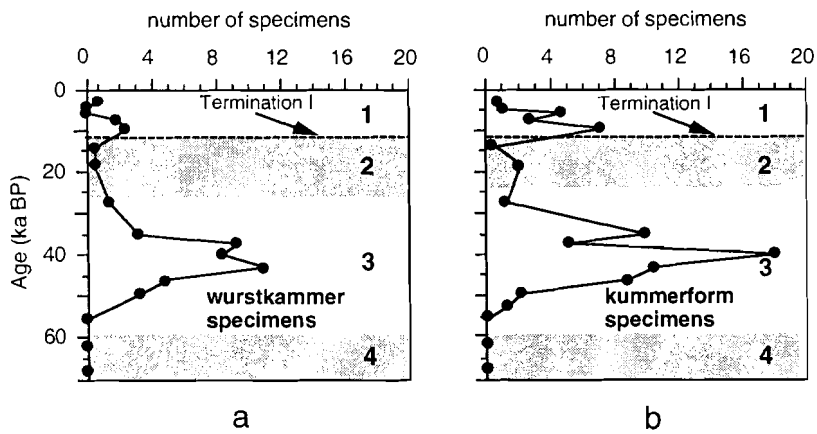


Figure 5a,b. Concentration of wurstkammer and kummerform specimens of *Neogloboquadrina pachyderma* (sin.) in the fraction 250-500 µm/g dry sediment in Core PS2185, central Arctic Ocean (oxygen isotope Stages 4 to 1).

In Core PS1388 wurstkammer specimens can be observed mainly within Stage 5 (about 9%) and in the Holocene. Frequency minima appear at Termination II, Termination I and in the lower Holocene, a weak minimum occurs in Stage 4 (Fig. 4a).

Most of the kummerform specimens appear in Substage 5.5 (about 26%), in Stage 4 (about 9%) and in the Holocene (11%) (Fig. 4b). Frequency minima occur at Termination II, within Stage 5, at Termination I and in the Holocene (Fig. 4b).

Concentrations of wurstkammer/kummerform specimens in the subfraction 250-500 µm

In Core PS2185 no wurstkammer specimens are found in the upper part of Stage 4 and at stage boundary 4/3. The numbers increase throughout Stage 3 with highest test concentrations found in the middle part of Stage 3 (up to 11 specimens/g dry sediment) (Fig. 5a). At the end of Stage 3 the number of wurstkammer specimens decreases rapidly down to only 1 wurstkammer specimen/g in Stage 2. During the Holocene the concentration increases slightly up to 2.5 specimens/g (Fig. 5a). The corresponding plot of the kummerform concentrations shows a similar trend (Fig. 5b): Lowest concentrations of kummerform specimens are found in the upper part of Stage 4 and at stage boundary 4/3 (0 specimens/g). Highest concentrations occur in Stage 3 (up to 18 specimens/g, Fig. 5b). Concentrations here are on average twice as high as the wurstkammer specimens.

In contrast, concentrations of wurstkammer

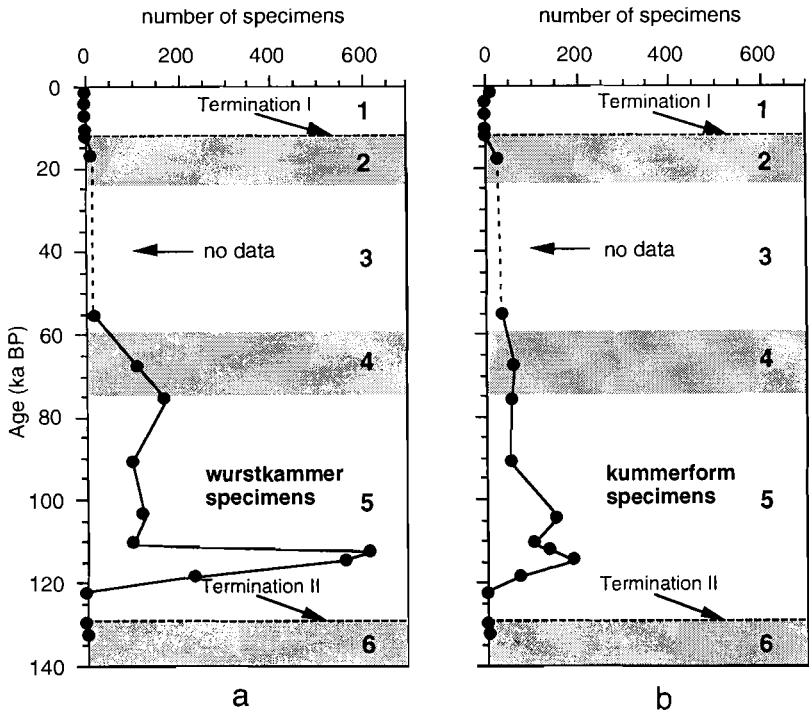


Figure 6a,b. Concentration of wurstkammer and kummerform specimens of *Neogloboquadrina pachyderma* (sin.) in the fraction 250-500 µm/g dry sediment in Core PS1388, eastern Weddell Sea (oxygen isotope Stages 6 to 1).

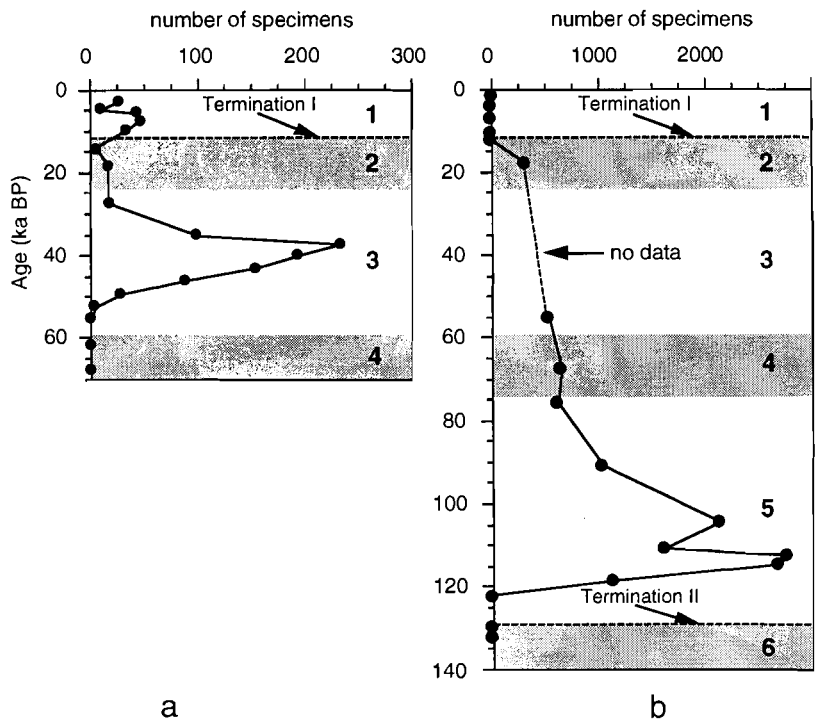


Figure 7a,b. Concentration of total specimens of *N. pachyderma* (sin.)/g dry sediment in the fraction 250-500 µm in Core PS2185, central Arctic Ocean (oxygen isotope Stages 4 to 1) and in Core PS1388, eastern Weddell Sea (oxygen isotope Stages 6 to 1).

specimens are very high in Core PS1388 (more than 600 wurstkammer specimens/g dry sediment near Substage 5.5 about 115 ka B.P.) (Fig. 6a). Concentrations decrease rapidly after this short maximum, although a minor maximum occurs at stage boundary 5/4 (about 150 wurstkammer specimens/g). Throughout Stage 4 a second decrease takes place. In Stages 3 and 2 concentrations are low (about 15 wurstkammer specimens/g). At Termination I and in the Holocene all wurstkammer specimens disappear (Fig. 6a). Kummerform specimens generally show lower concentrations than the wurstkammer specimens although they follow a similar trend to the wurstkammer speci-

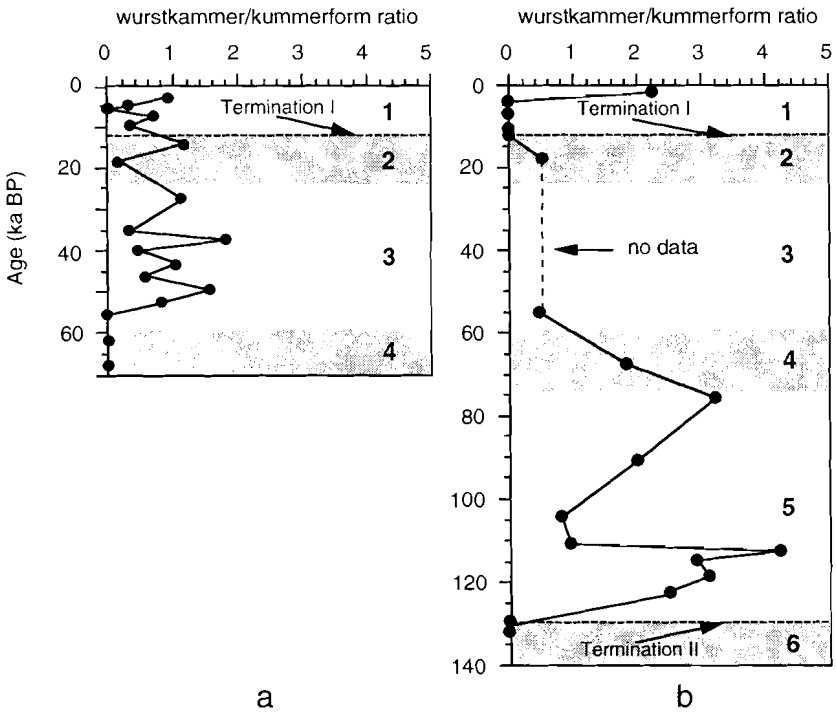


Figure 8a,b. Wurstkammer/kummerform ratio of specimens *N. pachyderma* (sin.) in the fraction 250-500 µm in Core PS2185, central Arctic Ocean (oxygen isotope Stages 4 to 1) and in Core PS1388, eastern Weddell Sea (oxygen isotope Stages 6 to 1).

mens. Maximum concentrations were observed in Stage 5 with 170 kummerform individuals/g (Fig. 6b).

The concentration of the total specimens of *N. pachyderma* (sin.) in the fraction 250-500 µm is up to 250 specimens/g dry sediment in Stage 3 in Core PS2185, a lower peak is observed in the Holocene with about 50 specimens/g (Fig. 7a). Lowest concentrations can be seen at stage boundary 4/3 (0 specimens/g) and in Stage 2 (about 20 specimens/g).

In Core PS1388 highest concentrations are seen in two maxima within Stage 5 with 2750 specimens/g at 115 ka B.P. and 2100 specimens/g at 105 ka B.P., minima occur at Terminations II and I (0 specimens/g) (Fig. 7b).

The highest concentration of total specimens of *N. pachyderma* (sin.) is up to 30 times higher in the Weddell Sea than in the Arctic Ocean (Fig. 7a, 7b). The concentration curve of total specimens of *N. pachyderma* (sin.) in the Arctic Ocean and the Weddell Sea (Fig. 7a, b) correlates well with the concentration of kummerform specimens in the fraction 250-500 µm in the same cores (Fig. 5b, 6b), whereas the correlation to the wurstkammer curves is not so evident (Fig. 5a, 6a).

The wurstkammer/kummerform ratio in the Arctic Ocean in the fraction 250-500 µm is low (up to 1.4 in Stage 5 and 1.7 in Stage 3) (Fig. 8a) compared with the wurstkammer/kummerform ratio in the Weddell Sea (up to 4.2 in Stage 5 and 2.2 in the Holocene) (Fig. 8b). In the Arctic Ocean lowest wurstkammer/kummerform ratios can be found in the upper part of Stage 4, at stage boundary 4/3 and in Stage 2 (0.05), highest values are seen in Stage 3 (up to 1.8, Fig. 8a). In the Weddell Sea maxima of the wurstkammer/kummerform ratio occur in Stage 5 at 112 ka B.P. (4.1), near stage boundary 5/4 (3.2) and in the upper Holocene (3.2).

DISCUSSION & CONCLUSION

The comparison of the quantitative analyses on the wurstkammer and kummerform specimens in the fraction 250-500 µm in Core PS2185 shows an excellent correlation between these two morphotypes (Fig. 3a, b). In this core, especially in Stage 3 and at Termination I, a high number of wurstkammer and kummerform specimens occur at the same time. The percentage of kummerform individuals is normally two to three times higher than that of the wurstkammer specimens. The ratio between wurstkammer and kummerform specimens is relatively low, indicating only a small difference in the number of wurstkammer and kummerform specimens (Fig. 8a).

These two special morphotypes can be interpretated as end-members of a morphological line and demonstrate the very high morphological variability of *N. pachyderma* (Kennett, 1968; Keller, 1978; Healy-Williams, 1992), clearly evident in the short time intervals between 56-50 and 18-8 ka B.P. (Fig. 3a, b).

In contrast, in Core PS1388 no general correlation between wurstkammer and kummerform

types can be found, for example some samples show a high number of wurstkammer specimens together with only a few kummerform specimens (Stage 5, about 90 ka B.P.; Fig. 4a, b).

Kummerform growth is probably due to two main reasons (Berberich, 1996):

a) Development of kummerforms in small specimens due to environmental stress, e.g. changes in temperature, salinity and food supply (Berger, 1971; Bé & Van Donk, 1971; Hecht & Savin, 1972).

b) Development of kummerforms in large specimens due to reproduction stress. Hemleben *et al.* (1987) discovered that specimens of the planktic foraminifer *G. sacculifer* form kummerform chambers instead of normally shaped last chambers shortly before reproduction.

If kummerform and wurstkammer specimens are considered as end-members of a morphological progression, then the reasons above i.e. environmental/reproduction stress need to be further analysed. If the formation of a wurstkammer is compared with the building of the sack-like chamber in specimens of *G. sacculifer*, then reproduction stress would be the most important reason for forming a wurstkammer. This is supported by the large number of wurstkammer specimens found in the fraction 250-500 µm in contrast to the fraction 125-250 µm where there are only a few such specimens. Therefore, the wurstkammers were formed mainly in the adult stage, when reproduction occurs. Secondary calcification of *N. pachyderma* tests formed shortly before reproduction (Kennett, 1968; Bé & Hemleben, 1977; Meggers, 1996) appears to be less well developed on wurstkammer individuals from either core (Plate 1: Fig. IIa, b, III; Plate 2: Fig. IIIa, b).

On the other hand the formation of wurstkammer specimens due to environmental stress is supported by:

1. their extensive appearance during time intervals of the last 140,000 years that are characterized by strong climate change, i.e. in very early Stage 3 and at Termination I (Nørgaard-Pedersen, 1996) the change of meltwater to normal salinity conditions could cause the appearance of large numbers of wurstkammer and kummerform specimens in the Arctic Ocean (Fig. 3a, b).

2. the abnormal shell growth of the wurstkammer individuals: the abnormality of the wurstkammer chambers is not only restricted to size and shape, as in the sack-like chambers of *G. sacculifer*, but there is also an abnormality in growth direction (often a second growth direction perpendicular to the main one). These specimens may terminate normal growth in one direction due to strong environmental stresses, and then build enlarged chambers with growth in a new direction. The different morphological shapes of the wurstkammer chambers in each of the two polar cores point to different strong environmental factors influencing *N. pachyderma* populations in the Arctic Ocean and the Weddell Sea.

Earlier works (Bé & Hutson, 1977; Boltovskoy, 1982) were unable to find causes for abnormal shell growth in planktic foraminifera.

To obtain more details about the formation of wurstkammer specimens additional studies of *N. pachyderma* shells in sediment surface samples, in samples from sediment traps and in plankton net tows need to be carried out. Especially the North Atlantic and the South Atlantic are interesting regions for further studies because of their different oceanic conditions and geological history to compare the biology and the fossil record of the bipolar populations of *N. pachyderma*. Culture experiments are also necessary to test the various conditions under which wurstkammer growth takes place.

ACKNOWLEDGEMENTS

Many thanks to H. Bauch, who supported this work on the wurstkammer specimens and with whom I had many helpful discussions. The manuscript was critically read and improved by M. Spindler. Thanks also go to A. v. Doetinchem for help at the scanning electron microscope, J. Heinze for SEM-photographs, U. Wollschläger for sample preparation, R. Spielhagen and N. Nørgaard-Pedersen for samples and stratigraphical data of Core PS2185 and H. Grobe, A. Mackensen and G. Kuhn for sample material from Core PS1388. C. Hass reviewed an earlier version of this paper. S. Kinsey and P. Goldschmidt corrected the English. This work is supported by the Deutsche Forschungsgemeinschaft (Schwerpunktprogramm „Antarktisforschung").

REFERENCES

Arikawa, R. 1983. Distribution and taxonomy of *Globigerina pachyderma* (Ehrenberg) off the Sanriku Coast, Northeast Honshu, *Science Reports of the Tohoku University, Sendai, Second Series (Geology)*, **53**, 103-157.

Bé, A.W.H. & Hemleben, C. 1977. Laboratory and field observations of living planktonic foraminifera. *Micropaleontology* , **23**, 155-179.

Bé, A.W. H. & Hutson, W. H. 1977. Ecology of planktonic foraminifera and biogeographic patterns of life and fossil assemblages in the Indian Ocean. *Micropaleontology*, **23**, 369-414.

Bé, A.W.H. & Van Donk, J. 1971. Oxygen-18 studies of recent planktonic foraminifera. *Science* , **173**, 167-168.

Berberich, D. 1996. Die planktische Foraminifere *Neogloboquadrina pachyderma* (Ehrenberg) im Weddellmeer, Antarktis. *Reports on Polar Research*, **195**, 1-193.

Berger, W.H. 1969. Kummerform foraminifera as clues to oceanic environments. *Bulletin of the American Association of Petroleum Geologists*, **53**, 706.

Berger, W.H. 1971. Sedimentation of planktonic

foraminifera. *Marine Geology*, **11**, 325-358.

Bijma, J., Faber, W.W. Jr. & Hemleben, C. 1990. Temperature and salinity limits for growth and survival of some planktonic foraminifers in laboratory cultures. *Journal of Foraminiferal Research*, **20**, 95-116.

Bijma, J., Hemleben, C., Oberhänsli, H. & Spindler, M. 1992. The effects of increased water fertility on tropical spinose planktonic foraminifers in laboratory cultures. *Journal of Foraminiferal Research* , **22**, 242-256.

Boltovskoy, E. 1982. Twinned and flattened tests in planktonic foraminifera. *Journal of Foraminiferal Research*, **12**, 79-82.

Carstens, J. & Wefer, G. 1992. Recent distribution of planktonic foraminifera in the Nansen Basin, Arctic Ocean. *Deep-Sea Research*, **39**, 507-524.

Dieckmann, G.S., Spindler, M., Lange, M.A., Ackley, S.F. & Eicken, H. 1991. Antarctic sea ice: a habitat for the foraminifer *Neogloboquadrina pachyderma*. *Journal of Foraminiferal Research*, **21**, 182-189.

Donner, B. & Wefer, G. 1994. Flux and stable isotope composition of *Neogloboquadrina pachyderma* and other planktonic foraminifers in the Southern Ocean (Atlantic sector). *Deep-Sea Research*, **41**, 1733-1743.

Fütterer, D.K. 1987. The Expedition ANT-IV of RV „Polarstern" 1985/86, Report of Legs ANT-IV/3-4. *Reports on Polar Research*, **33**, 1-204.

Fütterer, D.K. 1992. ARCTIC '91: The Expedition ARK-VIII/3 of RV „Polarstern" in 1991. *Reports on Polar Research*, **107**, 1-267.

Grobe, H. & Mackensen, A. 1992. Late Quaternary climatic cycles as recorded in sediments from the Antarctic continental margin. *In:* Kennett, J.P. & Warnke, D.A. (Eds.), *The Antarctic paleoenvironment: A perspective on global change. Antarctic Research Series*, **56**, 349-376, American Geophysical Union, Washington.

Grobe, H., Mackensen, A., Hubberten, H.-W., Spiess, V. & Fütterer, D. K. 1990. Stable isotope record and late Quaternary sedimentation rates at the Antarctic continental margin. *In:* Bleil, U. & Thiede, J. (Eds.), *Geological History of the Polar Oceans. NATO ASI Series*, C **308**, 539-572, Kluwer Academic Publishers, Dordrecht.

Healy-Williams, N. 1992. Stable isotope differences among morphotypes of *Neogloboquadrina pachyderma* (Ehrenberg): implications for high-latitude palaeoceanographic studies. *Terra Nova* , **4**, 693-700.

Hecht, A.D. & Savin, S.M. 1972. Phenotypic variation and oxygen isotope ratios in recent planktonic foraminifera. *Journal of Foraminiferal Research*, **2**, 55-67.

Hemleben, C., Spindler, M., Breitinger, I. & Ott, R. 1987. Morphological and physiological responses of *Globigerinoides sacculifer* (Brady) under varying laboratory conditions. *Marine Micropaleontology*, **12**, 305-324.

Hemleben, C., Spindler, M. & Anderson, O.R. 1989. Modern Planktonic Foraminifera. 363 pp, Springer-Verlag, Berlin.

Keller, G. 1978. Morphologic variation of *Neogloboquadrina pachyderma* (Ehrenberg) in sediments of the marginal and central northeast Pacific Ocean and paleoclimatic interpretation. *Journal of Foraminiferal Research*, **8**, 208-224.

Kennett, J.P. 1968. Latitudinal variation in *Globigerina pachyderma* (Ehrenberg) in surface sediments of the southwest Pacific Ocean. *Micropaleontology*, **14**, 305-318.

Martinson, D.G., Pisias, N.G., Hays, J.D., Imbrie, J., Moore, T.C. Jr. & Shackleton, N.J. 1987. Age dating and the orbital theory of the ice ages: development of a high-resolution 0 to 300,000-year chronostratigraphy. *Quaternary Research*, **27**, 1-29.

Meggers, H. 1996. Pliozän-quartäre Karbonatsedimentation und Paläozeanographie des Nordatlantiks und des Europäischen Nordmeeres - Hinweise aus planktischen Foraminiferengemeinschaften. *Berichte, Fachbereich Geowissenschaften, Universität Bremen*, **71**, 1-143.

Nørgaard-Pedersen, N., (in press). Late Quaternary Arctic Ocean sediment records: Surface ocean conditions and provenance of ice-rafted debris. *GEOMAR Report*.

Olsson, R.K. 1973. What is a kummerform foraminifer? *Journal of Paleontology*, **47**, 327-329.

Reynolds, L.A. & Thunell, R.C. 1986. Seasonal production and morphologic variation of *Neogloboquadrina pachyderma* (Ehrenberg) in the northeast Pacific. *Micropaleontology*, **32**, 1-18.

Spindler, M. 1996. On the salinity tolerance of the planktonic foraminifer *Neogloboquadrina pachyderma* from Antarctic sea ice. Proceedings of the NIPR Symposium on Polar Biology, **9**, 85-91.

Spindler, M. & Dieckmann, G. 1986. Distribution and abundance of the planktic foraminifer *Neogloboquadrina pachyderma* in sea ice of the Weddell Sea (Antarctica). *Polar Biology*, **5**, 185-191.

Spindler, M., Dieckmann, G.S. & Lange, M.A. 1990. Seasonal and geographic variations in sea ice community structure of the Weddell Sea, Antarctica. *In:* Kerry, K.R. & Hempel, G. *Antarctic Ecosystems. Ecological Change and Conservation*, Springer-Verlag, Berlin, 129-135.

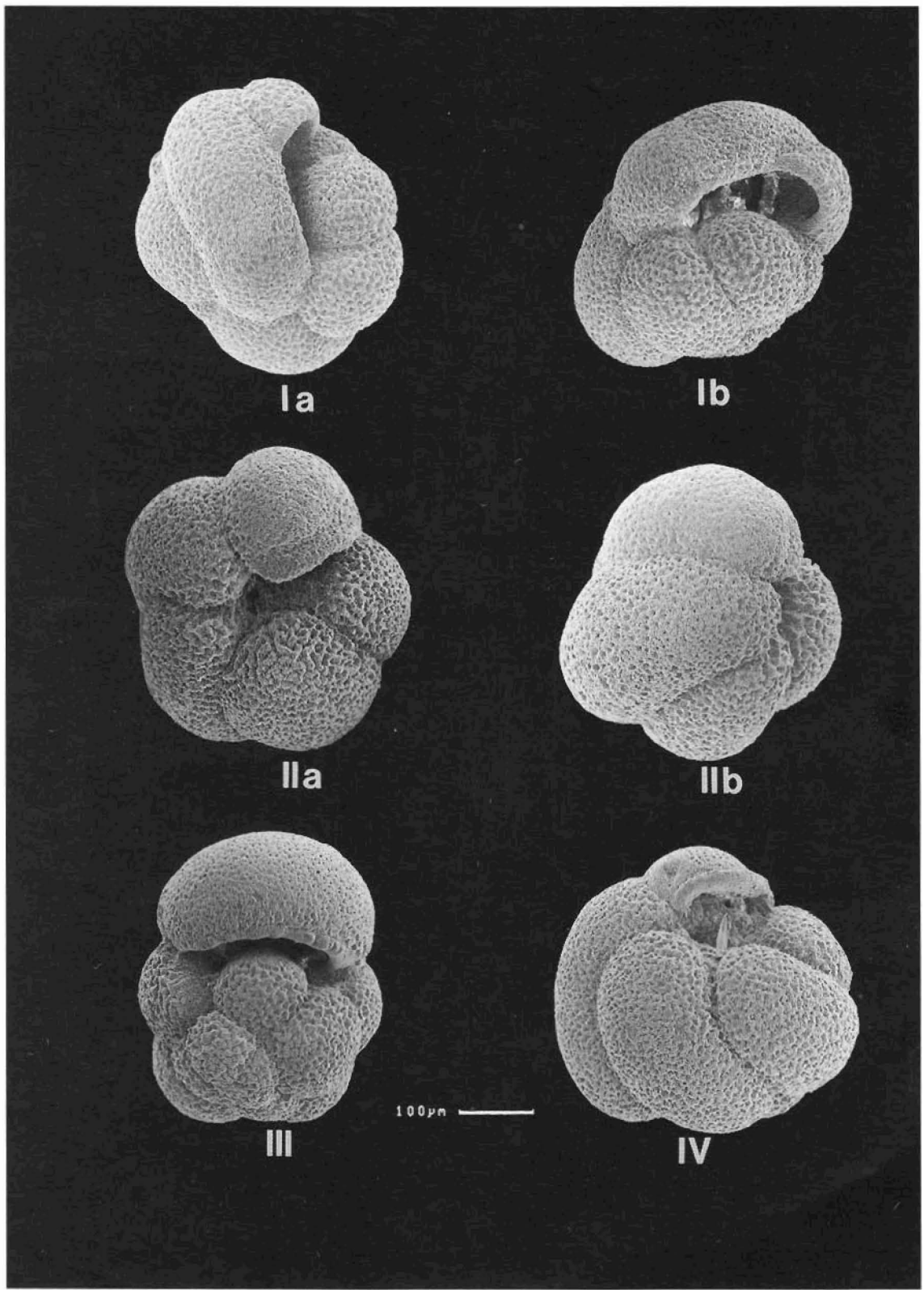


Plate 1. SEM-photographs of *Neogloboquadrina pachyderma* (sin.) wurstkammer specimens in Core PS2185 (central Arctic Ocean). Fig. Ia, b: Wurstkammer specimens in different views (49 ka B.P.). Fig. IIa, b: Wurstkammer specimens in different views (78 ka B.P.). Fig. III: Wurstkammer specimen (122 ka B.P.). Fig. IV: Wurstkammer specimen (78 ka B.P.).

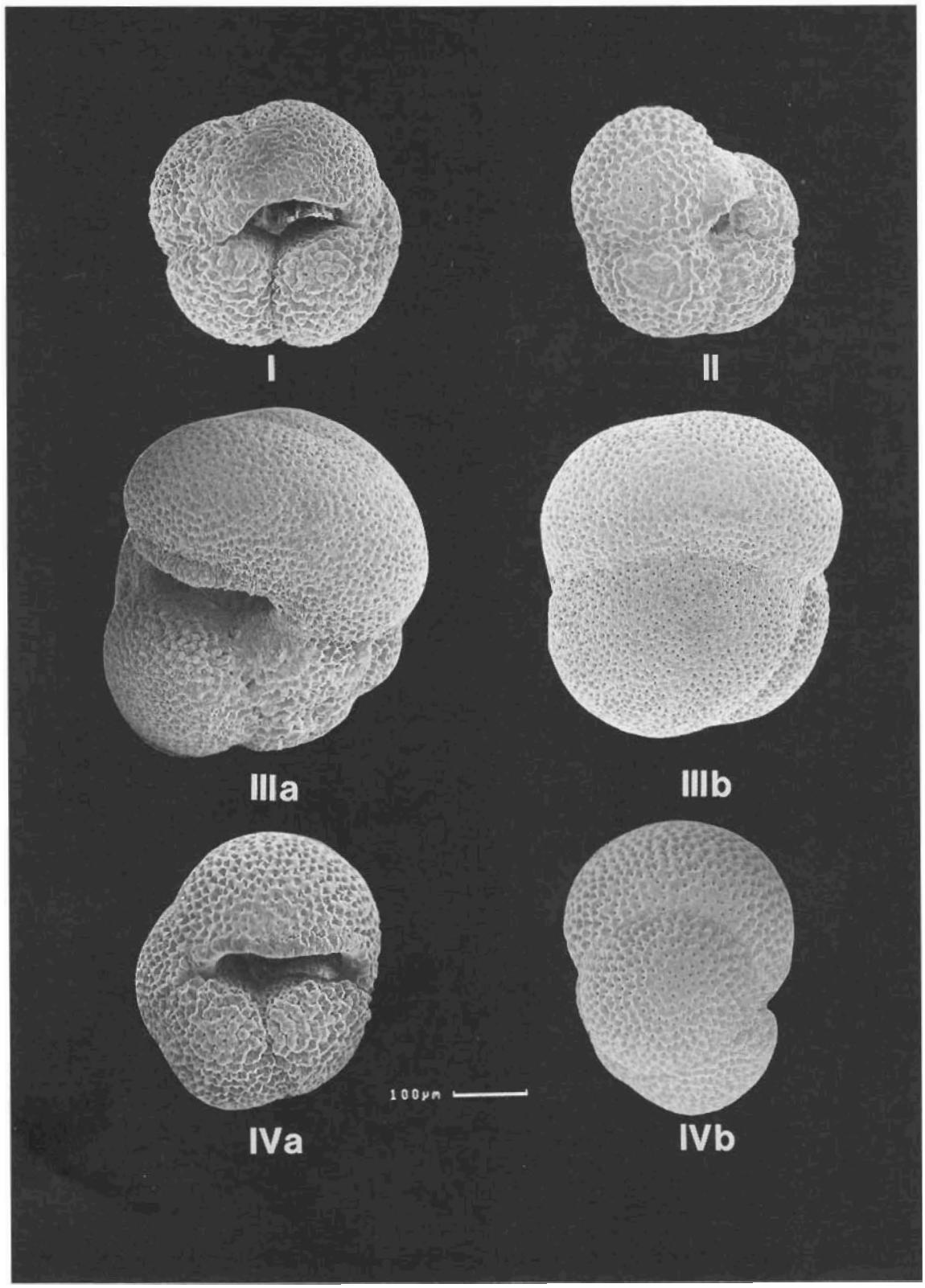


Plate 2. SEM-photographs of *Neogloboquadrina pachyderma* (sin.) wurstkammer specimens in Core PS1388 (Weddell Sea). Fig. I: Regular-formed specimen (122 ka B.P.). Fig. II: Kummerform specimen (15 ka B.P.). Fig. IIIa, b: Wurstkammer specimens in different views (18 ka B.P.). Fig. IVa, b: Wurstkammer specimens in different views (132 ka B.P.).

Effects of bed-load transport on planktonic foraminifer tests

KLAUS H. MICHELS[1] AND HELGE MEGGERS[2]

1. Bundesanstalt für Geowissenschaften und Rohstoffe, Stilleweg 2, D-30655 Hannover, Germany

2. Fachbereich Geowissenschaften, Universität Bremen, Klagenfurter Str., D-28359 Bremen, Germany

ABSTRACT

This investigation focuses on changes in the ultrastructure of planktonic foraminifer tests caused by sediment transport in the marine environment. Foraminifer tests that were unambiguously transported by bottom or turbidity currents (confirmed by sorting of the sediment) show changes in the ultrastructure of the crystalline part of tests. These changes can be distinguished from dissolution effects. Analysis of the ultrastructures by scanning electron microscopy clearly indicates physical abrasion of exposed parts of test surfaces during bottom-current transport; this may result in the disintegration of the test with persisting transport. In contrast, chemical dissolution acts upon the whole surface of the tests, both on exposed and more sheltered parts.

As a consequence, poor preservation and fragmentation of biogenic marine sediments must not necessarily be attributed to dissolution, but can be the result of bed-load transport. Moreover, the recognition of evidence for bed-load transport has important consequences on the assessment of the foraminifer tests as carriers of environmental signals.

INTRODUCTION

Foraminifers as sedimentary particles

Sediments can reveal important information about their formation. Evidence can be sedimentary structures on different scales or the occurrence of single grains with features that are characteristic of particular processes. Therefore, the detailed analysis and interpretation of marine sediment samples is an important method for increasing the knowledge of the formation processes of the sediment.

The study of foraminifer tests is crucial for a wide range of marine sedimentological investigations because foraminifers are important carriers of environmental signals such as stable isotope and geo- and biochemical signals that reveal information about water mass properties and nutrient contents. Because of the low density of empty (i.e. water-filled) foraminifer tests [e.g. 1.5 g/cm^3 for 250 µm planktic foraminifer tests (Berger & Piper, 1972); mean densities of 1.29 (*Globorotalia hirsuta*), 1.16 (*Globigerinoides ruber*), 1.30 (*Globigerinoides sacculifer*) and 1.48 g/cm^3 (*Orbulina universa*) (Fok-Pun & Komar 1983); 1.368 - 2.388 g/cm^3 for *Neogloboquadrina pachyderma* (Oehmig 1993)], they are transported by relatively slow currents as bed-load at the sediment surface or in suspension, together with medium to coarse silt and fine sand terrigenous particles. Thus, they may be found in places and environments that are not related to (or not immediately beneath) the surface waters where they originated. To interprete environmental signals indicated by these tests, it is essential to know the transport history of the tests and the physical influences (both physical abrasion and dissolution in the water column or in the sediment) that have acted on them on their way through the water column, whether bed-load transport is possible and the duration at the site of deposition where the sediment sample has been taken. Detailed investigations of the ultrastructure of foraminifer shells are a method to trace these influences.

Marine bottom currents and their effect on foraminifer tests

Sediment transport by thermohaline bottom currents and turbidites in the marine environment is a widely recognized phenomenon (e.g. Hollister & Nowell, 1991; Edwards, 1993). While there is continuous transport of fine grained particles in nearly

In: Hass, H.C. & Kaminski, M.A. (eds.) 1997. Contributions to the Micropaleontology and Paleoceanography of the Northern North Atlantic. *Grzybowski Foundation Special Publication*, no. 5, pp. 263-271

all parts of the oceans, transport of sand- and medium to coarse silt is principally restricted to events with higher current velocities ('deep sea storms', Kerr 1980; Gardner & Sullivan, 1981; Hollister & McCave, 1984), to areas with generally higher current velocities (e.g. 'contourite currents', Faugères & Stow, 1993), and to regions that generally show higher sediment transportation rates ('sediment drifts', e.g. McCave & Tucholke, 1986). During high current velocity events even foraminifer tests can be moved. This may result in accumulation of well-sorted foraminifer tests in distinct layers of mm to cm thickness in the sediment column. These are commonly referred to as contouritic layers. When these foraminifer tests are moved as bed-load, markings develop on the surface of the shells that are comparable to the rounding of fluvial and coastal sediment detrital grains. Due to the fragility of foraminiferal tests, abrasion may cause early break-up of the carbonate shell.

Until now, the disintegration and break-up of foraminifer shells has often been attributed to carbonate dissolution, either during settling through the water column or in the sediment due to dysoxic or undersaturated conditions. This investigation is dedicated to the recognition of the effects o bottom current transport on planktonic foramini feral tests before their disintegration. To evaluate this effect, detailed investigations were carried out using high-resolution scanning electron microscopy (SEM) methods. In our study, we concentrate on the planktonic foraminifer species *Neogloboquadrina pachyderma* (sinistral), a polar and subpolar species commonly present in large numbers in hemipelagic surface sediments of the northern North Atlantic (Henrich *et al.*, 1989). Whether or not the sediments were influenced by coarse-grained particle transport was inferred from the sorting of the sediment; this is indicated by the shape of the settling velocity distributions (Michels, 1995).

The investigations focus on the crystalline part of the foraminiferal test that was built up during gametogenesis (Ketten & Edmond, 1979). These crystalline areas allow the examination of physical and/or chemical effects on the tests under continuing physical and/or chemical stress (carbonate dissolution) that may lead to their disintegration.

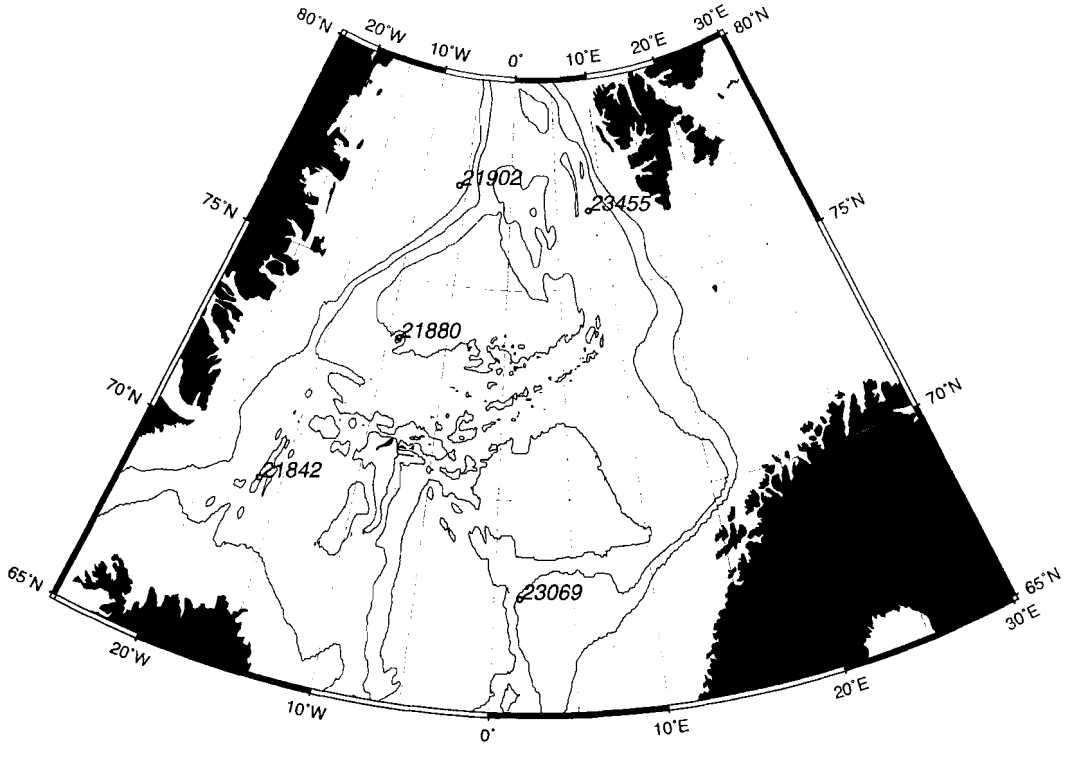


Figure 1. Map of the northern North Atlantic, including the locations of investigated surface sediment samples. Isolines indicate the 1000, 2000 and 3000 m isobaths.

The hypothesis that is tested in this study is that physical influences by bottom-current transport and attack by dissolution can be distinguished by the effect on sharp-edged and sharp cornered crystals of the ultrastructure of the foraminifer test's surface. The attack of dissolution ideally affects the whole surface that is exposed to corrosive seawater, causing stronger dissolution of corners and edges because of their larger exposed surface compared to the crystal planes. It is suggested that all edges, corners, and planes of a crystal should be corroded to the same extent. In contrast physical abrasion of a surface consisting of numerous crystals leads to the rounding or removal of most exposed corners and edges.

To highlight the differences of physical and chemical attack on the ultrastructure of the foraminifer test surface, the results are illustrated comparing SEM photographs of completely undissolved but not transported, slightly dissolved but not transported, and transported but undissolved foraminifer tests.

MATERIAL AND METHODS

Samples

Surface sediment samples (1 cm in thickness) were collected from several core sites that were obtained during the RV Meteor cruises M 2/2 in 1986 (Gerlach *et al.*, 1986), M 21/4 in 1992 (Pfannkuche *et al.*, 1993) and during RV Polarstern cruise ARK-VII/1 in 1990 (Thiede & Hempel, 1991) into the northern North Atlantic (Fig. 1).

The samples were taken from the sediment surface of box cores, freeze-dried, weighed, and split into the coarse (>63 µm) and fine fractions (<63 µm) by wet sieving. The fine and coarse fractions were split into halves. The grain size fraction 37-63 µm of one half of the fine fraction was separated according to Stokes' law using the Atterberg settling velocity method. The separated 37-63 µm fraction was then added to one half of the coarse fraction, resulting in a >37 µm fraction. This preparation of the coarse fraction provides samples with the full range of adult foraminifer tests and a grain size range of coarse-grained particles that, in case of current influence, are transported as single unaggregated grains (McCave *et al.*, 1995).

Terrigenous component

Carbonate was removed using hydrochloric acid. The carbonate percentage of the sample was determined by weighing the sample before and the residue after acid treatment. The carbonate-free >37 µm fraction was also subjected to a settling velocity analysis in order to gain additional information about the transport of noncalcareous, terrigenous material that can be correlated with the transport of foraminifer tests.

Settling velocity

To obtain a settling velocity distribution of the >37 µm fraction, a 0.5-1 g sample of both carbonate-free and carbonate-containing sediment was analysed in a Macrogranometer™ settling tube (Brezina, 1969). These settling velocity distributions were analyzed following the method described in Michels (1995). Although the settling velocities obtained for foraminifers cannot be compared to the settling velocities in the water column of the ocean, they reveal a high resolution record of the sediment sorting. This can be interpreted with regard to bottom current influences that may have changed the grain size distribution of the sediment (Michels, 1995). Since every foraminifer species has its own characteristic settling velocity distribution and settling velocity range (Michels, 1995), even slight changes can be attributed to current influence.

Ultrastructure of shells

For the SEM investigations of the ultrastructure of the crystalline part of the tests, microscope slides were prepared with at least 30 specimen of *N. pachyderma* randomly taken from the coarse fraction (>37 µm) of the sample. These specimens were studied in detail for the ultrastructure of their crystalline surfaces.

Preservation

Preservation of *Neogloboquadrina pachyderma* sin. tests (usually ca. 40 tests) was studied using the SEM. Five-step progressive stages of dissolution (0 - undissolved to 4 - strongly dissolved) of two principal surface types, reticulate and crystalline, were distinguished. Reticulate tests are composed of nannocrystals in an initial tiny primary microcrystalline layer and a secondary agglomerated layer with crystals arranged as diffuse palisades. Crystalline morphotypes develop tertiary calcitic crusts composed of large rhombohedra at the surface. This crust may completely or partly cover the surface. The differentiation between morphotypes in dissolution studies is important because of the lower preservation potential of the microgranular morphotype relative to the crystalline one. Finally, a composite dissolution index was calculated for each sample (*cf.* Henrich, 1989; Baumann & Meggers, *in press*).

It cannot be completely ruled out that the wet-sieving process influenced the ultrastructure of the foraminifer test's surface, although this procedure was carried out carefully. It is, however, of minor importance when compared with the bottom-current transport or the dissolution effects.

RESULTS AND INTERPRETATION

Transported *N. pachyderma* tests unaffected by dissolution

Figure 2 shows the settling velocity distributions (>37 µm) of two well-sorted surface sediments from location 23455 (southern Fram Strait) and 21880 (Greenland Basin, Vesteris Banken Seamount) and a moderately sorted surface sample from the Greenland continental shelf (21902). Distributions of carbonate and terrigeneous material are indicated by different curves.

The percentage of the >37 µm fraction compared to the bulk sediment and the $CaCO_3$ content is quoted in the figure caption. Dissolution indices of the *N. pachyderma* tests are approximately 0.9 for all three samples, thus the tests are very well preserved in terms of carbonate dissolution.

In case of no current influence and thus no sorting, *N. pachyderma* generally occurs in the settling velocity range between 1 and 2 cm/s according to its natural growth size distribution. This distribution is indicated by the shaded peak (marked with *N. pachyderma* reference peak).

The sediment of location 23455 in the Fram Strait shows the best grain size sorting (i.e. the sharpest peak). This is the settling velocity distribution of a sediment that has been very well sorted during current transport of both carbonate and terrigenous particles (indicated by the same settling velocity range of the carbonate and terrigenous peaks) as bed-load or in suspension. The sorting is a function of either duration of transport or intensity of the process. When transported, the sediment particles, even the *N. pachyderma* tests, must have been strongly moved. The fact that the *N. pachyderma* reference peak is near the bulk sediment peak merely indicates that the grain-size range that was involved in the transport process includes the whole grain-size spectrum of *N. pachyderma*. It does not indicate, however, that the sediment was not sorted by bottom currents. This type of sediment typically appears in areas of contourite currents or as a turbidite deposit.

The sediments of core positions 21880 and 21902 are generally coarser. The sorting of the sediment in location 21880 is better than that of location 21902, which suggests different processes: a depletion of the fine fraction due to strong currents and the generation of a residual sediment is assumed to be the reason for the shape of the settling velocity distribution of the 21902 curve. In this curve, the grain size range is broader and more discontinuous than that in 21880, which points to the formation of a residual sediment with coarse grain sizes, where the fine fraction has been depleted by winnowing. The settling velocity distribution at 21880 is most probably the result of transport and subsequent deposition of a coarse-grained sediment (i.e. accumulation sediment, e.g. by a turbidite); this is indicated by its smoother curve, a narrower grain size range and a clearly defined upper limit in the grain-size range. However, both sediments have certainly been affected by strong currents.

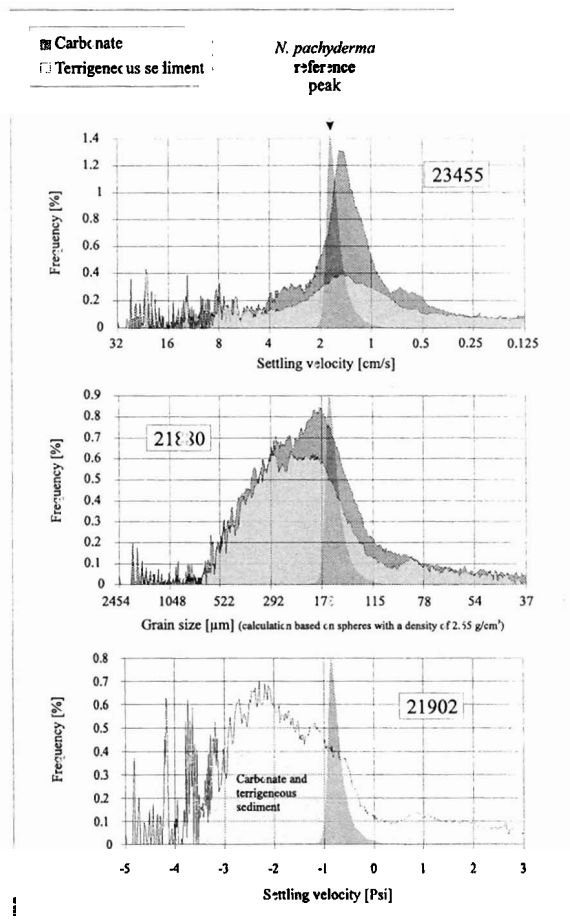


Figure 2. Settling velocity distributions of the >37 µm fraction of the surface sediments from locations 23455, 21880, and 21902. Unimodal settling velocity distributions with more or less narrow peaks indicate very well- to well-sorted sediments. The >37 µm distributions of carbonate and terrigeneous sediment fractions of locations 23455 and 21880 are depicted by different shades of gray. The settling velocity distribution of a *N. pachyderma* peak unaffected by current influence ("*N. pachyderma* reference peak") is represented by the shaded area. The dissolution index of all samples is low (~ 0.9); the >37 µm fraction portions of the bulk sediments and the carbonate contents of the coarse fractions make up 43%/46% at location 23455, 90%/20% at location 21880, and 47%/10% at location 21902. The scales of the three diagrams are equal, however, they provide settling velocities in cm/s, in Psi (the negative logarithm to a base of 2 of the settling velocity in cm/s), and as the corresponding grain size (calculated on the basis of round spheres with a density of 2.65 g/cm³) as further information.

SEM investigations of the crystalline surfaces of the *N. pachyderma* tests reveal differences in the surface ultrastructures of exposed rhombohedra (Plate 1). Uncorroded crystal planes are smooth while crystal edges and corners in protected places are sharp. However, the more exposed edges and corners there are, the more they are rounded and eroded. There is evidence that shaping of the edges and corners takes place through different processes: abrasion of exposed crystal edges and corners occurs mainly during low-energy transport (i.e. rolling transport) of the foraminiferal tests (Plate 1, upper and lower left photographs), but corners may completely break off at the top of the crystals only during high-energy movement of the tests (i.e. saltation transport) when they hit other sediment particles (Plate 1, upper and lower right photographs).

Partly dissolved *N. pachyderma* tests unaffected by currents

The settling velocity distribution from location 21842 sediments (Kolbeinsey Ridge, Iceland Plateau, Fig. 3) reveals a large percentage of finer grains in the >37 µm fraction. This is inferred to be the result of the deposition of fines from decelerating currents. The percentage of the >37 µm fraction makes up just 13% of the bulk sediment. Carbonate dissolution has a significant effect on the sediment, which is reflected by the dissolution index of 2.05. The investigation of the crystalline ultrastructures of the test surfaces shows that corners and edges of all rhombohedra in both exposed and protected positions are moderately to strongly corroded (Plate 2, lower left and right photographs). Crystals exhibit rough, corroded surfaces; their edges are more dissolved than the planes because of their larger surfaces (compared to the crystal's volume) and corners are even more affected than edges.

***Neogloboquadrina pachyderma* tests, not affected by currents and dissolution**

Figure 4 shows the settling velocity distribution of the coarse-grained fraction of a sample from the outer Vøring Plateau (23069). The sediment is very well preserved in terms of carbonate dissolution (dissolution index = 0.77). According to the polymodal settling velocity distribution with several distinct peaks of different foraminifer species (in Fig. 4 the main planktonic and benthic foraminifer species in the sediment are assigned to the main peaks in the distribution according to Michels 1995), there was little influence of bottom currents on the sediment. SEM investigations yield that the majority of the rhombohedra of the crystalline areas of the test surfaces are characterized by very sharp corners and edges in exposed as well as in sheltered positions (Plate 2, upper left and right photographs).

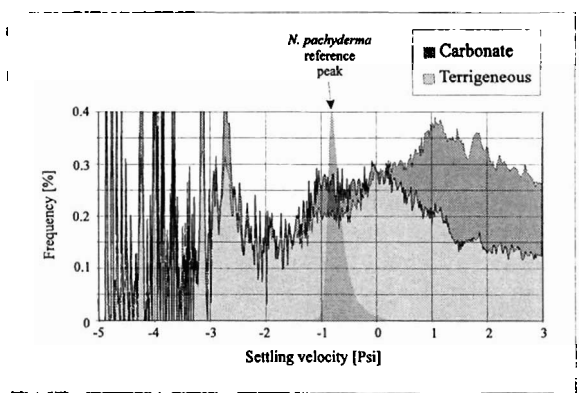


Figure 3. Settling velocity distributions of the >37 µm fraction of the surface sediment of location 21842. The >37 µm distributions of carbonate and terrigeneous sediment fractions are depicted by different shades of gray. A high peak of current-accumulated carbonate in the low settling velocity range between 0 and 3 Psi indicates that *N. pachyderma* tests (which settle in the range of the shaded reference peak) have probably not been moved by currents. Carbonate dissolution has had a significant influence on the *N. pachyderma* tests; the index is 2.06. The >37 µm fraction portion of the bulk sediment makes up 13% and the carbonate content of the >37 µm fraction 21%.

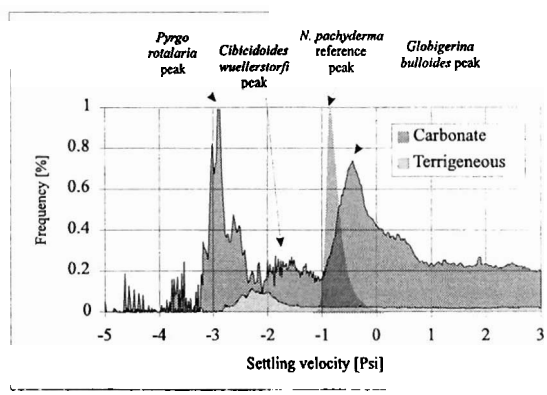


Figure 4. Settling velocity distribution of the >37 µm fraction of the surface sediment from location 23069. The >37 µm distributions of carbonate and terrigeneous sediment fractions are depicted by different shades of gray. The settling velocity distribution of a *N. pachyderma* peak unaffected by current influence ("*N. pachyderma* reference peak") is represented by the shaded area. The polymodal carbonate curve and low contents of terrigeneous material indicate a sediment type that is not affected and sorted by currents. Because of the low dissolution index of 0.77, the sediment can be viewed as unaffected by dissolution. The >37 µm fraction portion of the bulk sediment makes up 16% and the carbonate portion of the >37 µm fraction is about 9%.

DISCUSSION

Dissolution

A sediment assemblage of planktonic foraminifera contains a complex mixture of environmental information including biological, chemical and physical parameters. Different methods have been used to decipher the physical and chemical effects on foraminifer tests.

To quantify the effects of dissolution, different planktonic foraminifera species traditionally have been ranked according to their dissolution potential (Ruddiman & Heezen, 1967; Berger, 1968; Boltovskoy & Totah, 1992) or fragmentation indices have been defined (Thunell, 1976; Le & Shackleton, 1992). It was assumed in these investigations that no processes other than dissolution have an effect on the preservation of the tests.

However, our results demonstrate that *N. pachyderma*, which is very resistant to dissolution (Berger, 1968; Boltovskoy & Totah, 1992), clearly can show abrasion as a result of bed-load transport. The effect of current transport on the ultrastructure of less resistent fragile planktonic foraminifers, like *G. sacculifer* or *G. ruber*, which are the most prominent species in tropical water masses (Vincent & Berger, 1981), must be much higher and could as well initiate the complete fragmentation of the tests. Therefore, a failure to recognise transport of foraminifera tests may lead to a systematic false interpretation of carbonate dissolution, derived from fragmentation indices of different planktonic foraminifer species. Effects of transport and dissolution should therefore be carefully studied.

A combination of the investigations carried out in this study with a method of quantifying dissolution effects by the recognition of progressive dissolution stages on the crystalline surface of planktonic foraminifera with the SEM, like that proposed by Bé *et al.* (1975), Henrich (1989), and Meggers (1996), could achieve a qualitative and quantitative description of abrasion and dissolution effects on foraminifer tests.

Bed-load transport

Abrasion and fragmentation of foraminifer tests is mainly controlled by the intensity of particle transport by currents and the duration of current influence. For the extent of the physical impact on the foraminifer tests, it is important whether

- foraminifer tests are transported as bed-load or in suspension (related to the energy of the current),
- transportation takes place as a persistent (contour current) or ephemeral (turbidity current) event,
- grain sizes, that are transported simultaneously, are coarse or fine,
- many or few other particles are transported simultaneously as bed-load or in suspension.

The listed factors show that the abrasion and fragmentation of foraminifer tests are closely related to the hydrodynamic parameters of the current. For sediment samples, it is very difficult to reconstruct all of the listed parameters from grain size or settling velocity distributions. But the interpretation of granulometric data may indicate which sedimentary processes took place. For example in the description of our samples, we pointed out that the granulometric data support (a) the interpretation as a turbidite and (b) that rolling transport as a low energy form may mainly have led to the abrasion of the most exposed crystals of the crystalline foraminifer test surface, whereas saltation as a high energy form of particle movement may have led to a complete removal of the tip of the crystals.

However, the quantification of the processes that influence the abrasion and fragmentation of foraminifer tests could probably only be achieved by experiments in a flume (or more simply in a tumbler).

CONCLUSIONS

The hypothesis that physical (abrasion) and chemical (dissolution) impacts can be differentiated in the ultrastructure of a crystalline surface of foraminifer tests has been corroborated by SEM observations of foraminiferal test surfaces. Especially the crystalline part of the shell built up during gametogenesis is well suited to give a differentiated imprint of the stress foraminiferal shells are exposed to during the sedimentation processes. The described method can be used in addition to other methods to verify and increase the knowledge of sediment transport and carbonate dissolution.

Physical impacts, caused by sediment transport, and chemical impacts, caused by dissolution, can be distinguished by means of different effects on the crystalline ultrastructure of the shells. While physical impact during transportation of the shells only affects the exposed crystals of the outer surface, chemical impact by dissolution acts upon the whole surface, including the crystalline edges and planes in more sheltered positions. Thus, the investigation provides insights into the depositional history of foraminifer shells that is crucial for the interpretation of foraminiferal data. In particular biogeochemical and isotope data that are based on foraminiferal analyses may be very sensitive to changes caused by dissolution or bed-load transport and should therefore be reinterpreted carefully after dissolution or bed-load transport has been proved. Perhaps conflicting results between carbon isotope data, carbonate dissolution

data and sedimentological can then be solved without inconsistency.

ACKNOWLEDGEMENTS

The authors gratefully acknowledge the helpful comments and constructive remarks of Christian Hass and one anonymous referee. Thanks are given to Helga Heilmann who provided technical assistance in preparation of the plates. This work was supported by the „Deutsche Forschungsgemeinschaft" (DFG Grant no. He 1671/4-1,2) and the „Sonderforschungsbereich (SFB) 313" at the University of Kiel. This is SFB 313 contribution no 327.

REFERENCES

Baumann, K.H. & Meggers, H. 1996. Palaeoceanographic changes in the Labrador Sea during the past 3.0 My: Evidence from calcareous plankton records. *In:* Whatley, R. & Moguilevsky, A. (eds.), *Microfossils and oceanic environments*, The University of Wales, Aberystwyth Press, 131-153.

Bé, A.W.H., Morse, J.W. & Harrison, S.M. 1975. Progressive dissolution and ultrastructural breakdown of planktonic foraminifera. *In:* Sliter, W.V., Bé, A.W.H. & Berger, W.H. (eds.), Dissolution of Deep-Sea Carbonates. *Cushman Found. Foram. Res. Spec. Publ.*, **13**, 27-55.

Berger, W.H. 1968. Planktonic foraminifera: selective solution and paleoclimatic interpretation. *Deep-Sea Research*, **15**, 31-43.

Berger, W.H. & Piper, D.J.W. 1972. Planktonic foraminifera: differential settling, dissolution and redeposition. *Limnology and Oceanography*, **17**, 275-287.

Boltovskoy, E. & Totah, V.I. 1992. Preservation index and preservation potential of some foraminiferal species. *Journal of Foraminiferal Research*, **22**, 267-273.

Brezina, J. 1969. Granulometer - a sediment analyzer directly writing grain size distribution curves. *Journal of Sedimentary Petrolology*, **39**, 1627-1631.

Edwards, D.A. 1993. *Turbidity currents: dynamics, deposits, and reversals*. 173 pp., Springer, Berlin.

Faugères, J.-C. & Stow, D.A.V. 1993. Bottom-current-controlled sedimentation: A synthesis of the contourite problem. *Sedimentary Geology*, **82**, 287-297.

Fok-Pun, L. & Komar, P.D. 1983. Settling-velocities of planktonic foraminifera: density variation and shape effects. *Journal of Foraminiferal Research*, **13**, 60-68.

Gardner, W.D. & Sullivan, L.G. 1981. Benthic storms: Temporal variability in a deep ocean nepheloid layer. *Science*, **213**, 329-331.

Gerlach, S.A., Thiede, J., Graf, G., & Werner, F. 1986. Forschungsschiff Meteor, Reise 2 vom 19. Juni bis 16. Juli 1986, Forschungsschiff Poseidon, Reise 128 vom 7. Mai bis 8. Juni 1986. *Berichte aus dem Sonderforschungsbereich 313*, **4**, 1-140.

Henrich, R. 1989. Glacial/interglacial cycles in the Norwegian Sea: Sedimentology, paleoceanography, and evolution of Late Pliocene to Quarternary Northern Hemisphere climate. *In:* Eldholm, O., Thiede, J., Taylor, E., *et al.* (eds.), *Proc. ODP, Sci. Results*, **104**, 189-232, College Station, TX (Ocean Drilling Program).

Henrich, R., Kassens, H., Vogelsang, E. & Thiede, J. 1989. Sedimentary facies of glacial-interglacial cycles in the Norwegian Sea during the last 350 ka. *Marine Geology*, **86**, 283-319.

Hollister, C.D. & McCave, I.N. 1984. Sedimentation under deep-sea storms. *Nature*, **309**, 220-225.

Hollister, C.D. & Nowell, A.R.M. 1991. Prologue: Abyssal storm as a global geologic process. *Marine Geology*, **99**, 275-280.

Kerr, R.A. 1980. A new kind of storm beneath the sea. *Science*, **208**, 484-486.

Ketten, D.R. and Edmond, J.M. 1979. Gametogenesis and calcification of planktonic foraminifera. *Nature*, **278**, 546-548.

Le, J. & Shackleton, N.J. 1992. Carbonate dissolution fluctuations in the western equatorial Pacific during the Late Quaternary. *Paleoceanography*, **7**, 21-42.

McCave, I.N., Manighetti, B., & Beveridge, N.A.S. 1995. Circulation in the glacial North Atlantic inferred from grain-size measurements. *Nature*, **374**, 149-152.

McCave, I.N. & Tucholke, B.E. 1986. Deep current-controlled sedimentation in the western North Atlantic. *In:* Vogt, P.R. & Tucholke, B.E. (eds.), *The Geology of North America, Volume M, The Western North Atlantic Region*, 451-468, Geological Society of America.

Meggers, H. 1996. Pliozän-Quartäre Karbonatsedimentation und Paläozeanographie des Nordatlantik und des Europäischen Nordmeeres - Hinweise aus planktischen Foraminiferengemeinschaften. *Berichte aus dem Fachbereich Geowissenschaften der Universität Bremen*, **71**, 1-143.

Michels, K.H. 1995. The decomposition of polymodal settling velocity distributions for a comprehensive sedimentological description of sand-sized samples. *Sedimentology*, **42**, 31-38.

Oehmig, R. 1993. Entrainment of planktonic foraminifera: effect of bulk density. *Sedimentology*, **40**, 9-14.

Pfannkuche, O., Duinker, J.C., Graf, G., Henrich, R., Thiel, H., & Zeitzschel, B. 1993. Meteor Reise Nr. 21, Nordatlantik 92, 16. März - 31. August 1992. *Meteor-Berichte*, **93-4**, 1-281.

Ruddiman, W.F. & Heezen, B.C. 1967. Differential dissolution of planktonic foraminifera. *Deep-Sea Research*, **14**, 801-808.

Thiede, J. & Hempel, G. 1991. Die Expedition ARKTIS-VII/1 mit FS „Polarstern" 1990. *Berichte zur Polarforschung*, **80**, 1-137.

Thunell, R.C. 1976. Optimum indices of calcium carbonate dissolution in deep-sea sediments. *Geology*, **4**, 525-528.

Vincent, E. & Berger, W.H. 1981. Planktonic foraminifera and their use in paleoceanography. *In:* Emiliani, C., *The oceanic lithosphere*, 1025-1119, Wiley, New York.

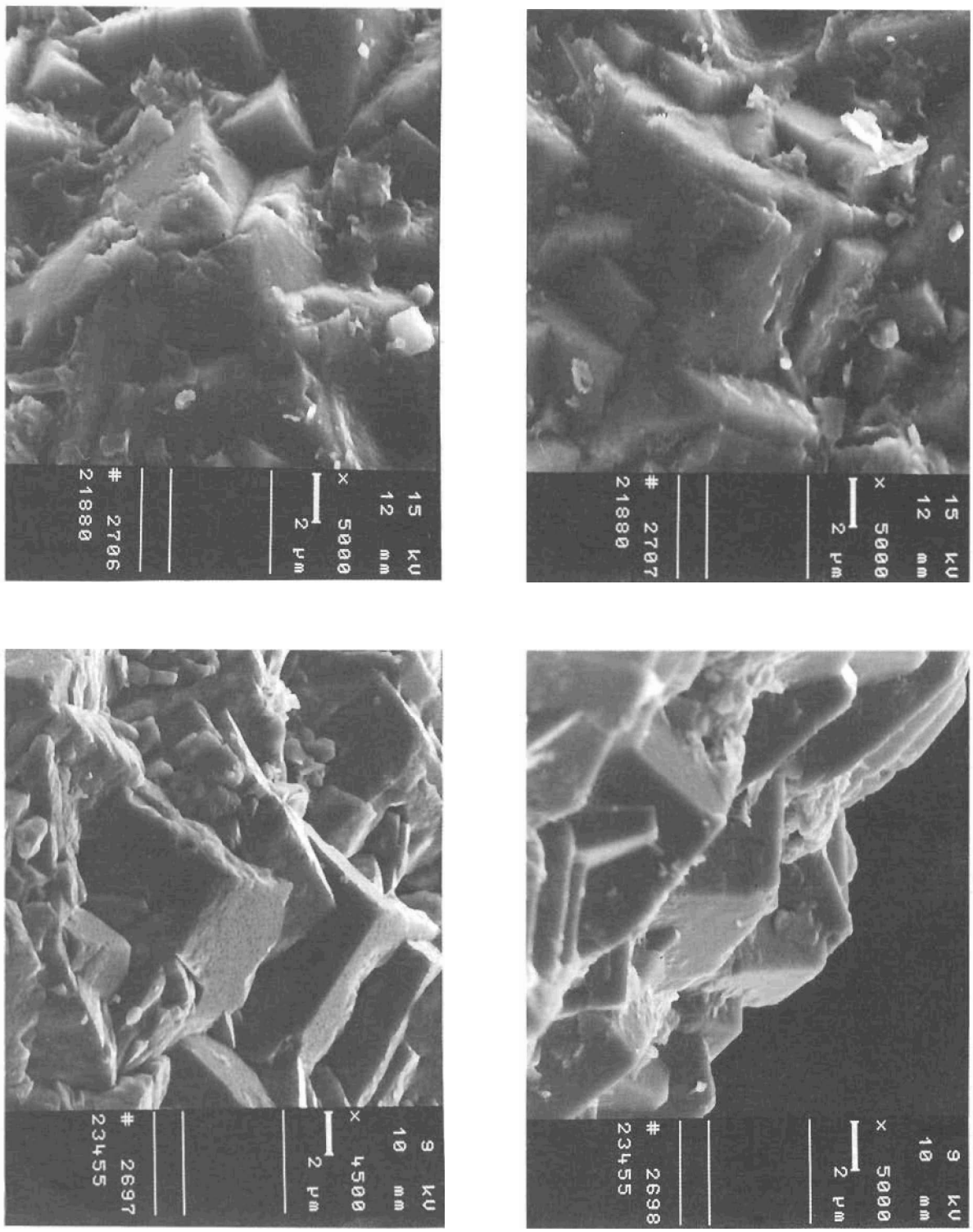


Plate 1. SEM photographs of the crystalline surface ultrastructures of transported *N. pachyderma* tests from the sediment surface samples of locations 23455 and 21880 that are not affected by carbonate dissolution. The upper and lower left pictures show crystals where the exposed crystal edges and corners were abraded during rolling transport of the foraminiferal test; the upper and lower right pictures show crystals where corners were completely broken off the top of the crystals during saltation-transport of the test when it hit other sediment particles.

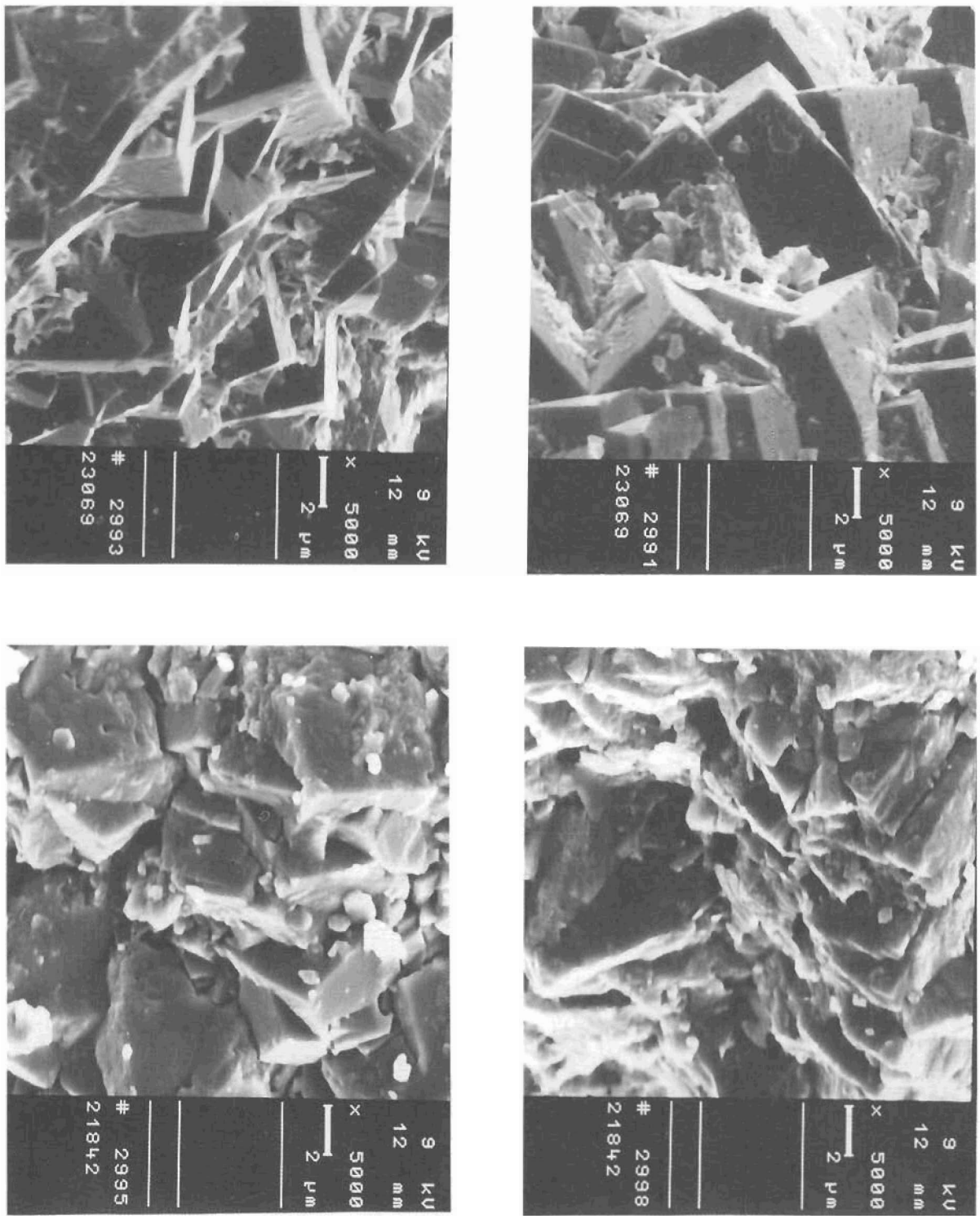


Plate 2. The upper left and right SEM photographs show ultrastructures of the crystalline surface of *N. pachyderma* tests from the sediment surface sample of location 23069 that are affected neither by sediment transport nor by carbonate dissolution. The lower left and right SEM photographs show ultrastructures of the crystalline surface of *N. pachyderma* tests that were not transported but were affected by carbonate dissolution (sediment surface sample from location 21842).